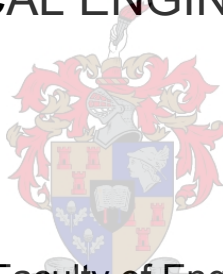


Kinetic and Economic Potential Evaluation of Grubbs-type Precatalysts for 1-Octene Metathesis

by
Chaney Gene Visser

Thesis presented in partial fulfilment
of the requirements for the Degree
of

MASTER OF ENGINEERING
(CHEMICAL ENGINEERING)



in the Faculty of Engineering
at Stellenbosch University

Supervisor
Prof. P. Van der Gryp

Co-Supervisor/s
Dr N. Goosen
Prof. H.C.M. Vosloo

December 2017

Declaration

By submitting this thesis electronically, I declare that the entirety of the work contained therein is my own, original work, that I am the sole author thereof (save to the extent explicitly otherwise stated), that reproduction and publication thereof by Stellenbosch University will not infringe any third-party rights and that I have not previously in its entirety or in part submitted it for obtaining any qualification

Date: December 2017

Abstract

The RSA olefins programme of the DST-NRF Centre of Excellence in Catalysis (c*change) aims to upgrade low-value linear 1-alkenes (also known as alpha-olefins) to high-value Guerbet-type surfactants via a proposed reaction sequence of which the initial step is the organometallic catalytic reaction of metathesis. Metathesis enables atom-efficient, green chemistry synthesis by reducing the number of synthesis steps required with current industry methods. Metathesis research has yielded a library of ruthenium carbene precatalysts, each with its own attributes and shortcomings. Previous work has designed and investigated the performance, kinetics, and industrial viability of precatalysts with the aim of improving thermal stability and efficiency for the metathesis of 1-octene, but has not compared precatalysts from an economic point of view. With the emergence of each new synthesised precatalyst, information such as the kinetic behaviour and performance is required before any economic evaluation can be made. In this study the combined catalytic, kinetic and economic performance of two chelating pyridinyl alcholato (O^N) ruthenium carbene precatalysts of the Grubbs 2nd generation type [RuCl(H₂IMes)(O N) (=CHPh)] where O N = 1-(2'-pyridinyl)-1-(cyclopentyl)-methanolato (**GCYC**) and O N = 1-(2'-pyridinyl)-1-(2'-methyl-phenyl),1-phenyl-methanolato (**GMPP**) was evaluated for 1-octene metathesis.

Metathesis reactions were conducted in a batch reactor with neat 1-octene (C₈) while investigating the effects of temperature (40 - 100°C) and precatalyst load (C₈/Ru: 5 000 - 14 000). Kinetic parameters were obtained by measuring concentration profiles for seven hours and fitting these profiles to fundamental kinetic models. The Douglas method was utilised for designing a conceptual process and estimating the economic potential of each precatalyst

Peak performance was observed at 70°C for the **GCYC** precatalyst with turnover numbers (TONs) of 6631, 80% conversion of 1-octene (C₈) and 42% selectivity towards primary metathesis products. In comparison, for the **GMPP** precatalyst TONs of 5888, 60% C₈ conversion and 37% selectivity was obtained at peak temperatures between 70 and 90 °C. Latent thermo-switchable behaviour was observed where activation only occurred beyond the switching temperatures.

Various reaction kinetic models were developed and could account for experimentally observed thermal precatalyst deactivation and competing isomerisation reactions with reasonable accuracy. Activation energies for 1-octene consumption were determined as 30.24 kcal.mol⁻¹ and 13.10 kcal.mol⁻¹ for the **GCYC** and **GMPP** precatalysts respectively. Similarly, the deactivation energies found for the precatalysts were 22.81 and 5.84 kcal.mol⁻¹ respectively. The **GMPP**

precatalyst was found to follow step-function behaviour and the Arrhenius relationship was followed where complete precatalyst deactivation did not occur.

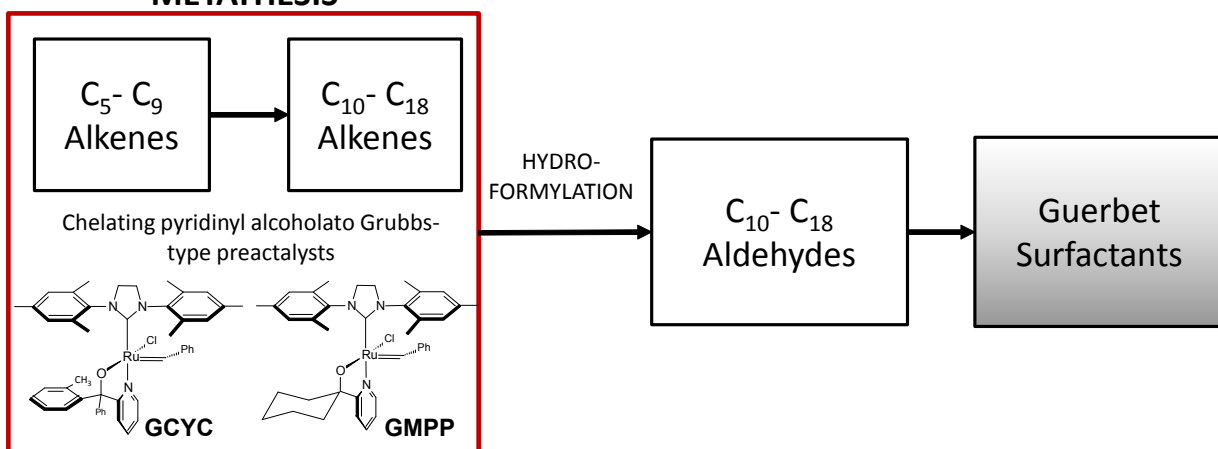
Economic evaluation over a Continuously Stirred Tank metathesis reactor – (CSTR -metathesis reactor) was found to be favourable for both precatalysts with an internal rate of return (IRR) of 73 and 53% respectively making them feasible choices for upgrading linear 1-alkenes to surfactants. The precatalyst with the best overall performance was found to be the **GCYC** precatalyst but the **GMPP** precatalyst still offers benefits of less stringent temperature control. Comparison studies with a commercial Hoveyda Grubbs 2nd generation catalyst **HG2** proved the commercial catalyst to still be the best at low temperatures with an IRR of 91%. Future studies are recommended to conduct Density Functional Theory (DFT) investigations into the precatalysts, expand the scope of precatalysts for the economic potential evaluation and to consider development studies towards piloting the proposed process.

Keywords:

Thermo-switchability, kinetics, economic evaluation, precatalyst deactivation, metathesis reactor.

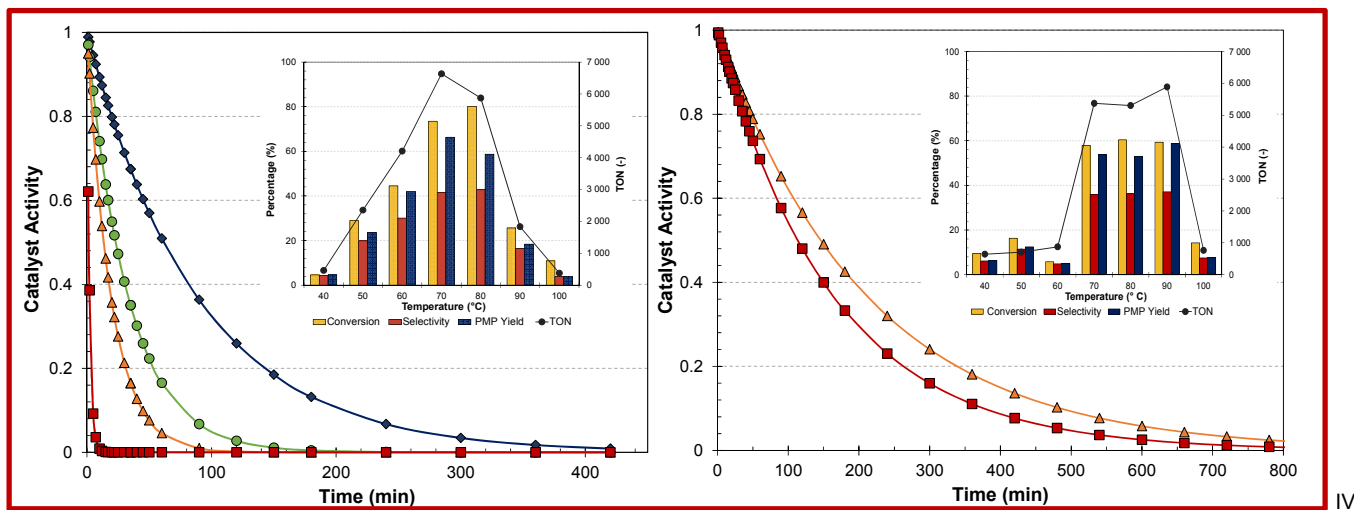
Graphical Abstract

METATHESIS



GCYC: IRR 73%

GMPP: IRR 53%



Opsomming

Die RSA Olefiene program van die DST-NRF Sentrum vir Uitnemendheid in Katalise (c*change) beoog om lae-waarde lineêre alkene (ook bekend as alpha-olefiene) (LLA) na hoë-waarde Guerbet-surfaktante om te skakel deur 'n voorgestelde reaksienetwerk waarvan die organometaal katalisereaksie van metatese die eerste stap is. Metatese bemagtig "groen-chemie", atoomdoeltreffende sinstese om opgradering van alkene te bewerkstelling deur die aantal stappes wat in huidige industriële metodes gebruik word te verminder. Navorsing in metatese het geleid tot die ontwikkeling van 'n reeks ruteniumkarbeen prekatalisators, met elk sy eie kenmerke en tekortkominge. Vorige navorsing het gefokus op die ontwerp en ondersoek van ruteniumkarbeen prekatalisators se prestasievermoë, kinetika, en industriële lewensvatbaarheid om die termiese stabilitet en effektiwitiet van die prekatalisator vir metatese met 1-okteen te verbeter, maar het nie die prekatalisators vergelyk van 'n ekonomiese oogpunt af nie. Met die opkoms van elke nuwe prekatalisator word inligting rakend die prekatalisator se kinetiese gedrag, en prestasievermoë benodig voordat 'n ekonomiese evaluering voltooi kan word. In hierdie studie is die ekonomiese en kinetiese prestasie van twee chelerende piridiniel alkoholato rutenium karbeen prekatalisators van die Grubbs 2^{de} generasie tipe [RuCl(H₂IMes)(O^N)(=CHPh) waar O^N =1-(2'-piridiniel)-1-(siklopentiel)-metanolato (**GCYC**) en O^N =1-(2'-piridiniell)-1-(2'-metiel-pheniel),1-pheniel-metanolato (**GMPP**) vir 1-okteen metatese geëvalueer.

Metatese reaksies was uitgevoer in 'n enkellading reaktor met skoon 1-okteen terwyl die effekte van temperatuur (40-100°C) en prekatalisator lading (C₈/Ru: 5 000 - 14 000) ondersoek was. Kinetiese parameters was bepaal deur die konsentrasie profiele te meet vir 7 uur, en gevvolglik die resultate te pas met fundamentele kinetiese modelle. Die Douglas metode was gebruik om 'n konseptuele proses te ontwerp en gevvolglik die ekonomiese potensiaal van elke prekatalisator te beraam.

Optimale gedrag was waargeneem vir die **GCYC**-katalisator met 'n omsettingsgetal (TON) van 6631, 80% omskakeling van 1-okteen (C₈) en 41% selektiwitiet teenoor primêre produkte by 70°C. In vergelyking, het die **GMPP**-katalisator 'n omsettingsgetal van 5888, 60% omskakeling van C₈ en 37% selektiwitiet teenoor primere metatese produkte behaal by 'n temperature tussen 70 en 90°C. Latente termo-skakelbare gedrag was waargeneem waar aktivering eers plaasgevind het bo die aktiveringstemperature. Verskeie kinetiese reaksiemodelle is ontwikkel en kon verduideliking bied (binne redelike voorspelbaarheid) vir die eksperimentele waarneming van termiese katalisatordeaktivering en kompeterende isomerisasie reaksies. Aktiveringsenergië van die **GCYC**-en **GMPP**-katalisators vir die verbruik van 1-okteen was 30.24 kcal.mol⁻¹ en 13.10

$\text{kcal}\cdot\text{mol}^{-1}$ onderskeidelik. Deaktiveringsenergië vir die katalisators is as 22.81 en 5.84 $\text{kcal}\cdot\text{mol}^{-1}$ onderskeidelik bepaal. Die **GMPP**-katalisator het trapfunksiegedrag gevvolg sowel as die Arrhenius verhouding by temperatuur waar volledige katalisatordeaktivering nie plaasgevind het nie.

Na 'n ekonomiese evaluering met 'n gemengde deurlopende tenk reaktor (CSTR) is dit bevind dat metatese gunstig was vir beide katalisators met 'n interne opbrengskoers (IRR) van 73% en 53% onderskeidelik, dus maak dit hulle moontlik uitvoerbare keuses vir die upgradering van LLA's na Guerbet-surfaktante. Daar is bevind dat die **GCYC**-katalisator die algeheel beste presastie lewer, maar die **GMPP**-katalisator bied steeds heelwat voordele waar minder streng temperatuur beheer benodig is. Vergelykings met 'n kommersiële 2^{de} generasie Hoveyda-Grubbs katalisator het getoon dat die kommersiële katalisator steeds die beste is by lae temperatuur met 'n interne opbrengskoes van 91%. Daar word voorgestel dat toekomstige studies uitgevoer word met die fokus op Digtheid Funksionele Teorie (DFT)-navorsing vir die verskeie katalisators, die uitbreiding van die omvang van katalisators beskou vir die ekonomiese potensiaal evaluering asook om ontwikkelings studies te oorweeg vir die implementering van 'n proef proses.

Kernwoorde

Termiese-skakeling, kinetika, ekonomiese evaluering, katalisatordeaktivering, metatesereaktor.

Acknowledgements

*"You don't write because you want to say something,
you write because you have something to say."*
— F. Scott Fitzgerald

To God all the glory and honour forever. Through the work of Christ, I have been able to complete this thesis. To Him, I owe all the glory, thanks and praise.

To my supervisors: Percy van der Gyp: thank you for your patience and the valuable lessons I have learnt under your leadership. Your academic insights were highly valued throughout the completion of this work. Professor Manie Vosloo; thank you for the opportunity to contribute to your research programme and your continued support. Dr Goosen for the use of your temperature controlled heating mantle.

I also want to thank the following individuals in the Department of Process Engineering at Stellenbosch University for their technical, moral and academic support:

- Ms Hanlie Botha and Mr Jaco van Rooyen at the analytical laboratory -the GC whisperers of our department.
- Ms Juliana Steyl and Ms Francis Layman for all the orders you had to place.
- Mr Alvin Petersen and Mr Jos Weerdenburg for their technical assistance with the reaction setup.
- My colleagues in the c*change and Separations Technology research groups. Monday coffee and fun times in the office made the long hours worthwhile.
- Dr JP Barnard and Dr LJ du Preez for help with the kinetic regression algorithm.
- Dr Leonard Santana at NWU for valuable insight into bootstrap statistics and Matlab fault finding.

Financially I would like to thank the (DST-NRF) Centre of Excellence in Catalysis and Stellenbosch University Department of Process Engineering for funding.

Lastly, but not least, I would like to thank my friends, family and loved ones for their support. Thank you for accommodating me so far from home. Without your love and understanding, this work would not have been possible.

Contents

<i>Declaration</i>	II
<i>Abstract</i>	III
<i>Opsomming</i>	V
<i>Acknowledgements</i>	VII
<i>Contents</i>	VIII
<i>Nomenclature</i>	X
<i>List of precatalysts</i>	XIII
1 INTRODUCTION	XV
1.1 Overview	XV
1.2 Background and motivation.....	1
1.3 Objectives	5
1.4 Scope	6
1.5 References	9
2 CATALYST PERFORMANCE	11
2.1 Overview	11
2.2 Metathesis literature	12
2.3 Experimental procedures	37
2.4 Precatalyst performance results	45
2.5 Catalyst comparison.....	58
2.6 Concluding remarks	59
2.7 References	60
3 METATHESIS REACTION KINETICS	65
3.1 Overview	65
3.2 Alkene metathesis kinetic literature	66
3.3 Kinetic modelling	78
3.4 Regression results and discussion.....	93
3.5 Concluding remarks	109
3.6 References	110
4 ECONOMIC POTENTIAL EVALUATION	115
4.1 Overview	115
4.2 Economic considerations: literature review.....	116
4.3 Economic evaluation methodology.....	128
4.4 Results and discussion	139
4.5 Concluding comments	157
4.6 References	158
5 CONCLUSION	161
5.1 Overview	161

5.2	Introduction	162
5.3	Catalyst performance and product distribution.....	162
5.4	Kinetic reaction modelling	164
5.5	Economic evaluation	167
5.6	Future research recommendations and contributions.....	170
5.7	References	171
	APPENDIX A: Supplementary literature.....	172
	APPENDIX B: Raw Data.....	175
	Chapter 2	175
	Chapter 3	187
	Chapter 4	190
	APPENDIX C: Methods, Constants & Assumptions.....	202
	Chapter 2	202
	Chapter 4	205
	APPENDIX D: Calculated Data	208
	Chapter 2	208
	Chapter 3	219
	Chapter 4	225
	APPENDIX E: Simulations and Regression algorithms.....	285

Nomenclature

Abbreviation	Description
ADMET	Acyclic Diene Metathesis Polymerization
ANOVA	Analysis of Variance
Bn	Billion= 1000 000 000
C ₈ /Ru	1-octene to ruthenium molar ratio or precatalyst load
CEI, C _e	Chemical Engineering Index
C _j	1-octene or alpha alkene carbon chain where j = the number of carbon atoms e.g. C ₈ is 1-octene C ₂ is ethene, C ₇ is 1-heptene etc.
CM	Cross-Metathesis
CV	Coefficient of variation
DEDAM	diethyl diallyl malonate
DFT	Density Functional Theory
DST-NRF	Department of Science and Technology-National Research Foundation
EP	Economic potential
EP-1 or EP ₁	Economic potential at level 1
EVE	Ethyl Vinyl Ether
EYM	Enyne Metathesis
FCI	Fixed Capital Investment
FID	Flame Ionisation Detector
GC	Gas Chromatography
H ₂ lmes	1,3-bis-(2,4,6-trimethylphenyl)-2-imadazolidinylidene
HNMR	Hydrogen Nuclear Magnetic Resonance
iMes	1,3-bis-(2,4,6-trimethylphenyl), Mesitylene
IMP	Isomerisation Metathesis Products
IRR	Internal Rate of Return
M	Million= 1000 000
M&S	Marshall and Swift index
NHC	N-Heterocyclic Carbene
NPV	Net Present Value
NWU	North-West University
OB	Objective function
PBP	Pay Back Period
PCy ₃	Tricyclohexyl phosphine
Ph	Phenyl group C ₆ H ₅
PID	Proportional Integral Derivative
PMP	Primary Metathesis Products
PSSHT	Pseudo Steady State Hypothesis Theory
R&D	Research and development
RCM	Ring-Closing Metathesis
RF	Response Factor
ROCM	Ring-Opening Cross-Metathesis
ROI	Return on Investment
ROMP	Ring-Opening Metathesis Polymerization
SASOL	South African Coal Oil and Gas Corporation (<i>Suid Afrikaanse Steenkool Olie en Gas Korporasie</i>)
SHOP	Shell Higher Olefins Process
SM	Self-Metathesis

Abbreviation	Description
SMP	Secondary Metathesis Products
TCI	Total Capital of Investment
TCP	Total Cost of Production
THF	Tetrahydrofuran
TOF	Turnover frequency
TOI	Total Operating Income
TON	Turnover Number
tpa	Tons per annum
USD	US Dollars

Symbol	Description	Units
A	Area	m ²
A	Catalyst activity	-
B	Coefficient matrix	-
C _{cat}	Catalyst concentration	mol. L ⁻¹
C _i	Concentration of species <i>i</i>	M (mol. L ⁻¹) or mol%
C _{pi}	Heat capacity of species <i>i</i>	J.mol ⁻¹
D	Diameter	m
E	Error or residuals	-
E	Weld joint efficiency	
E _a	Activation energy	kcal.mol ⁻¹
E _o	Column efficiency	-
F _{A0}	Molar Flow rate of Species A	mol.h ⁻¹
F _i	Material factors	-
H	Height	m
H _{Rxn}	Enthalpy of reaction	J.mol ⁻¹
ΔH _{vap}	Enthalpy of vaporisation	J.mol ⁻¹
<i>i</i>	Interest rate	%
[<i>i</i>]	Matrix <i>i</i>	-
k _d	Deactivation rate constant	mol.min ⁻¹
k _{-i}	Reverse reaction rate constant	min ⁻¹
K _i	Arrhenius kinetic constant	mL.mol ⁻¹ .min ⁻¹
k _i or k _{iobs}	Observed reaction rate constant of species <i>i</i>	min ⁻¹
MW _i	Molar weight of species <i>i</i>	g.mol ⁻¹
N	Number of bootstrap trials	-
N _i or n _i	Mole of species <i>i</i>	mol
N _m	Minimum number of stages in distillation column	-
P	Pressure	bar
P _i	Internal pressure	bar
r	Radius	m

Symbol	Description	Units
R	Universal Gas Constant	J.mol ⁻¹ .K ⁻¹
\dot{Q}	Heat rate	W
r _i	Reaction rate of species <i>i</i>	mol.min ⁻¹
S	Selectivity	%
s ,σ or SD	Standard Deviation	-
t	Time	min, h
T	Temperature	°C, K
t _w	Wall thickness	mm
U	Heat transfer Coefficient	W.(°C) ⁻¹ .m ²
\dot{v}	Volumetric flow rate	m ³ .h ⁻¹
V	Volume	m ³ , L, mL
\dot{W}_s	Shaft Work	W
X	Overall Conversion	%
X _{single pass}	Single pass conversion	%
\bar{X}	Mean or average	-
Y	Yield	%
y _i	Response matrix	-
ρ	Density	kg.m ⁻³

List of precatalysts

Abbreviation	Description	Structure
G1	Commercially available Grubbs 1 st Generation precatalyst $\text{RuCl}_2(\text{=CHPh})(\text{PCy}_3)_2$ <i>[Benzylidene-bis (tricyclohexyl phosphine) Dichloro ruthenium]</i>	
G2	Commercially available Grubbs 2 nd Generation precatalyst $\text{RuCl}_2(\text{=CHPh})(\text{PCy}_3)(\text{H}_2\text{IMes})$ <i>[1,3-Bis-(2,4,6 trimethyl-phenyl-2-imidazolidinylidene)dichloro(phenylmethylene) (tricyclohexylphosphine)ruthenium]</i>	
HG1	Commercially available Hoveyda Grubbs 1 st generation $\text{RuCl}_2(\text{=CH-o-OiPrC}_6\text{H}_4)(\text{PCy}_3)$ <i>[Dichloro(o-isopropoxypyphenylmethlene) (tricyclohexylphosphine)ruthenium(II)]</i>	
HG2	Commercially available Hoveyda Grubbs 2 nd Generation $\text{RuCl}_2(\text{=CH-o-OiPrC}_6\text{H}_4)(\text{H}_2\text{IMes})$ <i>[1,3-Bis-(2,4,6-trimethylphenyl)-2-imidazolidinylidene)dichloro(o-isopropoxypyphenyl)methylene ruthenium]</i>	
GCYC	Synthesised precatalyst from NWU $\text{RuCl}(\text{O}^{\wedge}\text{N})(\text{=CHPh}) (\text{H}_2\text{IMes})$ $\text{O}^{\wedge}\text{N} = 1\text{-}(2'\text{-pyridinyl})\text{-}1\text{-}(cyclopentyl)\text{-}methanolato$	
GMPP	Synthesised precatalyst from NWU $\text{RuCl}(\text{O}^{\wedge}\text{N})(\text{=CHPh}) (\text{H}_2\text{IMes})$ $\text{O}^{\wedge}\text{N} = 1\text{-}(2'\text{-pyridinyl})\text{-}1\text{-}(2'\text{-methylphenyl}),1\text{-phenyl-methanolato}$	

1 INTRODUCTION

"It is a dangerous business, Frodo, going out your door. You step onto the road, and if you don't keep your feet, there's no knowing where you might be swept off to." ~J.R.R. Tolkien, the Lord of the Rings.

1.1 Overview

In this chapter, a broad overview of the contents of this study is explained in three sections. Section 1.2 consists of a brief background and a motivation for the study followed by a description of the objectives that the study aims to address in Section 1.3. Finally, this chapter is concluded with an outline of this thesis and a scope of the investigation.

1.2 Background and motivation

1.2.1 Global alkenes market

Since the oil industry's recent and sharp downturn in prices, the profit margins of fuel producing companies have been affected. Compensating for changes such as these is a challenge that the petroleum industry must deal with on a regular basis [1]. Not only is adding value to a low value feed the primary purpose of refining [2], it is also one of the main drivers that lead to process innovation [3]. Since fuel prices are not likely to become favourable for them soon [1], relying on secondary metathesis products would allow oil and petroleum companies to alleviate pressure on their fuel production sections as a main source of revenue.

Secondary products in the fuel industry appear in various forms and have several different origins, but one particular feedstock of interest is alkenes (also known as "olefins"). This work will use the term "alkenes". Alkenes are produced in the refinery industry as a result of processing activities and are not present in the feed from the start, which is why utilising it to make higher value products are beneficial [5]. Other fuel production techniques such as gas to liquids and coal to liquids also produce alkene-rich side streams [6].

Terminal alkenes are the starting materials from which a range of different fine chemicals can be produced. Typically, alcohols, paint, solvents, plasticisers, surfactants and detergents [7-9]. Some surfactants have market values that are six times higher than that of fuel due to their *inter alia* biodegradability, efficiency and stability [10]. Furthermore, the global surfactant market demand is expected to grow at a rate of 4.5% within the next three years due to increased interest in biodegradable products and growing economies in developing countries [11]. There is, therefore, an overwhelming incentive to convert these low-value alkenes to higher value products. Industry examples of processes that produce finer chemicals from alkenes are the Shell Higher Olefins Process (SHOP), The Albemarle Process in Texas and Belgium, the Chevron-Gulf process in USA and UK, Idemitsu in Japan and Godrej-Lurgi in India to name a few [12].

In South Africa, SASOL is a producer of linear 1-alkenes as a side-product from their Fischer Tropsch process which can account for up to 12% of their total production cost [6]. Above all, the company has recently experienced lower income due to fuel price drops [13]. Keeping this in mind it is evident that there is drive and opportunity to increase the revenue that SASOL generates via side-products.

To facilitate alternative income the low-value 1-alkenes need to be chemically manipulated to yield higher value hydrocarbons.

The RSA Olefins programme of the DST-NRF Centre of Excellence in Catalysis (*c^{*}change*) has proposed a simple reaction network to address this issue and particularly look at the catalytic reactions of metathesis and hydroformylation as shown in Figure 1.1 [14].

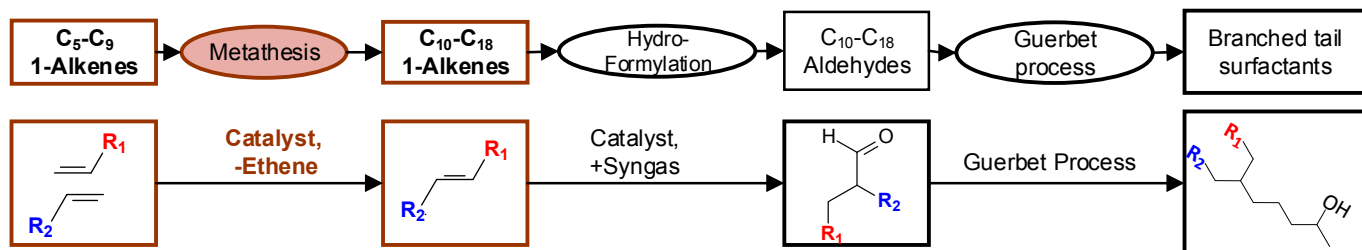


Figure 1.1: *c^{*}change* proposed reaction scheme for the upgrade of low-value alkene feedstock.

In this scheme, the chain length of the alkene is first increased via metathesis, after which the alkenes are converted to aldehydes via hydroformylation. After the hydroformylation step, they are typically hydrogenated to yield alcohol products which are processed further to produce the high-value surfactant molecules [14].

1.2.2 Alkene Metathesis: a revolution in Synthetic Organic Chemistry

In the hydrocarbon industry, the first industrial process to use metathesis was the Phillips Tri-Olefin Process. This process produced high quality ethylene and 2-butene from a propene feed. After this, many other processes were also successfully commissioned. The one that is the most significant in the fine chemicals industry is the Shell Higher Olefins Process. This process uses oligomerisation in combination with metathesis and ethenolysis to convert ethene into higher chain alkenes [15].

Metathesis was first discovered by industrial chemists in the 1950s and the first discovery at the time was made by H.S. Eleuterio in 1956. His discovery entailed the production of the propylene-ethylene copolymer by passing a propylene feed over a molybdenum precatalyst. What the study discovered was that 1-butene had formed as well. Repeated experiments with cyclopentene also resulted in a range of unexpected compounds [16] Peters and Evering recorded similar results under a patent in 1960 alongside Banks and Bailey in 1964 where propylene was converted into ethene and butene in the presence of a molybdenum precatalyst on alumina [16].

These discoveries led many other researchers to experiment with their own metathesis reactions which created the interest in metathesis.

Alkene Metathesis can be defined as the exchange of alkylidene fragments between two alkenes promoted by a metal carbene precatalyst as shown in Figure 1.2 [17].

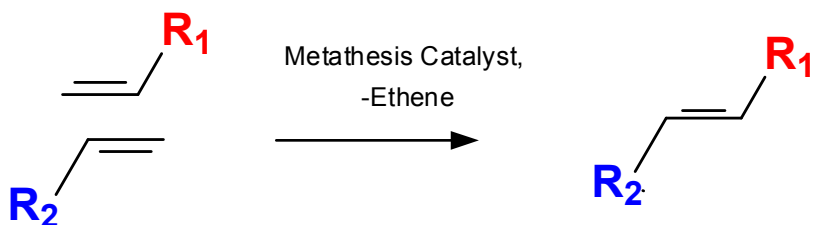


Figure 1.2: General alkene metathesis reaction scheme

Throughout history, many studies were conducted on metathesis in pursuit of well-defined catalysts and a better understanding of the reaction mechanisms. Significant work was conducted by Chauvin, Schrock and Grubbs who won the Nobel Prize for their work in the field in 2005. Chauvin (and Hérrison) was mainly responsible for elucidating and developing an accurate mechanism in 1971 [16], Schrock for the development of highly active molybdenum precatalysts and Grubbs for his development of active yet tolerant and stable precatalysts. An example of what these precatalysts typically look like is shown in Figure 1.3

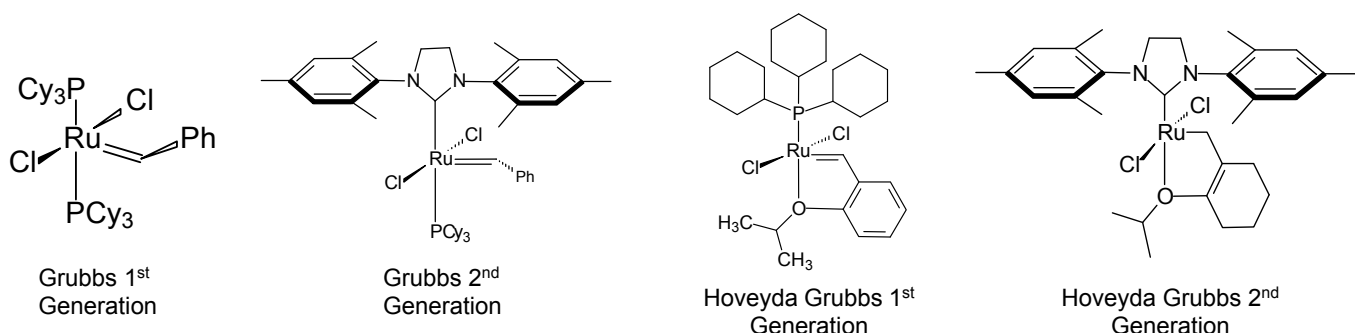


Figure 1.3: Typical Grubbs-type precatalysts

Grubbs and his fellow researchers' discovery has led the organic chemistry community to further experimentation with these well-defined catalytic compounds [18]. New precatalysts were created in the same style but different ligands allowed researchers to gain higher activity, selectivity and lifetime for their specific application. With so many similar precatalysts available, and each at its own cost it became a difficult task to select the best one.

Universal catalysts do not exist in metathesis and thus target specificity is the key [19]. Whether a precatalyst is target-specific or not, the capital expenditure on equipment must still make economic sense. Therefore, the challenge in evaluating precatalysts is determining whether they are target-specific and economically viable to implement. Some information regarding each precatalyst is needed to do so i.e. the product distribution, precatalyst performance and the reaction kinetics. Only once this information has been gathered an informed economic potential evaluation can be conducted.

This investigation aims to gather this information for two synthesised precatalysts for the metathesis of 1-octene. These catalysts have been designed so that the expensive ligands remain attached during the reaction- a benefit that distinguishes them from their competitors, moreover the ligands have been designed to increase their optimal performance temperature [20]. Since the Fischer Tropsch process operates at temperatures above 300 °C [2] and cooling down the feed stream would be costly. A catalyst that can withstand elevated temperatures would ultimately be beneficial in such circumstances. With this in mind, the question arises as to how these precatalysts compare in their performance? The aim is to answer this question by evaluating the economic potential of each catalyst by comparing the reactor size that would be required to yield worthwhile products. The precatalysts of interest for this study are presented in Figure 1.4

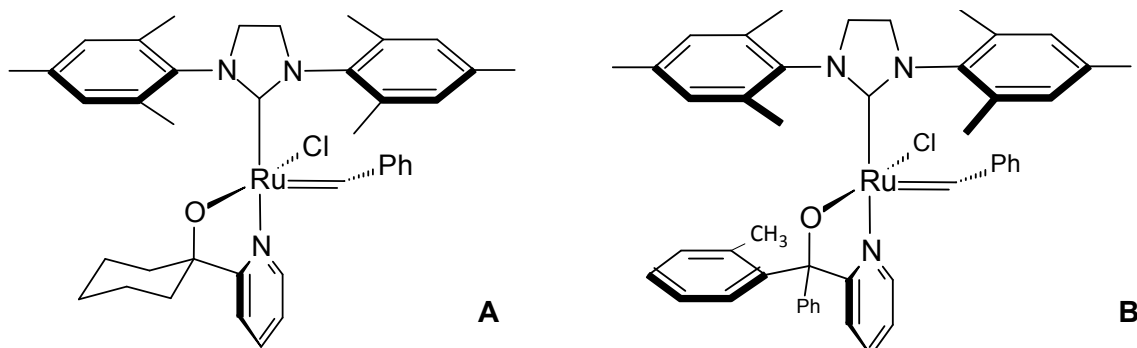


Figure 1.4: Precatalysts studied in this work. [(A) GCYC, (B) GMPP].

1.3 Objectives

This study aims to address the following questions in the field of metathesis as well as reactor design engineering:

1. How do the studied catalysts compare with regards to performance?
2. What kind of kinetic model would describe the system, and what value will the constants hold?
3. How does each of the catalysts' economic performance compare in a conceptual reactor system?

This will be achieved by drawing a comparison between the economic potential of two different precatalysts based on reactor size and the potential for income. The objectives of the study can be divided into 3 subsections corresponding to each question, i.e. precatalyst performance, reaction kinetics and economic potential evaluation.

The precatalyst performance objectives are as follows:

- a) Understand the catalytic performance of 2 different Grubbs-type precatalysts synthesised by NWU for the metathesis reaction of 1-octene. This includes characterising the product distribution of each precatalyst.
- b) Determine the effect of temperature and precatalyst load on each precatalyst's performance and product distribution.
- c) Draw a comparison between the synthesised precatalysts' performance and the performance of a typical commercial precatalyst.

The objectives for to the Reaction Kinetics are:

- a) Develop reaction models based on fundamental reaction engineering.
- b) Fit the reaction model to empirical data to determine the corresponding reaction constants and kinetic parameters (reaction order, reaction rate constants and activation energies) that will be able to predict the reaction behaviour

The objectives with regards to the Reactor economics are:

- a) Conceptually design a reactor system for the reaction of 1-octene using the catalytic system and the results obtained in objective one and two.
- b) Complete an economic analysis for optimum reactor conditions.
- c) Evaluate each catalytic system based on temperature, conversion, selectivity, and precatalyst load.

1.4 Scope

To achieve the above-mentioned objectives, a range of research activities have been carried out which are described throughout this work in detail. The contents of this thesis are subdivided into 5 Chapters of which 3 are main subsections that each subsequently address the three main objectives of the study. A schematic diagram (Figure 1.5) of the scope is also provided in this section to demonstrate the relationship between topics, chapters and objectives.

The content of Chapter 2 focusses on the precatalyst performance and reaction behaviour. The chapter is subdivided into sections as follows: *Section 1* aims to provide the necessary terminology, concepts, and background knowledge in the field of linear alkene metathesis and to compare and analyse work done in the field by others. The content of *Section 2* describes and motivates the methodologies and materials used to collect the empirical performance and kinetic data. The results of the activities described in *Section 2* are provided in *Section 3* which will also continue with a discussion and comparison. This includes evaluating each precatalyst's performance in terms of the effects of varied temperature and precatalyst load. Chapter 2 is concluded in *Section 4*, with concluding remarks on the chapter.

In Chapter 3 the focus is the kinetic considerations behind the metathesis reaction. This chapter follows the same structure of Chapter 2. Starting with background (*Section 2*) in the available literature, providing the necessary terminology and theoretical concepts on the reaction and the mechanism. Continuing to compare and analyse the available information in literature on the topic of kinetics. *Section 3* will include a description of the methodologies, algorithms and equations applied in modelling the empirical data. *Section 4* will contain and explain the results obtained from the kinetic modelling activities. *Section 4* then briefly concludes the chapter with comments on the results obtained.

Chapter 4 consists of the theoretical reactor design evaluation. The aim is to design reactors using theoretical design equations and the performance parameters that were obtained by modelling the reaction data in Chapter 2 and 3. *Section 1* of this chapter will address the literature and terminologies required to understand the sections that follow. In *Section 2* the methods, equations and choices made to conduct the economic evaluation are elucidated.

In *Section 3*, the results are presented, explained and motivated clearly as each precatalyst's corresponding reactor design is evaluated on an economic potential basis. The economic potential is evaluated focussing on conversion, selectivity, reactor volume and temperature. After which the chapter is briefly concluded in a commentary section (*Section 4*).

Finally, this work is concluded in Chapter 5, where all the principal conclusions of the study are drawn, summarised and recommendations for future research and industrial applications are made. A schematic presentation of the scope of the investigation is provided in Figure 1.5.

INVESTIGATION SCOPE

Catalyst Performance & Product distribution



CHAPTER 2

Metathesis Reactions
Characterise 1-Octene metathesis reaction with Grubbs type catalysts

Empirical Evaluation
Describe the reaction behaviour with 2 new catalysts

Temperature
Effects on reaction
40°C -100°C

Catalyst Molar load
Effects on reaction
C8/Ru: 7000-14000



CHAPTER 3

Theoretical Eulicidation
Describe both the reaction systems mathematically from 1st principles

Kinetic Rate law modelling
Fit reaction curves to a rate law

Estimate Rate law constants
Using a statistical regression algorithm

Model Validation
Validate the model by comparing results to literature

Parameter validation
Validate parameters with confidence intervals (bootstrap)



CHAPTER 4

Design a reactor
Evaluate the catalysts by sizing a basic reactor

Performance Equation
Formulate an equation used to determine Economic Potential

Analysis
Describe the effect of the following parameters on the performance equation:

- Temperature
- Conversion
- Reactor size
- Activity and Selectivity

Figure 1.5: Schematic of the scope of this Investigation

1.5 References

- [1] C. Krauss, Oil Prices: What's behind the drop? simple economics, New York Times. (2016). <http://www.nytimes.com/interactive/2016/business/energy-environment/oil-prices.html> (accessed April 1, 2016).
- [2] M.E. Dry, The Fischer -Tropsch process: 1950-2000, Catal. Today. 71 (2002) 227–241.
- [3] M.A. Fahim, T.A. Alsahhaf, A. Elkilani, Fundamentals of petroleum refining, Elsevier, 2010.
- [4] T. Ren, Barriers and drivers for process innovation in the petrochemical industry: A case study, J. Eng. Technol. Manag. 26 (2009) 285–304.
- [5] R.E. Maples, Petroleum refinery process economics, 2nd ed., Penwell Books, Tulsa, (2000).
- [6] O.O. James, A.M. Mesubi, T.C. Ako, S. Maity, Increasing carbon utilisation in Fischer-Tropsch synthesis using H₂-deficient or CO₂-rich syngas feeds, Fuel Process. Technol. 91 (2010) 136–144, (2009).
- [7] J.M. Behan, J.N. Ness, P.C. Traas, J.S. Vitsas, B.J. Willis, Aqueous perfume oil microemulsions, US5,374,614, (1994).
- [8] M.C. Jensen, G.E. Culver, Detergent-making process using a high active surfactant paste containing mid-chain branched surfactants, US6,294,513 B1, (2001).
- [9] T.A. Cripe, D.S. Connor, P.K. Vinson, J.C.T.R. Laurent, K.W. Willman, Mid-Chain branched alkoxylated sulfate surfactants, US6,008,181, (1999).
- [10] A.J. O'Lenick Jr., A.J. O'Lenick, Guerbet chemistry, J. Surfactants Deterg. 4 (2001) 311–315.
- [11] Research and Markets, Global surfactant market for personal care products industry 2015-2020: trends, forecast, and opportunity analysis, (2015). http://www.researchandmarkets.com/research/4ct3rc/global_surfactant (accessed February 8, 2016).
- [12] G.R. Lappin, L.H. Nemec, J.D. Sauer, J.D. Wagner, Olefins, Higher., in Kirk-Othmer Encycl. Chem. Technol., John Wiley and Sons, Hoboken New Jersey, 2005: p. vol 17.
- [13] S. Mantshantsha, Sasol's earnings in doldrums as oil price hits the skids, Bus. Day Live. (2016). <http://www.bdlive.co.za/business/energy/2016/01/29/sasols-earnings-in-doldrums-as-oil-price-hits-the-skids> (accessed April 1, 2016).
- [14] M. Claeys, S. Harrison, H.C.M. Vosloo, B. Zeelie, R. Weber, c*change DST-NRF Centre of Excellence in Catalysis, (2016). www.cchange.ac.za/rsa-olefins/ (accessed April 4, 2016)
- [15] O.M. Singh, Metathesis catalysts: historical perspective, recent developments and practical applications, J. Sci. Ind. Res. 65 (2006) 957–965.
- [16] A.M. Rouhi, Olefin metathesis: the early years, Chem. Eng. News. 80 (2002) 34–38.
- [17] S.J. Connon, S. Blechert, Recent developments in olefin cross-metathesis, Angew. Chemie Int., Ed. 42 (2003) 1900–1923

- [18] A.M. Thayer, Making metathesis work, commercially available metathesis catalysts may help a powerful synthesis tool move into drug manufacturing, *Chem. Eng. News.* (2007) 1–8.
- [19] R.H. Grubbs, Olefin metathesis, *Tetrahedron. Org. Chem. Ser.* 60 (2004) 7117–7140.
- [20] T. Tole, J. du Toit, C. van Sittert, J. Jordaan, H. Vosloo, Synthesis and application of novel ruthenium catalysts for high temperature alkene metathesis, *Catalysts.* 7 (2017) 22.

2 CATALYST PERFORMANCE

"The author who benefits you most is not the one who tells you something you did not know before, but the one who gives expression to the truth that has been dumbly struggling in you for utterance." ~ Oswald Chambers

2.1 Overview

The aim of the following chapter is to present the literature, methods and results pertaining to metathesis and catalyst performance. The aim is also to look at the available information and evaluate it critically. In Section 2.2 metathesis will be covered in general highlighting chelating pyridinyl alcoholato ruthenium type complexes and the typical product distributions. Section 2.3 includes the experimental procedures followed in the reaction performance tests. The last major sections, Section 2.4 and 2.5, present the results obtained from the experimental activities and discusses, explains and clarifies the trends and phenomena occurring in the empirical data. The chapter is concluded with a summary.

2.2 Alkene Metathesis literature

2.2.1 Introduction and general theory

Metathesis is a powerful reaction in the chemical synthesis field largely due to its low waste generation, atom-efficiency and elimination of lengthy multi-step synthesis reactions [1]. The meaning of metathesis is derived from the Greek word (<μετάθεσις>) meaning rearrangement or transposition. The second description is more closely related to Latin (trānspositiō) and the term can be applied in both linguistics and chemistry. In the chemistry sense, it refers to an exchange of ions in a salt ion exchange reaction or the exchange of alkylidene groups in alkene metathesis [1]. The general alkene metathesis reaction scheme is presented in Figure 2.1.

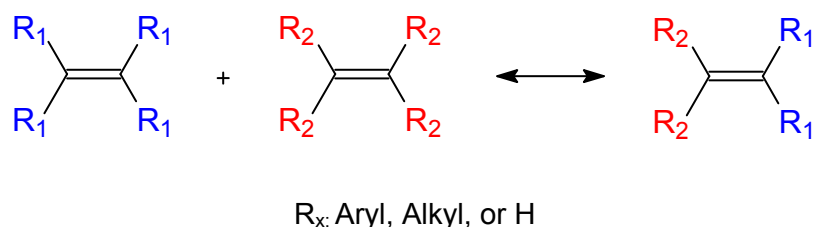


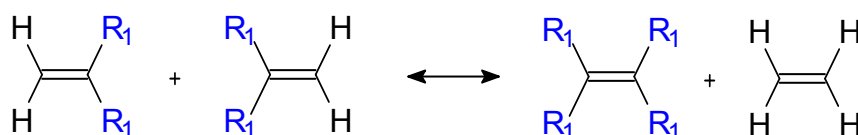
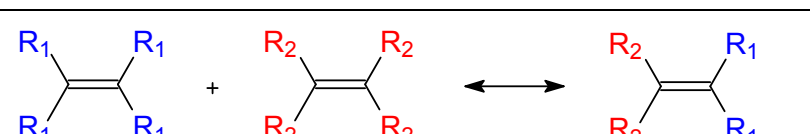
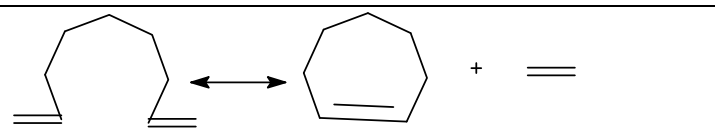
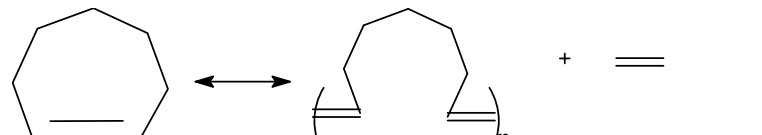
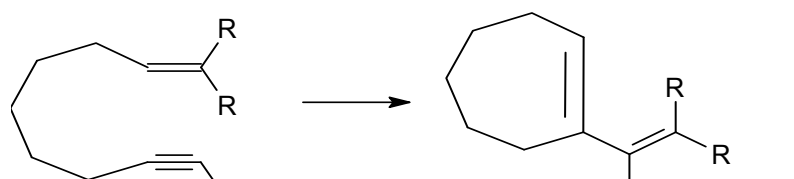
Figure 2.1: Generalised alkene metathesis reaction.

During this reaction, new carbon-carbon bonds are formed that would otherwise have been thermodynamically too energetically intensive to achieve, which is why these types of reactions are typically catalysed reactions [2].

2.2.1.1 Classification

Applications in alkene metathesis reactions have increased due to the wide variety of different classes the reaction is attributed to and its modification abilities. The reaction is classified into 7 different types based on the reacting species as illustrated in Table 2.1 (adapted from [3]) which include: Self-metathesis (SM), Cross-metathesis (CM), Ring-opening Metathesis Polymerization (ROMP), Ring-closing Metathesis (RCM), Acyclic Diene Metathesis Polymerization (ADMET), Enyne Metathesis (EYM), and lastly Ring-opening Cross-metathesis (ROCM).

Table 2.1: Classification of alkene metathesis reactions [3]

Class	Schematic
Self-metathesis (SM)	
Cross-metathesis (CM)	
Ring-closing Metathesis (RCM)	
Ring-opening Metathesis Polymerization (ROMP)	
Acyclic Diene Metathesis Polymerization (ADMET)	
Enyne Metathesis (EYM)	
Ring-opening Cross-metathesis (ROCM)	

2.2.1.2 Historical Overview

The first metathesis reaction was, in fact, an uncatalysed reaction. The discovery was accidental in 1931 by Schneider and Frolich [4] who reported a conversion of propene to butene and ethene at high temperatures. The publication was unfortunately ignored at the time and neither was the reaction term “metathesis” coined yet. Recognition of these types of reactions only started to rise when Ziegler and Natta’s discoveries on ethylene and propene polymerization reactions came to the fore in 1953 [5].

Around the same time chemists working at the Du Pont, Standard Oil and Phillips Petroleum, Euleterio *et al.*, also accidentally discovered the first *catalysed* metathesis reaction [6]. The precatalyst was a molybdenum oxide on an alumina support. Euleterio and Truett *et al.* were also independently responsible for the discovery of the polymerization of norbornene [6]. In 1960 Peters and Evering recorded in a patent that propene could be converted to butene and ethene with a molybdenum oxide catalyst on alumina [7]. 1964, Banks and Bailey reported a reaction with similar results in the presence of molybdenum hexacarbonyl also supported on alumina [8]. To the researchers, at that time, the chemistry became interesting as more reports were emerging on these seemingly inexplicable reactions [8]. It was Calderon at Goodyear Tire and Rubber who realised that all these reactions had something in common: the cleavage and reformation of carbon-carbon double bonds. Calderon’s finding was confirmed when Mol and his team reached the same conclusion independently in that same year of 1967 [1].

In the years that followed many had tried unsuccessfully to elucidate the metathesis mechanism. Chauvin and Hérrison finally came up with the best solution when they proposed a metal carbene mechanism in 1971 [9]. The following years of experimental research found proof for the theory and the mechanism has been accepted ever since [9].

Chauvin and Hérrison’s breakthrough allowed chemists a better understanding of the chemistry and shortly after Schrock came up with the first single component metal complex precatalyst [10]. He expanded his work further with the highly active Mo-alkylidene precatalyst group known as Schrock carbenes. Schrock complexes were well-performing precatalysts, but their tolerance and stability weren’t competitive enough [10]. Eventually, in the 1990s Grubbs synthesised a ruthenium benzylidene complex that brought metathesis to the forefront of synthetic chemistry [10].

As expected research continued beyond these discoveries and has led to a range of different (easily modifiable precatalysts) that exist in literature and industry today.

A short descriptive schematic timeline (adapted from [2]) of the milestones in alkene metathesis is presented in Figure 2.2

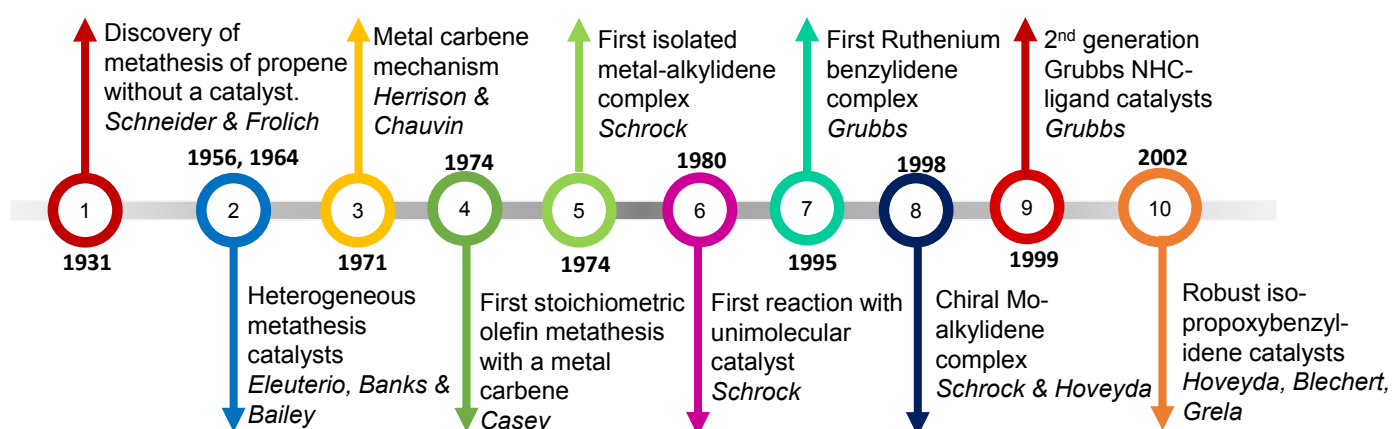


Figure 2.2: Metathesis milestones [2].

2.2.2 Linear alkene metathesis

The field of synthetic organic chemistry is an increasingly important one as the fields of medicine, fine chemicals and fuels continuously need new solutions. Alkene metathesis is a versatile reaction that has the ability to create otherwise difficult to obtain carbon molecules. Specifically, the focus of this study is the linear 1-alkenes [11]. Terminal linear alkenes are relatively easy to prepare but n-substituted alkenes are more cumbersome, and metathesis simplifies this conversion. Alkenes are often used to interconvert molecules due to their stability and reactivity [11]. Clearly, there is ample incentive towards the usage of linear 1-alkenes in metathesis, and this study specifically focuses on the metathesis of 1-octene (as model substrate) using Grubbs 2nd generation type precatalysts.

2.2.2.1 Product Distributions

Ideally 1-octene would react with itself exclusively in self-metathesis to yield a product that only consists of substrate and the desired primary metathesis products (PMP) namely 7-tetradecene and ethylene gas (Figure 2.3), but the catalytic presence and energy addition that is required for these reactions can often result in isomerisation taking place, allowing the alkene to form structural isomers (IMPs) or isomerisation metathesis products [12]. These isomers would then

typically participate in a cross-metathesis reaction as intermediates or undergo metathesis with themselves (secondary self-metathesis) and produce a range of secondary metathesis products (SMP) which can also be of value [12].

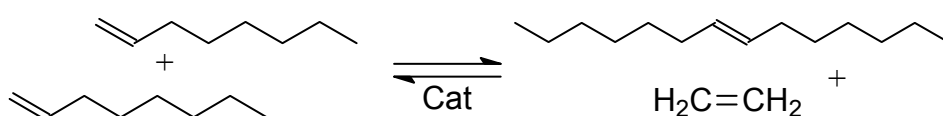


Figure 2.3: 1-Octene self-metathesis

. A summary of the possible products is illustrated in the reaction scheme below (Figure 2.4)

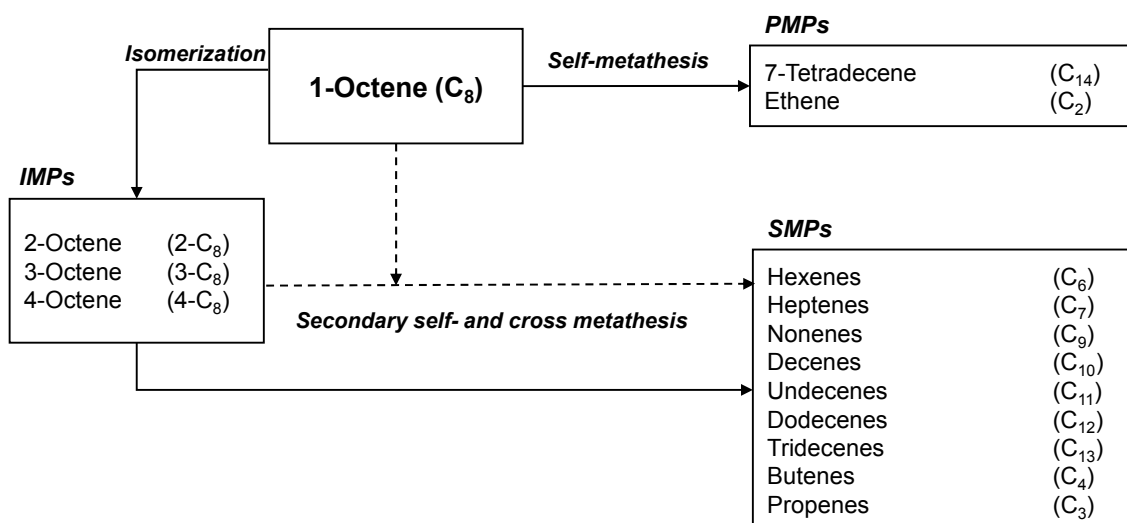


Figure 2.4: 1-Octene metathesis reaction network.

2.2.2.2 Alkene Metathesis Precatalysts

Catalytic reactions can be classified into homogeneous catalysis and heterogeneous catalysis. Heterogeneous precatalysts have dominated the industry despite the more superior capabilities of homogeneous catalysis on certain platforms [13]. Homogeneous Catalysis has its downfalls as well, but in lieu of increasing environmental concerns homogeneous catalysis is becoming more popular due to its mild operating conditions and superior performance [13].

Table 2.2 (adapted from [13]) provides a summarising comparison between these two catalytic systems.

Metathesis falls into the class of homogeneous catalysis and the attractiveness of metathesis is attributed to the superiority of homogeneous catalysis. In many respects, the issues with homogeneous metathesis precatalysts in the past have been resolved such as thermal stability and functional group tolerance [1]. The versatility of the different possibilities that homogenous catalysis affords has given metathesis a superiority in the synthetic chemistry industry [11]

Table 2.2: Comparison between homogeneous and heterogeneous catalysis.

Characteristic	Homogenous	Heterogeneous
Effectivity		
Active sites	All metal atoms	Only surface atoms
Concentration	low	High
Selectivity	High	Lower
Mass transfer	Virtually absent	Pronounced
Reaction conditions	Mild	Severe
Applicability	Limited	Wide
Deactivation	Clustering; Poisoning	Sintering; Poisoning
Catalyst characteristics		
Modification possibilities	High	Low
Thermal stability	Low	High
Separation	Sometimes difficult	Relatively easy
Recycling	Possible	Relatively easy
Cost of losses	High	Low

2.2.3 Alkene metathesis precatalysts

2.2.3.1 *Historical development*

The accidental nature of the discovery of metathesis explains the lack of well-defined metathesis precatalysts at the time. Today, however, there are multiple well-defined precatalysts available due to the pioneering work of Grubbs and his fellow Nobel laureates. In general alkene metathesis precatalysts fall in one of the three phases of development; i.e. the black-box phase, the Schrock complexes phase and finally the Grubbs complexes phase [14]. The Black-Box phase owes its name to the fact that the mechanisms and exact behaviour of these precatalysts were mostly not understood [15]. Typically, the precatalysts consisted of group 6 metal chlorides and either required supports or alkylating agents of a Lewis acidic nature e.g. $\text{WCl}_6/\text{EtAlCl}_2$ [15].

These and other classical systems were implemented industrially, but the systems were operated under harsh conditions with poor stability and selectivity [15].

Once metal carbene species were discovered the first well-defined and isolated complexes were developed. Metal carbenes fall into one of two categories: the Fischer-type ($\text{LnM=CRXR}'$) and the Schrock type complexes ($\text{LnM=CRR}'$). The main difference between the two is their oxidation states and electron donating or accepting properties [16]. As a result, a roll-out of what was known as the Schrock-type precatalysts (Figure 2.5) took place. Shortly after, ruthenium carbene complexes came to the fore in the third phase known as the Grubbs-type complexes [16].

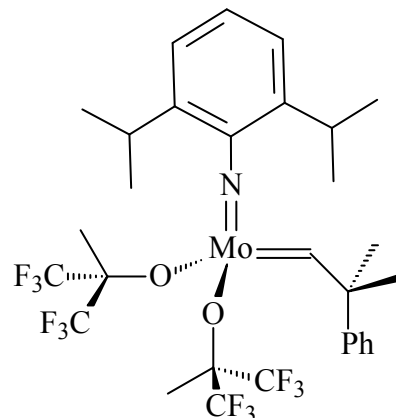


Figure 2.5: Schrock's precatalyst

Grubbs complexes were the most groundbreaking in terms of alkene metathesis because of their high tolerance for functional groups [16]. Table 2.3 provides a quick comparison of the functional group tolerance of late and early transitional metal alkene precatalysts as well as the argument for the favour awarded to ruthenium complexes [17].

Table 2.3 Transition metal-carbene reactivity to different functional groups [17]

Titanium	Tungsten	Molybdenum	Ruthenium
Acids	Acids	Acids	<u>Alkenes</u>
Alcohols & water	Alcohols & water	Alcohols & water	Acids
Aldehydes	Aldehydes	Aldehydes	Alcohols & water
Ketones	Ketones	<u>Alkenes</u>	Aldehydes
Esters & Amides	<u>Alkenes</u>	Ketones	Ketones
<u>Alkenes</u>	Esters & Amides	Esters & Amides	Esters & Amides

Increase in reactivity of metal carbene complexes with alkenes compared to other

Increasing Reactivity

At first, ruthenium salts were studied but these species did not perform very well [16]. Grubbs observed, however, that some ruthenium systems could improve in the presence of water and then continued the search for the ruthenium alkylidene complexes. The breakthrough came when the synthesis methodology for tungsten systems was applied to ruthenium i.e. by the addition of diphenylcyclopropene to $\text{RuCl}_2(\text{PPh}_3)_3$ to yield the first active ruthenium alkylidene species [16]. The complex's reactivity was limited but it led the research towards modifying the ligands. Consequently, the researchers discovered that bulky and basic phosphines increased the reactivity of the precatalyst. Nevertheless, the benzylidene complex (Figure 2.6) became the notorious first-generation Grubbs precatalyst **G1** primarily because it was the first isolated metathesis-active methylidene complex [16].

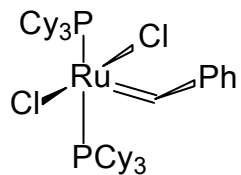


Figure 2.6: Grubbs 1st generation precatalyst [16]

By further altering the ligands of the ruthenium complexes Grubbs [1-3] added an N-heterocyclic carbene (NHC) ligand to the first-generation Grubbs precatalyst to stabilise the complex. The increase in stability could mainly be attributed to the non-labile, σ -donating characteristics of the NHC ligand [2]. The saturated nature of the backbone of this complex proved to be more reactive to its unsaturated counterpart, this, together with the stericity and basicity of the complex plays a role in the dissociation of the phosphine ligand (which is the necessary activation step) and in stabilizing the electron deficient intermediate products that form [3].

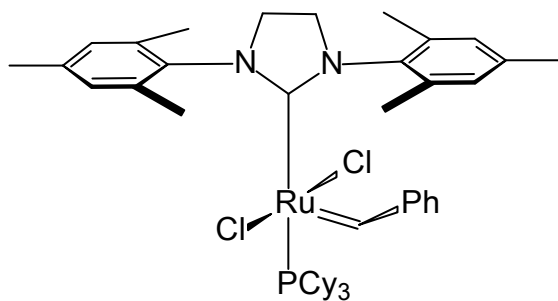


Figure 2.7: Grubbs 2nd generation precatalyst

The aim of the resulting research was to further improve the activity, stability and selectivity of the precatalysts by modifying the ligands.

Ligands are defined as atoms that can form chemical bonds with transition metals to form complexes. To bond to the metal, ligands need to have a lone pair of electrons to donate to the metal's empty d-orbital [17]. Ligands can be classified based on the number of such bonds that are able to be made. Monodentate ligands can form one coordinate bond, bidentate ligands can form 2 and multidentate ligands can form 3 or more coordinate bonds with the metal [17]. Altering the ligands would ultimately alter the steric bulk and electronic properties of the precatalyst [17].

The general format of the Grubbs system has 3 main group types. Firstly, the alkylidene moiety ($=\text{CHR}$), the anionic ligands (X) and finally the ancillary ligands (L) as depicted in Figure 2.8.

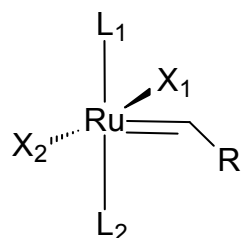


Figure 2.8: General Ru-alkylidene complex structure

The next generation of precatalysts that were developed are probably the most widely applied and the most successful ones to date. Adding a metal-oxygen chelate to the alkylidene moiety of **G1** resulted in the Hoveyda-Grubbs 1st generation **HG1** complex. The result was a precatalyst that has exceptional tolerance towards air and water with increased yield. Further modification by replacing the **PCy₃** ligand with the N-Heterocyclic carbene (NHC) ligand yielded a precatalyst with improved activity towards electron poor alkenes [14].

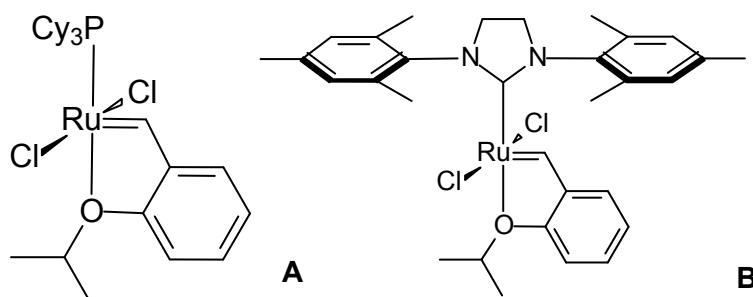


Figure 2.9: Hoveyda Grubbs 1st (A) and 2nd (B) generation precatalysts

2.2.3.2 Commercial Grubbs-type precatalysts for linear alkene metathesis

A whole library of Grubbs based precatalysts is available in literature and each of them has their own attributes and performance characteristics. When new precatalyst structures are being evaluated the benchmarks that literature provide is often the first means by which a precatalyst's performance can be compared. Each precatalyst is unique in its properties and fortunately classification based on these properties is possible which narrows down the spectrum of precatalysts in literature that comparisons can be made with. Additionally, the aspect of commercial application is also as criteria by which novel precatalysts and their performance are measured. Since the focus of this work is that of commercial application, a brief review and evaluation of commercial precatalysts will be made with focus placed upon the effects of temperature and precatalyst load on the catalytic performance. Additional attention is granted to the class of latent, hemilabile Grubbs-type precatalysts (following the same design concept of the **GMPP** and **GCYC** catalysts) in which findings from literature are presented and discussed.

The availability of literature on commercial precatalysts with respect to RCM is widespread [2] which can be attributed to the speciality of Grubbs and his team in those applications. For linear alkene metathesis, many studies were conducted on which only a number reported the catalytic performance and product distribution of the reactions [18-25].

The following sections aim to provide an in-depth background on past work in the field of linear alkene metathesis in the presence of commercial Grubbs-type precatalysts with the specific focus towards temperature and precatalyst load.

2.2.3.2.1 Effect of temperature

The effects of temperature have for the most part played the largest role in the catalytic activity of metathesis precatalysts. Grubbs-type complexes have been shown to be sensitive to slight changes in temperature and as a result, undesired side-product formation occurs [15]. Dinger and Mol [26-27] investigated the effects of temperature on the TONs of **G1** and **G2** precatalysts with 1-octene. The results reported showed that the **G1** precatalyst was much less reactive than the **G2** precatalyst and that the **G1** precatalyst's TONs peaked around 28 000 at 60°C.

Temperatures beyond 60°C resulted in a sharp downturn in activity which was presumed as the decomposition temperature of the precatalyst [26]. Similar trends were reported for the **G2** precatalyst except for the fact that the maximum TONs reached were considerably higher at approx. 295 000 [26].

The **G2** precatalyst also only succumbed to thermal degradation at temperatures beyond 100°C. A more interesting trend that the authors observed was the sharp increase in TONs with the **G2** precatalyst between 50 and 52°C. The conclusion was made that this temperature was the threshold at which the precatalyst's initiation rate increased but the underlying reason for this was reported as "unclear" [26]. A possible explanation was attributed to steric bulk differences leading to faster initiation rates. Longer reaction times resulted in a loss of selectivity due to cross-metathesis reactions taking place, but more attention was given to the performance of a bulkier analogue of the **G2** precatalyst [26].

A second study by the same authors [27] investigated the degradation of the **G2** precatalyst in the presence of alcohol and oxygen with 1-octene as a substrate. Their findings showed an increase in double bond isomerisation because of thermal decomposition. This explains a loss in selectivity at higher temperatures and the simultaneous cross metathesis product formation.

Catalyst decomposition often leads to the formation of isomers, probably because transition metal precatalysts are known for being used to produce isomers [28]. Several possibilities have been proposed in literature as to why isomerisation occurs in ruthenium carbene precatalysts and what the actual intermediates are that cause decomposition and/ or isomerisation [28-30]. A popular explanation has much to do with the formation or presence of ruthenium hydride- which is a known isomerisation catalyst. It has been reported that the presence of the dissociated phosphine ligand in the reaction environment is a possible cause [31]. A number of plausible mechanisms are suggested and proven in literature [28-31,34-35]. A brief explanation of the most popular decomposition mechanisms is provided in Appendix A.

Lehman *et al.* [30] demonstrated the occurrence of isomerisation and reported the resulting product distribution from the cross-metathesis reactions with 1-octene and 2-octene. They did not report the activity of the precatalysts tested but similar trends to Dinger and Mol [27] were reported where both **G1** and **G2** reactions with 1-and 2-octene respectively yielded higher PMP conversions at lower temperatures (81.8% and 90.8%). It was found that the 2-octene reacted analogously to the 1-octene in terms of performance and the cross-metathesis product distributions confirming the findings of Dinger and Mol [27].

Mtshatsheni [21], however, reported a higher amount of conversion (62%) for the **G1** precatalyst at 100°C (versus 54% at 25°C) but accompanied it with a reported loss in selectivity (74%). The reactions were, however, only carried out for 4 hours.

As for the **G2** precatalyst, Mtshatsheni reported data consistent with the previous findings i.e. a decrease in PMP conversion as temperature increased accompanied by a loss in selectivity.

Buchowitz and Mol [32] investigated the effects of temperature on cis and trans-4-nonene in the presence of different solvents with the **G1** precatalyst and observed an increase in conversion up to 70° C. Precatalyst decomposition at longer reaction times was also observed.

Ajam [33] also investigated metathesis of 1-octene with **HG2** and **G2** complexes in ionic liquids as solvents. Ethene was continuously removed by purging the reaction environment with argon. The **HG2** complex yielded a 93% conversion at 40°C and precatalyst load of 1:5000, while at the same time maintaining high selectivity (91%). In the case of **G2** the reaction temperature was increased to 60°C and the precatalyst load of 1:8500 a 99% conversion was achieved but the selectivity only peaked at 70%.

Jordaan [18-19] investigated the performance of different precatalysts in their performance of 1-octene metathesis reactions and compared it to the performance of commercial precatalysts. The reactions were conducted at a precatalyst load of 9000 and between 35-80°C. At 35°C, the conversion achieved with the **G1** precatalyst was 41% and a selectivity of 98.3 was reported. At higher temperatures, the reported conversion and selectivity declined to 21% and 44.5% respectively. Concurrently the highest TON for the **G1** precatalyst that Jordaan [18] reported was 4136. In comparison Jordaan reported an improved conversion for the **G2** precatalyst at the same conditions tested as with the **G1** precatalyst, and even more interesting the conversion attained increased from 61% at 35° up to 82% at 70° C. At the same time the selectivity and TON decreased from 97.9% to 69.9% as the temperature increased Jordaan's findings proved the superior performance of the second-generation Grubbs precatalysts compared to the first-generation analogue in terms of thermal stability.

Soon after Jordaan's study Loock [22] studied the metathesis of 6 to 9 carbon chain alkenes between 55-80°C and at 1:7000 precatalyst molar ratio in the presence of **G1** and **G2**. The effect of temperature on the precatalyst performance was proven to follow the trends previously reported in literature. At first, an increase in temperature resulted in an increased conversion and a simultaneous increase in selectivity, up until a threshold temperature was exceeded.

Beyond this temperature, the conversion typically continued to increase but the selectivity decreased as isomerisation and cross metathesis products were forming. Overall, the **G2** precatalyst outperformed the **G1** precatalyst in terms of higher conversions and TONs [22].

More recently in 2012, Van der Gryp *et al.* [24] reported results on the effect of temperature and precatalyst load on the performance of the **HG2** precatalyst in a 1-octene metathesis reaction. Van der Gryp *et al.* [24] observed a similar trend as Loock [22] with an increase in conversion (19.3-70.68%) as temperature increased from 30 °C to 80 °C after which (at temperatures >90°C) the conversion declined to 19.55%. At temperatures beyond 50 °C, Van der Gryp *et al.* [24] reported a decline in selectivity and TONs and recommended an optimal reaction temperature of 50-60 °C.

In the youngest report published by du Toit *et al.* [36] in 2016, only 1 commercial precatalyst was studied for the metathesis reaction of 1-octene at 60 and 80°C. At 60°C the **G2** precatalyst performed better in all aspects as opposed to 80°C where selectivity, conversion and activity started to decline, thus concluding that the **G2** precatalyst's peak performance temperature is between the temperatures of 55 and 65 °C

The effects of temperature on the performance of commercial precatalysts in different reaction environments and with different substrates have been studied comprehensively in the past. Throughout literature, the trends observed indicated an increase in performance as temperature increased up until a point where the precatalyst started to either produce side-products and compromise on selectivity or completely decompose and produce less product [20-22]. The **G2** precatalyst is also known for its thermal stability as opposed to the **G1** precatalyst explaining why its performance peaks at higher temperatures than the **G1** precatalyst [37]. The literature as discussed above is summarised and briefly expanded for comparison purposes in Table 2.4

2.2.3.2.2 Effect of precatalyst load

When evaluating a precatalyst's performance, the amount of precatalyst added to the reaction is a critical parameter considering the high cost of ruthenium-based metal complexes. In their review of NHC-ruthenium based precatalysts in metathesis reactions, Samojlowicz *et al.* [38] reported the effect of precatalyst loading on the conversion of RCM of N,N-diallyl-4-toluene-sulfonamide promoted by **HG2**. The findings indicated that the conversion directly correlated with the precatalyst loading. At 0.05 mol% (alkene/catalyst = 50 000:1) 100% conversion was achieved, and as the precatalyst loading decreased the conversion decreased as well.

The next obvious question is whether the same trend would be observed in the case of linear alkene self-metathesis?

Dinger and Mol's [27] study also investigated the effect of precatalyst load on catalytic performance. They reported the conversion and maximum effective turnover numbers achievable as a function of the substrate concentration at 22°C (the inverse of precatalyst concentration). Their results indicated a plateau in the TON that the **G2** precatalyst could achieve. The threshold precatalyst concentration was reported as 145 000 equivalents of 1-octene. Simultaneously they reported a decrease in conversion when 1-octene was additionally added to the reaction mixture to keep the TONs as high as possible [27]. It was noted however that without additional 1-octene, conversion would increase as the precatalyst concentration increased but the precatalyst use will ultimately be inefficient. The suggestion was made that according to their findings the **G2** precatalyst is best operated at a 63% conversion and 145 000 equivalents of 1-octene Mtshatsheni [21] observed a similar trend with their reaction of 1-octene with **G1** and **G2** complexes. The reactions were carried out at 25°C and 100, 1000 and 10 000 1-octene to precatalyst molar ratio. Both precatalysts indicated an increase in TON as the precatalyst concentration decreased but a decrease in conversion to below 10% was observed.

Jordan [19], Loock [22] and Stark [39] all investigated the effect of precatalyst load on the performance of the **G1** precatalyst. Jordan's tests were conducted at 60° C and C₈/Ru ratios of 2000, 9000, and 100 000. Jordan reported an increase in TON from 1728 to 3569 and an increase in selectivity of 69.6-97.8% as the precatalyst load increased (i.e. a decrease in the amount of precatalyst) simultaneously the conversion declined from 68 to 32%, thus also confirming that more precatalyst might improve conversion but not necessarily all efficiency of the precatalyst. An interesting analogy would be to compare the precatalyst performance to that of a car's engine (disregarding external factors such as drag, lubrication, maintenance etc.). Higher speed (in this case conversions) do not necessarily imply fuel efficiency or better performance [28] (TON). Interestingly the results Loock [22] reported for the same precatalyst and temperature with 1-Hexene only correlated with Jordan's trends in terms of conversion. The conversion decreased from 55.3-19.7% but the TONs reported at a higher precatalyst concentration (C₈/Ru = 7000) were closer to the values obtained by Jordan at lower precatalyst concentration (3873 at C₈/Ru = 7000 ~Loock vs 3569 at C₈/Ru = 100 000~Jordan). The trends Loock observed with 1-hexene closely resembled those of the reactions conducted with 1-heptene.

In the case of the second-generation precatalysts Loock [22] reported similar results, for 1-hexene at 60°C and precatalyst load at 7000 and 9000 TONs were reported as 5113 and 5351 respectively. Conversion remained almost constant but a slight increase in selectivity from 73.3 - 83% was observed. They attributed the change in selectivity to the decrease in secondary metathesis products as a result of less precatalyst available to initiate conversion to primary metathesis products. Similar trends were observed in the case of 1-heptene. Van der Gryp was one of few to report the effect of precatalyst load on 1-octene reaction performance in the presence of the **HG1** complex. Temperatures were kept constant at 50°C and the precatalyst loadings were varied between 5 000 and 14 000 [14].

Van der Gryp only reported a change in TON (2686-4779) and conversion (53.96-39.7) at a precatalyst load of 9000 however, the lowest conversion of 4.3 % was reported. Van der Gryp *et al.* soon published on the same reaction but instead of **HG1** used the **HG2** [24] precatalyst to evaluate and characterise in their DFT and kinetic study of the reaction. Once again, no changes were reported in selectivity as the precatalyst load was varied, but TONs reportedly increased from 4802 at C₈/Ru = 7000 to 5334 at 14000. Conversion decreased from 68.3 to 38.1%. The optimal performance point for the **HG2** precatalyst was however at a precatalyst load of 9000. Indicating an increase in performance up to an optimal point and a steady decline thereafter.

With the focus on metathesis with terminal longer chain alkenes promoted by Grubbs-type precatalysts, a summary of previous literature is presented in Table 2.4. The content of the table has been drawn from the discussion above with relevant additions thereto.

Table 2.4 Summary of literature on the performance of commercial Grubbs-type precatalysts

Author	Product Dist.	Year	Catalyst	Substrate	Activity TON (-)	Selectivity (%)	Conversion/ PMP mol%	Temperature °C	Catalyst load/ [Substrate]	Time (h)
Dinger & Mol [26] ^l	Y	2002	G2	1-octene	295000	91%	60	55	60000	24
			G1	1-octene	28500	>98	27		12000	
			G2	4-decene	570000	>98	48		140000	
			G1	4-decene	1250	>98	30		500	
Lehman <i>et al.</i> [30]	Y	2003	G2	1-octene	-	-	81.8	RT	1000	24
			G2	1-octene	-	-	29.3	60		
			G2	2-octene	-	-	~57	55		
			G1	1-octene	-	-	90.8	45		
			G1	2-octene	-	-	91.1	45		
Mshatsheni [21]	Y	2005	G1	1-octene	30	84	54%	25	100	4
			G1		120	81	22%	25	1000	
			G1		150	50	<10	25	10000	
			G1		-	57	50%	50	100	
			G1		-	74	62%	100	100	
			G2		65	81	62%	25	100	
			G2		350	72	38%	25	1000	
			G2		710	67	<10	25	10000	
			G2		-	72	47%	50	100	
			G2		-	18	<10	100	100	
Forman <i>et al.</i> [41]	Y	2005	G1	1-octene	2100	-	26	50	9000	3
			G2		-	-	55	50	9000	3
Jordaan [64]	Y	2006	G1	1-octene	-	91	62	25	1000	7
Ajam <i>et al.</i> [33]	N	2006	HG2	1-octene	-	91	93*	40	5000	-
			G2		-	70	99*	60	8500	
Stark <i>et al.</i> [39]	N	2006	G1	1-octene	2520	-	48.2	RT	1.22x10^-3 M	4
			G1		4920	-	41.1		6.10x10^-6 M	
			G1		-	-	60.2		1.22x10^-3 M	
			G2		-	-	83.4		1.22x10^-3 M	
			HG1		-	-	86.5		1.22x10^-3 M	
Jordaan [19]		2007	G1	1-octene	4136	98.3	41	35	9000	7
			G1		2175	80.6	21	60		
			G1		2020	67.4	19	70		
			G1		2056	44.5	21	80		

Table 2.4-Cont'd Summary of literature on the performance of commercial Grubbs-type precatalysts

Author	Product Dist.	Year	Catalyst	Substrate	Activity TON (-)	Selectivity (%)	Conversion/ PMP mol%	Temperature °C	Catalyst load/ [Substrate]	Time (h)
Jordaan [19]	Y	2007	G2	1-octene	6601	97.9	61	35	9000	7
			G2		8881	95.8	82	60		
			G2		8929	87.9	82	70		
			G2		8988	85.9	79	80		
Jordaan [19]	Y	2007	G1	1-octene	1728	69.6	68	60	2000	7
Jordaan [19]	Y	2007	G1		3569	97.86	32	60		
Van der Gryp [14]	Y	2008	HG1	1-octene	3777	96.08	20.82	30	7000	7
					2686	92.58	53.96	50	7000	
					2051	40.42	38.36	80	7000	
					301	16.12	29.3	100	7000	
					3573	93.28	4.3	50	9000	
					4779	93.04	39.7	50	14000	
Loock [22]	Y	2009	G1	1-hexene	1123	100	34.8	55	7000	2.5 to 336
			G1	1-hexene	3873	99.8	55.3	60	7000	
			G1	1-hexene	1380	99.8	19.7	60	9000	
			G2	1-hexene	4727	77.5	67.5	55	7000	
			G2	1-hexene	5113	73	80.3	60	7000	
			G2	1-hexene	5351	83.3	76.4	60	9000	
			G1	1-heptene	1370	86.3	19.6	60	9000	
			G1	1-heptene	2631	94.5	37.6	60	7000	
			G1	1-heptene	966	98.2	13.8	70	7000	
			G1	1-heptene	1129	56.8	48.9	80	7000	
			G2	1-heptene	4044	61.9	57.8	60	9000	
			G2	1-heptene	3278	52.7	46.8	60	7000	
			G2	1-heptene	4783	85.8	68.3	70	7000	
			G2	1-heptene	3420	56.8	48	80	7000	
			G1	1-nonene	2642	86.9	37.7	60	7000	
			G2	1-nonene	5438	96.1	77.7	60	7000	
			G1	1-decene	3979	90.5	56.8	60	7000	
			G2	1-decene	4648	71.9	66.4	60	7000	

Table 2.4-Cont'd Summary of literature on the performance of commercial Grubbs-based precatalysts

Author	Product Dist.	Year	Catalyst	Substrate	Activity TON (-)	Selectivity (%)	Conversion/ PMP mol%	Temperature °C	Catalyst load/ [Substrate]	Time (h)
Van der Gryp <i>et al.</i> [24]	Y	2012	HG2	1-octene	1351	97.26	19.3	30	7000	7
					4802	98.22	68.6	50	7000	
					4947	76.81	70.68	80	7000	
					1368	24.65	19.55	100	7000	
					6324	98.19	70.26	50	9000	
					5334	98	38.1	50	14000	
Du Toit <i>et al.</i> [36]	Y	2014	G2	1-octene	7254	96.3	80.6	60	9000	7
		2016	G2	1-octene	5278	82	75.5	60	7000	7
					4410	66	63	80	7000	

* Overall conversion

2.2.3.3 Chelating pyridinyl alcholato precatalysts

2.2.3.3.1 Hemilabile ligands

Chelating ligands have become a topic of interest recently due to their ability to aid in fine tuning the thermal stability of precatalysts. Chelates are defined as ligands that bind to metals through more than one atom, which allows them to form a cyclic compound by donating lone pairs of electrons (from the donor atoms) to the metal atom [43]. A particular class of chelating ligands, hemilabile ligands, enable chemists to place two or more donor atoms (with diverse electronic properties) close to the metal centre [43]. The interest in hemilabile ligands is attributed to their ability to create or occupy a vacant coordination site on the metal. This stabilises the active intermediate species, thereby enhancing the catalytic activity. Figure 2.10 explains this phenomenon graphically, where one ligand is labile (B) and the other (A) tightly bound to the metal centre (M).

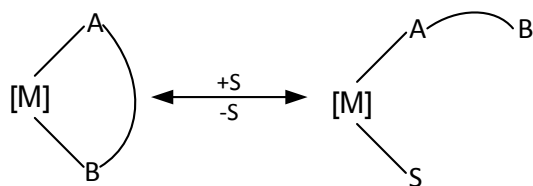


Figure 2.10: Hemilability concept

Different design concepts exist for the creation of precatalysts with hemilabile ligands (Figure 2.11). The intention behind these designs is to slow down or prevent the L₂ ligand from dissociating [44].

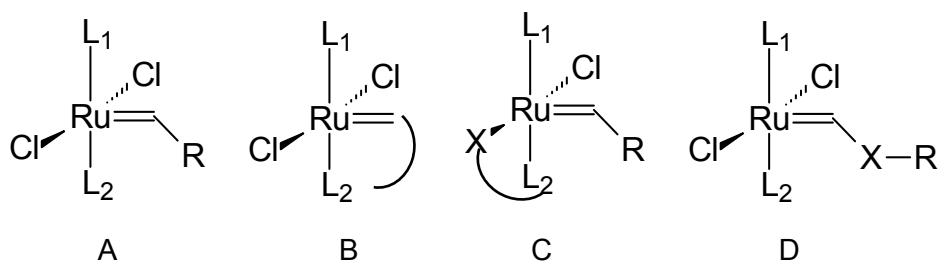


Figure 2.11: Design concepts for hemilabile precatalysts

The classical system is represented in motif A [45], which occurs in the typical Grubbs precatalysts where L₂ is either PCy₃ or H₂IMes. Precatalysts designed on Motif B are highly stable and can be used in reagent grade solvents or in the presence of air [45]. Motif C was first achieved by Grubbs *et al.* [46] and later by Verpoort *et al.* [47] with precatalysts where the X in motif C was typically an oxygen atom. This allows the chelating ligand to compete in the initiation and coordination with the incoming alkene for an open coordination site.

Typically, precatalysts that follow these design motifs would not react at ambient conditions until they are subjected to a stimulus such as a temperature increase, light or the addition of a co-catalyst [45]. Chelated complexes have found wide applications especially in the polymerization class of metathesis reactions but have the potential to be applied in multicomponent synthetic sequences because of the high amount of control that can be attained. This attribute is useful in systems that employ a wide range of operating parameters [44]

2.2.3.3.2 Performance of hemilabile latent precatalysts

Commercial precatalysts might be easy to come by but aren't always the best choice when a task-specific precatalyst is needed, and even more so when high operating temperatures will lead to costly precatalyst degradation.

The development of latent precatalysts found its source behind the need to create task-specific precatalysts that could be activated by an external stimulus. An even stronger driving force for the development of latent precatalysts was to increase the thermal stability lifetime. One of the applications of latent precatalysts that contributed immensely to their design was that of ROMP. There was a need for precatalysts that could be mixed with monomers without concomitant polymerization [44].

Latent precatalysts started off as ill-defined complexes that were formed *in situ* [44]. A major shortcoming of these ill-defined complexes is their inefficient initiation, which results in wide product distributions and requires costly high precatalyst loadings. However, with the advent of well-defined, highly active, ruthenium precatalysts with the Grubbs–catalyst system, a ruthenium alkylidene motif was incorporated into the latent class of precatalysts. In the search for highly active intermediates, the Grubbs team exchanged the chlorine ligands in the first-generation Grubbs precatalyst with pi-donating and sterically demanding tertiary alkoxides.

At room temperatures, these complexes displayed no activity towards the RCM reaction with diethyl diallyl malonate (DEDAM) and only moderate activity was obtained at 60°C and precatalyst decomposition was still taking place. Upon addition of hydrochloric acid, however, resulted in almost quantitative conversion for the DEDAM reaction. Following Grubb's report researchers started to explore by adding different N-donating groups such as pyridine, phosphoric acid and dimethylamino pyridine. Not only was the latency effect achieved but higher activation rates were

also observed. Consequently, other groups with different atoms such as S and O were added and explored [1,48-51].

Hemilabile ligands have gained interest since the hemilabile mechanism allowed an active site on the metal centre to be accessed while the tightly bound group and dangling ligand would stabilise the active species. These dangling/hemilabile ligands could also be sterically and electronically modified, allowing researchers to fine-tune the precatalysts with relative ease [44,45, 48-51].

It is beyond the scope of this work to discuss the details of the synthesis, and rationale behind hemilabile precatalysts, but the reader is referred to Monsaert *et al.* [44] who has published an excellent review on the topic.

The class of precatalysts that forms primarily the focus of this study is that of complexes bearing a pyridinyl alcoholato ligand. Typically, precatalysts of this class are identified as a 5-membered ring alternative to those with Schiff base ligands [52]. Herrmann *et al.* [53] were the first to report on them for the ROMP reaction of norbornene and cyclooctene. Work by de Clerq and Verpoort [47] included the NHC ligand as opposed to the first-generation Grubbs catalysts that were used by previous authors at the time. In doing so, the thermal stability and latency of the catalysts were increased. Low activity was observed at room temperatures but was enhanced by thermal activation. Jordaan and Vosloo extended this approach to the application of 1-octene and the result was a precatalyst of which the selectivity is temperature dependent [19]. Hahn tried to improve further by exchanging Halide ligands with bidentate carboxylato ligands which required the addition of HCl to initiate the reaction [54]. Limbach's group also employed the concept of pyridinyl oxygen chelates to first and second-generation ruthenium carbenes [55]. One of the goals in a recent study of theirs was to improve reaction residue separation with silica. Their approach focussed on ROMP of cyclooctene and CM of 5-decene with acetates [4].

Many more adaptions were made on these precatalysts and each reported complex had its own application, activation and style of ligands, what is important to note is that the lifetime of the precatalysts increased dramatically, that is where similar reactions with the commercial precatalysts would only last for two to seven hours at best, some of these precatalysts would still display activity at the 24-hour mark. Furthermore, the dramatic increase in reaction rate and activity due to the addition of external stimuli is almost impossible to miss. A summary of the activity performance of these hemilabile and chelating complexes as adapted from [44] is provided in Table 2.5.

Table 2.5: Summary of literature on hemilabile catalysts designed with motif C

Author	Year	Catalyst	Reaction	Substrate	Temperature (°C)	TON (-)	Conversion (%)
De Clercq <i>et al.</i> [47]	2002		ROMP	Bicyclo [2,2,1] hept-2-ene	70 ⁱ	2000-440	100
Allaert <i>et al.</i> [65]	2006			Cyclo-octene	70 ⁱ	800-632	100
Ledoux <i>et al.</i> [66]	2006			1,5-Cyclo-octadiene	25 ^d	- ^f	99
				1,5-Cyclo-octadiene	90 ⁱ	300	99
				DEDAM ^e	25 ^j	3000	>95
				1,5-Cyclo-octadiene	25 ⁱ	630000	100
De Clercq <i>et al.</i> [47]	2002		RCM	DEDAM ^e	55 ^m	20	87
Lozano <i>et al.</i> [44]	2009		RCM	DEDAM ^e	100 ⁱ	1000-1500	-
					25 ^j	>800	>50
Denk <i>et al.</i> [52]	2002		ROMP	Bicyclo [2,2,1]hept-2-ene	25 ⁱ	57-65	14
					60 ⁱ	98-100	99
			CM	Cyclo-octene	25 ^d	-90 ^f	65
					60 ^d	360-400	72
Jordaan <i>et al.</i> [19]	2007		CM	1-Octene	35 ^g	1143	10.2
					80 ^g	10119	90.3
					35 ^g	379	3.3
					70 ^g	10428	91.8
Hahn <i>et al.</i> [54]	2005		RCM	DEDAM ^e	20 ^d	20	100
				DAA•HCl ⁿ	40 ^o	14	70

Table 2.5 Cont'd: Summary of literature on hemilabile catalysts designed with motif C

Author	Year	Catalyst	Reaction	Substrate	Temperature (°C)	TON (-)	Conversion (%)
Limbach <i>et al.</i> [55]	2011		ROMP	Cyclo-octene	25	-	40-100
			CM	5-decene 5-hexenyl acetate	25	-	81-99
Du Toit <i>et al.</i> [36]	2016		SM	1-octene	60	7785	86.7
Tole <i>et al.</i> [45]	2017		SM	1-octene	110	8160	91
^a Turn-over number, calculated based on literature data. ^b Turn-over frequency, calculated based on literature data. ^c Solvent: CH ₂ ClCH ₂ Cl. ^d Solvent: dichloromethane. ^e Diethyl diallyl malonate. ^f No activity observed. ^g No solvent. ^h ‘Switching temperature’. ⁱ Solvent: toluene. ^j Photoacid generator. ^l Solvent: CDCl ₃ . ^m Solvent: C6D6. ⁿ Diallyl amine hydrochloride. ^o Solvent: CD3OD. ^p Diallyl malononitrile.							

Since most of the reactions mentioned are related to the polymer industry the purposes of the table are to give the reader an idea of how the performance of the precatalysts change because of varying ligands and the application of external stimuli.

2.2.3.3.3 Synthesis of chelating pyridinyl alcholato precatalysts (GCYC & GMPP)

The nature of this study is a collaboration between two fields of study –chemistry and engineering. A description of how the precatalysts for this work are typically synthesised is thus needed. The procedure for the synthesis of the precatalyst is required in cost estimation calculations that will be covered in Chapter 4. Precatalyst synthesis is beyond the scope of this study and focus will thus be given to the **GCYC** precatalyst. A similar approach is applied for the synthesis of the **GMPP** precatalyst.

The **GCYC** precatalyst is formally named as benzylidene-chloro (1, 3-bis-(2, 4, 6-trimethylphenyl)-2-imidazolidinylidene)-[1-(2'-pyridinyl)-1-(cyclopentyl)-methanolato] ruthenium and was first developed and introduced in 2002 by Denk *et al.* [52] for the RCMP of cyclo-octene. In 2007 the efforts of Jordaan and Vosloo used the **GCYC** precatalyst in a SM/CM application with 1-octene. The precatalyst synthesis is a 3-step process illustrated in Figure 2.12 [19].

The first step synthesizes the pyridinyl alcohols. 2-Bromopyridine is reacted with butyllithium in cooled diethyl ether, the desired ketone is then added to the reaction mixture. The ether phase is extracted, treated with activated charcoal and filtered to obtain the alcohol crystals. The second step entails adding tetrahydrofuran (THF) to the alcohol [19]. Butyllithium is then added dropwise to the mixture which is stirred for 2 hours at ambient conditions until precipitate forms. The solvent is then removed to yield the lithium salt [19].

The third and final step of the synthesis scheme entails adding the salt to the starting ruthenium alkylidene complex (**G2**). A solution of the salt in THF is added to a solution of the ruthenium complex in THF. The reaction is heated to the desired temperature until the reagents are consumed. The solvent is then evaporated from the mixture and the residue is dissolved in a small amount of toluene. The lithium chloride is removed by filtration. A small amount of THF is added to the residue and pentane is layered onto the THF in a Schleck flask which is refrigerated until precipitation occurs. The resulting solid is then washed and treated to remove impurities.

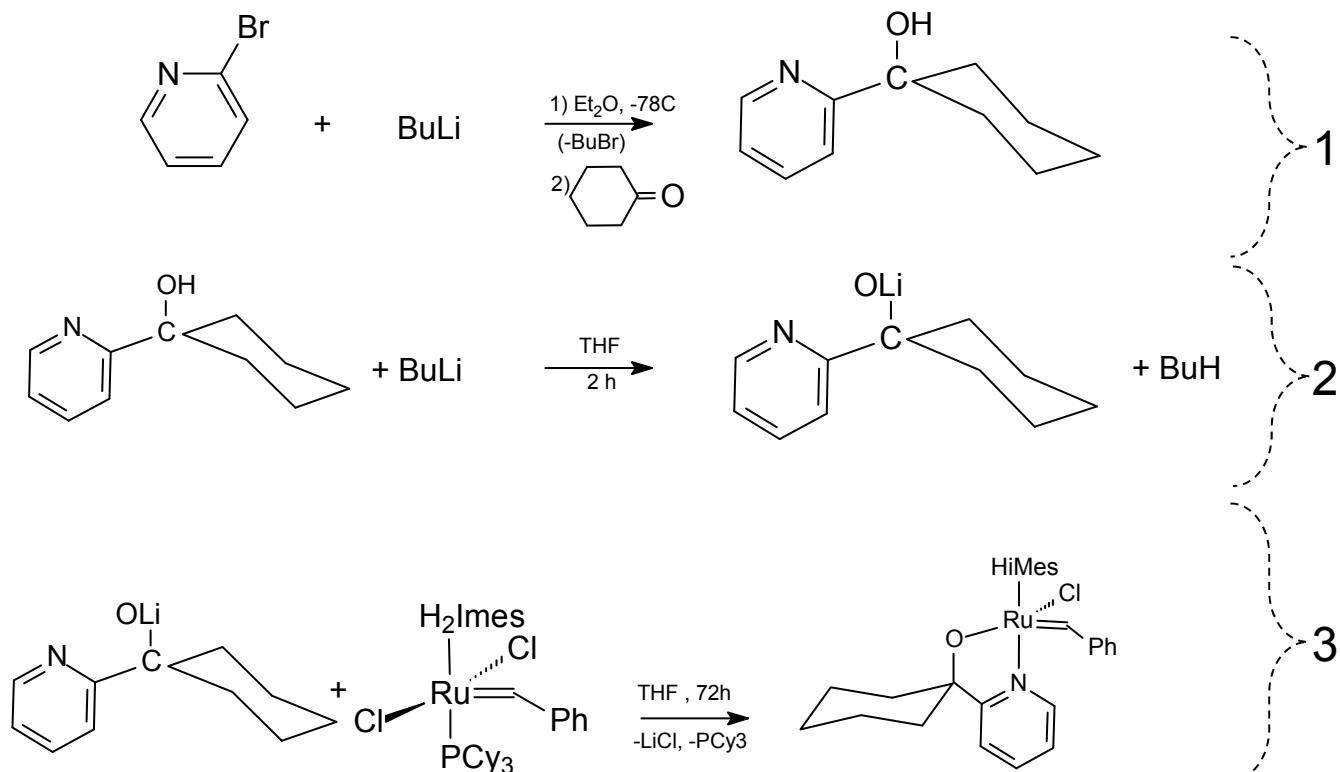


Figure 2.12: Precatalyst synthesis procedure for the GCYC catalyst [19]

2.2.4 Critical comments and concluding remarks

The efforts of precatalyst synthesis studies generally aim towards improving the precatalysts' overall performance. There are numerous descriptions and criteria for the ideal catalyst but one that could probably be viewed as the most comprehensive was the description that Gladysz [57] gave in 2001. The ideal catalyst needs to have the following attributes:

- Infinite production of product from a single catalyst molecule (which implies no deactivation and (high turnover number TON))
- Rapid reaction (high Turnover frequency TOF)
- Rapid reaction at ambient pressures
- Has no inert atmosphere requirements
- Tolerance towards impurities
- Full conversion and yield
- Readily available and inexpensive
- Non-hazardous

Throughout this study, the precatalyst performance will be evaluated based on the turnover number (TON), (TOF), selectivity (S), conversion (X) and yield (Y) which are defined in equations 2.1 through to 2.5 respectively.

$$TON = \frac{\text{Moles PMP produced}}{100} * \text{Catalyst Load} \quad (2.1)$$

$$TOF = \frac{TON}{t_{420}} \quad (2.2)$$

$$S = \frac{\text{Moles Desired Products}}{\text{Moles Undesired Products}} \quad (2.3)$$

$$X = \frac{\text{Moles } C_8 \text{ Reacted}}{\text{Moles } C_8 \text{ Fed}} \quad (2.4)$$

$$Y = \frac{\text{Moles Desired Products}}{\text{Moles } C_8 \text{ Reacted}} \quad (2.5)$$

The attributes mentioned above are too demanding when looking for a suitable precatalyst, but serve as good benchmarks by which synthesis communities can measure their precatalysts' performance. That said, it is evident that a large amount of information is available on the topics of precatalyst performance and the effects of temperature, precatalyst loading, co-catalysts and applications the field of alkene metathesis. What is even more evident is the effects that differences in the ligand environment create between precatalysts. Ultimately all these factors contribute to the success of a precatalyst in achieving the desired conversion, selectivity, and activity.

Alkene metathesis research has reached success on many fronts in this regard with much of literature directed towards the characterization and fine-tuning of catalysts. Less attention was spent on linear alkene metathesis in comparison to the fields of RCM and ROMP. Additionally, few authors have focussed on the economic impacts or used economic evaluations to aid in catalyst comparison. It is the focus of this study to conduct such a comparison with the **GCYC** and **GMPP** catalysts.

2.3 Experimental procedures

The layout of the sections to follow are mainly guided by the works of Van der Gryp [14,24], Jordaan [18,19], du Toit [20,36], Forman [41], Loock [22], Dinger and Mol [26] since the most information about Linear alpha-alkene metathesis has been generated by these authors.

2.3.1 Materials used

In Table 2.6 a summary of the solvents and reactants used throughout the experiments and the analyses is provided. Each of the compounds was used without further purification or processing. The chemical structures of each compound are also provided along with the supplier and the purity.

Table 2.6: Chemicals and solvents used for metathesis of 1-octene

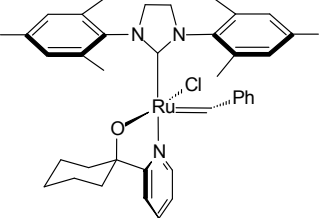
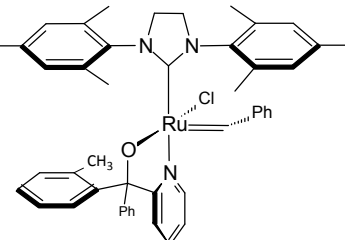
Compound	Purity/ Assay	Supplier	Use
1-octene	>98%	Sigma-Aldrich	Metathesis reaction feedstock
Dichloromethane	Analytical Grade	Associated chemical enterprises (ACE)	Solvent for GC analysis
Toluene	Analytical Grade	Associated chemical enterprises (ACE)	Solvent for GC Analysis
Tert-butyl hydroperoxide solution	0.5-0.6 M in Decane	Sigma- Aldrich	Used to quench the reaction after sampling
Nonane	>99.5%	Sigma- Aldrich	Standard for GC analysis
Air, Hydrogen & Helium	-	Afrox	GC Analysis

Table 2.7 lists all the different precatalysts that were used throughout the course of this study as well as their suppliers and structures.

Table 2.7: Precatalysts used for the metathesis of 1-octene

Precatalyst & abbreviation	Structure	Supplier
Hoveyda-Grubbs 2 nd Generation [1,3-Bis-(2,4,6-trimethylphenyl)-2-imidazolidinylidene)dichloro(o-isopropoxyphenyl)methylene ruthenium] HG2		Sigma-Aldrich

Table 2.7-cont'd: Precatalysts used for the metathesis of 1-octene

Precatalyst & abbreviation	Structure	Supplier
Benzylidene-chloro(1,3-bis(2,4,6-trimethylphenyl)-2-imidazolidinylidene)- [1-(2'-pyridinyl)-1-(cyclopentyl)-methanolato] ruthenium GCYC		North-West University
Benzylidene-chloro(1,3-bis-(2,4,6-trimethylphenyl)-2-imidazolidinylidene)-[1-(2'-pyridinyl)-1-(2'-methyl-phenyl),1-phenyl-methanolato] ruthenium GMPP		North-West University

2.3.2 Apparatus and experimental procedure

The reaction setup used corresponds to the setup used by authors in literature [20, 24, 36,45] The catalytic experiments were conducted in a 250mL three-necked round-bottomed flask fitted with a Davies condenser, mechanical stirrer and a thermometer. The condenser was fitted with rubber tubing to the water supply. The reaction vessel was heated with a temperature controlled (PID) heating mantle. Samples were drawn with a 1mL analytical glass syringe fitted with 11cm bevel-tip needles. Figure 2.13 provides a schematic of the setup and an accompanying photograph one. Reactions were carried out by first heating neat 1-octene to the desired temperature and then adding the precatalyst.

Once the precatalyst was added the reaction time was started and continued for 420 minutes. Samples were withdrawn at first every 2.5 minutes until the reaction time reached the 25-minute mark. The samples were subsequently withdrawn every 5 minutes until 60 minutes have passed after which the sampling times were lengthened to every 30 minutes for the next 2 hours. The final 4 hours of samples were taken at the end of every hour.

Samples were prepared for analysis by adding 3-4 drops of tert-butyl hydroperoxide solution to the 0.3 mL sample. 0.1 mL nonane was added as an external standard and the mixture was diluted to a total volume of 4 mL with dichloromethane.

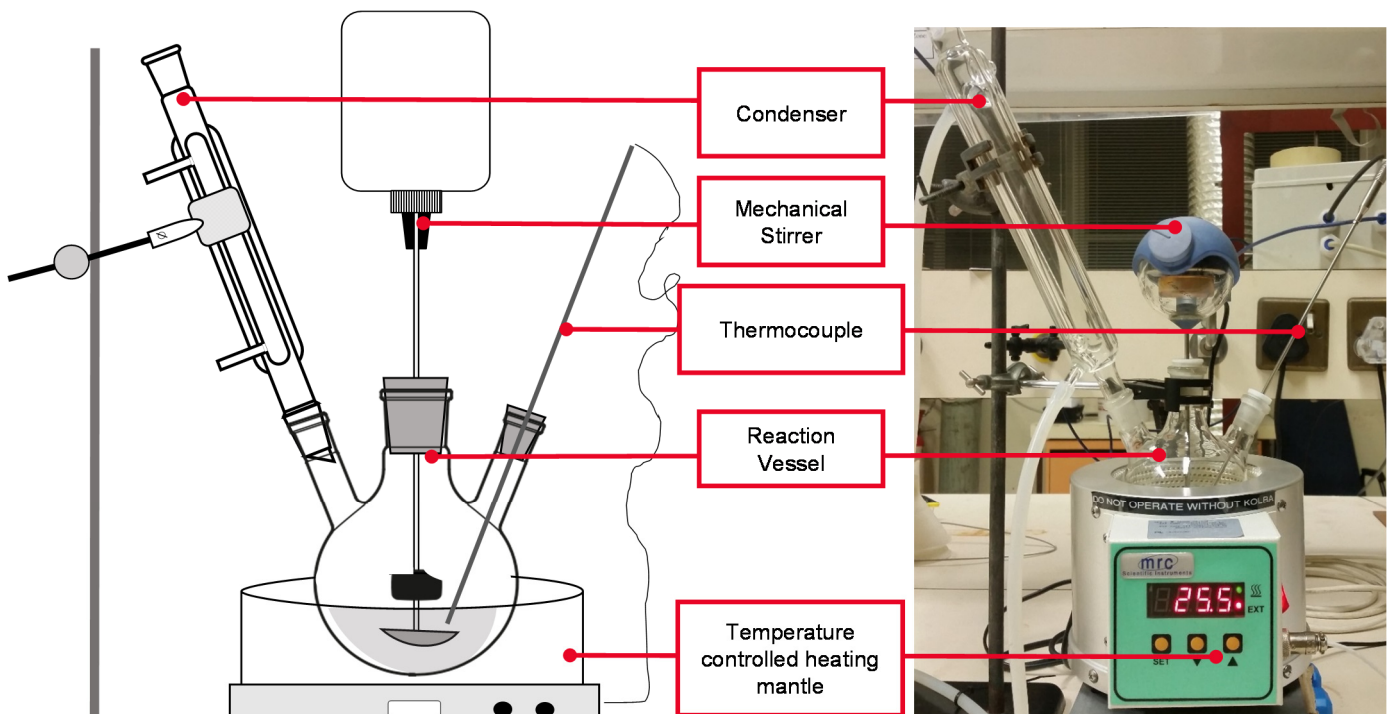


Figure 2.13: Experimental setup for metathesis reactions

Photograph 1.

2.3.3 Experimental design

The purpose of these metathesis experiments is to obtain data that will elucidate the reaction kinetics for the synthesised precatalysts.

A traditional empirical study was followed, and the varied parameters were the molar ratio of 1-octene to precatalyst and the temperature. Similar to the research conducted in literature [19,20,24,50,58-59], the temperature was varied between 40 and 100 °C and the precatalyst load was varied between a ratio of 5 000 and 14 000. The upper limit of 40 °C was chosen due to the low likelihood of formation of products under this temperature [58-59] and the upper limit was chosen based on the optimum formation of the primary metathesis product [20] and the temperature sensitivity of chelating pyridinyl alcoholato ruthenium complexes [19,20,24]. The precatalyst load was kept constant in the middle of the desired range first. Once the precatalysts' best operating temperature ranges were determined, a communal optimal temperature was selected at which the varied precatalyst load experiments were conducted. Table 2.8 provides an overall summary of this experimental design.

Table 2.8: Experimental design

Temperature (°C)	Catalyst Loadings (C₈/Ru)				
40	-	-	10 000	-	-
50	-	-	10 000	-	-
60	-	-	10 000	-	-
70	5 000	7 000	10 000	12 000	14 000
80	-	-	10 000	-	-
90	-	-	10 000	-	-
100	-	-	10 000	-	-

2.3.4 Analytical methodology

2.3.4.1 Gas chromatography analysis

2.3.4.1.1 Equipment

The analysis method used was based on the method used by various authors in literature [19,20,24,50,58-59], however, the choice of solvent and dilution methods were modified to suit the constraints of the available equipment.

Reaction samples were analysed with a Thermo Scientific Trace Ultra GC equipped with an autosampler, a ZB-5 capillary column (30m x 0.32 m x mm x 0.25 µF.T.), a programmable temperature vaporiser (PTV) and a Flame Ionisation Detector (FID).The GC oven settings were as follows:

Inlet temperature:	50 °C
He carrier gas flow rate:	1.5 mL·min ⁻¹
Injection volume:	1.0 µL
Split ratio:	30:1
Oven programming:	50 °C hold for 1 min, ramp to 180°C at 15°C·min ⁻¹ . Hold at 180 °C for 1 min.
Detector (FID) temperature:	270 °C
H ₂ flow rate:	40 mL·min ⁻¹ at RT
Air flow rate:	300 mL·min ⁻¹ at RT

2.3.4.1.2 Species identification and product distribution

Species were identified by assuming that the alkanes of the same carbon number would elute at generally the same retention time as their corresponding alkenes [60, 61]. The rationale behind this assumption was based on the larger availability of GC grade alkanes compared to that of the alkenes-this was also tested experimentally by comparing decene to decane's elution time on the equipment. The chromatograms were compared and verified against those provided in literature [19] that employed the same method. A typical chromatogram of these species is provided in Figure 2.14. Additionally, the species were quantified using nonane as an external standard which suits the prerequisites for a standard well due to its similar functional group, boiling point range and low likelihood of being present in the sample itself [61].

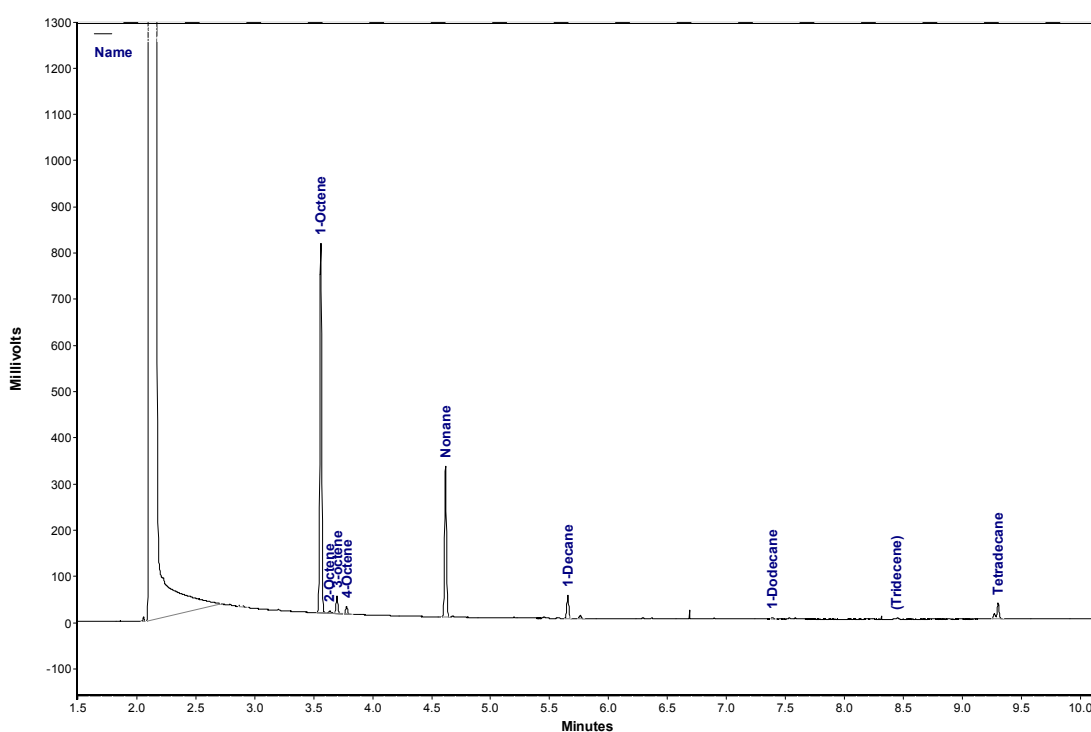


Figure 2.14: Typical chromatogram

2.3.4.1.3 Calibration

Samples were diluted for analysis by adding 100 µL of the 4-mL diluted sample mixture to 1.5 mL dichloromethane in GC vials.

The volume (V) of a given component (i) was determined by using Equation 2.6.

$$V_i = V_{Nonane} \times \left(\frac{A_i}{A_{Nonane}} \right) \times \left(\frac{1}{RF} \right) \quad (2.6)$$

where:

V_i = Component volume in the GC vial

V_{Nonane} = External Standard volume (0.1mL) in the GC vial

A_i = Component Area from the GC Chromatograph

A_{Nonane} = External Standard Area obtained from the GC Chromatograph

RF = GC Response factor

The GC response factor was obtained by developing a calibration curve shown in Figure 2.15. The volume ratio of 1-octene to nonane (which was kept constant at 0.1 mL) was plotted against the area ratio of these components obtained from the GC chromatograms.

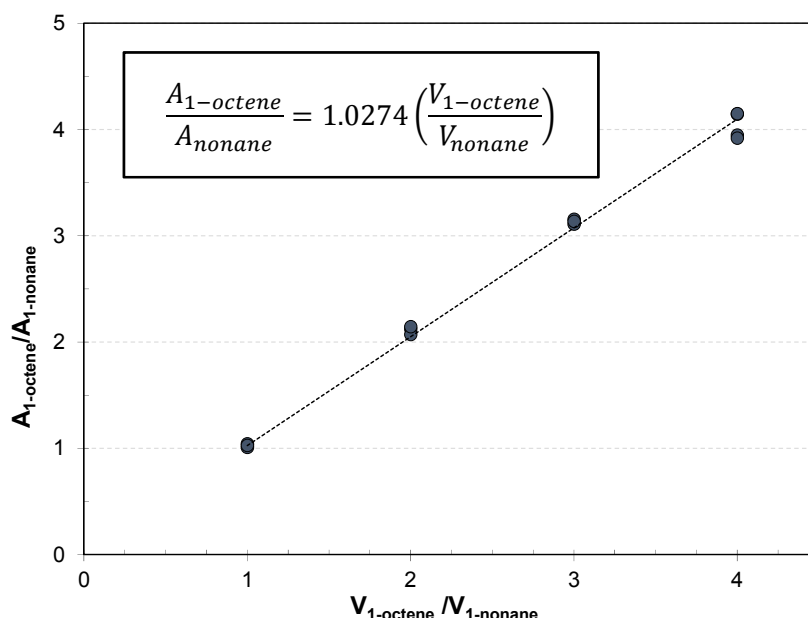


Figure 2.15: GC calibration curve for 1-octene [●experimental; ⋯trendline]

The mole percentages (n_i) were calculated consecutively with Equation 2.7 as follows:

$$n_i = \frac{V_i \times \rho_i}{MW_i} \cdot 100 \quad (2.7)$$

where:

V_i = Component volume in the GC vial

n_i = Moles of component i

ρ_i = Component i density

MW_i = Component i molar weight

A GC response factor of 1 was assumed for the analyses of all the components present in the samples. This assumption can be justified by literature where the same procedure is followed due to the similar response on FID's that alkenes display [24].

2.3.4.1.4 Measurement precision

In an ideal world, measurement instruments will always give an accurate representation of the reality, unfortunately, that is not the case. The best that scientists can do is to provide a measure of deviation from reality and the degree of precision of the measurements. To determine the measurement precision, the relative standard deviation or otherwise known as the coefficient of variation was determined for each set of calibration points. The sample coefficient of variation is a method for assessing the extent of variance relative to the mean [62].

The coefficient of variation (CV) was determined using equation

$$CV = 100 * \frac{s}{\bar{x}} \quad (2.6)$$

where:

- s = Standard deviation between values
- \bar{x} = average or mean of values

The results obtained from applying Equation 2.6 to the calibration data is presented Table 2.9:

Table 2.9: Statistical parameters from calibration data

Calibration point	Standard deviation (σ)	Mean (\bar{x})	CV (%)
1	0.02	1.03	1.67
2	0.04	2.11	1.76
3	0.02	3.13	0.74
4	0.12	4.04	3.07

The coefficient of variance of all four the data points lie between 3 and 0% and therefore the conclusion is made that the measurement instrument is sufficiently precise, and the calibration is satisfactory for this study.

2.4 Precatalyst performance results

In this section, the results obtained from each of the precatalysts considered in this study are presented. Namely the **GCYC** precatalyst and the **GMPP** precatalyst. Each of the precatalysts' performances is evaluated based on the influences that temperature and precatalyst load exert on the catalytic performance parameters related to activity and selectivity mentioned in section 2.2.3.

Repeatability

The experimental error in this investigation was determined by conducting a repeatability metathesis reaction experiment with the **GCYC** catalyst at 70 °C and with a molar C₈/Ru ratio of 12 000. A number of points in the time lapse of the reaction were selected as the sampling points for the repeat runs. Descriptive statistical concepts have been applied to these data points to determine the experimental error, a summary of which is available in Table 2.10.

Table 2.10: Statistical parameters of repeatability experiments

	Mean (\bar{X})	Lower limit	Upper limit	Standard deviation (σ)	Standard Error of \bar{X}	95% Confidence Interval of \bar{X}
C ₈ (%)	46.15	41.36	51.25	2.23	0.56	2.37
PMP (%)	46.00	41.31	48.70	1.80	0.45	1.92
IMP (%)	0.17	0.00	0.63	0.17	0.04	0.18
SMP (%)	7.61	6.63	9.94	0.79	0.20	0.84

Based on the results in Table 2.10, the conclusion can be drawn that the maximum value of the experimental error (standard deviation) of 2% is acceptable. The conclusion is drawn with 95% confidence that the values will fall within a maximum interval of $\pm 2.4\%$ from the sample mean.

2.4.1 1-Octene metathesis with GCYC precatalyst

The results of the **GCYC** precatalyst are presented and this section and it has displayed some interesting trends and phenomena. Although this precatalyst has been presented before in literature [18-20], little was available on its performance over a range of different conditions and its kinetic behaviour. This section will, therefore, present the results obtained in this study in the following sections.

2.4.1.1 Temperature effects

The effect of temperature on the performance of the **GCYC** precatalyst was investigated by varying temperature between 40 and 100 °C and keeping the precatalyst load constant at a 1-octene/Ru ratio of 10 000. Reaction samples were taken throughout the reaction and analysed using GC/FID as discussed in Section 2.3.4. The reaction was carried out at atmospheric conditions and no solvents were used. The results are summarised in Table 2.11.

Table 2.11: Catalytic performance of GCYC precatalyst at different temperatures towards 1-octene metathesis. (No solvent, C₈/Ru = 10 000).

Temperature (°C)	C ₈ (%)	PMP (%)	IMP (%)	SMP (%)	S (%)	TON (-)	C ₈ -X (%)	Y- PMP (%)
40	93.1	4.61	0.00	0.00	4.51	461	6.94	4.61
50	71.1	23.6	0.43	1.26	19.9	2356	28.9	23.6
60	55.5	42.1	0.34	2.12	30.1	4207	44.5	42.1
70	26.5	66.3	0.35	15.3	41.6	6631	73.5	66.3
80	19.9	58.7	0.00	21.4	42.8	5873	80.1	58.7
90	74.4	18.3	7.08	0.22	16.4	1834	25.7	18.3
100	89.1	3.77	6.90	0.23	3.87	377	10.9	3.77

Table 2.11 shows the product distribution (C₈, PMP, IMP, and SMP) obtained after 420 mins of metathesis reaction as percentages. The table also displays the selectivity, TON, conversion of 1-octene (C₈-X) and the yield towards primary metathesis products (Y-PMP). The results of Table 2.11 are expanded to display the product distribution as a function of time for the **GCYC** precatalyst in Figure 2.16 and Figure 2.17.

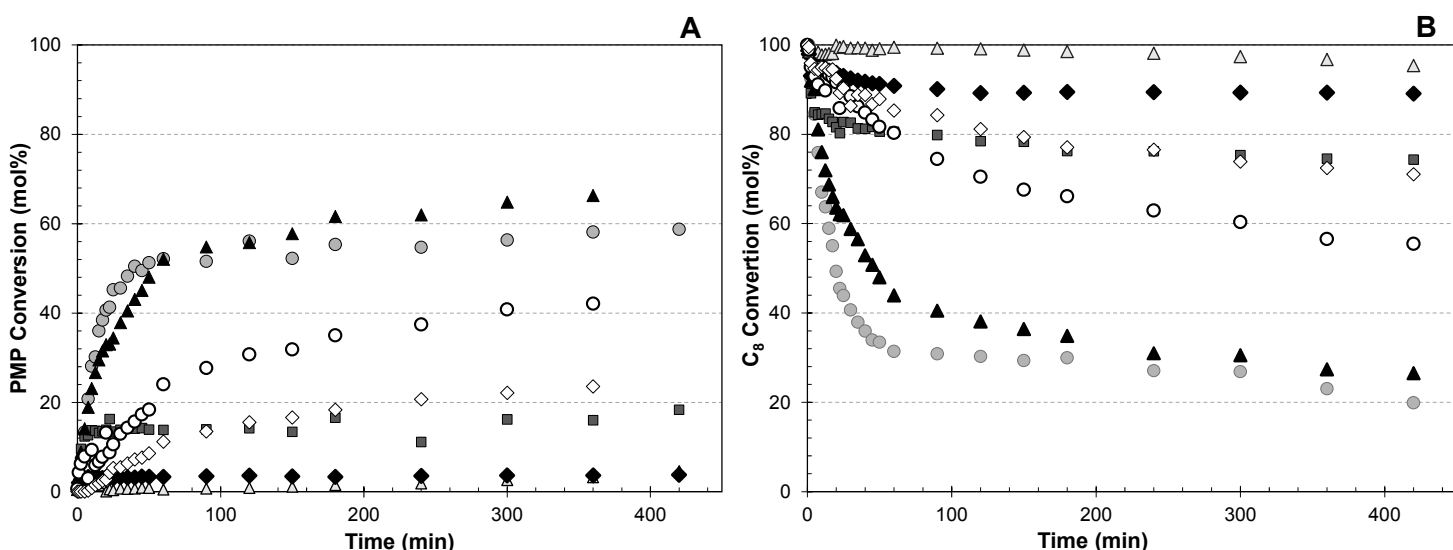


Figure 2.16: Effect of temperature on catalytic performance on (A) PMP formation, (B) 1-octene consumption, during 1-octene metathesis with GCYC precatalyst for 420 min without a solvent [△40°C ◇50°C ○60°C ▲70°C ●80°C ■90°C ◆100°C].

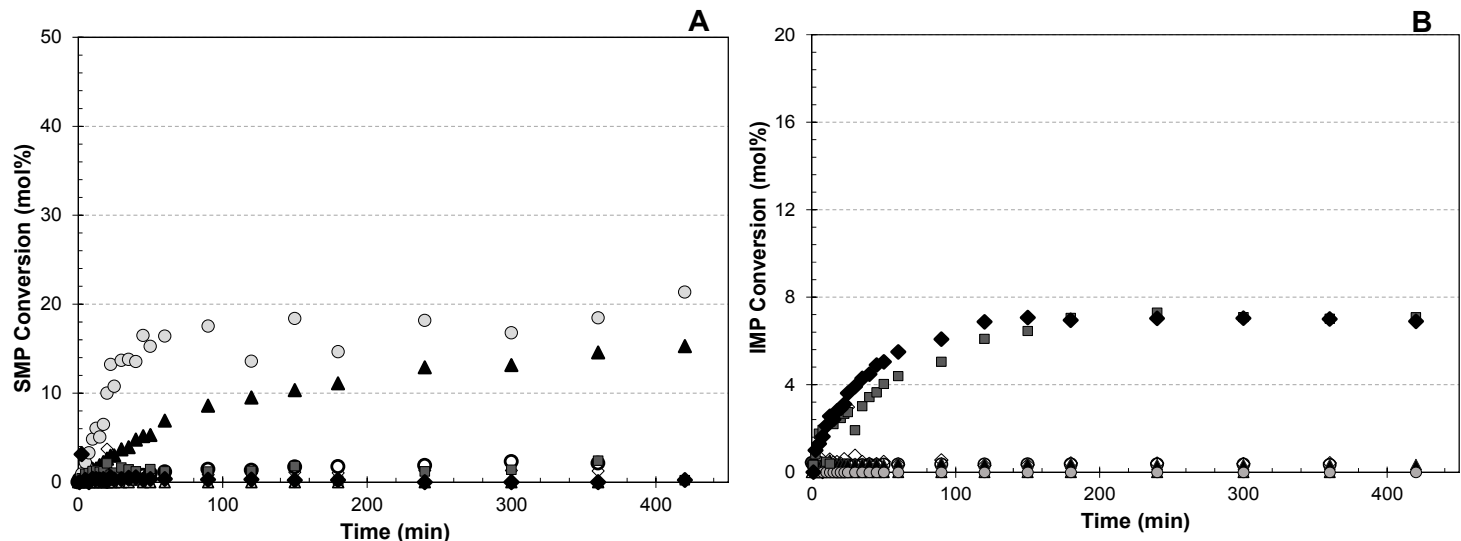


Figure 2.17 : Effect of temperature on catalytic performance on (A) IMP formation and (B) SP formation during 1-octene metathesis with GCYC precatalyst for 420 min without a solvent [Δ 40°C \diamond 50°C \circ 60°C \blacktriangle 70°C \bullet 80°C ■90°C◆100°C].

The results summarised in Table 2.11, Figure 2.16 and Figure 2.17 provide a clear picture of the effects of temperature on the catalytic performance of the **GCYC** precatalyst. It is evident that the primary metathesis product (PMP) formation is minuscule at 40°C (<5%). However, as temperature increases from 50 to 70°C, the primary metathesis product formation increases gradually (from ~24%-66%) and peaks around 70°C.

The side-product formation remains small at the lower temperatures as well. At higher temperatures, the primary metathesis product formation declines from ~58% down to below 4% at 100°C. Around the peak temperatures (70-80°C) the side-product formation increases as well but remains below 22%.

At temperatures higher than 80°C, the SMP and PMP formation becomes almost insignificant and a sudden but small increase in isomerisation metathesis products is observed (~7%). The observations indicate that this specific precatalyst is very selective towards the primary metathesis product since low amounts of SMP and IM products are formed throughout all the temperatures in the range. However, these products do occur, albeit on a small scale, and this indicates that two competing mechanisms are present, namely the isomerisation mechanism and the metathesis mechanism.

This phenomenon has been observed in the past [19-20,24,30] and the isomerisation can most likely be attributed to the formation of ruthenium hydride species [31]. Literature has suggested that the existence of these species is explained by the occurrence of thermal precatalyst degradation, thus promoting the formation of isomers via an alkyl mechanism [63]. The

explanation, however, is at best based on commercial catalysts, and suspicions of catalyst decomposition for the **GCYC** catalyst will have to be confirmed in future NMR studies. Nonetheless, the possible presence of these ruthenium hydride species explains the formation of side-products which are formed as a result of the cross-metathesis reaction between 1-octene and IMPs. More specifically, it explains why IMP formation only occurs between (70 and 80 °C). The isomerisation and metathesis reactions, therefore, occur in parallel.

The precatalyst displays latent behaviour, which can be substantiated by the low production of PMPs at 40 °C. Other studies could obtain more significant product formation for Grubbs 2nd generation precatalysts at temperatures below 40 °C, (>19% PMP conversion) as reported by Van der Gryp *et al.* for the **HG2** precatalyst.

The activity of the **GCYC** precatalyst was reported by Jordaan [19] to increase beyond 35 °C until a peak was reached at 70 °C after which Jordaan noted a sharp decrease in catalytic activity. The same activity trends were observed in this study. Jordaan attributed the sharp decrease in activity to thermal precatalyst deactivation.

Taking a broader look at the effect of temperature on product formation, by comparing the yield, conversion and the selectivity obtained from each reaction temperature the following figure, Figure 2.18 is obtained:

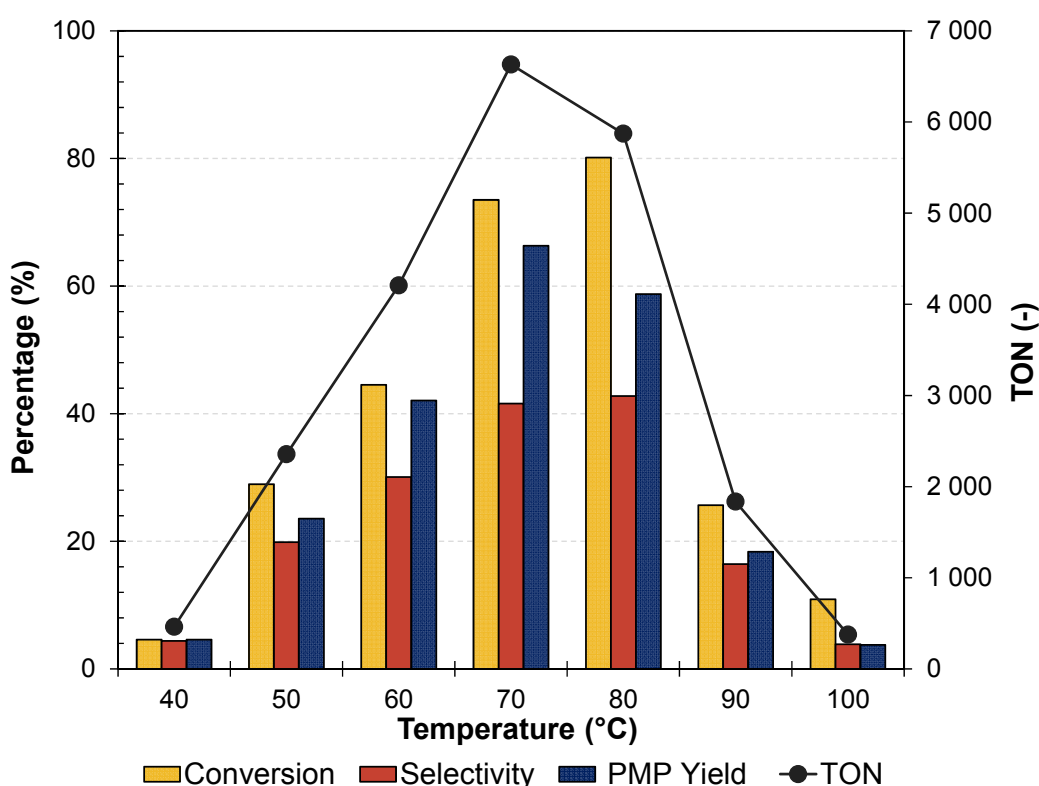


Figure 2.18: Effect of temperature on conversion, selectivity, PMP yield, and turnover number (TON) for GCYC precatalyst 1-octene metathesis reactions at C₈/Ru = 10 000.

Figure 2.18 displays the clear trend that is observed in Figure 2.16 and Figure 2.17 and Table 2.11. As the temperature increases, the conversion, yield and selectivity also increase gradually, peaking at its optimum point (with respect to all the parameters plotted) at 70° C. The typical latency of the precatalyst is also displayed well when comparing the optimal temperature of the **GCYC** precatalyst to the peak temperature of the **HG2** precatalyst (50 °C) [24].

Figure 2.18 also provides the effect of temperature on activity, i.e. the turnover number. The turnover numbers for the **GCYC** precatalyst confirm the optimal operating point as 70°C as is clearly presented by the black line in Figure 2.18. The catalytic activity is temperature dependent and increases as the temperature increases until the maximum TON (6631) is reached, after which it declines. This proves that the catalytic activity gradually diminishes at higher temperatures and substantiates the occurrence of possible precatalyst deactivation. The trends observed with the **GCYC** precatalyst are consistent with second-generation Grubbs-type precatalyst's behaviour as discussed in Section 2.2.3.2.

2.4.1.2 Catalyst load effects

Once the optimum reaction temperature with respect to low isomerisation and high activity and selectivity was obtained, the effect of the precatalyst load was tested by keeping the reaction temperature constant at 70° C. The precatalyst load (C_8/Ru) was varied between 5 000 and 14 000. The results obtained are presented in the figures and tables that follow:

Table 2.12: Effect of precatalyst load on catalytic performance of the GCYC precatalyst at 70°C and $C_8/Ru = 12\,000$ without a solvent

C_8/Ru	C_8 (%)	PMP (%)	IMP (%)	SMP (%)	S (%)	TON (-)	C_8-X (%)	Y- PMP (%)
5000	22.5	64.9	0.00	10.9	42.6	3244	77.5	64.9
7000	30.4	62.5	0.00	5.14	40.2	4377	69.4	62.5
10000	26.5	66.3	0.35	5.15	41.6	6631	73.5	66.3
12000	41.4	52.1	0.00	3.67	35.8	6251	58.6	52.1
14000	46.2	47.9	0.00	2.94	33.8	6706	53.8	47.9

Similar to the case for temperature, Table 2.12, shows the product distribution (C_8 , PMP, IMP, and SMP) obtained after 420 mins of metathesis reaction as percentages. The table also displays the selectivity, TON, conversion of 1-octene (C_8-X) and the yield towards primary metathesis products (Y-PMP).

The results of Table 2.12 are expanded to display the change of the product distribution as time progresses for the **GCYC** precatalyst in Figure 2.19.

The trends in Figure 2.19 clearly indicate the effect of the precatalyst concentration on the precatalyst performance. The most notable observation that can be made is the fact that the isomerisation product formation is completely unaffected by the precatalyst concentration, thus confirming the strong correlation between the temperature and isomerisation product formation. The precatalyst concentration does, however, influence the number of primary metathesis products and secondary metathesis products that form as pointed out by Loock [22]. Figure 2.20 indicates a slight increase in PMP formation from 47% at a C₈/Ru ratio of 14 000 to ~65% at a C₈/Ru ratio of 5 000. The increase in product formation with an increase in precatalyst load can be explained by the increased amount of precatalyst present, albeit a small change of ~18% over the whole range. Secondary product formation also remains below 10% throughout the range of precatalyst load conditions.

The question is whether the precatalyst load affects the conversion, yield and selectivity and if so, to what extent? Figure 2.20 provides a presentation of these effects.

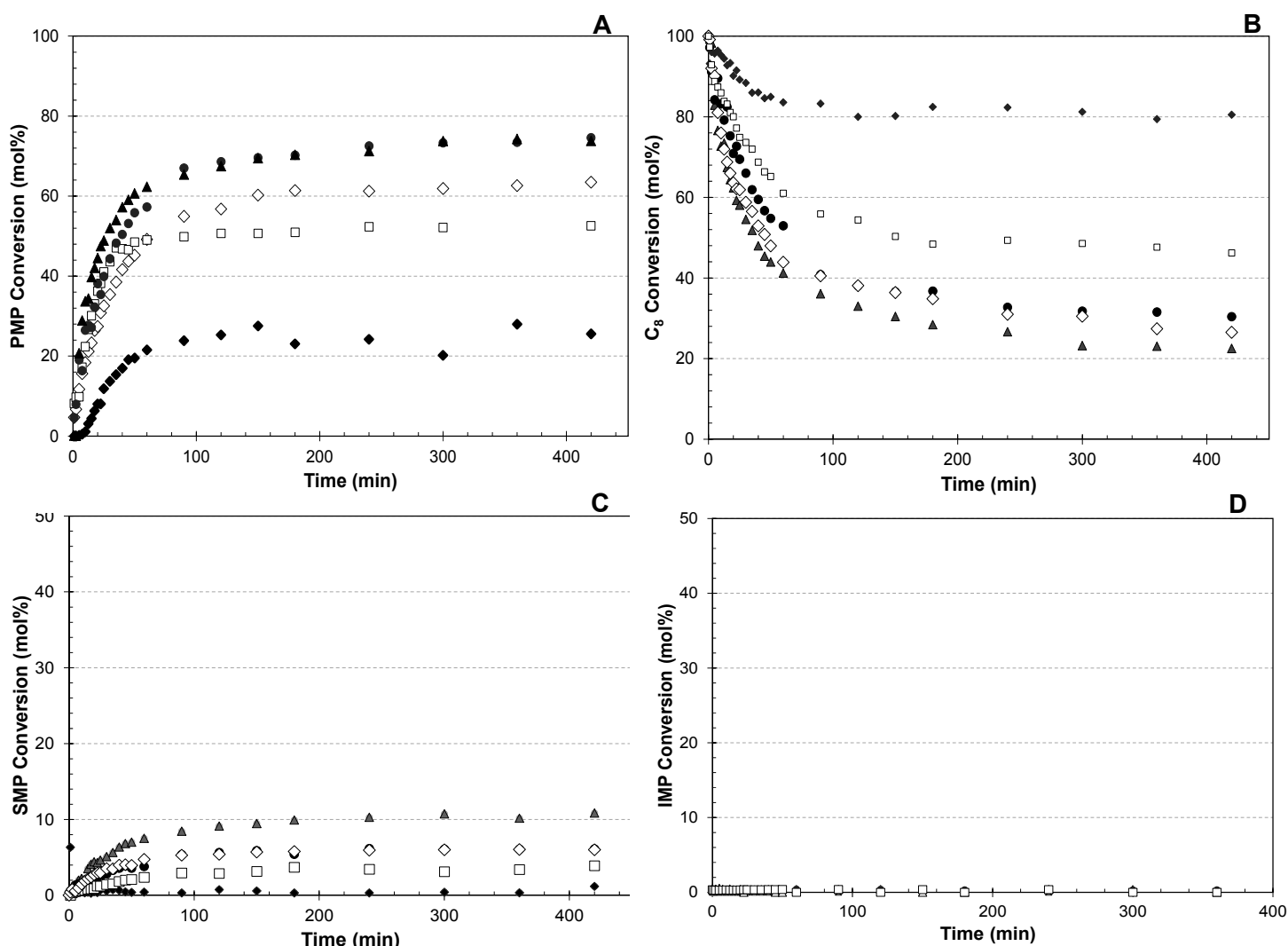


Figure 2.19: Effect of precatalyst load on catalytic performance on (A) PP formation, (B) 1-octene Consumption, (C) IMP formation and (D) SMP formation during 1-octene metathesis with GMPP precatalyst for 420 min without a solvent [▲5000 ●7000 ◇10000 ◆12000 □ 14000].

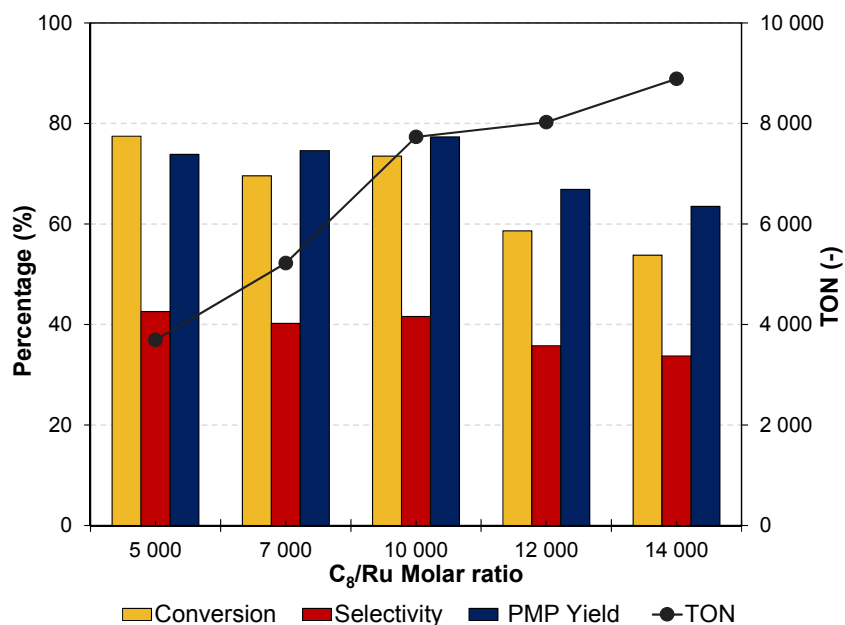


Figure 2.20: Effect of precatalyst load on conversion, selectivity, yield and turnover number (TON) during 1-octene metathesis at 70° C.

At the lower precatalyst loads, the effect on selectivity is not significant over the whole range and the same applies to conversion and yield for the lower precatalyst loads (i.e. higher amount of added precatalyst), but from 12000 to 14000 a slight decline in selectivity and conversion is observed. A possible explanation could be the smaller amount of precatalyst present in the system, leading to an overall smaller amount of product converted.

In Figure 2.20 the effect of the precatalyst load on the activity (TON) is plotted and shown to increase as the amount of precatalyst decreases. This trend shows that the precatalyst is more efficient at higher precatalyst loads. At first, the trend of the TON is contradicting to that of the conversion, selectivity and yield since the selectivity and conversion slightly decline at higher precatalyst loads, but the turnover numbers increase at higher precatalyst loads.

2.4.2 1-Octene metathesis with GMPP precatalyst

In the following section, the results for the **GMPP** precatalyst are presented and discussed. Compared to the previous precatalyst the results of the **GMPP** precatalyst are quite interesting and very intriguing phenomena were found to be present. To the author's knowledge, this specific precatalyst has not been reported in the literature yet and the characteristics that it displays are remarkable.

2.4.2.1 Temperature effects

The effect of temperature on the performance of the **GMPP** precatalyst was investigated by varying temperature between 40 and 100 °C and keeping the precatalyst load constant at a 1-octene/Ru ratio of 10 000. Reaction samples were taken throughout the reaction and analysed using GC/FID as discussed in Section 2.3.2. The reaction was carried out at atmospheric conditions and no solvents were used. The results are summarised in Table 2.13 and Figure 2.21.

Table 2.13: Summary of the effects of temperature on GMPP catalytic performance for 1-octene metathesis reaction at C₈/Ru = 10000

Temperature (°C)	C ₈ (%)	PMP (%)	IMP (%)	SMP (%)	S (%)	TON (-)	C ₈ -X (%)	Y-PMP (%)
40	90.5	6.41	0.00	0.42	6.19	641	9.53	6.41
50	83.7	12.5	0.00	0.52	11.5	704	16.3	12.5
60	94.2	5.07	0.00	0.42	4.85	874	5.80	5.07
70	42.1	53.7	0.00	1.95	35.9	5373	57.9	53.7
80	39.6	53.1	0.01	6.96	36.3	5306	60.4	53.1
90	40.7	58.9	0.00	6.97	37.2	5888	59.4	58.9
100	85.8	7.63	0.05	2.23	7.50	763	14.2	7.63

Table 2.13 shows the product distribution (C₈, PMP, IMP, and SMP) obtained after 420 mins of metathesis reaction as percentages. The table also displays the selectivity, TON, Conversion of 1-octene (C₈-X) and the yield towards primary metathesis products (Y-PMP).

The results of Table 2.13 are expanded to display the change of the product distribution as time progresses for the **GMPP** precatalyst in Figure 2.21 and Figure 2.22.

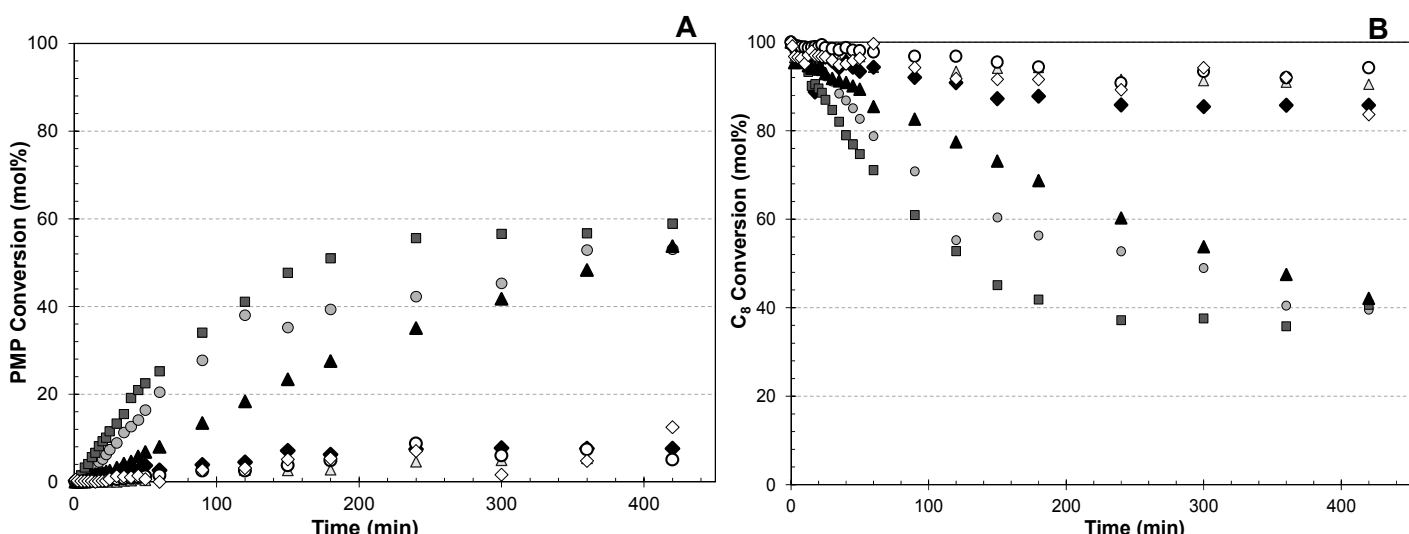


Figure 2.21: Influence of reaction temperature on (A) PMP formation, (B) 1-octene consumption during 1-octene metathesis with GMPP precatalyst for 420 min without a solvent. [△40°C ◇50°C ○60°C ▲70°C ●80°C ■90°C ◆100°C]

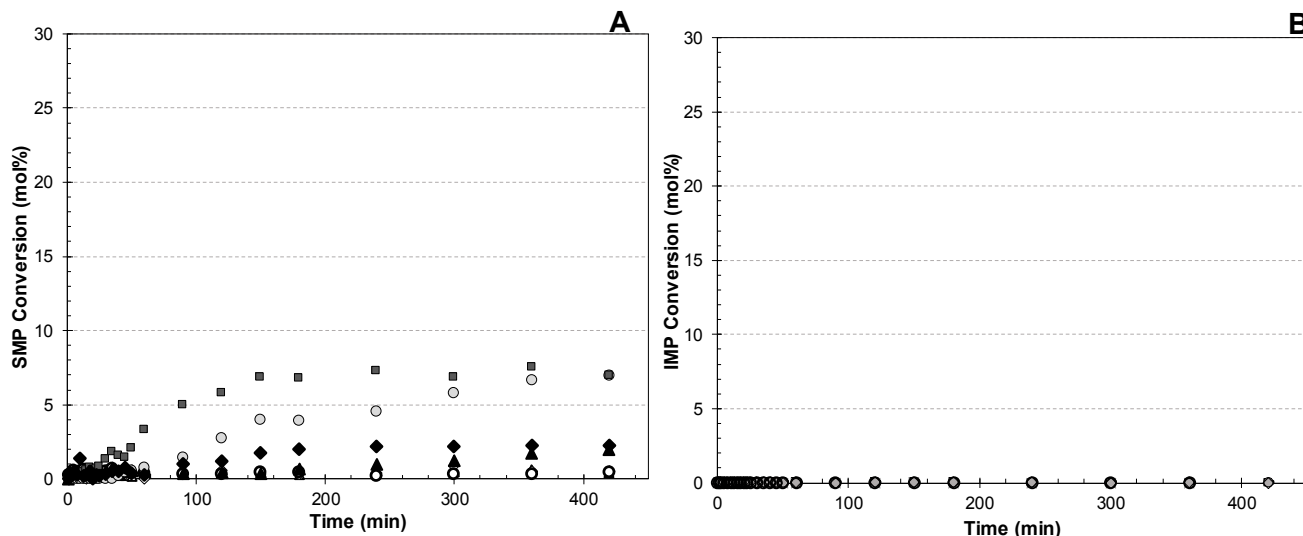


Figure 2.22 : Influence of reaction temperature on (A) SMP formation and (B) IMP formation during 1-octene metathesis with GMPP precatalyst for 420 min without a solvent. [Δ 40°C \diamond 50°C \circ 60°C \blacktriangle 70°C \bullet 80°C \blacksquare 90°C \blacklozenge 100°C]

The results in Figure 2.21, Figure 2.22 and Table 2.13 display the typical behaviour that can be expected from Latent thermo-switchable precatalysts [48]. This behaviour can be clearly seen in the small amount of product formation at temperatures below 70 °C. Typically in terms of primary metathesis products the highest number of products formed below 70 °C was ~12% (at 50 °C). The same trend was visible across all the other product types. Secondary metathesis products remained below 11% and virtually no isomerisation metathesis products were detected. Between 70°C and 90 °C however, products suddenly start to form and at values considerably higher than compared to the lower temperatures (typically 53-58%).

Another observation that can be made is the small difference between the product formation at temperatures 70, 80 and 90 ° C. The side-product formation at these conditions increase slightly but remain below 10%, all the while the Isomerisation metathesis products (IMPs) remain insignificant.

Once the temperature increases to 100 °C the reaction yields a very low amount of product again ~8%. The low product formation at these high temperatures can be explained by the precatalyst's degradation. The precatalyst does not lose all activity at these conditions since a small amount of side-product formation is still detected. In general, the **GMPP** precatalyst has displayed very selective behaviour due to the low percentages of side and isomerisation metathesis products formed, thus the competition between the isomerisation and the metathesis mechanism is not significant. Compared to commercial precatalyst this precatalyst only starts to react at moderate to high temperatures, combined with its high selectivity towards primary metathesis products it could prove to be advantageous in industry.

At 90 °C however, the highest amount of Isomerisation metathesis products is observed. Double bond migration typically takes place when ruthenium hydride species are present to catalyse the reaction. The ruthenium hydride species is known to be a result of precatalyst degradation as discussed in Section 2.2.3, thus the results prove that the precatalyst is starting to degrade at 90 °C. Based on this the best reaction temperature for conducting the precatalyst concentration tests was chosen as 70°C. The rationale behind the choice of temperature was attributed to maintaining consistency throughout the comparative tests between the precatalysts.

A similar bar graph to the **GCYC** precatalyst was constructed for the **GMPP** precatalyst to compare the performance of the precatalyst over the whole temperature range. The results are presented in Figure 2.23:

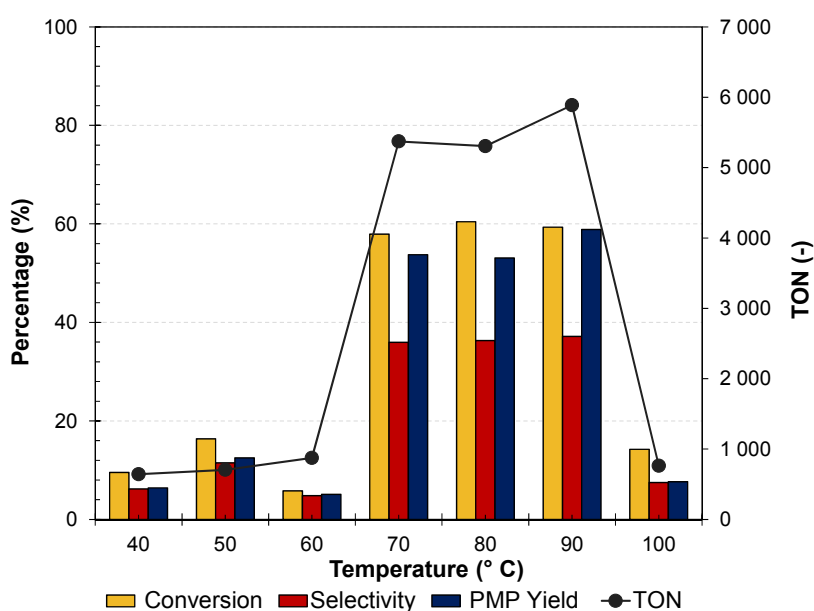


Figure 2.23: Effect of temperature on conversion, selectivity, and PMP yield with GMPP precatalyst 1-octene metathesis reactions at C₈/Ru = 10 000 in the absence of a solvent

The **GMPP** precatalyst's latency is clearly shown in Figure 2.23 where the conversion, yield and selectivity obtained after 420 mins of reaction time is plotted across the temperature range. Little conversion occurs at temperatures below 70°C and above 90°C.

Interestingly, in the range where the precatalyst is indeed active (70°-90°C), the conversion, yield and selectivity do not differ much between temperatures. Beyond 90°C precatalyst degradation is clearly visible with the loss of conversion, yield and selectivity at 100°C.

The next aspect to consider would be the activity of the precatalyst and how the activity compares over a range of temperatures. According to the trend displayed in Figure 2.23 the precatalyst's activity follows a similar trend. Although the activity increases slightly at the lower temperatures (40-60°C) the TON's remain below 1000.

When the temperature is increased to 70 ° C and above the catalytic activity suddenly increases to above 5000. There is little difference between the TON's achieved between 70° and 90°C. At 100° C, the activity diminishes again almost instantly back to TON's below 1000. Thus, the **GMPP** precatalyst has displayed typical latent behaviour, explaining why the activity only starts to take place beyond 70°C.

Under similar conditions, Dinger and Mol [27] reported a decline in TON's beyond the 100° C mark for 1-octene metathesis in the presence of the classical Grubbs 2nd generation precatalyst. They attributed the decline in activity to the decomposition of the precatalyst. Their investigation goes further to describe the activity of a more steric backbone analogue of the **G2** precatalyst. The result is a precatalyst that is less sensitive to changes in temperature. Their study couldn't provide concise explanations from a thermal point of view for their divergent results.

2.4.2.2 Catalyst load effects

Since the optimum reaction temperature with respect to low degradation, high activity and selectivity was obtained the effect of the precatalyst load was tested by keeping the reaction temperature constant at 70° C. The precatalyst load (C_8/Ru) was varied between 5 000 and 14 000. The results obtained are summarised in Table 2.14 and Figure 2.24.

Table 2.14: Performance of 1-octene metathesis reactions with GMPP precatalyst at 70°C without a solvent.

C_8/Ru	C_8 (%)	PMP (%)	IMP (%)	SMP (%)	S (%)	TON (-)	C_8-X (%)	Y-PMP (%)
5000	23.3	71.1	0.00	3.27	43.0	3556	76.8	71.1
7000	29.9	65.9	0.00	2.17	40.8	4616	70.1	65.9
10000	42.1	53.7	0.00	1.95	35.9	5373	57.9	53.7
12000	49.0	45.5	0.82	1.08	32.4	5464	51.0	45.5
14000	66.1	29.9	0.00	1.11	23.7	4181	33.9	23.0

Table 2.14 provides a summary of the product distribution (C_8 , PMP, IMP, and SMP) obtained after 420 mins of metathesis reaction as percentages. Table 2.14 also displays the selectivity, TON, Conversion of 1-octene (C_8-X) and the yield towards primary metathesis products (Y-PMP).

As can be seen from the table the effects of the precatalyst load are larger than in the case of the previous precatalyst. At the highest precatalyst concentration (i.e. the lowest precatalyst load) the PMP formation is 71 % the primary metathesis product formation then gradually decreases to 29.8% as the precatalyst load increases. Isomerisation almost doesn't take place at all with percentages below 1% which, when compared to the experimental error of 1.8% can be considered negligible.

Side-product formation is also very low and once compared to the experimental error the same conclusion that applies to isomerisation metathesis products can be reached for the side-products. The results presented in Table 2.14 are presented for visual reference in Figure 2.24 that displays the typical trends in the change of the product distribution over time observed with the **GMPP** precatalyst. Figure (A) through (D) presents a visual presentation of the effect of precatalyst load on the product distribution over time. The precatalyst load has a linear effect on the product formation, i.e. as the precatalyst load increases the product formation diminishes.

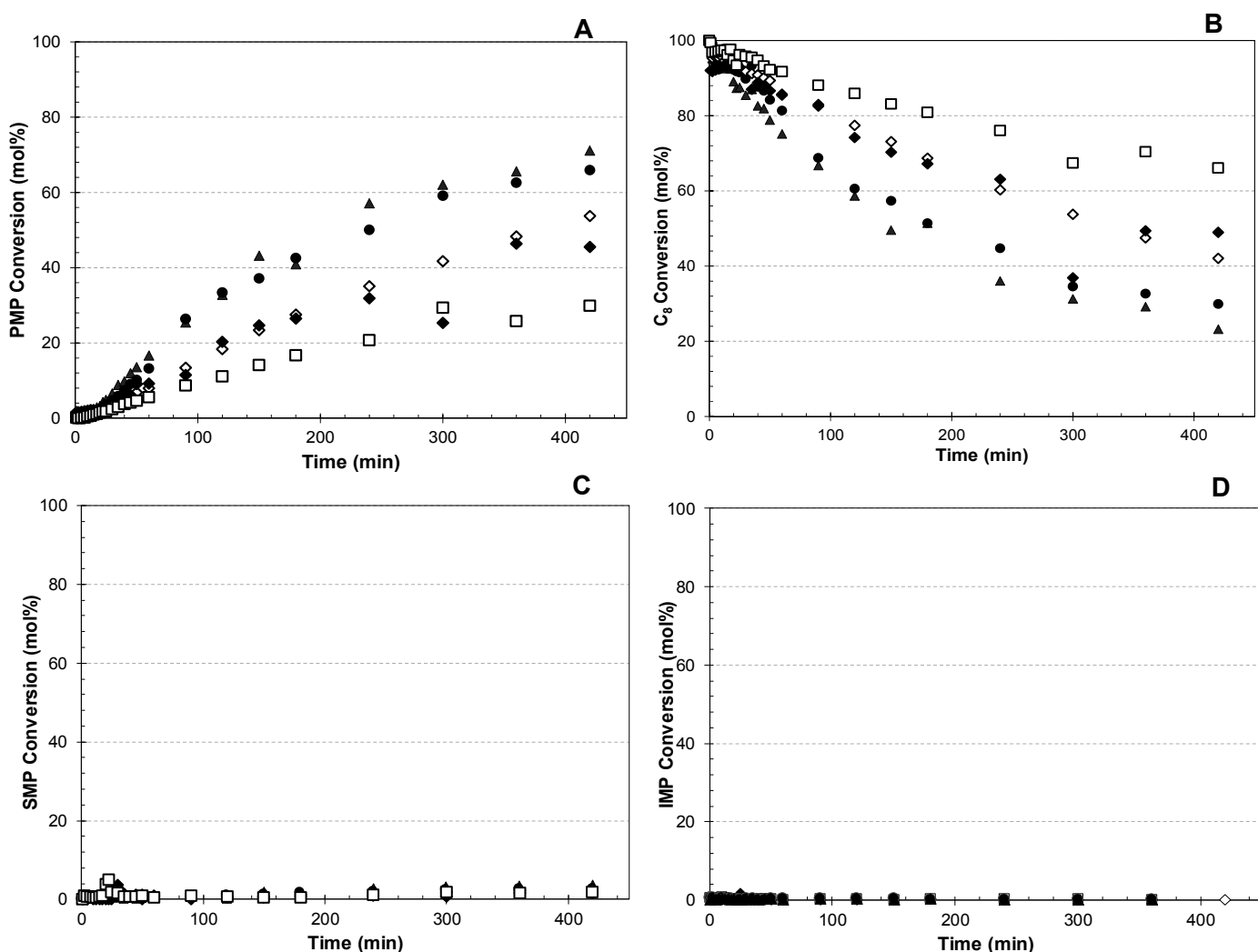


Figure 2.24: Influence of precatalyst load on (A) PMP formation, (B) 1-octene consumption, (C) SMP formation and (D) IMP formation during 1-octene metathesis with GMPP precatalyst for 420 min without a solvent [▲5000 ●7000 ◇10000 ◆12000 □14000]

The same trend but, in reverse, is observed for the 1-octene consumption in (B). Similarly, to the **GCYC** precatalyst, the precatalyst load has little to no effect on the formation of side- and isomerisation metathesis products, thus confirming that the temperature has a stronger effect on the formation of isomers, and consequently that larger amounts of isomerisation correlate to larger amounts of side-products formed due to cross-metathesis taking place. The next aspect to consider in the precatalyst's performance is the selectivity conversion and yield.

The results obtained with the **GMPP** precatalyst at 70 °C and varied precatalyst loadings are presented in Figure 2.25.

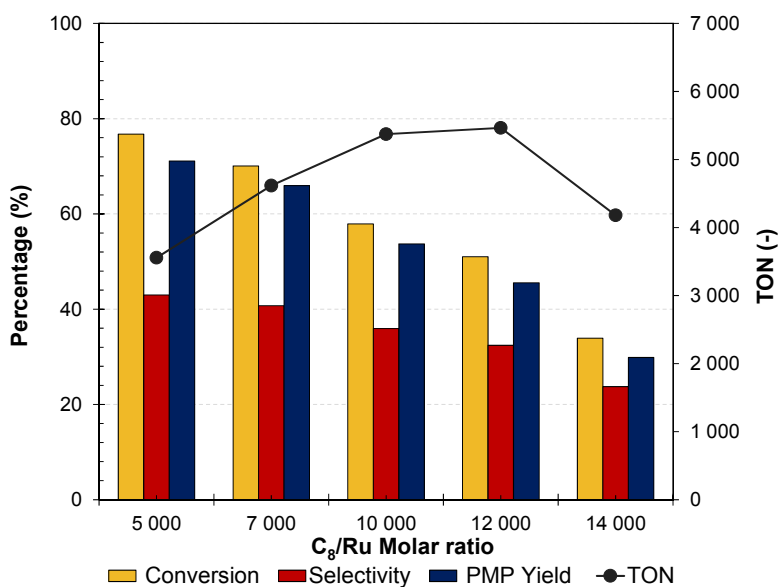


Figure 2.25: Effect of precatalyst load on conversion, selectivity, PMP yield and TON for 1-octene metathesis with GMPP precatalyst at 70°C

As can be seen in Figure 2.25 there is a clear linear decreasing trend in all three the parameters (conversion selectivity and yield). The precatalyst performs better at lower precatalyst loadings with selectivity above 40% and conversion and yield between 70 and 80%. Conversion, selectivity and yield gradually decrease to 23, 33 and 29 % respectively as the precatalyst load increases to 14 000. The trend can easily be explained in the fundamentals of basic chemistry.

Since the reaction was operated at an excess amount of substrate the assumption is made that there should not be any other limiting factors that affect the rate of product formation. In this case, the formation of products is directly dependent on the amount of precatalyst present in the mixture. More precatalyst would speed up the reaction and thus produce more products, up to the point where the substrate or other agents become the rate limiting. These agents can shift the equilibrium towards the right or the left depending on the scale of their presence and the mechanisms involved [63]. The next basis on which the precatalyst can be evaluated is the activity as measured by the Turnover number (TON). Figure 2.25 shows a linearly increasing trend in TON as the precatalyst load is increased. The TON obtained starts at approximately 3500:1 precatalyst loading and increases linearly towards 6000 up to 12000, after which the TONs slightly decrease back to 4100. It is evident that optimal operation is achieved at 12000, thus proving that optimal performance in terms of activity is favoured at medium to high precatalyst loadings (i.e.

less precatalyst). These results compare well with the results obtained by Van der Gryp *et al.* [24] that conducted their reactions at similar conditions with 2nd generation Grubbs precatalysts.

2.5 Catalyst comparison

In the following section, the aim is to draw a comparison between the **GCYC** and the **GMPP** precatalysts key performance results and discuss the differences, and phenomena observed compared to observations in literature. In order to make an easy comparison, Table 2.15 is drawn up to display the direct differences and similarities between the results from both precatalysts.

Table 2.15: precatalyst performance comparison

Catalyst	S (%)	TON	X (%)	Temperature
GCYC	41.6	6631	73.5	70°C
GMPP	35.9	5373	57.9	70°C
HG2 [24]	98.3	6648	64.5	50°C

At the same conditions the **GCYC** precatalyst outperforms the **GMPP** precatalyst, higher conversions are achieved, and the TONs prove the **GCYC** precatalyst to be the more efficient precatalyst. The steric bulk of the **GMPP** precatalyst could possibly be the reason as to why the conversion and activity of the **GMPP** precatalyst don't match up to the **GCYC** precatalyst. From literature, the **GCYC** precatalyst delivered a higher conversion of 91% and selectivity at 77% in the work by Jordaan at 60°C and C₈/Ru = 9000. The TONs that Jordaan [19] reported were also much higher at 10428. du Toit's work [20] on the same precatalyst reported an 80.6% conversion and a selectivity of 85.5% and a TON more comparable to the findings of this work at 7236. There is some discrepancy between the reports which could be attributed to the fact that both authors synthesised their own precatalysts. Which accounts for the discrepancy in the performance data with literature of the precatalysts in this work.

Overall the **GCYC** and **GMPP** precatalysts with respect to second generation commercial precatalysts Jordaan [19] reported a conversion of 87.9 and a selectivity of 82% from the **G2** precatalysts at similar conditions. du Toit [20] reported a higher conversion of 96.3% and 80.6 % selectivity for **G2**. In terms of the TON, the work of Jordaan reported a higher value than Jordaan. In comparison to the **G2** precatalyst, the **GCYC** and **GMPP** precatalysts do not perform well. Selectivity wise and in terms of conversion and TONs. Van der Gryp's work on **HG2** [24] at 80°C also yielded better results.

What should be mentioned, however, is the low values of isomerisation metathesis products that both the **GCYC** and **GMPP** precatalysts yielded in comparison to the Commercial precatalysts at low temperatures-alluding to their increased stability. By direct comparison, the author recommends the **GCYC** precatalyst for further application, but much information is still needed to make a sure-fire and informed recommendation.

2.6 Concluding remarks

The purpose of this chapter was to gather information and evaluate two different precatalysts based on their catalytic performance. Literature was consulted and some key phenomena that were mentioned that have a large effect on the performance of Grubbs-based precatalysts are temperature, precatalyst loading, the nature of the ligands and finally the precatalyst deactivation. The **GMPP** and **GCYC** precatalysts each have their own unique profile. The **GCYC** precatalyst proved to perform better (~15% higher conversion at the optimal temperature) than the **GMPP** precatalyst. The distinction between which precatalyst would be the best requires a comparison based on economics and kinetics. These will be treated in the chapters that follow.

2.7 References

- [1] K. Grela, Olefin Metathesis: Theory and Practice, 1st ed., Wiley, New Jersey, 2013.
- [2] T.M. Trnka, R.H. Grubbs, The development of $L_2X_2RU=CHR$ olefin metathesis catalysts: An organometallic success story, *Acc. Chem. Res.* 34 (2001) 18–29.
- [3] W.A. Vogt, D., Cornils, B., Herrman, Applied homogeneous catalysis with organometallic compounds - a comprehensive handbook in two volumes, Elsevier, 2000.
- [4] V. Schneider, P.K. Frolich, Mechanism of formation of aromatics from lower paraffins, *Ind. Eng. Chem.* 23 (1931) 1405–1410
- [5] A.M. Thayer, Making metathesis work, commercially available metathesis catalysts may help a powerful synthesis tool move into drug manufacturing, *Chem. Eng. News.* (2007) 1–8.
- [6] H.S. Eleuterio, Olefin metathesis: chance favours those minds that are best prepared, *J. Mol. Catal.* 65 (1991) 55–61.
- [7] A.M. Rouhi, Olefin metathesis: the early years, *Chem. Eng. News.* 80 (2002) 34–38.
- [8] R.L. Banks, G.C. Bailey, Mechanism of formation of aromatics from lower paraffins, *Ind. Eng. Chem. Prod. Res. Dev.* 3 (1964) 170–173.
- [9] Y. Chauvin, Olefin metathesis: The early days, *Angew. Chemie - Int. Ed.* 45 (2006) 3760–3765.
- [10] R.H. Grubbs, Olefin metathesis, *Tetrahedron.* 60 (2004) 7117–7140.
- [11] A.H. Hoveyda, A.R. Zhugralin, The remarkable metal-catalysed olefin metathesis reaction. *Nature.* 450 (2007) 243–251.
- [12] M.M. Kirk, Ruthenium Based Homogeneous Olefin Metathesis. University of the Free State, 2005.
- [13] J. Hagen, Industrial catalysis. A practical approach, Third, Wiley-VCH Verlag GmbH & Co, Weinheim, 2015.
- [14] P. Van Der Gryp, Separation of Grubbs-based catalysts with nanofiltration, PhD Thesis, North-West University, Potchefstroom, 2008.
- [15] R.H. Grubbs, Handbook of metathesis vol 1: catalyst development, Wiley-VCH Verlag GmbH & Co, 2003.
- [16] A. Furstner, Olefin metathesis and beyond, *Angew. Chemie - Int. Ed.* 39 (2000) 3013–3043.
- [17] A.K. Chatterjee, T.L. Choi, D.P. Sanders, R.H. Grubbs, A general model for selectivity in olefin cross metathesis, *J. Am. Chem. Soc.* 125 (2003) 11360–11370
- [18] M. Jordaan, Experimental and Theoretical Investigation of new Grubbs-type Catalysts for the metathesis of alkenes, PhD thesis, North-West University Potchefstroom, 2007.
- [19] M. Jordaan, H.C.M. Vosloo, Ruthenium catalyst with a chelating pyridinyl-alcoholato ligand for application in linear alkene metathesis, *Adv. Synth. Catal.* 349 (2007) 184–192.
- [20] J.I. Du Toit, M. Jordaan, C.A.A. Huijsmans, J.H.L. Jordaan, C.G.C.E. Van Sittert, H.C.M. Vosloo, Improved metathesis lifetime: chelating pyridinyl-alcoholato ligands in the second generation Grubbs precatalyst, *Molecules.* 19 (2014) 5522–5537.

-
- [21] Mtshatsheni Kgomotsong, Metathesis of alkenes using ruthenium carbene complexes, PhD Thesis, North-West University, 2005.
 - [22] M.M. Loock, The alkene metathesis reactivity of the PUK-Grubbs 2-precatalyst, PhD Thesis, North-West University, 2009.
 - [23] R. Spronk, F.H.M. Dekker, J.C. Mol, Metathesis of 1-alkenes in the liquid phase over a Re₂O₇/Al₂O₃ catalyst. II. Kinetics of deactivation, *Appl. Catal. A*, Gen. 83 (1992) 213–233.
 - [24] P. Van der Gryp, S. Marx, H.C.M. Vosloo, Journal of Molecular Catalysis A: Chemical Experimental, DFT and kinetic study of 1-octene metathesis with Hoveyda – Grubbs second generation precatalyst, "Journal Mol. Catal. A, Chem. 355 (2012) 85–95
 - [25] M. Ulman, R.H. Grubbs, Relative reaction rates of olefin substrates with ruthenium (II) carbene metathesis initiators, *Organometallics*. 17 (1998) 2484–2489.
 - [26] M.B. Dinger, J.C. Mol, High turnover numbers with ruthenium-based metathesis catalysts, *Adv. Synth. Catal.* 344 (2002) 671–677.
 - [27] M.B. Dinger, J.C. Mol, Degradation of the second-generation Grubbs metathesis catalyst with primary alcohols and oxygen –isomerization and hydrogenation activities of monocarbonyl complexes, *Eur. J. Inorg. Chem.* 2003 (2003) 2827–2833.
 - [28] F. Ding, S. Van Doorslaer, P. Cool, F. Verpoort, Olefin isomerization reactions catalyzed by ruthenium hydrides bearing Schiff base ligands, *Appl. Organomet. Chem.* 25 (2011) 601–607.
 - [29] H.H. Soon, A.G. Wenzel, T.T. Salguero, M.W. Day, R.H. Grubbs, Decomposition of ruthenium olefin metathesis catalysts, *J. Am. Chem. Soc.* 129 (2007) 7961–7968.
 - [30] S.E. Lehman, J.E. Schwendeman, P.M. O'Donnell, K.B. Wagener, Olefin isomerization promoted by olefin metathesis catalysts, *Inorganica Chim. Acta*. 345 (2003) 190–198.
 - [31] B. Schmidt, An olefin metathesis/double bond isomerization sequence catalysed by an in situ generated ruthenium hydride species, *Eur. J. Org. Chem.* (2003) 816–819.
 - [32] W. Buchowicz, J.C. Mol, Catalytic activity and selectivity of Ru(=CHPh) Cl₂(PCy₃)₂ in the metathesis of linear alkenes, *J. Mol. Catal. A Chem.* 148 (1999) 97–103. -1169(99)00145-4.
 - [33] M. Ajam, Metathesis and hydroformylation reactions in Ionic liquids, University of Johannesburg, 2005.
 - [34] B.J. Ireland, B.T. Dobigny, D.E. Fogg, Decomposition of a phosphine-free metathesis catalyst by amines and other bronsted bases: metallacyclobutane deprotonation as a major deactivation pathway, *ACS Catal.* 5 (2015) 4690–4698.
 - [35] J.A.M. Lummiss, W.L. McClellan, R. McDonald, D.E. Fogg, Donor-induced decomposition of the Grubbs catalysts: an intercepted intermediate, *Organometallics*. 33 (2014) 6738–6741.
 - [36] J.I. du Toit, P. van der Gryp, M.M. Loock, T.T. Tole, S. Marx, J.H.L. Jordaan, H.C.M. Vosloo, the Industrial viability of homogeneous olefin metathesis: Beneficiation of linear alpha olefins with the diphenyl-substituted pyridinyl alcoholato ruthenium carbene precatalyst, *Catal. Today.* (2016).
 - [37] M.M.D. Mahahle, Isomerisation of Alkenes using metal carbenes and related transitional metal complexes, Potchefstroom Universiteit vir Christelike Hoër onderwys, PhD Thesis, 2005.
 - [38] C. Samojlowicz, M. Bieniek, K. Grela, Ruthenium-based olefin metathesis catalysts bearing N-heterocyclic carbene ligands, *Chem. Rev.* 109 (2009) 3708–3742.

- [39] A. Stark, M. Ajam, M. Green, H.G. Raubenheimer, A. Ranwell, B. Ondruschka, Metathesis of 1-octene in ionic liquids and other solvents: Effects of substrate solubility, solvent polarity and impurities, *Adv. Synth. Catal.* 348 (2006) 1934–1941..
- [40] J. Henry, 6 Myths about Gas Mileage, CBS Moneywatch. (2009). <http://www.cbsnews.com/news/6-myths-about-gas-mileage/> (accessed January 1, 2016).
- [41] G.S. Forman, A.E. McConnell, R.P. Tooze, W.J. Van Rensburg, W.H. Meyer, M.M. Kirk, C.L. Dwyer, D.W. Serfontein, A convenient system for improving the efficiency of first-generation ruthenium olefin metathesis catalysts, *Organometallics*. 24 (2005) 4528–4542.
- [42] F.T.I. Marx, J.H.L. Jordaan, H.C.M. Vosloo, DFT investigation of the 1-octene metathesis reaction mechanism with the Phobcat precatalyst, *J. Mol. Model.* 15 (2009) 1371–1381..
- [43] D.J. Nelson, S. Manzini, C.A. Urbina-Blanco, S.P. Nolan, Key processes in ruthenium-catalysed olefin metathesis., *Chem. Commun. (Camb)*. 50 (2014) 10355–75.
- [44] S. Monsaert, A. Lozano Vila, R. Drozdak, P. Van Der Voort, F. Verpoort, Latent olefin metathesis catalysts., *Chem. Soc. Rev.* 38 (2009) 3360–3372.
- [45] T. Tole, J. du Toit, C. van Sittert, J. Jordaan, H. Vosloo, Synthesis and application of novel ruthenium catalysts for high temperature alkene metathesis, *Catalysts*. 7 (2017) 22.
- [46] R.M. Thomas, A. Fedorov, B.K. Keitz, R.H. Grubbs, Thermally stable, latent olefin metathesis catalysts, *Organometallics*. 30 (2011) 6713–6717.
- [47] B. De Clercq, F. Verpoort, Activity of a new class of ruthenium based ring-closing metathesis and ring-opening metathesis polymerization catalysts coordinated with a 1, 3-dimesityl-4,5-dihydroimidazol-2-ylidene and a Schiff base ligand, *Tetrahedron Lett.* 43 (2002) 9101–9104.
- [48] A. Szadkowska, X. Gstlein, D. Burtscher, K. Jarzembska, K. Woźniak, C. Slugovc, K. Grela, Latent thermo-switchable olefin metathesis initiators bearing a pyridyl-functionalized chelating carbene: Influence of the leaving group's rigidity on the catalyst's performance, *Organometallics*. 29 (2010) 117–124.
- [49] F. Boeda, M. Jordaan, W.H. Meyer, S.P. Nolan, Phosphabicyclononane-Containing Ru Complexes: Efficient Pre-Catalysts for Olefin Metathesis Reactions, (2008) 259–263.
- [50] C.A.A. Huijsmans, Modelling and synthesis of Grubbs -type complexes with hemilabile ligands, North West University, PhD Thesis, 2009.
- [51] A. Michrowska, R. Bujok, S. Harutyunyan, V. Sashuk, G. Dolgonos, K. Grela, Nitro-substituted Hoveyda-Grubbs ruthenium carbenes: Enhancement of catalyst activity through electronic activation, *J. Am. Chem. Soc.* 126 (2004) 9318–9325.
- [52] K. Denk, J. Fridgen, W.A. Herrmann, N-heterocyclic carbenes, part 33. Combining stable NHC and chelating pyridinyl-alcoholato ligands: A ruthenium catalyst for applications at elevated temperatures, *Adv. Synth. Catal.* 344 (2002) 666–670.
- [53] J.I. Toit, C.G.C.E. Van Sittert, H.C.M. Vosloo, Metal carbenes in homogeneous alkene metathesis : computational investigations, *J. Organomet. Chem.* 738 (2013) 76–91
- [54] F.E. Hahn, M. Paas, R. Fröhlich, Synthesis, characterization, and catalytic activity of a ruthenium carbene complex coordinated with bidentate 2-pyridine-carboxylato ligands, *J. Organomet. Chem.* 690 (2005) 5816–5821.
- [55] M. Limbach, A Ru-Vinylvinylidene Complex : Straightforward synthesis of a latent olefin metathesis catalyst, *Chem. Cat. Chem.*,(2011) 297–301.

-
- [56] A. Schachner, R. Padilla, C. Fischer, P.A. Van Der Schaaf, R. Pretot, F. Rominger, M. Limbach, A Set of olefin metathesis catalysts with extraordinary stickiness to silica, (2011) 872–876..
 - [57] J.A. Gladysz, Recoverable Catalysts. Ultimate goals, criteria of evaluation, and the green chemistry interface, *Pure Appl. Chem.* 73 (2001) 1319–1324.
 - [58] K.M.A. Booyens, Metathesis and transalkylation in tandem catalysis metathesis and transalkylation in tandem catalysis, PhD Thesis, North west University 2007.
 - [59] M.P. Motoboloi, Synthesis and modelling of imine derivatives as ligands for Grubbs-type pre-catalysts, North West University, 2010.
 - [60] D.A. Carlson, U.R. Bernier, B.D. Sutton, Elution patterns from capillary gc for methyl-branched alkanes, *J. Chem. Ecol.* 24 (1998) 1845–1865.
 - [61] H. Brevard, E. Cantergiani, T. Cachet, A. Chaintreau, J. Demyttenaere, L. French, K. Gassenmeier, D. Joulain, T. Koenig, H. Leijjs, P. Liddle, G. Loesing, M. Marchant, K. Saito, F. Scanlan, C. Schippa, A. Scotti, F. Sekiya, A. Sherlock, Guidelines for the quantitative gas chromatography of volatile flavouring substances, from the working group on methods of analysis of the International Organization of the Flavor Industry (IOFI), *Flavour Fragr. J.* 26 (2011) 297–299.
 - [62] R. Peck, C. Olsen, J.L. Devore, introduction to statistics and data analysis, Cengage learning, Boston, 2016.
 - [63] H.S. Fogler, Elements of chemical reaction engineering, Prentice-Hall, 2011.
 - [64] M. Jordaan, P. van Helden, C.G.C.E. van Sittert, H.C.M. Vosloo, Experimental and DFT investigation of the 1-octene metathesis reaction mechanism with the Grubbs 1 precatalyst, *J. Mol. Catal. A Chem.* 254 (2006) 145–154.
 - [65] B. Allaert, N. Dieltiens, N. Ledoux, C. Vercaemst, P. Van Der Voort, C. V. Stevens, A. Linden, F. Verpoort, Synthesis and activity for ROMP of bidentate Schiff base substituted second generation Grubbs catalysts, *J. Mol. Catal. A Chem.* 260 (2006) 221–226.
 - [66] N. Ledoux, B. Allaert, D. Schaubroeck, S. Monsaert, R. Drozdak, P.V.D. Voort, F. Verpoort, In situ generation of highly active olefin metathesis initiators, *J. Organomet. Chem.* 691 (2006) 5482–5486.

3 METATHESIS REACTION KINETICS

"And above all, watch with glittering eyes the whole world around you because the greatest secrets are always hidden in the most unlikely places. Those who don't believe in magic will never find it." ~Roald Dahl

3.1 Overview

The aim of this chapter is to present the literature, methods and results pertaining to metathesis reaction kinetics. The aim is also to look at the available kinetic information and evaluate it critically. In Section 3.2 reaction kinetics for alkene metathesis will be covered in general highlighting Grubbs 2nd generation catalysts and chelating pyridinyl alcoholato ruthenium-based complexes. Section 3.3 describes and elucidates the modelling procedures followed in the regression activities. The last major section, Section 3.4 presents the results obtained from the modelling activities and discusses, explains and compares the results with the empirical findings of Chapter 2. Chapter 3 is concluded with concluding remarks.

3.2 Alkene metathesis kinetic literature

3.2.1 Introduction

Once a catalyst's performance is assessed more detailed information is typically required from a kinetic standpoint [1]. Chemical kinetic data is necessary to predict, compare and implement chemical reactions and their applications. Little can be achieved with a new synthesised precatalyst from an industrial standpoint if the kinetics are not available. Kinetic rate laws allow the empirical data to be translated into mathematical laws that are used to design complex reactor systems [1]. Understanding the kinetics of the catalysts studied in this work will provide the bridge between the catalyst synthesis and the conceptual process design. The purpose of the following section is to review the kinetics that has been described in previous literature for typical 1-octene metathesis reactions with Grubbs 2nd generation type precatalysts. The section is then expanded to briefly describe the theoretical background that is needed to understand the basis from which the rate laws for the system have been developed.

3.2.2 Alkene metathesis mechanism

3.2.2.1 General mechanism

Generally, metathesis reaction rate laws are derived from the catalytic mechanisms [2], since these mechanisms can provide insights into the rate limiting steps and the roles that the catalyst ligands have therein. Additionally, precatalysts are known to initiate reactions in a number of steps, whether the steps entail principles of mass transfer as in the case of heterogeneous catalysis or catalytic initiation mechanics as with homogeneous precatalysts [2]. The importance of describing and understanding the mechanism of a catalytic reaction is therefore expressed.

As mentioned before, the exact mechanism for alkene metathesis was somewhat of a mystery until the insights of Hérrison and Chauvin in 1971 [3]. The mechanism of Chauvin involves 2 steps, the first of which results in the formation of an active metal carbene specie and the second involves transalkylation [4] (Figure 3.1). The mechanism starts with an alkene coordinating onto the active metal carbene specie (A). [2+2]-cycloaddition between the carbene and the metal-carbene then takes place to yield the metallacyclobutane intermediate (C) [5]. The metallacyclobutane intermediate then re-coordinates and breaks up to form an alkene. To propagate the cycle the coordinated alkene is replaced with a new alkene (F) [5].

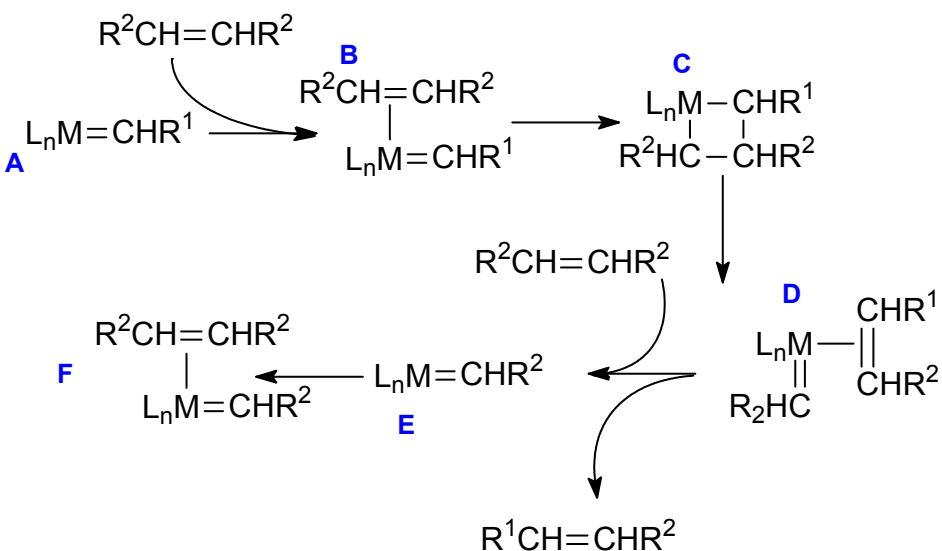


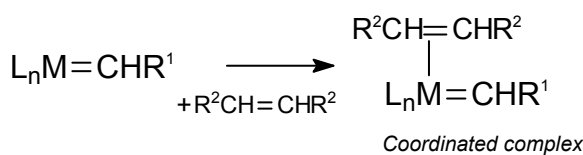
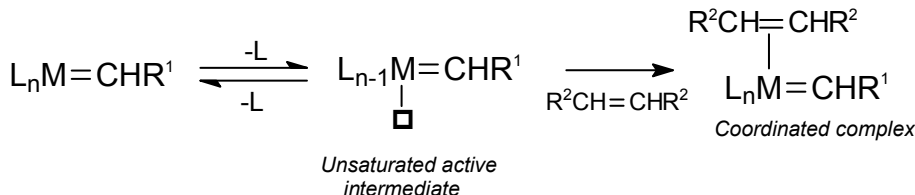
Figure 3.1: Chauvin mechanism adapted from [6]

Initiation

The metallacyclobutane mechanism of Chauvin and Hérisson does not specify as to how the active metal carbene is formed initially and only describes the propagation cycle of the reaction. The active metal carbene species are typically formed by initiation mechanisms. Two types of mechanisms are usually possible; the associative and the dissociative mechanisms [5]. The alkene coordinates directly onto the metal-carbene in the associative mechanism, whereas with the dissociative mechanism a ligand first has to dissociate before the alkene will coordinate to the metal-carbene [5]. The associative pathway entails the alkene associating onto the carbene to form an 18e⁻ intermediate species. For dissociative precatalysts, the 16e⁻ species need to lose a ligand to yield a 14e⁻ alkylidene [5].

Understanding the initiation process is the first step to develop a mechanistically based kinetic model. Du Toit *et al.* [6] provided a review on the topic of metal carbenes in terms of their mechanistic aspects. They discussed two main types of metal carbenes, the Fischer carbenes (low valent, 18e⁻ complexes) and the Schrock carbenes which are high valent complexes with less than 18 electrons- the authors pointed out that classification becomes complicated with the advent and study of more catalysts as time progresses- and the activities and structures should rather be seen as points along a spectrum [6]. The nature of these metal carbenes and their electronic properties provide a means towards understanding the initiation mechanisms.

A brief illustration of these initiation mechanisms is available in Figure 3.2 [6]

Associative Mechanism**Dissociative Mechanism****Figure 3.2: Alkene metathesis initiation mechanisms adapted from [6]**

The mechanisms presented in Figure 3.2 and 3.1 have been the topic of extensive consideration in research. Therefore, they will briefly be discussed to provide an understanding of the kinetic effects that these mechanisms produce.

3.2.2.2 Mechanistic aspects of commercial Grubbs-type precatalysts

Initiation

The initial belief with the initiation mechanism of 1st and 2nd generation Grubbs-type precatalysts was that it proceeds via the association mechanism. Dias *et al.* [7] explored the mechanisms for phosphine containing 1st generation precatalysts and proposed both the association and dissociation mechanisms. Evidence for the dissociation pathway was stronger in the presence of bulkier complexes, yet some results indicated a favour toward the associative pathway when phosphine concentrations were high (excess added to the reaction).

Later work by Sanford *et al.* [8] included the **G2** precatalyst in their mechanistic reactions with EVE and found stronger evidence for the dissociation pathway. Opposing expectations Sanford *et al.* reported higher initiation rates for the **G1** precatalyst compared to the **G2** precatalyst. The premise was that the larger steric bulk of the NHC ligand would favour dissociation. What Sanford's work demonstrated above all was that the sheer steric bulk of the ligands aren't always the only affecting factor, but that phosphine electronics also contribute to the reaction initiation rate [8].

Even so, changes to the initiation rate did not necessarily change the propagation. Nelson's review highlighted that the initiation constants for both the **G1** and the **G2** precatalysts span over a considerable range which can be attributed to a number of key factors, such as the type of solvent, phosphine concentration and the alkene substrate [9].

Propagation

The precatalyst's activity and selectivity have much to do with the $14e^-$ intermediate complex [9]. The effects of the substrate on the propagation cycle had to be explored since it was shown that there were some differences between the 1st and 2nd generation complexes (see Section 1.2.2.2) . For this reason Grubbs [10] set out to experiment with the precatalysts using ethyl vinyl ether and additional phosphine. The observed initiation constants that they found was a function of the phosphine concentration, the substrate concentration, the metathesis propagation rate and the rate at which the phosphine rebinds to the complex (Equation 3.1).

$$\frac{1}{k_{obs}} = \frac{k_{rebind} * [PCy_3]}{k_{init} * k_{metathesis} * [Alkene]} + \frac{1}{k_{init}} \quad (3.1)$$

Their results showed that the **G2** precatalyst was more likely to enter into the propagation cycle, given the **G1** precatalyst's propensity to get trapped and deactivated by excess phosphine. Grubbs *et al.* [11,12] realised that the precatalysts react differently to different substrates during the substitution patterns of the propagation cycle and developed a system by which these behaviours could be classified. The alkenes were grouped into 4 different types (I-IV) according to their relative ability to homodimerise during cross metathesis and the likelihood of these homodimers to undergo secondary metathesis [12]. Terminal alkenes were classified as Type I which are very reactive and therefore produce consumable homodimers rapidly. As a result, a statistical distribution of Primary and secondary metathesis products would result from reactions with Type I alkenes [12].

The difference between the performance of **G1** and **G2** precatalysts was explored from the viewpoint of the metallacyclobutane (MCB) formation as well as precatalyst initiation by Cavallo *et al.* [13]. Cavallo's calculations on the formation of MCB showed that the second-generation complexes have lower energy barriers, which lead to low energy MCB complexes that are lower in energy. The NHC ligands also provide a steric driving force that makes phosphine and alkene bound complexes unstable, therefore making the MCB formation energetically favoured [13]. Further research has shown that the first generation precatalysts yielded an MCB with a higher energetic state than the 2nd generation precatalysts, explaining the superior performance of the **G2** precatalysts. **G2** precatalysts have been shown to react with the initial pure alkenes as well as the products that result from the metathesis of the initial substrate and are therefore able to reach equilibrium sooner [13].

Many in-depth studies on the metathesis mechanism exist for 1st and 2nd generation precatalysts and although there is still some debate on many fronts the literature is fairly saturated with mechanistic studies on this commercial 1st and 2nd phosphine containing Grubbs precatalyst.

Vorlafldt *et al.* was one of the teams that investigated the RCM of DEDAM with **HG2** [14]. Their results indicated a pseudo first-order dependence of the reaction rate on the concentration- even at higher concentrations indicating the absence of saturation behaviour. At higher concentration, however, the reaction behaviour was not linear, and they concluded from further experiments that the concentration of the alkene, determines the rate-limiting step. Furthermore, the reaction rate is dependent on the nature of the alkene as well and Vorlafldt [14] therefore preferred the association mechanism.

In contrast, Vougioukalakis *et al.* [15] conducted kinetic experiments on Grubbs and Hoveyda type complexes with Butyl Vinyl Ether (BVE). Their results displayed a first-order dependence on substrate concentration for the HG type complexes [15]. The phosphine containing precatalysts, however, shown to be dependent on the substrate concentration and that the phosphine dissociation step was the rate-limiting step. Thiel *et al* conducted a kinetic study with 1-hexene (among others) and Hoveyda-Grubbs type catalysts as substrates [16] The data Thiel *et al.* obtained indicated a preliminary dissociative mechanism and further investigation either a dissociative or an interchange mechanism with an associative mode of activation [16].

Van der Gryp [17, 18] used DFT to determine the preferential mechanism in the case of **G1** and **G2** as opposed to the **HG1** and **HG2** for the reaction with 1-octene. The dissociation mechanism was generally accepted for the **G2** and **G1** precatalysts [9] but Van der Gryp questioned whether the release return mechanism of the ether group was the dominant pathway or whether the basic PCy₃ or H₂IMes ligands would rather dissociate from the complex to yield an open site [17]. Van der Gryp proved in their study that the release return-dissociative mechanism was the preferred mechanism for **HG2** and **HG1** complexes [17] and investigated their **GrPh** precatalyst with the O^N chelate's behaviour as well [18]. They found that the O^N group did not completely leave the complex as in the case of the **HG2** precatalyst, but that the hemilabile ligand would rather remain tightly bound to the complex throughout the reaction affording it a higher degree of stability[18].

Chelating pyridinyl alcoholato precatalysts is defined by their propensity to only initiate upon the introduction of a stimulus [9]. DFT studies have shown that the most energetically favourable mechanistic pathway is one where the nitrogen and ruthenium remain bound to each other,

however, the same studies have shown that the energy requirements for the alternative mechanism where the N and Ru bond breaks only differ slightly from the alternate mechanism [19].

In her study of the initiation rates of the **GCYC** precatalyst along with other 1st and 2nd generation analogues, Jordaan [20, 21] found that the stability of the hemilabile precatalysts improved in comparison to **G1** systems although the initiation rates were slower. Jordaan [21] attributed this phenomenon to the increased steric bulk of the **GCYC** precatalyst since an increase in steric bulk was shown to lead to an increase in initiation rates. In her study, free rotation of the phenyl ring in the **G1Ph** precatalyst was proposed to cause the drop in catalytic activity of the precatalyst since it results in an increased amount of steric bulk around the ruthenium centre obstructing the entrance of the substrate. Jordaan expanded her investigation to the 2nd generation precatalysts to show that the 2nd generation analogues of the chelating hemilabile pyridinyl alcoholato ruthenium precatalysts have displayed decreased initiation rates but higher activity during the catalytic cycle and improved stability and lifetime [21]. Unfortunately, despite the promising results on activity and stability the 2nd generation precatalysts displayed less selective behaviour towards PMP. Jordaan proposed the association and the dissociation initiation pathways for the GCYC catalyst and also investigated the reaction mechanism with DFT calculations and H-NMR studies [20, 21]. The proposed initiation and activation cycle for the GCYC catalyst was based on the works of Grubbs [8] and Chen [5] in combination with their experimental results. A schematic illustration of the resulting cycle is provided in Figure 3.3 [21].

At first, the 16e- precatalyst (A) is initiated with the release of the nitrogen atom resulting in an open position and active 14e- species (B). The catalyst is then activated in one of two directions as the 1-octene is coordinated onto the active ruthenium species in two stereochemical approaches (C₁ and C₂) [21]. [2+2]-cycloadditions then successively take place resulting in the formation of a metallacyclobutane complex after which cycloreversions form the propagating methylidene and heptylidene species (F1 and F2) [21].

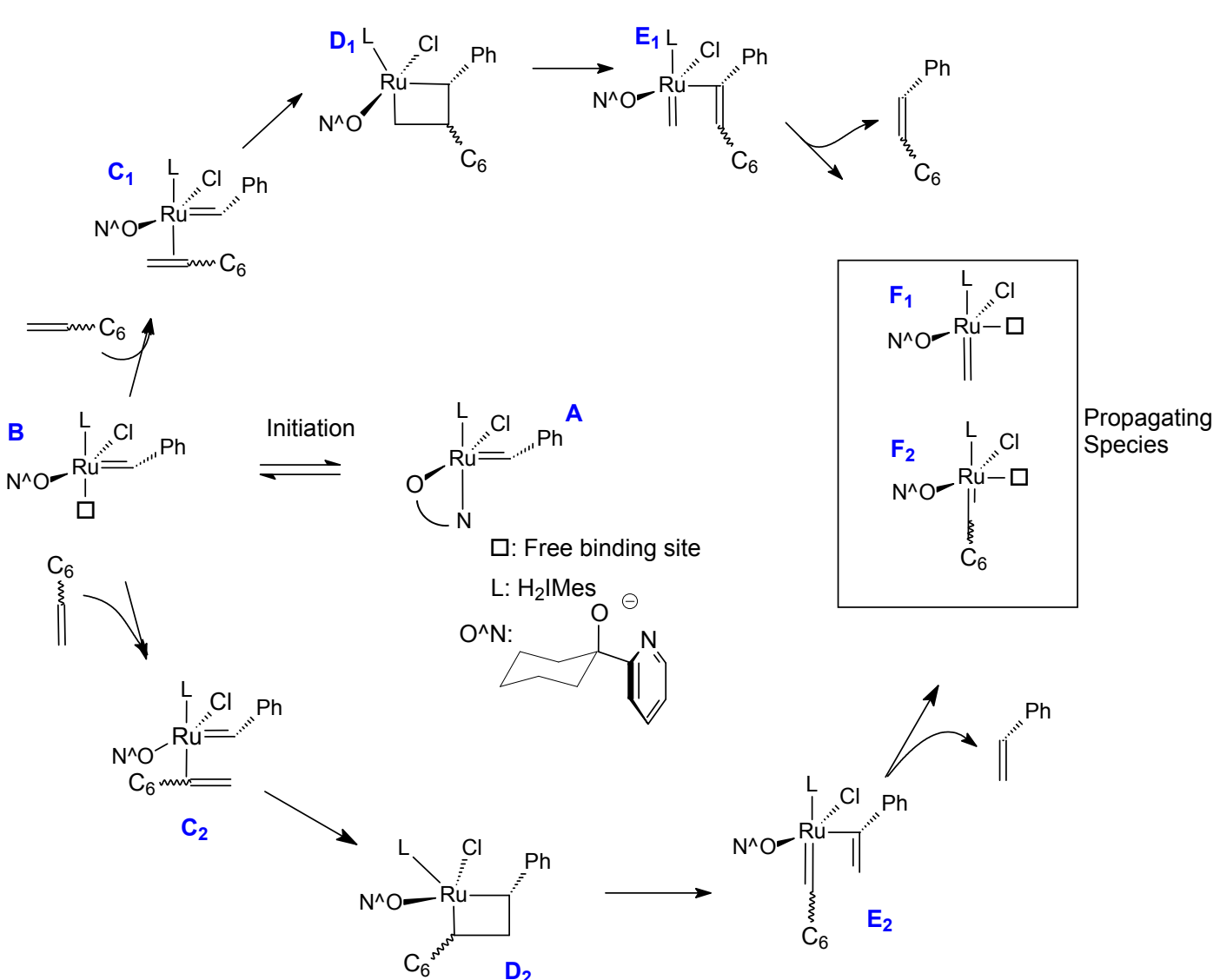


Figure 3.4: Full proposed initiation and activation mechanism for GCYC precatalyst (adapted from [21])

One of the big differences between the commercial systems and the latent hemilabile systems is the fact that the labile ligand remains attached to the metal centre during the propagation cycle [19]. In some cases, this can lead to a decreased initial reaction rate with the advantage of an increase in the catalytic lifetime. Szadkowska [22-23] has aimed to explain the latency that is afforded to bidentate ligands as they have observed in their experiments. Their explanation was that due to the π -bond nature of the chelates, the catalytic structure is more stable, affording it its latency, as opposed to sigma bonds that can easily buckle or bend when external forces are present.

Vorpaltd *et al.* [14] found that there was an increase in the reaction rate between the Grela complex and the **HG2** complex and as such made the conclusion that the leaving group has an effect on the reaction rate. Surprisingly the authors that studied the differences between the initiation rates

for a range of different substituted ligands found that the addition of an alkoxy group to the precatalyst ligands alters the initiation rate by at least 2 orders of magnitude [14].

Jordaan proposed the catalytic propagation cycle as illustrated in Figure 3.5: for the GCYC catalyst by applying the concepts applicable to the parent structure (G2). Depending on the coordination orientation of the 1-octene relative to the phenyl ring either the heptylidene or the methylidene species enter the catalytic cycle first [20-21]. Within the cycle, the heptylidenes (J) are converted to methylidenes (F_1) which are subsequently converted back to the heptylidenes and vice versa. This cycle continues until all the substrate is consumed or the catalyst decomposes [21]. Since the commencement of metathesis precatalyst development studies scientist have realised that the ligands attached to the precatalyst have a role to play in the reaction kinetics.

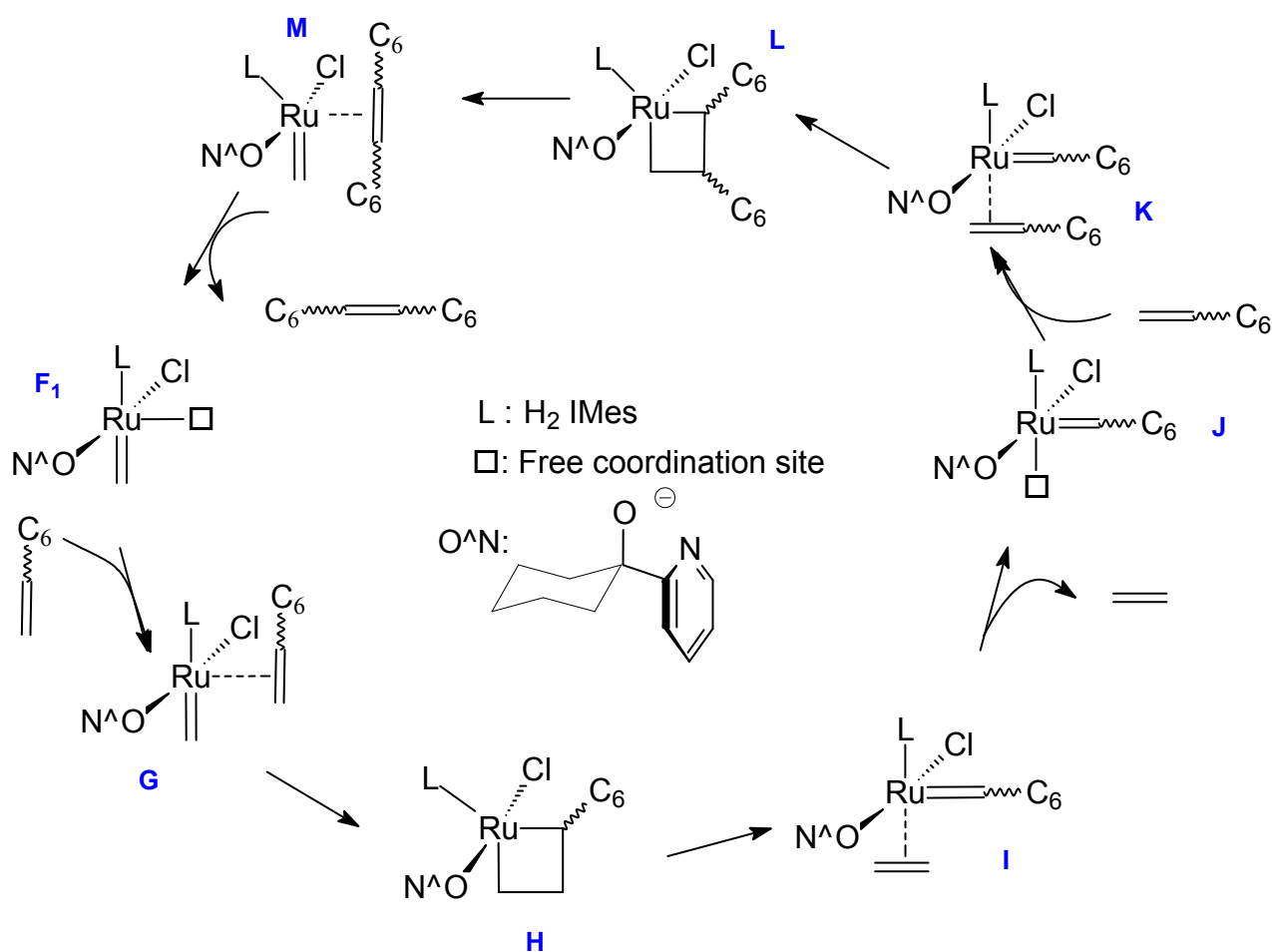


Figure 3.6: Proposed precatalyst catalytic cycle with chelating pyridinyl alcoholato precatalysts and 1-octene [21]

After the catalytic cycle, the precatalysts typically return to their stable state or deactivate by thermal decomposition or the interference alternative sources that cause the formation of

Ruthenium Hydride species, which have been shown across literature to be isomerisation precatalysts [24-27].

3.2.3 Kinetic literature evaluation

One of the prominent and early works in literature that explored the kinetics of Grubbs based precatalysts was the work of Dias in 1997 [7]. Dias and Grubbs explored the effects of different ancillary ligand identities on the precatalyst activity. Their work sought to explore the reaction rate and the mechanistic pathway with which the reaction with **G1** and DEDAM would proceed further [9]. A rate law was developed, and it was found that the consumption of the DEDAM followed a pseudo first-order rate in the presence of excess phosphine. The rate law also indicated that the rate was dependent upon the ruthenium and the phosphine concentration. Furthermore, the investigation showed that a combination of the dissociative and the associative mechanism described their system best.

Since Grubbs and Dias' work, Grubbs and Ullman [27] investigated the rate of reaction of different linear alkenes shortly thereafter. For 1-hexene they reported a relative reaction rate constant of $6.1 \times 10^{-4} \text{ s}^{-1}$. Their work also found that the kinetically favoured product during the reaction was the alkylidene complex rather than the methylidene and that the bulkier the alkene substrates were the slower the reaction was [27].

In 2001 Grubbs included the **G2** precatalyst into the kinetic investigation with EVE and reported the reaction rate constants and the activation energy. The values were compared to the results obtained for the **G1** precatalyst [28].

A little later in 2005 Mahahle [29] investigated the decomposition kinetics in the presence of **G1** and **G2** since these precatalysts were known for their sensitivity to temperature and their propensity to catalyse isomerisation reactions at high temperatures. Mahahle used NMR between the ranges of 20°C and 120°C to determine the deactivation rate constant by investigation on a molecular level. A reversible decomposition reaction scheme was proposed to explain the isomerisation kinetics of the reaction with internal and terminal octenes [29]. A linear Arrhenius fit was carried out and deactivation activation energy was determined to be 12.6 kcal.mol⁻¹ for the forward reaction and 5.45 for the reverse reaction. The kinetic rate constant for the deactivation of the **G2** precatalyst was reported to be 4×10^{-6} . Mahahle made the conclusion from statistical regression tests that the forward reaction was better defined than the reverse reaction [29].

Janse van Rensburg [30] subsequently estimated the decomposition rate based on a substrate induced decomposition reaction but reported kinetic rate parameters that were higher than what Mahahle has determined experimentally for the **G1** and **G2** precatalysts at 29.5 and 27.2 kcal.mol⁻¹. Possible explanations could be that the reactions investigated were dissimilar [29] i.e. thermal decomposition and substrate induced decomposition thus meaning that the thermal decomposition would take place sooner than substrate induced decomposition. Janse van Rensburg's explanation for the decomposition from a mechanistic standpoint suggested β-hydride transfer from the ruthenacyclobutane intermediate [30].

Jordaan investigated the initiation reaction rates of 1-octene metathesis in combination with chelating pyridinyl alcoholato precatalysts that have been synthesised to increase catalytic stability. A linear relationship between the initiation rate constant and temperature was observed for the precatalysts considered [31]. The initiation rates were fitted to the Arrhenius equation which display a curved trend. A typical linearised Arrhenius equation would rather display a direct linear relationship, but Jordaan explained the curvature by the presence of two competing mechanisms, the mechanisms were deduced from two separate regimes which were obtained by separating the curved region into two linear regions [31]. Jordaan also mentioned the possibility that precatalyst decomposition was taking place for the **GCYC** precatalyst but the decomposition rates were not included in the study. Jordaan attempted to estimate the activation energy for the **G1** system beforehand and reported an activation energy value of 33.94 kcal.mol⁻¹. The estimated value and the experimentally determined value was found to differ significantly in that the experimental value was considerably lower at 10.05 kcal.mol⁻¹ [31]. Loocke [32] followed the approach of Jordaan and expanded the study to the PUK-Grubbs 2 precatalyst (a) synthesised precatalyst with an O-N hemilabile ligand with two phenyl groups coordinated to the metal centre b) as well as different alpha alkenes. HNMR investigations were conducted and the reported kinetic constants are summarised in Table 3.1.

Vorfalt [14] and Thiel [16] both studied the reaction kinetics of **HG2** with DEDAM and BuVE. Vorfalt obtained an excellent linear fit and suggested second-order rate constants from the linear correlation, the study was later expanded to include a Grela complex that yielded rate constants for DEDAM and EVE as 0.00764 L.mol⁻¹.s⁻¹ and 0.192L.mol⁻¹.s⁻¹ The Grela complex displayed higher rate constants as compared to **HG2**. Thiel used 1-hexene to estimate the rate constants for the reaction system as well. The experimental data fitted the proposed hyperbolic model well only once a first order dependence on the alkene concentration term was included in the model. Their findings are summarised in Table 3.1.

Van der Gryp [17-18] did an in-depth kinetic study of the **G1**, **G2**, **HG2** and the **Gr2Ph** precatalysts before conducting a membrane separation test [18] on the reaction residue to recover the precatalyst in 2008. Van der Gryp expanded the kinetic parameters to account for the forward and reverse reactions and reported the activation energy for the forward reaction as $23.8 \text{ kcal.mol}^{-1}$. The reverse reaction rate was found to require less activation energy thus preferring lower reaction temperatures. As such at higher temperatures, Van der Gryp observed competing mechanisms taking place i.e. the PMP reaction, IMP and SMP reactions [17]. The most recent work reporting kinetic parameters for a latent Grubbs based reaction with 1-octene is presented by Du Toit in 2016 [33]. The precatalyst used was an O-N chelate precatalyst and the activation energy for the forward reaction was reported to be $24.19 \text{ kcal.mol}^{-1}$. Which was quite similar to the value for **HG2** as reported by Van der Gryp [17].

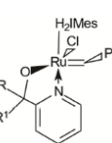
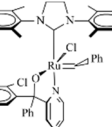
The nature of the **GMPP** precatalyst has not been reported before from a kinetic point of view, however, precatalysts that were synthesised using the same design base were reported by Tole *et al.* [34] in 2017. Tole noted that the precatalysts only started reacting at 70°C . Precatalyst 13 as Tole reported on is identical in structure to the **GMPP** precatalyst except for the fact that the methyl group on the benzene ring of the labile group is a chlorine atom. Tole reported a maximum initiation reaction constant of 14.84×10^{-3} . Tole *et al.* [34] did not consider the precatalyst decomposition or the reaction rate towards the formation of secondary metathesis products. The authors did, however, explain why the precatalysts were so latent and stable: the precatalyst stability was attributed to shorter bond lengths between the Ru and the N atom in the hemilabile ligand, therefore, increasing the energy required to activate the reaction making the precatalyst latent and stable at higher temperatures [34].

Key results of literature are summarised in Table 3.1. From the background provided, several lacks in literature have been identified for the reaction kinetics of 1-octene metathesis with chelating pyridinyl alcoholato ruthenium precatalysts:

- 1) Mostly, works in literature only estimate the initiation rates for the reaction system and do not consider the side-product reaction rates
- 2) A full kinetic study has not been conducted on the **GMPP** precatalysts and the studies on the **GCYC** catalyst had only described the initiation kinetics from a mechanistic standpoint.
- 3) Catalyst deactivation kinetics have not been included in the rate laws developed for these reaction systems

The aim of this work is to address these issues in the following sections of this chapter.

Table 3.1: Kinetic literature evaluation summary (** deactivation rate constants).

Author	Year	Catalyst	Linear alkene	Temperature (°C)	Rate constant	Units	Ea k₁	Units
Ullman & Grubbs [27]	1997	G1	1-hexene	35	6.10×10^{-4}	s ⁻¹	-	-
Mahale [29]	2005	G1	1/2/4-octene	-	7.04×10^{-3}	s ⁻¹	12.36	kcal.mol ⁻¹
		G1	1/2/4-octene	-	1.1×10^{-1}	s ⁻¹	5.45	kcal.mol ⁻¹
		G2	1/2/4-octene	-	$0.4 \times 10^{-7} **$	min ⁻¹	-	-
Janse van Rensburg [30]	2006	G1	ethene	-	-	-	29.5	kcal.mol ⁻¹
		G2	ethene	-	-	-	27.2	kcal.mol ⁻¹
		G1	1-octene	-	1.70×10^{-2}	min ⁻¹	10.05	kcal.mol ⁻¹
Jordaan [21]	2007	G2	1-octene	-	2.98×10^{-6}	min ⁻¹	15.61	kcal.mol ⁻¹
		GCYC	1-octene	70	$1.35 \times 10^{-5} **$	mol.s ⁻¹	-	-
		G1	1-hexene	55	3.58×10^{-4}	mol.s ⁻¹	-	-
Loocke [32]	2009	G2	1-hexene	55	3.82×10^{-4}	mol.s ⁻¹	-	-
		G1	1-heptene	60	6.37×10^{-4}	mol.s ⁻¹	-	-
		G1	1-heptene	60	$0.21 \times 10^{-2} **$	s ⁻¹	-	-
		G2	1-heptene	60	1.09×10^{-3}	mol.s ⁻¹	-	-
Van der Westhuizen [35]	2010	G1	1-octene	25	3.46×10^{-2}	s ⁻¹	-	-
		G1	ethene	25	4.75×10^{-2}	s ⁻¹	-	-
		G1	-	53	3.20×10^{-4}	s ⁻¹	-	-
Thiel [14]	2012	HG2	1-hexene	30	1.00×10^{-1}	s ⁻¹	-	-
Van der Gryp [17]	2012	HG2	1-octene	-	$3.79 \times 10^{+14}$	min ⁻¹ .mmol ^a .mL ^a	23.8	kcal.mol ⁻¹
Du Toit [33]	2016		1-octene	-	$1.79 \times 10^{+11}$	min ⁻¹ .mmol ^a .mL ^a	24.19	kcal.mol ⁻¹
Tole [34]	2017		1-octene	90	14.84×10^{-4}	mol.s ⁻¹	-	-

3.3 Kinetic modelling

Countless models and expressions have been developed mathematically to describe kinetic rate laws, but finding a model that fits experimental data is a challenge. Experimental data most often include some element of variation or randomness that is difficult to predict. Ideally, mathematics and statistics would be able to account for all variations in experimental observations but there are computational limitations to that ideology. Technological advancements have been able to overcome the limits as far as computations go, but that doesn't speak for the issue of resources which is also a factor to account for. The aim of data modelling is therefore to make reasonable compromises. Compromise is essentially applied by making assumptions that would simplify the model and statistics is often the tool that is used to aid the modeller in their choice of assumptions. The aim of this section is to briefly elucidate and describe the assumptions, methods used, and choices made during the development process. Thereafter the developed rate laws and kinetic models are put to the test using statistical regression techniques.

3.3.1 Kinetic rate law development

Kinetic rate laws are typically designed to predict the rates of consumption or production of species during the reaction. It is particularly useful for the engineering discipline to determine these rates to be able to design reactor equipment and systems effectively. The rates of consumption or production are mostly dependent on the presence of relevant species as the reaction progresses [1], but it doesn't end there, temperature, pressure and the presence of a precatalyst are the other obvious factors that contribute to the rate of a chemical reaction [1]. In the case of multi-step catalytic reactions, the relevance of undesired side reactions is a factor that the engineer is required to consider, not to mention the possibility of precatalyst decay and intermediate species. The key to developing a good kinetic rate law, however, is to account for these factors were relevant but also to keep the model as simple as necessary by making suitable assumptions [1].

In this section the development of a model for the reaction of 1-octene metathesis in the presence of the **GCYC** and **GMPP** precatalysts is presented and explained, a basic methodology was adopted from [1] and is presented in Figure 3.7

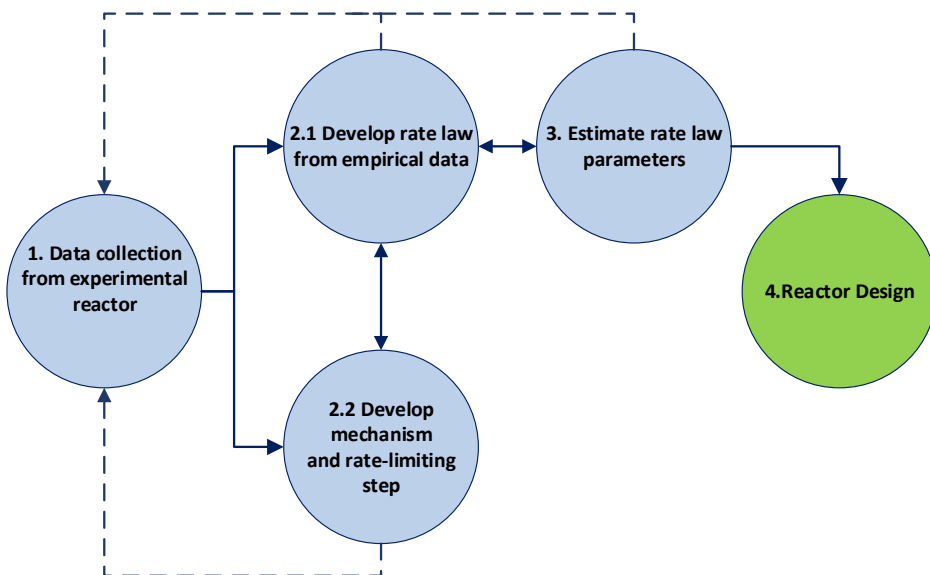


Figure 3.7: Proposed algorithm for rate law development (adapted from [1])

According to Fogler [1] and Levenspiel [36], there are two different approaches that can be followed in the process of estimating the rate law parameters by data analysis. The first is the integral method, where a rate law is estimated and then compared to the data to see if a linear fit can be obtained, the fit is not appropriate the law is amended, and the process is repeated. The differential method is usually used in cases where the mechanisms present in the reactions are more complicated and directly compares the rate law to the experimental reaction rate data. In this study, the integral method is applied [36].

Step 1 of Fogler's algorithm has been completed by the activities and data obtained in chapter two, which brings the next step to the fore; developing a rate law that fits the experimental data and can be described mechanistically. Literature is abundant with proposed rate laws and mechanisms and as such the following sections will apply the knowledge from literature to the system of this work [1].

Initiation Mechanisms

Catalytic cycles are known to include multi-step reactions but usually, only a number of these steps are actually rate determining [1], furthermore multistep reactions also entail intermediate species. The (pseudo-steady state hypothesis) theory (PSSH) that an intermediate species' active lifetime is negligible has been applied in the rate development of the studied system. The assumption is therefore that the rate of formation of intermediate species is negligible since the participation of the active species has been accounted for throughout all the reaction steps. The assumption has been applied to metathesis in past work [11].

The PSSH can be expressed mathematically as follows [1]:

$$r_i^* = \sum_{k=1}^n r_{ki}^* \quad (3.2)$$

To apply this theory, however, the rate laws need to consist of well-defined mechanistic considerations. Luckily literature has provided possible reaction mechanisms to choose from, the most prominent ones are the associative and the dissociation mechanisms [21]. The Release return mechanism has also been suggested [37], but since the associative mechanism is closely related to the release-return mechanism in the initial stages only these two mechanisms will be considered for the rate law development.

In this work, the assumption is made that the rate determining step is the initiation rate, especially since the catalytic systems that are being considered are classified as latent. First considering the Associative mechanism: it can be expressed as follows



Assume the PSSH

$$R_X = 0 = k_i C_{C_8} C_{Ru} - k_{-i} C_X - k_j C_X \quad (3.6)$$

$$C_X = \frac{k_i C_{C_8} C_{Ru}}{k_i + k_j} \quad (3.7)$$

$$r_{C_8} = -k_i C_{C_8} C_{Ru} + k_{-i} C_X \quad (3.8)$$

$$r_{C_8} = -k_i C_{C_8} C_{Ru} + \frac{k_i k_{-i} C_{C_8} C_{Ru}}{k_i + k_j} \quad (3.9)$$

$$r_{C_8} = \left(-k_i + \frac{k_i k_{-i}}{k_i + k_j} \right) C_{C_8} C_{Ru} \quad (3.10)$$

let

$$-k = \left(-k_i + \frac{k_i k_{-i}}{k_i + k_j} \right) \quad (3.11)$$

$$r_{C_8} = -k C_{C_8} C_{Ru} \quad (3.12)$$

Equation 12 could be a possible rate law to model the reaction rate, however, it only models the initiation rate and measuring the concentration of the precatalyst throughout the reaction is challenging since the propagating species (14e⁻intermediate) is often unobservable [9]. To overcome these limitations the assumption was made that the initiation rate is only dependent upon the initial precatalyst concentration i.e. (C_{Ru_0}) to give:

$$r_{C_8} = -k C_{Ru_0} C_8 \quad (3.13)$$

Similarly, the dissociation initiation mechanism can be expressed as follows:



Applying the PSSH theory to develop the rate law:

$$R_X = 0 = -k_i C_{Ru} - k_{-i} C_X - k_j C_{C_8} C_X \quad (3.18)$$

$$C_X = \frac{k_i C_{Ru}}{k_{-i} + k_j C_{C_8}} \quad (3.19)$$

$$r_{C_8} = -k_j C_{C_8} C_X \quad (3.20)$$

$$r_{C_8} = -k_j C_{C_8} \left(\frac{k_i C_{Ru}}{k_{-i} + k_j C_{C_8}} \right) \quad (3.21)$$

At excess 1-octene concentrations, the reverse initiation rate can be assumed to be infinitesimally small ($k_{-i} \ll k_j C_{C_8}$) and the equation reduces to:

$$r_{C_8} \approx k_i C_{Ru} \quad (3.22)$$

The same assumption was made for Equation 23 as for Equation 13 in that the precatalyst concentration is only that of the initial stage. Therefore:

$$r_{C_8} = k_i C_{Ru_0} \quad (3.23)$$

The difference between the dissociation and the associative mechanism only constitutes of the Alkene concentration term and as such the associative mechanism was chosen to account for all possibilities.

The rate law in equation 2.13 only predicts the rate in 1-octene consumption during initiation, but since secondary metathesis products are formed during the reaction, the question arises; how is the rate of consumption of 1-octene distributed between the primary and secondary reactions? Furthermore, how does the precatalyst decay affect the reaction rate?

Pseudo first order reaction system

According to one of the works of the team led by Grubbs [38,42] the relative stability of a precatalyst can be determined by constructing a semi-log plot of the starting material against time. A straight linear line indicates that the reaction follows a pseudo-first-order rate law and a curved line indicates the presence of precatalyst decomposition. To screen between experiments where precatalyst decay occurred and the ones where pseudo first-order kinetics were present linearised plots of 1-octene vs time have been constructed to compare and identify the runs and conditions under which precatalyst decay was present. The results are available in Figure 3.8 and as can clearly be seen the **GMPP** precatalyst's behaviour is predominantly linear except for the cases of 80 and 90°C .

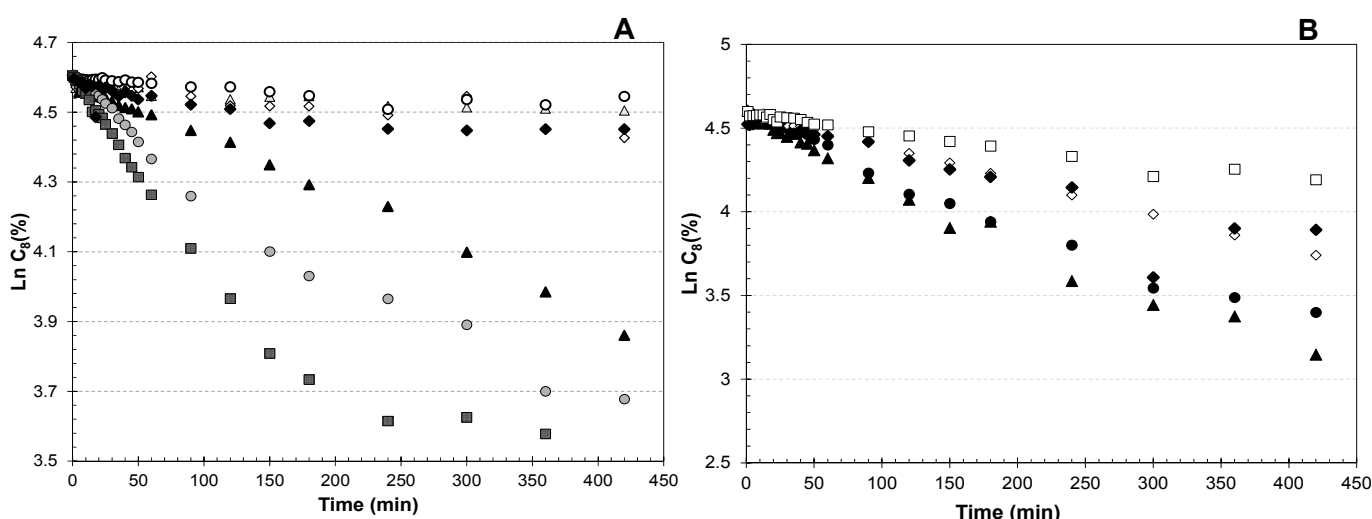


Figure 3.8: Linearised 1-octene consumption for (A) varied temperature [Δ 40°C \diamond 50°C \circ 60°C \blacktriangle 70°C \bullet 80°C \blacksquare 90°C \blacklozenge 100°C] and (B) varied precatalyst load [\blacktriangle 5000 \bullet 7000 \diamond 10000 \blacklozenge 12000 \square 14000] with GMPP precatalyst.

Similarly, for the **GCYC** precatalyst, the following linearised graphs were obtained:

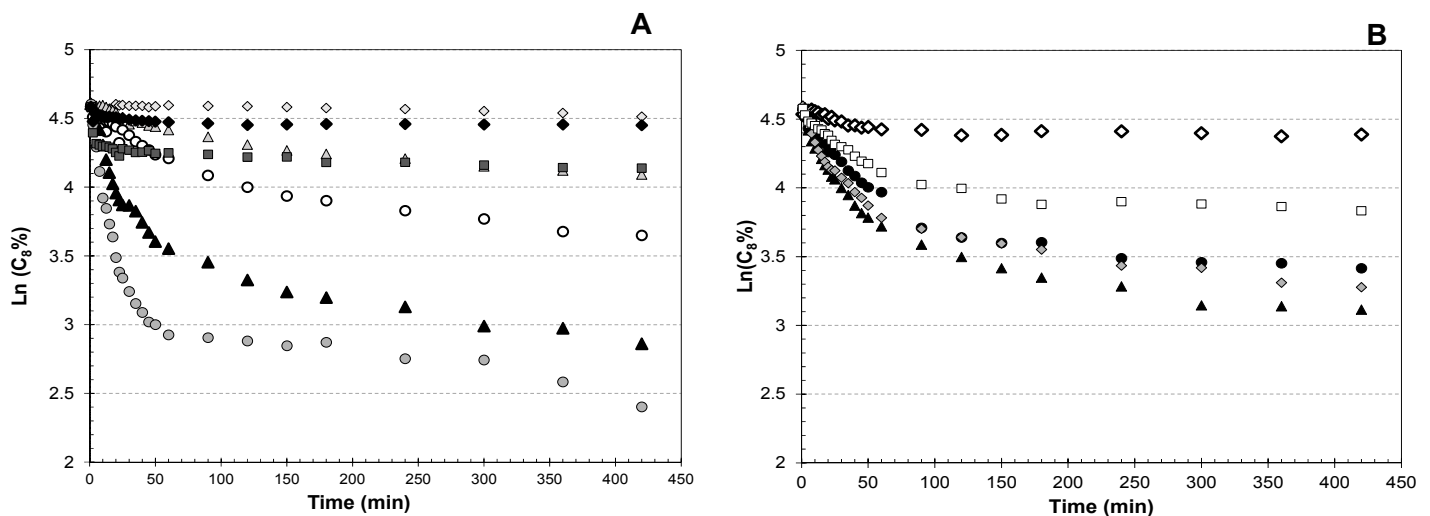


Figure 3.9: Linearised 1-octene consumption for (A) varied temperature [\triangle 40°C \diamond 50°C \circ 60°C \blacktriangle 70°C \bullet 80°C \blacksquare 90°C \blacklozenge 100°C] and (B) varied precatalyst load [\blacktriangle 5000 \bullet 7000 \diamond 10000 \blacklozenge 12000 \square 14000] with GCYC precatalyst.

The **GCYC** precatalyst showed a higher propensity to decompose at temperatures above 50°C up until the precatalyst almost completely disintegrated above 100 °C. Figure 3.9 B shows how the precatalyst concentration affects the likelihood that the precatalyst would decompose. At lower concentrations

The plots are predominantly linear indicating that the precatalyst concentration could possibly affect the decomposition [42]. The occurrence of precatalyst decomposition has to be accounted for in the reaction rate law and there are two possible ways to do so. The first requires specific knowledge of the decomposition mechanism, which for the field of metathesis has been explored for other classes of metathesis reactions and precatalysts in detail, but for the specific precatalysts of this study, the decomposition mechanism is still unknown. The kinetic details of such mechanisms fall into the class of non-separable kinetics [1] and are generally defined as:

$$-r_i = -r_i(\text{past history}, \text{fresh catalyst}) \quad (3.24)$$

The second method by which the precatalyst decomposition can be accounted for is separable kinetics. This method is a simpler approach because it separates the kinetic rate law from the precatalyst activity and creates an empirical catalytic activity parameter by which the catalyst decay over time can be measured [1]. The approach defines the precatalyst activity as follows: Generally

$$-r_i = -r_i(\text{fresh catalyst}) * a(\text{past history}) \quad (3.25)$$

And more specifically the activity (a) is defined as the ratio of the rate of reaction at time t to the rate of reaction at the start of the run

$$a(t) = \frac{r_i(t)}{r_i(t=0)} \quad (3.26)$$

A first-order precatalyst decay law will be assumed for the efforts of this work and such a law can be expressed as follows:

$$\frac{da}{dt} = k_d * a \quad (3.27)$$

Integrated to give:

$$a(t) = EXP(-k_d t) \quad (3.28)$$

Combining the dissociative mechanism's rate law with the precatalyst decomposition:

$$r_{C_8} = \frac{dC_{c_8}}{dt} * a(t) = -k C_{c_8} C_{Ru_0} * EXP(-k_d t) \quad (3.29)$$

If we assume that the initial precatalyst concentration remains constant throughout the reaction equation 29 reduces to:

$$r_{C_8} = \frac{dC_{c_8}}{dt} * a(t) = -k_{obs} C_{c_8} * EXP(-k_d t) \quad (3.30)$$

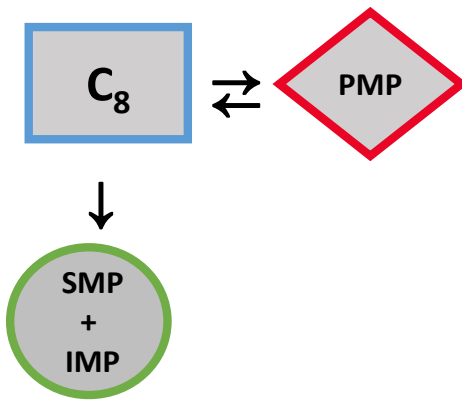
where k_{obs} represents the pseudo-kinetic constant for the reaction in (t^{-1}).

Thus far a model was obtained to account for the 1-octene consumption, precatalyst concentration and the decay thereof, the only aspect still unaccounted for is the distribution of products formed and their rates of reaction.

From the findings of chapter 2 the following main product distribution was obtained:



To simplify the reaction network the components were grouped together to create a set of pseudo-components as follows: $7-C_{14}$ and C_2 are lumped as primary metathesis products, all isomerisation, secondary self-metathesis and cross metathesis side-products are lumped as side-products (SMP) and the 1-octene remains as is.



The next step is to use this reaction network and accounts for the reversibility, as well as secondary product formation. For an irreversible system without the presence of precatalyst decay the set of equations used are similar to those of Van der Gryp [17]:

$$\frac{dC_{C8}}{dt} = -k_1 C_{C8} + k_2 C_{PMP} - k_3 C_{C8} \quad (3.32)$$

$$\frac{dC_{PMP}}{dt} = k_1 C_{C8} - k_2 C_{PMP} \quad (3.33)$$

$$\frac{dC_{SMP}}{dt} = k_3 C_{C8} \quad (3.34)$$

Including the precatalyst decay term:

$$\frac{dC_{C8}}{dt} = -k_1 C_{C8} * EXP(-k_d t) + k_2 C_{PMP} - k_3 C_{C8} * EXP(-k_d t) \quad (3.35)$$

$$\frac{dC_{PMP}}{dt} = k_1 C_{C8} * EXP(-k_d t) - k_2 C_{PMP} \quad (3.36)$$

$$\frac{dC_{SMP}}{dt} = k_3 C_{C8} * EXP(-k_d t) \quad (3.37)$$

Should the system be an irreversible process due to the possible escape of gasses formed during sampling then:

$$\frac{dC_{C8}}{dt} = -k_1 C_{C8} * EXP(-k_d t) - k_3 C_{C8} * EXP(-k_d t) \quad (3.38)$$

$$\frac{dC_{PMP}}{dt} = k_1 C_{C8} * EXP(-k_d t) \quad (3.39)$$

$$\frac{dC_{SMP}}{dt} = k_3 C_{C8} * EXP(-k_d t) \quad (3.40)$$

Typically observed reaction rate constants have an inherent dependence on temperature. According to Grubbs the kinetic constants for **G1** and **G2** are generally dependent upon the precatalyst concentration (related to the dissociated phosphine ligand concentration) [27]. Van der Gryp, however, pointed out that literature failed to describe the dependence of the observed rate constants on temperature [17].

Grubbs precatalysts are sensitive to temperature and as a result, the dependence of the temperature and precatalyst concentration on the observed reaction rate constants will be explored.

The temperature dependence of the observed rate constants is assumed to follow the Arrhenius rate law and the original precatalyst concentration is included in the pre-exponential factor of the observed rate constants. The resulting Arrhenius equation is:

$$k_{obs} = k_i C_{Ru_0} \text{EXP}\left(-\frac{E_a}{R * T}\right) \quad (3.41)$$

Now that the possible rate laws have been developed, they have to be tested by regression.

3.3.2 Mathematical and statistical methods

In order to determine the constant parameters for the kinetic rate law a number of mathematical methods were applied. The rate law (mathematical model) was regressed to fit the experimental data using a nonlinear least squares method employed in the MATLAB® computational software suite. The Idea behind the algorithm is to effectively minimise the distance between the estimated model and the actual experimental data points as far as possible [39]. This is a common technique used for non-linear curve fitting problems [39]. The algorithm followed to obtain the kinetic model parameters will briefly be discussed. The problem, of course, is the differential nature of the rate law and the three state variables that need to be fitted simultaneously. The problem can thus be defined mathematically as:

$$r_i = \frac{dC_i}{dt} = f(k_i(T), (C_i \dots n), C_{cat}, a(t)) \quad (3.42)$$

where:

r_i = rate of reaction of species i (min^{-1})

C_i = concentration of species i in mol (%)

k_i = kinetic model parameters

C_{cat} = catalyst concentration

a = precatalyst activity

T = temperature

t = time.

The experimental data obtained from the activities of Chapter 2 are concentration (mol %) versus time graphs and represent the solution of the differential equation that is defined in equation 3.1. Mathematically the rate law function first has to be solved so as to start fitting the model to the data but since there are more than one species included in the rate equations the equation is a

matrix rather than a single scalar equation and equation 3.1 rather becomes a system of equations defined as follows:

$$\mathbf{r} = \frac{d\mathbf{C}}{dt} = f(\mathbf{k}(T), C_i, \dots, C_{cat}, a(t)) \quad (3.42)$$

where the parameters in bold represent matrices. The system first had to be solved before it could be compared to the experimental data. This was achieved via numeric integration by applying the 4th and 5th order Runge-Kutta algorithm [39]. The Runge-Kutta algorithm (ode45) was chosen based on a decision table (Table 3.2) as provided in the MATLAB documentation [40]. This algorithm is well suited to non-stiff systems with medium level accuracy. The solution was obtained by providing the Ordinary Differential Equation (ODE) solver with an initial estimate and specifying the chosen mathematical model under investigation.

Once the algorithm has iteratively solved the system of ODEs the solution response can be represented as \mathbf{y}_i and the regression model as follows [41]:

$$\mathbf{y} = g(\boldsymbol{\beta}; \mathbf{x}_i) + \mathbf{e}_i \quad i = 1, 2, \dots, n \quad (3.43)$$

where \mathbf{y}_i = the response of the original experimental data

$\boldsymbol{\beta}$ = the model coefficients which can be related to $[\mathbf{k}]$ in Eq 3.42

\mathbf{x}_i = the model predictors or $[\mathbf{C}]$,

\mathbf{e}_i = the model error

The next step is to apply the least squares fit to compare the model response to the reaction data. The comparison is made by a simple elementwise subtraction of the model value from the value of the experimental data value at the corresponding time. The result is a list of residuals which are used as the objective function. The function effectively squares the residuals and aims to minimise the sum of those residuals to obtain the optimal parameter estimates ($\hat{\boldsymbol{\beta}}$). It can be expressed as follows [41]:

$$\text{Min}(OB) = \sum (y_i - g(\boldsymbol{\beta}; \mathbf{x}_i))^2 = \hat{\boldsymbol{\beta}} \quad (3.43)$$

Naturally, an optimisation algorithm needs to be selected that would suit the problem. A Simple comparison table [42] was used to determine which algorithm would be suitable for this study. Since the algorithm needed to be able to handle constraints and the function is non-linear, the least squares options were considered applicable. The smooth non-linear functions could also be used, but the degree of accuracy and the speed of the *fminsearch* and *fminunc* solvers were not

desirable when resampling had to be applied [40]. As a result, to account for any constraints and obtain reasonable accuracy without the loss of speed the *lsqlnonlin* solver was chosen.

Table 3.2: Solver decision table [42]

Constraint type	Objective		
	Least Squares	Smooth Nonlinear	Non-smooth
<i>None</i>	mldivide, lsqcurvefit, lsqlnonlin	lminsearch, fminunc	fminsearch
<i>Bound</i>	lsqcurvefit, lsqlin, lsqlnonlin, lsqnonneg	fminbnd, fmincon, fseminf	fminbnd
<i>Linear</i>	lsqlin	fmincon, fseminf.	-
<i>General smooth</i>	fmincon	lmincon, fseminf	-

In the least-squares non-linear algorithm as provided by MATLAB, the Function is based on the trust-region-reflective algorithm for constrained cases and the Levenberg-Marquardt equation for unconstrained cases [43]. In brief, the trust-region-reflective algorithm searches for a direction in which it should move inside a certain environment around a given starting point. The algorithm only progresses along a chosen direction if the latest function value of the objective function is less than the previous iteration's result. If the constraint is not satisfied the algorithm reflects the region in which it is searching to find an alternative direction [42].

The Levenberg-Marquardt equation is more robust and less sensitive to initial parameter guesses but it has a drawback in that it cannot accept bound constraints, furthermore the sparsity encountered in some datasets of this work warrants the use of the trust-region-reflective algorithm [43]. The Levenberg-Marquardt algorithm and the trust-region reflective algorithms are both trust-region algorithms, however the trust-region-reflective algorithm is very effective in the respect that it can follow negative curvatures well resulting in a faster and more efficient solution. [44-47]

The principle behind these algorithms are to minimise the objective function using a directional derivative method. The method is rather a combination of the Gauss-Newton method and the steepest descent direction method, therefore, making the algorithm more robust and efficient [44].

The results obtained from the regression algorithm can often vary depending on the starting point of the function, moreover, the confidence intervals and goodness of fit must be determined before an estimated parameter could be accepted.

Traditionally the way to determine the goodness of fit for a regression is by the use of the Pearson squared correlation coefficient, but Rhinehart suggests to rather use statistical tests for bias (for non-linear regression) since the traditional methods are designed upon assumptions of ideal linear regression situations.

Rhinehart [41] recommends repeating the regression runs for n amount of data sets n times in order to create a statistical distribution of estimated values from which the optimal parameters could be chosen. There is also the issue of over-parameterizing [41]. In such cases, the obtained regression parameters are meaningless and often do not make fundamental sense, for that reason several models were compared in the Model framework (Appendix E). The characteristics of each are listed in the framework as well.

Time and resources make it unreasonable to repeat N number of experiments and regressing the same set of empirical data N -times would only yield the same optimal parameter results [41]. By adding a normalised error term and resampling the data, however, a number of new “synthetic” data sets can be created to which the model can be compared so as to find the bounds of the fit, the statistical mean and standard deviation of the parameter estimates [41]. The bootstrap algorithm is an elegant resampling method and is the method of choice employed in the regression of the kinetic parameters for the model equations developed. The bootstrap algorithm is a resampling with replacement technique that provides an added advantage of higher accuracy as compared to classical resampling techniques. The bootstrap algorithm was employed by first finding the residuals from the initial vertical least squares fit defined as follows:

$$\hat{y} = g(\hat{\beta}; x_i) \quad (3.44)$$

and subtract from the original response to get:

$$e = y_i - \hat{y}_i \quad (3.45)$$

centre these residuals by taking the mean of the residuals

$$\tilde{e} = e - \bar{e} \quad (3.46)$$

where:

$$\bar{e} = \frac{1}{m} \cdot \sum (e_i) \quad (3.47)$$

Sample with replacement from

$$\tilde{e} = \{\tilde{e_1}, \tilde{e_2}, \dots, \tilde{e_m}\} \quad (3.48)$$

To get

$$\tilde{\mathbf{e}}^* = \{\tilde{\mathbf{e}}_1^*, \tilde{\mathbf{e}}_2^*, \dots, \tilde{\mathbf{e}}_m^*\} \quad (3.49)$$

Create the bootstrap samples

$$\mathbf{y}^* = g(\hat{\boldsymbol{\beta}}; \mathbf{x}) + \tilde{\mathbf{e}}^* \quad (3.50)$$

Recalculate the model parameters with the bootstrap data set

$$\text{Min}(OB) = \sum (\mathbf{y}_i^* - g(\boldsymbol{\beta}; \mathbf{x}_i))^2 = \hat{\boldsymbol{\beta}}^* \quad (3.51)$$

Equations 6 to 9 are recalculated repeatedly n times to get

$$\{\hat{\boldsymbol{\beta}}_1^*, \dots, \hat{\boldsymbol{\beta}}_n^*\} \quad (3.52)$$

The dataset of estimated model parameters can then be used to determine basic statistic parameters i.e. 95% confidence interval, standard deviation and sample mean [48].

The overall algorithm is presented in Figure 3.10

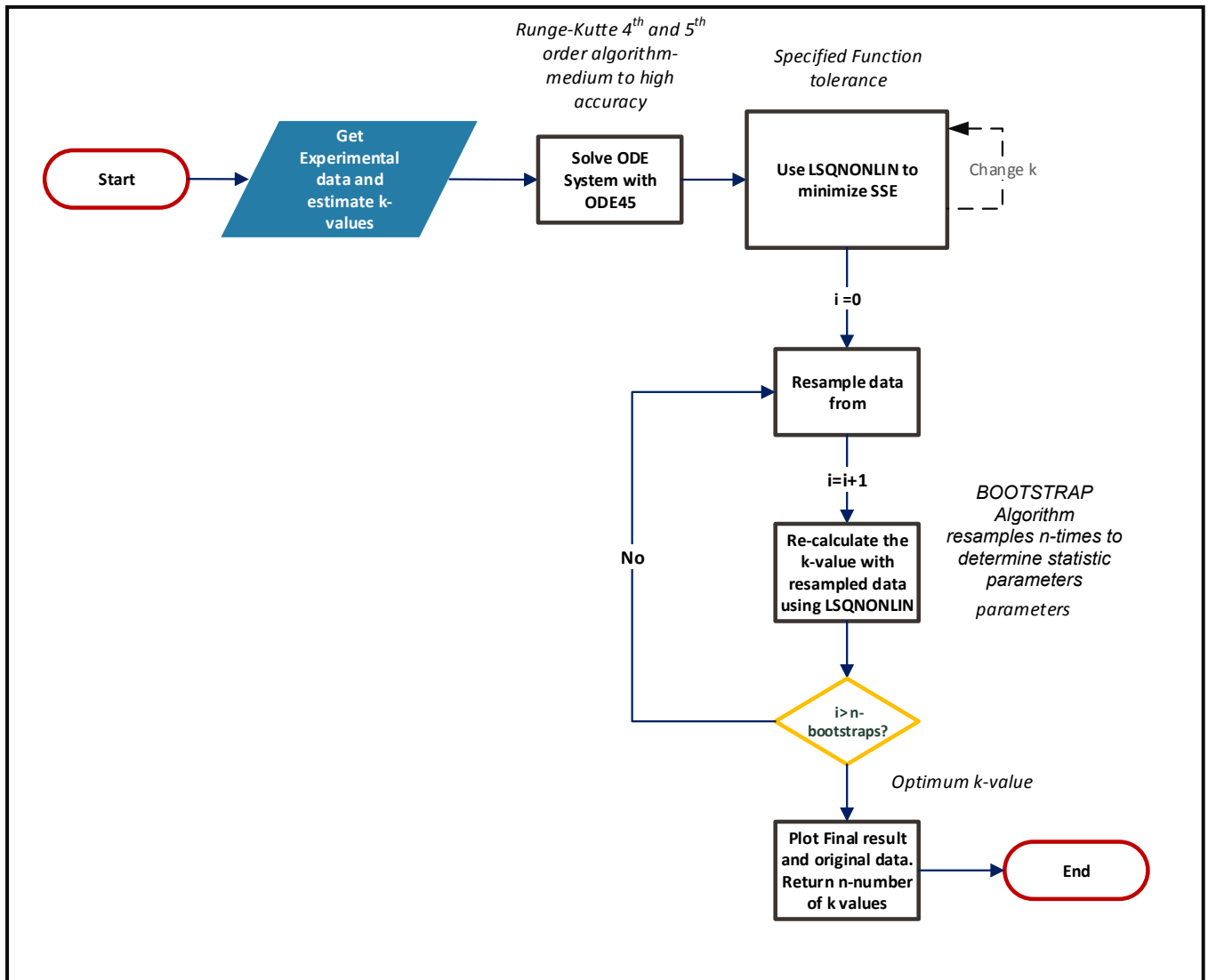


Figure 3.10: Regression algorithm

Naturally, the algorithm's effectiveness had to be validated before any regression results could be trusted. As a result, a dummy set of data was developed based on a hypothetical reaction scheme mimicking the reaction system of the current study. A simple randomised scatter was applied to the data which was used as the input to the regression algorithm. The known parameters were compared to the estimated parameters and the results obtained are presented

in the following tables and figures. Similarly, the irreversible rate law in combination with precatalyst deactivation kinetics was used to mimic the behaviour of the system. The regressed results and statistics are presented in Table 3.3 -Table 3.4 and Figure 3.11- Figure 3.12.



Table 3.3: Comparison between parameters obtained and defined

	k₁	k₂	k₃
Defined	0.030	0.020	0.001
Estimated	0.0341	0.0243	0.0012
\bar{x}	0.0341	0.0242	0.0012
SD	0.001	0.0009	0.0001

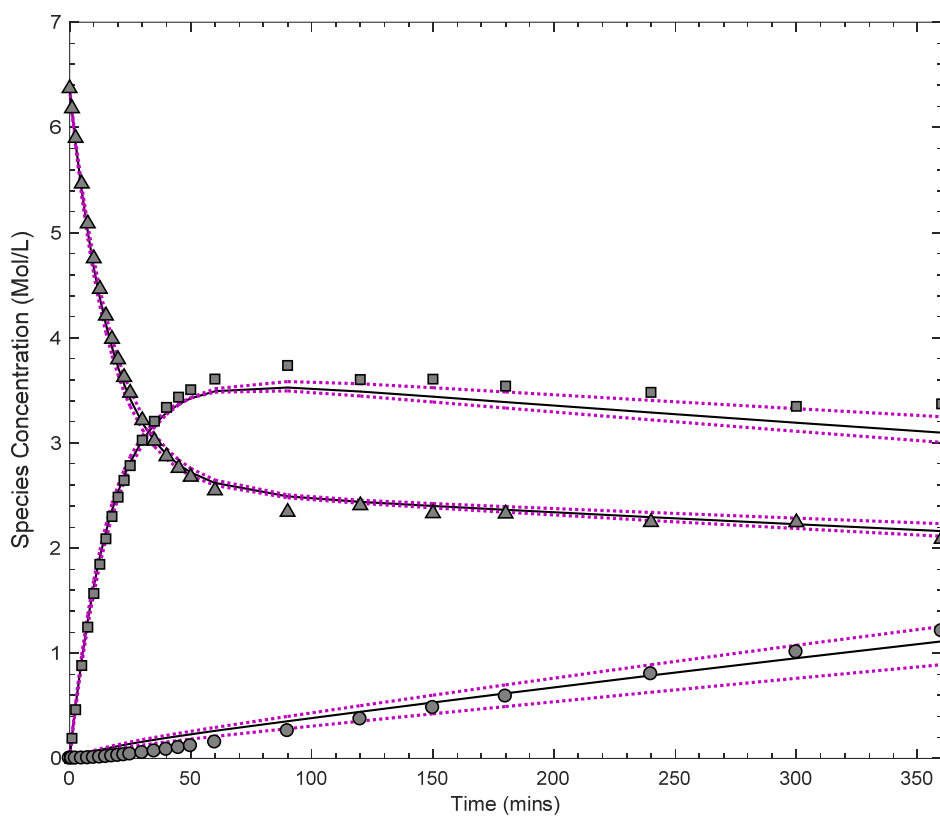


Figure 3.11 Reversible reaction rate regression tool verification

Figure 3.11 and Table 3.3 represent the results obtained by applying the model rate laws in equations 3.32-3.34 to the simulated concentration curves. Consequently, for the catalyst deactivation model rate laws Table 3.4 and Figure 3.12 was obtained.

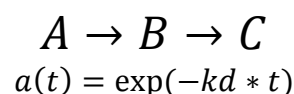


Table 3.4 Comparison of parameters obtained and defined for the catalyst deactivation model rate laws

	k_1	k_3	k_d
Defined	0.03	0.004	0.03
Estimated	0.031	0.004	0.034
\bar{x}	0.034	0.044	0.036
SD	0.001	0.001	0.001

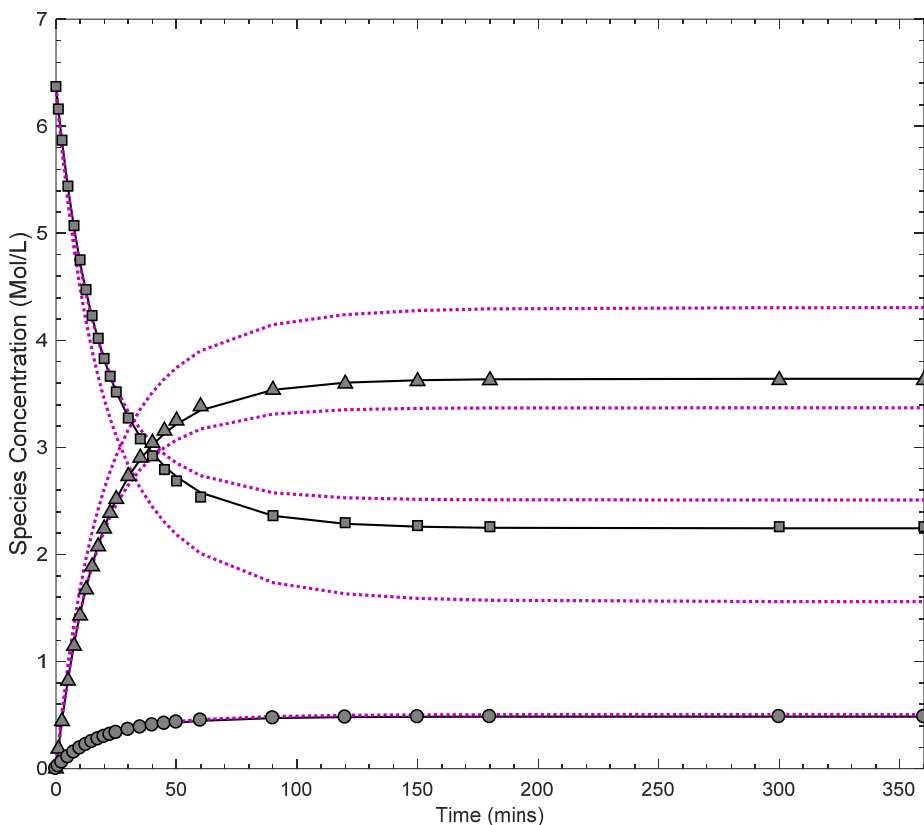


Figure 3.12: Irreversible reaction rate with precatalyst deactivation regression tool verification

From the results shown in Figure 3.11-Figure 3.12 and Table 3.3 and Table 3.4 it is evident that the regression algorithm is able to find the estimated parameters with accuracy and precision. Comment on the non-linearity aspect of the data can be made here when comparing the concentration profile for species C. The reversible model in Figure 3.11 predicts the formation of side-products as a positive linear trend, whereas the irreversible and deactivated precatalyst model predicts a logarithmic trend in Figure 3.12

Consequently, each model was applied to the empirical data for the **GCYC** and **GMPP** precatalysts, and the solution with the least deviation in the predicted regression constants was selected.

Once the observed kinetic constants were determined the Arrhenius equation was linearised yield:

$$\ln\left(\frac{k_{i,obs}}{C_{Ru}}\right) = \left(-\frac{E_a}{R}\right) * \left(\frac{1}{T}\right) + \ln(K_i) \quad (3.53)$$

The observed kinetic constant parameters were regressed to fit equation 3.53 using a two-way ANOVA regression [48]. The results of which are provided in section 3.4

3.4 Regression results and discussion

The results obtained from the kinetic model regressions for each of the precatalysts studied in this work are presented. The kinetic behaviour of the precatalysts is compared based on the influence of temperature and precatalyst load on the rate of species formation, activation energy, and precatalyst decomposition. Possible behaviour is explained, mechanisms are proposed and discussed, and results are compared to commercial precatalysts

3.4.1 GCYC precatalyst

This following section will briefly present and discuss the results of the kinetic regression activities. Overall the **GCYC** precatalyst has displayed deactivation behaviour. The empirical data obtained in chapter 2 was used in combination with models developed in section 3.3 to obtain the observed rate constants. The calculated regression results for varied temperature are presented in Figure 3.13. The calculated optimal observed rate constants were used to compare the model prediction to the original data sets. A summary of the final optimal constants is provided in Table 3.5 along with the standard deviations of the bootstrap results and the 95% confidence intervals.

3.4.1.1 Varied temperature

Table 3.5: Calculated observed rate constants for varying temperature with the GCYC precatalyst at C₈/Ru =10 000

	Observed Rate Constant (min ⁻¹)	Standard Deviation (σ)	95% Confidence Interval
40 °C			
k ₁	0.00016	0.02180	4.31×10 ⁻⁴
k ₂	-0.00140	1.05195	7.76×10 ⁻³
k ₃	3.80×10 ⁻⁷	0.00003	6.26×10 ⁻⁵
50 °C			
k ₁	0.00348	0.00033	1.32×10 ⁻³
k ₂	0.00667	0.00094	3.60×10 ⁻³
k ₃	0.00011	0.00008	3.78×10 ⁻⁴
60 °C			
k ₁	0.00954	0.00133	4.97×10 ⁻³
k ₃	0.00041	0.00040	1.58×10 ⁻³
k _d	0.01125	0.00160	6.12×10 ⁻³
70 °C			
k ₁	0.04275	0.00299	1.07×10 ⁻²
k ₃	0.00290	0.00102	3.80×10 ⁻³
k _d	0.02998	0.00184	7.08×10 ⁻³
80°C			
k ₁	0.07563	0.00357	1.40×10 ⁻²
k ₃	0.02148	0.00271	1.05×10 ⁻²
k _d	0.05150	0.00222	8.64×10 ⁻³
90°C			
k ₁	0.231589	0.08547	3.47×10 ⁻¹
k ₃	0.031981	0.02214	9.25×10 ⁻²
k _d	0.476339	0.09828	3.99×10 ⁻¹
100°C			
k ₁	0.00526	0.00216	8.88×10 ⁻³
k ₃	0.00420	0.00094	3.47×10 ⁻³
k _d	0.14593	0.01565	6.10×10 ⁻²

The results from Table 3.5 were used to create the predicted reaction profiles and the predicted confidence bounds. These are visible in Figure 3.13 and Figure 3.14.

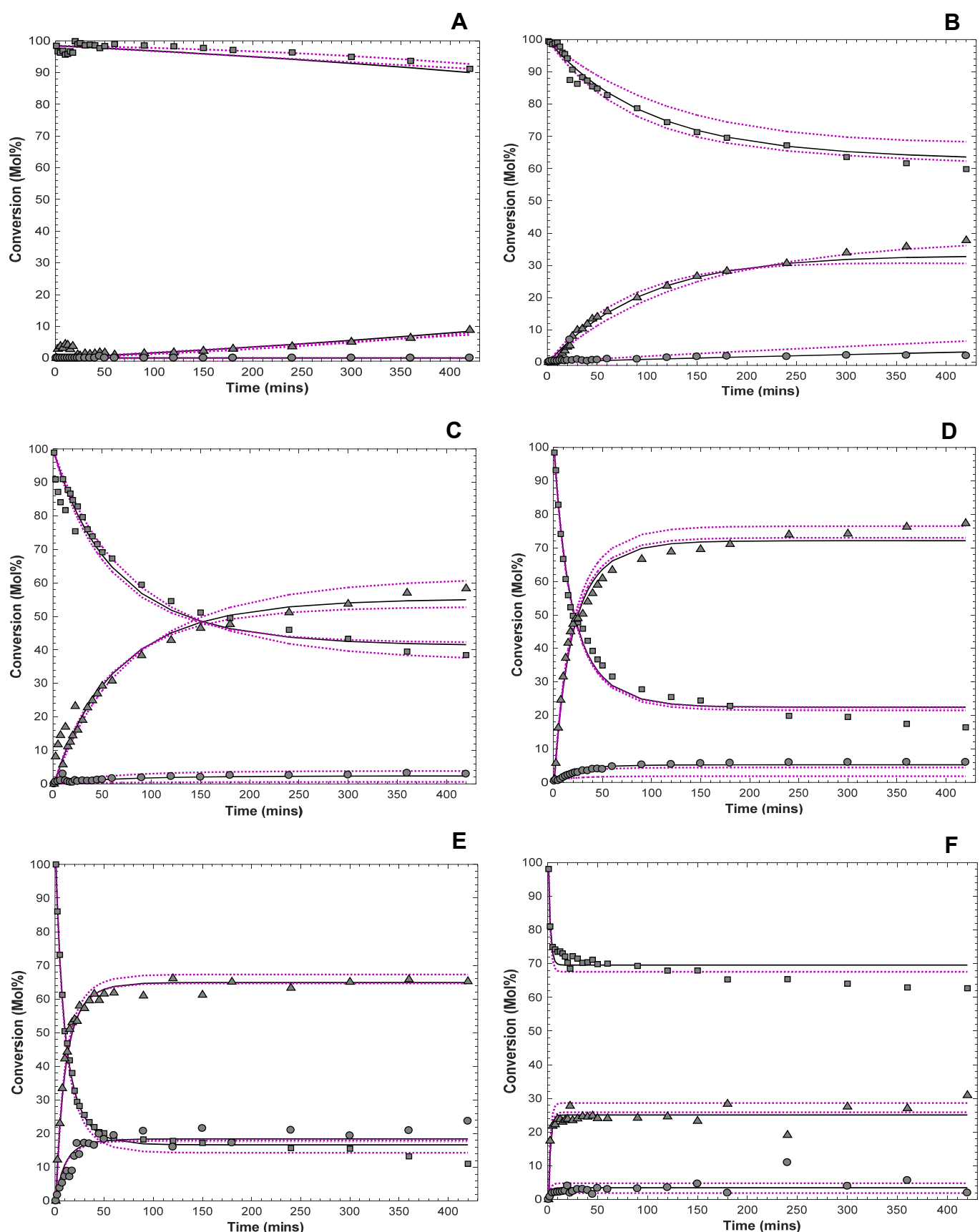


Figure 3.13: Experimental data compared to predicted rate laws for the metathesis of 1-octene with GCYC precatalyst at (A) 40 (B) 50 (C) 60 (D) 70 (E) 80 and (F) 90° C at C₈/Ru: 10 000. [■ 1-octene consumption, ▲ Primary metathesis product formation, ● Secondary product formation, — Predicted rate law, Prediction bounds]

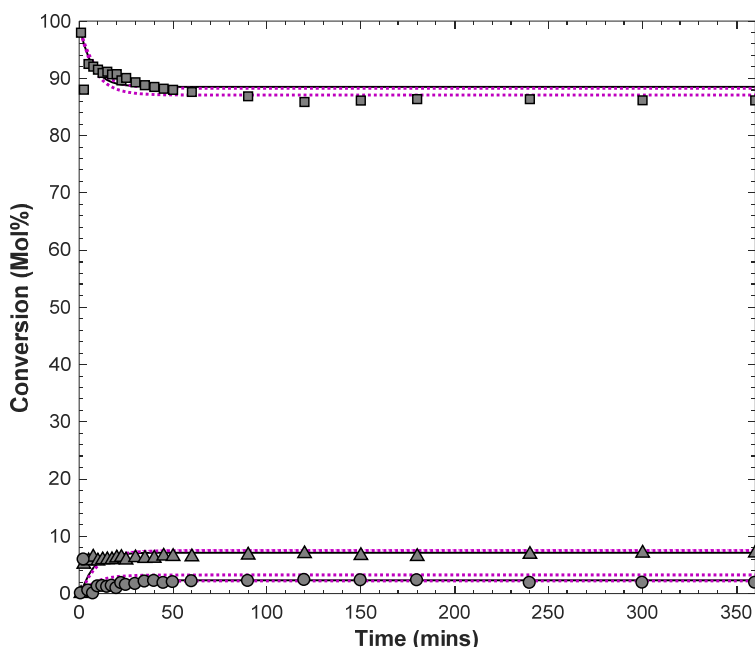


Figure 3.14: Experimental data compared to predicted rate laws for the metathesis of 1-octene with GCYC precatalyst at 100°C at C₈/Ru: 10 000. [■ 1-octene consumption, ▲ Primary metathesis product formation, ● Secondary product formation, — Predicted rate law, Prediction bounds]

It is clear that the regressed model parameters are suitable to describe the empirical data's behaviour. The precatalyst deactivation rate laws proved to be more accurate in predicting the non-linearity of the side-product formation in combination with the damped product formation after decomposition has taken place. The deactivation rate model fitted the data better for reactions higher than 50 °C. Thus, indicating that the precatalyst deactivation is indeed largely temperature dependent as hypothesised in Chapter 2.

Hong [26] reported a deactivation rate constant of 0.126 min⁻¹ at 55°C for the **G2** precatalyst in comparison to the deactivation constant obtained at 60°C for the **GCYC** precatalyst as 0.012 min⁻¹. The **GCYC** precatalyst is more stable since the decomposition rate for the **GCYC** precatalyst is almost an order of 10 smaller than the **G2** precatalyst. Hong attributed the decomposition to a nucleophilic attack and phosphine dissociation mechanism that results in ruthenium hydride complexes.

The presence of these complexes could possibly explain the production of side-products. The question is rather since there are no phosphine species present in the **GCYC** precatalyst, what mechanism would explain the precatalyst deactivation at higher temperatures?

Work by Louie [49] has shown that thermal degradation could be a possible cause for the formation of isomers and Van der Gryp attributed the isomers formed by the **Gr2Ph** precatalyst to an alkyl-based isomerisation mechanism.

Van der Gryp's work [17], however, did not model the reaction system with precatalyst deactivation, but rather expanded the number of kinetic parameters and rate laws to regress to the data. At 50°C, the authors reported the pseudo-kinetic rate constant for 1-octene consumption as $0.01962 \pm 0.00009 \text{ min}^{-1}$ at $C_8/\text{Ru} = 10000$. The **GCYC** precatalyst's results at the same conditions yield a K_1 value of $0.00348 \pm 0.00033 \text{ min}^{-1}$ [17] by direct comparison it is evident that the rate of 1-octene consumption of **HG2** is possibly larger than that of the **GCYC** precatalyst, possibly explaining the reduced conversion of the **GCYC** precatalyst pointing to a more stable precatalyst. Jordaan [31] considered the initiation rates of the **GCYC** precatalyst but nonetheless reported a peak K_{init} as $2.82 \times 10^{-5} \text{ min}^{-1}$ at 80°C, thus confirming that the **GCYC** precatalyst's reaction rate is rather small in comparison to the commercial precatalysts.

3.4.1.2 Varied precatalyst load

The results from the regressions for the varied precatalyst load experiments with the **GCYC** precatalyst are presented in Table 3.6.

Table 3.6: Calculated observed rate constants for varying precatalyst load with the GCYC precatalyst at 70°C

	Observed Rate Constant (min^{-1})	Standard Deviation (σ)	95% Confidence Interval
$C_8/\text{Ru} = 5000$			
k_1	0.03219	0.00286	1.18×10^{-2}
k_3	0.00411	0.00108	4.23×10^{-3}
k_d	0.02532	0.00209	7.93×10^{-3}
$C_8/\text{Ru} = 7000$			
k_1	0.01896	0.00131	5.24×10^{-3}
k_3	0.00103	0.00045	1.77×10^{-3}
k_d	0.01647	0.00116	4.76×10^{-3}
$C_8/\text{Ru} = 12000$			
k_1	0.00499	0.00085	3.38×10^{-3}
k_2	0.01806	0.00369	1.38×10^{-2}
k_3	-0.00011	0.00008	2.85×10^{-4}
$C_8/\text{Ru} = 14000$			
k_1	0.01526	0.00080	3.13×10^{-3}
k_2	0.01112	0.00084	3.26×10^{-3}
k_3	-0.00003	0.00011	4.35×10^{-4}

The results of the model fits for varied precatalyst load are presented in Figure 3.15

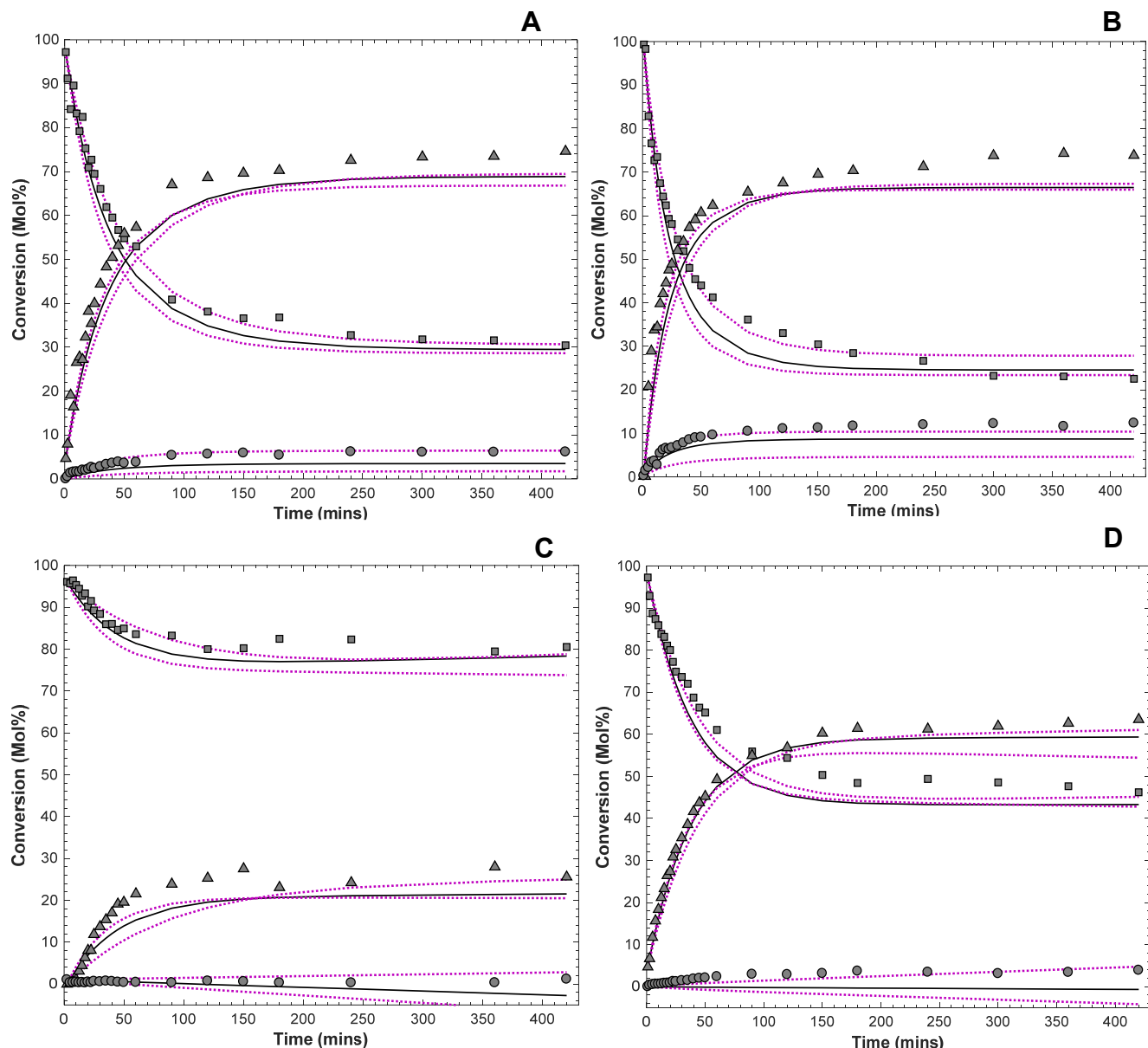


Figure 3.15 Experimental data compared to predicted rate laws for the metathesis of 1-octene with GCYC precatalyst at (A) 5000, (B) 7000 (C) 12000 and (D) 14000 at 70°C [■ 1-octene consumption, ▲ Primary metathesis product formation, ● Secondary product formation, — Predicted rate law, Prediction bounds]

It can easily be deduced that proposed reaction rate laws fit the experimental data well since the most data is found in the prediction bounds. The non-linear behaviour of the secondary product formation rates is better described by the rate models that account for the precatalyst deactivation.

The cases where the reversible rate reaction as proposed by Van der Gryp [17] were better suited to describe the data where the formation of secondary metathesis products was rather small in comparison to the primary metathesis products. At lower precatalyst concentrations, the precatalyst deactivation model did not describe the system well, even though precatalyst decomposition was found to be present in cases of higher precatalyst concentration at identical temperatures.

In such cases, the traditional irreversible reaction rate law was better suited to predicting the system behaviour

A possible reason for this occurrence could be that the deactivation is related to the amount of precatalyst present in the reaction environment. This means that the mechanism involves the decomposition of the methylidene complex as literature has shown to take place in **G2** type precatalysts [24-26].

However, the regression data also indicates that the precatalyst deactivation is temperature dependent. Thus, further exploration into the deactivation rate and the dependence thereof on precatalyst concentration and temperature is needed.

3.4.1.3 Describing the observed reaction rate constants.

It is postulated that, as in Van der Gryp's work [17], the observed rate constants will follow the relationship of Arrhenius as defined in Section 1.3.2.

The coefficients of the relationship (E_a and K_i) have been determined using regression and the linearised Arrhenius relationship from the observed parameter values between 40° and 90°C. The trends and parameters obtained are presented for the **GCYC** precatalyst in Table 3.7.

The key results of the regression and two-way ANOVA analyses is summarised in Table 3.7 and detailed information on the ANOVA analyses is provided in Appendix D.

Table 3.7: Regressed Arrhenius equation constants for GCYC precatalyst

	Coefficients	Units	MSE	F-Significance
K_1	7.073×10^{20}	$\text{mL} \cdot \text{mol}^{-1} \text{min}^{-1}$	0.378	0.001
E_a	30.24	$\text{kcal} \cdot \text{mol}^{-1}$		
K_2	1.728×10^{12}	$\text{mL} \cdot \text{mol}^{-1} \text{min}^{-1}$	0.171	0.039
E_a	16.86	$\text{kcal} \cdot \text{mol}^{-1}$		
K_3	1.635×10^{31}	$\text{mL} \cdot \text{mol}^{-1} \text{min}^{-1}$	1.724	0.002
E_a	48.28	$\text{kcal} \cdot \text{mol}^{-1}$		
K_d	1.04984×10^{16}	$\text{mL} \cdot \text{mol}^{-1} \text{min}^{-1}$	0.763	0.054
E_a	22.81	$\text{kcal} \cdot \text{mol}^{-1}$		

The results in Table 3.7 provide an overall picture of the temperature dependence of the observed kinetic parameters. From the different results in Table 3.5, it can be concluded that the optimal temperature range in which to operate the reactor is a very narrow 70°-80°C.

This will favour the forward reaction in producing PMPs but hamper the secondary product formation since the activation energy required to produce SMPs is higher. Lower temperatures will favour the reverse reaction. One aspect to point out, however, is that the reaction will marginally almost always experience precatalyst deactivation even at the optimum temperature of 70°C.

The key lies in minimising the precatalyst deactivation but maximising the PMP formation. The **GCYC** precatalyst is highly sensitive to temperature and because the precatalyst deactivation reaction requires less energy to proceed than the forward reaction ($E_f > E_d$) precatalyst deactivation is inevitable but can be kept at a minimum by stringent temperature control.

To display the effect of precatalyst deactivation and the temperature dependence of the observed K values an example of the linearised Arrhenius regression plot is provided in Figure 3.16.

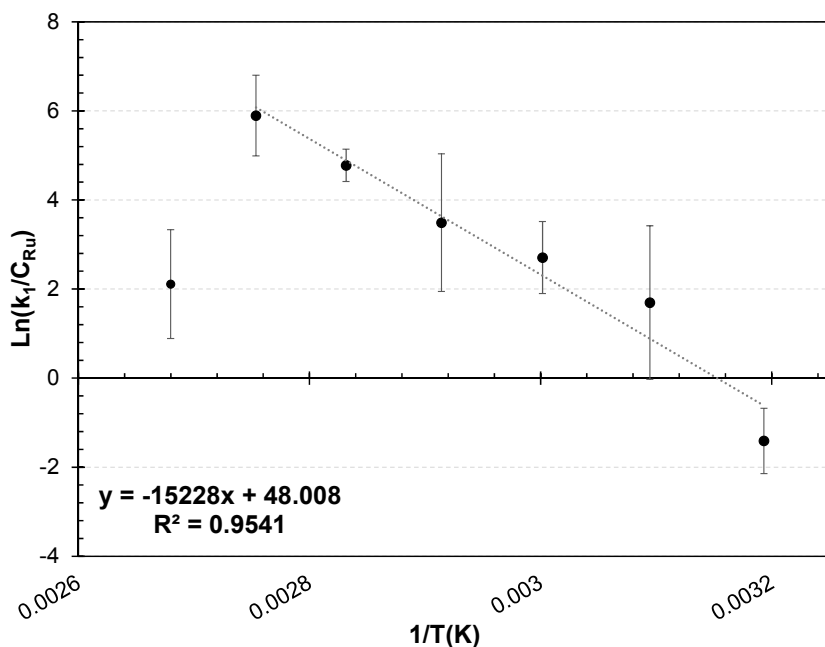


Figure 3.16: Linearised Arrhenius plot of K_1

Jordaan [31] noted an exponential trend for k_{init} . The same trend has been observed for k_1 as is evident in Figure 3.16 for this work resulting in a linear semi-log Arrhenius relationship. Jordaan investigated the H-NMR spectra for neat 1-octene reactions with the **GCYC** precatalyst to gain a better understanding of the mechanism. Three important species were identified in their work as complexes that would influence the mechanism, i.e. benzylidene, heptylidene and methylidene species (coordinated, uncoordinated, and open) [31]. During the NMR reactions, they observed a sharp decrease in the benzylidene carbene species to yield either an uncoordinated benzylidene or methylidene and heptylidene species.

The heptylidene signal was found to increase up to 24 mins but the methylidene signal continued to increase up to 3 hours, thereafter a gradual decrease was observed which was attributed to either precatalyst decomposition or the formation of uncoordinated methylidene intermediates [31].

Jordaan [31] also reported that the SMP for the **GCYC** precatalyst increases exponentially beyond 70 °C for the **GCYC** precatalyst. The K_3 value of the rate model that relates to the forward isomerisation and secondary product metathesis for this work displayed a linear semi-log Arrhenius plot within the margin of prediction errors (Appendix C). This means that the K_3 values also follow an exponential trend as temperature increases, however at temperatures from 90 °C to 100 °C a sharp decrease in the reaction rate constant is observed, showing that the reaction has slowed down considerably, which as Jordaan has hypothesised [31] could be because of precatalyst deactivation and was confirmed by the rate laws modelled in this work.

A similar structural precatalyst as investigated by du Toit [33] have shown a K_3 value of 49.59 kcal.mol⁻¹ which is very close to the value obtained for the **GCYC** precatalyst. It is possible that the mechanism that proceeds towards the formation of side metathesis products for du Toit is precatalyst and the **GCYC** precatalyst correspond. du Toit suggested a dissociation mechanism and compared to the work of Jordaan the results indicated towards the dissociation mechanism being more energetically favourable.

Some comment is to be made on the aspect of the irreversibility of the rate law model that fitted the decomposed precatalyst data the best. Literature has shown that the presence of ethene could contribute to the deactivation process in substrate induced precatalyst deactivation, but the presence of ethene could also favour the reverse reaction [35]. The activation energies obtained indicated however that at lower temperatures the latter case would be more likely since less energy is required for the reverse reaction to occur, but for higher temperatures, the precatalyst deactivation mechanism is temperature related and the occurrence thereof is dominant as opposed to the reversible reaction.

When considering the effects of precatalyst load on the reaction constants the effect was mostly observed in the nonlinear regression trends. Lower precatalyst concentrations did not show precatalyst deactivation in comparison to the higher concentrations. This could mean that the amount of precatalyst present affects the deactivation since there would be more active species available in the reaction environment and the presence of these increased numbers could indicate that the precatalyst decomposition also takes place via the interaction between precatalyst species

3.4.2 GMPP precatalyst

This following section will briefly present and discuss the results of the kinetic regression activities for the **GMPP** precatalyst. Overall the **GMPP** precatalyst has displayed less deactivation in comparison to the **GCYC** precatalyst. The empirical data obtained in Chapter 2 was used in combination with rate laws developed in Section 3.3 to obtain the observed rate constants. The calculated regression results for varied temperature are presented in Figure 3.17 and Figure 3.19. The calculated optimal observed rate constants were used to compare the model prediction to the original data sets. A summary of the final optimal constants is provided in Table 3.8 along with the standard deviations of the bootstrap results and the 95% confidence intervals.

3.4.2.1 Varied temperature

Table 3.8: Calculated observed rate constants for varying temperature with the GMPP precatalyst at C₈/Ru = 10 000

	Observed Rate Constant (min-1)	Standard Deviation (σ)	95% Confidence Interval
40°C			
k ₁	0.00063	0.04888	8.18×10 ⁻²
k ₂	0.00537	2.19920	3.36
k ₃	2.38×10 ⁻⁵	3.53×10 ⁻⁵	1.45×10 ⁻⁴
50°C			
k ₁	0.00072	0.04135	1.30×10 ⁻¹
k ₂	0.00430	0.55556	1.65
k ₃	1.59×10 ⁻⁵	6.92×10 ⁻⁵	3.32×10 ⁻⁴
60°C			
k ₁	0.00062	0.00025	1.30×10 ⁻³
k ₂	0.00443	0.00290	1.40×10 ⁻²
k ₃	-3.30×10 ⁻⁵	3.69×10 ⁻⁵	1.66×10 ⁻⁴
70°C			
k ₁	0.00272	0.00037	1.43×10 ⁻³
k ₂	0.00038	0.00063	2.47×10 ⁻³
k ₃	-1.19×10 ⁻⁴	1.22×10 ⁻⁴	4.84×10 ⁻⁴
80°C			
k ₁	0.00528	0.00081	2.94×10 ⁻³
k ₃	-0.00010	0.00026	1.04×10 ⁻³
k _d	4.59×10 ⁻³	9.53×10 ⁻⁴	3.69×10 ⁻³
90°C			
k ₁	0.00784	0.00079	-3.97×10 ⁻⁴
k ₃	0.00108	0.00029	6.07×10 ⁻⁴
k _d	5.78×10 ⁻³	9.19×10 ⁻⁴	-2.77×10 ⁻⁴

Table 3.8 (cont'd): Calculated observed rate constants for varying temperature with the GMPP precatalyst at C₈/Ru = 10000

	Observed Rate Constant (min ⁻¹)	Standard Deviation (σ)	95% Confidence Interval
100°C			
k ₁	0.00174	0.00042	1.98×10 ⁻³
k ₂	0.01250	0.00366	1.67×10 ⁻²
k ₃	1.57×10 ⁻⁴	5.28×10 ⁻⁵	2.34×10 ⁻⁴

The parameters in Table 3.8 correspond to the data curve fits presented in Figure 3.17 and Figure 3.18

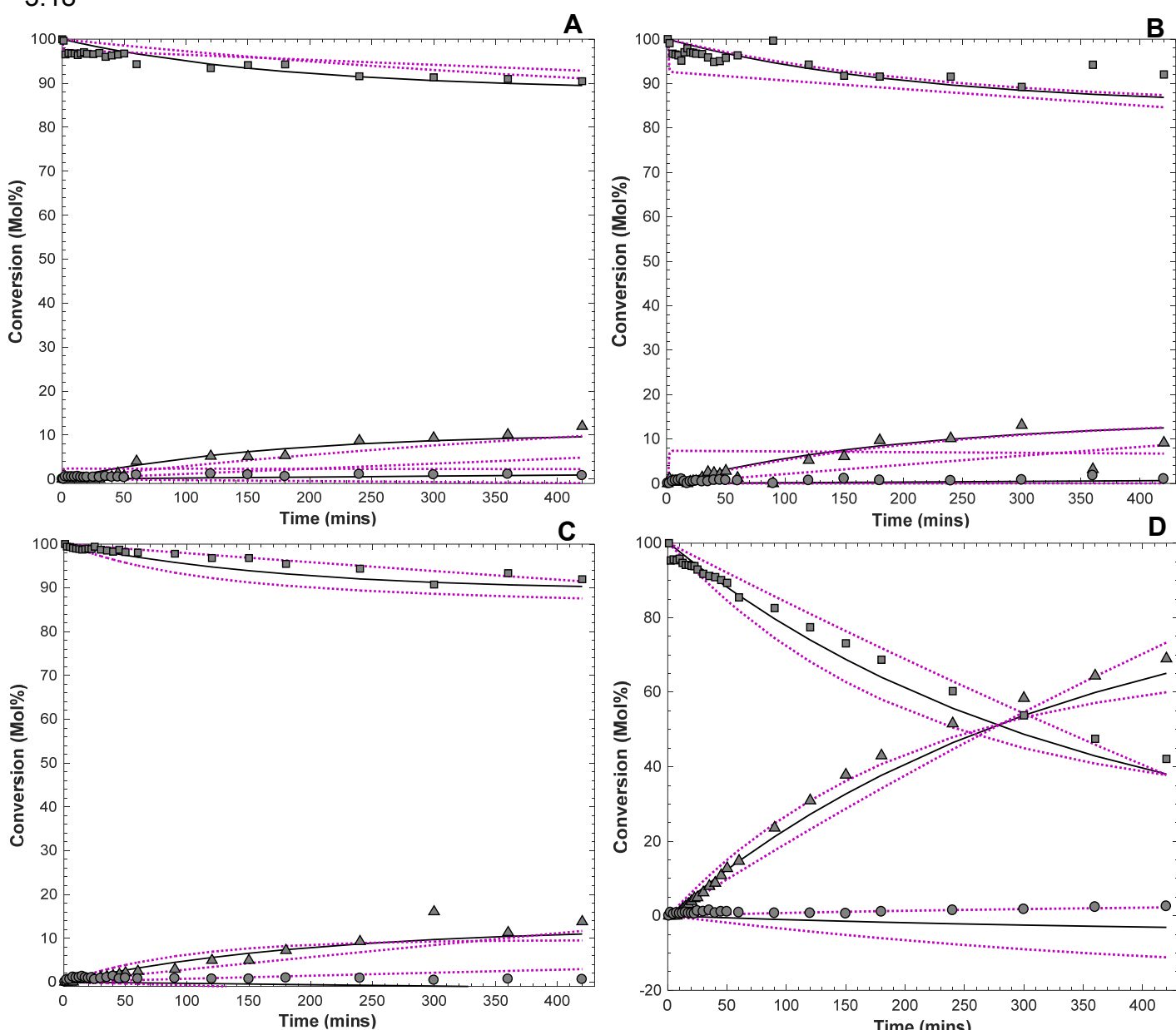


Figure 3.17: Experimental data compared to predicted rate laws for the metathesis of 1-octene with GCYC precatalyst at (A) 40°C, (B) 50°C (C) 60°C and (D) 70°C at C₈/Ru: 10 000. [■ 1-octene consumption, ▲ Primary metathesis product formation, ● Secondary product formation, — Predicted rate law, Prediction bounds]

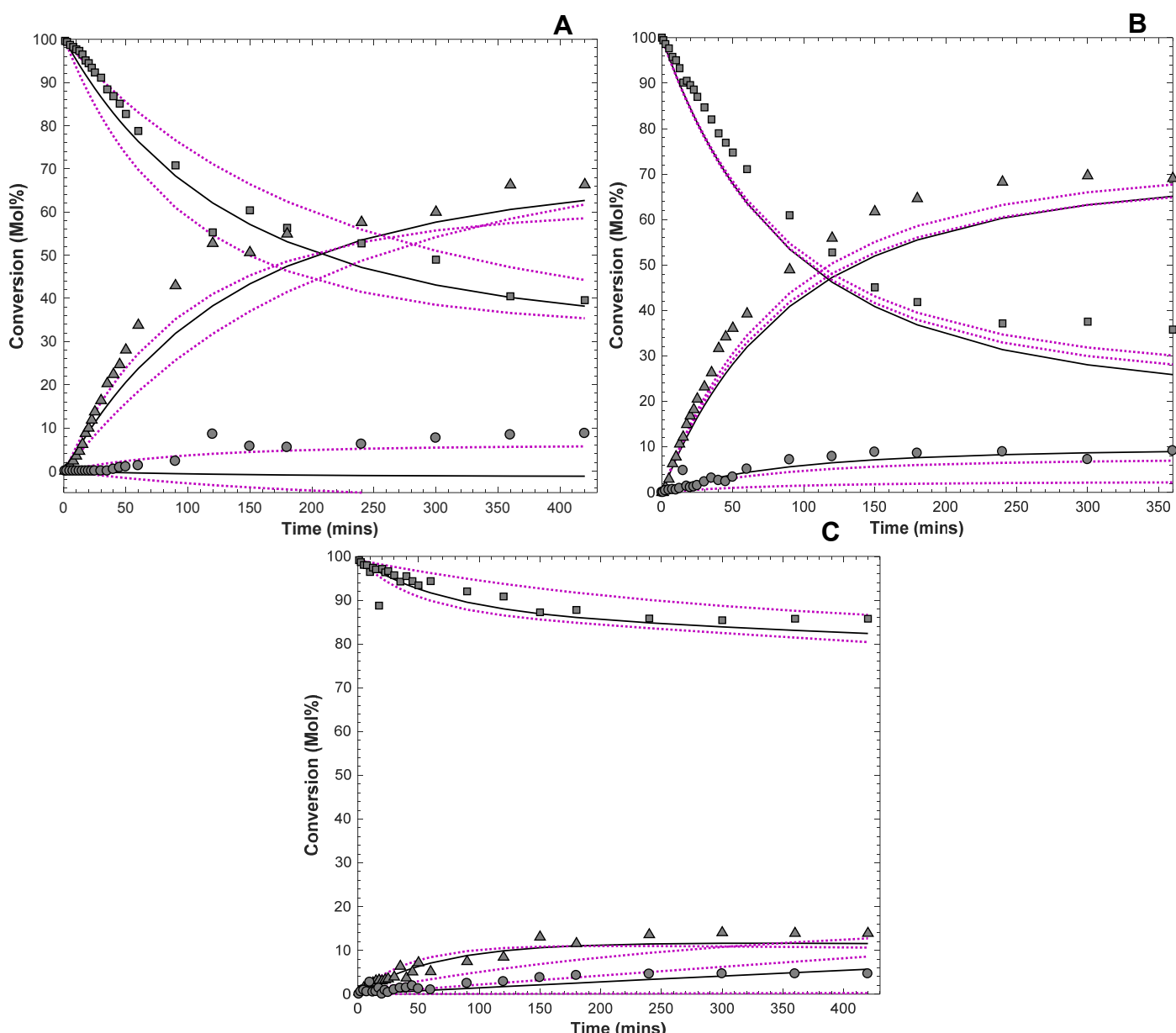


Figure 3.18: Experimental data compared to predicted rate laws for the metathesis of 1-octene with GMPP precatalyst at (A) 80 °C, (B) 90 °C (C) 100 °C at C₈/Ru: 10 000 [■ 1-octene consumption, ▲ Primary metathesis product formation, ● Secondary product formation, — Predicted rate law, Prediction bounds

The results from the **GMPP** precatalyst did not show as much precatalyst decomposition as for the **GCYC** precatalyst at varying temperatures. If any, precatalyst decomposition rate laws only described reactions at 80 °C and 90 °C better than the irreversible rate law. The results indicate that the rate laws used describe the reaction behaviour well since the predicted trends follow the shape of the data and most data falls within the confidence interval of the predicted trends.

The **GMPP** precatalyst showed small forward reaction rates at lower temperatures almost all around the same order of magnitude and value (between 0.00062 and 0.0072 min⁻¹). Only beyond 70°C the observed reaction rate increases dramatically, thus indicating a thermal switchable reaction mechanism and a very latent precatalyst.

Examples of a thermal switchable precatalyst have been reported [19, 23, 47], but structurally and electronically the precatalysts could not be compared much. In comparison to commercial precatalysts, the **GMPP** precatalyst displays a smaller decomposition rate (0.00459min^{-1}) in comparison to 0.126min^{-1} as reported by Hong [26] for the **G2** precatalyst at $55\text{ }^\circ\text{C}$. At a much higher temperature, the **GMPP** precatalyst decomposes 2 orders of magnitude slower than the parent precatalyst **G2**. Thus, the **GMPP** precatalyst is a worthy opponent for the **GCYC** precatalyst albeit that the **GMPP** precatalyst provides lower yields and conversion (Chapter 2) the **GMPP** precatalyst is much more stable.

The influence of precatalyst load should also be considered in the precatalyst kinetics and the results of the non-linear activities are presented as an auxiliary to gaining understanding for the **GMPP** precatalyst's kinetic behaviour.

3.4.2.2 Varied precatalyst load

Table 3.9 summarises the regressed parameters for the non-linear data fits the rate laws and rate equations defined in Section 3.3.1.

Table 3.9: Calculated regression constants for GMPP precatalyst at various precatalyst loads at 70°C

	Observed rate constant (Min^{-1})	SD	95% CI
$C_8/\text{Ru} = 5000$			
k_1	0.00530	0.00048	1.92×10^{-3}
k_3	0.00093	0.00033	1.35×10^{-3}
k_d	-0.00004	0.00015	6.01×10^{-4}
$C_8/\text{Ru} = 7000$			
k_1	0.00426	0.00064	2.31×10^{-3}
k_3	0.00058	0.00047	1.81×10^{-3}
k_d	-0.00011	0.00016	6.47×10^{-4}
$C_8/\text{Ru} = 12000$			
k_1	0.00228	0.00048	1.79×10^{-3}
k_2	0.00017	0.00068	2.64×10^{-3}
k_3	-0.00024	0.00012	4.69×10^{-4}
$C_8/\text{Ru} = 14000$			
k_1	0.00172	0.00027	1.06×10^{-3}
k_2	0.00124	0.00074	2.91×10^{-3}
k_3	-0.00010	0.00008	3.19×10^{-4}

The predicted parameters summarised above were used to construct prediction plots and compared to the reaction data in a visual presentation. These plots are available in Figure 3.19.

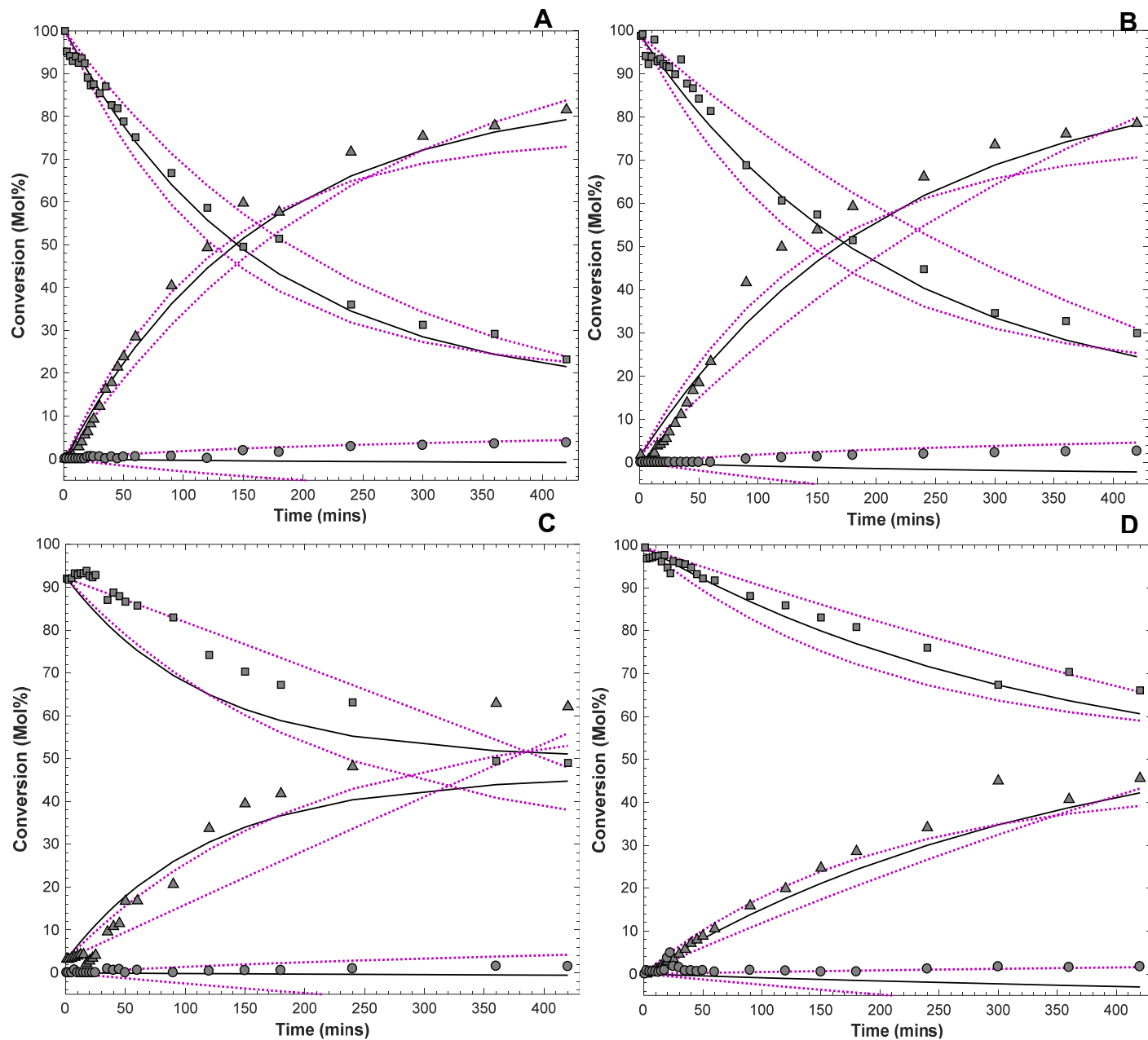


Figure 3.19: Modelled versus experimental data for the GMPP precatalyst at (A) 5000, (B) 7000 (C) 12000 and (D) 14 000 at 70°C . [■ 1-octene consumption, ▲ Primary metathesis product formation, ● Secondary product formation, — Predicted rate law, Prediction bounds]

3.4.2.3 Describing the observed reaction rate kinetics

The coefficients of the relationship (E_a and K_i) have been determined by the use of regression and the linearised Arrhenius relationship from the observed parameter values between 40° and 90°C. The trends and parameters obtained are presented for the GMPP precatalyst in the following Table 3.10. The key results of the regression and two-way ANOVA analyses are also summarised in Table 3.10.

Table 3.10: Regressed Arrhenius parameters for GMPP precatalyst

Coefficients		Units	MSE	F-Significance
K_1	$1.05 \times 10^{+9}$	$\text{mL} \cdot \text{mol}^{-1} \text{min}^{-1}$	0.010	0.083
E_a	13.10	$\text{kcal} \cdot \text{mol}^{-1}$		
K_2	$3.13 \times 10^{+3}$	$\text{mL} \cdot \text{mol}^{-1} \text{min}^{-1}$	0.097	0.139
E_a	3.84	$\text{kcal} \cdot \text{mol}^{-1}$		
K_3	$1.89 \times 10^{+13}$	$\text{mL} \cdot \text{mol}^{-1} \text{min}^{-1}$	0.392	0.017
E_a	22.07	$\text{kcal} \cdot \text{mol}^{-1}$		
K_d	$3.03 \times 10^{+4}$	$\text{mL} \cdot \text{mol}^{-1} \text{min}^{-1}$	0.026	-
E_a	5.84	$\text{kcal} \cdot \text{mol}^{-1}$		

The regressed activation energies for the **GMPP** precatalyst indicate that the **GMPP** precatalyst for temperatures between 70 and 90°C follows the Arrhenius relationship, but for the upper and lower temperature ranges the Arrhenius equation is unable to describe the trend. As an example, K_1 has been plotted against $1/T$ to demonstrate the Step function behaviour of the observed rate parameters. The fact that the **GMPP** precatalyst is so latent in its reaction indicates that the initiation reaction is the rate-determining step in the catalytic cycle.

Once the reaction has commenced the forward reaction requires much more energy than the reverse reaction ($E_1 > E_2$) thus the **GMPP** precatalyst will favour the reverse reaction at lower temperatures. In contrast, the forward reaction would continue until enough energy is added to supply the SMP reaction (E_3) with enough to produce the observed production of secondary metathesis products, but higher temperatures will favour the side-product formation since the activation energy for that reaction is the largest. The precatalyst deactivation activation energy is very low meaning that at even at the milder reaction temperatures where the activity does occur the precatalyst will decompose, albeit very slowly. A comparison between the **GCYC** and **GMPP** precatalyst proves that the decomposition rate of the **GCYC** precatalyst is higher than that of the **GMPP** proving that as far as stability goes the **GMPP** precatalyst is the best choice

Tole *et al.* [34], synthesised precatalysts of similar hemilabile structures and varied the identity and the position of different functional groups on the hemilabile ligand, thus creating precatalysts of different levels of stability, steric bulk and electronic properties. Tole *et al.* [34] reported that activity only took place at 70 °C and higher, which compares well with the observations of the **GMPP** precatalyst.

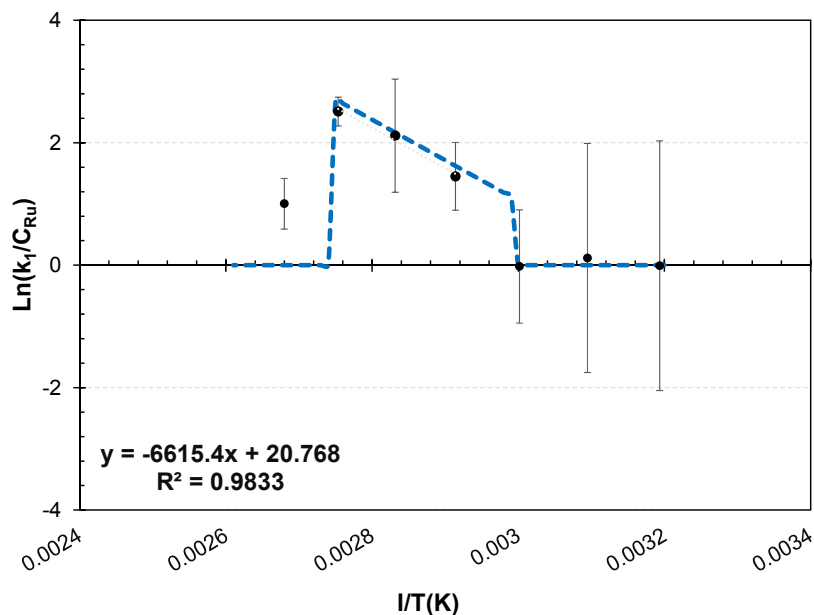


Figure 3.20: Step function Arrhenius behaviour of GMPP precatalyst observed kinetic parameters

The results from the linear regression fit for the linearised Arrhenius equation for K_i as shown in Figure 3.20 display step function behaviour, the step function behaviour has been observed for a sulphur substituted **HG2** type complex in literature [51], although the step-behaviour was only observed for conversion-time plots. The authors have attributed the step-behaviour to thermal switchability but did not investigate the kinetics of the system further to determine whether the step-behaviour was present in the reaction rate constant too.

The **GMPP** precatalyst has shown step behaviour for conversion and for the kinetic rate law parameters too. The linear decreasing section of the regression equation explains the variation in the parameters well with a variation in temperature (Pearson square correlation coefficient of 0.98) showing that at least for a temperature range between 70 and 90 °C the kinetic rate law parameters follow the Arrhenius equation. Beyond 90 °C, the kinetic constant no longer follows the linear trend and rather drastically decreases again showing that the precatalyst degrades swiftly at those temperatures.

The F-significance statistic for the regression activities for K_1 indicates that the probability of the trend being purely by chance is lower than 10% [44] indicating that for an empirical description of the observed kinetics the regression trends are suitable. A step function was formulated for future use when describing the kinetic behaviour of this precatalyst as follows:

$$k_{1obs} = \begin{cases} 0; T < 70^\circ C \\ 1.05E + 09e^{-\frac{13.10}{R.T}}; 70^\circ C < T < 100^\circ C \\ \leq 2; T \geq 100^\circ C \end{cases} \quad (3.53)$$

The **GMPP** precatalyst displayed typical latent behaviour, closely related to the work by Tole *et al.* [34], however, deactivation does take place beyond 90 °C as opposed to what Tole found for their precatalysts. The obvious question is now: what is the implication of the deactivation kinetics and how does it compare to the **GCYC** precatalyst?

3.5 Concluding remarks

The findings in this chapter have provided some interesting trends and relationships. The first is that including precatalyst deactivation kinetics require comparison against traditional models to screen for the presence of deactivation. Precatalyst deactivation only takes place at certain conditions.

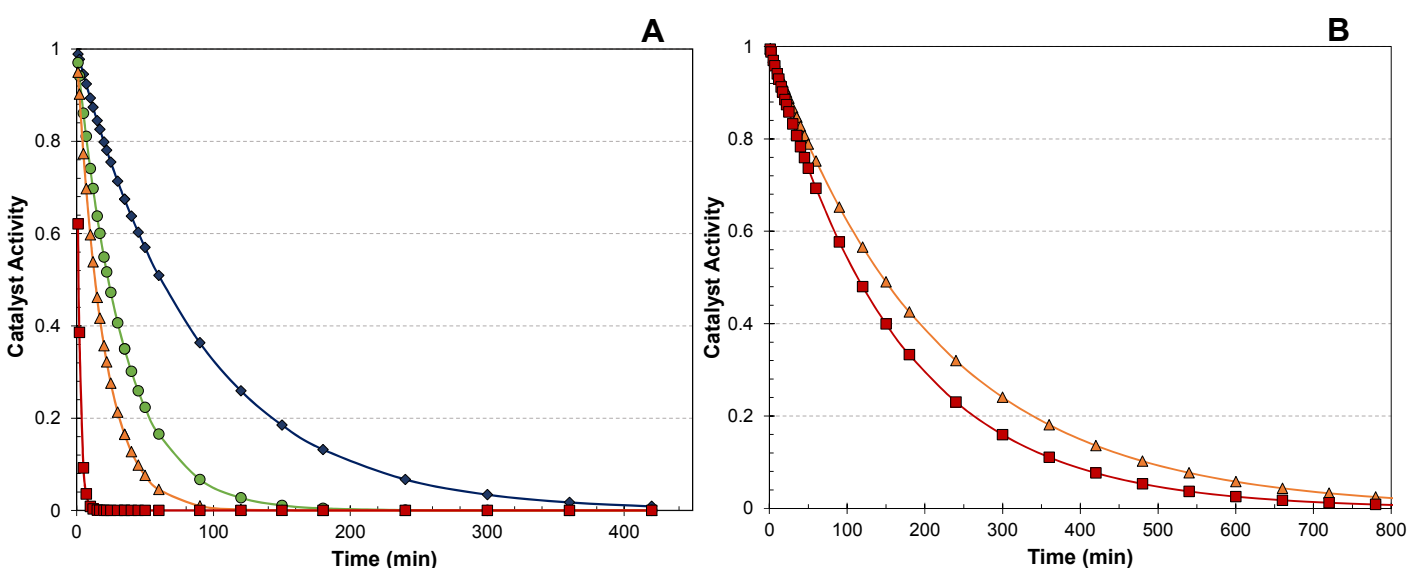


Figure 3.21: Estimated catalytic activity vs time for the A) GCYC and B) GMPP precatalysts at
◆ 60°C ● 70°C ▲ 80°C ■ 90°C

The **GCYC** precatalyst requires a very narrow operation range within which optimal results can be obtained. Precatalyst decomposition is inevitable even at optimum temperatures, however, the **GCYC** precatalyst reacts sooner than the **GMPP** precatalyst and produces higher conversions and yield. The **GCYC** precatalyst starts to deactivate at lower temperatures demonstrating that it is less stable than the **GMPP** precatalyst.

As a comparison, the precatalyst activity was plotted against time for both the **GCYC** and the **GMPP** precatalyst at the temperatures at which each has experienced deactivation. The result is displayed in Figure 3.21. It is evident that the **GMPP** precatalyst takes twice as long to deactivate compared to the **GCYC** precatalyst.

Mahahle [29] has constructed similar plots to fit the systems in her work and has found that the deactivation rates start at lower temperatures and the deactivation rate also increases with an increase in temperature.

Some comment is to be made on the use of the terms “deactivation”, “decomposition”, “decay” or “degradation”. The nature of the description of this phenomenon in the scope of this work is an empirical one and the term is used interchangeably to describe the observed loss in conversion and activity. The best theoretical model to describe the observed loss in activity and conversion of the empirical data was that of an assumed first-order decay model. In describing the empirical results and quantifying the kinetic parameters related to those results the models applied have succeeded. What was not explored however, is the characterising the exact species in the propagation and/or activation cycle that are decomposing. Whether it is the precatalyst itself or the active catalytic species inside the propagation mechanism, and further investigation would be required. Furthermore- a lifetime study in which the catalysts are re-used and recycled in subsequent reactions would also be able to provide a clearer indication of the exact catalytic species that are decomposing and if such decomposition is irreversible.

Now that the kinetic behaviour, activity, selectivity, conversion and yield has been determined for both these precatalysts the best way to compare their performance is to determine the economic potential that they hold.

3.6 References

- [1] H.S. Fogler, Elements of Chemical Reaction Engineering, Prentice-Hall, 2011.
- [2] D. Y. Murzin and T. Salmi, Catalytic Kinetics: Chemistry and Engineering, Elsevier, 2016.
- [3] Y. Chauvin, Olefin metathesis: the early days, *Angew. Chemie - Int. Ed.* 45 (2006) 3760–3765.
- [4] K. Grela, Olefin metathesis: theory and practice, 1st ed., Wiley, New Jersey, 2013.
- [5] C. Adlhart, P. Chen, Mechanism and activity of ruthenium olefin metathesis catalysts: the role of ligands and substrates from a theoretical perspective, *J. Am. Chem. Soc.* 126 (2004) 3496–3510.
- [6] J.I. Toit, C.G.C.E. Van Sittert, H.C.M. Vosloo, Metal carbenes in homogeneous alkene metathesis : computational investigations, *J. Organomet. Chem.* 738 (2013) 76–91.
- [7] E.L. Dias, S.T. Nguyen, R.H. Grubbs, Well-defined Ru olefin metathesis catalysts: mechanism and activity, *J. Am. Chem. Soc.* 119 (1997) 3887.
- [8] M.S. Sandford, J.A. Love, R.H. Grubbs, Mechanism and activity of ruthenium olefin metathesis catalysts, *J. Am. Chem. Soc.* 123 (2001) 6543–6554.

- [9] D.J. Nelson, S. Manzini, C.A. Urbina-Blanco, S.P. Nolan, Key processes in ruthenium-catalysed olefin metathesis., *Chem. Commun. (Camb)*. 50 (2014) 10355–75.
- [10] K.M. Engle, G. Lu, S.X. Luo, L.M. Healing, M.K. Takase, P. Liu, K.N. Houk, R.H. Grubbs, Origins of initiation rate differences in ruthenium olefin metathesis catalysts containing chelating benzylidenes, *J. Am. Chem. Soc.* 137 (2015) 5782–5792.
- [11] I.W. Ashworth, I.H. Hillier, D.J. Nelson, J.M. Percy, M.A. Vincent, Olefin metathesis by grubbs–hoveyda complexes: computational and experimental studies of the mechanism and substrate-dependent kinetics, (2013).
- [12] A.K. Chatterjee, T.L. Choi, D.P. Sanders, R.H. Grubbs, A general model for selectivity in olefin cross metathesis, *J. Am. Chem. Soc.* 125 (2003) 11360–11370.
- [13] E. Pump, A. Poater, M. Zirngast, A. Torvisco, R. Fischer, L. Cavallo, C. Slugovc, Impact of electronic modification of the chelating benzylidene ligand in cis-dichloro-configured second-generation olefin metathesis catalysts on their activity, *Organometallics*. 33 (2014) 2806–2813.
- [14] T. Vorfalt, K.-J. Wannowius, H. Plenio, Probing the mechanism of olefin metathesis in Grubbs-Hoveyda and Grela type complexes, *Angew. Chem. Int. Ed. Engl.* 49 (2010) 5533–6.
- [15] G.C. Vougioukalakis, R.H. Grubbs, Ruthenium-based heterocyclic carbene-coordinated olefin metathesis catalysts, *Chem. Rev.* 110 (2010) 1746–1787.
- [16] V. Thiel, M. Hendann, K.-J. Wannowius, H. Plenio, On the mechanism of the initiation reaction in Grubbs- Hoveyda complexes, *J. Am. Chem. Soc.* 134 (2012) 1104–1114.
- [17] P. Van der Gryp, S. Marx, H.C.M. Vosloo, Journal of Molecular Catalysis A : Chemical Experimental , DFT and kinetic study of 1-octene metathesis with Hoveyda – Grubbs second generation precatalyst, "Journal Mol. Catal. A, Chem. 355 (2012) 85–95.
- [18] P. Van Der Gryp, Separation of Grubbs-based catalysts with nanofiltration, North-West University, Potchefstroom, Phd Thesis, 2008.
- [19] R.M. Thomas, A. Fedorov, B.K. Keitz, R.H. Grubbs, Thermally Stable, Latent Olefin Metathesis Catalysts, *Organometallics*. 30 (2011) 6713–6717.
- [20] M. Jordaan, H.C.M. Vosloo, Ruthenium catalyst with a chelating pyridinyl-alcoholato ligand for application in linear alkene metathesis, *Adv. Synth. Catal.* 349 (2007) 184–192.
- [21] M. Jordaan, P. van Helden, C.G.C.E. van Sittert, H.C.M. Vosloo, Experimental and DFT investigation of the 1-octene metathesis reaction mechanism with the Grubbs 1 precatalyst, *J. Mol. Catal. A Chem.* 254 (2006) 145–154.
- [22] A. Szadkowska, A. Makal, K. Woz, R. Kadyrov, K. Grela, Ruthenium olefin metathesis initiators bearing chelating sulfoxide ligands, *Organometallics* (2009) 2693–2700.
- [23] A. Szadkowska, X. Gstrein, D. Burtscher, K. Jarzembska, K. Woźniak, C. Slugovc, K. Grela, Latent thermo-switchable olefin metathesis initiators bearing a pyridyl-functionalized chelating carbene: Influence of the leaving group's rigidity on the catalyst's performance, *Organometallics*. 29 (2010) 117–124.
- [24] H.H. Soon, A.G. Wenzel, T.T. Salguero, M.W. Day, R.H. Grubbs, Decomposition of ruthenium olefin metathesis catalysts, *J. Am. Chem. Soc.* 129 (2007) 7961–7968.
- [25] A. Young, M.A. Vincent, I.H. Hillier, J.M. Percy, T. Tuttle, Forming a ruthenium isomerization catalyst from Grubbs II: a DFT study, *Dalton Trans.* 43 (2014) 8493–8498.

- [26] S.H. Hong, D.P. Sanders, C.W. Lee, R.H. Grubbs, Prevention of olefin isomerization during olefin metathesis reactions., Abstr. Pap. 229th ACS Natl. Meet. San Diego, CA, United States, March 13–17, 2005. (2005) ORGN-080.
- [27] M. Ulman, R.H. Grubbs, Relative reaction rates of olefin substrates with ruthenium (II) carbene metathesis initiators, *Organometallics*. 17 (1998) 2484–2489.
- [28] J.A. Love, M.S. Sanford, M.W. Day, R.H. Grubbs, Synthesis, structure, and activity of enhanced initiators for olefin metathesis, *J. Am. Chem. Soc.* 125 (2003) 10103–10109.
- [29] M.M.D. Mahahle, Isomerisation of alkenes using metal carbenes and related transitional metal complexes, Potchefstroom Universiteit vir Christelike Hoër onderwys, PhD Thesis 2005.
- [30] W. Janse, V. Rensburg, P.J. Steynberg, M.M. Kirk, W.H. Meyer, G.S. Forman, Mechanistic comparison of ruthenium olefin metathesis catalysts: DFT insight into relative reactivity and decomposition behaviour, *J. Organomet. Chem.* 691 (2006) 5312–5325.
- [31] M. Jordaan, Experimental and Theoretical Investigation of New Grubbs-type Catalysts for the Metathesis of Alkenes, PhD Thesis, North-West University, Potchefstroom, 2007.
- [32] M.M. Loock, The alkene metathesis reactivity of the PUK-Grubbs 2-precatalyst, North-West University, PhD-Thesis, 2009.
- [33] J.I. du Toit, P. van der Gryp, M.M. Loock, T.T. Tole, S. Marx, J.H.L. Jordaan, H.C.M. Vosloo, the Industrial viability of homogeneous olefin metathesis: Beneficiation of linear alpha olefins with the diphenyl-substituted pyridinyl alcoholato ruthenium carbene precatalyst, *Catal. Today*. 275 (2016) 191–200.
- [34] T. Tole, J. du Toit, C. van Sittert, J. Jordaan, H. Vosloo, Synthesis and application of novel ruthenium catalysts for high-temperature alkene metathesis, *Catalysts*. 7 (2017) 22.
- [35] H.J. Van Der Westhuizen, A. Roodt, R. Meijboom, Kinetics of thermal decomposition and of the reaction with oxygen, ethene and 1-octene of first generation Grubbs' catalyst precursor, *Polyhedron*. 29 (2010) 2776–2779.
- [36] O. Levenspiel, *Chemical Reaction Engineering*, Wiley, 1999, 566-609.
- [37] A.H. Hoveyda, A.R. Zhugralin, The remarkable metal-catalysed olefin metathesis reaction, *Nature*. 450 (2007) 243–251.
- [38] T. Ritter, A. Hejl, A.G. Wenzel, T.W. Funk, R.H. Grubbs, A Standard System of Characterization for Olefin Metathesis Catalysts, (2006) 5740–5745.
- [39] M.E. Davis, *Numerical Modelling for chemical engineers*, John Wiley & Sons, Ltd, New York, 1984.
- [40] L.F. Shampine, M.W. Reichelt, The Matlab ode suite, (2016) 1–22.
- [41] R.R. Rhinehart, *Nonlinear Regression Modeling for Engineering Applications*, John Wiley & Sons, Ltd, Chichester, UK, 2016.
- [42] MATHWORKS Inc., Constrained Nonlinear Optimization Algorithms - MATLAB & Simulink, <https://www.mathworks.com/help/optim/ug/constrained-nonlinear-optimization-algorithms.html> (accessed April 27, 2017).

-
- [43] MATHWORKS Inc., Solve nonlinear least-squares (nonlinear data-fitting) problems - MATLAB lsqnonlin, <https://www.mathworks.com/lsqnonlin.html?requestedDomain=www.mathworks.com> (accessed April 27, 2017).
 - [44] Coleman, T.F. and Y. Li. "On the Convergence of Reflective Newton Methods for Large-Scale Nonlinear Minimization Subject to Bounds." *Mathematical Programming*, 67 (1994) 189–224.
 - [45] Moré, J. J. "The Levenberg-Marquardt Algorithm: Implementation and Theory." *Numerical Analysis*, ed. G. A. Watson, Notes in Mathematics 630, Springer Verlag, 1977, pp. 105–116.
 - [46] F. Van den Berghen, Levenberg-Marquardt algorithms vs Trust Region algorithms, *Methods*. (2004) 3–6.
 - [47] Y. Yuan, A Review of Trust Region Algorithms for Optimization, *Iciam*. 99 (2000) 271–282.
 - [48] R. Peck, C. Olsen, J.L. Devore, *Introduction to Statistics and Data Analysis*, Cengage Learning, Boston, 2016.
 - [49] J. Louie, R.H. Grubbs, Reactivity of Electron-Rich Carbene Complexes, *Organometallics*. (2002) 2153–2164.
 - [50] J.I. Du Toit, M. Jordaan, C.A.A. Huijsmans, J.H.L. Jordaan, C.G.C.E. Van Sittert, H.C.M. Vosloo, Improved metathesis lifetime: Chelating pyridinyl-alcoholato ligands in the second-generation Grubbs precatalyst, *Molecules*. 19 (2014) 5522–5537.
 - [51] A. Ben-Asuly, E. Tzur, C.E. Diesendruck, M. Sigalov, I. Goldberg, N.G. Lemcoff, A thermally switchable latent ruthenium olefin metathesis catalyst, *Organometallics*. 27 (2008) 811–813.

4 ECONOMIC POTENTIAL EVALUATION

“A man who could afford fifty dollars had a pair of boots that'd still be keeping his feet dry in ten years' time, while the poor man who could only afford cheap boots would have spent a hundred dollars on boots in the same time and would still have wet feet.”

~Terry Pratchett, Men at Arms: The Play

4.1 Overview

The aim of this chapter is to evaluate the GCYC and the GMPP catalysts on the basis of their economic potential. In section 4.2 the fundamental principles and industrial applications will be discussed and critically evaluated. Section 4.3 describes and elucidates the costing procedures and assumptions made for the economic potential evaluation at Level 1 through to 3. The last major section, Section 4.4, presents the results obtained from the Economic potential evaluations, discusses and compares the results from each catalyst. Chapter 4 is concluded with a summary.

4.2 Economic considerations: literature review

4.2.1 Introduction

Before a reaction or process can be commissioned to large-scale operations the process feasibility has to be questioned [1]. In the past economic aspects alone may have been sufficient for developments in the industry but modern processes have developed a new set of criteria on top of these. The core of these new criteria has mostly to do with the environmental impact of a process and the competitiveness thereof in relation to other processes [1].

Industrial chemists very often develop chemistry and reactions that are favourable from an R&D perspective but when process engineering becomes part of the development two core aspects need to be confronted in order of importance [1]:

- 1) Would the process be able to make money and is there a market?
- 2) What impact does the process have on the environment?

Some qualities that the field of metathesis has shown in this regard is that the reactions are equilibrium reactions, solvents are not necessary, the reactions are atom-efficient and nearly thermo-neutral. Stoichiometric waste is not created as in traditional synthetic processes and low-value feedstock can be used to create value-added products [1].

Process engineers ultimately need to answer the above questions in order to make key choices between alternatives and optimise the design [2]. In the proposed pathway of the conversion of low-value alkenes to Guerbet-type surfactants, this work focusses on the metathesis step. The purpose of this work is to evaluate the **GCYC** and **GMPP** catalysts on an economic level as well since it would be able to clearly distinguish one catalyst above the other. This chapter will address the design base and economic costing and evaluation process that has been followed around the metathesis reactor section.

4.2.2 Design approach

The first step that has to be taken in order to design a process is to choose an appropriate design base with which decisions will be made [3]. To find the best process, the design engineer is required to generate process flowsheets and evaluate them in order to determine which is best [2]. Many different strategies exist, and these can be classified into two main groups: the first is knowledge-based and the second is optimisation based [4].

Each of these process synthesis classes has their own advantages and disadvantages, but it is important to keep the definition of the problem in mind when choosing a design base. Since the purpose of this work is to gain knowledge about the best option between two catalysts, the focus is placed on the knowledge-based process design synthesis methods. A number of popular synthesis methods available are;

- Douglas's hierarchical approach [5]
- Smith and Linnhoff's onion-model approach [6]
- Turton *et al.*'s revolutionary approach [3]
- Sirola and Rudd's systematic approach [7]

The Douglas approach was followed for the economic evaluation in this chapter since it allows the designer to identify dominant design variables and facilitates the creation and evaluation of process alternatives with a hierarchical approach [8]. It also uses the concept of economic potential as a short-cut method to evaluate these process alternatives, an advantage compared to reducible methods such as the onion model. The major merit of the hierarchical approach is, therefore, that it creates a consistent framework [8] for developing and evaluating process alternatives. It is well suited to aid the development of the conceptual base-case design by assisting the decision-making process, it also provides room for design optimisation by means of eliminating non- or less-feasible designs [8]. This attribute of the Douglas method makes it suitable for the purposes of academia and this work: a comparative study between two metathesis precatalysts.

Douglas's hierarchical approach is defined by a selection of different design levels, approaching the design from the outside in. Typically, each level adds complexity to the design as the design progresses. The Douglas method consists of a number of questions that need to be answered in order to determine the direction in which the process design will flow. The levels and questions are summarised in Figure 4.1.

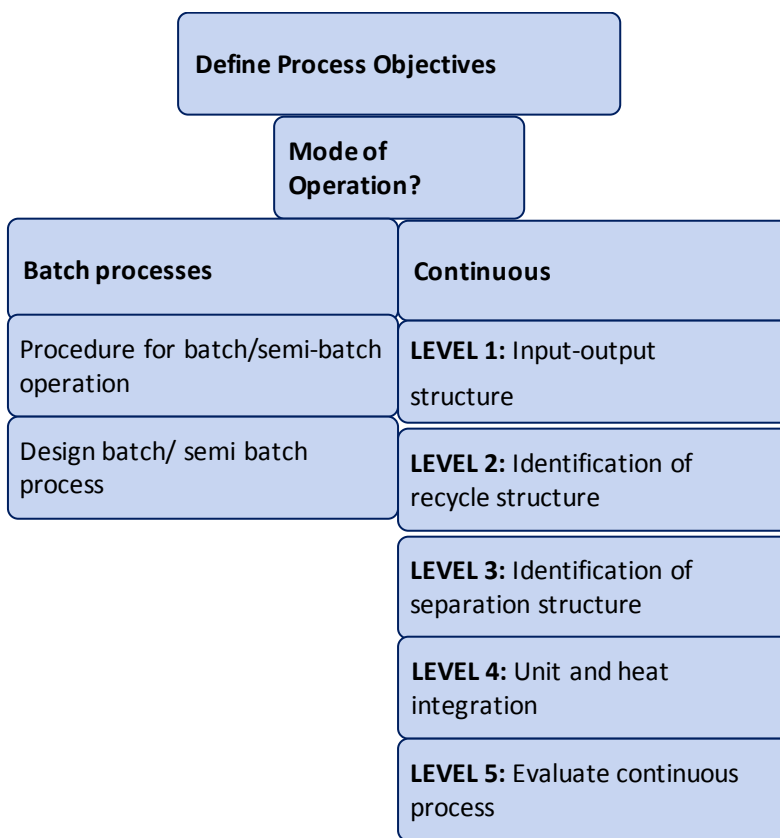


Figure 4.1: Hierarchical Douglas design method [5,8]

For the purposes of this work, the Douglas method has been applied up to level 3 in order to obtain a quick comparison between the **GCYC** and **GMPP** catalysts.

Levels of design and cost estimation

According to Douglas [5], there are a number of different levels of design in engineering; each level has its own estimation accuracy. The design methods range from rapid and simple but decreased levels of accuracy to detailed estimates that are as accurate as possible. The first design level is known as an order-of-magnitude estimate [5], which is based on similar previous cost data, the second level of cost estimation is known as the factored / study estimate which is based on the knowledge of major items of equipment [5]. Since the scope of the economic potential evaluation is purely for comparison between catalysts, the level of cost estimation followed in this work will be an order of magnitude estimation based on the known items of equipment that is chosen in the design process. The purpose of these order-of magnitude costings is to establish a short-cut comparison technique to facilitate discussions between the relevant fields' researchers (i.e. catalyst synthesis chemists and process engineers) to that end the objective is to obtain a brief comparison between two non-commercial and 1 commercial catalyst. Since more non-commercial catalysts exist, this order-of-magnitude costing technique

provides a quick way of filtering out catalysts that are not feasible enough to warrant a detailed techno-economic analysis.

The economic evaluation of the **GMPP** and **GCYC** catalysts is subdivided into two sections. The first section evaluates the economic potential against the reaction conversion using the empirical data obtained in chapter 2. Conversion versus economic potential plots are constructed and optimal reaction conditions are chosen for each respective catalyst.

The second section conducts a brief profitability analysis (discounted cash flow) for those optimal conditions and compares conversions, internal rates of return (IRR), returns on investment (ROI) and payback periods between the two catalysts.

4.2.3 Olefin metathesis in industry

Olefin metathesis is not a new concept and examples of applications in the industry do exist, but they are few in comparison to other synthetic chemistry methods. Improvements in the technology and identification of processes that focus on smaller and high-value products have kept the research interest on-going [10].

A comparison between the commercial processes discussed in literature [11] is presented in Table 4.1

Olefin metathesis may not be able to compete with the large-scale petrochemical operations but reactions such as ROMP provide niche products [9] that are favoured in markets such as the automotive and the sporting industries, some large niche-market operations have however found their place in the light olefins industry

A basic olefin that is in high demand globally, propene, is originally obtained from naphtha steam crackers [12]. It is usually produced as a co-product with ethylene as a result of catalytic cracking at refineries [12]. The global demand for propene is, however, too high for these processes to satisfy it. The Philips triolefin process produces propene from ethene and 2-butene. In the past, the Philips triolefin process was used to produce butene and ethene, but demand for these products have diminished [12]. Consequently, the process is currently operating in the reverse direction to produce propene and is known as the Olefins Conversion Technology process offered by CB&I Lummus Global [12].

The process (Figure 4.2) is fed with fresh and recycled butene which is then mixed with ethene before it is sent through a guard bed to remove the impurities [13]. The feed is then heated before it is sent to the metathesis reactor [13]. The reaction takes place in the presence of a heterogeneous fixed bed reactor over a mixture of WO_3/SiO_2 and MgO (for isomerization) at $>260^\circ\text{C}$ and 30-35 bar [13]. The plant can produce propylene with $>60\%$ conversion and approximately 92% selectivity towards propene. In 2004 upgrades to the process was completed to increase the propene output. The plant currently produces 350 ktpa at a cost of 200 USD per ton of propylene produced [14].

Other expansion projects and joint ventures utilising the OCT technology have been commissioned in Cajong, China, Osaka, Japan and Singapore [12].

Drawbacks of the OCT process are that the metathesis reactor requires high temperatures and pressures, and catalyst coking takes place.

The Shell Higher Olefins Process is the metathesis process that would stand in competition to the proposed reaction scheme of the research behind c^* change because of the specific range of alkenes that the SHOP produces. The SHOP process produces lighter $<\text{C}_6$ and heavier $>\text{C}_{18}$ terminal alkenes [15] by nickel-catalysed oligomerization of ethylene that is isomerised over a potassium metal catalyst. The resulting mixture is then metathesized over $\text{MoO}_3/\text{Al}_2\text{O}_3$ catalyst at $100^\circ\text{C}-125^\circ\text{C}$ and 10 bar to give a Schultz-Flory distribution of C_{11} to C_{14} linear alkenes [15].

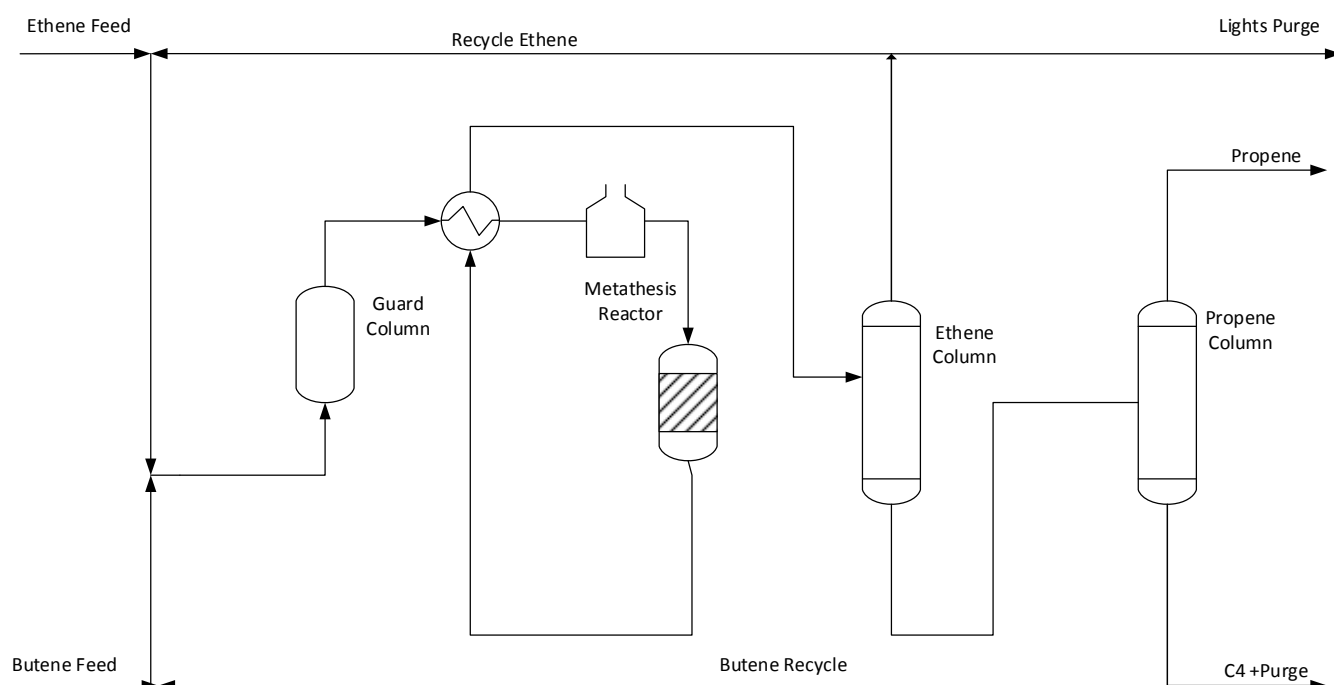


Figure 4.2: OCT Metathesis process [12]

Shell sells this product as Neodene [16] or the mixture is distilled to separate the alkenes to be sold individually. The catalyst, products and solvent are immiscible with each other and the catalyst and solvent can therefore easily be recycled. Shell's total worldwide production of Neodene amounts to 1190 000 000 tons per annum.

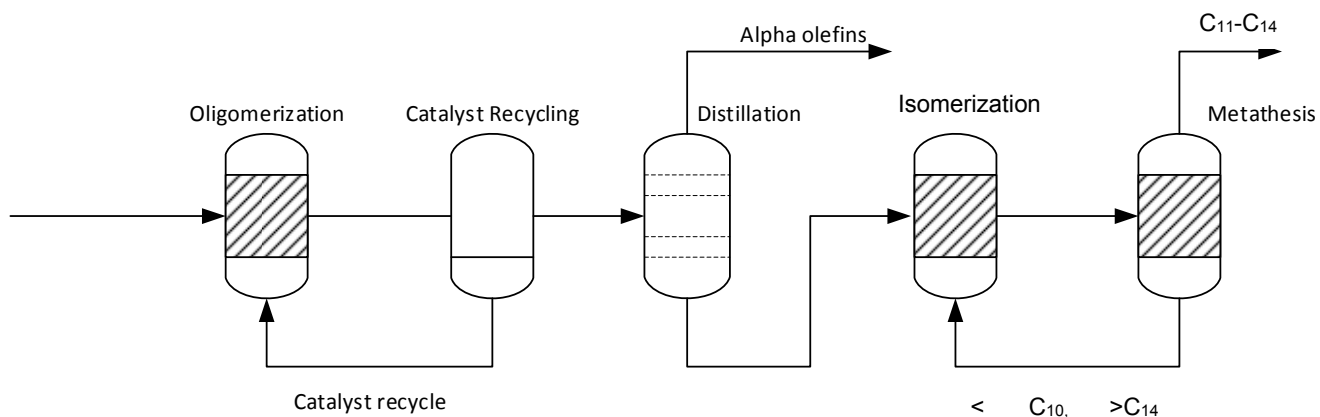


Figure 4.3: Basic SHOP process [15]

The French Institute of Petroleum (IFP) and the Chinese petroleum corporation have joined efforts to develop a process to produce propene known as the Meta-4 process [12]. Ethene and 2-Butene are reacted in the liquid phase over a $\text{Re}_2\text{O}_7/\text{Al}_2\text{O}_3$ at 35 °C and 60 bar. A 63% single pass conversion is specified for the process, but it hasn't yet reached commercialization due to the cost of the catalyst and high feed purity requirements [12]. It is currently offered by Axen4, a French subsidiary of IFP formed in a joint venture with IFP's licensing department and Procatalyse & Catalysis and Adsorbents.

The Neo hexene process produces an intermediate in the synthesis of a musk perfume and Terbafine which is an anti-fungal agent. A process located in Chevron Philips Chemical company is based on the dimer of isobutene [12, 14]. The dimer consists of a mixture of 2, 4, 4, -trimethyl-2-pentene and 2, 4, 4-trimethyl-1-pentene. Cross-metathesis of the 2,4,4-trimethyl-2-pentene with ethene yields the neohexene, the 2,4,4-trimethyl-1-pentene is used by employing a dual catalyst that would facilitate isomerization to 2,4,4-trimethyl-2-pentene which in turn could be used during the metathesis reaction [12, 13]. A 1:3 catalyst mixture with WO_3/SiO_2 and MgO is used to facilitate a 65-70% conversion and 85% selectivity to neohexene at 370 °C and 30 bar. In The neohexene process, di-isobutene is first fractionated to remove a catalyst poison. The fractionated di-isobutene and ethene is sent to a reactor that contains the catalyst [12]. The make-up and recycled ethene is compressed before it enters the reactor and products are separated using fractionation and stripping columns.

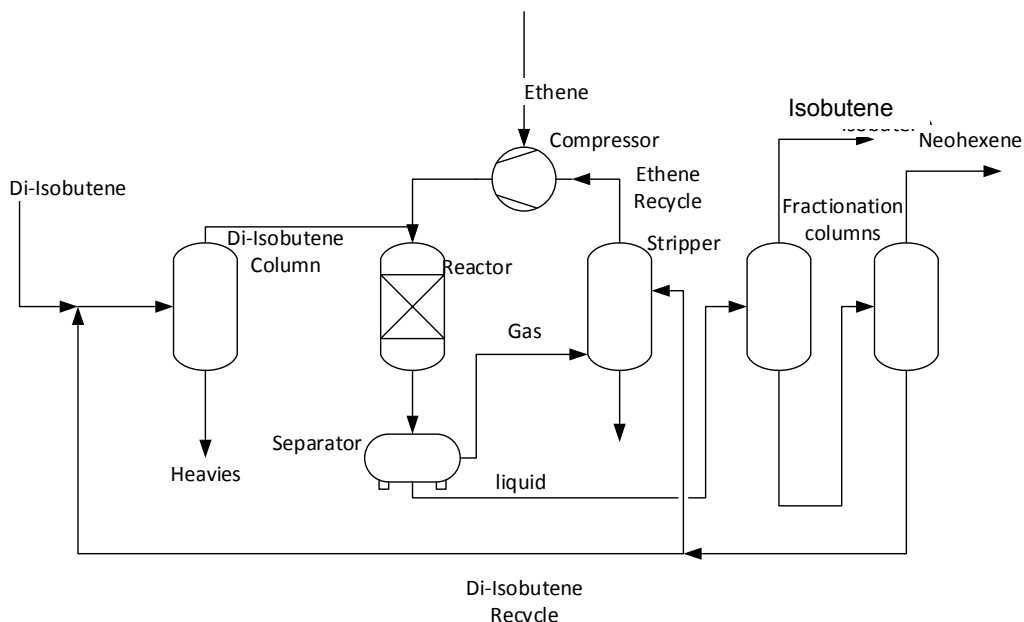


Figure 4.4: The Neohexene Process [10]

The Polynorbornene process was the first to produce a commercial metathesis polymer. It was put on the market in the late 1970's by CdF-Chimie in France as well as the USA and Japan and sold as Norsorex [11]. The ROMP reaction combines 2-norbornene, dicyclopentadiene and ethene to give a 90% trans-polymer with a very high molecular weight. The product has a glass transition temperature of 37 °C. A RuCl₃/HCl catalyst in butanol is used [11]. Catalyst losses are kept at a bare minimum since the butanol in which the catalyst is contained differs greatly in density to the product and separation processes are relatively easy.

Probably the most well-known process that uses Grubbs-type catalysts is the poly dicyclopentadiene process that is operated by Materia. The technology is also used by Cymetech to produce polymers.

SASOL technology has successfully used a heterogeneous WO₃/SiO₂ catalyst to pilot a process that upgrades low-value 1-heptenes from the Fischer–Tropsch effluent streams to detergent range olefins [1]. High temperatures were required, and modifications were necessary to reduce isomerization [17]. In recent years SASOL has developed a pilot-scale plant to generate their surfactant alcohol product ISOFOL from linear alpha alkenes [18].

Table 4.1: Comparison between commercial metathesis processes (adapted from [17])

Process	Company	Feed	Product	Production rate	Conditions	Catalyst
Phillips Triolefin Process	Phillips; 1966-1972	propene	ethene, butene	15 ktpa	400°C	WO ₃ /SiO ₂
Reverse Phillips Triolefin process	Lyondell Petrochemical Co. since 1985	ethene 2-butene	propene	136 ktpa	400°C	WO ₃ /SiO ₃
ABB Lummus and OCT	BASF fine petrochemicals	ethene 2-butene	propene	400 ktpa	350°C 20 bar	WO ₃ /SiO ₄
	Mitsui Chemicals	ethene 2-butene	propene	140 ktpa	-	-
	Korea Petrochemical Co.	ethene 2-butene	propene	110 ktpa	-	-
Axens Meta-4	Not commercialised yet	ethene 2-butene	propene	-	35°C 60 bar	Re ₂ O ₇ /Al ₂ O ₃
SHOP	Shell - 3 different locations	butene and >C ₁₈ Olefins	C ₁₁ -C ₁₄ alkenes	1190 ktpa	100-125°C 10 bar	MoO ₃ /CoO /Al ₂ O ₃
Phillips neohexene	Phillips since 1980	di-Isobutene ethene	neohexene	1.4 ktpa	370 °C 30 bar	WO ₃ /MgO/ SiO ₂
Cyclooctene polymerization	Degussa-Huls since 1980	Cyclooctene	polyoctenamer	12 ktpa	100-125 °C	RuCl ₃ /HCl/ BuOH
Norbornene polymerization	CdF Chimie; Elf Atochem; since 1976	norbornene	polynorbornene	-	25-100 °C	-
	Nippon Zeon since 1991	norbornene	hydrogenated norbornene	-	25-100 °C	[R ₃ NH] ₂ y- 6xMo xOy/ EtAlCl/RO H/SiCl ₄
Telene Process	BF Goodrich	dicyclopenta-diene	polydicyclopenta-diene	-	25-100 °C	[R ₃ NH] ₂ y- 6xMoxOy/ EtAlCl/RO H/SiCl ₅
	Nippon Zeon	dicyclopenta-diene	polydicyclopenta-diene	> 13.6 ktpa	25-100 °C	WCl ₆ /WOC I ₄ / EtAlCl/RO H

Table 4.1-cont'd: Comparison between commercial metathesis processes (adapted from [17])

Process	Company	Feed	Product	Production rate	Conditions	Catalyst
DCPD Processes	Materia, Cymetech, Hitachi chemical Co.	dicyclopentadiene	Polydicyclo-pentadiene	-	25-100 °C	Grubbs based. catalysts
Pheromone production	Materia	5-decene, 1,10-diacetoxy-5-decene	peach twig borer pheromone	-	25-100 °C	Grubbs based. catalysts
Fragrance production	Symrise	cyclooctene	Cyclohexa-decenone cyclohexadecadiene	-	25-100 °C	Grubbs based. catalysts
Metton Process	Hercules Inc.	dicyclopentadiene	polydicyclopentadiene	-	25-100 °C	WCl ₆ /WOC I ₄ /EtAlCl/ROH

4.2.4 Future outlook and market trends

When a process is considered, it is important to realise whether there is a market for the product it produces. The PMP and SMPs of the metathesis reaction with 1-octene are both considered as intermediates to produce branched Guerbet surfactants. SASOL's international operations offer a similar product called ISOFOL [18], which consists of a distribution of different Guerbet alcohols. SASOL points out in their technical data sheet that the advantages of these alcohols are that they remain liquid at lower temperatures compared to linear saturated and unsaturated alcohols, making them suitable for all kinds of fine chemical industry applications. It is important to reiterate that the expected annual global growth in demand for surfactants of this sort is 4.5% [19]. Furthermore, the expected annual growth in demand for linear 1-alkenes between 2006 and 2020 was reported as 3.5% [14]. The advantage that the proposed process by c*change offers is the scale of value addition to the linear 1-alkene feed and the abundance of linear 1- alkene feedstocks.

The environmental friendliness and green chemistry nature of metathesis is an ongoing reason for interest in the field [1]. Development in the homogeneous metathesis field is large and intense but heterogeneous catalysis is also showing some improvement in the metathesis department. The future of industrial processes in metathesis will depend on market trends and the availability of feedstock [21]. Fischer-Tropsch and linear alkene oligomerization will only yield a certain product distribution. In future, the industry may need to rely on metathesis to fill the gap. Research into renewable feedstock for synthesis via metathesis is becoming an interest further relevant trends in the production of polymers are looking at self-healing products, and depolymerization processes as well [12]. CM and RCM will feature in important steps towards creating fine chemicals and pharmaceuticals. It is, however, important that research finds cheaper and more efficient catalysts that will facilitate a favourable environment in the metathesis field for further commercialization [17].

4.2.5 Continuous metathesis reactors in literature

As an extra consideration, literature on continuous flow reactors for metathesis was sought that were only operated for R&D purposes. As a result, valuable operation information could be extracted from such sources.

Lysenko *et al.* [21] have studied the stability of the first-generation Grubbs catalyst in a continuous flow reactor. They investigated the cross-metathesis reaction of ethylene and cis-2-butene to form propylene. The first important point mentioned in their work was the role that the methyldene

and alkylidene species play in the catalytic cycle and the effects thereof in the number of turnovers. Catalyst deactivation during the CM reaction of ethylene and cis-2 butene could be expanded by two factors, decomposition due to the presence of ethene or thermal decomposition of the catalyst itself leading to an irreversible loss in catalyst activity [20].

The reactor setup that Lysenko *et al.* used was made of a number of 100mL glass containers. A small reactor was charged with the catalyst solution [21]. Temperatures and pressures were regulated as the feed gasses were supplied to the reactors in excess. Both reacted and unreacted gasses were vented out of the reactor, analysed via GC analysis and discarded. It was reported that the flow reactor could effectively separate the substrate and product inhibition effect from the original catalyst decomposition [21].

In an attempt to expand on the proof of the versatility of their multi-jet oscillating disc reactor technology, Bjørsvik and Liguori [22] used **HG2** catalyst and the RCM reaction of a number of olefins. Their results were comparable to traditional batch studies and they could obtain similar or higher yields and selectivities. The reactor, however, is somewhat specialised and would need to be tested for linear alkene metathesis as well, before something similar could be evaluated for commercial applications

Some studies also focus on the combination of reactors and separation units into a single equipment unit. Membrane reactors and reactive distillation [23] modules have been proved to work for the respective systems the researchers have chosen to study. Their studies are mostly focussed towards the production of propene given the high number of commercial processes producing propene via metathesis.

4.2.6 Critical discussion

The commercial processes for linear alkenes mostly all require high temperatures and pressures, which is why the research trends lean towards the more forgiving Grubbs and Hoveyda-Grubbs-type catalysts. Their tolerance to different functional groups, low temperature and pressure requirements make them attractive alternatives to such processes. Homogeneous catalyst applications in the pharmaceutical and fine chemicals industry are widespread. Usually, the high catalyst costs and catalyst decomposition effects aren't of much concern since the product values are typically high [12]. So far, large-scale continuous commercial processes that use Grubbs-type catalysts for linear alkenes are mostly only under consideration and is, as such, the purpose of

this work; to explore the alternatives and evaluate process alternatives to find a catalyst that would ultimately be beneficial for the production of high-value Guerbet surfactants from linear1-alkenes.

Laboratory tests have well displayed that specialised reactor systems are able to deliver satisfactory results that compare or improve upon traditional batch tests. Effectively very little open literature is available on cost evaluations regarding metathesis processes. To the author's knowledge, few academic researchers consider cost evaluations as a prime focus of their work for the metathesis industry. The only known work (to the author's knowledge) in the field of upgrading linear 1-alkenes and evaluating the process economics is that of Denhere [9]. Denhere studied the upgrade of low-value alpha olefins to 2-hexyl nonanal via metathesis and hydroformylation using the **HG2** catalyst. Denhere also employed the works of Van der Gryp [24] in evaluation between distillation and membrane separation methods and also used the kinetic parameters of Van der Gryp for the metathesis reactor [25]. Denhere demonstrated that the process that employed membrane separation was the economic choice with an IRR of 83% and an NPV of \$ 563 M with a payback period of 3 years [9]. Sensitivity analysis by Denhere reported that the factors with the largest influence on the economic potential of the process are the cost of the catalysts, selling price of the product, tax rate and the feed costs [9].

Market trends have displayed that there is ample opportunity for the production of high-quality surfactants that make use of green chemistry methods if the process can compete with current production systems in meeting the demands of a niche market such as the speciality detergent industry.

The efforts of this chapter will follow the principles that Denhere used to compare the results of the economic potential for each catalyst and make a recommendation on the best performing catalyst for the metathesis of 1-octene.

4.3 Economic evaluation methodology

In engineering economics, the design engineer uses economic indicators, (cost, ROI, IRR, NPV) to choose between process alternatives [3]. Economic potential can be defined in layman's terms as the estimated highest level of output that can be sustained by the process [26]. The economic potential is evaluated at each level of complexity to determine whether the process idea is still feasible. The different design levels for the economic evaluation evaluated in this project is listed and the methodology followed at each level is explained. The overall decision levels and workflow are briefly illustrated in the schematic at the end of this section.

4.3.1 Process objectives

The process objectives to produce 7-tetradecene in a metathesis reactor are defined as follows in Table 4.2:

Table 4.2: Process design objectives

Design Parameter	Value/Description	Rationale
Desired product	7-Tetradecene at constant production rate	7-tetradecene is the primary product of the 1-octene metathesis reactions and is also an important intermediate for the production of high-value Guerbet alcohols/ surfactants [27]
Feed rate	Minimum feed rate of 10000 tpa	According to Arnoldy [28], the minimum production rate for petrochemical processes is 1000 tpa, but values between 10 000 and 500 000 tpa is considered favourable
Feedstock	1-octene	1-octene is a linear alkene that is relatively cheap and is also an α -olefin in the C ₅ -C ₉ range that is a by-product of the Fischer-Tropsch Process.
Catalyst	Latent O-N chelated 2 nd generation Grubbs-type catalyst (GCYC & GMPP)	Latent systems are more stable at higher temperatures [29]
Nature of Process	Continuous	Feed rate is too high for batch systems [5]

A description of the process and method followed in the economic evaluation hierarchy is presented in the following schematic:

Economic Evaluation Process

An illustration of the methodology followed through the Douglas design hierarchy for the economic evaluation of the continuous metathesis reactor system

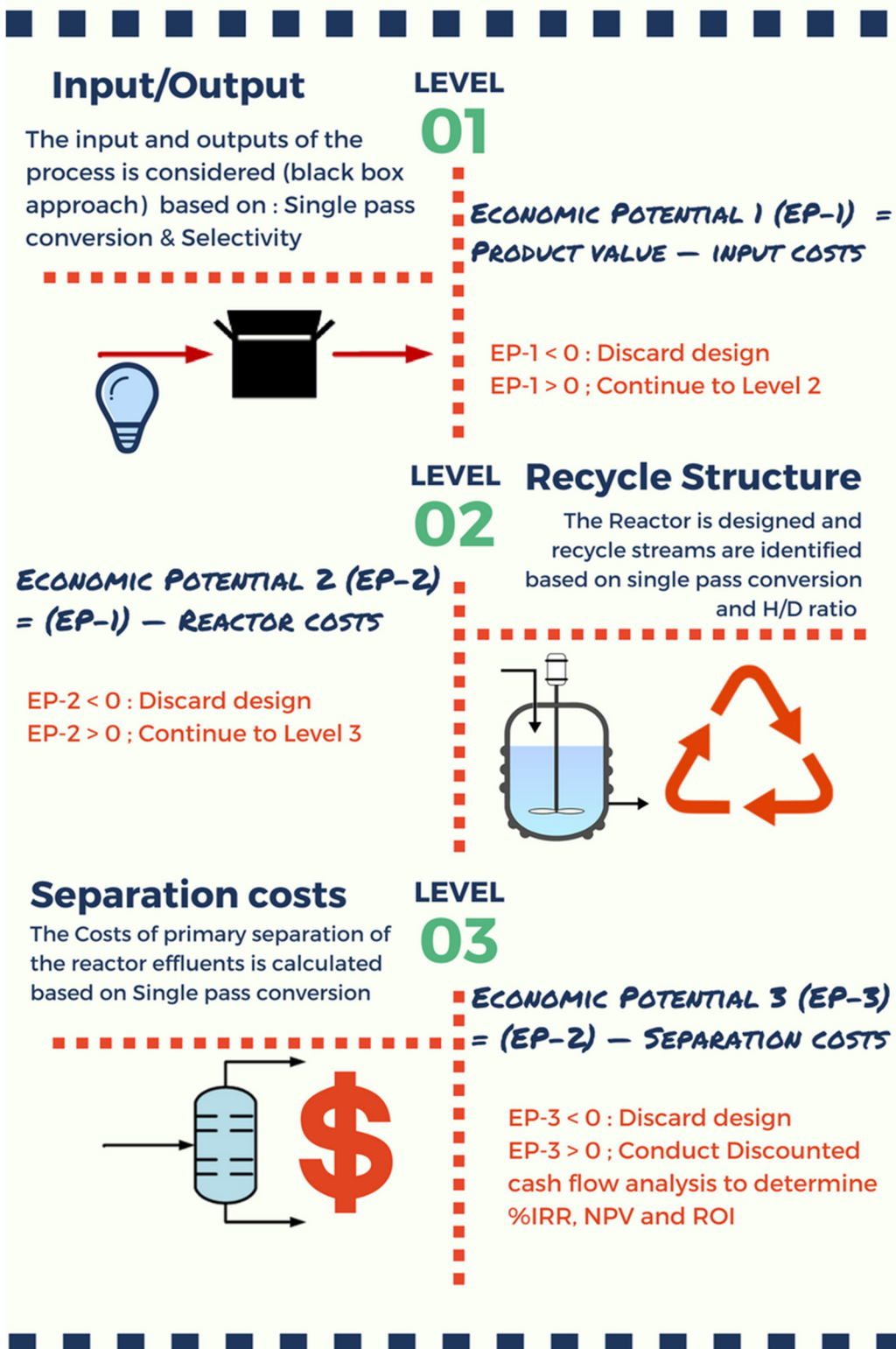


Figure 4.5: Flow diagram of the economic evaluation process

4.3.2 Economic potential level 1 (EP-1)

According to Douglas [5], the first decision to make before considering the input-output structure of the process is to decide whether the process should be operated continuously or on a batch basis. He suggested that a feed rate above 500 tpa should warrant a continuous process above batch [5]. Since the minimum specified feed rate for this system is defined as 1000 tpa the process is operated continuously in a continuously stirred tank reactor.

The input-output structure of the process can be described as the black box approach since the designer only looks at the process feed and the process effluent [5]. The raw materials costs are in the range of 33 to 83% [5] of the total processing costs and it is important to calculate these costs before any other calculations are made.

It is assumed that all the recycled products are recovered and that a 100% overall conversion is taking place in the process.

The input-output structure for this process is illustrated as follows:

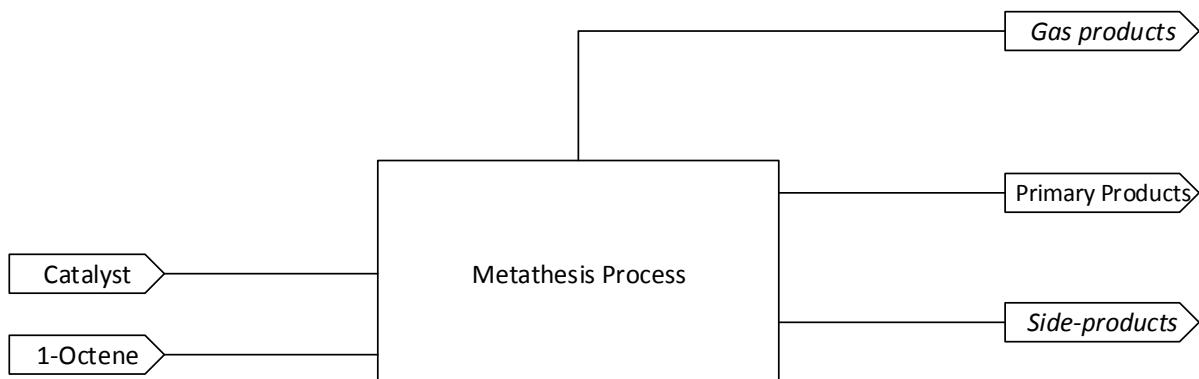


Figure 4.6: Input-output flow diagram

The next question is what the costs of the raw materials and products are per unit? The costs of the products were estimated as a preliminary evaluation for comparison between the catalysts.

Since the catalysts are not commercially available the costs had to be estimated via the synthesis process. The materials necessary to create the catalysts along with the reported yield of the synthesis process was used to estimate the cost per unit of catalyst, based on the Sigma-Aldrich prices of the raw materials and the cost of the **G2** catalyst as reported by [9].

The catalyst cost for the **GCYC** catalyst was calculated as 22516.9 \$/ kg complex and the price of the **GMPP** catalyst was calculated as 20995.7 \$/kg. For comparison against the commercial HG2 catalyst the catalyst price for HG2 was estimated as 28746 \$/kg [9]. The price per unit of catalyst was estimated by adding the raw material cost for the three preparation steps described in Chapter 2, Section 2.2.3.3.3 of which the first is the preparation of the bidentate ligand, secondly a lithium salt is prepared and lastly the complex is synthesised from the **G2** complex. Detailed calculation steps and results of the catalyst cost estimation activities are provided in Appendix D. Additionally, all other raw chemical costs were based on non-commercial prices to ensure uniformity within the economic evaluation, with the estimation of these synthesised catalyst costs based on non-commercial values.

The variables and costs for the input and output of the process are listed in Table 4.3.

Table 4.3 Costs of input & output materials

Variable	Description	Reference
Overall 1-octene conversion	100%	[30]
Selectivity to 7-tetradecene	100%	[25]
1-octene	1.8 \$/kg	[9]
7-tetradecene (97%)	334.1\$/kg	[31]
GMPP catalyst	20995.7 \$/g	[31]
GCYC catalyst	22516.9 \$/g	[31]

The economic potential of dollars per annum on a level 1 basis is calculated with the following equation:

$$EP_1 = \text{Product value} - \text{Raw material cost} \left(\frac{\$}{\text{yr}} \right) \quad (4.1)$$

where:

$$\text{Raw material cost} = \text{catalyst cost} + C_8 \text{ Costs} \left(\frac{\$}{\text{yr}} \right) \quad (4.2)$$

The EP₁ can also be expressed as a function of a number of variables as follows:

$$EP_1 = f(C_8 \text{ Feedrate}, C_{Ru}, \text{commodity prices}) \left(\frac{\$}{\text{yr}} \right) \quad (4.3)$$

The EP₁ value was calculated disregarding the secondary and gas products. The ethene and secondary products are assumed to be utilised in other downstream processes which are beyond

the scope of this work, as such only the 7-tetradecene is considered as a source of revenue estimation.

4.3.3 Economic potential level 2 (EP-2)

Douglas' methodology lists a number of questions that the designer is confronted within Level 2 [5]. These questions are related to whether purification is required before the feed is introduced, whether a product should be removed, purged or recycled and whether valuable reactants can be recycled [5]. The 1-octene and catalysts obtained from Sigma-Aldrich were used without further purification during the experiments and as a result, purification was deemed unnecessary before processing.

One of these questions (recycle streams) is fairly easy to answer considering that the most valuable raw material utilised is that of the catalyst. The specifications made in the process objectives requires an overall conversion of 100 % of the 1-octene feed. Experimental data from Chapter 2 has shown, however, that single pass conversion ($X_{\text{single pass}}$) of 100% after 7 hours of operation could not be obtained, therefore a 1-octene recycle stream is necessary. The process flow diagram at level 2 for the metathesis reactor is shown in Figure 4.7.

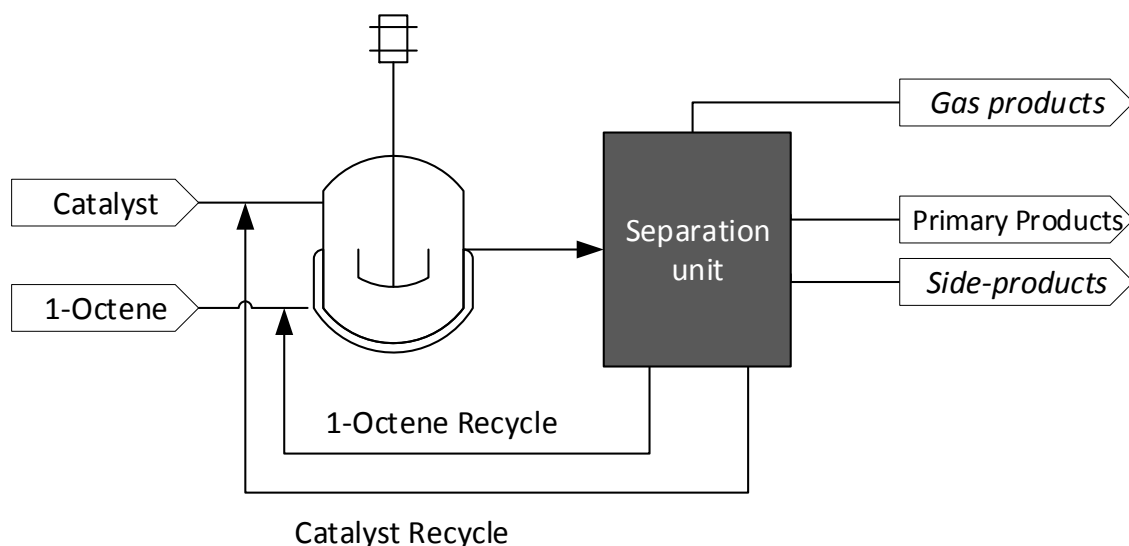


Figure 4.7: Recycle structure process flow diagram

At level 2 the economic potential is defined as:

$$EP_2 = EP_1 - \text{Reactor Cost} \left(\frac{H}{D} \right) \quad (4.4)$$

The reactor costs were estimated using a Guthrie [5] correlation defined as:

$$\text{installed cost}(\$) = \left(\frac{M\&S}{282} \right) * (101.9D^{1.066}H^{0.82}(2.18 + F_C)) \quad (4.5)$$

where:

$$F_C = F_M * F_P$$

$M\&S$ = Marshall & Swift Cost Index (2016) [36]

D = Diameter (m)

H = height (m)

F_m and F_p are correction factors that are included in the correlation to account for pressure and the choice of material. Towler & Sinnott [2] provide an easy method for choosing the material based strength and the chosen material carbon steel clad with 304 Stainless steel [2]. The corresponding correction factor F_m as suggested [2] was selected as 2.25. In Denhere's study, the design pressure for the metathesis reactor was specified as 1 bar. The reaction experiments were conducted at atmospheric conditions and as such the design pressure for Denhere's Study was applied in this work as well. Pressure vessel design practices recommend at least a 10% overdesign factor [2] as such the correction factor for pressure was selected based on a pressure of 1.15 bar. Consequently $F_p=1.15$.

A Height to diameter ratio of 1 was assumed for the reactor well within recommended ranges [2]. The results of the Economic potential for Level 2 are provided and discussed in Section. 4.4.

4.3.4 Economic potential level 3 (EP-3)

Economic potential evaluation on a level 3 basis would require an estimation of the primary costs around separation. The EP at level 3 process flow diagram is displayed in Figure 4.7 and defined in Equation 4.6 as:

$$EP_3 = EP_2 - \text{Primary separation cost} - \text{Energy cost} \quad (4.6)$$

Douglas [5] suggests two main recovery and separation considerations during design, vapour recovery and liquid separation. Vapour recovery is employed by means of a flash drum. The flash drum size and cost were estimated based on an assumed flash time of 0.083 hours based on Denhere's simulation [9]. Once the volume was obtained and a design pressure of 1.5 bar was

assumed based on Denhere's design and an additional overdesign factor, the flash drum cost was calculated based on shell mass using a correlation by Towler and Sinnott [2].

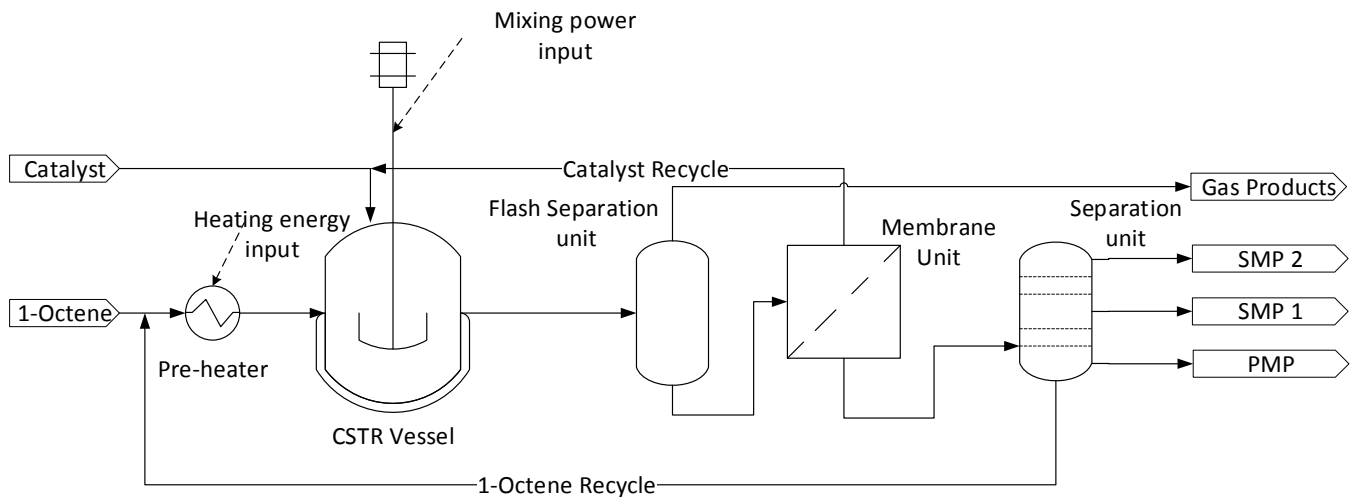


Figure 4.8: EP-level 3 process flow diagram

$$\text{Shell Mass} = \pi D_{vessel} L t_w \rho \quad (4.7)$$

where

$$t_w = \frac{P_i D_i}{2SE - 1.2P_i} \quad (4.7a)$$

D_i = internal diameter

P_i = internal Pressure

S = Maximum allowable stress

E = weld joint efficiency

First, the maximum allowable stress was chosen based on a maximum allowable temperature of 260°C for 304 Stainless steel resulting in a value of 8.9 N.m⁻² [2]. Weld joint efficiency was selected as 1 and an H/D ratio for the Flash drum was assumed to be 2. Once the shell mass was determined equation 17 was used to calculate the cost of the flash drum [2] and chemical engineering cost indices (CEI) were applied to the equation to account for inflation [32].

$$C_e = a + bS^n * \left(\frac{\text{CEI (2016)} [32]}{478.6} \right) \quad (4.8)$$

The correlation constants for the calculated Shell mass values were selected as:

$$a = -10\ 000; b = 600 \text{ and } n = 0.6 \quad (4.8a)$$

Before liquid recovery could be applied the catalyst needed to be recovered. Two separation options were available for the catalyst, but since high temperatures lead to isomerization and loss of precious catalyst activity due to thermal decomposition [32]. The proven method of OSN was preferred. OSN has benefits of lower energy requirements above high-temperature distillation towers. An experimental correlation equation obtained from [9] was used to determine the flux across the membrane as a function of the 1-octene mass fraction (X). Consequently, the area was calculated and an estimated (non-commercial) flat-sheet membrane cost factor of 1970 \$/m² (2016) [9] was used to determine the cost of the membrane in Equations 4.9.

$$Flux = 9.422X_{C_8} - 2.5102X_{C_8} + 1.0856 \quad (4.9)$$

$$Membrane\ Area = \frac{\dot{v} \left(\frac{m^3}{hr} \right) * \rho \left(\frac{kg}{m^3} \right)}{flux \left(\frac{kg}{m^3 hr} \right)} \quad (4.9a)$$

$$Membrane\ Cost = 1970 * membrane\ Area \quad (4.9b)$$

The last separation unit to consider in the separation sequence is how the liquid products would be separated. Separation processes exploit the physical property differences between components to achieve separation [2]. The property difference that would facilitate separation the best is the boiling point. Distillation is an effective separation method for such cases [6].

For the purposes of this work, a shortcut distillation column was designed at the selected optimal process operating conditions. Perfect separation between the primary products were assumed but in reality, only the octenes would be separated from the liquid products for recycle and the 7-tetradecene along with other similar products would be sent to the hydroformylation section. The distillation column was therefore designed with this in mind. A conceptual process was simulated in Aspen Plus ® software to obtain an estimate of the number of required stages and the reflux ratio. (User Input and process design details are provided in Appendix E). The distillation column was designed with a short-cut DSTWU model. The design objectives of the 1-octene column were defined as follows:

- 1) Recover 99.8% of the unreacted 1-octene
- 2) Ensure 95% octenes purity in the distillate

Once the simulation completed successfully the column height and diameter could be estimated based on the minimum number of stages estimated in the process simulation. The relationships are defined as follows from Guthrie's correlations [5]:

$$N = \frac{N_m}{E_o} \quad (4.10)$$

where:

- N_m = minimum number of stages
- N = actual number of stages
- E_o = column efficiency = 0.5 (simulation results)

The height was calculated as follows:

$$H (ft) = 2.3 \left(\frac{N}{E_o} \right) \quad (4.11)$$

The diameter was calculated based on a simple H/D ratio assumption of 15. According to Douglas, Guthrie recommends any assumed value between 10 and 20 [5]. Higher than 20 would result in very tall and narrow distillation columns. Material-and pressure correction factors were selected where $F_m = 3.67$ for a distillation from solid stainless steel and $F_p = 1$ for a column specified to operate at atmospheric conditions the resulting cost correction factor $F_c = F_p * F_m$.

The Guthrie correlation for the column cost is [5]:

$$\text{Column cost} (\frac{\$}{yr}) = \left(\frac{M\&S}{280} \right) (F_c)(101.9) D^{1.066} H^{0.82} \quad (4.12)$$

where

- D = column diameter
- H = column height

The condenser cost is calculated as follows [5]:

$$\text{Condenser cost} (\frac{\$}{yr}) = \left(\frac{M\&S}{280} \right) (F_c)(101.3) \left(\frac{\Delta H_{vap}}{U \Delta T} \right)^{1.066} V^{0.65} \quad (4.13)$$

where

- ΔH_{vap} = enthalpy of vaporisation (Btu)
- U = heat transfer coefficient (100 Btu. h⁻¹. ft⁻². °F⁻¹)
- V = Volumetric flow (ft³.h⁻¹)
- ΔT = Temperature change (°F)

And the reboiler cost correlation [5]:

$$\text{Reboiler cost } (\frac{\$}{\text{yr}}) = \left(\frac{M\&S}{280}\right)(F_c)(101.3)\left(\frac{\Delta H}{11250}\right)^{0.92} V^{0.65} \quad (4.14)$$

The metathesis reaction is known to be endothermic [33], as a result, heat has to be applied and in order to prevent operation in the mass transfer limited regime sufficient mixing is required. As a result, a preliminary energy balance was conducted over the reactor as follows [34]:

$$(\dot{Q} - \dot{W}_s) - F_{A_0} \sum_{i=1}^n \theta C_{p_i} [T_i - T_{i_0}] - \Delta H_{rxn}(T) * F_{A_0} X = 0 \quad (4.15)$$

where:

$$\theta = \frac{F_{i_0}}{F_{A_0}} \quad (4.15a)$$

Heat capacity correlation data for species i was determined using the Joback prediction method commonly used in Aspen simulation software ® [35]. Sample equations and calculation tables are available in Appendix C and D.

Once the heat and shaft work required for the reaction was determined the costs of the mixing equipment, energy and heater were estimated.

The heat exchange area for the heater was determined with Equation 4.10a and 4.10b [6]. Once the area was estimated the cost was calculated with an assumed [5,9] heat transfer coefficient of 200 W.°C⁻¹. m⁻².

$$A(m^3) = Q / (U \Delta T_m) \quad (4.16)$$

$$\Delta T_m = \frac{[(T_1 - t_2) - (T_2 - t_1)]}{\left[\ln\left(\frac{T_1 - t_2}{T_2 - t_1}\right)\right]} \quad (4.16a)$$

where

$$t_1 = 25^\circ\text{C}, t_2 = \text{design } T, T_1 = t_2 + 10, T_2 = t_2 - 10 \quad (4.16b)$$

Hot water was chosen to heat the reaction since reaction temperatures would not exceed 100°C and since organics are used steam is unnecessary [26]. The heated water was assumed to be heated to 10°C above the design temperature and the exit temperature was specified as 10°C below the design temperature.

A stainless-steel spiral tube heater was selected, and the cost estimation equation was obtained from [36]

$$\text{Log}C_p = (K_1 + K_2 \text{Log}(A) + K_3 (\text{Log}(A))^2) * \left(\frac{\text{CEI}(2016)}{394} \right) \quad (4.17)$$

where

$$K_1 = 3.99, K_2 = 0.0668 \text{ & } K_3 = 0.2430 \quad (4.17\text{a})$$

The mixing power was determined from the shaft work required as calculated in the energy balance. Silla [26] recommends a 0.03kW.m^{-3} mixing power requirements for a homogeneous reaction. The volumetric flow was multiplied by the power requirements and the power costs were calculated based on the business rates that Eskom charges. These details are available in Appendix C.

The costs calculated were all determined as a function of the single pass reactor conversion, combined and plugged into Equation 4.6. For each subsequent level, the value of the economic potential would ultimately determine whether the design should further be pursued. The results of these evaluations are several plots that are related to the empirical data. The effects of temperature and catalyst load on the economic potential are explored as a result in Section 4.4. A preliminary cash flow analysis is also evaluated and the results of which are discussed in Section 4.4 to obtain a comparison on an economic scale between the catalysts.

Additionally, a commercial analogue of the **GMPP** and **GCYC** catalysts are included in the profitability analysis. The same methodologies and equations applied to the **GMPP** and the **GCYC** catalysts are applied to the **HG2** data obtained from [25]. Details of the costs and calculations for the **HG2** catalyst are included in Appendix D and E.

4.4 Results and discussion

This section presents the results of the economic potential evaluations conducted as a function of the reactor single pass conversion for each level of the Douglas hierarchical design approach. The effects of temperature, catalyst load and selectivity are explored for each of the catalysts and a comparison is drawn to establish optimum operating parameters for the reactor based on the economic potential. The results of a cash flow analysis based on these optimum parameters is also conducted by which the results are presented as discussed in the final subsections of this chapter.

4.4.1 Economic potential of GCYC precatalyst

The results of the Economic potential for the **GCYC** precatalyst are presented and summarised. Most notably the optimal single pass conversion and conditions are pointed out. The optimal residence time of the reactor is also determined and according to the experimental batch reactor, the reaction only needs to proceed about 5% of the duration of the experimental reactions to be profitable. This topic and other optimal conditions, as well as the economic potential thereof, will be treated in the subsequent sections.

4.4.1.1 *GCYC precatalyst EP-1*

The constant parameters and assumptions made in section 1.2 and 1.3.1 were applied to the economic potential equation for the **GCYC** catalyst. Stoichiometry was used to determine the 7-tetradecene production rate and the amount of catalyst required. The annual EP value at level 1 results are summarised in Table 4.4.

Table 4.4: Economic potential level 1 for the GCYC catalyst:

EP-1		
Input	rate (kg/hr)	cost (\$/kg)
1-octene	1201	1.80
GCYC catalyst	0.760	22517
Output	rate (kg/hr)	cost (\$/kg)
7-tetradecene	1051	334
EP1 (\$/h)	331648	
EP1 (Bn \$/y)	2. 761	

Stoichiometry and sample calculations conducted during the EP-1 analysis are available in Appendix D. Clearly the economic potential for the **GCYC** catalyst on level 1 is favourable as is displayed in Table 4.4 with an annual value of \$2.76 billion. The analysis can therefore proceed to the next level.

4.4.1.2 GCYC precatalyst EP-2

The economic potential evaluation on level 2 was conducted as a function of conversion and the kinetic behaviour of the catalysts as obtained from empirical experiments, was used to facilitate the calculation. The recycle structure and the reactor cost was accounted for as described in the equations defined in section 1.3.3. Figure 4.9 displays the effects of temperature and conversion on the cost of the reactor is displayed in Figure 4.7A and the corresponding effects on the economic potential is displayed in Figure 4.7B

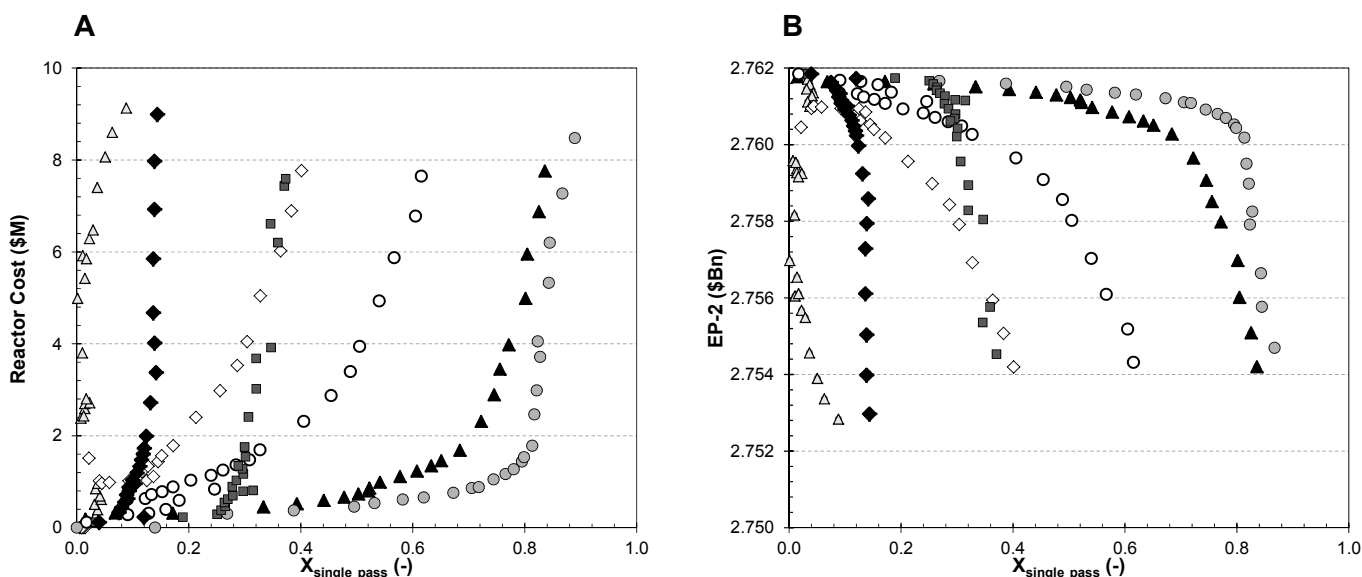


Figure 4.9: Effect of temperature and conversion ($X_{\text{single pass}}$) on (A) reactor cost and (B) EP-2 for GCYC [$\triangle 40^{\circ}\text{C}$ $\diamond 50^{\circ}\text{C}$ $\circ 60^{\circ}\text{C}$ $\blacktriangle 70^{\circ}\text{C}$ $\bullet 80^{\circ}\text{C}$ $\blacksquare 90^{\circ}\text{C}$ $\blacklozenge 100^{\circ}\text{C}$]

The trends in Figure 4.9 A shows how the reactor costs exponentially increase and peak around \$ 9 million as the conversion increases. This trend is understandable since a higher conversion would require the reaction to proceed longer which results in a larger residence time and consequent reactor size [33]. As the reactor size increases standard pipes and fittings are no longer suitable and the reactor must be custom-made, driving up the price. In Figure 4.9 A the reactor price shoots up vertically with an increase in conversion between 40°C -50 °C and at 90-100°C. This trend is related to the poor performance of the catalyst under these conditions and reactor size will not be able to compensate for the low conversion that these conditions result in. The inverse of the same trend is visible when the effect of temperature and conversion on the EP2 economic potential is considered (Figure 4.9 B). Although the economic potential at this level

remains positive for all the cases, the vertical downward trends of the economic potential over the reactor occur at 40, 90 and 100°C, which indicates that these conditions are not favourable for the reaction. The optimal temperature that would result in high single pass conversion over the reactor without unreasonably large reactor sizes is 70 and 80°C. Operation at 80°C will result in higher conversion but the margin between optimal conversion and higher reactor costs is very narrow. A more gradual trend as observed for 70°C is perhaps the better alternative. Further analysis is necessary to explore the effects of catalyst load and selectivity. The effects of catalyst load on the EP-2 value are summarised in Figure 4.10 A and B.

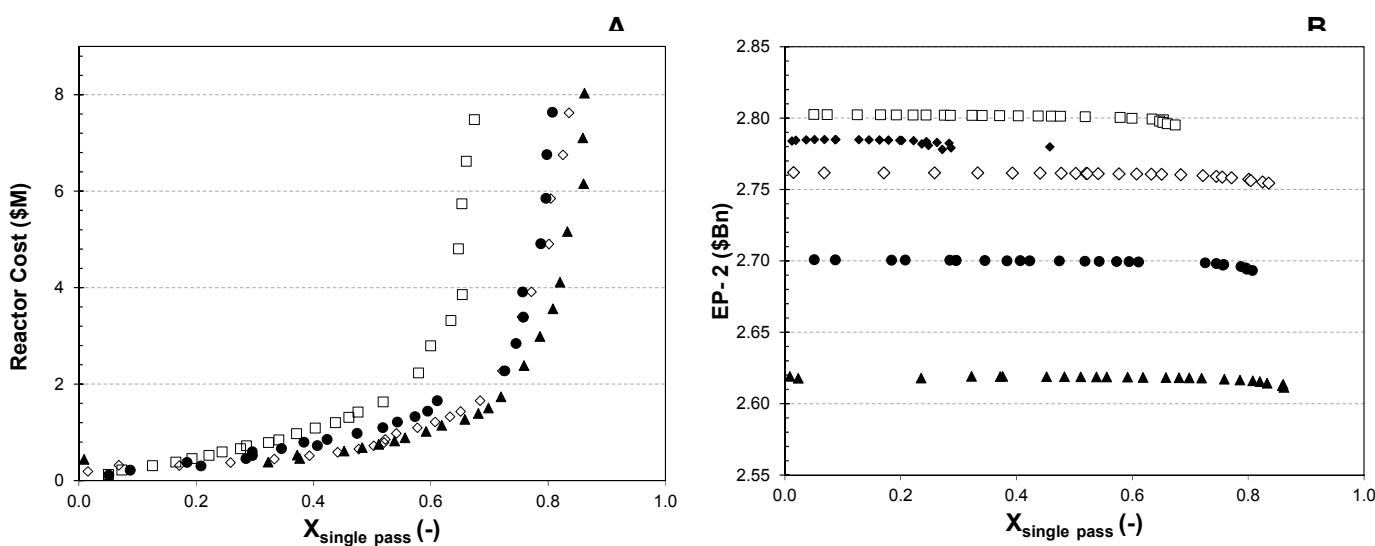


Figure 4.10: Effects of catalyst load and conversion ($X_{\text{single pass}}$) on (A) Reactor Costs and (B) EP-2 [▲5000 ●7000 ◇10000 ◆12000 □ 14000]

Figure 4.10 B shows how the economic potential increases with an increase in catalyst load. As the catalyst concentration is lowered (higher catalyst load) the economic potential varies between \$ 2.6 billion and \$ 2.81 billion. The economic potential remains constant as the conversion increases. At the upper limits of the conversion, a small decrease in the economic potential is observed. The maximum economic potential in Figure 4.10 B is around \$ 2.76 billion, even at the lower molar catalyst load conditions. As for the effects on the reactor cost with varying catalyst concentration, Figure 4.10 A shows that the reactor costs follow an exponential trend but remain below the \$ 2 million mark for as long as the single pass conversion remains below 60%. The costs start to increase beyond 65-70 % conversion. Beyond that, the reactor costs again increase sharply, as was observed when the temperature was varied. Less catalyst results in a larger economic potential but at the lower limits (12 000 and 14 000) the conversion peaks around 60%. To illustrate this a bar chart with the average economic potential for each catalyst was constructed (Figure 4.11).

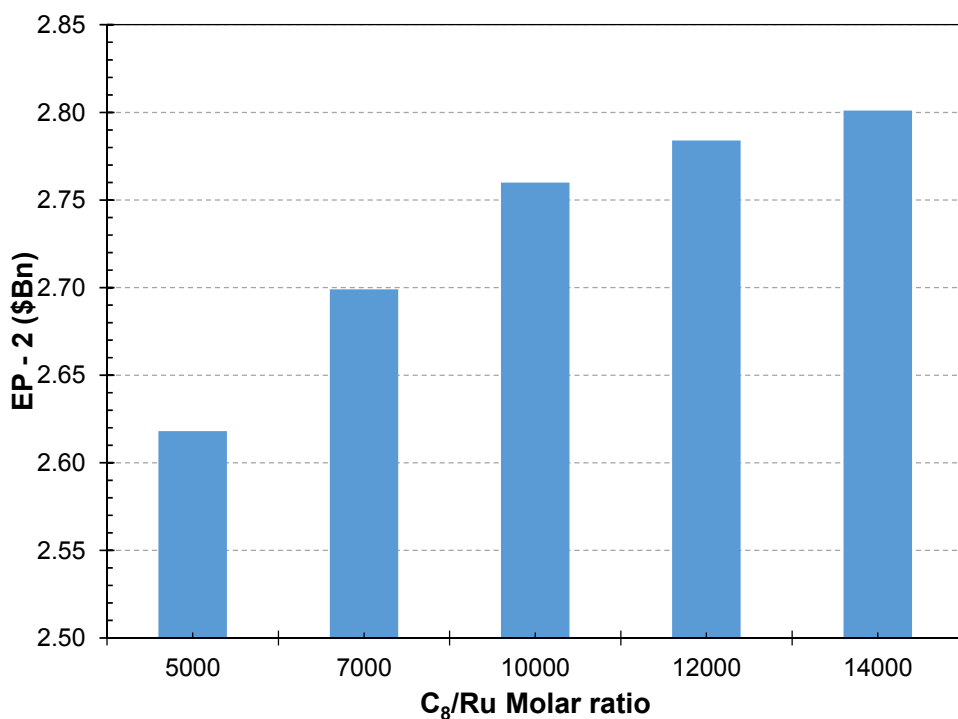


Figure 4.11: Maximum EP 2 at different catalyst loads (C₈/Ru)

The effects of decreased catalyst load (increase in catalyst concentration) reduce the economic potential. Denhere's study attributes this trend to the cost of the catalyst [9]. The catalyst is the largest production expense as shown in Figure 4.11, the amount of revenue achieved with less catalyst remains closely similar at the final conversion values. When combining that observation with the fact that the reactor costs are increased exponentially towards the upper conversion limits it can be deduced that an increase in reactor size (to attain higher conversion) will not necessarily have the desired results of higher economic return. It is thus better to operate the reactor at a lower catalyst concentration and conversion, and still obtain economic revenue.

Thus far, the economic potential has shown positive values for all conditions and the next level of complexity can be added.

4.4.1.3 GCYC precatalyst EP-3

The economic potential at level 3 will aid in the selection of an optimal single pass conversion over the reactor. The effects of the temperature and catalyst load on the separation costs as a function of conversion will also be explored. The economic potential evaluation at level 3 was evaluated for preliminary separation costs by applying short-cut design methods in the separation system development.

Effect of Separation cost

The effects of catalyst load, temperature and conversion on the total separation cost is summarised in Figure 4.12 where a nonlinear decreasing trend is observed between \$ 400 million and \$ 40 million. As the conversion increases the separation cost decreases until a local minimum is reached between 40 and 60% single pass conversion. The possible explanation that accounts for the high costs at low conversion argues that the volume required in the flash drum would be larger at lower conversions since larger amounts of liquid (unreacted 1-octene) are entering the flash drum pool. Higher amounts of liquid could lead to flooding and entrainment and consequently affect the size of the designed flash drum as well. Likewise, at higher conversions, more gas products (SMPs) are present and less liquid volume is present in the flash drum. More liquid would also require a larger membrane area which would explain the high separation costs at lower conversions [35].

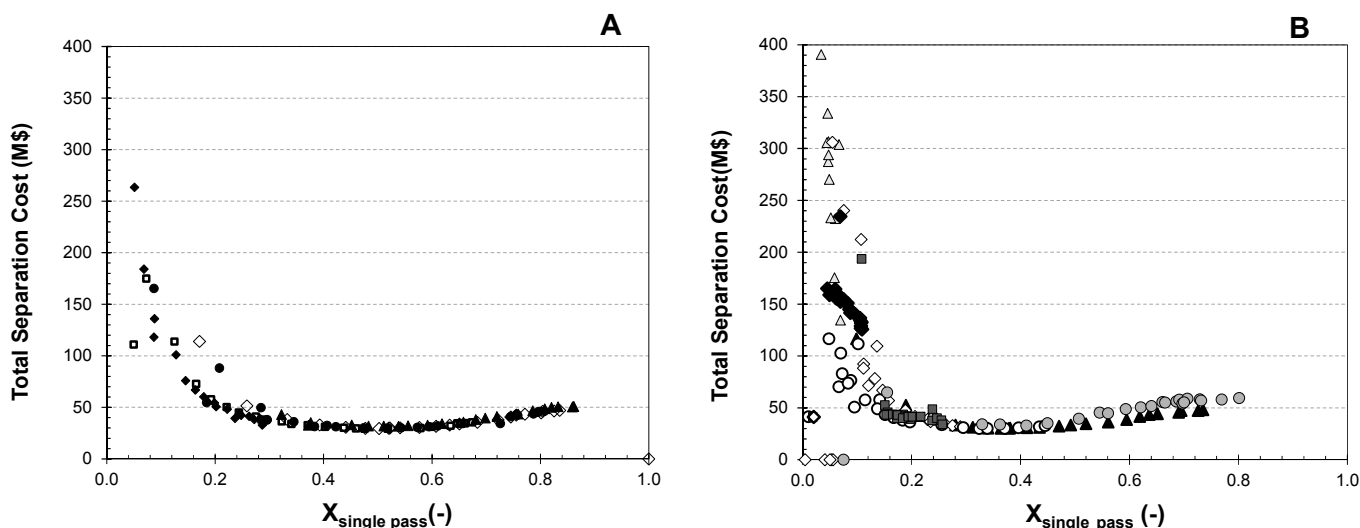


Figure 4.12: Effect of conversion on (A) catalyst load [▲5000 ●7000 ◇10000 ◆12000 □ 14000 (C₈/Ru)] and (B) temperature ([△40°C ◇50°C ○60°C ▲70°C ●80°C ■90°C◆100°C] on separation costs for GCYC catalyst]

Effect of Temperature

The effect of temperature and conversion on the Level 3 economic potential was studied to not only gain information on the optimal reaction temperature but also the optimal reaction conversion.

Figure 4.13 A displays the economic potential as a function of temperature and conversion and Figure 4.13 B displays a rescaled version of A to illustrate the trends clearly. It is evident in B that the economic potential, albeit positive, is low (< \$ 400 million) in comparison with the lower limits of the temperatures studied. This trend is clearer in B, displaying the optimal conversion and temperature for the **GCYC** catalyst. The economic potential again continues to increase as the conversion increases and as the temperature increases up until the peak is reached around 40-50% after which the economic potential starts to decline. The decline is attributed to the catalyst decomposition at higher temperatures.

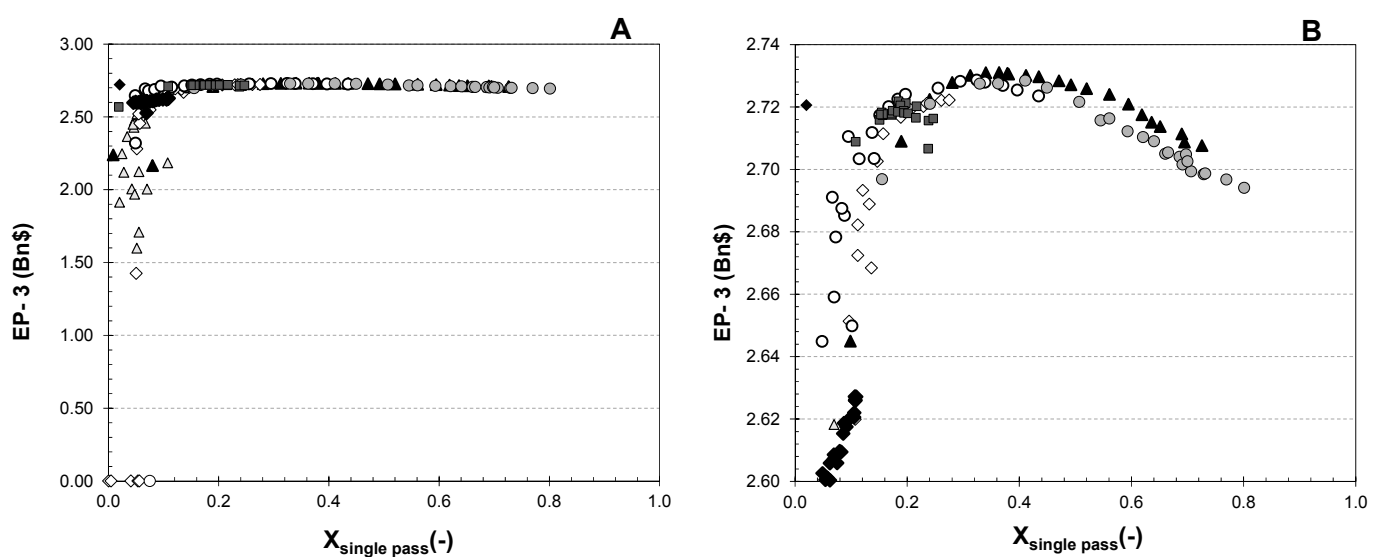


Figure 4.13: Effect of conversion and temperature on EP 3 for GCYC [$\triangle 40^{\circ}\text{C}$ $\diamond 50^{\circ}\text{C}$ $\circ 60^{\circ}\text{C}$ $\blacktriangle 70^{\circ}\text{C}$ $\bullet 80^{\circ}\text{C}$ $\blacksquare 90^{\circ}\text{C}$ $\blacklozenge 100^{\circ}\text{C}$]

Effect of catalyst load

The effect of catalyst load on the economic potential was also evaluated in the same manner. A comparison between the different catalyst loads against conversion is depicted in Figure 4.14 the same parabolic trend is observed in Figure 4.13, but less catalyst is favourable for the economic potential in this case due to the higher prices of the catalyst.

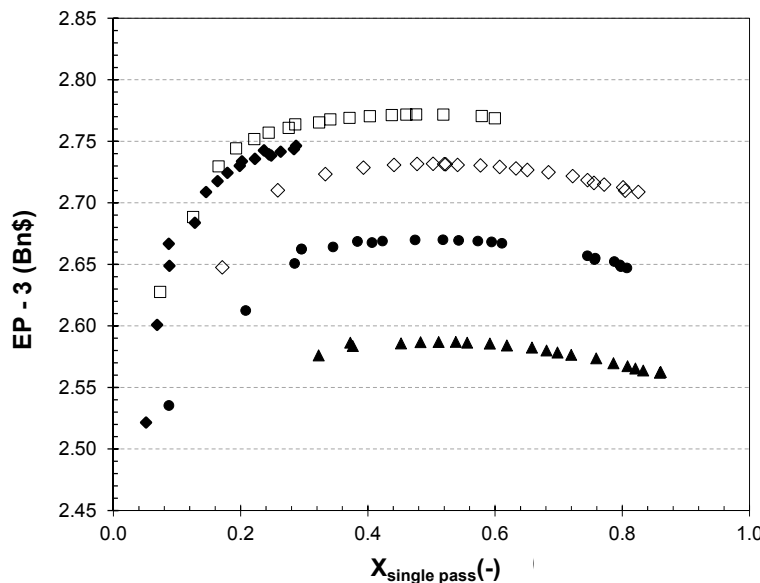


Figure 4.14: Effect of conversion and catalyst load on EP-3 [▲5000 ●7000 ◇10000 ◆12000 □ 14000 (C₈/Ru)]

From the results of the economic potential for a level 3 analysis, optimal operation conditions from an economic perspective were determined to be at the lowest catalyst concentration, i.e. C₈/Ru = 14 000 and 70 °C for the **GCYC** catalyst. Optimal conversion at which the reaction should be operated for the **GCYC** catalyst was determined to be 50 % single pass conversion. At these conditions, the reaction time in the reactor is recommended to be only 20 minutes. With these optimal conditions, and a favourable economic potential as a result of the design decisions made in the hierarchical design approach of Douglas, the next step required is to draw a comparison between the catalysts and evaluate the cash flow of the project over its lifetime to determine the return on investment, internal rate of return and the net present value thereof. This will be treated in section 4.5. As such the performance of the **GMPP** catalyst will consequently be evaluated for comparison.

4.4.2 Economic potential of GMPP precatalyst

The results of the Economic potential for the GMPP precatalyst is presented and summarised. The optimal single pass conversion and conditions are pointed out and the optimal residence time of the reactor is also determined. This topic and other optimal conditions, as well as the economic potential thereof, will be treated in the subsequent sections as the levels of design of the Douglas approach are sequentially processed. The GMPP catalyst has displayed latent thermos-switchable behaviour in the catalyst performance experiments. Similar step-function trends were observed in the kinetic evaluations the effects of which will be explored in this section.

4.4.2.1 GMPP precatalyst EP-1

The constant parameters and assumptions made in section 1.2 and 1.3.1 were applied to the economic potential equation for the GMPP catalyst. Stoichiometry was used to determine the 7-tetradecene production rate and the amount of catalyst required. The annual EP value at level 1 results are summarised in Table 4.5.

Table 4.5 Summary of EP1 inputs and outputs for the GMPP catalyst

EP-1		
Input	rate (kg/hr)	cost (\$/kg)
1-octene	1201	1.80
GMPP catalyst	0.760	20996
Output		
7-tetradecene	1051	334
EP1 (\$/hr)	332 804	
EP1 (Bn \$/yr.)	2 .771	

Table 4.5 displays the costs and feed rates of the process inputs, as well as the selling price and the output production rate of the primary product. As a result, the economic potential was calculated by application of the equation defined in section 1.3.2. A positive economic potential value of \$2.77 billion is a clear indication of positive potential in the process and the design can proceed to the next level.

4.4.2.2 GMPP precatalyst EP-2

The economic potential evaluation on level 2 was conducted as a function of conversion and the kinetic behaviour of the catalysts as obtained from empirical experiments was used to conduct the calculation. The recycle structure and the reactor cost was accounted for as described in the equations defined in section 1.3.3. Figure 4.15 A displays the effects of temperature and conversion on the cost of the reactor as and the corresponding effects on the economic potential is shown in Figure 4.15 B.

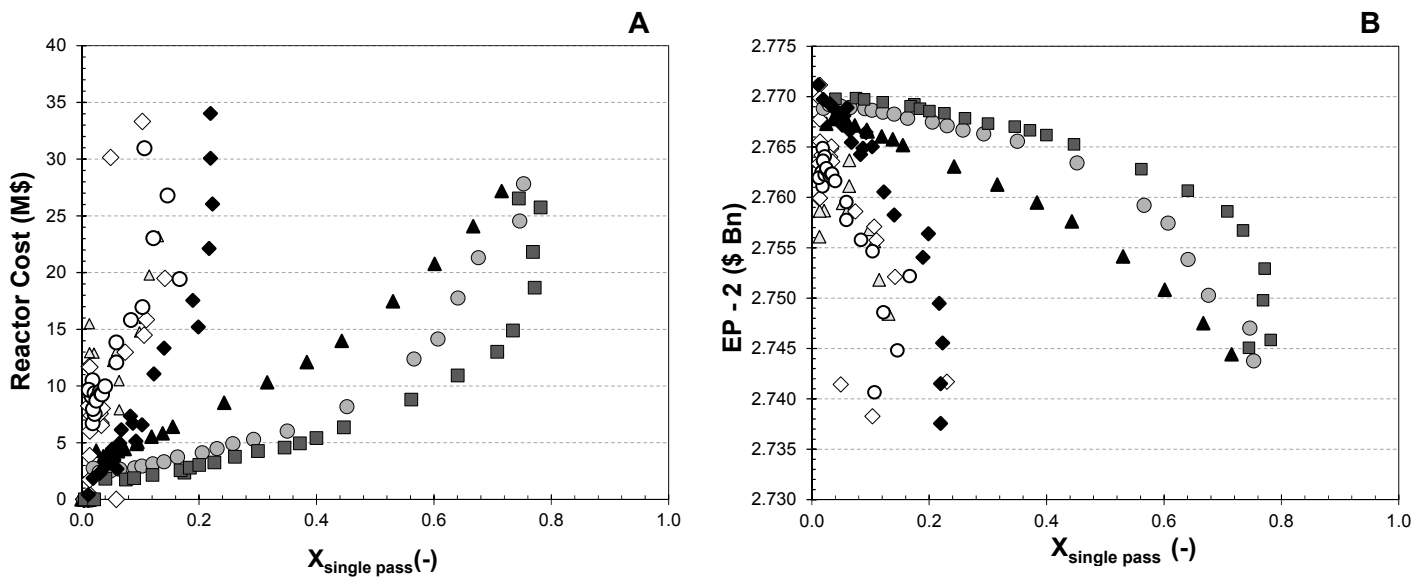


Figure 4.15 Effect of temperature and conversion for GMPP on (A) Reactor Cost and (B) EP-2 [\triangle 40°C \diamond 50°C \circ 60°C \blacktriangle 70°C \bullet 80°C \blacksquare 90°C \blacklozenge 100°C]

The trends in Figure 4.15 A show how the reactor cost exponentially increase and peak around 30-35 million US dollars as the conversion increases this is most visible at temperatures 70-80 °C. For temperatures, 40-60 °C and 100 °C low conversions are achieved and the costs for the reactor at these conditions are higher (< 35 million US dollars). This trend is understandable since a higher conversion would ultimately require the reaction to proceed longer, which results in a larger residence time and consequently reactor size [33]. The peak cost of the reactor for the **GCYC** catalyst was considerably lower than that for the **GMPP** catalyst, the most probable reason is the poor production performance of the **GMPP** catalyst. The linearly increasing trend at 40-60 °C and 100 °C in Figure 4.14 A is related to the poor performance of the catalyst under these conditions and its thermo-switchable nature that requires higher temperatures as a stimulus, and reactor size will not be able to compensate for the low conversion that these conditions result in.

The inverse of the same trend is visible when the effect of temperature and conversion on EP-2 is explored (Figure 4.14 B). Although the economic potential at this level remains positive for all the cases, the vertical downward trends of the economic potential over the reactor at 40, 50, 60 and 100°C indicates that these conditions are not favourable for the reaction. The optimal temperature that would result in high single pass conversion over the reactor without unreasonably large reactor sizes is 70, 80 or 90°C, the overall performance of the catalyst across these optimal temperatures remain mostly constant. Operation at 80°C will result in higher conversion but the margin between optimal conversion and higher reactor costs is very narrow thus 70 °C is selected.

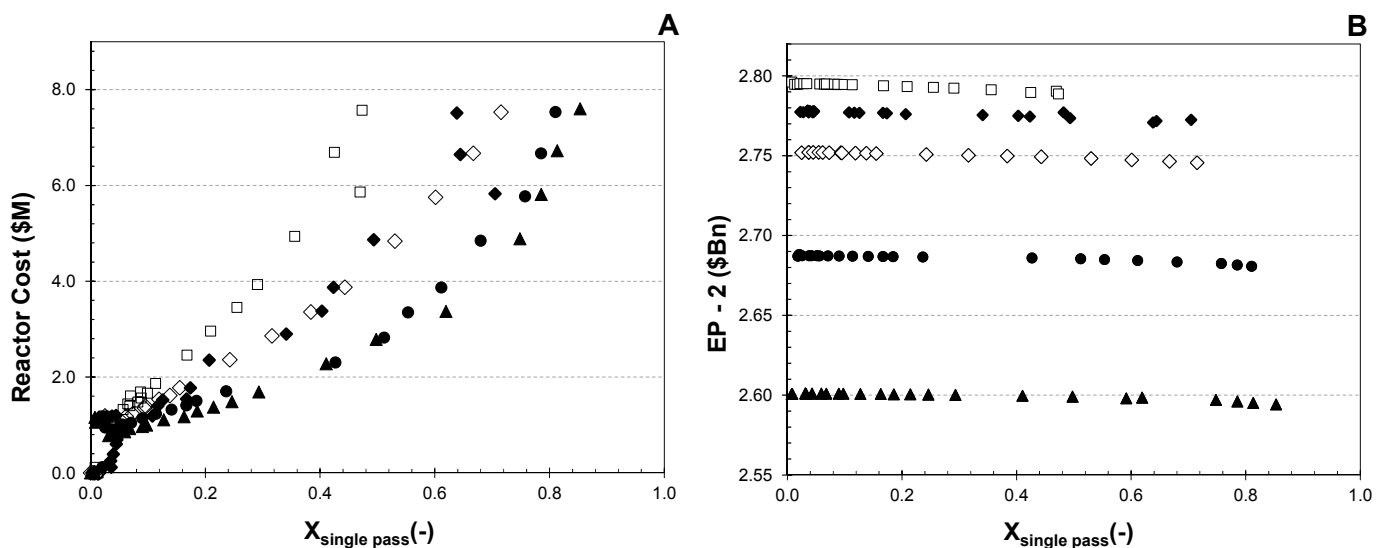


Figure 4.16: Effect of conversion and catalyst load for GMPP on (A) Reactor cost [$\triangle 40^{\circ}\text{C}$ $\diamond 50^{\circ}\text{C}$ $\circ 60^{\circ}\text{C}$ $\blacktriangle 70^{\circ}\text{C}$ $\bullet 80^{\circ}\text{C}$ $\blacksquare 90^{\circ}\text{C}$ $\blacklozenge 100^{\circ}\text{C}$] and (B) EP-2 [$\blacktriangle 5000$ $\bullet 7000$ $\diamond 10000$ $\blacklozenge 12000$ $\square 14000$ (C₈/Ru)]

Figure 4.16 B shows how the economic potential increases with a decrease in catalyst load. As the catalyst concentration is lowered the economic potential varies between \$ 2.6 billion and \$ 2.78 billion. The economic potential remains fairly constant as the conversion increases. At the upper limits of the conversion, a small decrease in the economic potential is observed. The maximum economic potential. As for the effects on the reactor cost with varying catalyst concentration the Figure 4.16 A shows that the reactor costs have a linearly increasing or slightly exponential trend as the conversion increases. Lower catalyst concentrations also have a lower conversion as a result and consequently, a larger reactor is required to achieve higher conversion, thus explaining the higher reactor costs under these conditions. Less catalyst is not necessarily the best option, but the economic potential thereof would have a deciding role. To illustrate this a bar chart with the average economic potential for each catalyst is provided in Figure 4.17.

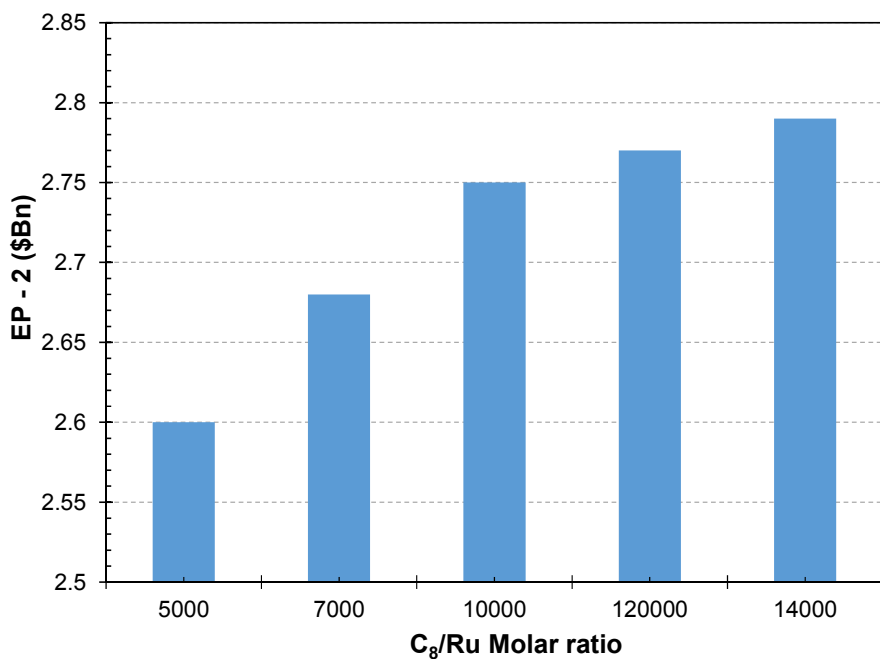


Figure 4.17: Maximum EP-2 at different catalyst loads (C₈/Ru)

4.4.2.3 GMPP precatalyst EP-3

The economic potential at level 3 will aid in the selection of an optimal single pass conversion over the reactor. The effects of the temperature and catalyst load on the separation costs as a function of conversion will also be explored. The economic potential evaluation at level 3 was evaluated for preliminary separation costs by applying short-cut design methods in the separation system development.

Effect of Separation cost

The effects of catalyst load, temperature and conversion on the total separation cost is summarised in Figure 4.18 A and B, where a nonlinear decreasing trend is observed between 400 million and 50 million US dollars. As the conversion increases the separation cost decreases until a local minimum is reached between 40 and 60% single pass conversion. The possible explanation that accounts for the high amount of separation costs at low conversion argues that the liquid pool volume required in the flash drum would be larger at lower conversions since larger amounts of 1-octene remain unreacted. More liquid would also cause entrainment and flooding and consequently higher volumes and larger membrane area, resulting in increased separation costs.

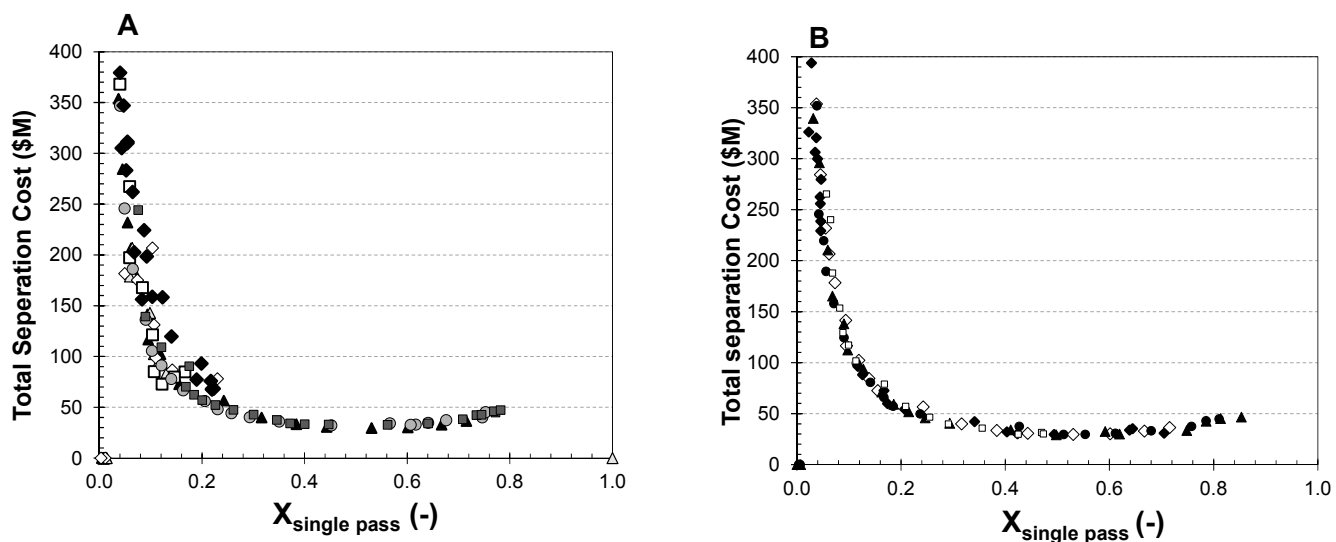


Figure 4.18 Effect of conversion, temperature (A) and catalyst load (B) on separation costs for GMPP [\triangle 40°C \diamond 50°C \circ 60°C \blacktriangle 70°C \bullet 80°C \blacksquare 90°C \blacklozenge 100°C] and [\blacktriangle 5000 \bullet 7000 \diamond 10000 \blacklozenge 12000 \square 14000 (C_8/Ru)]

Effect of Temperature

The effect of temperature and conversion on the level 3 economic potential was studied not only to gain information on the optimal reaction temperature but also the optimal reaction conversion.

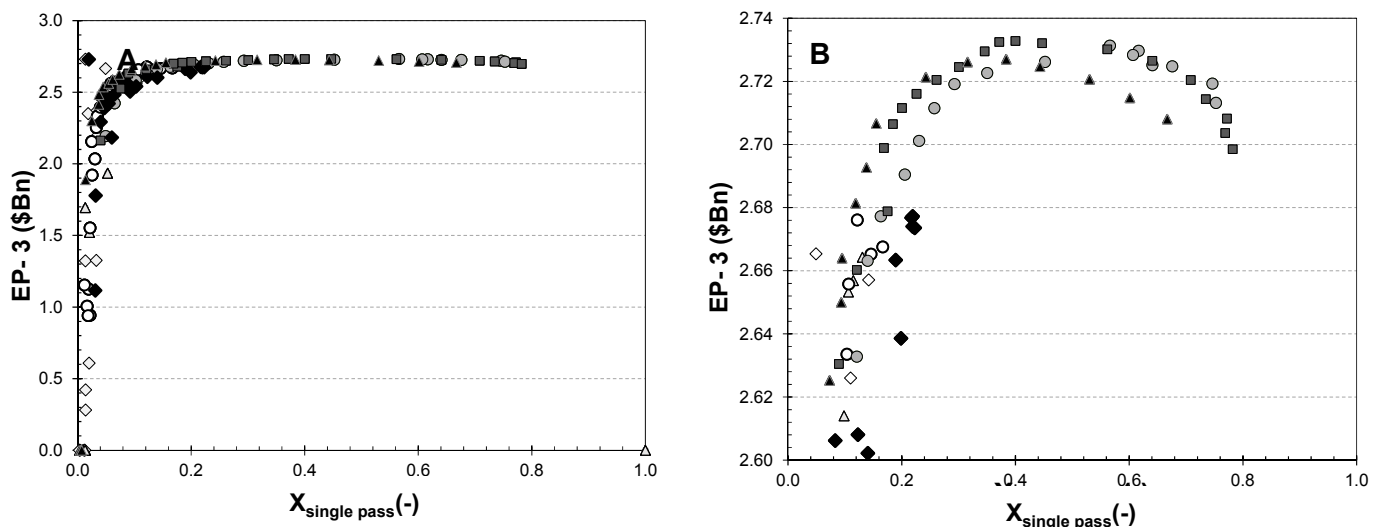


Figure 4.19: Effect of conversion (A) and temperature (B) on EP-3 [\triangle 40°C \diamond 50°C \circ 60°C \blacktriangle 70°C \bullet 80°C \blacksquare 90°C \blacklozenge 100°C]

Figure 4.19 A displays the economic potential as a function of temperature and conversion and B displays a rescaled version of A to illustrate the trends clearly. It is evident in A that the economic potential, albeit positive, is low in comparison to the **GCYC** catalysts at the lower and upper limits of the temperatures studied. This trend is clearer in 4.19 B displaying the optimal conversion and temperature for the **GMPP** catalyst.

The economic potential again continues to increase as the conversion up until the peak is reached between 40-50% after which the economic potential starts to decline. The decline is attributed to the catalyst decomposition at higher temperatures. The latency of the catalyst affords it the optimum operating temperature of 80°C.

Effect of catalyst load

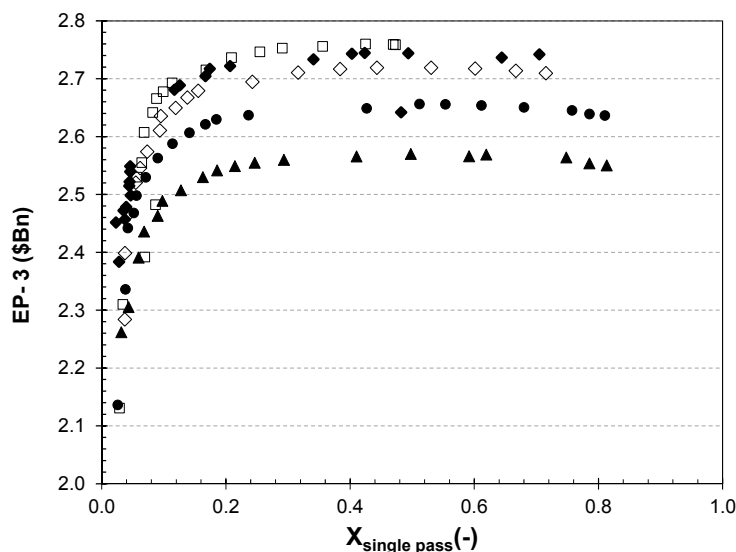


Figure 4.20: Effect of catalyst load on EP-3 with GMPP [▲5000 ●7000 ◇10000 ◆12000 □ 14000 (C₈/Ru)]

Similar to the effect of temperature, the effect of catalyst load on the economic potential was also evaluated. A comparison between the different catalyst loads against conversion is depicted in Figure 4.20. The same parabolic trend is observed as seen for the **GCYC** catalyst in the sense that less catalyst is favourable for the economic potential, probably due to the high prices of the catalyst.

4.4.3 Profitability analysis: catalyst comparison

Silla [25] describes economic evaluation as a continuous process. The economic potential of a process must be evaluated continually as new information becomes available to the engineer. Even if the initial information is insufficient to design a new plant or give a full techno-economic feasibility study, the intermittent economic analysis would enable the design engineer to work with chemists and researchers to obtain information where it lacks, or as such proceed the process to the pilot or commissioning stage. A project is economically feasible when the profits it will generate outperform those of the competing alternatives, even so, a process may be abandoned if the initial capital requirement is too high despite predictions of high profit. In such cases, unless alternative investors are sought to share the risk, the project will most likely be abandoned.

In his future work recommendations, Denhere [8] pointed out key focusses for the process of upgrading linear terminal alkenes via metathesis and hydroformylation of which one is to develop a data bank of kinetic data for more commercially available catalysts [8] and to employ more selective catalysts. The aim of this section is to take the analysis further and use the economic potential evaluation to screen between the non-commercial catalysts of this study and compare their profitability to a commercial catalyst for the same conceptual design over the reactor system. In doing so a method is developed that could be used in future synthesis studies to determine the feasibility of new complexes as they are developed.

Economic data can vary considerably, which could make it difficult to conduct such economic evaluations over time, as a result, standardised methods have been developed that are widely applied. The method used in this work is that of the methods described by Silla [25], Towler and Sinnott [2], Seader [35], and Timmerhaus.

To determine the financial position of the process over time a discounted cash flow analysis was conducted [35]. The cash flow analysis takes the capital investment, direct, indirect and overhead costs as well as the income generated to determine the rate at which the process has to return the investment to break even by the end of the project lifetime (Internal Rate of Return %). Similarly, the cash flow analysis is used to determine the current financial position (Net Present Value) of the process after the project lifetime has expired. If these values are found to be favourable the process can be kept in consideration for commercial application.

A workflow that describes the approach of the cash flow analysis is briefly illustrated in Figure 4.21

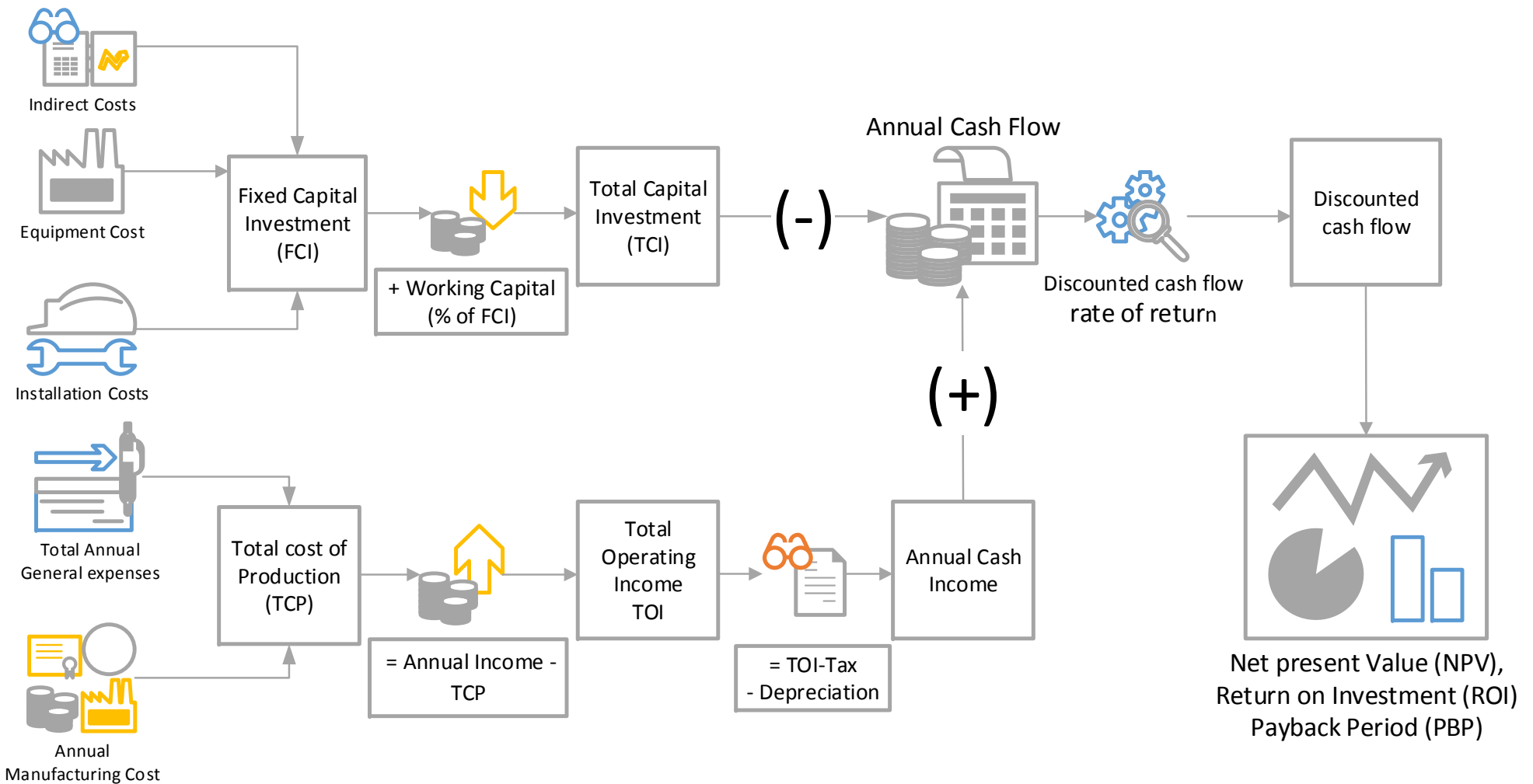


Figure 4.21: Discounted cash flow analysis work flowchart

Timmerhaus describes a number of methods by which the total capital investment and subsequent production and overhead costs can be estimated. The first is a detailed estimate. Such an estimate requires information from suppliers, contractors, engineers, detailed drawings etc. but this method would require many resources and is usually not used in preliminary cost estimation studies. Unit cost estimates are a widely applied method and are fairly accurate without the laborious efforts of the detailed method. This method, however, also requires the detailed cost estimation of equipment as determined from quotations or accurate cost records and published data. The other costs are then added to the unit cost as a number of factors to determine the overall cost. The third method and method of choice for this work is the percentage of delivered equipment cost method. The production, construction and secondary plant costs are determined as a percentage of the delivered equipment costs and total capital costs.

A list of assumptions and factors used for the cash flow analysis in this work is summarised in Table 4.6. Detailed sample calculations and assumption elucidation of the total investment cost, overhead costs, indirect costs etc. are provided in Appendix C and D.

Table 4.6 Assumed cash flow analysis constants

Assumption	Value
Discount rate	15%
Tax rate	28%
Project lifetime	15 Years

The cash flow analysis as depicted in Figure 4.21 was used in order to determine economic performance indicators. These indicators are a means by which the process can be evaluated, and the catalysts compared against each other. The indicators used in this work will briefly be listed and explained.

The Net present value is the total present value of future cash flows

$$NPV = \sum_{n=1-t} \left(\frac{\text{Cash Flow in year } n}{(1 + i)^n} \right) \quad (4.18)$$

where

$$n = \text{year}; i = \text{interest rate}; t = \text{project life time}$$

The Return on investment is defined as the percentage return in income the investors of the project can expect on their initial capital investment.

$$ROI = \frac{\text{Cumulative Net Profit}}{\text{Plant life} \times \text{initial investment}} \times 100\% \quad (4.19)$$

The Discounted cash flow rate of return (i') is a method used to estimate the current value of future earnings the process will generate. It is also the interest rate at which the NPV of the process is equal to 0 after the project lifetime has expired. The relationship can be expressed mathematically as:

$$0 = NPV = \sum_{n=1-t} \left(\frac{\text{Cash Flow in year } n}{(1 + i')^n} \right) \quad (4.20)$$

The final economic performance indicator is the Payback period which is the time it takes for the project to break even and has paid back its initial investment. All revenues generated after this point is considered profits.

$$PBP = \frac{\text{Total depreciable capital}}{\text{Net earnings} + \text{ann. depreciation}} \quad (4.21)$$

The economic indicators described have been calculated and are summarised in Table 4.7 for the **GCYC** and the **GMPP** catalysts. The values of the project are then compared to acceptable norms and the outcome of Denhere's study [8]. The profitability analysis was also applied to the **HG2** catalyst to provide a commercial measure by which the **GCYC** and **GMPP** catalyst can be compared. The differences and trends observed will be discussed and possible reasons for the differences will be provided.

Table 4.7 compares the results of the cash flow analysis for the **HG2**, **GCYC** and the **GMPP** catalysts. For both alcoholato pyridinyl precatalysts the operating conditions that were selected as the optimal were similar, however, the NPV (\$ 5.7 billion) of the **GCYC** catalyst was higher with a higher rate of return at 73.3% and a shorter payback period (3.6 years) compared to 4.8 required for the **GMPP** catalyst. Consequently, the **GMPP** catalyst is the less favourable choice in terms of economics because of the same value and amount of conversion achieved in both cases, but a higher reactor cost for the **GMPP** catalyst does not necessarily result in higher financial output. Despite the catalyst's thermal stability, it fails to compete with the **GCYC** catalyst on a financial basis.

Table 4.7: Economic Comparison of Cash flow results for GMPP and GCYC catalysts

Parameter	GCYC	GMPP	HG2
Single pass X	0.50	0.47	0.54
1-octene feed rate (tpa)	10 000	10 000	10 000
Temperature (°C)	70	70	50
catalyst load (C ₈ /Ru)	14000	14000	14000
Overall X C ₈	1	1	1
NPV (Bn \$)	5.777	4. 936	4.870
PBP Depreciable (yrs.)	3.65	4.71	3.53
IRR (%)	73.3	53.6	90.6
ROI (%)	78.34	50.1	107.81
TCI (Bn \$)	1. 637	2. 355	0.976

The **GMPP**, **HG2** and **GCYC** catalysts have been compared based on their discounted cash flow for the project in Figure 4.22. Figure 4.22 clearly shows how the **GCYC** catalyst outperforms. The **GMPP** catalyst, in payback period, the rate of return and the NPV. If the thermal switchable characteristics of the **GMPP** catalyst are preferred in the industry, it would require a longer reaction time than the seven hours specified in this work. Perhaps in such a case, it would be better to apply the **GMPP** catalyst on a batch basis.

When including the **HG2** catalyst, the results indicate that the **HG2** catalyst is still commercially the better choice in terms of the IRR (91%) and the ROI (107.8%). The temperature at which the **HG2** catalyst reactions are the most favourable (50 °C) is lower than the **GMPP** and the **GCYC** catalysts and temperature influences the cost of energy used in the process. Therefore, the process using **HG2** is cheaper to operate than the **GMPP** and **GCYC** catalysts if the feed has to be heated from room temperature. In the scope of SASOL's Fischer-Tropsch process, this may not be the case since energy would be required to lower the reactor effluent from >300 °C down to the reactor temperature and energy would be wasted if the **HG2** catalyst was selected. In contrast, the **HG2** catalyst is much more selective and catalyst decomposition only takes place at temperatures beyond 50 °C.

This means that the project using **HG2** would produce more and would consequently be able to repay the investment back sooner, resulting in higher IRR% and ROI%. Additionally, the **GMPP** and **GCYC** catalysts cost more than the **HG2** catalyst and a process using the **HG2** catalyst would spend less on operating and capital costs. Despite the **HG2** catalyst's high returns the NPV of the project is less than the **GCYC** which is explained by the high initial capital cost of the **GCYC** and **GMPP** catalysts.

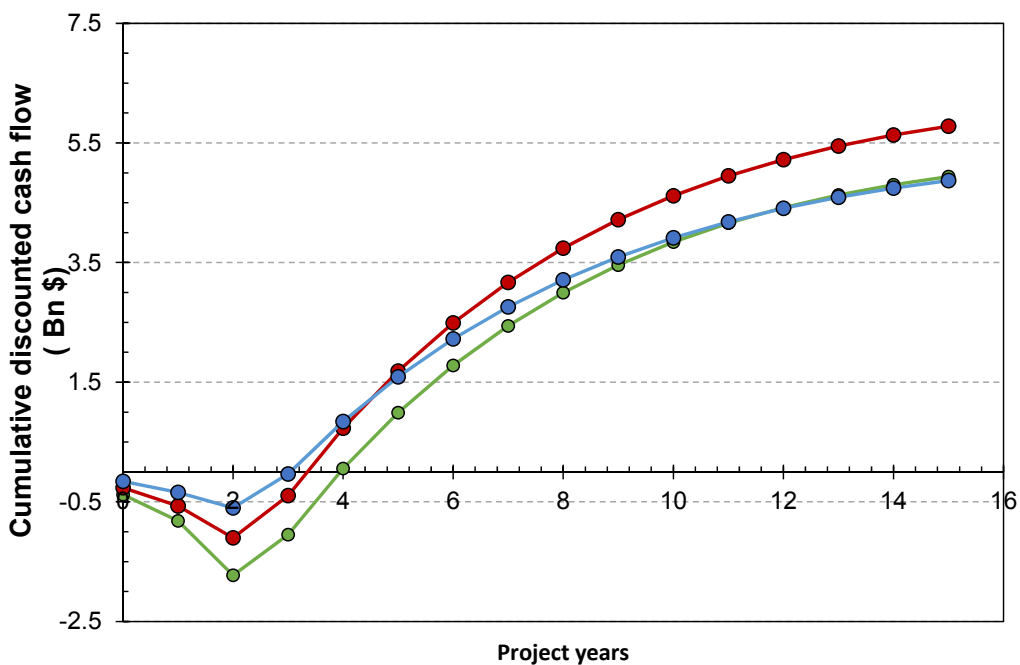


Figure 4.22: Discounted cash flow for 1-octene metathesis reactions in the presence of **GCYC** ● **GMPP** ● and **HG2** ●

4.5 Concluding comments

The efforts of this chapter sought to compare the **GCYC** can the **GMPP** precatalysts based on their reaction performance in a designed reaction process that would form part of a project to upgrade low-value alkenes to high-value surfactants. The work in this chapter has displayed that both the **GMPP** and the **GCYC** precatalysts prove to be feasible choices from an order-of-magnitude perspective, but when faced with a choice the **GCYC** precatalyst promises higher returns on investment than the **GMPP** catalyst, but higher NVP than the **HG2** catalyst. It is important to know that this doesn't render the **GMPP** precatalyst impractical. It only qualifies the conditions under which the **GMPP** catalyst should be applied.

A sensitivity analysis investigating the effects of a variation in the costs of the 7-tetradecene and the catalysts is summarised in Appendix D. The sensitivity analysis motivates the fact that the outcomes of the comparison study would not be affected but the only difference would be the scale at which the comparison is drawn. That said, with the NPVs of the **HG2** and **GMPP** catalyst so close to one another in value, it is difficult to distinguish the one from the other on this basis alone and the other profitability parameters thus need to be included.

4.6 References

- [1] R. Streck, Economic and ecological aspects in applied olefin metathesis, *J. Mol. Catal.* 76 (1992) 359–372
- [2] G. Towler, R.K. Sinnott, Costing and project evaluation, in Coulson Richardson Chem. Eng. Des. 2009: pp. 291–388.
- [3] R. Turton, R.C. Bailie, W.B. Whiting, J.A. Shaeiwitz, D. Bhattacharyya, Analysis, synthesis, and design of chemical processes Fourth Edition, 2012.
- [4] C.A. Cardona, Ó.J. Sánchez, Fuel ethanol production: Process design trends and integration opportunities, *Bioresour. Technol.* 98 (2007) 2415–2457.
- [5] J.M. Douglas, Conceptual design of chemical processes, McGraw-Hill, New York, 1988.
- [6] R. Smith, Chemical process: design and integration, 2014.
- [7] J.J. Siirila, D.F. Rudd, Computer-Aided synthesis of chemical process designs. from reaction path data to the process task network, *Ind. Eng. Chem. Fundam.* 10 (1971) 353–362.
- [8] M.C. Dimian, Process synthesis by hierarchical approach, *Integr. Des. Simul. Chem. Process.* 13 (2003) 229–298
- [9] S.F. Denhere, Process development for upgrading low value α C₈-olefin from Fischer-Tropsch to 2-hexyl-nonal, Stellenbosch University, 2016.
- [10] R.H. Grubbs, D.J. O'Leary, Handbook of Metathesis, Volume 2: Applications in Organic Synthesis, Wiley-VCH Verlag GmbH & Co, 2015.
- [11] C.L. Dwyer, Metathesis of Olefins, *Met. Ind. Org. Process.* (2006) 201–217.
- [12] J.C. Mol, Industrial applications of olefin metathesis, 213 (2004) 39–45.
- [13] B. de Jose, Olefins conversion technology applications. *Proc. World Pet. Congr.* 17th (2002) 503–511.
- [14] A. Inratecsolutions, Recent Publication Unveils the Economics of Propene Production via Metathesis ; (2012) 11–12. <http://www.einpresswire.com/article/94741415/propylene-production-via-metathesis-publication-is-announced-by-inratec> (date Accessed: June 2017)
- [15] K. Grela, Olefin Metathesis: Theory and Practice, 1st ed., Wiley, New Jersey, 2013.
- [16] W. Keim, Oligomerization of Ethylene to α -Olefins : Discovery and Development of the Shell Higher Olefin Process (SHOP), (2013) 12492–12496.
- [17] C.L: Dwyer, Metathesis : An Industrial Perspective, (2007) 1–7.
- [18] Sasol, Sasol Olefins & Surfactants, (2012) 1–24.
- [19] Research and Markets, Global Surfactant Market for Personal Care Products Industry 2015-2020: Trends, Forecast, and Opportunity Analysis, (2015). http://www.researchandmarkets.com/research/4ct3rc/global_surfactant (accessed February 8, 2016).

-
- [20] G.S. Forman, A.E. McConnell, R.P. Tooze, W.J. Van Rensburg, W.H. Meyer, M.M. Kirk, C.L. Dwyer, D.W. Serfontein, A Convenient System for Improving the Efficiency of First-Generation Ruthenium Olefin Metathesis Catalysts, *Organometallics*. 24 (2005) 4528–4542.
 - [21] Z. Lysenko, B.R. Maughon, T. Mokhtar-Zadeh, M.L. Tulchinsky, Stability of the first-generation Grubbs metathesis catalyst in a continuous flow reactor, *J. Organomet. Chem.* 691 (2006) 5197–5203.
 - [22] L. Liguori, H.-R. Bjorsvik, Continuous flow olefin metathesis using a multijet oscillating disk reactor as the reaction platform, *Org. Process Res. Dev.* 18 (2014) 1509–1515.
 - [23] A. Eldridge, Separations Division (76d) Olefin Production via Reactive Distillation-Based Olefin Metathesis, (2015) 20–23.
 - [24] P. van der Gryp, A. Barnard, J.P. Cronje, D. de Vlieger, S. Marx, H.C.M. Vosloo, Separation of different metathesis Grubbs-type catalysts using organic solvent nanofiltration, *J. Memb. Sci.* 353 (2010)
 - [25] P. Van der Gryp, S. Marx, H.C.M. Vosloo, Journal of Molecular Catalysis A: Chemical Experimental, DFT and kinetic study of 1-octene metathesis with Hoveyda–Grubbs second generation precatalyst, "Journal Mol. Catal. A, Chem." 355 (2012) 85–95.
 - [26] H. Silla, *Chemical process engineering: design and economics*, 2003.
 - [27] A.J. O'Lenick Jr., A.J. O'Lenick, Guerbet chemistry, *J. Surfactants Deterg.* 4 (2001) 311–315.
 - [28] P. Arnoldy, *Process aspects of rhodium-catalyzed hydroformylation*, Kluwer Academic Publishers, 2000.
 - [29] A. Szadkowska, X. Gstrein, D. Burtscher, K. Jarzembska, K. Woźniak, C. Slugovc, K. Grela, Latent thermo-switchable olefin metathesis initiators bearing a pyridyl-functionalized chelating carbene: Influence of the leaving group's rigidity on the catalyst's performance, *Organometallics*. 29 (2010) 117–124.
 - [30] P. Van Der Gryp, Separation of Grubbs-based catalysts with nanofiltration, North-West University, Potchefstroom, 2008.
 - [31] Sigma-Aldrich, Sigma-Aldrich, (2016). <http://www.sigmaaldrich.com/south-africa.html> (accessed August 10, 2016).
 - [32] C. Engineering, P. Cost, *Economic Indicators 2013 2014 2015*, (2015) 1–6.
 - [33] M.B. Dinger, J.C. Mol, Degradation of the second-generation Grubbs metathesis catalyst with primary alcohols and oxygen-isomerization and hydrogenation activities of monocarbonyl complexes, *Eur. J. Inorg. Chem.* 2003 (2003) 2827–2833.
 - [34] H.S. Fogler, *Elements of chemical reaction engineering*, Prentice-Hall, 2011.
 - [35] K.G. Joback, R.C. Reid, Estimation of pure-component properties from group-contributions, *Chem. Eng. Commun.* 57 (1987) 233–243.
 - [36] W.D. Seider, J.D. Seader, D.R. Lewin, *Product and process design principles: Synthesis, Analysis and Design*, (2004) 736.
 - [37] J.T. Sommerfeld, Tracking the Marshall & Swift equipment cost index, *Cost Eng.* 41 (1999) 29–31.

5 CONCLUSION

"Whatever our struggles and triumphs, however we may suffer them, all too soon they bleed into a wash, just like watery ink on paper." Arthur Golden, *Memoirs of a Geisha*

5.1 Overview

The contents of this chapter conclude and summarises the findings drawn from the investigations of this thesis. The conclusion breakdown in this chapter is as follows; in Section 5.1 the empirical studies in Chapter 2 are concluded, Section 5.2 is based on the kinetic studies conducted in Chapter 3 and Section 5.3 contains conclusions from the economic potential evaluation of Chapter 4. Chapter 5 is concluded with the contributions this work has made towards the research of c*change and the RSA-olefins programme and future research recommendations.

5.2 Introduction

The goals of this thesis were to compare two new Grubbs-type precatalysts on the basis of reactor size and economic potential in a conceptual design based on upgrading linear 1-alkenes to higher value Guerbet surfactants. The goals were divided into 3 objectives each of which was addressed in their own corresponding chapters. The conclusions obtained from these chapters is compiled, summarised and provided further in Chapter 5.

5.3 Precatalyst performance and product distribution

The objective of Chapter 2 was to understand the catalytic performance of the **GMPP** and **GCYC** precatalysts for the metathesis reaction of 1-octene. The metathesis reactions were conducted in a batch reactor setup with a temperature control facility. Precatalyst load was varied between 5 000 and 14 000 molar ratio of olefin to precatalyst (C_8/Ru) and the temperature was varied from 40 to 100 °C. The reactions ran for 7 hours and intermittent samples were taken and analysed via GC-FID to determine the product distribution of the precatalysts.

The species identified in the products followed the reports in literature, [1–5] and is summarised in Figure 5.1.

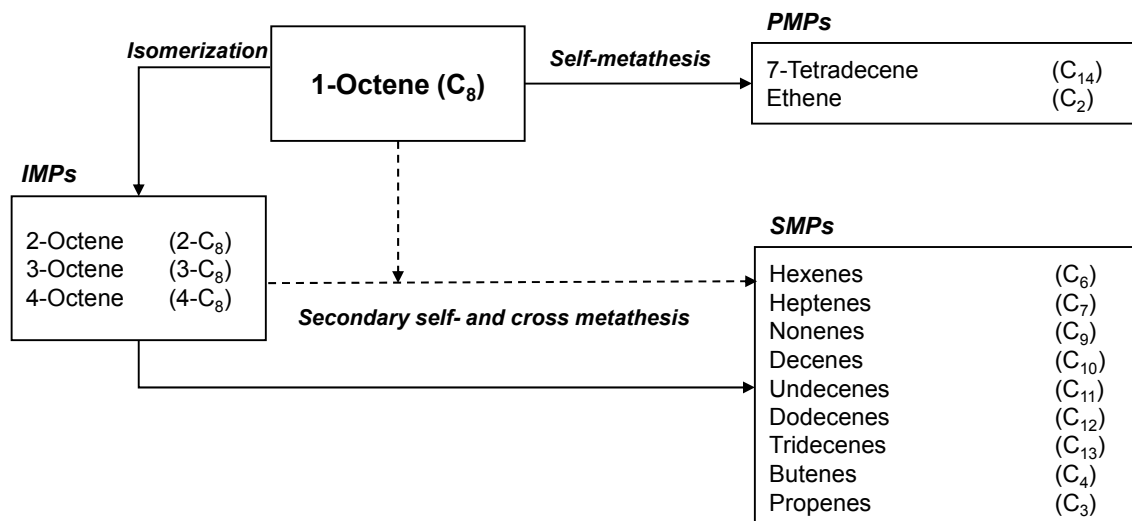


Figure 5.1: Possible products and reaction networks for 1-octene metathesis

In terms of catalytic performance, the **GCYC** precatalyst has shown a higher overall conversion of ~ 80.0 % at its optimal temperature (70 °C) compared to the GMPP precatalyst that only obtained 60% conversion at its peak temperature (80°C). Both precatalysts formed isomers that were ascribed to the possibility of precatalyst degeneration at higher temperatures [6–8], most of which underwent cross-metathesis (CM) to yield side metathesis products (SMPs). Both

precatalysts displayed latency towards the reaction since their performance only peaked/ initiated at 70 °C compared to the peak performance temperature of 50 °C for the commercial precatalyst of **HG2** [9]. Similar behaviour was observed by previous works on the **GCYC** precatalyst specifically [2, 10]. The **GMPP** precatalyst displayed thermal switchability in a step-function type trend. Conversion, selectivity and yield remained constant across the temperature range of 70–90 °C, before and after these temperatures the catalytic activity of the **GMPP** precatalyst was significantly lower, owing to its thermal switchable nature [5, 11].

This latent characteristic might make the precatalyst beneficial in reaction temperature control since the reaction is not very sensitive to changes in temperature in its operating range. The **GCYC** precatalyst's activity follows a classical bell curve trend where the conversion, yield and selectivity slowly increase up to 70 °C after which the performance starts to decline as temperature rises. The effects of precatalyst load showed that less precatalyst resulted in fewer products furthermore, the catalytic activity (TON) declined as the amount of precatalyst added declined. Since the 1-octene was in excess it can, therefore, be concluded that the load is the factor limiting the catalyst's efficiency.

The performance results of the **GCYC** and **GMPP** catalysts showed that the better performing precatalyst was found to be the **GCYC** precatalyst, but specific application may favour the **GMPP** precatalyst.

When compared to results from literature on the commercial **HG2** [9] precatalyst the **GCYC** precatalyst performed at a higher conversion but with decreased selectivity, indicating that a large portion of the **GCYC** precatalyst's side and isomerisation products contributed to the overall C₈ conversion. Thermal precatalyst decomposition was, therefore, suspected [10].

More information was required from a kinetic and mechanistic viewpoint to find the better precatalyst. The key results as discussed are summarised in Table 5.1.

Table 5.1: Summary of precatalyst performances from Chapter 2

Precatalyst	S (%)	TON	X (%)	Temperature
GCYC	41.6	6631	80.1	70 °C
GMPP	35.9	5373	60.0	80 °C
HG2 [9]	98.3	6648	64.5	50 °C

5.4 Kinetic reaction modelling

The aims of Chapter 3 were to develop a kinetic reaction rate law from first principles, design and develop the regression algorithm necessary to find the kinetic rate constants and compare the findings with literature. The different possible reaction mechanisms available in literature was explored and the reaction rate law was developed based on pseudo-steady state conditions. The Trust-region-reflective and Bootstrap algorithms were used to determine the kinetic constants and their confidence intervals. Precatalyst deactivation kinetics have not been described for the **GMPP** and the **GCYC** [1] precatalysts in literature yet.

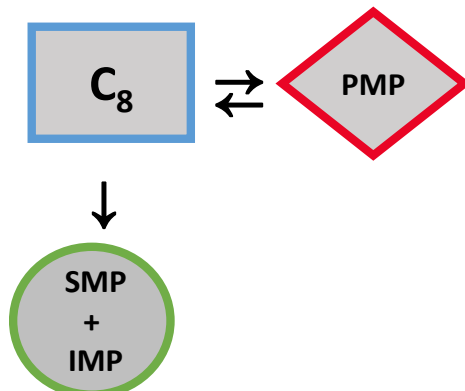
It was found that separable kinetics for catalyst deactivation could reasonably predict the reaction behaviour, especially in the formation of the secondary metathesis products (SMPs). Two possible rate laws were found to reasonably predict the reaction system based on the occurrence of catalyst deactivation and the irreversible nature thereof at higher temperatures. The observed kinetic parameters were fitted to the Arrhenius relationship to determine the dependence of the kinetic rates on temperature.

The deactivation rate of the **GCYC** precatalyst was found to be slower than findings in literature [1], explaining the increased stability of the **GCYC** precatalyst. The **HG2** precatalyst's consumption of 1-octene was reported [9] to be faster than the **GCYC** precatalyst which explained the reason why the **HG2** precatalyst's reactions reached equilibrium sooner at lower temperatures. The **GCYC** precatalyst's observed kinetic parameters followed the Arrhenius relationship up until complete precatalyst deactivation occurred at 100 °C. Closely corresponding activation energy between the **GCYC** precatalyst and the precatalyst in a previous report of similar structure [4] explained that the two precatalysts may be following the same mechanistic pathway, which was concluded to be a dissociation mechanism. The dissociation mechanism corresponded to the results as found by Jordaan [1] on the same precatalyst. The kinetic results indicate that the **GCYC** precatalyst has a very narrow region of optimal operation in terms of temperature, reduction of decomposition and peak performance, therefore, suggesting careful control requirements for temperature should the precatalyst be implemented industrially.

The results of the kinetic regression activities for the **GMPP** precatalyst was interesting since the step-function behaviour observed in the empirical experiments translated to the observed kinetic parameters as well. Step function behaviour for latent and thermo-switchable precatalysts have (to the author's knowledge) only been observed but not investigated kinetically in metathesis literature [14].

The decomposition rates of the **GMPP** precatalyst was found to be 2-orders of magnitude smaller than the deactivation of the **GCYC** precatalyst. Making the **GMPP** precatalyst a viable choice when prevention of precatalyst decomposition is the largest concern, as it brings the question of whether this precatalyst will be reusable for consecutive reactions. In terms of the observed kinetic rate parameters, the Arrhenius relationship was followed between the ranges of 70-100 °C resulting in the step function equation as formulated in Equation 5.7. Reaction rates were generally found to be considerably smaller than commercial precatalysts [9] and the initiation step was concluded to be the rate-limiting step for both precatalysts in the dissociation mechanism. Key findings for the precatalysts are summarised as follows:

Reaction network:



Rate Laws:

First order precatalyst deactivation cases

$$\frac{dC_{c8}}{dt} = -k_1 C_{c8} * \text{EXP}(-k_d t) - k_3 C_{c8} * \text{EXP}(-k_d t) \quad (5.1)$$

$$\frac{dC_{PMP}}{dt} = k_1 C_{c8} * \text{EXP}(-k_d t) \quad (5.2)$$

$$\frac{dC_{SMP}}{dt} = k_3 C_{c8} * \text{EXP}(-k_d t) \quad (5.3)$$

Cases where the deactivation does not occur.

$$\frac{dC_{c8}}{dt} = -k_1 C_{c8} + k_2 C_{PP} - k_3 C_{c8} \quad (5.4)$$

$$\frac{dC_{PMP}}{dt} = k_1 C_{c8} - k_2 C_{PMP} \quad (5.5)$$

$$\frac{dC_{SMP}}{dt} = k_3 C_{c8} \quad (5.6)$$

Arrhenius relationship:

Step function relationship for GMPP 1-octene Consumption:

$$k_{1obs} = \begin{cases} 0; T < 70^{\circ}C \\ 1.05E + 09 e^{-\frac{13.10}{R.T}}; 70^{\circ}C < T < 100^{\circ}C \\ \leq 2; T \geq 100^{\circ}C \end{cases} \quad (5.7)$$

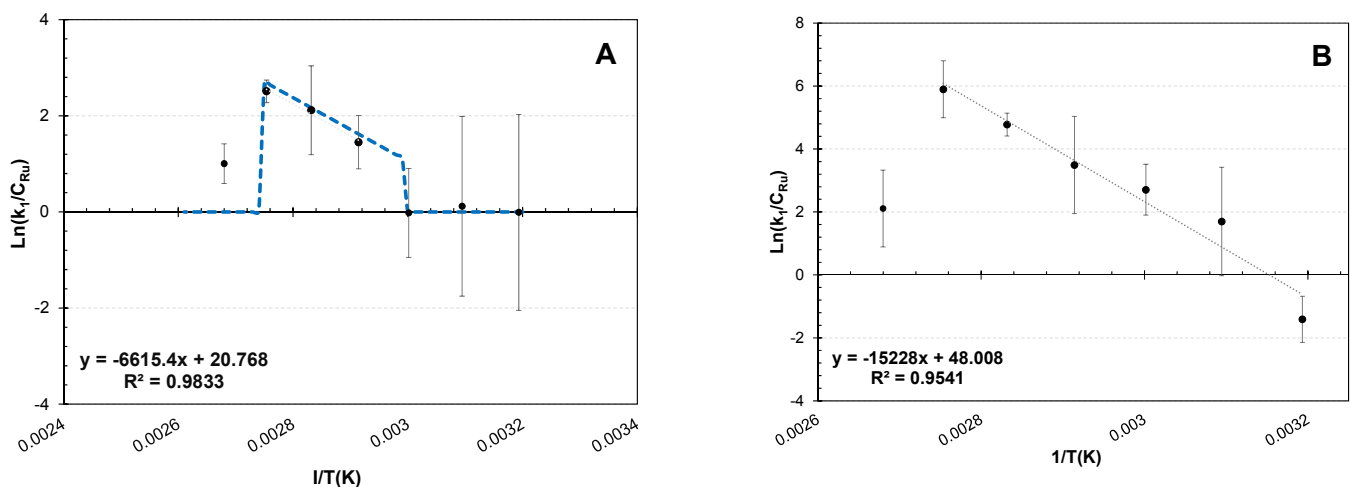


Figure 5.2: Arrhenius relationship fits for the GMPP (A) and the GMPP (B) catalysts 1-octene consumption

Table 5.2: Summary of key Arrhenius relationship parameters for GMPP and GCYC precatalysts

Precatalyst	Average activation energy (kcal.mol ⁻¹)	Average rate constant for C ₈ consumption (mL.mol ⁻¹ .min ⁻¹)	Average thermal decomposition rate (mL.mol ⁻¹ .min ⁻¹)
GCYC	30	7×10^{20}	1×10^{16}
GMPP	13	1×10^9	3×10^4

Deactivation rates

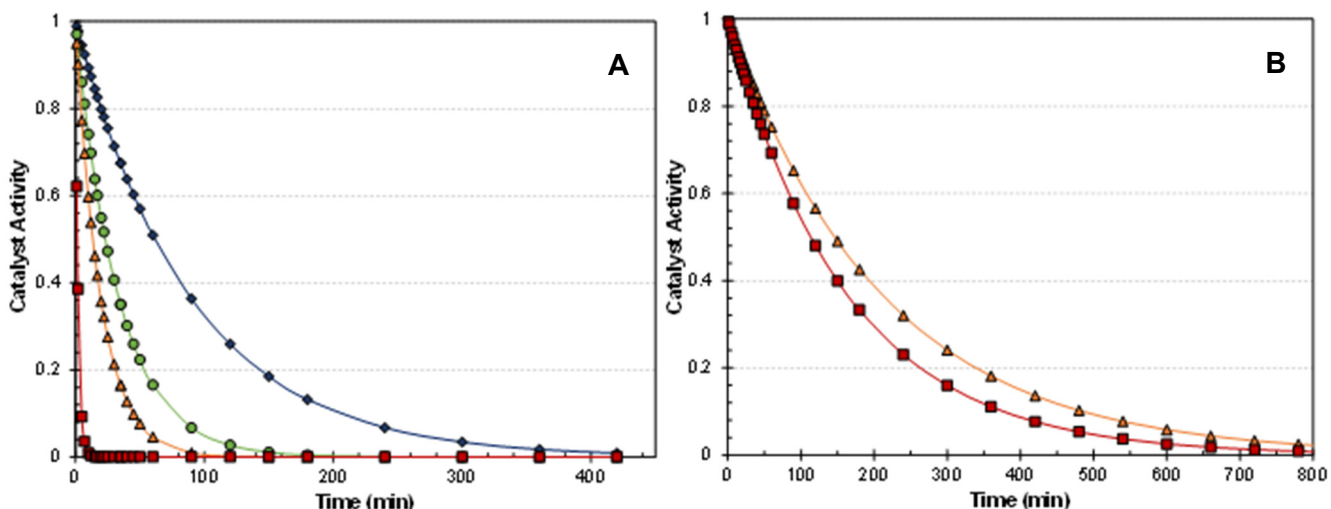


Figure 5.3: Precatalyst activity (a) as a function of time for the GCYC (A) and GMPP (B) catalysts at \blacklozenge 60°C
● 70°C ▲ 80°C ■ 90°C

The kinetic investigation of the **GMPP** and **GCYC** precatalysts provided insight into the precatalyst deactivation and decreased reaction rates obtained for latent precatalyst systems. The **GMPP** precatalyst has shown interesting behaviour and further exploration thereof is necessary for studies to lead to development and implementation in industry since it offers the prospects of less stringent temperature control and slower deactivation.

5.5 Economic evaluation

The objectives of the economic evaluation were to obtain a financial perspective on the difference between the **GMPP** and the **GCYC** precatalysts and determine their industrial viability towards beneficiation of low-value alkene feedstocks with metathesis. The aim was to obtain an estimation of the reactor size required and determine the economic potential of each precatalyst, by also investigating the effects of temperature, conversion and precatalyst load.

The economic potential analysis was conducted following the design approach suggested by Douglas up to level 3 [14] where the primary separation steps, recycle structure and reactor inputs & products were considered in a conceptual process.

Empirical correlations for cost estimations were used to design the conceptual process equipment [16]. Correlations were related to modern values by implementing cost indices [17]. Designed equipment included a stainless steel CSTR-reactor, separation by OSN membrane [3] was used to retrieve the catalyst, a flash drum designed to facilitate gas-liquid separation and a distillation column to retrieve the unreacted 1-octene and products.

Positive economic potential values were obtained for both precatalysts. The optimal operating temperature was found to be 70 °C and the least amount of precatalyst added to the system proved to be the most economic choice (C_8/Ru molar ratio = 14 000). The single pass conversion for the highest economic potential was determined to be 50 and 47 % for the **GCYC** and the **GMPP** precatalysts respectively. Economic indicators found that the **GCYC** precatalyst's production rate would favour investment above that of the **GMPP** precatalyst with an internal rate of return (**IRR**) of 73.3% and 53.6% for the two precatalysts respectively. The same set of equations, conditions and assumptions were applied to empirical data results obtained in [9] to obtain economic profitability parameters for the **HG2** precatalyst as well. Overall the **HG2** precatalyst could generate revenue faster with an IRR of 91 % and a 107.81 % ROI but yielded less revenue at the end of the project lifetime with the lowest **NPV** of the three. This trend is attributed to the high precatalyst costs and lower selectivity of the **GMPP** and **GCYC** precatalysts compared to the **HG2**. The higher selectivity of the **HG2** precatalyst results in a smaller and cheaper reactor and consequently cheaper initial start-up costs. Additionally, the **HG2** precatalyst operates at lower process temperatures which also influence the project cost, increasing the percentage of return on initial investment (**ROI%**).

Both precatalysts were found to be profitable, however, the **GCYC** precatalyst offered higher investment return, with a shorter payback period.

It is important to keep in mind that the economic values in the conceptual design are heavily dependent on the cost of the precatalysts and the price of the 7-tetradecene products. In reality, the 7-tetradecene would not be the final product but rather an intermediate and as such, the project viability can change considerably when looking at the whole proposed reaction network of c*change [18]. This work has served its purpose in comparing precatalysts based on economic evaluations aiding in the collaboration between chemists and engineers in the prospects of future research recommendations. What can be said of the **GMPP** and **GCYC** precatalysts is that their latency provides a higher temperature stability than the **HG2** precatalyst cannot.

A summary of the key results is available in Figure 5.4.

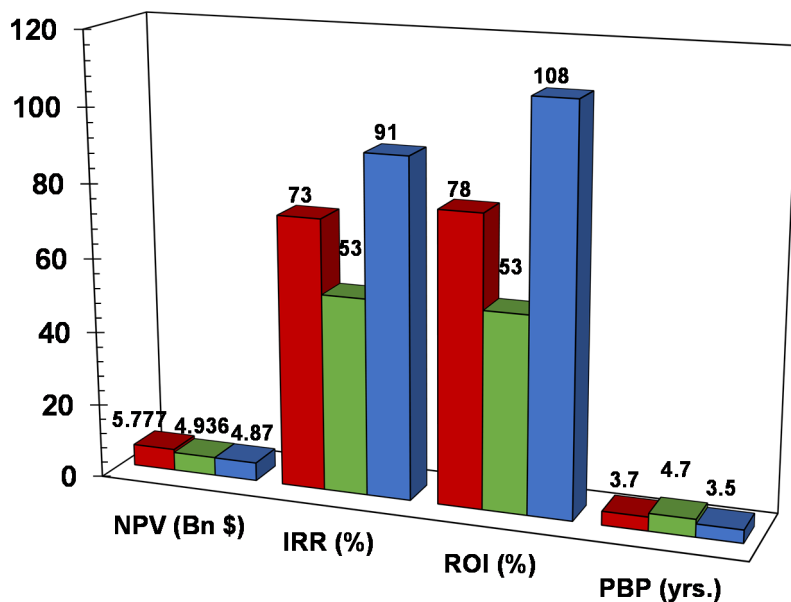


Figure 5.4: Profitability analysis summary for GCYC ● GMPP ● HG2 ●

Taking all the evaluations together, that is: performance, kinetics and economics into account, the **GCYC** precatalyst has displayed more favourable results compared to the **GMPP**, the only drawbacks are that it would require stringent temperature control and prevention of precatalyst deactivation. An important aspect to question is how the precatalyst performs under recycled consecutive reaction tests, it is suspected that recycling decomposed precatalyst into the reactor would possibly increase the deactivation of fresh precatalyst.

The **GMPP** precatalyst still proved to be a profitable choice where temperature control is required, and higher temperatures need to be endured. The precatalyst stability may prove the precatalyst to be a better choice in consecutive reactions. Overall the **HG2** precatalyst is still the better choice at low temperatures.

5.6 Future research recommendations and contributions

Key results from this work have been presented at the 22nd International Symposium of Olefin Metathesis (ISOM) in Zurich, July 9-12, 2017. It has contributed to the research of c*change by providing insight into the kinetic deactivation behaviour of latent precatalysts as well as providing the step function behaviour of the **GMPP** precatalyst.

The novel **GMPP** precatalyst's product distribution, reaction rate and overall kinetic behaviour was evaluated and compared to the **GCYC** precatalyst. A reaction kinetic model that describes deactivation behaviour of the reaction for chelating pyridinyl alcoholato ruthenium precatalysts was developed. An economic potential analysis was conducted to determine the industrial viability of the new precatalysts assisting further research into improving on their shortcomings and proving that such a process is viable. Perhaps further research should be directed towards the development of more selective precatalysts, scale-up studies, and the comparison of catalysts, proved feasible enough with the techniques applied in this work, from a techno-economic perspective.

DFT and NMR studies are necessary to determine whether the precatalysts are indeed following a dissociation mechanism and understand the mechanistic aspects of precatalyst deactivation for these latent chelating pyridinyl alcoholato precatalysts. Also, to characterise the decomposing species within the catalytic cycle. In terms of economic potential, the analysis can be used in future studies towards screening more precatalysts for industrial application, identifying the problem areas of each precatalyst compared to the next. The precatalysts have been developed to a high level of thermal stability but decomposition is still taking place. A lifetime study in which the catalysts are re-used and recycled in subsequent reactions would also be able to provide a clearer indication of the exact catalytic species that are decomposing and if such decomposition is irreversible. Future synthesis research should try to improve the precatalyst efficiency/activity (TON) and selectivity capabilities of the precatalysts towards primary product formation.

5.7 References

- [1] M. Jordaan, H.C.M. Vosloo, Ruthenium catalyst with a chelating pyridinyl-alcoholato ligand for application in linear alkene metathesis, *Adv. Synth. Catal.* 349 (2007) 184–192.
- [2] J.I. Du Toit, M. Jordaan, C.A.A. Huijsmans, J.H.L. Jordaan, C.G.C.E. Van Sittert, H.C.M. Vosloo, Improved metathesis lifetime: Chelating pyridinyl-alcoholato ligands in the second-generation Grubbs precatalyst, *Molecules*. 19 (2014) 5522–5537.
- [3] C. Van Schalkwyk, H.C.M. Vosloo, J.M. Botha, An investigation into the activity of the in-situ ruthenium(III) chloride catalytic system for the metathesis of 1-octene, *J. Mol. Catal. A Chem.* 190 (2002) 185–195.
- [4] J.I. du Toit, P. van der Gryp, M.M. Loock, T.T. Tole, S. Marx, J.H.L. Jordaan, H.C.M. Vosloo, Industrial viability of homogeneous olefin metathesis: Beneficiation of linear alpha olefins with the diphenyl-substituted pyridinyl alcoholato ruthenium carbene precatalyst, *Catal. Today.* (2016).
- [5] T. Tole, J. du Toit, C. van Sittert, J. Jordaan, H. Vosloo, Synthesis and application of novel ruthenium catalysts for high-temperature alkene metathesis, *Catalysts*. 7 (2017) 22.
- [6] S.H. Hong, D.P. Sanders, C.W. Lee, R.H. Grubbs, Prevention of olefin isomerization during olefin metathesis reactions., *Abstr. Pap. 229th ACS Natl. Meet. San Diego, CA, United States, March 13-17, (2005)*.
- [7] H.H. Soon, A.G. Wenzel, T.T. Salguero, M.W. Day, R.H. Grubbs, Decomposition of ruthenium olefin metathesis catalysts, *J. Am. Chem. Soc.* 129 (2007) 7961–7968.
- [8] M.B. Dinger, J.C. Mol, Degradation of the second-generation Grubbs metathesis catalyst with primary alcohols and oxygen – isomerization and hydrogenation activities of monocarbonyl complexes, *Eur. J. Inorg. Chem.* 2003 (2003) 2827–2833.
- [9] P. Van der Gryp, S. Marx, H.C.M. Vosloo, Journal of Molecular Catalysis A: Chemical Experimental, DFT and kinetic study of 1-octene metathesis with Hoveyda – Grubbs second generation precatalyst, "Journal Mol. Catal. A Chem. 355 (2012) 85–95.
- [10] M. Jordaan, Experimental and Theoretical Investigation of new Grubbs-type catalysts for the metathesis of alkenes, North-West University Potchefstroom, 2007.
- [11] A. Szadkowska, X. Gstrein, D. Burtscher, K. Jarzembska, K. Woźniak, C. Slugovc, K. Grela, Latent thermo-switchable olefin metathesis initiators bearing a pyridyl-functionalized chelating carbene: Influence of the leaving group's rigidity on the catalyst's performance, *Organometallics*. 29 (2010) 117–124.
- [12] F. Ding, S. Van Doorslaer, P. Cool, F. Verpoort, Olefin isomerization reactions catalyzed by ruthenium hydrides bearing Schiff base ligands, *Appl. Organomet. Chem.* 25 (2011) 601–607.
- [13] M. Jordaan, P. van Helden, C.G.C.E. van Sittert, H.C.M. Vosloo, Experimental and DFT investigation of the 1-octene metathesis reaction mechanism with the Grubbs 1 precatalyst, *J. Mol. Catal. A Chem.* 254 (2006) 145–154.
- [14] A. Ben-Asuly, E. Tzur, C.E. Diesendruck, M. Sigalov, I. Goldberg, N.G. Lemcoff, A thermally switchable latent ruthenium olefin metathesis catalyst, *Organometallics*. 27 (2008) 811–813.
- [15] J.M. Douglas, Conceptual design of chemical processes, McGraw-Hill, New York, 1988.
- [16] G. Towler, R.K. Sinnot, Costing and project evaluation, in Coulson Richardson Chem. Eng. Des. 2009: pp. 291–388.

-
- [17] C. Engineering, P. Cost, Economic indicators 2013 2014 2015, (2016) 1–6.
 - [18] M. Claeys, S. Harrison, H.C.M. Vosloo, B. Zeelie, R. Weber, c*change DST-NRF Centre of Excellence in Catalysis, (2016). www.cchange.ac.za/rsa-olefins/ (accessed April 4, 2016)

APPENDIX A: Supplementary literature

CATALYST DECOMPOSITION

Catalysts are wonderful resources to increase reaction rates but precatalyst decomposition or poisoning is one of the drawbacks that precatalysts experience. The Grubbs-type precatalysts are not immune to decomposition and loss of performance. In the case of these benzylidene complexes, many different reasons have been proposed about the cause of decomposition although, all instances of decomposition aren't necessarily a complete disadvantage. Some authors have managed to take advantage of the propensity of the precatalysts to decompose in tandem reactions [1-2] to selectively produce desirable stereo-isomers. Nevertheless, the importance of a clear understanding of the decomposition reactions and mechanisms cannot be emphasised more. The largest motivation is to prevent the formation of unwanted side reactions and reduce precatalyst replacement costs [3]. A brief layout of precatalyst decomposition in Grubbs-type precatalysts will thus be covered

Typically, highly unstable methylidene complexes form once the catalytic turnover with terminal alkenes has taken place. During the propagation phase in the catalytic cycle, the phosphine can re-coordinate to the metal complex forming the methylidene complex that decomposes quite swiftly. Decomposition of the methylidene takes place by the dissociation of the phosphine that reacts with the alkylidene moiety, forming a phosphine ylide species and a binuclear ruthenium hydride species. [3] Grubbs *et al.* [4] proposed this mechanism for the formation of the binuclear ruthenium hydride species from the **G2** precatalyst.

The team went even further to screen the stability of a range of different complexes. Decomposition rates were reported, and it was found that not only does the ligand structure play a large role in the decomposition mechanism, but that the presence of ethylene also led to the formation of the isomerising ruthenium hydride species. The methylidene complex has also displayed sensitivity towards pyridine [4].

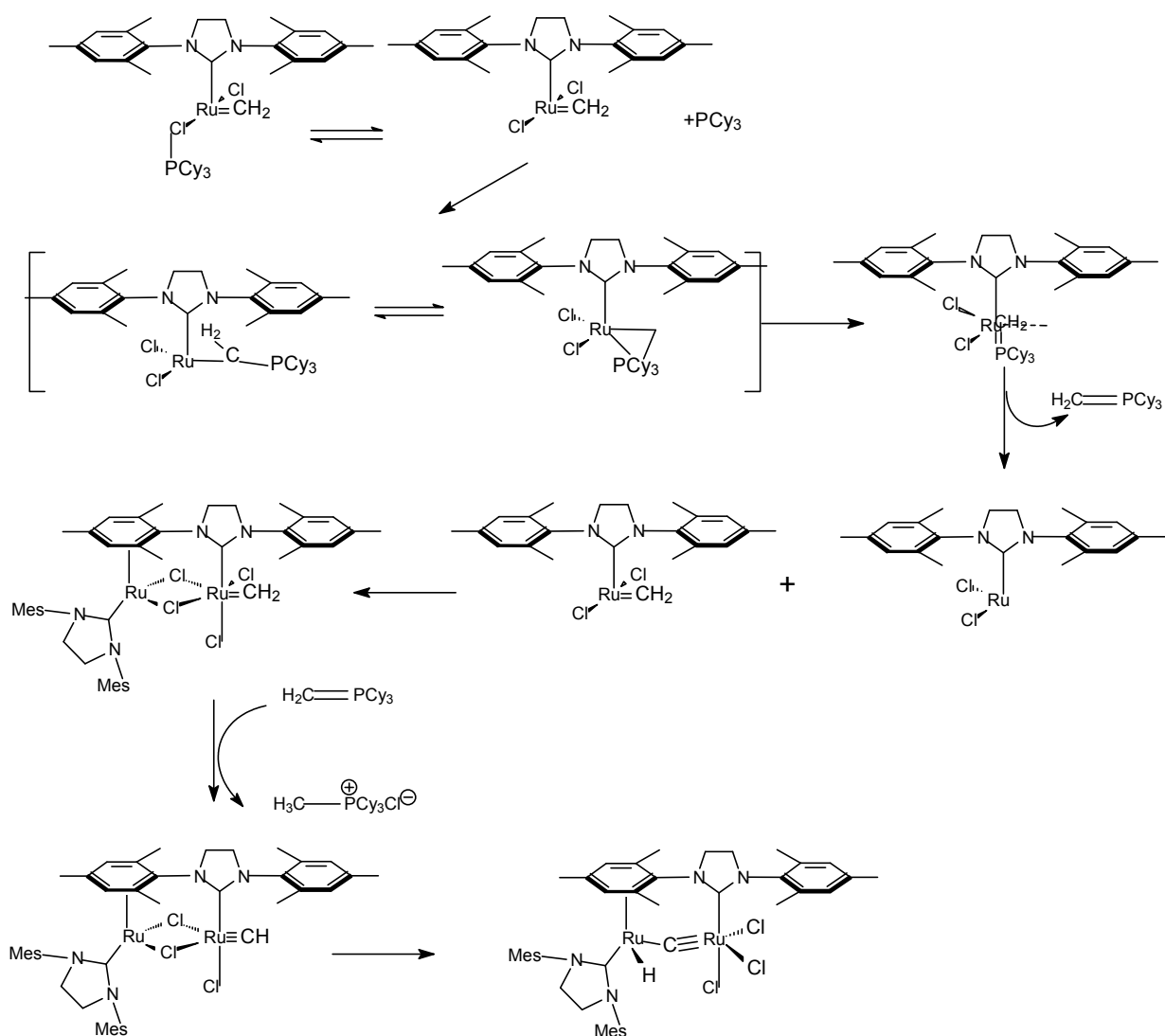
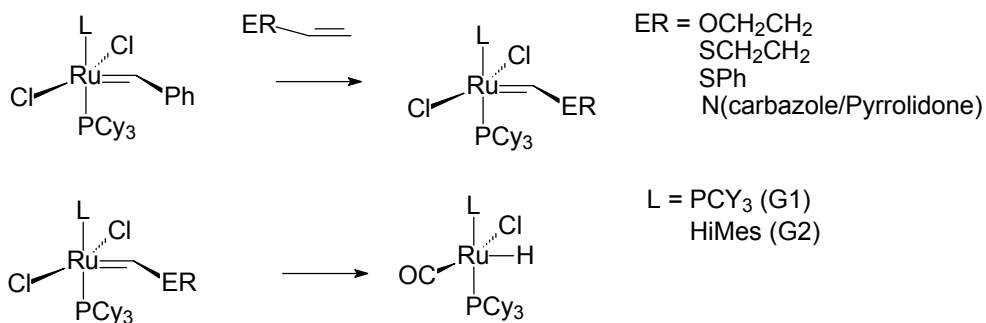


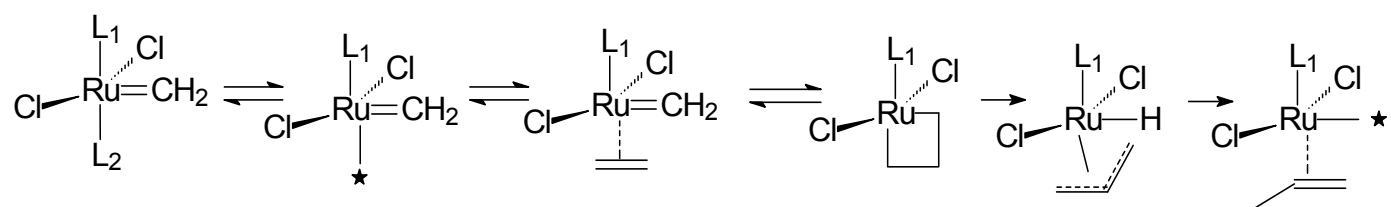
Figure A.1: Decomposition mechanism of methylidene species [4]

Substrates have also been reported to cause decomposition, of which electron-rich alkenes are the typical culprit. In another study by Grubbs *et al.* [5] using vinyl ethers as a substrate, the resulting decomposition complexes required high temperatures to initiate, even higher temperatures led to thermolysis of these species which in turn caused the formation of ruthenium hydride species [5]. As depicted in the scheme of Figure A.. In application Lehman *et al.* [1] showcased this isomerisation with 1-octene as a substrate, using both the **G1** and **G2** precatalysts. The results yielded significant isomerisation metathesis products forming as well as the corresponding side-product formation for temperatures between 50-60°C. High temperatures and long reaction times were ascribed to the formation of side-products and isomers by Dinger and Mol's study of the efficiency of the Ruthenium Hydride species formed when using the **G1** precatalyst. A range of temperatures and reaction times were tested and a high degree of selectivity towards 2-Octene was reported alongside high isomerisation conversion at 100°C (97%).

**Figure A.2: Metathesis reaction of electron-rich alkenes**

Ruthenium Hydride species could also be formed by the addition of external hydrogen sources or co-catalysts. Schmidt [5] has used the addition of external hydrogen sources such as NaH and NaOH to a metathesis reaction sequence to promote alkene isomerisation. Once again it was found that the ruthenium hydride species was responsible for the isomerisation activity.

Janse van Rensburg [5] has studied the decomposition of the ruthenacyclobutane species that forms during the dissociation mechanism in the presence of ethene. Their DFT calculations were consistent with the substrate induced decomposition mechanism as shown in Figure A 2

**Figure A.3: Dissociation mechanism and substrate-induced decomposition of ruthenacyclobutane intermediate with ethylene [1]**

There have been other suggestions as to how and why precatalyst decomposition takes place. *inter alia* alcoholysis, C-H insertion, π -Acids, and bases have been shown to be possible causes towards precatalyst deactivation, each with their own pathway [5].

REFERENCES

- [1] S.E. Lehman, J.E. Schwendeman, P.M. O'Donnell, K.B. Wagener, Olefin isomerization promoted by olefin metathesis catalysts, *Inorganica Chim. Acta*. 345 (2003) 190–198.
- [2] Mtshatsheni Kgomotsong, Metathesis of alkenes using ruthenium carbene complexes, North-West University, 2005.
- [3] W. Buchowicz, J.C. Mol, Catalytic activity and selectivity of $\text{Ru}(\text{=CHPh})\text{Cl}_2(\text{PCy}_3)_2$ in the metathesis of linear alkenes, *J. Mol. Catal. A Chem.* 148 (1999) 97–103.
- [4] H.H. Soon, A.G. Wenzel, T.T. Salguero, M.W. Day, R.H. Grubbs, Decomposition of ruthenium olefin metathesis catalysts, *J. Am. Chem. Soc.* 129 (2007) 7961–7968.
- [5] D.J. Nelson, S. Manzini, C.A. Urbina-Blanco, S.P. Nolan, Key processes in ruthenium-catalysed olefin metathesis., *Chem. Commun. (Camb)*. 50 (2014) 10355–75.
- [6] F. Ding, S. Van Doorslaer, P. Cool, F. Verpoort, Olefin isomerization reactions catalyzed by ruthenium hydrides bearing Schiff base ligands, *Appl. Organomet. Chem.* 25 (2011) 601–607.

APPENDIX B: Raw Data

The Data included in Appendix A is that data which was used as input into calculations that yield the final results and was obtained from the efforts of experimentation and mathematical modelling

Chapter 2

GCYC REACTIONS FOR VARIED TEMPERATURE

T	40	C8/Ru	10000	A ₁ -Octene	A ₂ -Octene	A ₃ -Octene	A ₄ -Octene	A _n onane	A ₁ -decene	A ₁ -dodecene	A ₁ -Tridecene	A ₇ -Tetradecene
Time												
0				0	0	0	0	0	0	0	0	0
1	1348981			0	0	0	421433	44442	11942	0	0	34615
2.5	2498861		12075	0	0	917727	86555	0	0	0	0	60156
5	1268892			0	0	0	426658	80068	0	0	0	40039
7.5	1388319			0	0	0	484870	55164	0	0	0	36897
10	1558309			0	0	0	542513	53876	0	0	0	57972
12.5	1601923			0	0	0	505604	82008	0	0	0	55975
15	1925977		10865	0	0	0	672892	69422	0	0	0	45388
17.5	1217099			0	0	0	363820		0	0	0	38580
20	2514936			0	0	0	911508	44413	0	0	0	2230
22.5	2492143			0	0	0	1169027	192436	0	0	0	21815
25	2131818			0	0	0	739950	96984	0	0	0	12395
30	2784604			0	0	0	928805	130442	0	0	0	32404
35	2797231			0	0	0	1125000	172514	0	0	0	28265
40	2290922			0	0	0	802322	127570	0	0	0	26703
45	2935431			0	0	0	1139994	188571	12021	0	0	42413
50	802792			0	0	0	380536	59937	0	0	0	11133
60	2374252			0	0	0	830838	108173	0	0	0	19415
90	2049266			0	0	0	759860	128292	0	0	0	24382
120	1157477			0	0	0	453962	32428	0	0	0	16473
150	1439290			0	0	0	608248	69436	0	0	0	26946
180	969735			0	0	0	320156	23642	0	0	0	23642
240	1019050			0	0	0	297610	23642	0	0	0	31479
300	1014530			0	0	0	382045	34002	0	0	0	44257
360	889135			0	0	0	324724	30286	0	0	0	48982
420	1131204			0	0	0	514449	35818	0	0	0	89612

T	50	C8/Ru	10000	A ₁ -Octene	A ₂ -Octene	A ₃ -Octene	A ₄ -Octene	A _n onane	A ₁ -decene	A ₁ -dodecene	A ₁ -Tridecene	A ₇ -Tetradecene
Time												
0	-			0	0	0	0	0	0	0	0	0
1	25847266		88537	30578	0	8611736	1617735	75254	0	0	0	0
2.5	20784952		72078	25188	0	6775053	906927	45306	0	0	0	0
5	23647208		169577	61603	0	8151987	1255939	84438	0	0	0	0
7.5	24810790		176136	0	0	8463405	1498632	73084	0	0	0	0
10	22408250		0	0	0	7761901	1308160	61054	0	0	88707	
12.5	23135275		11762	0	0	8500495	1201304	85620	0	0	308200	
15	25541418		152714	0	0	9505665	1121611	109043	0	0	623924	
17.5	25257776		116021	0	0	8412932	981808	83088	0	0	771880	
20	36464636		176563	0	0	13348870	2129013	165358	0	0	1504186	
22.5	22625236		99619	0	0	10941487	1276132	88184	0	0	1088017	
25	24836955		157617	0	0	9185329	1574254	116238	0	0	1819546	
30	24574938		375553	426598	0	11678033	1845111	175124	0	0	2328375	
35	26604834		216976	0	0	10231228	1796276	115255	0	0	2557319	
40	25998765		134941	0	0	9891045	1587608	82559	0	0	2885593	
45	21244468		91017	0	0	9181808	1685044	114520	0	0	2742763	
50	24310395		101833	0	0	11404717	1349590	76903	78219	0	3296956	
60	25668630		136018	0	0	10500486	2036850	136137	89341	0	3997328	
90	20144701		78864	0	0	7954585	1208831	87538	86340	0	4194070	
120	21205658		136695	0	0	10164781	1465659	109072	197578	0	5515356	
150	16138472		59085	0	0	9459512	1117613	80503	209405	0	4940883	
180	15164986		61956	0	0	7098639	1398339	90577	213270	0	5042484	
240	17090541		88145	0	0	9691229	1249811	83824	246418	0	6382704	
300	15966014		83308	0	0	8518222	1241265	76289	325969	0	6972818	
360	15560990		79387	0	0	7764841	1246355	103351	297284	0	7409752	
420	13812213		78566	0	0	9034959	1161033	65117	284228	0	7130907	

T	60	C8/Ru	10000						
Time	A ₁ -Octene	A ₂ -Octene	A ₃ -Octene	A ₄ -Octene	A _{nonane}	A _{1-decene}	A _{1-dodecene}	A _{1-<u>Tridecene</u>}	A _{7-Tetradecene}
0	-	0	0	0	0	0	0	0	0
1	31906240	108700	31956	0	11079877	1728905	82068	0	342583
2.5	34642022	120564	0	0	14187001	2009679	101319	63033	2548001
5	35314169	117106	0	0	13356658	1793318	92705	140792	3901835
7.5	62061871	205269	65515	32908	26883966	39075	202087	325536	8774775
10	24554634	72856	0	0	10230145	1389320	72473	532762	1274527
12.5	31688097	107409	0	0	14348606	1926208	103480	181377	5397863
15	42955674	129123	32667	0	17465658	2592772	141354	99626	4484702
17.5	25752269	79990	0	0	10117500	1444979	62943	52600	3050093
20	24075962	75435	0	0	10192068	1334720	55227	54590	3357714
22.5	31575105	113409	0	0	18321320	1832461	97917	243405	7959027
25	20025066	71703	0	0	9632215	1704928	75391	55614	3191594
30	19117450	70558	0	0	8877318	1737308	97927	74374	3747614
35	14841564	55442	0	0	7561562	1101645	57549	70254	3644709
40	15184026	59440	0	0	8196498	1049529	38351	98465	4190838
45	15277794	65266	0	0	8771732	1300710	55640	130228	4712448
50	18029686	73696	0	0	8783688	1309354	57091	190579	6247038
60	14809871	65385	0	0	7812158	1540051	81847	185205	5548652
90	14459915	70093	0	0	9486951	1210435	62208	274927	7641649
120	13879915	71627	0	0	9628520	1117143	82090	343076	8932117
150	13439866	73022	0	0	13649059	1336531	70298	327296	10013763
180	11882065	66516	0	0	9576388	1225655	55411	406388	9368794
240	12223624	71479	0	0	9439554	1252700	50437	459995	11133303
300	10760617	65668	0	0	8117285	1017098	50109	450995	10927728
360	9614734	61390	0	0	7996620	941046	113653	471824	11361755
420	10345890	64085	0	0	9201054	1276719	59792	536445	12849838

T	70	C8/Ru	10000						
Time	A ₁ -Octene	A ₂ -Octene	A ₃ -Octene	A ₄ -Octene	A _{nonane}	A _{1-decene}	A _{1-dodecene}	A _{1-<u>Tridecene</u>}	A _{7-Tetradecene}
0	-	0	0	0	0	0	0	0	0
1	33974459	11820	38009	0	9346214	2208267	93735	108157	271551
2.5	22345552	67241	0	0	8870011	1314187	53557	84693	1129589
5	27503804	89079	0	0	10946650	154182	66730	67268	4427351
7.5	21528920	76897	0	0	9603274	1496707	57538	151510	5849772
10	21779697	90190	0	0	11624004	1678024	79094	278207	8442416
12.5	15546010	73032	0	0	9271761	1200887	64738	294601	7787316
15	19606873	94881	0	0	10061063	1362553	70404	505803	11959557
17.5	14873471	77081	0	0	9464375	1020618	52489	465479	10489361
20	14198750	79879	0	0	9746606	1107019	44084	539821	11049279
22.5	14770877	86166	0	0	14366263	1154013	57266	626419	12300098
25	13349261	77307	0	0	12996315	1055620	53149	575720	11207452
30	8426335	54220	0	0	6812807	1093629	77992	407406	7564941
35	10701171	73011	0	0	8643516	1082598	57091	607234	11177083
40	9288906	70128	0	0	8749736	1261562	67378	641042	10937064
45	10352446	79908	0	0	9486153	1288510	71394	785058	13610389
50	9058749	62625	0	0	8256162	1629702	56075	713461	12927454
60	7342557	67140	0	0	8095085	1695389	51324	779437	12047377
90	6637407	67217	0	0	8702592	1307448	67173	885177	13028344
120	5364622	54501	0	0	8385056	1009350	35286	825952	11873799
150	5504748	59307	0	0	10932893	1309073	66442	901396	12823559
180	5572281	62707	0	0	8785955	1179796	65122	998042	14198275
240	4319873	46429	0	0	6947210	1069270	60283	916913	13165040
300	4866929	53340	0	0	8941178	1255758	68842	1057932	15125956
360	3785466	44957	0	0	7277289	1291876	45320	943128	13528565
420	4966007	60991	0	0	15631887	1349548	59022	1312976	19126182

T	80	C8/Ru	10000					6.7	
Time	A ₁ -Octene	A ₂ -Octene	A ₃ -Octene	A ₄ -Octene	A _{nonane}	A _{1-decene}	A _{1-dodecene}	A _{1-<u>Tridecene</u>}	A _{7-Tetradecene}
1	812125	0	0	0	278469	0	0	0	0
2.5	835573	0	0	0	297136	0	0	11950	97300
5	758386	0	0	0	353356	31059	0	14703	195724
7.5	614048	0	0	0	315083	42044	0	25450	274807
10	473190	0	0	0	279338	28090	0	27169	324845
12.5	368195	0	0	0	238706	21560	0	27675	285299
15	357191	0	0	0	269906	24878	0	14207	357404
17.5	308933	0	0	0	255029	14618	0	38900	353053
20	506787	0	0	0	445653	58117	0	82066	684058
22.5	267599	0	0	0	353709	26166	0	49277	397647
25	319954	0	0	0	326490	71324	0	68457	538532
30	268772	0	0	0	335200	38795	0	62339	492836
35	279687	0	0	0	390352	22926	0	76173	582685
40	254733	0	0	0	313654	33865	0	78680	584420
45	266419	0	0	0	390321	63545	0	91515	635394
50	274588	0	0	0	374916	44877	0	95066	688409
60	188751	0	0	0	292419	27615	0	70409	513132
90	199669	0	0	0	351838	53719	0	81322	545467
120	244836	0	0	0	358526	44665	0	78244	742904
150	201037	0	0	0	458348	36635	0	84731	585045
180	184188	0	0	0	278631	24326	0	79241	555795
240	222455	0	0	0	402678	44513	0	104012	734691
300	203829	0	0	0	331518	46584	0	100148	699217
360	185840	0	0	0	357384	493002	0	106843	755817
420	167496	0	0	0	506454	47529	0	113206	809568

T	90	C8/Ru	10000						
Time	A ₁ -Octene	A ₂ -Octene	A ₃ -Octene	A ₄ -Octene	A _{nonane}	A _{1-decene}	A _{1-dodecene}	A _{1-<u>Tridecene</u>}	A _{7-Tetradecene}
1	19529538	66240	0	0	7422007	1268338	51432	0	500210
2.5	18746137	65251	106422	0	7809573	1303081	46985	87412	3295631
5	12257170	47762	162628	43532	5523966	898489	62438	141440	2923328
7.5	13970361	57254	211079	51944	7035050	201652	52131	200053	3431528
10	16020551	90190	0	0	7712901	1678024	79094	270712	4270610
12.5	15717747	73032	0	0	7978161	1200887	64738	260415	4157240
15	16814829	75481	292315	74490	8352205	1248844	62808	290345	4339013
17.5	16187233	81079	317340	89324	8579409	1169201	54155	287210	4326717
20	16167091	73715	327123	90128	8532457	1731345	82300	304476	4499930
22.5	25906351	130379	564728	166932	16014008	2080198	105199	546298	8597979
25	15171854	71683	330868	101132	7445721	1170078	53859	297039	4040830
30	16382268	244058	95706	40738	7781800	44740	217776	240199	4501670
35	13176805	34962	340287	113583	8142950	1108503	58024	258803	3789981
40	14599835	74306	404841	137911	7392805	1054949	52304	285040	4164583
45	13426553	68707	394304	137293	7594431	1021921	81578	270060	3836261
50	14967709	85786	487045	176020	8107071	1106736	58861	27822	4228334
60	16912207	98637	599692	224002	8856630	1244292	60044	345923	4755436
90	16349855	96465	670289	266610	8132755	1108153	46919	317924	4672968
120	15979563	107941	807411	326419	8433323	1171368	42406	317957	4736009
150	16735442	114870	893229	369879	10196054	1787502	89845	341188	4692108
180	19239873	137843	1165599	477344	14201496	1442445	59764	487783	6834630
240	3745906	0	260891	97939	1718921	247508	0	0	895268
300	16172037	126511	992448	403533	9960500	1376421	44039	401290	5689884
360	16172037	126511	992448	403533	9960500	1376421	44039	401290	5689884
420	26583114	223316	1644594	664700	16345196	79394	111310	744658	10739810

T	100	C8/Ru	10000	A ₁ -Octene	A ₂ -Octene	A ₃ -Octene	A ₄ -Octene	A _n onane	A ₁ -decene	A ₁ -dodecene	A ₁ -Tridecene	A ₇ -Tetradecene
Time												
1	7615390	0	0	0	2651363	404824	0	0	257289			
2.5	7449715	0	80244	0	3075425	472181	354215	0	354215			
5	9745387	35523	96787	0	3505270	668921	37566	0	493468			
7.5	7359066	0	126066	0	2978967	345300	0	0	416514			
10	15371972	63615	200284	80302	6373968	888243	37202	54019	782933			
12.5	9081163	40657	146231	60087	3713448	1141077	48607	0	481617			
15	7673784	0	149619	47075	3365155	865001	34021	0	407733			
17.5	9065313	41620	165726	63906	3118082	785342	48667	0	483275			
20	6960430	0	163928	51912	2855492	894669	12920	0	389694			
22.5	6421898	0	159931	54229	3890824	799741	53057	0	370105			
25	7764785	37998	186522	76870	3674127	1035552	34941	0	413188			
30	7908310	40112	206914	87576	2981739	1117868	41041	0	453520			
35	7314982	38927	207707	93985	3097739	1277045	54079	0	413623			
40	8170000	44453	248942	105192	3631170	1675419	67346	0	464997			
45	10014134	56848	334067	146016	4578978	1064165	43130	0	607805			
50	8648124	49004	300844	127832	4066798	1084322	45998	0	520930			
60	8189929	50883	310008	134893	3721104	948703	43823	0	491050			
90	7623008	49330	322914	141937	3751731	563363	33820	0	483194			
120	10242077	85415	491199	212270	6261518	811274	46869	0	679417			
150	10437001	89139	512702	224320	4412431	705308	35923	0	658122			
180	8680304	71438	419051	183343	3692859	581007	32666	0	531230			
240	8373633	70095	410384	177743	3485424	561398	0	0	543564			
300	8699697	68757	429948	186804	3471935	531606	0	0	582202			
360	8794826	67928	433602	188459	3908832	614607	0	0	592576			
420	9369641	69178	459071	197052	4751067	658544	34963	0	649175			

GCYC REACTIONS FOR VARIED CATALYST LOADING

T	70	C8/Ru	5000	A ₁ -Octene	A ₂ -Octene	A ₃ -Octene	A ₄ -Octene	A _n onane	A ₁ -decene	A ₁ -dodecene	A ₁ -Tridecene	A ₇ -Tetradecene
Time												
0	-	-	-	-	-	-	-	-	-	-	-	-
1	31263995	102479	47731	0	12147990	1580565	102337	58712	40616			
2.5	66866915	230809	310170	59277	23679067	66007	228711	450672	59035			
5	19937361	75798	87593	0	11054037	1172431	89418	326535	4432083			
7.5	6903517	0	0	0	3860176	559834	61349	192990	2411954			
10	10157780	44456	0	0	6271640	869132	56375	387089	4498350			
12.5	2745827	0	0	0	1670183	214534	0	92119	1233188			
15	5384168	0	0	0	3552658	455563	73380	325146	3200284			
17.5	4385226	0	0	0	3428852	453629	90159	303637	2921406			
20	4597935	0	0	0	3368734	445098	94449	366897	3432442			
22.5	3403250	0	0	0	4982062	428678	38206	311167	2867562			
25	3670687	0	0	0	2951785	424300	42088	374951	3309703			
30	3590705	0	0	0	3531569	470375	32600	443985	3746484			
35	2675013	0	0	0	3039060	382028	35220	377253	3103114			
40	2748479	0	0	0	3090466	404940	50461	466322	3767590			
45	2719363	0	0	0	2919775	442667	55226	522109	4123008			
50	2632908	0	0	0	2900457	371353	55045	544218	4336889			
60	2363081	0	0	0	3159614	401484	57063	554039	4304330			
90	1873732	0	0	0	3379517	440548	57882	556133	4164570			
120	1696168	0	0	0	3335288	391523	61991	600045	4381957			
150	2047254	0	0	0	3582124	445746	71332	836608	6073367			
180	1346564	0	0	0	1346564	381268	60273	600171	4317017			
240	1449541	0	0	0	3157246	458158	74387	708414	5057750			
300	1415135	0	0	0	3654724	379221	83470	852031	6129562			
360	1433436	0	0	0	3663108	493233	36015	856915	6190235			
420	1136245	0	0	0	3592704	438500	73895	691069	4974232			

T	70	C8/Ru	7000						
Time	A ₁ -Octene	A ₂ -Octene	A ₃ -Octene	A ₄ -Octene	A _{nonane}	A ₁ -decene	A ₁ -dodecene	A ₁ -Tridecene	A ₇ -Tetradecene
0	-	-	-	-	-	-	-	-	-
1	27405870	92536	33307	0	10950013	1340825	85484	0	1094677
2.5	17011357	52946	0	0	2104241	980351	65976	0	1210455
5	21205643	69535	31328	0	10629239	1375851	91920	174035	4180330
7.5	136051183	459975	331301	48615	68821972	100877	894524	972991	22371970
10	62920642	210914	92565	0	32502048	41701	342845	710864	19093900
12.5	18585532	69098	0	0	8725114	1151582	84142	220989	5995463
15	96215675	361141	180276	0	46666072	63843	511763	1506557	30384480
17.5	10192274	44816	0	0	6667023	771057	56987	167706	4117963
20	16067508	66960	0	0	9491643	1288157	80215	371287	8458132
22.5	48075598	199473	44286	0	37418781	3597843	282018	1256139	22603291
25	7484024	0	0	0	2408821	658759	38088	190413	4241227
30	10323371	51959	0	0	2782369	763731	53285	358188	7127485
35	13202196	65371	0	0	6211421	1204405	97341	576801	10830339
40	12748858	73185	0	0	9333954	1294535	97415	650502	11515899
45	7197271	45239	0	0	16237840	784839	64142	425291	7333837
50	3054316	0	0	0	3447329	338592	0	203987	3444602
60	2140567	0	0	0	2028413	269452	0	157777	2579403
90	6768786	59285	0	0	8812213	986717	80905	915758	13550205
120	5449895	52089	0	0	9311800	1052031	75806	833077	12008267
150	5489400	54861	0	0	9447009	1111312	85226	919535	12906690
180	1275428	0	0	0	1933914	259136	0	214530	3010356
240	3458545	0	0	0	5524152	850450	64627	692065	9662224
300	6052205	63145	0	0	11221562	1373735	97512	1265576	17825286
360	7983505	88457	0	0	13750864	1852883	140860	1667497	23732915
420	2433536	0	0	0	5470708	571627	39938	543625	7709134

T	70	C8/Ru	12000						
Time	A ₁ -Octene	A ₂ -Octene	A ₃ -Octene	A ₄ -Octene	A _{nonane}	A ₁ -decene	A ₁ -dodecene	A ₁ -Tridecene	A ₇ -Tetradecene
0	-	-	-	-	-	-	-	-	-
1	20044204	66509	0	0	6873423	864943	960063	0	0
2.5	17122309	59852	0	0	5760807	660306	127735	0	0
5	31074408	104713	35431	0	10450734	1408608	73234	0	52265
7.5	16623519	58349	0	0	6606726	585205	45719	0	68729
10	17120100	56630	0	0	5750913	781970	57438	0	157105
12.5	24097598	74158	0	0	7958732	1106582	57466	0	633173
15	18900926	57590	0	0	6929658	1127799	56980	0	722538
17.5	23736612	70810	0	0	8346239	952171	49298	0	1316187
20	25002627	75282	0	0	9388903	1778473	94681	0	1807835
22.5	16473671	49852	0	0	8314098	864223	46493	0	1192279
25	20504835	62341	0	0	7893680	1135036	75363	38030	2281290
30	22084307	67422	0	0	9105010	1178468	68020	39889	2903008
35	21730654	68322	0	0	8783028	1673137	91902	44867	3271362
40	20555993	65176	0	0	9085989	1284730	82085	34054	3488643
45	15933094	52030	0	0	7822904	1089223	65870	0	3113983
50	14924035	49213	0	0	6420780	883829	51218	0	2994872
60	21125549	70286	0	0	10171036	1322925	80798	0	4794970
90	16905623	58471	0	0	8443645	771144	50237	0	4375089
120	19430690	68835	0	0	8693182	1635782	102687	36928	5461899
150	21580764	72865	0	0	13657411	1226539	77643	49543	6794659
180	14886048	54534	0	0	7345717	1002148	42332	0	3686728
240	15920712	57543	0	0	7448869	925566	45132	0	4199781
300	20201060	70757	36335	0	9261036	1233158	68565	42388	6166005
360	15374003	55716	32612	0	9877250	1011057	48775	0	4940790
420	13298384	54286	29393	0	5808740	836041	52972	106547	3825848

T	70	C8/Ru	14000	A ₁ -Octene	A ₂ -Octene	A ₃ -Octene	A ₄ -Octene	A _{nonane}	A _{1-decene}	A _{1-dodecene}	A _{1-Tridecene}	A _{7-Tetradecene}
Time												
0	-	-	-	-	-	-	-	-	-	-	-	-
1	14800446	48884	0	0	8528039	995868	58740	0	598761			
2.5	21597006	66510	0	0	8081466	930533	55326	0	1275610			
5	21826222	65473	0	0	8747960	1419641	89290	0	2398222			
7.5	21807632	66720	0	0	9345594	1152522	75048	40506	3345960			
10	23207651	75677	0	0	10525565	1204488	70633	58314	4327661			
12.5	17388843	60092	0	0	8461591	1021878	58934	51157	3876388			
15	21691247	73697	0	0	10088051	1033747	69904	100122	5478662			
17.5	18621601	66715	0	0	8318124	937135	59103	101330	5560021			
20	14400184	51830	0	0	7918689	831294	53842	80369	4524375			
22.5	16714129	65554	0	0	10712874	1101770	76105	147054	6232117			
25	9108320	37020	0	0	4633760	821483	57995	64438	3688598			
30	13003002	53993	0	0	8331522	953574	57087	163563	5991911			
35	14753164	63202	0	0	8751133	875196	53859	222577	7796912			
40	14440826	66322	0	0	9013725	1118179	75520	273865	8750822			
45	13290210	65170	0	0	9588322	1266090	78343	290204	8817244			
50	11686823	60570	0	0	8400373	1104003	70215	277344	8255724			
60	8493258	47476	0	0	7030054	995361	69631	242324	7109463			
90	4282081	0	0	0	3744566	522885	50787	172377	4575085			
120	10866101	70449	0	0	9931485	1152729	74908	510688	12613286			
150	3367094	0	0	0	4567452	487079	44037	172666	4541594			
180	17635123	119283	0	0	16455983	2531107	190888	1222679	25587779			
240	4257325	0	0	0	4634150	556820	70372	239159	6050175			
300	7112898	49168	0	0	7976952	998221	56239	423718	10387247			
360	3901099	0	0	0	4384924	597043	59453	232051	5890614			
420	3882018	0	0	0	5063531	608193	99473	245836	6194869			

GMPP REACTIONS WITH VARIED TEMPERATURE

T	40	C8/Ru	10000						
Time	A ₁ -Octene	A ₂ -Octene	A ₃ -Octene	A ₄ -Octene	A _{nonane}	A _{1-decene}	A _{1-dodecene}	A _{1-Tridecene}	A _{7-Tetradecene}
0	-	0	0	0	0	0	0	0	0
1	13855560	46920	0	0	5562791	692594	78935	0	0
2.5	16609512	58505	0	0	6236412	591780	66297	0	0
5	16362914	58195	0	0	4553474	521104	59229	0	0
7.5	16579902	57483	0	0	6011983	547114	60431	0	0
10	18574121	65629	0	0	6236869	617541	66979	0	0
12.5	14056000	50520	0	0	5956697	521691	60324	0	0
15	14664017	49147	0	0	5528866	487654	45703	0	0
17.5	15703467	55267	0	0	5641213	470668	43518	0	0
20	14164832	50597	0	0	5366283	485150	44525	0	0
25	15999004	52571	0	0	6939241	568932	49201	0	0
30	13383208	45924	0	0	5287347	432399	38237	0	0
35	14057872	44793	0	0	5312763	562382	62552	0	52587
40	14056010	46329	0	0	5391168	511753	43156	0	64652
45	16226332	50557	0	0	6486824	466051	54348	0	180815
50	14797870	46127	0	0	5373919	451975	35388	0	84424
60	12275099	38982	0	0	4527391	452847	85079	0	429945
120	11006631	0	0	0	4433290	479532	54993	46653	501288
150	13930005	42229	0	0	4524129	453734	55521	49993	623613
180	10507640	0	0	0	4253145	368949	45447	0	490257
240	10806854	0	0	0	4972623	486236	53598	40579	860597
300	11713996	39061	0	0	4851235	476655	37642	56197	1005480
360	12778854	42787	0	0	5079670	502338	45809	70535	1194175
420	14056171	45508	0	0	5367806	483458	39952	53521	1590107

T	50	C8/Ru	10000						
Time	A ₁ -Octene	A ₂ -Octene	A ₃ -Octene	A ₄ -Octene	A _{nonane}	A _{1-decene}	A _{1-dodecene}	A _{1-Tridecene}	A _{7-Tetradecene}
0	-	0	0	0	0	0	0	0	0
1	13329000	48511	0	0	4525864	423472	52961	0	113662
2.5	11182602	43076	0	0	4292606	335643	37826	0	47152
5	14080103	52863	0	0	4353207	452650	65776	0	41544
7.5	14368127	53086	0	0	4941586	497570	73218	0	39066
10	13734436	48803	0	0	4985322	670593	92647	0	42894
12.5	13533780	50493	0	0	4655286	365322	41151	0	43756
15	10773230	42804	0	0	3959881	219296	0	0	0
17.5	12657525	47231	0	0	4797816	348946	36976	0	36713
20	11308813	41405	0	0	3703644	318484	36361	0	42361
22.5	13730111	47987	0	0	4400060	409709	57869	0	52352
25	11627276	39382	0	0	4798983	314441	33652	0	125756
30	11834839	39351	0	0	4403124	346345	35841	0	254239
35	10844397	37192	0	0	4026565	454737	56634	0	213081
40	13488159	45731	0	0	5156992	551967	74962	0	233222
45	9458820	0	0	0	4035844	291999	47894	0	223587
50	11327615	0	0	0	4378157	388602	50726	0	113575
60	14092046	45635	0	0	5391485	0	0	0	0
90	11270070	0	0	0	3221168	400308	54679	0	514655
120	13025601	40916	0	0	10035468	752880	105491	0	699353
150	15341024	48596	0	0	11448790	566194	81053	0	1363170
180	11685375	39881	0	0	4904431	402775	54867	0	1086736
240	11769735	41071	0	0	5343128	510210	75494	0	1471935
300	9744522	0	0	0	5343128	519591	93816	70443	333683
360	10400128	31360	0	0	66624	340775	35986	43762	865932
420	8862252	0	0	0	3870979	493058	74787	0	2081088

T	60	C8/Ru	10000						
Time	A ₁ -Octene	A ₂ -Octene	A ₃ -Octene	A ₄ -Octene	A _n onane	A ₁ -decene	A ₁ -dodecene	A ₁ -Tridecene	A ₇ -Tetradecene
0	-	0	0	0	0	0	0	0	0
1	18291625	59566	0	0	6543829	950721	69426	72562	0
2.5	18594527	66561	0	0	8387536	1174140	81630	0	0
5	16044076	54534	0	0	6255807	774630	57479	73579	0
7.5	20079147	66282	0	0	6940902	864441	61982	80654	77945
10	18137691	63725	0	0	7017979	899251	66998	75127	75218
12.5	16962900	56994	0	0	6275855	1011479	79376	85619	82873
15	20842072	70191	0	0	8169815	993785	72589	84560	105036
17.5	14948353	51246	0	0	6141658	760618	55206	37550	64025
20	16394223	56000	0	0	6534656	883488	61163	56779	76864
22.5	9642330	0	0	0	5379536	445425	38486	0	52176
25	15351405	51471	0	0	5792039	762763	45902	47487	138432
30	17163262	57423	0	0	6165214	913436	68912	60155	181779
35	15635634	51707	0	0	6655060	1116575	82550	73006	190496
40	10199221	0	0	0	3855566	524128	53045	0	152175
45	16365922	51752	0	0	6832519	849528	61622	48251	292233
50	17263814	56606	0	0	6837531	832410	50858	43039	358681
60	16355493	50409	0	0	6712520	810291	60407	40021	405075
90	17883071	54785	0	0	6160123	790017	47494	45702	769544
120	17883071	54785	0	0	6160123	790017	47494	45702	769544
150	14792800	45467	0	0	6601556	774386	53903	53903	952550
180	16666724	53052	0	0	7946158	847589	49732	66970	1406661
240	17899067	56024	0	0	7191541	859515	59829	0	2822113
300	15549956	48090	0	0	6206527	751922	46947	36730	1638792
360	17954748	57849	0	0	7395481	750055	55004	32685	2371180
420	13500419	43466	0	0	4963913	728485	49059	39585	1190375

T	70	C8/Ru	10000						
Time	A ₁ -Octene	A ₂ -Octene	A ₃ -Octene	A ₄ -Octene	A _n onane	A ₁ -decene	A ₁ -dodecene	A ₁ -Tridecene	A ₇ -Tetradecene
0	-	0	0	0	0	0	0	0	0
1	7597923	0	0	0	2704785	69550	41762	0	0
2.5	12922203	47464	0	0	4864031	637074	46980	31972	0
5	10393846	0	0	0	4204380	546205	31703	0	0
7.5	10349916	0	0	0	4021317	552299	53290	0	0
10	11258325	0	0	0	5279025	500080	47277	0	75254
12.5	9763929	0	0	0	3785312	510091	46618	0	150071
15	11721078	42602	0	0	4549874	581056	43086	35413	246201
17.5	10498922	0	0	0	4363531	537144	48255	0	276893
20	10430231	0	0	0	3968695	516903	47259	0	348178
22.5	11417639	37441	0	0	4580638	481340	45179	0	457945
25	8498868	0	0	0	2940582	443481	42919	40705	364157
30	9649124	0	0	0	4666838	582215	80490	0	530609
35	10521744	0	0	0	4359021	566902	79572	41248	753509
40	9404641	0	0	0	4467661	543098	52579	0	748025
45	8696333	0	0	0	4044439	442339	42607	34002	876579
50	10350682	0	0	0	3569549	487633	45937	47423	1252631
60	9520402	0	0	0	4414616	899842	66577	0	1355645
90	8084034	0	0	0	4088664	493096	49784	0	2062535
120	5804575	0	0	0	3442535	422090	40868	0	2149087
150	6057401	0	0	0	3622173	409609	39235	0	3043272
180	7840947	39060	0	0	4577728	519717	55361	52811	4954861
240	4936257	0	0	0	4604006	561598	55052	57221	4438682
300	3662654	0	0	0	4104287	465047	45839	70662	4392407
360	4107466	0	0	0	3621084	518793	51074	159935	6502241
420	3030827	0	0	0	4024284	437552	43212	156247	6017958

T	80	C8/Ru	10000					6.7	
Time	A ₁ -Octene	A ₂ -Octene	A ₃ -Octene	A ₄ -Octene	A _{nonane}	A _{1-decene}	A _{1-dodecene}	A _{1-Tridecene}	A _{7-Tetradecene}
1	11830422	44942	0	0	4169074	533297	75997	0	49059
2.5	15138438	55769	0	0	5310870	393438	61388	0	61764
5	13259956	53105	32413	0	4514548	367053	45080	0	146705
7.5	14988280	57339	34616	0	5377494	348718	42246	0	298040
10	13815794	48650	27913	0	5026739	375183	42399	0	413438
12.5	13410945	46728	0	0	4990921	419987	62812	0	531125
15	13786513	47133	0	0	5048939	573482	74786	0	746657
17.5	11106114	37884	0	0	4286931	351465	37668	0	873250
20	14220751	46977	0	0	6001238	392326	47989	0	1290115
22.5	12827195	41193	0	0	6580943	448869	66868	0	1413065
25	10328477	36295	0	0	4424558	472685	57392	0	1348768
30	8918110	0	0	0	4141439	312998	54370	0	1425428
35	10484639	39447	0	0	5184476	477464	71219	0	2188556
40	10072896	38172	0	0	5159784	393919	61152	36279	2399313
45	10352439	40500	0	0	4912159	386950	86799	46078	2815069
50	9906735	39495	0	0	4998983	337095	93696	51947	3217776
60	7440335	0	0	0	4322709	273222	46104	59606	3167925
90	6497098	0	0	0	4415621	292453	89852	133035	4167952
120	4246642	43844	0	0	7800913	71034	84845	448286	4783634
150	6066953	43627	0	0	5603443	81575	106875	263695	5794659
180	5423437	43052	0	0	5357535	78531	72094	298251	6203518
240	5812186	47587	0	0	5994763	75891	97647	398815	7631608
300	3786238	0	0	0	4610875	79590	59245	343920	5735771
360	3583691	0	0	0	5273908	71021	77116	468693	7667169
420	4012386	42227	0	0	5637985	74965	76799	530820	8811028

T	90	C8/Ru	10000					6.7	
Time	A ₁ -Octene	A ₂ -Octene	A ₃ -Octene	A ₄ -Octene	A _{nonane}	A _{1-decene}	A _{1-dodecene}	A _{1-Tridecene}	A _{7-Tetradecene}
0	-	0	0	0	0	0	0	0	0
1	14340094	51682	28107	0	5534425	575759	59169	0	0
2.5	16568122	63771	47707	0	6871325	514914	43749	0	153398
5	16159502	53801	44504	0	2540503	572405	61376	0	403833
7.5	11033943	39025	32190	0	4143033	413472	52743	0	618755
10	18339292	61053	53359	0	7263089	777073	78069	0	1289401
12.5	10993793	38384	33461	0	4601025	425568	33469	0	1091166
15	14627540	48888	46236	0	6648494	554641	554641	45112	1765797
17.5	13085602	44296	43007	0	5289025	509361	97145	52526	1927460
20	12396422	42215	41725	0	5795461	715989	59733	56150	2094944
22.5	11651268	42734	43650	0	5235555	378665	44142	58864	2173896
25	10590798	38666	40227	0	5166131	483893	61078	87275	2300568
30	8214031	33242	33421	0	4209780	544336	58338	88974	2113472
35	8832481	36034	37060	0	5344250	386170	48403	132070	2723437
40	11918023	51617	0	0	5703196	835488	82354	248507	4724722
45	10668157	48693	47500	0	6132237	652036	52551	273364	4757711
50	8248386	37702	37203	0	4769444	600471	64244	249431	4063427
60	6822120	37034	0	0	5119266	715717	73690	280464	3966392
90	5111765	0	0	0	4173182	499875	49416	399312	4675782
120	4712245	33750	0	0	4537464	529324	45689	581516	6005934
150	3993051	34692	0	0	5120842	483221	50394	734628	6912995
180	3983413	37193	0	0	5043912	543857	48720	862894	7944620
240	3363029	0	0	0	5222720	508663	45257	926964	8235594
300	3398083	0	0	0	4891919	593889	53205	949108	8384465
360	2610617	0	0	0	5027861	387842	34259	747767	6768559
420	2601305	0	0	0	5947817	485999	42362	793566	6169767

T	100	C8/Ru	10000						
Time	A ₁ -Octene	A ₂ -Octene	A ₃ -Octene	A ₄ -Octene	A _{nonane}	A _{1-decene}	A _{1-dodecene}	A _{1-Tridecene}	A _{7-Tetradecene}
1	14426122	56143	32734	0	4983809	332308	38050	0	59306
2.5	11476575	44533	32474	0	4879568	374703	46002	0	70624
5	14421546	57462	52145	0	5328772	922252	92269	0	179962
7.5	12766555	46493	55761	0	5276763	480960	49580	0	201704
10	8601934	0	83784	0	3165944	205991	176936	0	176936
12.5	13203858	52472	85308	0	4953213	364904	44419	0	290641
15	10329698	41451	77497	0	4594911	359496	43822	0	269812
17.5	11736567	47196	102910	0	31383	4437230	91606	0	325395
20	9331556	0	126352	0	3600001	284481	0	0	241403
22.5	14352490	60578	143135	50341	5895854	516237	56496	0	404267
25	13336367	142547	49296	0	5263929	440585	35225	0	403173
30	10676111	48785	128935	41842	4439556	386002	50607	0	364674
35	10389509	44193	126010	40270	4209515	407993	82716	0	597187
40	11381584	50001	147105	52036	4832731	515166	41486	50359	368304
45	12469932	56984	182271	60299	4963656	502872	98070	44513	567036
50	12540681	62594	203271	66011	5196550	478161	38327	37038	821825
60	10549335	54842	193875	57881	5092230	351920	38729	0	485257
90	9747915	54022	213126	57733	5281987	470163	46935	111769	677313
120	13732913	82878	353101	85196	6036539	672043	63172	212922	1105990
150	9187512	67499	282374	58002	4527631	397414	57678	222570	1225003
180	8682665	58872	274317	55153	4863576	420897	72400	226763	1014645
240	9170724	70951	343175	70911	4041800	402622	46354	303562	1303845
300	7987665	70172	299530	65205	4384929	417887	37026	272161	1182564
360	8548044	65239	307910	62364	4281190	397336	46087	287867	1245361
420	8548044	65239	307910	62364	4281190	397336	46087	287867	1245361

GMPP REACTIONS WITH VARIED CATALYST LOAD.

T	70	C8/Ru	5000						
Time	A ₁ -Octene	A ₂ -Octene	A ₃ -Octene	A ₄ -Octene	A _{nonane}	A _{1-decene}	A _{1-dodecene}	A _{1-Tridecene}	A _{7-tetradecene}
0	-	-	-	-	-	-	-	-	-
1	9750496	0	0	0	4134371	655225	0	0	0
2.5	12730435	43238	0	0	4976675	696938	0	0	39223
5	11939014	42915	0	0	4678047	813369	0	0	49052
7.5	10882839	0	0	0	4620118	943911	0	0	68096
10	11552794	39246	0	0	4384356	631618	0	0	285792
12.5	12536592	41159	0	0	5299443	947021	0	0	300435
15	10939208	36767	0	0	4357595	580875	0	0	373780
17.5	13253887	43994	0	0	4918182	779123	0	0	648122
20	10774876	0	0	0	501182	1118876	0	40501	600457
22.5	12683385	42020	0	0	5366200	1443525	0	54423	935055
25	8975060	0	0	0	3812819	953240	0	34504	758099
30	9287205	0	0	0	3967966	1088735	0	37088	1071219
35	9006672	0	0	0	4237718	562970	0	0	1435411
40	9672359	37743	0	0	4065665	1095105	0	39439	1734034
45	8555588	0	0	0	4270396	869058	0	0	1912913
50	8804336	37409	0	0	4544990	1092279	0	38117	2283703
60	9304283	40118	0	0	5007620	1356127	0	50424	3074055
90	6669016	0	0	0	4215923	1200376	0	50525	3747026
120	6748683	42808	0	0	5503878	1675832	0	10858	5429729
150	5842348	38560	0	0	6079462	1414917	0	222958	7509481
180	4486698	0	0	0	4694662	1187837	0	127248	5186010
240	3393222	35951	0	0	4769058	1152201	0	292523	7910813
300	3002250	0	0	0	4924956	1316712	0	335137	8638249
360	1973603	0	0	0	4594972	583982	0	278540	6738106
420	1855037	0	0	0	5370347	891122	0	358663	8431705

T	70	C8/Ru	7000	A ₁ -Octene	A ₂ -Octene	A ₃ -Octene	A ₄ -Octene	A _{nonane}	A _{1-decene}	A _{1-dodecene}	A _{1-Tridecene}	A _{7-Tetradecene}
Time												
0	-	-	-	-	-	-	-	-	-	-	-	-
1	12111886	46068	0	0	4801898	840604	0	0	0	0	173443	
2.5	11794400	45889	0	0	4594536	70866	0	0	0	0	0	
5	12586006	45266	0	0	5209030	900925	0	0	0	0	0	
7.5	10036959	0	0	0	4271791	983139	0	0	0	0	49352	
10	11080358	37849	0	0	4539587	716242	0	0	0	0	138072	
12.5	12813094	46128	0	0	5578631	105867	0	0	0	0	236594	
15	10809598	0	0	0	4988980	741025	0	0	0	0	352034	
17.5	10409142	0	0	0	4154918	618630	0	0	0	0	372893	
20	10894567	38477	0	0	3978969	731387	0	0	0	0	452252	
22.5	9646849	0	0	0	4638223	699862	0	0	0	0	466947	
25	10693757	0	0	0	4663715	704683	0	0	0	0	667342	
30	10865771	0	0	0	4574860	834244	0	0	0	0	881836	
35	11337314	39892	0	0	5296300	82068	0	0	0	0	1160269	
40	10836870	40797	0	0	4808835	737291	0	0	0	0	1423620	
45	9069045	0	0	0	4421394	597234	0	0	0	0	1487515	
50	8924600	0	0	0	4152602	799764	0	0	0	0	1654675	
60	9356677	36917	0	0	4743488	816310	0	0	0	0	2342067	
90	8868127	43357	0	0	5262852	846721	0	0	91996	0	5270631	
120	6767701	38261	0	0	5081306	1004443	0	0	113195	0	5655788	
150	6317848	37826	0	0	5355764	915314	0	0	134140	0	6236356	
180	6562920	44555	0	0	6125445	1218395	0	0	210276	0	8192133	
240	4289906	0	0	0	5261249	893505	0	0	196014	0	7253380	
300	2994733	0	0	0	4007369	1192170	0	0	209495	0	7428435	
360	2525623	0	0	0	4148118	700235	0	0	220801	0	7324471	
420	2731339	0	0	0	4841610	678545	0	0	282068	0	9249190	

T	70	C8/Ru	12000	A ₁ -Octene	A ₂ -Octene	A ₃ -Octene	A ₄ -Octene	A _{nonane}	A _{1-decene}	A _{1-dodecene}	A _{1-Tridecene}	A _{7-Tetradecene}
Time												
0	-	-	-	-	-	-	-	-	-	-	-	-
1	13923156	52144	0	0	5089641	1110159	0	0	0	0	381438	
2.5	12859075	46738	0	0	4758075	1080575	0	0	0	0	343779	
5	16031784	62598	32449	0	6091203	1197370	0	0	0	0	461588	
7.5	13542977	48755	0	0	5426855	754069	65590	0	0	0	424976	
10	15431356	57063	33205	0	5614686	934175	0	0	0	0	518618	
12.5	14271250	48347	0	0	5176708	800539	0	0	0	0	521501	
15	14271250	48347	0	0	5176708	800539	0	0	0	0	521501	
17.5	9362196	0	0	0	4131511	612916	0	0	0	0	177836	
20	10675643	0	0	0	4452858	832987	0	0	0	0	250414	
22.5	12197515	39310	0	0	5359814	916862	0	0	0	0	355272	
25	13485197	45747	0	0	6061783	845999	0	0	0	0	473876	
30	1037981	36312	0	0	4304313	785299	0	0	54297	0	703140	
35	12116731	39953	0	0	6065506	1271365	0	0	92737	0	1063768	
40	10817816	38370	0	0	4560298	763390	0	0	54006	0	1083821	
45	11300462	39343	0	0	4714228	870303	0	0	75085	0	1218528	
50	7992417	0	0	0	3126197	521082	0	0	0	0	1312904	
60	9664175	0	0	0	5801864	715127	0	0	51828	0	1609757	
90	9789981	0	0	0	5160795	889804	0	0	0	0	2087577	
120	7963785	0	0	0	4862713	857470	0	0	36530	0	3334863	
150	7713414	40902	0	0	4597673	762921	0	0	51715	0	4174910	
180	5819647	0	0	0	3414224	846205	0	0	42127	0	3454391	
240	7196471	41652	0	0	4668478	817093	0	0	100725	0	5599105	
300	3283427	0	0	0	3278621	488451	0	0	57416	0	3672250	
360	4129411	0	0	0	4548246	585229	0	0	135225	0	5979713	
420	5971694	43172	0	0	5631398	1113556	0	0	184096	0	8401016	

T	70	C8/Ru	14000						
Time	A ₁ -Octene	A ₂ -Octene	A ₃ -Octene	A ₄ -Octene	A _{nonane}	A ₁ -decene	A ₁ -dodecene	A ₁ -Tridecene	A ₇ -Tetradecene
0	-	-	-	-	-	-	-	-	-
1	14934473	55268	0	0	5070760	419322	76693	0	46808
2.5	16195008	58924	0	0	5657556	490989	89766	0	0
5	12027229	42890	0	0	4505059	328271	49437	0	38218
7.5	14160214	50624	0	0	5148323	363016	56566	0	42456
10	19002795	6813	34930	0	7210241	373598	65608	0	165152
12.5	17022113	64318	33963	0	5133614	253486	49592	0	172900
15	13812644	48219	0	0	5194419	392156	64377	0	216898
17.5	13207062	44579	0	0	4573797	76982	83198	0	245980
20	14287817	48698	0	0	5252504	290897	63217	364374	363758
22.5	10404008	37465	0	0	4669377	268830	72696	346226	319939
25	15553235	50366	0	0	5606094	146831	104104	109105	481940
30	13185262	43171	0	0	5003082	126737	68270	85864	537018
35	12972374	42877	0	0	5045044	135567	73289	0	655625
40	12894926	42114	0	0	4868781	143879	74875	0	822365
45	12811617	41265	0	0	5269814	356325	56524	0	915246
50	11076950	34899	0	0	4331543	373951	69395	0	887502
60	12021070	40872	0	0	5472910	354775	44340	0	1171750
90	8411359	0	0	0	3689524	345183	61654	0	1316727
120	14004154	47342	0	0	5905304	507874	88117	0	2886183
150	10367388	38283	0	0	6899478	381176	47685	0	2813818
180	7786983	0	0	0	4093028	298531	38102	0	2567815
240	10293748	42963	0	0	5158507	459187	75020	61157	4463229
300	7738665	37649	0	0	4590407	358839	63072	118385	5375355
360	7755576	36253	0	0	68966	456508	77395	70122	4492536
420	4274485	0	0	0	4478778	329466	53666	46789	3029133

Chapter 3

This section of Appendix A includes data related to the obtained K-values from the application of the bootstrap and other algorithms discussed in Chapter 3

Due to the volume of information included in the bootstrap trial result tables, it will not be included in this document. The tables will, however, be included in supplementary data packages available on request.

BOOTSTRAP RESULTS FOR GCYC CATALYST AT VARIOUS TEMPERATURES

40° C C8/Ru: 10000			
	K1	K2	K3
UL	0.000172	-0.00096	-1.58E-05
LL	-0.00026	-0.00872	-7.8358E-05
Mean	0.004083	0.176701	-0.0000192
Std dev	0.0218	1.051953	0.0000318

50° C C8/Ru: 10000			
	K1	K2	K3
UL	0.004096	0.008423	0.000222305
LL	0.002774	0.004819	-0.00015587
Mean	0.003476	0.006673	0.000105226
Std dev	0.000333	0.000937	8.20817E-05

60° C C8/Ru: 10000			
	K1	K2	kd
UL	0.011526	0.001169	0.013872503
LL	0.006556	-0.00041	0.007751877
Mean	0.009536	0.000409	0.011247293
Std dev	0.001327	0.0004	0.00159975

70° C C8/Ru: 10000			
	K1	K2	K3
UL	0.04836	0.004699	0.033635
LL	0.037691	0.0009	0.026555
Mean	0.043013	0.002902	0.030089
Std dev	0.002988	0.00102	0.001837

80° C C8/Ru: 10000			
	K1	K2	K3
UL	0.082937	0.026785	0.055472
LL	0.068959	0.016271	0.046835
Mean	0.075803	0.021403	0.051539
Std dev	0.003574	0.002711	0.002223

90° C C8/Ru: 10000			
	K1	K2	K3
UL	0.479783	0.077924	0.734815
LL	0.133186	-0.01459	0.33566
Mean	0.249325	0.033525	0.490146
Std dev	0.085474	0.022142	0.098281

100° C C8/Ru: 10000			
	K1	K2	K3
UL	0.013768	0.004989	1.37E-01
LL	0.004888	0.001519	0.07595107
Mean	0.009518	0.003101	0.104570896
Std dev	0.002164	0.00094	0.015652895

BOOTSTRAP RESULTS FOR GCYC CATALYST AT VARIOUS CATALYST LOADINGS

70° C C8/Ru: 5000			
	K1	K3	kd
UL	0.038771	0.005973	3.00E-02
LL	0.027009	0.001743	0.022103
Mean	0.031619	0.004089	0.026089
Std dev	0.002861	0.001075	0.002092

70° C C8/Ru: 7000			
	K1	k3	kd
UL	0.021238	0.002193	1.88E-02
LL	0.016	0.000423	0.013997
Mean	0.018085	0.001487	0.016
Std dev	0.001309	0.000454	0.001163

70° C C8/Ru: 12000			
	K1	K2	K3
UL	0.006375	0.022993	5.62E-05
LL	0.003	0.00922	-0.000228765
Mean	0.00446	0.015159	-7.41E-05
Std dev	0.000845	0.00369	7.7964E-05

70° C C8/Ru: 14000			
	K1	K2	K3
UL	0.016214	0.012846	2.36E-04
LL	0.013083	0.009588	-0.000199
Mean	0.014784	0.011333	0.000035
Std dev	0.000795	0.000842	0.000112

BOOTSTRAP RESULTS FOR GMPP CATALYST AT VARIOUS TEMPERATURES

40° C C8/Ru: 10000			
	K1	K2	K3
UL	0.082098231	3.362595	0.000121895
LL	0.000320575	0.0013	-2.29374E-05
Mean	0.008295409	0.34748	3.04939E-05
Std dev	0.048879314	2.199196	3.53015E-05

50° C C8/Ru: 10000			
	K1	K2	K3
UL	0.130293	1.644876	0.000231929
LL	0.000297	-0.00023	-0.000100329
Mean	0.008202	0.104488	1.86078E-05
Std dev	0.04135	0.555556	6.92108E-05

60° C C8/Ru: 10000			
	K1	K2	K3
UL	0.001012978	0.009278354	7.67897E-05
LL	-0.000288576	-0.004758242	-8.91515E-05
Mean	0.000624062	0.004425294	-3.30013E-05
Std dev	0.00025268	0.002898725	3.69064E-05

70° C C8/Ru: 10000			
	K1	K2	K3
UL	0.003458	0.001501888	9.13E-05
LL	0.00203	-0.000966208	-0.000392245
Mean	0.002775	0.000232023	-1.44E-04
Std dev	0.000366	0.000632111	0.000121662

80° C C8/Ru: 10000			
	K1	k3	kd
UL	0.006684	0.000651	0.006593682
LL	0.003746	-0.00039	0.002906922
Mean	0.005252	0.000227	0.004749921
Std dev	0.000806	0.000265	0.000953184

90° C C8/Ru: 10000			
	K1	k3	kd
UL	0.008274	0.000889	0.006538
LL	0.008672	0.000282	0.006815
Mean	0.007987	0.000841	0.006117
Std dev	0.000794	0.000294	0.000919

100° C C8/Ru: 10000			
	K1	K2	K3
UL	0.002544	0.019454	0.000240141
LL	0.000561	0.002766	6.43402E-06
Mean	0.001738	0.012497	0.000156564
Std dev	0.000421	0.003665	5.27599E-05

BOOTSTRAP RESULTS FOR GMPP CATALYST AT VARIOUS CATALYST LOADS

70° C C8/Ru: 5000			
	K1	K2	K3
UL	0.00613057	0.001658646	2.44E-04
LL	0.004214983	0.000307322	-0.000357041
Mean	0.005294698	0.000968512	-4.92E-05
Std dev	0.000479567	0.000333783	0.000149002

70° C C8/Ru: 7000			
	K1	K2	K3
UL	0.005190716	0.001505945	2.35E-04
LL	0.002877453	-0.000301538	-0.000411525
Mean	0.004200358	0.00062106	-1.05E-04
Std dev	0.000639931	0.000470653	0.000161834

70° C C8/Ru: 12000			
	K1	K2	K3
UL	0.003148811	1.63E-03	1.78E-04
LL	0.001360514	-0.001015253	-0.000290834
Mean	0.002347129	0.000280243	-7.42E-05
Std dev	0.000483517	0.000679071	0.000119287

70° C C8/Ru: 14000			
	K1	K2	K3
UL	0.002282335	0.002784404	5.22E-05
LL	0.001218044	-0.000125002	-0.000266673
Mean	0.001724944	0.001240965	-9.51E-05
Std dev	0.000269943	0.000740887	7.69626E-05

Chapter 4

The data included in this section lists the input data used for the economic evaluation of the **GMPP** and **GCYC** catalysts for the metathesis of 1-octene

SPECIES PERCENTAGE DATA FOR GCYC CATALYST AT VARIED TEMPERATURES

Time (min)	40°C Percentages							
	1-C8	C14	C2H4	2-C8	C12	C4H8	C13	C3H6
1	96.96	1.52	1.52	0.00	0.00	0.00	0.00	0.00
2.5	96.69	1.42	1.42	0.00	0.00	0.00	0.00	0.00
5	96.29	1.86	1.86	0.00	0.00	0.00	0.00	0.00
7.5	96.86	1.57	1.57	0.00	0.00	0.00	0.00	0.00
10	95.65	2.17	2.17	0.00	0.00	0.00	0.00	0.00
12.5	95.91	2.05	2.05	0.00	0.00	0.00	0.00	0.00
15	96.67	1.39	1.39	0.00	0.00	0.00	0.00	0.00
17.5	96.27	1.86	1.86	0.00	0.00	0.00	0.00	0.00
20	99.89	0.05	0.05	0.00	0.00	0.00	0.00	0.00
22.5	98.94	0.53	0.53	0.00	0.00	0.00	0.00	0.00
25	99.29	0.35	0.35	0.00	0.00	0.00	0.00	0.00
30	98.60	0.70	0.70	0.00	0.00	0.00	0.00	0.00
35	98.78	0.61	0.61	0.00	0.00	0.00	0.00	0.00
40	98.60	0.70	0.70	0.00	0.00	0.00	0.00	0.00
45	97.71	0.86	0.86	0.00	0.28	0.28	0.00	0.00
50	98.33	0.83	0.83	0.00	0.00	0.00	0.00	0.00
60	99.01	0.49	0.49	0.00	0.00	0.00	0.00	0.00
90	98.57	0.72	0.72	0.00	0.00	0.00	0.00	0.00
120	98.29	0.85	0.85	0.00	0.00	0.00	0.00	0.00
150	97.76	1.12	1.12	0.00	0.00	0.00	0.00	0.00
180	97.11	1.45	1.45	0.00	0.00	0.00	0.00	0.00
240	96.36	1.82	1.82	0.00	0.00	0.00	0.00	0.00
300	94.94	2.53	2.53	0.00	0.00	0.00	0.00	0.00
360	93.70	3.15	3.15	0.00	0.00	0.00	0.00	0.00
420	91.18	4.41	4.41	0.00	0.00	0.00	0.00	0.00

Time (min)	50°C							
	Percentages							
1-C8	C14	C2H4	2-C8	C12	C4H8	C13	C3H6	
1	99.54	0.00	0.00	0.0009	0	0	0	0
2.5	99.23	0.00	0.00	0.0009	0.152865083	0.152865083	0	0
5	98.54	0.00	0.00	0.0018	0.248671842	0.248671842	0.00E+00	0
7.5	98.89	0.00	0.00	0.0013	0.20586224	0.20586224	0	0
10	99.14	0.24	0.24	0.0000	0.190901552	0.190901552	0	0
12.5	97.85	0.80	0.80	0.0001	0.255920771	0.255920771	0	0
15	95.98	1.43	1.43	0.0010	0.289607007	0.289607007	0	0
17.5	95.55	1.78	1.78	0.0009	0.222145332	0.222145332	0	0
20	94.20	2.37	2.37	0.0008	0.301884636	0.301884636	0	0
22.5	87.50	2.57	2.57	0.0006	3.487961391	3.487961391	0	0
25	90.71	4.06	4.06	0.0011	0.300027077	0.300027077	0	0
30	86.32	4.99	4.99	0.0043	0.434758913	0.434758913	0	0
35	88.37	5.19	5.19	0.0013	0.27054673	0.27054673	0	0
40	87.32	5.92	5.92	0.0008	0.195967294	0.195967294	0	0
45	85.50	6.74	6.74	0.0006	0.325740166	0.325740166	0	0
50	84.85	7.03	7.03	0.0006	0.189703309	0.189703309	0.179983794	0.179983794
60	82.81	7.87	7.87	0.0008	0.310402977	0.310402977	0.190015938	0.190015938
90	78.74	10.01	10.01	0.0006	0.241828715	0.241828715	0.222491186	0.222491186
120	74.43	11.82	11.82	0.0008	0.270549419	0.270549419	0.457152852	0.457152852
150	71.34	13.34	13.34	0.0004	0.251511539	0.251511539	0.610270555	0.610270555
180	69.58	14.13	14.13	0.0005	0.293726232	0.293726232	0.645125322	0.645125322
240	67.24	15.33	15.33	0.0006	0.23308453	0.23308453	0.639156216	0.639156216
300	63.60	16.96	16.96	0.0006	0.214790198	0.214790198	0.856087894	0.856087894
360	61.68	17.93	17.93	0.0006	0.289540294	0.289540294	0.77688258	0.77688258
420	59.88	18.88	18.88	0.0005	0.199521221	0.199521221	0.812364784	0.812364784

Time (min)	60°C							
	Percentages							
1-C8	C14	C2H4	2-C8	C12	C4H8	C13	C3H6	
1	98.28	0.64	0.64	0.00	0.00	0.00	0.00	0.00
2.5	90.92	4.08	4.08	0.00	0.19	0.19	0.11	0.11
5	87.17	5.88	5.88	0.00	0.16	0.16	0.23	0.23
7.5	84.10	7.26	7.26	0.05	0.19	0.19	0.29	0.29
10	90.98	2.88	2.88	0.00	0.19	0.19	1.30	1.30
12.5	81.73	8.50	8.50	0.00	0.19	0.19	0.31	0.31
15	87.80	5.60	5.60	0.00	0.20	0.20	0.13	0.13
17.5	86.66	6.27	6.27	0.00	0.15	0.15	0.12	0.12
20	84.77	7.22	7.22	0.00	0.14	0.14	0.13	0.13
22.5	75.42	11.61	11.61	0.00	0.17	0.17	0.38	0.38
25	82.84	8.06	8.06	0.00	0.22	0.22	0.15	0.15
30	79.65	9.53	9.53	0.00	0.29	0.29	0.20	0.20
35	76.03	11.40	11.40	0.00	0.21	0.21	0.24	0.24
40	73.91	12.45	12.45	0.00	0.13	0.13	0.32	0.32
45	71.57	13.48	13.48	0.00	0.18	0.18	0.40	0.40
50	69.17	14.63	14.63	0.00	0.15	0.15	0.48	0.48
60	67.28	15.39	15.39	0.00	0.26	0.26	0.55	0.55
90	59.48	19.19	19.19	0.00	0.18	0.18	0.75	0.75
120	54.59	21.45	21.45	0.00	0.23	0.23	0.89	0.89
150	51.16	23.27	23.27	0.00	0.19	0.19	0.82	0.82
180	49.50	23.83	23.83	0.00	0.16	0.16	1.12	1.12
240	46.01	25.59	25.59	0.00	0.13	0.13	1.14	1.14
300	43.33	26.87	26.87	0.00	0.14	0.14	1.20	1.20
360	39.51	28.51	28.51	0.00	0.33	0.33	1.28	1.28
420	38.47	29.17	29.17	0.00	0.16	0.16	1.31	1.31

Time (min)	70°C							
	Percentages							
1-C8	C14	C2H4	2-C8	C12	C4H8	C13	C3H6	
1	98.48	0.48	0.48	0.0003	0	0	0.206682133	0.206682133
2.5	93.19	2.88	2.88	0.0005	0.15784607	0.15784607	0.232838378	0.232838378
5	82.89	8.15	8.15	0.0005	0.142125542	0.142125542	1.34E-01	0.13364387
7.5	74.16	12.30	12.30	0.0005	0.140074856	0.140074856	0.344061627	0.344061627
10	66.69	15.78	15.78	0.0005	0.171163855	0.171163855	0.561598699	0.561598699
12.5	60.71	18.57	18.57	0.0005	0.17866237	0.17866237	0.758398643	0.758398643
15	55.90	20.82	20.82	0.0006	0.141868721	0.141868721	0.950736658	0.950736658
17.5	52.28	22.51	22.51	0.0005	0.130400774	0.130400774	1.078701997	1.078701997
20	49.74	23.63	23.63	0.0005	0.109143988	0.109143988	1.24668898	1.24668898
22.5	47.98	24.40	24.40	0.0004	0.131469777	0.131469777	1.34147789	1.34147789
25	47.77	24.49	24.49	0.0004	0.134406531	0.134406531	1.358082364	1.358082364
30	45.88	25.15	25.15	0.0005	0.300119915	0.300119915	1.462384909	1.462384909
35	42.29	26.97	26.97	0.0005	0.159451244	0.159451244	1.581997749	1.581997749
40	39.27	28.23	28.23	0.0005	0.201301218	0.201301218	1.786505223	1.786505223
45	36.73	29.48	29.48	0.0005	0.178995886	0.178995886	1.835999662	1.835999662
50	34.94	30.44	30.44	0.0005	0.152848642	0.152848642	1.814061724	1.814061724
60	31.62	31.68	31.68	0.0005	0.156201332	0.156201332	2.212762344	2.212762344
90	27.80	33.32	33.32	0.0005	0.1988313	0.1988313	2.444047525	2.444047525
120	25.48	34.43	34.43	0.0004	0.118426038	0.118426038	2.58576528	2.58576528
150	24.46	34.79	34.79	0.0003	0.208641728	0.208641728	2.640362885	2.640362885
180	22.85	35.56	35.56	0.0004	0.188768173	0.188768173	2.698605357	2.698605357
240	19.87	36.98	36.98	0.0004	0.195998104	0.195998104	2.780831429	2.780831429
300	19.56	37.12	37.12	0.0004	0.195522729	0.195522729	2.802793132	2.802793132
360	17.48	38.14	38.14	0.0004	0.147883242	0.147883242	2.870709311	2.870709311
420	16.44	38.67	38.67	0.0002	0.138133204	0.138133204	2.866358252	2.866358252

Time (min)	80°C							
	Percentages							
1-C8	C14	C2H4	2-C8	C12	C4H8	C13	C3H6	
1	100.00	0.00	0.00	0.00E+00	0.00E+00	0.00E+00	0.00E+00	
2.5	86.03	6.12	6.12	0.00	8.70E-01	8.70E-01	0.00E+00	0.00E+00
5	73.14	11.53	11.53	0.00	1.00E+00	1.00E+00	9.04E-01	9.04E-01
7.5	61.23	16.73	16.73	0.00	1.79E+00	1.79E+00	8.62E-01	8.62E-01
10	50.45	21.14	21.14	0.00	2.05E+00	2.05E+00	1.59E+00	1.59E+00
12.5	46.83	22.15	22.15	0.00	2.49E+00	2.49E+00	1.95E+00	1.95E+00
15	41.78	25.52	25.52	0.00	1.17E+00	1.17E+00	2.41E+00	2.41E+00
17.5	38.01	26.52	26.52	0.00	3.38E+00	3.38E+00	1.09E+00	1.09E+00
20	32.74	26.99	26.99	0.00	3.75E+00	3.75E+00	2.90E+00	2.90E+00
22.5	29.45	26.72	26.72	0.00	3.83E+00	3.83E+00	4.73E+00	4.73E+00
25	28.21	28.99	28.99	0.00	4.27E+00	4.27E+00	2.64E+00	2.64E+00
30	25.56	28.62	28.62	0.00	4.19E+00	4.19E+00	4.41E+00	4.41E+00
35	23.41	29.78	29.78	0.00	4.51E+00	4.51E+00	4.01E+00	4.01E+00
40	21.95	30.75	30.75	0.00	4.79E+00	4.79E+00	3.48E+00	3.48E+00
45	20.48	29.82	29.82	0.00	4.97E+00	4.97E+00	4.96E+00	4.96E+00
50	20.11	30.78	30.78	0.00	4.92E+00	4.92E+00	4.24E+00	4.24E+00
60	18.64	30.94	30.94	0.00	4.91E+00	4.91E+00	4.83E+00	4.83E+00
90	18.28	30.49	30.49	0.00	5.26E+00	5.26E+00	5.11E+00	5.11E+00
120	17.85	33.06	33.06	0.00	4.03E+00	4.03E+00	3.98E+00	3.98E+00
150	17.22	30.61	30.61	0.00	5.13E+00	5.13E+00	5.65E+00	5.65E+00
180	17.66	32.54	32.54	0.00	5.37E+00	5.37E+00	3.26E+00	3.26E+00
240	15.69	31.64	31.64	0.00	5.19E+00	5.19E+00	5.33E+00	5.33E+00
300	15.53	32.54	32.54	0.00	5.39E+00	5.39E+00	4.30E+00	4.30E+00
360	13.25	32.91	32.91	0.00	5.39E+00	5.39E+00	5.08E+00	5.08E+00
420	11.05	32.61	32.61	0.00	5.28E+00	5.28E+00	6.59E+00	6.59E+00

Time (min)	90°C							
	Percentages							
1-C8	C14	C2H4	2-C8	C12	C4H8	C13	C3H6	
1	96.65	1.51	1.51	0.00	0.00	0.00	0.00	0.00
2.5	81.07	8.70	8.70	0.00	0.14	0.14	0.25	0.25
5	74.94	10.91	10.91	0.27	0.27	0.27	0.57	0.57
7.5	74.24	11.13	11.13	0.28	0.20	0.20	0.70	0.70
10	73.51	11.96	11.96	0.00	0.26	0.26	0.82	0.82
12.5	73.65	11.89	11.89	0.00	0.21	0.21	0.90	0.90
15	73.03	11.51	11.51	0.33	0.19	0.19	0.82	0.82
17.5	72.15	11.77	11.77	0.40	0.17	0.17	0.89	0.89
20	70.32	11.95	11.95	0.39	0.25	0.25	1.57	1.57
22.5	68.52	13.89	13.89	0.44	0.20	0.20	0.52	0.52
25	72.24	11.75	11.75	0.48	0.18	0.18	0.75	0.75
30	71.51	12.00	12.00	0.18	0.67	0.67	0.74	0.74
35	70.27	12.34	12.34	0.61	0.22	0.22	1.00	1.00
40	70.42	12.26	12.26	0.67	0.18	0.18	0.86	0.86
45	71.18	12.42	12.42	0.73	0.31	0.31	0.10	0.10
50	69.88	12.05	12.05	0.83	0.19	0.19	1.06	1.06
60	70.04	12.03	12.03	0.93	0.18	0.18	0.87	0.87
90	69.35	12.10	12.10	1.14	0.14	0.14	0.89	0.89
120	67.96	12.30	12.30	1.39	0.13	0.13	0.96	0.96
150	67.99	11.64	11.64	1.51	0.26	0.26	1.31	1.31
180	65.33	14.17	14.17	1.63	0.14	0.14	0.00	0.00
240	65.41	9.54	9.54	1.72	0.00	0.00	4.62	4.62
300	64.09	13.77	13.77	1.61	0.12	0.12	1.05	1.05
360	62.96	13.52	13.52	1.58	0.12	0.12	1.91	1.91
420	62.71	15.47	15.47	1.58	0.19	0.19	0.00	0.00

Time (min)	100°C							
	Percentages							
1-C8	C14	C2H4	2-C8	C12	C4H8	C13	C3H6	
1	96.04	1.98	1.98	0.00	0.00	0.00	0.00	0.00
2.5	88.02	2.56	2.56	0.00	2.96	2.96	0.00	0.00
5	92.52	2.86	2.86	0.00	0.25	0.25	0.00	0.00
7.5	92.06	3.18	3.18	0.00	0.00	0.00	0.00	0.00
10	91.52	2.85	2.85	0.48	0.16	0.16	0.21	0.21
12.5	90.95	2.95	2.95	0.60	0.34	0.34	0.00	0.00
15	91.18	2.96	2.96	0.56	0.29	0.29	0.00	0.00
17.5	90.69	2.95	2.95	0.64	0.34	0.34	0.00	0.00
20	90.74	3.10	3.10	0.68	0.12	0.12	0.00	0.00
22.5	89.65	3.15	3.15	0.76	0.52	0.52	0.00	0.00
25	90.08	2.93	2.93	0.90	0.29	0.29	0.00	0.00
30	89.31	3.13	3.13	0.99	0.33	0.33	0.00	0.00
35	88.80	3.07	3.07	1.15	0.46	0.46	0.00	0.00
40	88.50	3.08	3.08	1.14	0.52	0.52	0.00	0.00
45	88.20	3.27	3.27	1.29	0.27	0.27	0.00	0.00
50	88.00	3.24	3.24	1.31	0.33	0.33	0.00	0.00
60	87.62	3.21	3.21	1.45	0.33	0.33	0.00	0.00
90	86.87	3.36	3.36	1.62	0.27	0.27	0.00	0.00
120	85.87	3.48	3.48	1.79	0.28	0.28	0.00	0.00
150	86.13	3.32	3.32	1.86	0.21	0.21	0.00	0.00
180	86.38	3.23	3.23	1.83	0.23	0.23	0.00	0.00
240	86.36	3.42	3.42	1.84	0.00	0.00	0.00	0.00
300	86.17	3.52	3.52	1.86	0.00	0.00	0.00	0.00
360	86.15	3.54	3.54	1.85	0.00	0.00	0.00	0.00
420	85.67	3.62	3.62	1.81	0.23	0.23	0.00	0.00

SPECIES PERCENTAGE DATA FOR GCYC CATALYST AT VARIED CATALYST LOADS

Time (min)	5000							
	Percentages							
1-C8	C14	C2H4	2-C8	C12	C4H8	C13	C3H6	
1	99.12	0.08	0.08	0.0008	0	0	0.122714809	0.122714809
2.5	97.68	0.05	0.05	0.0880	0.236118375	0.236118375	0.434003096	0.434003096
5	76.48	10.38	10.38	0.0009	0.242405994	0.242405994	8.26E-01	0.825729234
7.5	67.75	14.45	14.45	0.0000	0.425489614	0.425489614	1.248549602	1.248549602
10	62.37	16.87	16.87	0.0004	0.244649339	0.244649339	1.566959748	1.566959748
12.5	62.79	17.22	17.22	0.0000	0	0	1.388664937	1.388664937
15	54.80	19.89	19.89	0.0000	0.527860429	0.527860429	2.181771847	2.181771847
17.5	51.71	21.03	21.03	0.0000	0.751355617	0.751355617	2.36037313	2.36037313
20	48.88	22.28	22.28	0.0000	0.709604364	0.709604364	2.571299072	2.571299072
22.5	46.18	23.76	23.76	0.0000	0.366408138	0.366408138	2.783662576	2.783662576
25	44.41	24.45	24.45	0.0000	0.359840034	0.359840034	2.990303195	2.990303195
30	40.82	26.00	26.00	0.0000	0.261896631	0.261896631	3.327132747	3.327132747
35	38.15	27.02	27.02	0.0000	0.355001801	0.355001801	3.547018267	3.547018267
40	34.20	28.63	28.63	0.0000	0.443815509	0.443815509	3.825798086	3.825798086
45	31.91	29.54	29.54	0.0000	0.458065874	0.458065874	4.039569157	4.039569157
50	30.18	30.35	30.35	0.0000	0.445908478	0.445908478	4.112351938	4.112351938
60	28.03	31.17	31.17	0.0000	0.478364505	0.478364505	4.332456415	4.332456415
90	24.10	32.71	32.71	0.0000	0.526179867	0.526179867	4.715838057	4.715838057
120	21.40	33.76	33.76	0.0000	0.552753894	0.552753894	4.990872884	4.990872884
150	19.19	34.76	34.76	0.0000	0.472576303	0.472576303	5.170101522	5.170101522
180	17.97	35.17	35.17	0.0000	0.568352892	0.568352892	5.279098811	5.279098811
240	16.73	35.64	35.64	0.0000	0.606714337	0.606714337	5.389691007	5.389691007
300	13.95	36.90	36.90	0.0000	0.581671941	0.581671941	5.538505812	5.538505812
360	14.09	37.15	37.15	0.0000	0.250191982	0.250191982	5.552866504	5.552866504
420	13.81	36.92	36.92	0.0000	0.634854247	0.634854247	5.538216211	5.538216211

Time (min)	7000							
	Percentages							
1-C8	C14	C2H4	2-C8	C12	C4H8	C13	C3H6	
1	94.93	2.32	2.32	0.00	0.00	0.00	0.00	0.00
2.5	91.28	3.97	3.97	0.00	0.25	0.25	0.00	0.00
5	79.21	9.53	9.53	0.00	0.24	0.24	0.43	0.43
7.5	81.59	8.19	8.19	0.03	0.38	0.38	0.38	0.38
10	71.53	13.25	13.25	0.00	0.28	0.28	0.53	0.53
12.5	70.44	13.87	13.87	0.00	0.23	0.23	0.55	0.55
15	70.45	13.58	13.58	0.00	0.26	0.26	0.73	0.73
17.5	65.47	16.15	16.15	0.00	0.26	0.26	0.71	0.71
20	59.36	19.08	19.08	0.00	0.21	0.21	0.90	0.90
22.5	61.65	17.70	17.70	0.00	0.26	0.26	1.06	1.06
25	57.71	19.97	19.97	0.00	0.21	0.21	0.97	0.97
30	52.60	22.17	22.17	0.00	0.19	0.19	1.20	1.20
35	48.20	24.14	24.14	0.00	0.25	0.25	1.39	1.39
40	45.73	25.22	25.22	0.00	0.25	0.25	1.54	1.54
45	42.71	26.58	26.58	0.00	0.27	0.27	1.66	1.66
50	40.56	27.93	27.93	0.00	0.00	0.00	1.79	1.79
60	38.93	28.64	28.64	0.00	0.00	0.00	1.89	1.89
90	27.41	33.50	33.50	0.00	0.23	0.23	2.44	2.44
120	25.50	34.31	34.31	0.00	0.25	0.25	2.57	2.57
150	24.25	34.81	34.81	0.00	0.27	0.27	2.68	2.68
180	24.37	35.12	35.12	0.00	0.00	0.00	2.70	2.70
240	21.27	36.28	36.28	0.00	0.28	0.28	2.81	2.81
300	20.39	36.66	36.66	0.00	0.23	0.23	2.81	2.81
360	20.24	36.73	36.73	0.00	0.25	0.25	2.79	2.79
420	19.28	37.30	37.30	0.00	0.22	0.22	2.84	2.84

Time (min)	12000							
	Percentages							
1-C8	C14	C2H4	2-C8	C12	C4H8	C13	C3H6	
1	93.37	0.00	0.00	0.00	3.16	3.16	0.00	0.00
2.5	98.62	0.00	0.00	0.00	0.52	0.52	0.00	0.00
5	99.02	0.10	0.10	0.00	0.16	0.16	0.00	0.00
7.5	98.77	0.25	0.25	0.00	0.19	0.19	0.00	0.00
10	98.11	0.55	0.55	0.00	0.23	0.23	0.00	0.00
12.5	96.29	1.54	1.54	0.00	0.16	0.16	0.00	0.00
15	94.88	2.21	2.21	0.00	0.20	0.20	0.00	0.00
17.5	93.14	3.15	3.15	0.00	0.14	0.14	0.00	0.00
20	91.19	4.03	4.03	0.00	0.24	0.24	0.00	0.00
22.5	91.29	4.03	4.03	0.00	0.18	0.18	0.00	0.00
25	87.22	5.92	5.92	0.00	0.23	0.23	0.11	0.11
30	85.45	6.86	6.86	0.00	0.19	0.19	0.10	0.10
35	83.63	7.69	7.69	0.00	0.25	0.25	0.11	0.11
40	82.09	8.50	8.50	0.00	0.23	0.23	0.09	0.09
45	80.14	9.56	9.56	0.00	0.23	0.23	0.00	0.00
50	79.80	9.78	9.78	0.00	0.19	0.19	0.00	0.00
60	77.77	10.78	10.78	0.00	0.21	0.21	0.00	0.00
90	75.55	11.94	11.94	0.00	0.16	0.16	0.00	0.00
120	73.70	12.65	12.65	0.00	0.28	0.28	0.09	0.09
150	71.63	13.77	13.77	0.00	0.18	0.18	0.11	0.11
180	76.33	11.54	11.54	0.00	0.15	0.15	0.00	0.00
240	75.20	12.11	12.11	0.00	0.15	0.15	0.00	0.00
300	54.23	10.11	10.11	24.87	0.13	0.13	0.08	0.08
360	71.29	13.99	13.99	0.00	0.16	0.16	0.00	0.00
420	72.79	12.79	12.79	0.00	0.20	0.20	0.38	0.38

Time (min)	14000							
	Percentages							
1-C8	C14	C2H4	2-C8	C12	C4H8	C13	C3H6	
1	94.99	2.35	2.35	0.00	0.00E+00	0.00E+00	0.00E+00	0.00E+00
2.5	92.69	3.34	3.34	0.00	1.68E-01	1.68E-01	0.00E+00	0.00E+00
5	87.49	5.87	5.87	0.00	2.53E-01	2.53E-01	0.00E+00	0.00E+00
7.5	83.49	7.82	7.82	0.00	2.03E-01	2.03E-01	1.02E-01	1.02E-01
10	80.74	9.19	9.19	0.00	1.74E-01	1.74E-01	1.34E-01	1.34E-01
12.5	77.86	10.60	10.60	0.00	1.86E-01	1.86E-01	1.51E-01	1.51E-01
15	75.62	11.66	11.66	0.00	1.72E-01	1.72E-01	2.30E-01	2.30E-01
17.5	72.47	13.21	13.21	0.00	1.63E-01	1.63E-01	2.60E-01	2.60E-01
20	71.43	13.70	13.70	0.00	1.89E-01	1.89E-01	2.63E-01	2.63E-01
22.5	67.69	15.41	15.41	0.00	2.18E-01	2.18E-01	3.93E-01	3.93E-01
25	65.92	16.30	16.30	0.00	2.97E-01	2.97E-01	3.07E-01	3.07E-01
30	62.91	17.70	17.70	0.00	1.95E-01	1.95E-01	5.22E-01	5.22E-01
35	59.71	19.27	19.27	0.00	1.54E-01	1.54E-01	5.94E-01	5.94E-01
40	56.28	20.82	20.82	0.00	2.08E-01	2.08E-01	7.04E-01	7.04E-01
45	53.99	21.87	21.87	0.00	2.25E-01	2.25E-01	7.77E-01	7.77E-01
50	52.42	22.61	22.61	0.00	2.23E-01	2.23E-01	8.20E-01	8.20E-01
60	48.15	24.61	24.61	0.00	2.79E-01	2.79E-01	9.06E-01	9.06E-01
90	42.11	27.47	27.47	0.00	3.53E-01	3.53E-01	1.12E+00	1.12E+00
120	40.07	28.40	28.40	0.00	1.95E-01	1.95E-01	1.24E+00	1.24E+00
150	36.59	30.13	30.13	0.00	3.38E-01	3.38E-01	1.24E+00	1.24E+00
180	34.66	30.70	30.70	0.00	2.65E-01	2.65E-01	1.58E+00	1.58E+00
240	35.30	30.63	30.63	0.00	4.12E-01	4.12E-01	1.31E+00	1.31E+00
300	34.72	30.96	30.96	0.00	1.94E-01	1.94E-01	1.36E+00	1.36E+00
360	33.97	31.32	31.32	0.00	3.66E-01	3.66E-01	1.33E+00	1.33E+00
420	32.59	31.75	31.75	0.00	5.90E-01	5.90E-01	1.36E+00	1.36E+00

SPECIES PERCENTAGE DATA FOR GMPP CATALYST AT VARIED TEMPERATURES

Time (min)	40°C							
	Percentages							
1-C8	C14	C2H4	2-C8	C12	C4H8	C13	C3H6	
1	99.66	0.00	0.00	0.34	0.00	0.00	0.00	0.00
2.5	99.09	0.00	0.00	0.35	0.00	0.00	0.00	0.00
5	99.14	0.00	0.00	0.35	0.00	0.00	0.00	0.00
7.5	99.15	0.00	0.00	0.34	0.00	0.00	0.00	0.00
10	99.14	0.00	0.00	0.35	0.00	0.00	0.00	0.00
12.5	99.04	0.00	0.00	0.36	0.00	0.00	0.00	0.00
15	99.23	0.00	0.00	0.33	0.00	0.00	0.00	0.00
17.5	99.26	0.00	0.00	0.35	0.00	0.00	0.00	0.00
20	99.20	0.00	0.00	0.36	0.00	0.00	0.00	0.00
22.5	99.24	0.00	0.00	0.33	0.00	0.00	0.00	0.00
25	99.26	0.00	0.00	0.34	0.00	0.00	0.00	0.00
30	98.62	0.23	0.23	0.32	0.00	0.00	0.00	0.00
35	98.69	0.28	0.28	0.33	0.00	0.00	0.00	0.00
40	97.90	0.67	0.67	0.31	0.00	0.00	0.00	0.00
45	98.67	0.35	0.35	0.31	0.00	0.00	0.00	0.00
50	94.72	2.08	2.08	0.31	0.00	0.00	0.00	0.00
60	93.61	2.69	2.69	0.00	0.00	0.00	0.00	0.00
90	93.63	2.64	2.64	0.29	0.00	0.00	0.00	0.00
120	94.07	2.76	2.76	0.00	0.00	0.00	0.00	0.00
150	90.15	4.61	4.61	0.00	0.00	0.00	0.00	0.00
180	89.36	4.94	4.94	0.31	0.00	0.00	0.00	0.00
240	88.51	5.35	5.35	0.31	0.00	0.00	0.00	0.00
300	86.92	6.41	6.41	0.30	0.00	0.00	0.00	0.00

Time (min)	50°C							
	Percentages							
1-C8	C14	C2H4	2-C8	C12	C4H8	C13	C3H6	
1	98.61	0.51	0.51	0.0007	0	0	0	0
2.5	98.64	0.25	0.25	0.0006	0.235809789	0.235809789	0	0
5	98.62	0.18	0.18	0.0008	0.325611334	0.325611334	0.00E+00	0
7.5	98.60	0.16	0.16	0.0007	0.355095734	0.355095734	0	0
10	98.34	0.19	0.19	0.0006	0.468813896	0.468813896	0	0
12.5	98.82	0.20	0.20	0.0007	0.212348746	0.212348746	0	0
15	99.60	0.00	0.00	0.0007	0	0	0	0
17.5	98.87	0.18	0.18	0.0006	0.204129647	0.204129647	0	0
20	98.74	0.23	0.23	0.0007	0.224368843	0.224368843	0	0
22.5	98.61	0.23	0.23	0.0007	0.293728731	0.293728731	0	0
25	97.97	0.65	0.65	0.0005	0.200401018	0.200401018	0	0
30	96.73	1.27	1.27	0.0006	0.207025512	0.207025512	0	0
35	96.64	1.16	1.16	0.0006	0.356674378	0.356674378	0	0
40	96.87	1.02	1.02	0.0006	0.380466045	0.380466045	0	0
45	96.52	1.39	1.39	0.0000	0.345409146	0.345409146	0	0
50	98.18	0.60	0.60	0.0000	0.310712524	0.310712524	0	0
60	99.68	0.00	0.00	0.0005	0	0	0	0
90	94.11	2.62	2.62	0.0000	0.322681265	0.322681265	0	0
120	92.58	3.03	3.03	0.0003	0.529896568	0.529896568	0	0
150	89.35	4.85	4.85	0.0003	0.333646943	0.333646943	0	0
180	89.00	5.05	5.05	0.0005	0.295331033	0.295331033	0	0
240	85.82	6.55	6.55	0.0005	0.389023652	0.389023652	0	0
300	95.08	1.58	1.58	0.0000	0.515355488	0.515355488	0.360958568	0.360958568
360	89.68	4.56	4.56	0.0293	0.219294774	0.219294774	0.248760481	0.248760481
420	77.00	11.04	11.04	0.0000	0.459235897	0.459235897	0	0

Time (min)	60°C							
	Percentages							
1-C8	C14	C2H4	2-C8	C12	C4H8	C13	C3H6	
1	99.16	0.00	0.00	0.00	0.00	0.26	0.26	
2.5	99.03	0.00	0.00	0.31	0.31	0.00	0.00	
5	98.57	0.00	0.00	0.25	0.25	0.30	0.30	
7.5	98.26	0.23	0.23	0.21	0.21	0.26	0.26	
10	98.11	0.25	0.25	0.26	0.26	0.27	0.27	
12.5	97.79	0.29	0.29	0.32	0.32	0.33	0.33	
15	98.06	0.30	0.30	0.24	0.24	0.26	0.26	
17.5	98.31	0.26	0.26	0.26	0.26	0.16	0.16	
20	98.14	0.28	0.28	0.26	0.26	0.22	0.22	
22.5	98.79	0.33	0.33	0.28	0.28	0.00	0.00	
25	97.78	0.54	0.54	0.21	0.21	0.20	0.20	
30	97.41	0.63	0.63	0.28	0.28	0.23	0.23	
35	96.92	0.72	0.72	0.36	0.36	0.30	0.30	
40	97.51	0.89	0.89	0.36	0.36	0.00	0.00	
45	96.70	1.05	1.05	0.26	0.26	0.19	0.19	
50	96.52	1.22	1.22	0.20	0.20	0.16	0.16	
60	95.99	1.45	1.45	0.25	0.25	0.15	0.15	
90	94.10	2.47	2.47	0.18	0.18	0.16	0.16	
120	94.10	2.47	2.47	0.18	0.18	0.16	0.16	
150	91.60	3.60	3.60	0.24	0.24	0.22	0.22	
180	89.62	4.62	4.62	0.19	0.19	0.24	0.24	
240	83.31	8.02	8.02	0.20	0.20	0.00	0.00	
300	87.78	5.65	5.65	0.19	0.19	0.14	0.14	
360	85.38	6.88	6.88	0.18	0.18	0.10	0.10	
420	89.29	4.81	4.81	0.23	0.23	0.17	0.17	

Time (min)	70°C							
	Percentages							
1-C8	C14	C2H4	2-C8	C12	C4H8	C13	C3H6	
1	100.00	0.00	0.00	0.0000	0	0	0	0
2.5	98.81	0.00	0.00	0.253876873	0.253876873	0.161164525	0.161164525	
5	99.57	0.00	0.00	0.214642005	0.214642005	0.00E+00	0	
7.5	99.28	0.00	0.00	0.361258981	0.361258981	0	0	
10	98.61	0.40	0.40	0.292654435	0.292654435	0	0	
12.5	97.51	0.92	0.92	0.329037044	0.329037044	0	0	
15	96.30	1.24	1.24	0.250170403	0.250170403	0.191801495	0.191801495	
17.5	96.27	1.55	1.55	0.312726916	0.312726916	0	0	
20	95.50	1.95	1.95	0.305796775	0.305796775	0	0	
22.5	94.53	2.32	2.32	0.264359337	0.264359337	0	0	
25	93.83	2.45	2.45	0.334873818	0.334873818	0.296257175	0.296257175	
30	92.68	3.11	3.11	0.546404832	0.546404832	0	0	
35	90.64	3.96	3.96	0.484432691	0.484432691	0.23424244	0.23424244	
40	90.50	4.39	4.39	0.357564667	0.357564667	0	0	
45	88.09	5.42	5.42	0.305029673	0.305029673	0.227067572	0.227067572	
50	86.20	6.37	6.37	0.270369649	0.270369649	0.260359753	0.260359753	
60	84.48	7.34	7.34	0.417503794	0.417503794	0	0	
90	75.74	11.80	11.80	0.329654064	0.329654064	0	0	
120	68.40	15.46	15.46	0.340331501	0.340331501	0	0	
150	61.63	18.90	18.90	0.282107671	0.282107671	0	0	
180	55.69	21.49	21.49	0.277909861	0.277909861	0.247294206	0.247294206	
240	46.97	25.79	25.79	0.370198491	0.370198491	0.35892731	0.35892731	
300	39.88	29.20	29.20	0.352728466	0.352728466	0.507201839	0.507201839	
360	33.31	32.20	32.20	0.292729565	0.292729565	0.855066217	0.855066217	
420	28.47	34.51	34.51	0.286842301	0.286842301	0.967475636	0.967475636	

Time (min)	80°C							
	Percentages							
1-C8	C14	C2H4	2-C8	C12	C4H8	C13	C3H6	
1	99.62	0.00	0.00	0.00E+00	0.00E+00	0.00E+00	0.00E+00	
2.5	99.14	0.25	0.25	0.00E+00	0.00E+00	0.00E+00	0.00E+00	
5	98.04	0.66	0.66	0.00E+00	0.00E+00	0.00E+00	0.00E+00	
7.5	97.05	1.18	1.18	0.00E+00	0.00E+00	0.00E+00	0.00E+00	
10	95.96	1.75	1.75	0.00E+00	0.00E+00	0.00E+00	0.00E+00	
12.5	95.07	2.30	2.30	0.00E+00	0.00E+00	0.00E+00	0.00E+00	
15	93.50	3.09	3.09	0.00E+00	0.00E+00	0.00E+00	0.00E+00	
17.5	90.96	4.37	4.37	0.00E+00	0.00E+00	0.00E+00	0.00E+00	
20	89.76	4.97	4.97	0.00E+00	0.00E+00	0.00E+00	0.00E+00	
22.5	87.89	5.91	5.91	0.00E+00	0.00E+00	0.00E+00	0.00E+00	
25	85.99	6.86	6.86	0.00E+00	0.00E+00	0.00E+00	0.00E+00	
30	83.67	8.17	8.17	0.00E+00	0.00E+00	0.00E+00	0.00E+00	
35	79.45	10.13	10.13	0.00E+00	0.00E+00	0.00E+00	0.00E+00	
40	76.94	11.19	11.19	1.96E-01	1.96E-01	0.00E+00	0.00E+00	
45	74.26	12.33	12.33	2.34E-01	2.34E-01	1.63E-01	1.63E-01	
50	70.71	14.02	14.02	2.62E-01	2.62E-01	2.21E-01	2.21E-01	
60	64.97	16.89	16.89	3.68E-01	3.68E-01	2.59E-01	2.59E-01	
90	54.80	21.47	21.47	7.93E-01	7.93E-01	3.39E-01	3.39E-01	
120	38.34	26.37	26.37	2.86E+00	2.86E+00	1.40E+00	1.40E+00	
150	43.38	25.30	25.30	1.33E+00	1.33E+00	1.52E+00	1.52E+00	
180	39.31	27.46	27.46	1.53E+00	1.53E+00	1.20E+00	1.20E+00	
240	35.92	28.79	28.79	1.74E+00	1.74E+00	1.36E+00	1.36E+00	
300	32.41	29.98	29.98	2.08E+00	2.08E+00	1.73E+00	1.73E+00	
360	25.37	33.14	33.14	2.34E+00	2.34E+00	1.84E+00	1.84E+00	
420	24.73	33.16	33.16	2.31E+00	2.31E+00	2.04E+00	2.04E+00	

Time (min)	90°C							
	Percentages							
1-C8	C14	C2H4	2-C8	C12	C4H8	C13	C3H6	
1	99.45	0.00	0.00	0.00	0.00	0.00	0.00	0.00
2.5	97.87	0.55	0.55	0.00	0.18	0.18	0.00	0.00
5	95.97	1.46	1.46	0.00	0.26	0.26	0.00	0.00
7.5	92.45	3.17	3.17	0.00	0.31	0.31	0.00	0.00
10	91.07	3.91	3.91	0.00	0.27	0.27	0.00	0.00
12.5	87.92	5.33	5.33	0.00	0.19	0.19	0.24	0.24
15	82.49	6.08	6.08	0.00	0.21	0.21	0.20	0.20
17.5	83.15	7.48	7.48	0.00	0.44	0.44	0.24	0.24
20	81.55	8.41	8.41	0.00	0.28	0.28	0.26	0.26
22.5	79.97	9.11	9.11	0.00	0.21	0.21	0.39	0.39
25	77.40	10.27	10.27	0.00	0.32	0.32	0.43	0.43
30	73.88	11.61	11.61	0.00	0.37	0.37	0.78	0.78
35	69.95	13.17	13.17	0.00	0.27	0.27	1.30	1.30
40	65.43	15.84	15.84	0.00	0.32	0.32	0.99	0.99
45	62.84	17.11	17.11	0.00	0.22	0.22	0.97	0.97
50	60.01	18.05	18.05	0.00	0.33	0.33	1.35	1.35
60	55.31	19.64	19.64	0.00	0.42	0.42	2.13	2.13
90	43.85	24.49	24.49	0.00	0.30	0.30	3.29	3.29
120	35.93	27.96	27.96	0.00	0.25	0.25	3.69	3.69
150	29.19	30.86	30.86	0.00	0.26	0.26	4.16	4.16
180	26.53	32.31	32.31	0.00	0.23	0.23	4.07	4.07
240	22.82	34.13	34.13	0.00	0.22	0.22	4.25	4.25
300	23.12	34.83	34.83	0.00	0.26	0.26	3.35	3.35
360	21.81	34.52	34.52	0.00	0.20	0.20	4.37	4.37
420	25.51	36.95	36.95	0.00	0.29	0.29	0.00	0.00

Time (min)	100°C							
	Percentages							
1-C8	C14	C2H4	2-C8	C12	C4H8	C13	C3H6	
1	98.89	0.25	0.25	0.00	0.00	0.00	0.00	0.00
2.5	98.05	0.37	0.37	0.00	0.28	0.28	0.00	0.00
5	96.91	0.74	0.74	0.00	0.44	0.44	0.00	0.00
7.5	96.82	0.93	0.93	0.00	0.27	0.27	0.00	0.00
10	93.99	1.18	1.18	0.00	1.37	1.37	0.00	0.00
12.5	95.96	1.29	1.29	0.00	0.23	0.23	0.00	0.00
15	95.29	1.52	1.52	0.00	0.29	0.29	0.00	0.00
17.5	94.55	1.60	1.60	0.30	0.52	0.52	0.00	0.00
20	95.68	1.51	1.51	0.00	0.00	0.00	0.00	0.00
22.5	94.55	1.63	1.63	0.33	0.26	0.26	0.00	0.00
25	94.78	1.75	1.75	0.00	0.18	0.18	0.00	0.00
30	93.55	1.95	1.95	0.37	0.31	0.31	0.00	0.00
35	90.77	3.19	3.19	0.35	0.51	0.51	0.00	0.00
40	93.25	1.84	1.84	0.43	0.24	0.24	0.27	0.27
45	91.29	2.53	2.53	0.44	0.51	0.51	0.21	0.21
50	89.71	3.59	3.59	0.48	0.19	0.19	0.17	0.17
60	91.71	2.58	2.58	0.51	0.24	0.24	0.00	0.00
90	87.71	3.72	3.72	0.52	0.30	0.30	0.66	0.66
120	85.97	4.23	4.23	0.54	0.28	0.28	0.88	0.88
150	80.13	6.52	6.52	0.51	0.36	0.36	1.28	1.28
180	81.06	5.78	5.78	0.52	0.48	0.48	1.40	1.40
240	78.29	6.80	6.80	0.61	0.28	0.28	1.71	1.71
300	77.72	7.03	7.03	0.64	0.25	0.25	1.75	1.75
360	78.07	6.94	6.94	0.58	0.30	0.30	1.73	1.73
420	78.07	6.94	6.94	0.58	0.30	0.30	1.73	1.73

SPECIES PERCENTAGE DATA FOR GMPP CATALYST AT VARIED CATALYST LOADS

Time (min)	5000							
	Percentages							
1-C8	C14	C2H4	2-C8	C12	C4H8	C13	C3H6	
1	100.00	0.00	0.00	0.0000	0	0	0	0
2.5	99.29	0.19	0.19	0.0005	0	0	0	0
5	99.15	0.25	0.25	0.0006	0	0	0.00E+00	0
7.5	99.24	0.38	0.38	0.0000	0	0	0	0
10	96.75	1.46	1.46	0.0006	0	0	0	0
12.5	96.85	1.42	1.42	0.0005	0	0	0	0
15	95.69	2.00	2.00	0.0005	0	0	0	0
17.5	94.07	2.81	2.81	0.0006	0	0	0	0
20	93.20	3.17	3.17	0.0000	0	0	0.230939844	0.230939844
22.5	90.99	4.10	4.10	0.0005	0	0	0.25739427	0.25739427
25	90.24	4.65	4.65	0.0000	0	0	0.228694497	0.228694497
30	87.25	6.14	6.14	0.0000	0	0	0.229703353	0.229703353
35	83.71	8.15	8.15	0.0000	0	0	0	0
40	81.42	8.91	8.91	0.0006	0	0	0.218862376	0.218862376
45	78.55	10.72	10.72	0.0000	0	0	0	0
50	75.37	11.94	11.94	0.0005	0	0	0.2151273	0.2151273
60	70.68	14.26	14.26	0.0005	0	0	0.252505761	0.252505761
90	58.96	20.23	20.23	0.0000	0	0	0.294469206	0.294469206
120	50.23	24.67	24.67	0.0005	0	0	0.053274044	0.053274044
150	38.07	29.88	29.88	0.0004	0	0	0.957854649	0.957854649
180	40.83	28.82	28.82	0.0000	0	0	0.763489411	0.763489411
240	25.18	35.84	35.84	0.0005	0	0	1.431104905	1.431104905
300	21.46	37.69	37.69	0.0000	0	0	1.578937958	1.578937958
360	18.67	38.93	38.93	0.0000	0	0	1.737379235	1.737379235
420	14.69	40.78	40.78	0.0000	0	0	1.872939005	1.872939005

Time (min)	7000							
	Percentages							
1-C8	C14	C2H4	2-C8	C12	C4H8	C13	C3H6	
1	97.92	0.86	0.86	0.00	0.00	0.00	0.00	0.00
2.5	99.61	0.00	0.00	0.00	0.00	0.00	0.00	0.00
5	99.64	0.00	0.00	0.00	0.00	0.00	0.00	0.00
7.5	99.40	0.30	0.30	0.00	0.00	0.00	0.00	0.00
10	98.17	0.75	0.75	0.00	0.00	0.00	0.00	0.00
12.5	97.45	1.10	1.10	0.00	0.00	0.00	0.00	0.00
15	96.18	1.91	1.91	0.00	0.00	0.00	0.00	0.00
17.5	95.81	2.10	2.10	0.00	0.00	0.00	0.00	0.00
20	94.86	2.40	2.40	0.00	0.00	0.00	0.00	0.00
22.5	94.42	2.79	2.79	0.00	0.00	0.00	0.00	0.00
25	92.92	3.54	3.54	0.00	0.00	0.00	0.00	0.00
30	90.98	4.51	4.51	0.00	0.00	0.00	0.00	0.00
35	88.61	5.54	5.54	0.00	0.00	0.00	0.00	0.00
40	85.90	6.89	6.89	0.00	0.00	0.00	0.00	0.00
45	83.31	8.34	8.34	0.00	0.00	0.00	0.00	0.00
50	81.54	9.23	9.23	0.00	0.00	0.00	0.00	0.00
60	76.36	11.67	11.67	0.00	0.00	0.00	0.00	0.00
90	57.33	20.80	20.80	0.00	0.00	0.00	0.39	0.39
120	48.82	24.91	24.91	0.00	0.00	0.00	0.54	0.54
150	44.65	26.91	26.91	0.00	0.00	0.00	0.63	0.63
180	38.86	29.62	29.62	0.00	0.00	0.00	0.82	0.82
240	32.00	33.04	33.04	0.00	0.00	0.00	0.96	0.96
300	24.26	36.75	36.75	0.00	0.00	0.00	1.12	1.12
360	21.47	38.03	38.03	0.00	0.00	0.00	1.24	1.24
420	18.97	39.22	39.22	0.00	0.00	0.00	1.29	1.29

Time (min)	12000							
	Percentages							
1-C8	C14	C2H4	2-C8	C12	C4H8	C13	C3H6	
1	96.41	1.61	1.61	0.00	0.00	0.00	0.00	0.00
2.5	96.50	1.58	1.58	0.00	0.00	0.00	0.00	0.00
5	96.05	1.69	1.69	0.00	0.00	0.00	0.00	0.00
7.5	95.35	1.83	1.83	0.00	0.33	0.33	0.00	0.00
10	95.52	1.96	1.96	0.00	0.00	0.00	0.00	0.00
12.5	95.42	2.13	2.13	0.00	0.00	0.00	0.00	0.00
15	95.42	2.13	2.13	0.00	0.00	0.00	0.00	0.00
17.5	97.73	1.13	1.13	0.00	0.00	0.00	0.00	0.00
20	97.22	1.39	1.39	0.00	0.00	0.00	0.00	0.00
22.5	96.27	1.71	1.71	0.00	0.00	0.00	0.00	0.00
25	95.57	2.05	2.05	0.00	0.00	0.00	0.00	0.00
30	51.78	21.42	21.42	0.00	0.00	0.00	1.79	1.79
35	89.24	4.78	4.78	0.00	0.00	0.00	0.45	0.45
40	88.30	5.40	5.40	0.00	0.00	0.00	0.29	0.29
45	87.42	5.76	5.76	0.00	0.00	0.00	0.38	0.38
50	83.29	8.35	8.35	0.00	0.00	0.00	0.00	0.00
60	82.61	8.40	8.40	0.00	0.00	0.00	0.29	0.29
90	79.34	10.33	10.33	0.00	0.00	0.00	0.00	0.00
120	65.90	16.85	16.85	0.00	0.00	0.00	0.20	0.20
150	59.70	19.73	19.73	0.00	0.00	0.00	0.26	0.26
180	57.66	20.90	20.90	0.00	0.00	0.00	0.28	0.28
240	50.65	24.06	24.06	0.00	0.00	0.00	0.47	0.47
300	29.52	20.16	20.16	29.48	0.00	0.00	0.34	0.34
360	35.57	31.45	31.45	0.00	0.00	0.00	0.77	0.77
420	36.16	31.06	31.06	0.00	0.00	0.00	0.73	0.73

Time (min)	14000							
	Percentages							
1-C8	C14	C2H4	2-C8	C12	C4H8	C13	C3H6	
1	99.25	0.19	0.19	0.00	0.00E+00	0.00E+00	0.00E+00	0.00E+00
2.5	98.87	0.00	0.00	0.00	3.87E-01	3.87E-01	0.00E+00	0.00E+00
5	98.69	0.19	0.19	0.00	2.87E-01	2.87E-01	0.00E+00	0.00E+00
7.5	98.73	0.18	0.18	0.00	2.79E-01	2.79E-01	0.00E+00	0.00E+00
10	98.26	0.52	0.52	0.00	2.40E-01	2.40E-01	0.00E+00	0.00E+00
12.5	97.82	0.61	0.61	0.00	2.01E-01	2.01E-01	0.00E+00	0.00E+00
15	97.16	0.93	0.93	0.00	3.20E-01	3.20E-01	0.00E+00	0.00E+00
17.5	96.62	1.10	1.10	0.00	4.30E-01	4.30E-01	0.00E+00	0.00E+00
20	93.08	1.45	1.45	0.00	2.91E-01	2.91E-01	1.56E+00	1.56E+00
22.5	91.33	1.71	1.71	0.00	4.51E-01	4.51E-01	2.00E+00	2.00E+00
25	94.36	1.79	1.79	0.00	4.46E-01	4.46E-01	4.36E-01	4.36E-01
30	93.55	2.33	2.33	0.00	3.42E-01	3.42E-01	4.02E-01	4.02E-01
35	93.20	2.88	2.88	0.00	3.72E-01	3.72E-01	0.00E+00	0.00E+00
40	91.80	3.57	3.57	0.00	3.77E-01	3.77E-01	0.00E+00	0.00E+00
45	91.18	3.98	3.98	0.00	2.84E-01	2.84E-01	0.00E+00	0.00E+00
50	90.10	4.41	4.41	0.00	3.99E-01	3.99E-01	0.00E+00	0.00E+00
60	88.68	5.28	5.28	0.00	2.31E-01	2.31E-01	0.00E+00	0.00E+00
90	83.23	7.96	7.96	0.00	4.31E-01	4.31E-01	0.00E+00	0.00E+00
120	79.12	9.96	9.96	0.00	3.52E-01	3.52E-01	0.00E+00	0.00E+00
150	74.54	12.35	12.35	0.00	2.42E-01	2.42E-01	0.00E+00	0.00E+00
180	70.94	14.28	14.28	0.00	2.45E-01	2.45E-01	0.00E+00	0.00E+00
240	64.44	17.06	17.06	0.00	3.32E-01	3.32E-01	2.52E-01	2.52E-01
300	53.06	22.50	22.50	0.00	3.06E-01	3.06E-01	5.35E-01	5.35E-01
360	57.53	20.35	20.35	0.03	4.06E-01	4.06E-01	3.43E-01	3.43E-01
420	52.70	22.80	22.80	0.00	4.68E-01	4.68E-01	3.80E-01	3.80E-01

APPENDIX C: Methods, Constants & Assumptions

Chapter 2

DETAILED EXPERIMENTAL METHOD

STEP	TASK
1	Measure out 15 mL 1-octene with a syringe and add to clean glass flask
2	Fit condenser, stirrer and temperature probes to vessel ports
3	Open cooling water and ensure proper seal on vessel
4	Switch on mechanical stirrer
5	Heat 1-octene to desired temperature
6	Transfer catalyst to spatula
7	Add catalyst to 1-octene and close all the ports securely
8	Transfer 4-5 drops of Tert-butyl hydroperoxide to a 4 ml Vial with Pasteur pipette
9	Draw a sample from reaction flask with analytical syringe, add to 4 mL vial
10	Add 0.1mL Nonane to sample vial
11	Fill vial with Dichloromethane solvent
12	Dilute 4ml vial solution to 1.5 mL vials with dichloromethane

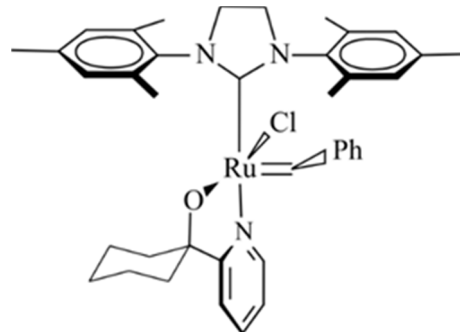
CONSTANTS & PARAMETERS

Chemical Data				
Chemical	MW (g/mol)	ρ (g/mL)	Formula	Category
1-Heptene	98.19	0.697	CH ₃ (CH ₂) ₄ CH=CH ₂	SP
1-Octene	112.21	0.715	CH ₃ (CH ₂) ₅ CH=CH ₂	R
2-Octene	112.21	0.715	CH ₃ (CH ₂) ₄ CH=CHCH ₃	IP
3-Octene	112.21	0.715	CH ₃ (CH ₂) ₃ CH=CHC ₂ H ₅	IP
4-Octene	112.21	0.715	CH ₃ CH ₂ CH ₂ CH=CHCH ₂ CH ₂ CH ₃	IP
Nonane	128.26	0.718	CH ₃ (CH ₂) ₇ CH ₃	ES
Decene	140.27	0.741	CH ₃ (CH ₂) ₇ CH=CH ₂	SP
Undecene	154.29	0.75	CH ₃ (CH ₂) ₈ CH=CH ₂	SP
Dodecene	168.32	0.758	CH ₃ (CH ₂) ₉ CH=CH ₂	SP
Tridecene	182.35	0.766	CH ₃ (CH ₂) ₁₀ CH=CH ₂	SP
Ethene	28.05	0.00118	CH ₂ =CH ₂	PP
7-Tetradecene	196.37	0.764	CH ₃ (CH ₂) ₅ CH=CH(CH ₂) ₅ CH ₃	PP
HGr2	626.62	-	C ₃₁ H ₃₈ Cl ₂ N ₂ ORu	C
Toluene	92.14	0.865	C ₆ H ₅ CH ₃	S
Dichloromethane	84.93	1.325	CH ₂ Cl ₂	S
Ruthenium	101.07	12.2	Ru	C
Gr1Cyc5	710	-	C ₃₉ H ₄₅ Cl ₁ N ₃ ORu	C
Gr2MPP	808.43	-	C ₃₅ H ₄₅ Cl ₁ N ₃ OPRu	C
Gr2MPM	746.36	-	C ₃₆ H ₄₅ Cl ₁ N ₃ OPRu	C
Gr2ClPP	828.85	-	C ₃₄ H ₄₂ Cl ₂ N ₃ OP ₂ Ru	C
Gr4ClPP	828.85	-	C ₃₄ H ₄₂ Cl ₂ N ₃ OP ₂ Ru	C
Gr4MeOPP	824.43	-	C ₃₅ H ₄₅ Cl ₁ N ₃ O ₂ PRu	C

CATALYST LOAD CALCULATIONS

Gcyc				
Catalyst load C8/Ru	Mol Ru	g Ru	Mass Precatalyst needed	mg catalyst needed
5000	0.000019	0.002	0.01357232	13.6
7000	0.000014	0.001	0.009694514	9.7
10000	0.000010	0.001	0.00678616	6.8
9000	0.000011	0.001	0.007540178	7.5
12000	0.000008	0.001	0.005655133	5.7
14000	0.000007	0.001	0.004847257	4.8

No. Of Experiments	Mass Cat needed
1	13.6
1	9.7
7	47.5
1	5.7
3	14.5
TOTAL (mg)	91.0



GMPP				
Catalyst load C8/Ru	Mol Ru	g Ru	Mass Precatalyst needed	mg catalyst needed
5000	0.000019	0.002	0.015453902	15.5
7000	0.000014	0.001	0.011038501	11.0
10000	0.000010	0.001	0.007726951	7.7
12000	0.000008	0.001	0.006439126	6.4
14000	0.000007	0.001	0.005519251	5.5

No. Of Experiments	Mass Cat needed
1	15.5
1	15.5
7	77.3
1	7.7
1	6.4
TOTAL (mg)	122.3

The chemical structure shows a Ru atom at the center. It is coordinated to a Cl ligand, a Ph ligand, and an oxazoline nitrogen atom. The oxazoline ring is further substituted with a 2-methylphenyl group and a 2-pyridyl group.

Chapter 4

HEAT CAPACITY CORRELATION CONSTANTS FOR JOBACK METHOD

Heat Capacity J/Mol K correlation parameters																
	C8		2-C8		C12		C13		C14		C2		C3		C4	
	Value	Units	Value	Units	Value	Units	Value	Units	Value	Units	Value	Units	Value	Units	Value	Units
C1	194042.6	J/kmol-K	332609.4	J/kmol-K	243058.3	J/kmol-K	475221.1	J/kmol-K	272353.6	J/kmol-K	72022.72	J/kmol-K	133146.7	J/kmol-K	130310.2	J/kmol-K
C2	-198.6302	J/kmol-K**2	-1705.43	J/kmol-K**2	115.7478	J/kmol-K**2	-1501.025	J/kmol-K**2	202.4168	J/kmol-K**2	21.59559	J/kmol-K**2	-865.1865	J/kmol-K**2	-624.1461	J/kmol-K**2
C3	1.545295	J/kmol-K**3	6.434974	J/kmol-K**3	1.147052	J/kmol-K**3	5.268038	J/kmol-K**3	1.177902	J/kmol-K**3	-1.14516	J/kmol-K**3	4.407376	J/kmol-K**3	3.00934	J/kmol-K**3
C4	-0.001405217	J/kmol-K**4	-0.00682	J/kmol-K**4	-0.000998161	J/kmol-K**4	-0.004313122	J/kmol-K**4	-0.001027811	J/kmol-K**4	0.0043	J/kmol-K**4	-0.007385419	J/kmol-K**4	-0.004567732	J/kmol-K**4
β	5413.983	J/kmol-K	12293.03	J/kmol-K	5848.692	J/kmol-K	7538.579	J/kmol-K	6087.869	J/kmol-K	1523.754	J/kmol-K	5412.138	J/kmol-K	10991.47	J/kmol-K
Tci	573.2	K	566.5827	K	661	K	673	K	690	K	282.3438	K	364.9487	K	419.29	K
Nterms	4	Unitless	4	Unitless	4	Unitless	4	Unitless	4	Unitless	4	Unitless	4	Unitless	4	Unitless
Lower T	179.15	K	171.4935	K	250	K	250.075	K	250	K	103.9662	K	87.85	K	60	K
Upper T	560	K	550	K	647.78	K	659.54	K	676.2	K	275.4367	K	344.2349	K	377.5689	K
heat of formation	-121.8	kJ/mol							-215.07	kJ/mol	52.88	kJ/mol				
heat of reaction	40705000				J/Kmol		Power constant		0.03	kW/m^3	Power Cost	\$/kwh				
									u						200	

Joback Method Equations

$$C_{p,i}^* = \frac{\beta}{\tau} + \sum_{m=1}^{nTerms} C_{mi} T^{m-1}$$

$$\tau = 1 - \frac{T}{T_{ci}}$$

$$\Delta \widehat{H} = \int_{T_1}^{T_2} C_{p,i} dT$$

admin charge	44 r/day
service charge	190.73 r/day
c/kwh	325.88
admin charge	0.002206177 \$/min
service charge/hr	0.009563277 \$/min
	\$/kwh
	0.235292419

Assumed Constants for equipment sizes	Value
Reactor H/D ratio	1
Flash Drum H/D ratio	2
Flash Time	0.8333 hr
Operating pressure for flash drum	1.5 Bar
Membrane cost per m ²	1970 \$.m ⁻³
Heat exchanger Reference Temperature	25 °C
Heat exchange transfer coefficient	200 W.m ⁻²

PROFITABILITY ANALYSIS ASSUMPTIONS

GCYC

Assumptions	
Years of Operation	15
Conditions	
T	70
Conversion	0.5
catalyst load	140000
Rates	
income tax	28%
inflation rate	6.30
Discount rate	15.00

GMPP

Assumptions	
Years of Operation	15
conditions	
T	70
Conversion	0.53
catalyst load	10000
Rates	
income tax	28%
inflation rate	6.30
Discount rate	15.00
Straight line depreciation over 15 years	

APPENDIX D: Calculated Data

Chapter 2

The Data in this section contains the data used in the Regression Algorithm

$C_1 = 1 - \text{Octene}$, $C_2 = \text{PPs}$, $C_3 = \text{SPs}$, $T = \text{sampling time}$
 EXPORTED DATA FOR THE **GCYC** CATALYST WHERE TEMPERATURE WAS
 VARIED

Temperatures in °C are indicated in the highlighted section of the data tables

40				50			
T	C1	C2	C3	T	C1	C2	C3
1	98.45741	0	0	1	99.54127	0	0
2.5	96.69	2.84	0.00	2.5	99.23	0.00	0.31
5	96.29	3.71	0.00	5	98.54	0.00	0.50
7.5	96.86	3.14	0.00	7.5	98.89	0.00	0.41
10	95.65	4.35	0.00	10	99.14	0.48	0.38
12.5	95.91	4.09	0.00	12.5	97.85	1.59	0.51
15	96.67	2.78	0.00	15	95.98	2.86	0.58
17.5	96.27	3.73	0.00	17.5	95.55	3.57	0.45
20	99.89	0.11	0.00	20	94.20	4.74	0.60
22.5	98.94	1.06	0.00	22.5	87.50	5.14	6.98
25	99.29	0.71	0.00	25	90.71	8.12	0.60
30	98.60	1.40	0.00	30	86.32	9.99	0.87
35	98.78	1.22	0.00	35	88.37	10.37	0.54
40	98.60	1.40	0.00	40	87.32	11.84	0.39
45	97.71	1.72	0.57	45	85.50	13.48	0.65
50	98.33	1.67	0.00	50	84.85	14.05	0.74
60	99.01	0.99	0.00	60	82.81	15.75	1.00
90	98.57	1.43	0.00	90	78.74	20.02	0.93
120	98.29	1.71	0.00	120	74.43	23.64	1.46
150	97.76	2.24	0.00	150	71.34	26.67	1.72
180	97.11	2.89	0.00	180	69.58	28.25	1.88
240	96.36	3.64	0.00	240	67.24	30.67	1.75
300	94.94	5.06	0.00	300	63.60	33.92	2.14
360	93.70	6.30	0.00	360	61.68	35.87	2.13
420	91.18	8.82	0.00	420	59.88	37.75	2.02

60				70			
T	C1	C2	C3	T	C1	C2	C3
1	98.91546	0	0	1	98.48	0.96	0.41
2.5	90.92	8.17	0.59	2.5	93.19	5.75	0.78
5	87.17	11.76	0.78	5	82.89	16.29	0.55
7.5	84.10	14.52	1.01	7.5	74.16	24.61	0.97
10	90.98	5.77	2.98	10	66.69	31.57	1.47
12.5	81.73	17.00	0.99	12.5	60.71	37.13	1.87
15	87.80	11.19	0.68	15	55.90	41.64	2.19
17.5	86.66	12.53	0.53	17.5	52.28	45.03	2.42
20	84.77	14.44	0.53	20	49.74	47.27	2.71
22.5	75.42	23.21	1.10	22.5	47.98	48.79	2.95
25	82.84	16.12	0.74	25	47.77	48.97	2.99
30	79.65	19.07	0.99	30	45.88	50.30	3.53
35	76.03	22.80	0.89	35	42.29	53.94	3.48
40	73.91	24.91	0.90	40	39.27	56.46	3.98
45	71.57	26.96	1.17	45	36.73	58.96	4.03
50	69.17	29.27	1.27	50	34.94	60.89	3.93
60	67.28	30.78	1.64	60	31.62	63.35	4.74
90	59.48	38.38	1.85	90	27.80	66.63	5.29
120	54.59	42.90	2.24	120	25.48	68.86	5.41
150	51.16	46.55	2.02	150	24.46	69.58	5.70
180	49.50	47.66	2.56	180	22.85	71.11	5.78
240	46.01	51.17	2.55	240	19.87	73.96	5.95
300	43.33	53.73	2.68	300	19.56	74.23	6.00
360	39.51	57.02	3.22	360	17.48	76.28	6.04
420	38.47	58.35	2.94	420	16.44	77.34	6.01

80				90			
T	C1	C2	C3	T	C1	C2	C3
1	100	0	0	1	98.13248	0	0
2.5	86.03	12.23	1.74	2.5	81.07	17.40	0.79
5	73.14	23.05	3.81	5	74.94	21.83	1.95
7.5	61.23	33.46	5.31	7.5	74.24	22.27	2.07
10	50.45	42.29	7.27	10	73.51	23.93	2.15
12.5	46.83	44.31	8.87	12.5	73.65	23.79	2.22
15	41.78	51.05	7.17	15	73.03	23.01	2.36
17.5	38.01	53.05	8.94	17.5	72.15	23.55	2.53
20	32.74	53.97	13.29	20	70.32	23.90	4.03
22.5	29.45	53.44	17.12	22.5	68.52	27.77	1.87
25	28.21	57.98	13.82	25	72.24	23.49	2.36
30	25.56	57.24	17.19	30	71.51	24.00	3.01
35	23.41	59.56	17.03	35	70.27	24.68	3.05
40	21.95	61.51	16.54	40	70.42	24.53	2.74
45	20.48	59.65	19.87	45	71.18	24.83	1.54
50	20.11	61.56	18.33	50	69.88	24.11	3.34
60	18.64	61.88	19.48	60	70.04	24.05	3.02
90	18.28	60.98	20.75	90	69.35	24.21	3.20
120	17.85	66.13	16.03	120	67.96	24.60	3.56
150	17.22	61.21	21.56	150	67.99	23.28	4.64
180	17.66	65.08	17.25	180	65.33	28.34	1.91
240	15.69	63.29	21.02	240	65.41	19.09	10.96
300	15.53	65.07	19.39	300	64.09	27.54	3.95
360	13.25	65.82	20.92	360	62.96	27.05	5.64
420	11.05	65.22	23.73	420	62.71	30.94	1.95

100			
T	C1	C2	C3
1	97.97882	0	0
2.5	88.02	5.11	5.92
5	92.52	5.72	0.51
7.5	92.06	6.36	0.00
10	91.52	5.69	1.22
12.5	90.95	5.89	1.29
15	91.18	5.92	1.13
17.5	90.69	5.90	1.33
20	90.74	6.20	0.92
22.5	89.65	6.31	1.81
25	90.08	5.85	1.47
30	89.31	6.25	1.65
35	88.80	6.13	2.07
40	88.50	6.15	2.18
45	88.20	6.54	1.83
50	88.00	6.47	1.97
60	87.62	6.42	2.11
90	86.87	6.72	2.17
120	85.87	6.96	2.34
150	86.13	6.63	2.28
180	86.38	6.46	2.29
240	86.36	6.85	1.84
300	86.17	7.04	1.86
360	86.15	7.09	1.85
420	85.67	7.25	2.26

EXPORTED DATA FOR THE **GCYC** CATALYST WHERE CATALYST LOAD WAS VARIED

5000				7000			
T	C1	C2	C3	T	C1	C2	C3
1	99.32	0.16	0.25	1	97.18	4.63	0.00
2.5	98.31	0.11	1.43	2.5	91.15	7.93	0.50
5	82.87	20.76	2.14	5	84.22	19.07	1.34
7.5	76.61	28.90	3.35	7.5	89.56	16.38	1.56
10	72.74	33.73	3.62	10	83.20	26.51	1.62
12.5	73.47	34.44	2.78	12.5	79.17	27.75	1.56
15	67.45	39.78	5.42	15	82.43	27.17	1.98
17.5	64.40	42.07	6.22	17.5	75.27	32.30	1.94
20	62.38	44.56	6.56	20	70.88	38.16	2.23
22.5	59.27	47.52	6.30	22.5	72.70	35.40	2.64
25	58.08	48.89	6.70	25	69.48	39.94	2.35
30	54.54	52.01	7.18	30	66.03	44.35	2.79
35	51.84	54.04	7.80	35	61.90	48.28	3.28
40	47.99	57.26	8.54	40	59.51	50.44	3.57
45	45.42	59.09	9.00	45	56.69	53.15	3.87
50	43.98	60.70	9.12	50	54.81	55.86	3.57
60	41.24	62.35	9.62	60	52.95	57.29	3.78
90	36.11	65.41	10.48	90	40.82	67.00	5.35
120	33.03	67.51	11.09	120	38.09	68.61	5.64
150	30.43	69.52	11.29	150	36.57	69.62	5.89
180	28.43	70.34	11.69	180	36.76	70.23	5.40
240	26.66	71.28	11.99	240	32.74	72.56	6.17
300	23.23	73.81	12.24	300	31.78	73.32	6.08
360	23.07	74.30	11.61	360	31.56	73.46	6.08
420	22.52	73.84	12.35	420	30.41	74.59	6.13

12000				14000			
T	C1	C2	C3	T	C1	C2	C3
1	93.20	0.00	6.32	1	97.28	4.69	0.00
2.5	96.09	0.00	1.04	2.5	92.88	6.69	0.34
5	95.71	0.20	0.33	5	88.74	11.74	0.51
7.5	96.42	0.50	0.38	7.5	87.40	15.64	0.61
10	95.32	1.10	0.47	10	85.91	18.39	0.62
12.5	94.44	3.09	0.33	12.5	83.85	21.20	0.68
15	92.77	4.43	0.40	15	83.16	23.32	0.81
17.5	93.32	6.31	0.27	17.5	81.07	26.42	0.85
20	90.19	8.05	0.49	20	80.02	27.41	0.90
22.5	91.52	8.07	0.36	22.5	77.20	30.82	1.22
25	89.23	11.85	0.67	25	74.89	32.60	1.21
30	88.42	13.72	0.58	30	73.65	35.40	1.43
35	85.97	15.37	0.73	35	72.01	38.54	1.50
40	86.02	17.00	0.64	40	68.73	41.64	1.82
45	84.59	19.13	0.47	45	66.33	43.74	2.00
50	84.94	19.55	0.39	50	65.16	45.22	2.09
60	83.57	21.55	0.42	60	61.03	49.22	2.37
90	83.24	23.87	0.32	90	55.91	54.95	2.94
120	80.00	25.30	0.74	120	54.38	56.80	2.87
150	80.21	27.54	0.58	150	50.34	60.26	3.15
180	82.46	23.08	0.31	180	48.43	61.41	3.70
240	82.31	24.23	0.30	240	49.39	61.26	3.44
300	81.22	20.21	25.28	300	48.55	61.92	3.12
360	79.44	27.98	0.32	360	47.65	62.64	3.40
420	80.50	25.57	1.18	420	46.21	63.51	3.90

EXPORTED DATA FOR THE GMPP CATALYST WHERE TEMPERATURE WAS VARIED

40				50			
Time	C1	C2	C3	Time	C1	C2	C3
0	100.00	0.00	0.00	0	100.00	0.00	0.00
1	99.66	0.00	0.00	1	99.12	1.03	0.00
2.5	96.54	0.00	0.56	2.5	96.74	0.51	0.47
5	96.85	0.00	0.51	5	96.57	0.36	0.65
7.5	96.77	0.00	0.51	7.5	96.37	0.33	0.71
10	96.74	0.00	0.51	10	95.17	0.38	0.94
12.5	96.40	0.00	0.60	12.5	97.07	0.39	0.43
15	96.79	0.00	0.44	15	97.96	0.00	0.00
17.5	97.06	0.00	0.39	17.5	97.05	0.35	0.41
20	96.69	0.00	0.44	20	96.94	0.45	0.45
25	96.62	0.00	0.43	22.5	96.75	0.46	0.59
30	96.88	0.00	0.40	25	96.67	1.29	0.40
35	95.99	0.45	0.62	30	95.89	2.54	0.41
40	96.30	0.55	0.43	35	94.89	2.32	0.71
45	96.52	1.33	0.46	40	95.07	2.05	0.76
50	96.75	0.69	0.33	45	95.82	2.79	0.69
60	94.34	4.05	0.93	50	96.36	1.20	0.62
120	93.44	5.21	1.18	60	99.68	0.00	0.00
150	94.11	5.12	0.97	90	94.27	5.25	0.65
180	94.28	5.36	0.58	120	91.78	6.07	1.06
240	91.58	8.77	1.08	150	91.60	9.70	0.67
300	91.33	9.37	0.97	180	91.57	10.11	0.59
360	90.98	10.10	1.09	240	89.26	13.11	0.78
420	90.47	12.01	0.79	300	94.24	3.17	1.75
				360	92.06	9.12	0.97
				420	83.65	22.08	0.92

60				70			
Time	C1	C2	C3	Time	C1	C2	C3
0	100.00	0.00	0.00	0	100.00	0.00	0.00
1	99.42	0.00	0.52	1	100.00	0.00	0.00
2.5	99.33	0.00	0.61	2.5	95.35	0.00	0.83
5	99.11	0.00	1.10	5	95.63	0.00	0.43
7.5	98.96	0.47	0.95	7.5	95.43	0.00	0.72
10	98.87	0.50	1.05	10	95.80	0.80	0.59
12.5	98.71	0.58	1.30	12.5	94.69	1.83	0.66
15	98.85	0.60	1.01	15	94.15	2.47	0.88
17.5	98.98	0.51	0.84	17.5	94.18	3.10	0.63
20	98.89	0.56	0.97	20	93.93	3.89	0.61
22.5	99.39	0.65	0.56	22.5	93.85	4.63	0.53
25	98.71	1.08	0.81	25	92.92	4.91	1.26
30	98.52	1.26	1.00	30	91.79	6.22	1.09
35	98.27	1.44	1.32	35	91.21	7.93	1.44
40	98.73	1.78	0.72	40	90.88	8.79	0.72
45	98.16	2.11	0.89	45	90.11	10.84	1.06
50	98.07	2.45	0.72	50	89.36	12.74	1.06
60	97.80	2.90	0.81	60	85.45	14.69	0.84
90	96.81	4.94	0.67	90	82.60	23.60	0.66
120	96.81	4.94	0.67	120	77.44	30.92	0.68
150	95.47	7.20	0.91	150	73.13	37.81	0.56
180	94.38	9.24	0.85	180	68.72	42.98	1.05
240	90.76	16.04	0.39	240	60.28	51.57	1.46
300	93.36	11.30	0.65	300	53.79	58.40	1.72
360	91.98	13.77	0.58	360	47.49	64.39	2.30
420	94.20	9.61	0.80	420	28.46695	69.02	2.51

80				90			
Time	C1	C2	C3	Time	C1	C2	C3
1	99.62	0.00	0.00	0	100.00	0.00	0.00
2.5	99.39	0.49	0.00	1	99.45	0.00	0.00
5	98.70	1.32	0.00	2.5	98.59	1.11	0.37
7.5	98.21	2.36	0.00	5	97.65	2.93	0.52
10	97.67	3.51	0.00	7.5	95.78	6.33	0.63
12.5	97.31	4.60	0.00	10	95.04	7.82	0.55
15	96.48	6.18	0.00	12.5	93.28	10.66	0.85
17.5	95.11	8.73	0.00	15	90.12	12.16	4.81
20	94.46	9.94	0.00	17.5	90.52	14.96	1.34
22.5	93.42	11.82	0.00	20	89.56	16.83	1.07
25	92.31	13.71	0.00	22.5	88.58	18.22	1.22
30	91.11	16.33	0.00	25	86.98	20.53	1.49
35	88.40	20.25	0.00	30	84.68	23.21	2.31
40	86.82	22.38	0.39	35	82.03	26.34	3.14
45	85.08	24.66	0.79	40	78.96	31.67	2.62
50	82.70	28.05	0.97	45	76.91	34.22	2.38
60	78.76	33.78	1.25	50	74.75	36.10	3.35
90	70.80	42.93	2.26	60	71.08	39.27	5.11
120	55.27	52.74	8.52	90	60.96	48.98	7.18
150	60.38	50.60	5.70	120	52.77	55.93	7.88
180	56.31	54.91	5.47	150	45.10	61.72	8.84
240	52.73	57.59	6.20	180	41.85	64.62	8.60
300	48.95	59.96	7.62	240	37.16	68.25	8.93
360	40.47	66.27	8.36	300	37.55	69.66	7.22
420	39.57	66.31	8.70	360	35.81	69.05	9.15

100			
Time	C1	C2	C3
1	99.14	0.50	0.00
2.5	98.68	0.74	0.56
5	98.06	1.48	0.88
7.5	98.00	1.87	0.53
10	96.44	2.36	2.73
12.5	97.44	2.58	0.46
15	97.04	3.04	0.57
17.5	88.75	3.20	1.34
20	97.15	3.02	0.00
22.5	96.37	3.25	0.86
25	96.64	3.50	0.36
30	95.71	3.90	1.00
35	94.25	6.37	1.38
40	95.50	3.68	1.45
45	94.36	5.07	1.89
50	93.40	7.18	1.21
60	94.36	5.15	0.98
90	92.02	7.44	2.45
120	90.86	8.45	2.85
150	87.24	13.05	3.78
180	87.78	11.57	4.27
240	85.83	13.59	4.59
300	85.42	14.05	4.64
360	85.77	13.89	4.64
420	85.77	13.89	4.64

EXPORTED DATA FOR THE GMPP CATALYST WHERE CATALYST LOAD WAS VARIED

5000				7000			
T	C1	C2	C3	T	C1	C2	C3
1	100.00	0.00	0.00	1	98.76	1.71	0.00
2.5	95.18	0.37	0.00	2.5	99.12	0.00	0.00
5	94.11	0.50	0.00	5	94.08	0.00	0.00
7.5	92.96	0.76	0.00	7.5	92.23	0.60	0.00
10	94.00	2.92	0.00	10	93.93	1.49	0.00
12.5	92.55	2.83	0.00	12.5	97.87	2.20	0.00
15	93.61	3.99	0.00	15	92.87	3.82	0.00
17.5	92.43	5.62	0.00	17.5	93.36	4.19	0.00
20	89.08	6.34	0.46	20	92.21	4.81	0.00
22.5	87.30	8.19	0.52	22.5	91.77	5.58	0.00
25	87.55	9.31	0.46	25	91.51	7.08	0.00
30	85.45	12.29	0.46	30	89.83	9.02	0.00
35	87.02	16.29	0.00	35	93.28	11.07	0.00
40	82.65	17.82	0.44	40	87.69	13.78	0.00
45	81.92	21.45	0.00	45	86.60	16.69	0.00
50	78.84	23.87	0.43	50	84.21	18.46	0.00
60	75.16	28.51	0.51	60	81.36	23.34	0.00
90	66.79	40.45	0.59	90	68.79	41.61	0.78
120	58.67	49.35	0.11	120	60.61	49.82	1.08
150	49.57	59.76	1.92	150	57.38	53.83	1.25
180	51.44	57.64	1.53	180	51.44	59.23	1.64
240	36.07	71.69	2.86	240	44.74	66.07	1.93
300	31.31	75.39	3.16	300	34.59	73.50	2.24
360	29.21	77.85	3.47	360	32.70	76.05	2.48
420	23.25	81.56	3.75	420	29.93	78.45	2.58

12000				14000			
T	C1	C2	C3	T	C1	C2	C3
1	92.03	3.23	0.00	1	99.44	0.38	0.00
2.5	91.77	3.15	0.00	2.5	96.83	0.00	0.78
5	92.13	3.38	0.00	5	96.99	0.38	0.57
7.5	93.25	3.65	0.65	7.5	97.14	0.36	0.56
10	92.89	3.92	0.00	10	97.44	1.04	0.48
12.5	93.27	4.26	0.00	12.5	97.43	1.21	0.40
15	93.27	4.26	0.00	15	96.16	1.86	0.64
17.5	93.82	2.27	0.00	17.5	97.65	2.20	0.86
20	92.68	2.78	0.00	20	94.72	2.89	3.71
22.5	92.31	3.42	0.00	22.5	93.40	3.43	4.91
25	92.86	4.10	0.00	25	96.21	3.57	1.77
30	47.39	42.84	3.57	30	95.78	4.65	1.49
35	87.04	9.57	0.90	35	95.53	5.75	0.74
40	88.77	10.80	0.58	40	94.74	7.15	0.75
45	87.91	11.51	0.77	45	93.20	7.95	0.57
50	86.63	16.71	0.00	50	92.21	8.82	0.80
60	85.72	16.80	0.58	60	91.74	10.56	0.46
90	82.95	20.66	0.00	90	88.12	15.91	0.86
120	74.19	33.70	0.40	120	85.93	19.91	0.70
150	70.31	39.46	0.53	150	83.12	24.70	0.48
180	67.22	41.79	0.55	180	80.87	28.57	0.49
240	63.12	48.12	0.94	240	76.05	34.12	1.17
300	36.88	40.32	30.16	300	67.42	45.00	1.68
360	49.43	62.90	1.54	360	70.41	40.70	1.53
420	48.99	62.11	1.47	420	66.11	45.60	1.70

Chapter 3

The calculated data tabulated and summarized in this section are the output results from the ANOVA analyses as obtained from the MS Excel ANOVA analysis tool pack

GCYC K1 ANOVA

	df	SS	MS	F	Significance F
Regression	1	31.37243308	31.37243308	83.10545682	0.000803216
Residual	4	1.510005926	0.377501482		
Total	5	32.88243901			

	Coefficients	Standard Error	t Stat	P-value	Lower 95%	Upper 95%	Lower 95.0%	Upper 95.0%
Intercept	48.00818049	4.958920396	9.681175873	0.000637033	34.24001023	61.77635075	34.24001023	61.77635075
X Variable 1	-15228.03039	1670.432627	-9.116219437	0.000803216	-19865.89488	-10590.16589	-19865.89488	-10590.16589

GCYC K2 ANOVA

	<i>df</i>	<i>SS</i>	<i>MS</i>	<i>F</i>	<i>Significance F</i>
Regression	1	4.156565668	4.156565668	24.31182979	0.038756762
Residual	2	0.341937707	0.170968854		
Total	3	4.498503375			

	<i>Coefficients</i>	<i>Standard Error</i>	<i>t Stat</i>	<i>P-value</i>	<i>Lower 95%</i>	<i>Upper 95%</i>	<i>Lower 95.0%</i>	<i>Upper 95.0%</i>
Intercept	28.17819543	5.219223125	5.398925234	0.03263697	5.721690807	50.63470006	5.721690807	50.63470006
X Variable 1	-8489.173916	1721.696544	-4.930702769	0.038756762	-15897.03625	-1081.311582	-15897.03625	-1081.311582

GCYC K3 ANOVA

	<i>df</i>	<i>SS</i>	<i>MS</i>	<i>F</i>	<i>Significance F</i>
Regression	1	79.9815349	79.9815349	46.39280385	0.002428194
Residual	4	6.896029407	1.724007352		
Total	5	86.87756431			

	<i>Coefficients</i>	<i>Standard Error</i>	<i>t Stat</i>	<i>P-value</i>	<i>Lower 95%</i>	<i>Upper 95%</i>	<i>Lower 95.0%</i>	<i>Upper 95.0%</i>
Intercept	71.87213798	10.59735208	6.782084567	0.002467376	42.44917168	101.2951043	42.44917168	101.2951043
X Variable 1	-24314.45285	3569.761412	-6.81122631	0.002428194	-34225.69945	-14403.20625	-34225.69945	-14403.20625

GCYC Kd ANOVA

	<i>df</i>	<i>SS</i>	<i>MS</i>	<i>F</i>	<i>Significance F</i>
Regression	1	7.304147829	7.304147829	9.576646517	0.05352016
Residual	3	2.288112384	0.762704128		
Total	4	9.592260213			

	<i>Coefficients</i>	<i>Standard Error</i>	<i>t Stat</i>	<i>P-value</i>	<i>Lower 95%</i>	<i>Upper 95%</i>	<i>Lower 95.0%</i>	<i>Upper 95.0%</i>
Intercept	34.64265964	9.744374309	3.555144593	0.037951208	3.631711619	65.65360766	3.631711619	65.65360766
X Variable 1	-10623.63079	3432.940214	-3.09461573	0.05352016	-21548.77868	301.5171137	-21548.77868	301.5171137

GMPP K1 ANOVA

	<i>df</i>	<i>SS</i>	<i>MS</i>	<i>F</i>	<i>Significance F</i>
Regression	1	0.563788294	0.563788294	58.84483342	0.082524666
Residual	1	0.009580931	0.009580931		
Total	2	0.573369225			

	<i>Coefficients</i>	<i>Standard Error</i>	<i>t Stat</i>	<i>P-value</i>	<i>Lower 95%</i>	<i>Upper 95%</i>	<i>Lower 95.0%</i>	<i>Upper 95.0%</i>
Intercept	20.76754227	2.443937454	8.497575189	0.074574822	-10.28562738	51.82071192	-10.28562738	51.82071192
X Variable 1	-6615.383879	862.38438	-7.671038614	0.082524666	-17573.01637	4342.248614	-17573.01637	4342.248614

GMPP K2 ANOVA

	<i>df</i>	<i>SS</i>	<i>MS</i>	<i>F</i>	<i>Significance F</i>
Regression	1	0.559826241	0.559826241	5.742384553	0.138790589
Residual	2	0.194980408	0.097490204		
Total	3	0.754806649			

	<i>Coefficients</i>	<i>Standard Error</i>	<i>t Stat</i>	<i>P-value</i>	<i>Lower 95%</i>	<i>Upper 95%</i>	<i>Lower 95.0%</i>	<i>Upper 95.0%</i>
Intercept	8.047405643	2.429032833	3.31300818	0.080288321	-2.403879105	18.49869039	-2.403879105	18.49869039
X Variable 1	-1941.185495	810.0669266	-2.396327305	0.138790589	-5426.622168	1544.251178	-5426.622168	1544.251178

GMPP K3 ANOVA

	<i>df</i>	<i>SS</i>	<i>MS</i>	<i>F</i>	<i>Significance F</i>
Regression	1	9.025796172	9.025796172	23.01982038	0.01722864
Residual	3	1.176264109	0.392088036		
Total	4	10.20206028			

	<i>Coefficients</i>	<i>Standard Error</i>	<i>t Stat</i>	<i>P-value</i>	<i>Lower 95%</i>	<i>Upper 95%</i>	<i>Lower 95.0%</i>	<i>Upper 95.0%</i>
Intercept	30.56906021	6.788437387	4.503107043	0.020452431	8.965222728	52.17289769	8.965222728	52.17289769
X Variable 1	-11147.97043	2323.511588	-4.797897496	0.01722864	-18542.4213	-3753.519562	-18542.4213	-3753.519562

GMPP Kd ANOVA

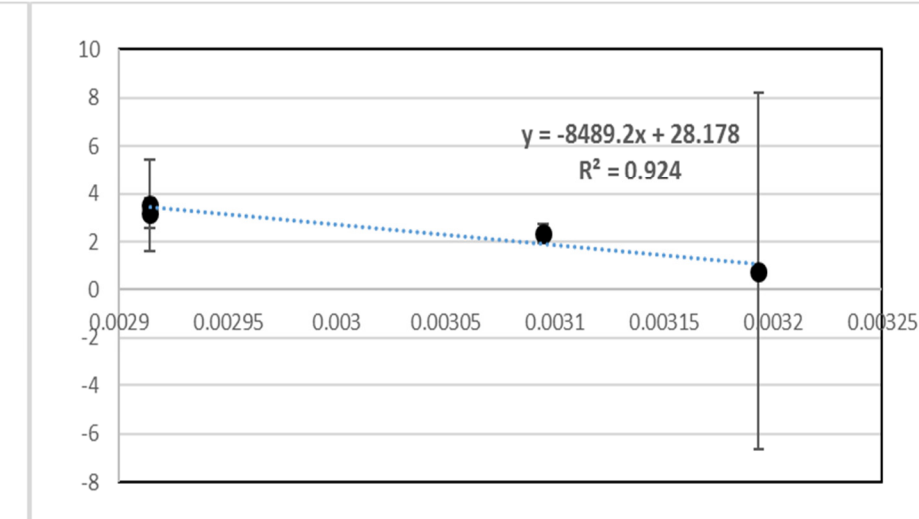
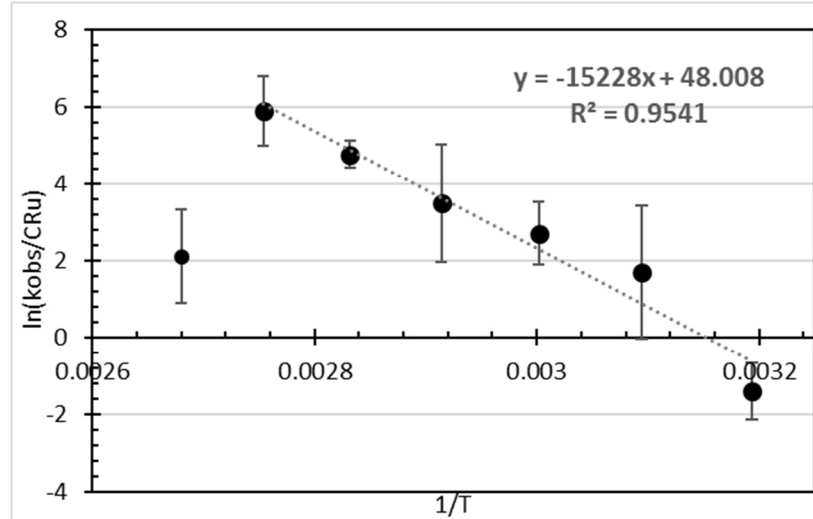
	<i>df</i>	<i>SS</i>	<i>MS</i>	<i>F</i>	<i>Significance F</i>
Regression	1	0.026402668	0.026402668	-	-
Residual	0	0	65535		
Total	1	0.026402668			

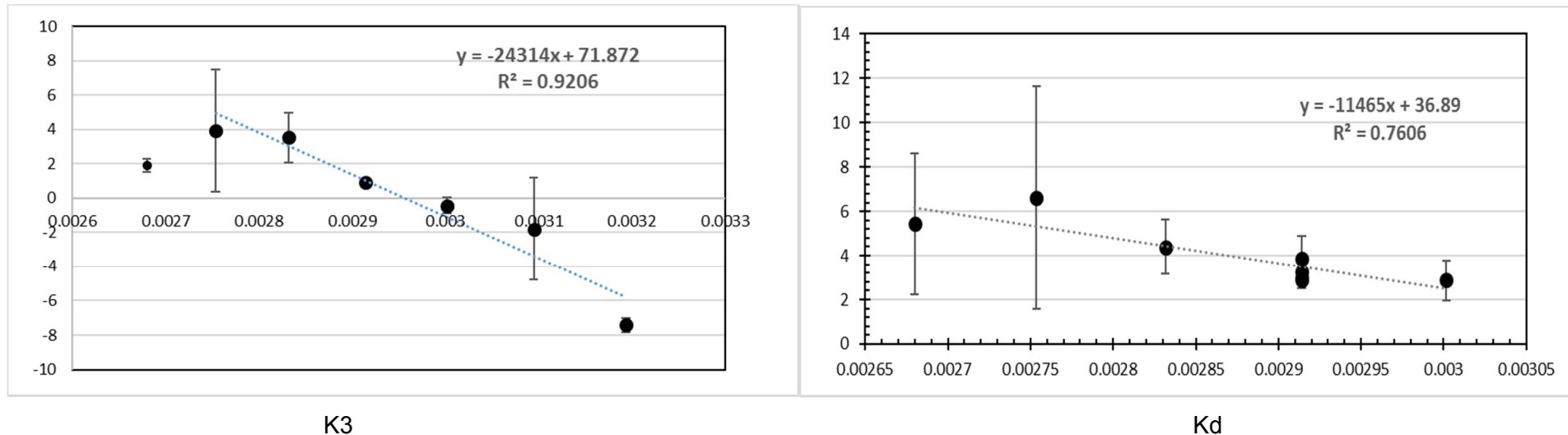
	<i>Coefficients</i>	<i>Standard Error</i>	<i>t Stat</i>	<i>P-value</i>	<i>Lower 95%</i>	<i>Upper 95%</i>	<i>Lower 95.0%</i>	<i>Upper 95.0%</i>
Intercept	10.31945033	0	65535	-	10.31945033	10.31945033	10.31945033	10.31945033
X Variable 1	-2947.027355	0	65535	-	-2947.027355	-2947.027355	-2947.027355	-2947.027355

GCYC K'S

CATALYST DEACTIVATION																
T(°C)	T(K)	K1	K1 SD	K3	K3 SD	Kd	Kd SD	c8/RU	CCAT	1/T(K)	Ln(K1/CCAT)	Ln(K1 SD/CCAT)	Ln(K3/CCAT)	Ln(K3 SD/CCAT)	Ln(Kd/CCAT)	Ln(Kd SD/CCAT)
70	343.15	0.04275	0.00299	0.00290	0.00102	0.02998	0.00184	10000	0.000637198	0.002914177	4.206158112	1.545308897	1.516977994	0.470303145	3.85134383	1.058912555
70	343.15	0.03219	0.00286	0.00411	0.00108	0.02532	0.00209	5000	0.001274396	0.002914177	3.229281488	0.808746271	1.170929787	-0.169913594	2.989009894	0.495815778
70	343.15	1.90E-02	1.31E-03	1.03E-03	4.54E-04	1.65E-02	1.16E-03	7000	0.000910283	0.002914177	3.036519994	0.363138494	0.122335564	-0.694783919	2.895633531	0.244838955
AVERAGE 70'S	343.15	3.13E-02	2.39E-03	2.68E-03	8.50E-04	2.39E-02	1.70E-03	-	0.000940626	0.002914177	3.490653198	0.905731221	0.936747782	-0.131464789	3.245329085	0.599855763
60	333.15	0.00954	0.00133	0.00041	0.00040	0.01125	0.00160	10000	0.000637198	0.003001651	2.705751603	0.733609671	-0.442504169	-0.465460409	2.870802153	0.920521873
80	353.15	0.07563	0.00357	0.02148	0.00271	0.05150	0.00222	10000	0.000637198	0.002831658	4.776513344	1.724025	3.517620617	1.447985559	4.392242183	1.249415846
90	363.15	0.231589	0.08547	0.031981	0.02214	0.476339	0.09828	10000	0.000637198	0.002753683	5.895639512	4.898883915	3.915812413	3.548164349	6.616804471	5.038506782
100	373.15	0.00526	0.00216	0.00420	0.00094	0.14593	0.01565	10000	0.000637198	0.002679887	2.110338134	1.222448471	1.886139589	0.389207015	5.433808571	3.201330547

REVERSIBLE NON-DEACTIVATING CATALYST																
T(°C)	T(K)	K1	K1 SD	K2	K2 SD	K3	K3 SD	c8/RU	CCAT	1/T(K)	Ln(K1/CCAT)	Ln(K1 SD/CCAT)	Ln(K2/CCAT)	Ln(K2 SD/CCAT)	Ln(K3/CCAT)	Ln(K3 SD/CCAT)
40	313.15	0.00016	0.02180	-0.00140	1.05195	0.00000	0.00003	10000	0.000637198	0.003193358	-1.408370812	3.532568415	0.784599659	7.409078403	-7.425264393	-2.997927259
50	323.15	0.00348	0.00033	0.00667	0.00094	0.00011	0.00008	10000	0.000637198	0.003094538	1.696468816	-0.650376281	2.348695505	0.385782615	-1.80097445	-2.049365179
70	343.15	0.00499	0.00085	0.01806	0.00369	-0.00011	0.00008	12000	0.000530998	0.002914177	2.239465204	0.464676108	3.526583575	1.938528639	-1.535615003	-1.918511725
70	343.15	0.015261	0.00080	0.011121	0.00084	-0.000034	0.00011	14000	0.000455142	0.002914177	3.512477319	0.558112104	3.195941866	0.615128548	-2.603995281	-1.405789807

GCYC DEACTIVATING & NON-DEACTIVATING K'S



K3

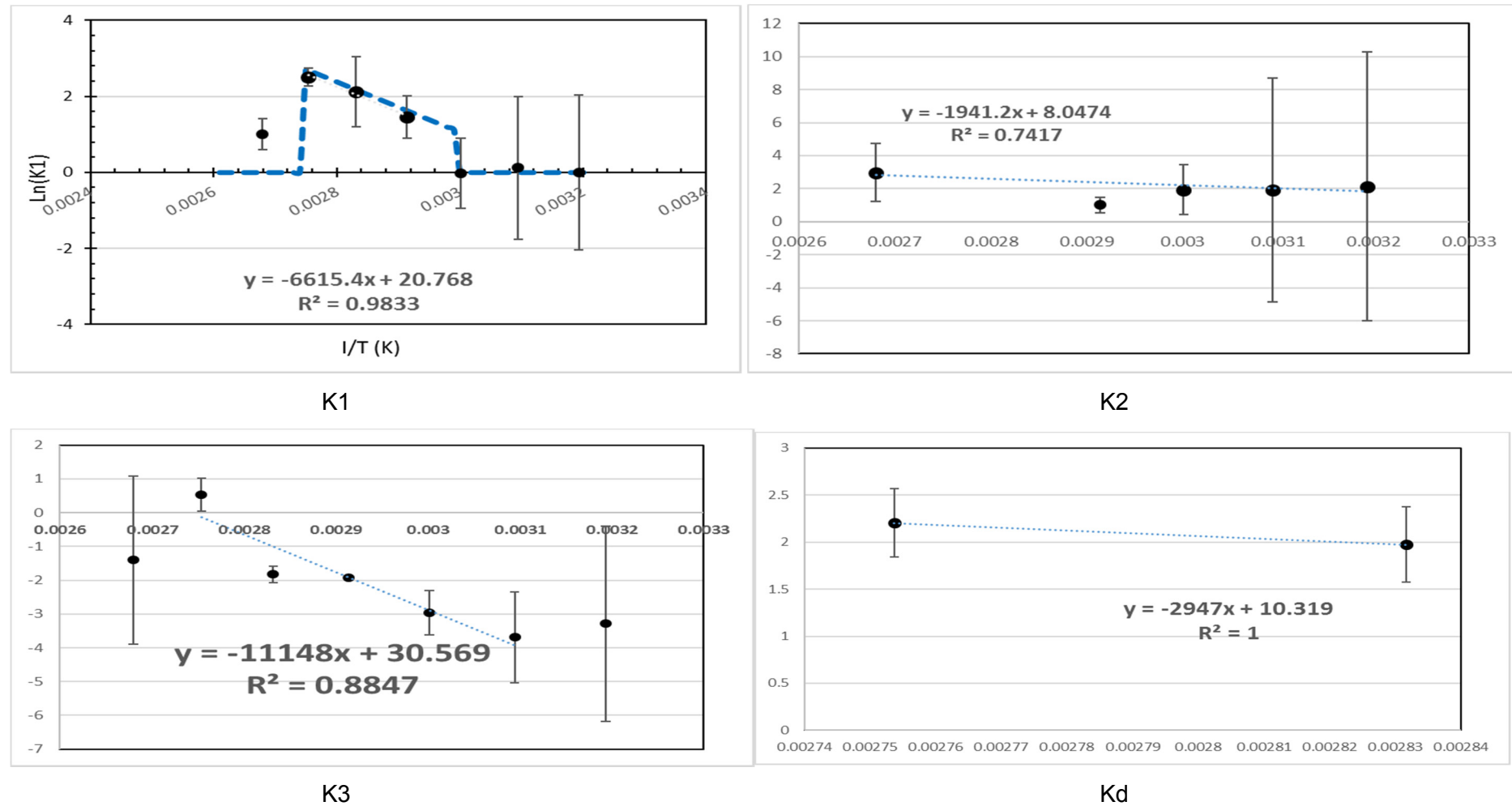
Kd

GMPP K'S

T(°C)	CATALYST DEACTIVATION															
	T(K)	K1	K1 SD	K2	K2 SD	K3	K3 SD	c8/RU	CCAT	1/T(K)	ln(K1/CCAT)	ln(K1 SD/CCAT)	ln(K3/CCAT)	ln(K3 SD/CCAT)	ln(Kd/CCAT)	ln(KD SD/CCAT)
80	353.15	0.00528	0.00081	-0.00010	0.00026	0.00459	0.00095	10000	0.000637	0.002832	2.114947842	0.234953554	-1.82539549	-0.878971576	1.974476937	0.402726927
90	363.15	0.007839	0.00079	0.001080	0.00029	0.005775	0.00092	10000	0.000637	0.002754	2.509785507	0.219584304	0.527380895	-0.773684644	2.204271055	0.366027515

T(°C)	REVERSIBLE NON-DEACTIVATING CATALYST															
	T(K)	K1	K1 SD	K2	K2 SD	K3	K3 SD	c8/RU	CCAT	1/T(K)	ln(K1/CCAT)	ln(K1 SD/CCAT)	ln(K2/CCAT)	ln(K2 SD/CCAT)	ln(K3/CCAT)	ln(K3 SD/CCAT)
70	343.15	0.00272	0.00037	0.00038	0.00063	-0.00012	0.00012	10000	0.000637	0.002914	1.450316066	-0.554047798	-0.505303389	-0.008015672	-1.680801066	-1.655831978
70	343.15	0.00530	0.00048	0.00093	0.00033	-0.00004	0.00015	5000	0.001274	0.002914	1.424295778	-0.977343495	-0.310012751	-1.339736857	-3.385334625	-2.146270325
70	343.15	4.26E-03	6.40E-04	5.85E-04	4.71E-04	-1.06E-04	1.62E-04	7000	0.00091	0.002914	1.542817509	-0.352395054	-0.442445442	-0.659633805	-2.154953304	-1.727185368
70	343.15	0.00228	0.00048	0.00017	0.00068	-0.00024	0.00012	12000	0.000531	0.002914	1.456721919	-0.093672643	-1.137254242	0.245965999	-0.803360078	-1.49322693
70	343.15	0.001725	0.00027	0.001241	0.00074	-0.000095	0.00008	14000	0.000455	0.002914	1.332341652	-0.522397347	1.00303634	0.487239944	1.565909598	1.77288235
AVERAGE 70'S	343.15	3.25E-03	4.48E-04	6.63E-04	5.71E-04	-1.20E-04	1.26E-04									
40	313.15	0.00063	0.00489	0.00537	2.19920	0.00002	0.00004	10000	0.000637	0.003193	-0.009358836	2.037443845	2.132258085	8.146521842	-3.288610809	-2.893153939
50	323.15	0.00072	0.00414	0.00430	0.55556	0.00002	0.00007	10000	0.000637	0.003095	0.116830797	1.870164042	1.908276334	6.770644587	-3.690593461	-2.21924414
60	333.15	0.00062	0.00025	0.00443	0.00290	-0.00003	0.00004	10000	0.000637	0.003002	-0.020830232	-0.924956453	1.938011418	1.514945497	-2.96053488	-2.84869598
100	373.15	0.00174	0.00042	0.01250	0.00366	0.00016	0.00005	10000	0.000637	0.00268	1.003296939	-0.415133059	2.976184472	1.749404782	-1.403616545	-2.491329977

GMPP DEACTIVATING & NON-DEACTIVATING K'S



Chapter 4

Catalyst cost was estimated based on Sigma Aldrich prices and the ZAR/USD exchange rate at the time of cost estimation which is specified as 13.89 ZAR/USD

Each of the synthesis steps was calculated based on yields that Jordaan reported and the method used. Only raw materials were used, and the amount of each material used per gram of product was calculated.

Step 1 Ligand cost:

$$\text{ligand cost} = \frac{\text{Raw materials cost}}{\text{Amount of ligand prepared}}$$

$$\text{Raw materials cost} = \text{Amount of material used} * \text{price per unit}$$

Step 2 Synthesis of Lithium Salt

Similarly, the price of the lithium salt was estimated by adding the raw materials cost per unit material used to the calculated ligand cost

$$\text{Salt cost} = \frac{\text{Raw materials for Salt preparation}}{\text{Amount of salt prepared}} + \text{Ligand cost}$$

Step 3 Complex Synthesis

The complex cost was finally calculated by adding the cost of **G2** catalyst per gram to the cost of the synthesised salt

$$\text{complex cost} = \text{G2 cost per unit} + \text{Salt cost}$$

The calculation steps for both the **GMPP** and the **GCYC** catalysts are summarized in the tables provided. Assumed yields, raw materials and costs are included in the tables.

RAW MATERIAL COSTS SENSITIVITY ANALYSIS

Since the prices of the raw materials in this study was based on non-wholesale values (i.e. prices not based on bulk unit size) a brief sensitivity analysis was conducted to determine whether a change in these values would result in a change of the overall outcome of the catalyst comparison. Catalyst, membrane and 7-tetradecene costs were incrementally varied and the resulting EP₃ values, and IRR percentages were recorded. The results are summarised in the following figures as follows:

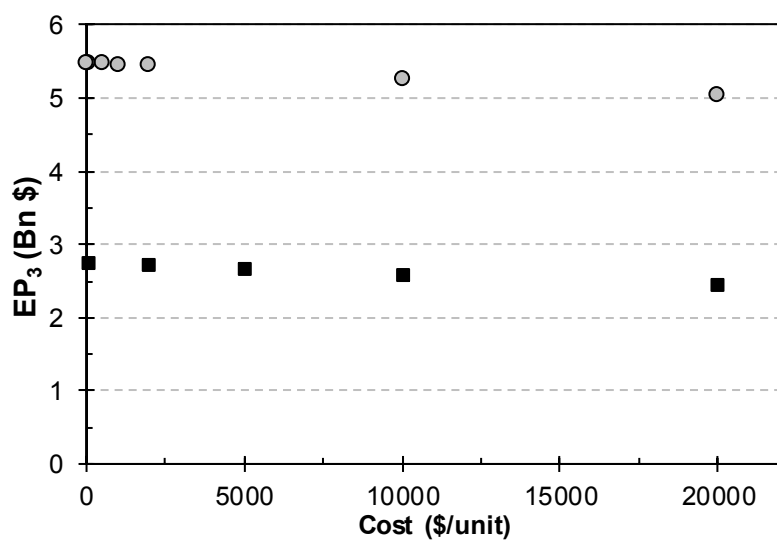


Figure D-1: Effect of catalyst cost ● (\$/kg) and membrane cost ■ (\$/m²) on Economic Potential (level 3)

Figure D-1 displays the effects of catalyst and membrane costs on the EP₃ values. A slight decrease is observed as the costs increase per unit, however, despite the costs per unit increasing at least 3 times in order of magnitude the EP values remain within the same order of magnitude, albeit at a slightly lower value. What can be concluded is that even with a large-scale variation in costs the EP remains profitable and only varies within the order of 1 billion USD. The effects of the 7-tetradecene costs on the IRR and the EP₃-values are consequently summarised as follows:

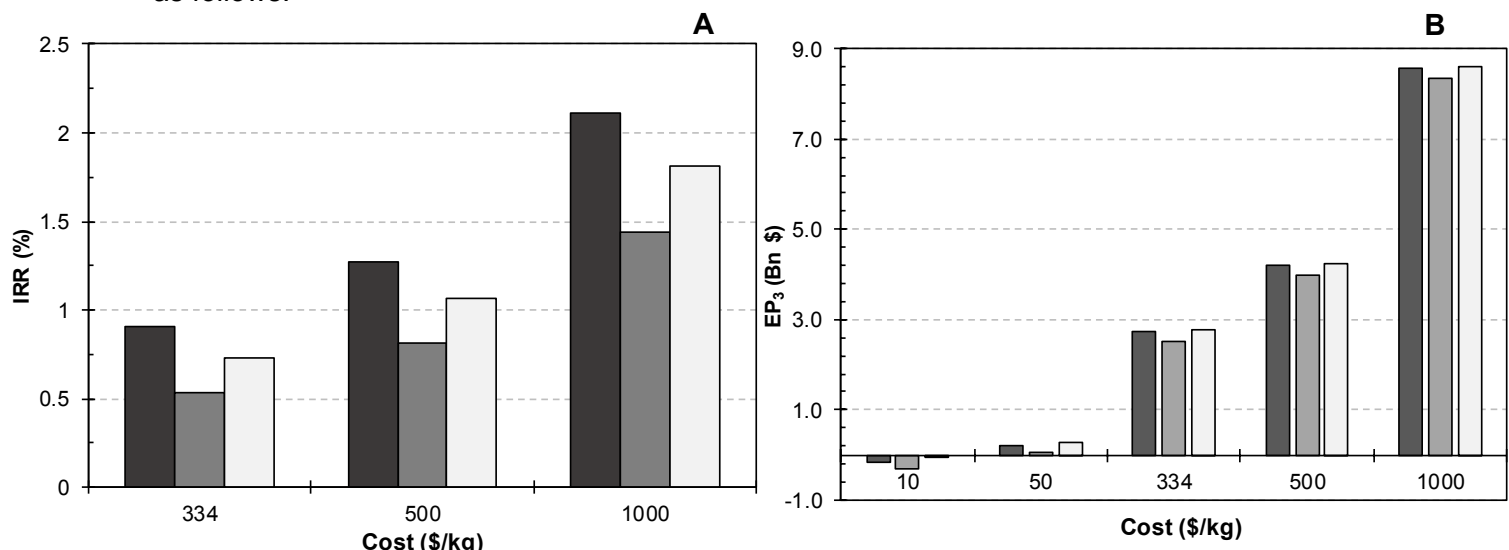


Figure D-2: Effect of 7-tetradecene prices (\$/kg) on (A) IRR and (B) Economic Potential (level 3) for HG2 ■, GMPP □ and GCYC □

Figure D2 indicates the effects the price of 7-tetradecene would have on the overall outcome of the comparison study between the catalysts. As is evident in Figure A the HG2 catalyst and GCYC catalysts still perform the best compared to the GMPP catalyst as the costs increase, but the scale with which the catalysts differ from each other remains the same despite the increase in IRR. The same conclusion applies to the EP₃ comparison in Figure B.

An increase in the price in the 7-tetradecene does not affect the overall comparison results between the catalysts only the scale at which those estimated comparisons are made. What is also clear is that lower range prices would render the project unfeasible. This is an expected result- and with the specialised nature of the product prices that low is unlikely to occur. It is also important to note that the product is only an intermediate for the beneficiation of short chain linear alkenes. Furthermore, the likelihood of a pure 7-tetradecene product stream is low, since the PMP and SMP liquid products would most probably be sent to the hydroformylation section as a mixture.

GCYC

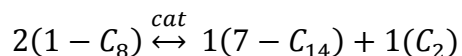
Step 1										Step 2						Step 3									
Preparation of pyridinyl ligand (OH)						Synthesis of lithium salt						Synthesis of complex from Gr 2													
Raw Material	CAS #	Specs	Amount	Price Sigma	% Yield	Raw Material	CAS #	Specs	Amount	Price Sigma	% Yield	Raw Material	CAS #	Specs	Amount	Price Sigma	% Yield	Raw Material	CAS #	Specs	Amount	Price Sigma	% Yield		
2-bromopyridine	109-04-6	in 25 mL diethyl ether	9.05mL	8.32	ZAR/g	density	1.657 g/mL	Butyllithium 109-72-8 10M sln in hexane	0.15 mL	9.5875 ZAR/mL	90	Grubbs 2nd Generation	246047-72-3		527mg	257.15 ZAR/g		Synthesized salt	-		120mg	21.12 ZAR/g		84	
Butyllithium	109-72-8	2.5M in Hexane	40mL	1.6325	ZAR/mL	assume 95%		ligand		0.28	13.87 ZAR/g														
Cyclohexanone	108-94-1	Neat	105mmol	0.69	ZAR/mL	Molar weight	98.14 g/mol					Price Step 2							Grubbs 2nd Generation			0.527 g	135.51805 ZAR		
		Conversion				Price for step 1		0.09814 g/mmol	Butyllithium		3.8836 ZAR								Synthesized salt			0.12 g	2.53 ZAR		
2-bromopyridine	14.9959	g		124.77	ZAR	Density	0.948 g/ml	ligand										Total Raw Materials cost	5.321725 ZAR						
Butyllithium				65.3	ZAR													Total Raw Materials cost	138.05245 ZAR						
Cyclohexanone	10.87 mL			7.50	ZAR													Price per g of salt	21.12 ZAR/g						
																		Amount of Salt prepared	0.252 g salt						
Total Raw Materials cost			197.57	ZAR														Amount of complex prepared	0.44268 g Cmplx						
						Price per g of Ligand		13.8681 ZAR/g										Price per g of Complex	311.86 ZAR/g						
Amount of ligand prepared			14.2460575	g Ligand																					

GMPP

Step 1										Step 2						Step 3										
Preparation of pyridinyl ligand (OH)						Synthesis of lithium salt						Synthesis of complex from Gr 2														
Raw Material	CAS #	Specs	Amount	Price Sigma	% Yield	Raw Material	CAS #	Specs	Amount	Price Sigma	% Yield	Raw Material	CAS #	Specs	Amount	Price Sigma	% Yield	Raw Material	CAS #	Specs	Amount	Price Sigma	% Yield			
2-bromopyridine	109-04-6	in 25 mL diethyl ether	9.05mL	8.32	ZAR/g	assume 95%		density	1.657 g/mL	Butyllithium 109-72-8 10M sln in hexane	0.15 mL	9.5875 ZAR/mL	95	Grubbs 2nd Generation	246047-72-3		164mg	257.15 ZAR/g		Synthesized salt	-		58mg	21.12 ZAR/g		91
Butyllithium	109-72-8	2.5M in Hexane	40mL	1.6325	ZAR/mL			ligand		0.4115	72.88 ZAR/g															
2-methyl benzophenone	131-58-8	Neat	105mmol	45.68	ZAR/g	Molar weight	196.24 g/mol					Price Step 2							Grubbs 2nd Generation			0.164 g	42.1726 ZAR			
		Conversion				Price for step 1		0.19624 g/mmol	Butyllithium		29.98823 ZAR							Synthesized salt			0.058 g	1.22 ZAR				
2-bromopyridine	14.9959	g		124.77	ZAR			Density	1.1098 g/ml	ligand							Total Raw Materials cost	31.426355 ZAR								
Butyllithium				65.3	ZAR												Total Raw Materials cost	43.39756 ZAR								
2-methyl benzophenone	18.57 mL			848.12	ZAR												Price per g of salt	80.39 ZAR/g								
																	Amount of Salt prepared	0.390925 g salt								
Total Raw Materials cost			1038.19	ZAR													Amount of complex prepared	0.14924 g Cmplx								
						Price per g of Ligand		72.87541 ZAR/g									Price per g of Complex	290.79 ZAR/g								
Amount of ligand prepared			14.2460575	g Ligand																						

CALCULATION OF EP1

The stoichiometry of the reaction for the calculation of EP 1 is defined as follows:



Calculations for EP 1

$$C_8 \text{ feedrate} = 1200.8 \text{ tpa} = 10.7 \text{ kmol/hr}$$

|

$$C_{14} \text{ Production rate} = \frac{C_8 \text{ Feedrate}}{2}$$

$$\text{Catalyst feedrate} = \frac{C_8}{R_u} * \dot{N}_{C_8} * MW_{Ru} * \frac{MW_{complex}}{MW_{Ru}}$$

$$EP_1 = (C_{14} \text{ Production rate} * C_{14} \text{ Price}) - ((C_8 \text{ feedrate} * C_8 \text{ cost}) + (\text{Complex Cost} * \text{Catalyst feedrate}))$$

SAMPLE TABLE OF HEAT CAPACITY ESTIMATION RESULTS WITH JOBACK METHOD

T	343.15	Delta T	45				
tref	298.15						
Hi @ Tdesign (J/kmol)							
1-C8	2-C8	C12	C13	C14	C2H4	C3H6	C4H8
8021879	12151134.68	10576741.64	19371921.9	8021878.719	1947.809	3030061	3178621

Similar results are available for each specified temperature condition upon request

CALCULATED EQUIPMENT COST

The calculated data in chapter 4 is summarised and tabulated in this section. It includes equipment cost estimations and economic potential values as a function of conversion and time

The data is listed according to varying temperature, catalyst load and catalyst structure.

ECONOMIC POTENTIAL AND EQUIPMENT COST FOR THE **GCYC** CATALYST AT VARIED TEMPERATURES

40°C

Reactor Cost (\$\$) & EP					
V (m3)	Conversion	D (m)	H (m)	Cost (\$) H/D based	EP
#DIV/0!	1.0000	#DIV/0!	#DIV/0!	#DIV/0!	#DIV/0!
2.1	0.0304	5.867660799	5.867660799	73 702.38	\$2 761 846 524.7
9.9	0.0331	27.0841398	27.0841398	1 319 037.46	\$2 761 707 517.5
19.0	0.0371	51.8347212	51.8347212	4 486 744.27	\$2 761 573 433.0
27.8	0.0314	75.84314875	75.84314875	9 197 690.59	\$2 761 455 611.7
36.1	0.0435	98.45750811	98.45750811	15 046 097.16	\$2 761 351 408.7
42.4	0.0409	115.7109543	115.7109543	20 402 378.99	\$2 761 275 148.2
56.1	0.0333	153.2107624	153.2107624	34 642 730.91	\$2 761 116 693.3
66.7	0.0373	182.201277	182.201277	48 034 859.16	\$2 760 999 546.0
555.1	0.0011	1516.05299	1516.05299	2 612 064 358.80	\$2 756 975 703.5
688.7	0.0106	1881.053205	1881.053205	3 923 530 077.37	\$2 756 047 305.0
216.6	0.0071	591.6133517	591.6133517	442 812 788.81	\$2 759 582 812.3
241.3	0.0140	659.0561929	659.0561929	542 805 552.87	\$2 759 373 391.6
222.3	0.0122	607.1899449	607.1899449	465 057 540.91	\$2 759 534 038.4
254.3	0.0140	694.4312232	694.4312232	599 058 584.03	\$2 759 265 278.2
256.2	0.0229	699.8363915	699.8363915	607 882 989.54	\$2 759 248 857.1
266.9	0.0167	728.9613924	728.9613924	656 473 635.31	\$2 759 160 804.8
393.3	0.0099	1074.139357	1074.139357	1 363 756 701.05	\$2 758 163 230.2
617.1	0.0143	1685.265084	1685.265084	3 188 987 513.60	\$2 756 540 315.9
679.2	0.0171	1854.897981	1854.897981	3 821 273 512.41	\$2 756 112 549.1
744.0	0.0224	2031.847947	2031.847947	4 537 737 421.50	\$2 755 674 592.5
772.1	0.0289	2108.608247	2108.608247	4 866 456 199.11	\$2 755 487 008.9
913.6	0.0364	2495.064947	2495.064947	6 684 253 748.73	\$2 754 562 173.5
1018.2	0.0506	2780.957743	2780.957743	8 201 762 119.67	\$2 753 896 510.1
1103.9	0.0630	3014.776559	3014.776559	9 550 623 499.46	\$2 753 362 256.0
1189.9	0.0882	3249.644842	3249.644842	11 002 187 840.32	\$2 752 833 890.6

Flash-drum								
Total volume flow (m ³ /hr)	Drum-volume	D (m)	H (m)	tw (m)	shell mass (kg)	cost (\$)	EP	
#DIV/0!	#DIV/0!	#DIV/0!	#DIV/0!	#DIV/0!	#DIV/0!	#DIV/0!	#DIV/0!	
128.90593	10.74173	1.89810	3.79619	0.00160	289.95787	8990.86505	205244.22112	
238.00327	19.83281	2.32856	4.65713	0.00196	535.35879	17980.22773	2761689537.25480	
227.75014	18.97842	2.29463	4.58927	0.00194	512.29564	17218.76623	2761556214.25364	
222.15852	18.51247	2.27570	4.55140	0.00192	499.71799	16797.72172	2761438813.95759	
216.30010	18.02429	2.25552	4.51103	0.00190	486.54021	16352.01375	2761335056.63736	
203.36319	16.94625	2.20962	4.41924	0.00186	457.44023	15350.30167	2761259797.87232	
224.39124	18.69852	2.28330	4.56659	0.00193	504.74022	16966.34647	2761099726.93690	
228.72901	19.05999	2.29792	4.59583	0.00194	514.49749	17292.04746	2760982253.99154	
1665.29918	138.76938	4.45374	8.90747	0.00376	3745.88364	82612.99163	2756893090.46218	
1836.65018	153.04806	4.60153	9.20307	0.00388	4131.31641	88292.28071	2755959012.74692	
519.88327	43.32187	3.02131	6.04263	0.00255	1169.41283	35445.17257	2759547367.17476	
482.62418	40.21707	2.94734	5.89468	0.00249	1085.60313	33408.65851	2759339982.94869	
381.12234	31.75892	2.72426	5.44852	0.00230	857.28737	27513.22025	2759506525.21321	
381.39688	31.78180	2.72491	5.44983	0.00230	857.90489	27529.95919	2759237748.22266	
341.65823	28.47038	2.62678	5.25357	0.00222	768.51775	25054.24107	2759223802.84858	
320.28928	26.68971	2.57084	5.14168	0.00217	720.45095	23675.34920	2759137129.42237	
393.29395	32.77318	2.75296	5.50592	0.00232	884.66588	28250.78847	2758134979.39866	
411.37093	34.27954	2.79451	5.58901	0.00236	925.32780	29329.57253	2756510986.34152	
339.58357	28.29750	2.62146	5.24291	0.00221	763.85105	24921.90982	2756087627.15601	
297.58280	24.79757	2.50859	5.01718	0.00212	669.37555	22169.16069	2755652423.31656	
257.35421	21.44533	2.39004	4.78007	0.00202	578.88633	19382.49464	2755467626.42067	
228.39074	19.03180	2.29678	4.59357	0.00194	513.73660	17266.73799	2754544906.81163	
203.64841	16.97002	2.21065	4.42131	0.00186	458.08179	15372.65630	2753881137.42955	
183.97572	15.33070	2.13705	4.27409	0.00180	413.83053	13799.98475	2753348456.03661	
169.97870	14.16432	2.08141	4.16283	0.00176	382.34596	12639.72723	2752821250.86733	

Membrane Cost							
C8 + 2-C8 (kg/hr)	C12-C14 (kg/hr)	wt frac C8	flux	Area	Membrane cost	EP-cost	
#DIV/0!	#DIV/0!	#DIV/0!	#DIV/0!	#DIV/0!	#DIV/0!	#DIV/0!	#DIV/0!
112.2	1050.65	0.096502977	0.925597	2093.901	41 249 849.97	-\$41 044 605.74	
78116.8	1050.65	0.98672882	7.784677	16949.42	333 903 618.81	\$2 427 785 918.44	
70785.8	1050.65	0.985374482	7.76289	15423.05	303 834 138.18	\$2 457 722 076.07	
66787.8	1050.65	0.984512539	7.749042	14590.72	287 437 228.34	\$2 474 001 585.62	
62599.1	1050.65	0.983493313	7.732685	13718.76	270 259 532.54	\$2 491 075 524.09	
53349.2	1050.65	0.980686593	7.687743	11793.62	232 334 381.68	\$2 528 925 416.19	
68384.2	1050.65	0.984868615	7.754761	14923.06	293 984 321.88	\$2 467 115 405.06	
71485.7	1050.65	0.985515602	7.765158	15568.77	306 704 731.72	\$2 454 277 522.27	
1098633.4	1050.65	0.999044593	7.984388	229548.8	4 522 111 666.68	-\$1 765 218 576.22	
1221149.4	1050.65	0.999140365	7.985952	255072.9	5 024 936 345.04	-\$2 268 977 332.30	
279661.0	1050.65	0.996257207	7.938937	58931.41	1 160 948 776.73	\$1 598 598 590.45	
253020.8	1050.65	0.995864762	7.93255	53381.62	1 051 617 869.61	\$1 707 722 113.34	
180447.0	1050.65	0.994211242	7.90567	38263.17	753 784 495.79	\$2 005 722 029.42	
180643.2	1050.65	0.994217496	7.905771	38304.06	754 590 024.55	\$2 004 647 723.68	
151847.9	1346.07	0.991213273	7.857065	32496.01	640 171 490.31	\$2 119 052 312.54	
136951.3	1050.65	0.992386734	7.87607	29202.8	575 295 130.46	\$2 183 841 998.96	
189149.7	1050.65	0.994476109	7.909972	40076.06	789 498 341.24	\$1 968 636 638.15	
202074.7	1050.65	0.994827599	7.915684	42768.54	842 540 261.57	\$1 913 970 724.77	
150746.7	1050.65	0.993078631	7.887287	32076.38	631 904 698.26	\$2 124 182 928.90	
120716.2	1050.65	0.99137166	7.859629	25821.16	508 676 827.44	\$2 246 975 595.88	
91952.7	1050.65	0.988703146	7.8165	19830.57	390 662 231.14	\$2 364 805 395.28	
71243.9	1050.65	0.985467144	7.764379	15518.41	305 712 740.91	\$2 448 832 165.90	
53553.1	1050.65	0.980758723	7.688896	11836.06	233 170 367.89	\$2 520 710 769.54	
39487.1	1050.65	0.974082301	7.58258	8910.285	175 532 611.49	\$2 577 815 844.55	
29479.3	1050.65	0.965586333	7.448504	6831.326	134 577 114.91	\$2 618 244 135.95	

50°C

Reactor Cost (\$\$) & EP						
V (m3)	Conversion	D (m)	H (m)	Cost (\$)	H/D based	EP
#DIV/0!	1.0000	#DIV/0!	#DIV/0!	#DIV/0!	#DIV/0!	#DIV/0!
#DIV/0!	0.0046	#DIV/0!	#DIV/0!	#DIV/0!	#DIV/0!	#DIV/0!
#DIV/0!	0.0077	#DIV/0!	#DIV/0!	#DIV/0!	#DIV/0!	#DIV/0!
#DIV/0!	0.0146	#DIV/0!	#DIV/0!	#DIV/0!	#DIV/0!	#DIV/0!
#DIV/0!	0.0111	#DIV/0!	#DIV/0!	#DIV/0!	#DIV/0!	#DIV/0!
#DIV/0!	0.0086	#DIV/0!	#DIV/0!	#DIV/0!	#DIV/0!	#DIV/0!
120.47	0.0215	329.0328711	329.0328711	146 443 414.19	\$2 760 452 490.6	
71.87	0.0402	196.2871831	196.2871831	55 277 800.43	\$2 760 943 999.1	
66.56	0.0445	181.775357	181.775357	47 823 303.40	\$2 761 001 238.7	
68.59	0.0580	187.3326319	187.3326319	50 618 059.05	\$2 760 979 214.7	
72.43	0.1250	197.8206464	197.8206464	56 095 086.11	\$2 760 938 001.0	
71.67	0.0929	195.7328515	195.7328515	54 983 746.90	\$2 760 946 169.7	
80.59	0.1368	220.0912457	220.0912457	68 597 039.25	\$2 760 851 896.5	
90.62	0.1163	247.483661	247.483661	85 582 567.06	\$2 760 748 339.0	
102.66	0.1268	280.3691536	280.3691536	108 286 861.03	\$2 760 626 991.4	
112.89	0.1450	308.3302118	308.3302118	129 551 032.70	\$2 760 526 048.5	
126.11	0.1515	344.4365257	344.4365257	159 641 022.62	\$2 760 398 361.5	
149.50	0.1719	408.3011795	408.3011795	220 021 958.77	\$2 760 178 818.8	
218.76	0.2126	597.4687246	597.4687246	451 114 693.27	\$2 759 564 448.0	
288.88	0.2557	788.9823683	788.9823683	762 123 711.83	\$2 758 981 521.0	
357.88	0.2866	977.413655	977.413655	1 141 417 209.52	\$2 758 435 265.8	
425.90	0.3042	1163.187321	1163.187321	1 584 790 313.90	\$2 757 917 098.6	
562.80	0.3276	1537.085818	1537.085818	2 680 829 511.49	\$2 756 921 076.0	
704.59	0.3640	1924.32042	1924.32042	4 095 469 581.56	\$2 755 939 771.6	
835.20	0.3832	2281.035668	2281.035668	5 644 086 302.28	\$2 755 070 514.6	
970.89	0.4012	2651.646371	2651.646371	7 497 336 117.45	\$2 754 195 810.1	

Flash-drum							
Total volume flow (m3/hr)	Drum-volume	D (m)	H (m)	tw (m)	shell mass (kg)	cost (\$)	EP
#DIV/0!	#DIV/0!	#DIV/0!	#DIV/0!	#DIV/0!	#DIV/0!	#DIV/0!	#DIV/0!
#DIV/0!	#DIV/0!	#DIV/0!	#DIV/0!	#DIV/0!	#DIV/0!	#DIV/0!	#DIV/0!
#DIV/0!	#DIV/0!	#DIV/0!	#DIV/0!	#DIV/0!	#DIV/0!	#DIV/0!	#DIV/0!
#DIV/0!	#DIV/0!	#DIV/0!	#DIV/0!	#DIV/0!	#DIV/0!	#DIV/0!	#DIV/0!
#DIV/0!	#DIV/0!	#DIV/0!	#DIV/0!	#DIV/0!	#DIV/0!	#DIV/0!	#DIV/0!
#DIV/0!	#DIV/0!	#DIV/0!	#DIV/0!	#DIV/0!	#DIV/0!	#DIV/0!	#DIV/0!
578.2786486	48.18795978	3.13	6.26	0.002640687	1300.765982	38523.11739	\$2 760 413 967.53
287.480616	23.95575973	2.48	4.96	0.002091899	646.6519329	21484.33439	\$2 760 922 514.77
228.1943256	19.01543315	2.30	4.59	0.001936895	513.2947876	17252.03504	\$2 760 983 986.69
205.7743898	17.1471799	2.22	4.44	0.001871263	462.8639271	15538.89269	\$2 760 963 675.79
193.1510093	16.0952736	2.17	4.34	0.001832188	434.4692009	14541.43665	\$2 760 923 459.58
172.0012479	14.33286398	2.09	4.18	0.001762713	386.8954399	12809.68269	\$2 760 933 359.97
161.1719265	13.43045663	2.04	4.09	0.001724915	362.5362267	11890.05881	\$2 760 840 006.41
155.3410981	12.9445737	2.02	4.04	0.001703858	349.4205026	11384.67474	\$2 760 736 954.29
153.9848954	12.83156134	2.01	4.03	0.001698885	346.3698933	11266.04517	\$2 760 615 725.35
150.5259756	12.54332955	2.00	4.00	0.001686068	338.5894828	10961.5792	\$2 760 515 086.89
151.3376824	12.61096908	2.00	4.00	0.001689093	340.4153164	11033.27757	\$2 760 387 328.24
149.4986488	12.4577224	1.99	3.99	0.001682223	336.2786387	10870.6129	\$2 760 167 948.22
145.8413079	12.15295618	1.98	3.96	0.001668392	328.0519046	10544.71846	\$2 759 553 903.33
144.442147	12.03636411	1.97	3.94	0.001663039	324.9046661	10419.18086	\$2 758 971 101.86
143.151211	11.92879041	1.97	3.93	0.00165807	322.0008659	10302.92144	\$2 758 424 962.88
141.9662262	11.83004563	1.96	3.92	0.001653482	319.3353898	10195.8341	\$2 757 906 902.72
140.7002137	11.72454881	1.95	3.91	0.001648552	316.487652	10081.02844	\$2 756 910 994.97
140.9172038	11.74263059	1.96	3.91	0.001649399	316.9757443	10100.73498	\$2 755 929 670.86
139.1994306	11.59948855	1.95	3.89	0.00164267	313.1118268	9944.396476	\$2 755 060 570.21
138.6992773	11.55781078	1.94	3.89	0.0016407	311.9867941	9898.731541	\$2 754 185 911.37

Membrane Cost						
C8 + 2-C8 (kg/hr)	C12-C14 (kg/hr)	wt frac C8	flux	Area	Membrane cost	EP-cost
#DIV/0!	#DIV/0!	#DIV/0!	#DIV/0!	#DIV/0!	#DIV/0!	#DIV/0!
#DIV/0!	#DIV/0!	#DIV/0!	#DIV/0!	#DIV/0!	#DIV/0!	#DIV/0!
#DIV/0!	#DIV/0!	#DIV/0!	#DIV/0!	#DIV/0!	#DIV/0!	#DIV/0!
#DIV/0!	#DIV/0!	#DIV/0!	#DIV/0!	#DIV/0!	#DIV/0!	#DIV/0!
#DIV/0!	#DIV/0!	#DIV/0!	#DIV/0!	#DIV/0!	#DIV/0!	#DIV/0!
#DIV/0!	#DIV/0!	#DIV/0!	#DIV/0!	#DIV/0!	#DIV/0!	#DIV/0!
#DIV/0!	1768.05	#DIV/0!	#DIV/0!	#DIV/0!	#DIV/0!	#DIV/0!
321039.1	1340.22	0.995842739	7.932192	67736.49	1 334 408 864.92	\$1 426 005 102.61
113257.4	1232.82	0.989232137	7.825039	24385.45	480 393 369.81	\$2 280 529 144.96
70958.3	1162.85	0.983876467	7.738832	15532.3	305 986 304.87	\$2 454 997 681.82
54924.9	1165.23	0.979225727	7.66441	12197.1	240 282 911.67	\$2 520 680 764.12
44465.8	2273.20	0.951363814	7.227105	10778.63	212 338 970.53	\$2 548 584 489.05
30839.2	1117.23	0.965038883	7.439912	7158.79	141 028 166.56	\$2 619 905 193.41
23081.0	1129.04	0.953364644	7.258021	5559.373	109 519 653.43	\$2 651 320 352.98
18952.6	1097.62	0.945256314	7.133201	4684.716	92 288 911.06	\$2 668 448 043.23
18005.1	1080.47	0.943388228	7.10462	4477.267	88 202 165.10	\$2 672 413 560.25
15514.2	1094.17	0.934119722	6.963786	3974.949	78 306 499.59	\$2 682 208 587.30
13818.1	1099.95	0.926267139	6.845734	3631.952	71 549 461.17	\$2 688 837 867.06
12622.0	1109.69	0.919187998	6.740307	3395.422	66 889 809.70	\$2 693 278 138.53
10195.9	1094.09	0.903092547	6.504121	2893.039	56 992 866.79	\$2 702 561 036.53
7718.9	1108.99	0.874376751	6.094877	2414.03	47 556 396.08	\$2 711 414 705.78
6164.4	1112.27	0.847145068	5.72115	2119.809	41 760 244.66	\$2 716 664 718.23
5323.3	1113.92	0.826957641	5.453126	1967.454	38 758 852.54	\$2 719 148 050.18
4782.4	1105.00	0.812309672	5.26346	1864.225	36 725 231.62	\$2 720 185 763.35
4150.7	1111.29	0.788808409	4.967613	1765.438	34 779 135.66	\$2 721 150 535.20
3561.4	1107.45	0.762800489	4.652354	1672.57	32 949 635.68	\$2 722 110 934.53
3235.7	1102.15	0.745922293	4.454588	1622.986	31 972 832.53	\$2 722 213 078.84

60°C

Reactor Cost (\$\$) & EP						
V (m3)	Conversion	D (m)	H (m)	Cost (\$) H/D based	EP	
#DIV/0!	1.0000	#DIV/0!	#DIV/0!	#DIV/0!	#DIV/0!	
2.1	0.0172	5.867707434	5.867707434	73 703.49	\$2 761 846 524.3	
11.6	0.0908	31.6660808	31.6660808	1 771 240.07	\$2 761 681 286.5	
13.6	0.1283	37.25102326	37.25102326	2 406 152.83	\$2 761 650 317.3	
19.3	0.1590	52.83459482	52.83459482	4 651 367.10	\$2 761 568 334.5	
36.4	0.0902	99.33997945	99.33997945	15 301 448.26	\$2 761 347 446.6	
34.7	0.1827	94.70026527	94.70026527	13 981 536.63	\$2 761 368 358.1	
37.7	0.1220	102.8834346	102.8834346	16 347 075.80	\$2 761 331 607.6	
45.0	0.1334	123.0370296	123.0370296	22 906 785.01	\$2 761 243 469.9	
50.4	0.1523	137.5854414	137.5854414	28 281 617.86	\$2 761 181 649.9	
55.3	0.2458	150.9766597	150.9766597	33 696 163.47	\$2 761 125 896.5	
59.6	0.1716	162.8760925	162.8760925	38 879 394.85	\$2 761 077 180.9	
73.0	0.2035	199.2833356	199.2833356	56 879 900.18	\$2 760 932 288.4	
83.3	0.2397	227.582049	227.582049	73 066 587.42	\$2 760 823 333.5	
94.2	0.2609	257.3405172	257.3405172	92 124 460.52	\$2 760 711 646.3	
105.6	0.2843	288.4230583	288.4230583	114 228 135.43	\$2 760 597 717.5	
116.8	0.3083	319.0927636	319.0927636	138 211 419.59	\$2 760 487 689.2	
139.8	0.3272	381.880291	381.880291	193 941 760.55	\$2 760 268 744.4	
208.6	0.4052	569.6841262	569.6841262	412 365 665.01	\$2 759 651 916.2	
275.7	0.4541	752.9936741	752.9936741	697 886 816.00	\$2 759 088 678.4	
340.8	0.4884	930.8574151	930.8574151	1 041 046 659.12	\$2 758 568 103.7	
412.2	0.5050	1125.707103	1125.707103	1 489 857 963.50	\$2 758 020 218.7	
547.4	0.5399	1495.034803	1495.034803	2 544 186 283.91	\$2 757 030 444.5	
682.4	0.5667	1863.858154	1863.858154	3 856 161 373.70	\$2 756 090 177.4	
817.6	0.6049	2232.945321	2232.945321	5 421 764 189.63	\$2 755 186 022.0	
952.1	0.6153	2600.399936	2600.399936	7 226 404 480.35	\$2 754 315 225.8	

Flash-drum							
Total volume flow (m3/hr)	Drum-volume	D (m)	H (m)	tw (m)	shell mass (kg)	cost (\$)	EP
#DIV/0!	#DIV/0!	#DIV/0!	#DIV/0!	#DIV/0!	#DIV/0!	#DIV/0!	#DIV/0!
128.9069506	10.74181619	1.90	3.80	0.001601142	289.9601717	8990.961442	\$2 761 837 533.35
278.2673103	23.18801497	2.45	4.91	0.002069308	625.9277464	20851.32346	\$2 761 660 435.13
163.6726394	13.63884104	2.06	4.11	0.00173379	368.1612699	12104.56023	\$2 761 638 212.74
154.7622379	12.89633729	2.02	4.03	0.001701738	348.1184286	11334.09165	\$2 761 557 000.40
218.238792	18.18583854	2.26	4.52	0.001908308	490.9010516	16500.0377	\$2 761 330 946.58
166.4366883	13.86916924	2.07	4.13	0.001743496	374.3786545	12340.13003	\$2 761 356 017.95
150.6822437	12.55635137	2.00	4.00	0.001686651	338.9409884	10975.39441	\$2 761 320 632.22
154.4563161	12.87084482	2.02	4.03	0.001700616	347.4302954	11307.32842	\$2 761 232 162.57
151.1298909	12.59365381	2.00	4.00	0.001688319	339.9479153	11014.93795	\$2 761 170 634.93
147.412794	12.28390812	1.98	3.97	0.001674363	331.5867675	10685.1447	\$2 761 115 211.31
143.1282022	11.92687309	1.97	3.93	0.001657981	321.9491106	10300.84551	\$2 761 066 880.04
145.9343783	12.16071175	1.98	3.96	0.001668746	328.2612551	10553.05195	\$2 760 921 735.38
142.8492097	11.90362465	1.96	3.93	0.001656903	321.3215516	10275.66329	\$2 760 813 057.87
141.3370627	11.77761743	1.96	3.91	0.001651036	317.9201647	10138.83116	\$2 760 701 507.51
140.8073571	11.73347707	1.95	3.91	0.001648971	316.7286578	10090.76048	\$2 760 587 626.71
140.2022019	11.68304948	1.95	3.90	0.001646605	315.3674362	10035.75414	\$2 760 477 653.47
139.824694	11.65159175	1.95	3.90	0.001645126	314.5182793	10001.39199	\$2 760 258 743.03
139.059125	11.58779688	1.95	3.89	0.001642118	312.7962267	9931.592941	\$2 759 641 984.66
137.8535533	11.4873366	1.94	3.88	0.001637359	310.0844431	9821.36522	\$2 759 078 856.99
136.3326219	11.36059738	1.93	3.87	0.001631315	306.6632967	9681.75191	\$2 758 558 421.95
137.3917909	11.44885794	1.94	3.88	0.001635528	309.045766	9779.043353	\$2 758 010 439.63
136.8509903	11.40379302	1.94	3.87	0.00163338	307.829302	9729.404988	\$2 757 020 715.11
136.4895766	11.37367642	1.93	3.87	0.00163194	307.0163469	9696.188235	\$2 756 080 481.19
136.2647334	11.35494024	1.93	3.87	0.001631044	306.5105901	9675.505631	\$2 755 176 346.48
136.0187375	11.33444414	1.93	3.86	0.001630062	305.9572528	9652.861607	\$2 754 305 572.93

Membrane Cost						
C8 + 2-C8 (kg/hr)	C12-C14 (kg/hr)	wt frac C8	flux	Area	Membrane cost	EP-cost
#DIV/0!	#DIV/0!	#DIV/0!	#DIV/0!	#DIV/0!	#DIV/0!	#DIV/0!
113.0	1050.65	0.097074143	0.925206	2096.111	41 293 387.09	\$2 720 544 146.26
104452.3	1118.15	0.98940848	7.827887	22477.42	442 805 203.11	\$2 318 855 232.03
21438.1	1113.42	0.950627787	7.215751	5208.868	102 614 705.85	\$2 659 023 506.89
14969.7	1113.73	0.930752861	6.913028	3877.558	76 387 885.21	\$2 685 169 115.19
23360.0	1550.22	0.937767584	7.019021	5914.924	116 524 009.00	\$2 644 806 937.58
23661.4	1106.02	0.955343602	7.288673	5663.44	111 569 775.25	\$2 649 786 242.71
13484.9	1106.90	0.924142212	6.813989	3569.071	70 310 690.33	\$2 691 009 941.89
16680.0	1090.32	0.938643848	7.032327	4211.589	82 968 311.89	\$2 678 263 850.68
14403.1	1084.92	0.929951166	6.900973	3740.531	73 688 470.53	\$2 687 482 164.41
10361.4	1095.68	0.904366562	6.522638	2927.525	57 672 237.14	\$2 703 442 974.17
8559.0	1093.62	0.886701787	6.268622	2566.38	50 557 681.52	\$2 710 509 198.51
10327.2	1098.79	0.903834452	6.5149	2923.041	57 583 912.51	\$2 703 337 822.86
8190.6	1087.41	0.882796718	6.213263	2488.753	49 028 424.61	\$2 711 784 633.26
6709.0	1084.93	0.860797671	5.90677	2199.151	43 323 278.29	\$2 717 378 229.22
5925.1	1092.06	0.844373078	5.683892	2057.621	40 535 131.35	\$2 720 052 495.36
5217.4	1092.31	0.826885109	5.452177	1928.807	37 997 489.24	\$2 722 480 164.23
4661.4	1101.18	0.808908466	5.219999	1839.904	36 246 108.00	\$2 724 012 635.02
3870.8	1097.03	0.779174	4.849341	1707.393	33 635 635.16	\$2 726 006 349.50
2771.5	1100.68	0.715747044	4.114406	1568.552	30 900 482.79	\$2 728 178 374.20
2242.3	1092.39	0.672415068	3.655937	1520.212	29 948 182.77	\$2 728 610 239.19
1963.9	1102.50	0.640457747	3.340506	1529.909	30 139 205.06	\$2 727 871 234.56
1778.9	1098.89	0.618148055	3.131718	1531.528	30 171 097.77	\$2 726 849 617.34
1524.9	1098.90	0.581181715	2.806426	1558.213	30 696 792.31	\$2 725 383 688.88
1331.9	1104.81	0.54660384	2.52548	1608.113	31 679 824.78	\$2 723 496 521.70
1141.9	1099.47	0.509474403	2.248909	1661.11	32 723 874.28	\$2 721 581 698.65

70°C

Reactor Cost (\$\$) & EP						
V (m3)	Conversion	D (m)	H (m)	Cost (\$)	H/D based	EP
#DIV/0!	1.000	#DIV/0!	#DIV/0!	#DIV/0!	#DIV/0!	#DIV/0!
5.9	0.015	\$16.2	\$16.2	497 603.39	\$2 761 774 217.0	
14.1	0.068	\$38.4	\$38.4	2 544 707.63	\$2 761 644 209.6	
13.8	0.171	\$37.7	\$37.7	2 465 334.76	\$2 761 647 684.3	
18.1	0.258	\$49.5	\$49.5	4 114 560.82	\$2 761 585 371.6	
23.5	0.333	\$64.2	\$64.2	6 707 539.52	\$2 761 511 870.9	
29.0	0.393	\$79.2	\$79.2	9 991 929.38	\$2 761 439 562.2	
34.7	0.441	\$94.6	\$94.6	13 965 516.00	\$2 761 368 618.7	
40.3	0.477	\$110.0	\$110.0	18 553 543.90	\$2 761 300 000.9	
46.1	0.503	\$125.9	\$125.9	23 911 932.78	\$2 761 231 318.9	
51.8	0.520	\$141.6	\$141.6	29 858 394.51	\$2 761 164 822.7	
57.6	0.522	\$157.2	\$157.2	36 375 840.78	\$2 761 100 210.9	
69.2	0.541	\$189.1	\$189.1	51 504 940.61	\$2 760 972 372.6	
80.7	0.577	\$220.3	\$220.3	68 703 200.85	\$2 760 851 205.8	
92.4	0.607	\$252.2	\$252.2	88 700 743.17	\$2 760 730 655.3	
103.6	0.633	\$283.0	\$283.0	110 213 818.08	\$2 760 617 397.7	
114.7	0.651	\$313.3	\$313.3	133 489 803.38	\$2 760 508 425.1	
138.8	0.684	\$379.1	\$379.1	191 263 247.61	\$2 760 278 365.3	
208.6	0.722	\$569.6	\$569.6	412 249 924.26	\$2 759 652 184.5	
278.1	0.745	\$759.6	\$759.6	709 495 951.86	\$2 759 068 904.3	
347.7	0.755	\$949.5	\$949.5	1 080 797 926.45	\$2 758 514 647.9	
417.0	0.771	\$1 139.0	\$1 139.0	1 523 256 716.27	\$2 757 983 519.1	
555.4	0.801	\$1 516.9	\$1 516.9	2 614 696 190.51	\$2 756 973 597.6	
693.9	0.804	\$1 895.2	\$1 895.2	3 979 427 942.63	\$2 756 012 053.2	
832.4	0.825	\$2 273.4	\$2 273.4	5 608 286 157.47	\$2 755 088 935.3	
969.6	0.836	\$2 648.1	\$2 648.1	7 478 568 806.40	\$2 754 204 001.1	

Flash-drum							
Total volume flow (m3/hr)	Drum-volume	D (m)	H (m)	tw (m)	shell mass (kg)	cost (\$)	EP
#DIV/0!	#DIV/0!	#DIV/0!	#DIV/0!	#DIV/0!	#DIV/0!	#DIV/0!	#DIV/0!
354.8465078	29.5693595	2.66	5.32	0.002243975	798.1831379	25888.05093	\$2 761 748 328.94
337.208318	28.09956914	2.62	5.23	0.002206161	758.508221	24770.00843	\$2 761 619 439.61
165.7949743	13.81569521	2.06	4.13	0.001741252	372.9351984	12285.57944	\$2 761 635 398.76
145.0196532	12.0844877	1.97	3.95	0.001665253	326.2036944	10471.05542	\$2 761 574 900.55
140.9361681	11.74421089	1.96	3.91	0.001649473	317.0184021	10102.4567	\$2 761 501 768.40
139.2793184	11.6061456	1.95	3.90	0.001642984	313.2915244	9951.684296	\$2 761 429 610.50
138.6129519	11.55061728	1.94	3.89	0.00164036	311.7926158	9890.843208	\$2 761 358 727.89
138.1244424	11.50990979	1.94	3.88	0.00163843	310.6937744	9846.166607	\$2 761 290 154.77
138.2619461	11.52136797	1.94	3.89	0.001638974	311.003072	9858.748383	\$2 761 221 460.16
138.2582517	11.52106011	1.94	3.89	0.001638959	310.9947618	9858.410403	\$2 761 154 964.31
138.1651005	11.51329782	1.94	3.88	0.001638591	310.7852298	9849.887399	\$2 761 090 361.01
138.4521635	11.53721879	1.94	3.89	0.001639725	311.4309424	9876.145286	\$2 760 962 496.45
138.2606852	11.5212629	1.94	3.89	0.001638969	311.0002357	9858.63303	\$2 760 841 347.17
138.5272198	11.54347322	1.94	3.89	0.001640021	311.5997721	9883.007149	\$2 760 720 772.27
138.1615688	11.51300353	1.94	3.88	0.001638577	310.7772856	9849.564214	\$2 760 607 548.17
137.6419068	11.46970009	1.94	3.88	0.00163652	309.6083705	9801.974249	\$2 760 498 623.14
138.7974331	11.5659901	1.95	3.89	0.001641087	312.2075834	9907.698541	\$2 760 268 457.59
139.0384288	11.58607227	1.95	3.89	0.001642036	312.7496732	9929.703882	\$2 759 642 254.75
139.0647221	11.58826329	1.95	3.89	0.00164214	312.8088168	9932.103805	\$2 759 058 972.22
139.0685077	11.58857874	1.95	3.89	0.001642155	312.817332	9932.449318	\$2 758 504 715.43
139.0163538	11.58423276	1.95	3.89	0.001641949	312.7000183	9927.688848	\$2 757 973 591.46
138.8490529	11.57029157	1.95	3.89	0.001641291	312.3236956	9912.413231	\$2 756 963 685.16
138.7858583	11.56502557	1.95	3.89	0.001641041	312.1815473	9906.64126	\$2 756 002 146.58
138.7305789	11.56041914	1.95	3.89	0.001640824	312.0572032	9901.591368	\$2 755 079 033.70
138.51508	11.54246162	1.94	3.89	0.001639974	311.5724652	9881.897396	\$2 754 194 119.16

Membrane Cost						
C8 + 2-C8 (kg/hr)	C12-C14 (kg/hr)	wt frac C8	flux	Area	Membrane cost	EP-cost
#DIV/0!	#DIV/0!	#DIV/0!	#DIV/0!	#DIV/0!	#DIV/0!	#DIV/0!
123023.5	1470.19	0.988190687	7.808233	26573.17	523 491 480.01	\$2 238 256 848.94
141711.4	1179.04	0.991748628	7.865732	30277	596 456 863.81	\$2 165 162 575.80
24993.7	1082.36	0.958492193	7.337594	5922.937	116 681 860.10	\$2 644 953 538.67
9107.8	1088.18	0.893274082	6.362443	2670.888	52 616 486.54	\$2 708 958 414.01
5504.6	1095.12	0.834064817	5.54661	1983.103	39 067 129.00	\$2 722 434 639.40
3848.2	1099.16	0.777830083	4.832982	1706.118	33 610 534.06	\$2 727 819 076.44
2942.2	1101.33	0.727632735	4.24635	1587.069	31 265 257.26	\$2 730 093 470.63
2392.0	1102.61	0.684485074	3.780084	1540.804	30 353 833.08	\$2 730 936 321.69
2057.2	1106.27	0.650296075	3.435562	1534.653	30 232 655.79	\$2 730 988 804.37
1852.6	1109.14	0.625512323	3.199599	1542.777	30 392 711.44	\$2 730 762 252.87
1743.1	1109.70	0.611011144	3.066907	1550.3	30 540 917.03	\$2 730 549 443.98
1699.8	1118.12	0.603204844	2.997119	1566.991	30 869 722.74	\$2 730 092 773.71
1523.9	1113.20	0.57786777	2.778523	1581.824	31 161 924.41	\$2 729 679 422.77
1297.5	1118.81	0.536981991	2.451312	1642.883	32 364 804.16	\$2 728 355 968.10
1127.6	1116.87	0.502399236	2.199157	1701.04	33 510 484.12	\$2 727 097 064.05
999.0	1113.30	0.472935001	2.002118	1758.358	34 639 657.97	\$2 725 858 965.18
902.9	1123.24	0.445639551	1.834192	1841.121	36 270 087.62	\$2 723 998 369.97
759.3	1127.59	0.402407536	1.596974	1969.226	38 793 756.86	\$2 720 848 497.89
624.0	1127.01	0.356379723	1.383158	2109.972	41 566 452.70	\$2 717 492 519.52
552.8	1130.09	0.328494315	1.273057	2203.249	43 404 010.80	\$2 715 100 704.63
516.2	1129.47	0.313689841	1.220563	2247.204	44 269 927.16	\$2 713 703 664.30
459.3	1128.78	0.289199654	1.1428	2316.01	45 625 405.63	\$2 711 338 279.53
385.6	1129.06	0.254579361	1.05217	2399.27	47 265 616.96	\$2 708 736 529.62
369.8	1127.57	0.246957654	1.035254	2410.605	47 488 910.91	\$2 707 590 122.80
319.4	1126.17	0.220970624	0.985812	2444.025	48 147 293.85	\$2 706 046 825.32

80°C

Reactor Cost (\$\$) & EP						
V (m3)	Conversion	D (m)	H (m)	Cost (\$)	H/D based	EP
#DIV/0!	1.0000	#DIV/0!	#DIV/0!	#DIV/0!	#DIV/0!	#DIV/0!
#DIV/0!	0.0000	#DIV/0!	#DIV/0!	#DIV/0!	#DIV/0!	#DIV/0!
#DIV/0!	0.1397	#DIV/0!	#DIV/0!	#DIV/0!	#DIV/0!	#DIV/0!
12.93	0.2686	35.31565865	35.31565865	2 175 819.66	\$2 761 660 936.4	
17.87	0.3877	48.80687485	48.80687485	4 005 269.25	\$2 761 588 994.7	
23.77	0.4955	64.92955907	64.92955907	6 861 562.40	\$2 761 508 071.9	
29.77	0.5317	81.30541816	81.30541816	10 486 773.89	\$2 761 429 931.8	
35.77	0.5822	97.68865748	97.68865748	14 825 269.62	\$2 761 354 866.4	
39.67	0.6199	108.3447473	108.3447473	18 022 049.40	\$2 761 307 407.4	
48.03	0.6726	131.1830845	131.1830845	25 850 809.82	\$2 761 208 685.5	
57.21	0.7055	156.2567273	156.2567273	35 953 103.40	\$2 761 104 188.8	
58.99	0.7179	161.1064842	161.1064842	38 086 556.27	\$2 761 084 379.3	
74.70	0.7444	204.0070018	204.0070018	59 449 356.50	\$2 760 913 896.8	
85.64	0.7659	233.8938782	233.8938782	76 935 381.29	\$2 760 799 411.9	
96.00	0.7805	262.1989799	262.1989799	95 432 128.82	\$2 760 693 664.3	
113.01	0.7952	308.6388112	308.6388112	129 795 687.69	\$2 760 524 944.9	
122.51	0.7989	334.5870573	334.5870573	151 140 475.03	\$2 760 432 915.7	
149.27	0.8136	407.6718033	407.6718033	219 382 752.97	\$2 760 180 947.2	
226.06	0.8172	617.4088933	617.4088933	479 929 011.13	\$2 759 502 176.6	
289.27	0.8215	790.0482826	790.0482826	764 066 752.88	\$2 758 978 362.4	
381.97	0.8278	1043.219638	1043.219638	1 290 664 075.40	\$2 758 249 635.8	
426.35	0.8234	1164.422464	1164.422464	1 587 965 616.74	\$2 757 913 711.7	
602.85	0.8431	1646.467493	1646.467493	3 051 938 732.21	\$2 756 639 338.6	
730.52	0.8447	1995.158458	1995.158458	4 384 437 810.44	\$2 755 764 751.3	
893.12	0.8675	2439.235611	2439.235611	6 404 970 384.10	\$2 754 693 902.5	
1083.41	0.8895	2958.932432	2958.932432	9 219 709 784.43		-\$8 143 212.33

Flash-drum							
Total volume flow (m3/hr)	Drum-volume	D (m)	H (m)	tw (m)	shell mass (kg)	cost (\$)	EP
#DIV/0!	#DIV/0!	#DIV/0!	#DIV/0!	#DIV/0!	#DIV/0!	#DIV/0!	#DIV/0!
#DIV/0!	#DIV/0!	#DIV/0!	#DIV/0!	#DIV/0!	#DIV/0!	#DIV/0!	#DIV/0!
#DIV/0!	#DIV/0!	#DIV/0!	#DIV/0!	#DIV/0!	#DIV/0!	#DIV/0!	#DIV/0!
155.1690815	12.93023956	2.02	4.04	0.001703228	349.0335726	11369.65114	\$2 761 649 566.79
142.9643059	11.91321561	1.96	3.93	0.001657348	321.5804462	10286.0544	\$2 761 578 708.62
142.6429582	11.88643771	1.96	3.93	0.001656105	320.8576144	10257.03411	\$2 761 497 814.89
142.895107	11.90744927	1.96	3.93	0.001657081	321.4247918	10279.80739	\$2 761 419 651.94
143.0740153	11.92235769	1.97	3.93	0.001657772	321.8272237	10295.95606	\$2 761 344 570.40
136.0121468	11.33389219	1.93	3.86	0.001630035	305.9424279	9652.254706	\$2 761 297 755.10
144.097261	12.00762476	1.97	3.94	0.001661714	324.1288878	10388.16186	\$2 761 198 297.30
152.5682235	12.71351006	2.01	4.02	0.001693659	343.1832657	11141.67907	\$2 761 093 047.13
141.5731499	11.79729058	1.96	3.92	0.001651955	318.4512135	10160.2328	\$2 761 074 219.03
149.3934999	12.44896035	1.99	3.99	0.001681829	336.0421193	10861.28824	\$2 760 903 035.53
146.8110328	12.23376336	1.98	3.96	0.001672081	330.2331804	10631.44308	\$2 760 788 780.48
144.0054371	11.99997307	1.97	3.94	0.001661361	323.9223414	10379.89823	\$2 760 683 284.42
150.676633	12.55588383	2.00	4.00	0.001686663	338.9283679	10974.89849	\$2 760 513 969.99
147.0100469	12.25034721	1.98	3.97	0.001672836	330.680838	10649.21297	\$2 760 422 266.54
149.268204	12.43851944	1.99	3.99	0.001681358	335.7602818	10850.1735	\$2 760 170 096.98
150.7086761	12.55855398	2.00	4.00	0.001686749	339.0004448	10977.73066	\$2 759 491 198.89
144.6372882	12.05262522	1.97	3.94	0.001663788	325.3436119	10436.7187	\$2 758 967 925.64
152.7891019	12.73191586	2.01	4.02	0.001694475	343.6801043	11161.09974	\$2 758 238 474.73
142.1169745	11.84260748	1.96	3.92	0.001654067	319.6744794	10209.47705	\$2 757 903 502.22
150.7126833	12.5588879	2.00	4.00	0.001686764	339.0094586	10978.08483	\$2 756 628 360.56
146.1046446	12.17490003	1.98	3.96	0.001669395	328.6442479	10568.292	\$2 755 754 183.05
148.8535287	12.40396454	1.99	3.98	0.0016798	334.8275212	10813.36188	\$2 754 683 089.17
154.7724441	12.89718777	2.02	4.03	0.001701776	348.1413862	11334.98416	\$2 753 477 742.28

Membrane Cost						
C8 + 2-C8 (kg/hr)	C12-C14 (kg/hr)	wt frac C8	flux	Area	Membrane cost	EP-cost
#DIV/0!	#DIV/0!	#DIV/0!	#DIV/0!	#DIV/0!	#DIV/0!	#DIV/0!
#DIV/0!	#DIV/0!	#DIV/0!	#DIV/0!	#DIV/0!	#DIV/0!	#DIV/0!
#DIV/0!	1178.66	#DIV/0!	#DIV/0!	#DIV/0!	#DIV/0!	#DIV/0!
11745.8	1205.43	0.90692583	6.559928	3290.499	64 822 836.43	\$2 696 826 730.36
5411.2	1197.43	0.818807935	5.347102	2059.877	40 579 579.12	\$2 720 999 129.50
3083.8	1210.99	0.718031323	4.139557	1729.152	34 064 290.25	\$2 727 433 524.64
2089.7	1237.48	0.628065173	3.223369	1720.316	33 890 234.39	\$2 727 529 417.55
1695.6	1184.30	0.588776608	2.871155	1671.774	32 933 945.18	\$2 728 410 625.22
1356.2	1205.54	0.529413252	2.394198	1783.33	35 131 608.76	\$2 726 166 146.33
1172.7	1280.37	0.478059556	2.035212	2008.875	39 574 832.30	\$2 721 623 465.00
974.3	1352.35	0.418755633	1.682533	2304.709	45 402 771.19	\$2 715 690 275.94
804.8	1272.11	0.387489173	1.523296	2272.354	44 765 371.93	\$2 716 308 847.11
756.5	1332.71	0.362091569	1.40752	2473.837	48 734 580.83	\$2 712 168 454.70
652.4	1318.14	0.331088995	1.282682	2560.494	50 441 730.22	\$2 710 347 050.25
567.6	1301.29	0.303696352	1.187465	2623.034	51 673 770.08	\$2 709 009 514.34
536.0	1363.09	0.282250649	1.122796	2819.028	55 534 847.50	\$2 704 979 122.49
483.9	1329.09	0.266916894	1.081875	2793.01	55 022 304.44	\$2 705 399 962.10
469.1	1345.88	0.258452462	1.061186	2850.517	56 155 189.07	\$2 704 014 907.91
434.5	1369.64	0.240824699	1.022437	2940.871	57 935 166.42	\$2 701 556 032.48
397.7	1277.92	0.237335828	1.015463	2750.148	54 177 907.64	\$2 704 790 018.00
407.9	1381.70	0.227933339	0.99781	2989.24	58 888 035.67	\$2 699 350 439.06
376.0	1296.87	0.224758784	0.992226	2809.951	55 356 028.99	\$2 702 547 473.23
392.7	1362.40	0.223736183	0.990468	2953.276	58 179 530.25	\$2 698 448 830.30
336.3	1328.94	0.201940864	0.957685	2897.985	57 090 304.31	\$2 698 663 878.74
327.9	1348.45	0.195602604	0.949833	2941.485	57 947 257.35	\$2 696 735 831.82
276.0	1393.40	0.165352258	0.922795	3015.204	59 399 526.46	\$2 694 078 215.81

90°C

Reactor Cost (\$\$) & EP					
V (m3)	Conversion	D (m)	H (m)	Cost (\$) H/D based	EP
#DIV/0!	1.0000	#DIV/0!	#DIV/0!	#DIV/0!	#DIV/0!
2.1	0.0335	5.867674775	5.867674775	73 702.72	\$2 761 846 524.6
8.1	0.1893	22.03055624	22.03055624	893 516.49	\$2 761 737 509.3
12.3	0.2506	33.673383	33.673383	1 988 929.37	\$2 761 670 039.0
18.3	0.2576	50.07578461	50.07578461	4 203 920.65	\$2 761 582 450.3
24.5	0.2649	66.79937962	66.79937962	7 238 979.58	\$2 761 498 965.9
30.7	0.2635	83.77507832	83.77507832	11 095 608.97	\$2 761 418 435.3
36.7	0.2697	100.3582664	100.3582664	15 598 606.12	\$2 761 342 883.5
43.0	0.2785	117.4551766	117.4551766	20 986 279.28	\$2 761 267 570.6
51.4	0.2968	140.2554412	140.2554412	29 325 615.73	\$2 761 170 449.9
53.0	0.3148	144.627156	144.627156	31 073 327.34	\$2 761 152 203.2
60.3	0.2776	164.5628396	164.5628396	39 642 247.92	\$2 761 070 334.1
72.7	0.2849	198.6057055	198.6057055	56 515 677.12	\$2 760 934 933.9
86.0	0.2973	234.9394296	234.9394296	77 585 291.52	\$2 760 795 461.9
97.2	0.2958	265.4426099	265.4426099	97 670 896.68	\$2 760 681 696.2
103.5	0.2882	282.6303757	282.6303757	109 939 884.00	\$2 760 618 755.6
123.6	0.3012	337.5601161	337.5601161	153 683 335.12	\$2 760 422 464.4
146.2	0.2996	399.2627847	399.2627847	210 926 286.28	\$2 760 209 446.9
219.5	0.3065	599.6060397	599.6060397	454 163 077.02	\$2 759 557 753.7
293.4	0.3204	801.3539439	801.3539439	784 818 674.16	\$2 758 944 911.9
377.6	0.3201	1031.36735	1031.36735	1 263 147 835.74	\$2 758 282 892.5
408.7	0.3467	1116.154887	1116.154887	1 466 104 381.15	\$2 758 046 609.0
792.0	0.3459	2162.930158	2162.930158	5 105 598 951.52	\$2 755 355 085.2
730.9	0.3591	1996.219808	1996.219808	4 388 837 673.56	\$2 755 762 138.6
918.6	0.3704	2508.835318	2508.835318	6 753 999 652.10	\$2 754 529 773.5
943.1	0.3729	2575.797209	2575.797209	7 097 999 368.75	-\$7 259 567.06

Flash-drum								
Total volume flow (m3/hr)	Drum-volume	D (m)	H (m)	tw (m)	shell mass (kg)	cost (\$)	EP	#DIV/0!
#DIV/0!	#DIV/0!	#DIV/0!	#DIV/0!	#DIV/0!	#DIV/0!	#DIV/0!	#DIV/0!	#DIV/0!
128.9062331	10.74175641	1.90	3.80	0.001601139	289.9585578	8990.893939	\$2 761 837 533.68	
193.5946437	16.13224166	2.17	4.35	0.00183359	435.4671014	14576.92528	\$2 761 722 932.42	
147.9532907	12.32894771	1.99	3.97	0.001676407	332.8025477	10733.30432	\$2 761 659 305.66	
146.6811758	12.22294238	1.98	3.96	0.001671588	329.9410832	10619.843	\$2 761 571 830.41	
146.7507442	12.22873952	1.98	3.96	0.001671852	330.0975688	10626.05803	\$2 761 488 339.84	
147.2355601	12.26913922	1.98	3.97	0.001673691	331.1881019	10669.33734	\$2 761 407 765.96	
146.9839027	12.24816862	1.98	3.97	0.001672737	330.6220299	10646.87912	\$2 761 332 236.66	
147.4490561	12.28692985	1.99	3.97	0.0016745	331.6683346	10688.37795	\$2 761 256 882.20	
154.062736	12.83804779	2.01	4.03	0.001699171	346.544986	11272.86531	\$2 761 159 177.07	
141.213173	11.7672937	1.96	3.91	0.001650553	317.6414901	10127.59465	\$2 761 142 075.63	
144.6104399	12.05038796	1.97	3.94	0.001663685	325.2832201	10434.30634	\$2 761 059 899.80	
145.4381526	12.11936125	1.98	3.95	0.001666853	327.1450569	10508.59556	\$2 760 924 425.30	
147.4673069	12.28845068	1.99	3.97	0.001674569	331.7093874	10690.00513	\$2 760 784 771.86	
145.7869099	12.1484232	1.98	3.96	0.001668184	327.9295432	10539.84671	\$2 760 671 156.35	
137.9793851	11.49782216	1.94	3.88	0.001637857	310.3674862	9832.88824	\$2 760 608 922.75	
148.3163423	12.3592008	1.99	3.98	0.001677777	333.6191871	10765.61363	\$2 760 411 698.78	
146.1892589	12.18195094	1.98	3.96	0.001669717	328.8345772	10575.86294	\$2 760 198 871.06	
146.3630236	12.19643075	1.98	3.96	0.001670379	329.2254393	10591.4052	\$2 759 547 162.33	
146.7070607	12.22509937	1.98	3.96	0.001671686	329.999308	10622.15561	\$2 758 934 289.70	
151.0532254	12.58726527	2.00	4.00	0.001688034	339.7754656	11008.16892	\$2 758 271 884.29	
136.2259495	11.35170837	1.93	3.87	0.001630889	306.4233504	9671.936637	\$2 758 036 937.04	
197.9881227	16.49835026	2.19	4.38	0.001847357	445.3496865	14926.64361	\$2 755 340 158.59	
146.1823668	12.18137663	1.98	3.96	0.001669691	328.8190744	10575.24633	\$2 755 751 563.36	
153.1008272	12.75789193	2.01	4.02	0.001695627	344.3812917	11188.48899	\$2 754 518 585.00	
134.7318463	11.22720475	1.93	3.85	0.001624905	303.0625509	9534.134701	\$2 754 363 188.40	

Membrane Cost						
C8 + 2-C8 (kg/hr)	C12-C14 (kg/hr)	wt frac C8	flux	Area	Membrane cost	EP-cost
#DIV/0!	#DIV/0!	#DIV/0!	#DIV/0!	#DIV/0!	#DIV/0!	#DIV/0!
112.4	1050.65	0.096674222	0.92548	2094.565	41 262 924.61	\$2 720 574 609.07
43772.5	1093.44	0.975628642	7.607129	9829.807	193 647 191.79	\$2 568 075 740.64
9009.0	1123.87	0.889086044	6.302564	2679.553	52 787 201.13	\$2 708 872 104.53
7145.9	1127.89	0.863679062	5.946394	2318.99	45 684 100.83	\$2 715 887 729.58
6697.2	1136.72	0.854898021	5.826127	2241.039	44 148 470.51	\$2 717 339 869.33
6422.0	1140.44	0.849197285	5.748828	2192.472	43 191 707.53	\$2 718 216 058.43
6597.6	1135.46	0.853167724	5.8026	2221.137	43 756 392.62	\$2 717 575 844.04
6527.5	1137.82	0.851562101	5.780819	2209.973	43 536 468.39	\$2 717 720 413.81
6298.3	1197.59	0.840233874	5.628527	2219.608	43 726 271.86	\$2 717 432 905.21
5544.2	1099.79	0.834468998	5.551955	1994.495	39 291 557.61	\$2 721 850 518.02
5556.8	1127.15	0.831365542	5.510993	2021.414	39 821 855.78	\$2 721 238 044.02
6290.7	1161.63	0.844126276	5.680582	2186.503	43 074 105.72	\$2 717 850 319.58
6067.5	1145.82	0.841151684	5.640775	2131.304	41 986 689.54	\$2 718 798 082.32
5874.9	1132.04	0.838439795	5.60463	2083.676	41 048 418.78	\$2 719 622 737.57
5867.7	1080.45	0.844498194	5.685571	2036.78	40 124 559.15	\$2 720 484 363.60
6036.1	1151.33	0.839812674	5.622911	2130.391	41 968 708.14	\$2 718 442 990.63
5967.8	1134.23	0.840294235	5.629332	2102.672	41 422 643.66	\$2 718 776 227.40
5980.4	1132.78	0.840748627	5.635394	2103.719	41 443 273.76	\$2 718 103 888.56
5839.9	1135.86	0.837170651	5.587761	2080.674	40 989 283.63	\$2 717 945 006.08
5837.6	1180.11	0.831839566	5.517238	2119.947	41 762 957.61	\$2 716 508 926.69
5334.5	1059.76	0.834264673	5.549253	1920.467	37 833 194.40	\$2 720 203 742.64
6025.7	1522.79	0.798266445	5.085424	2473.908	48 735 983.48	\$2 706 604 175.11
5613.3	1133.00	0.832056052	5.520091	2036.896	40 126 857.16	\$2 715 624 706.20
4706.1	1196.57	0.79728264	5.073091	1939.201	38 202 250.72	\$2 716 316 334.28
4264.0	1061.45	0.800684887	5.115819	1734.972	34 178 942.03	\$2 720 184 246.37

100°C

Reactor Cost (\$\$) & EP						
V (m3)	Conversion	D (m)	H (m)	Cost (\$)	H/D based	EP
#DIV/0!	1.0000	#DIV/0!	#DIV/0!	#DIV/0!	#DIV/0!	#DIV/0!
2.1	0.0396	5.867660799	5.867660799	73 702.38	\$2 761 846 524.7	
8.4	0.1198	22.90563464	22.90563464	961 629.51	\$2 761 732 224.9	
15.0	0.0748	41.01104786	41.01104786	2 884 613.18	\$2 761 629 994.6	
22.3	0.0794	60.86897968	60.86897968	6 074 736.54	\$2 761 528 030.7	
31.3	0.0848	85.51625579	85.51625579	11 534 542.03	\$2 761 410 370.8	
37.5	0.0905	102.3705814	102.3705814	16 193 730.97	\$2 761 333 893.2	
44.6	0.0882	121.8546797	121.8546797	22 493 392.54	\$2 761 248 556.3	
52.1	0.0931	142.3125531	142.3125531	30 142 081.78	\$2 761 161 850.0	
59.0	0.0926	161.0834767	161.0834767	38 076 298.74	\$2 761 084 473.0	
65.9	0.1035	179.9103142	179.9103142	46 902 099.40	\$2 761 008 660.1	
73.5	0.0992	200.6025838	200.6025838	57 592 142.04	\$2 760 927 143.2	
88.3	0.1069	241.2299756	241.2299756	81 549 617.96	\$2 760 771 769.9	
102.2	0.1120	279.0998562	279.0998562	107 364 122.69	\$2 760 631 620.2	
116.8	0.1150	318.9568029	318.9568029	138 100 374.35	\$2 760 488 172.2	
130.0	0.1180	355.0485148	355.0485148	169 043 763.35	\$2 760 361 352.6	
143.4	0.1200	391.7313126	391.7313126	203 485 028.22	\$2 760 235 074.6	
172.4	0.1238	470.9162974	470.9162974	287 957 508.49	\$2 759 970 172.9	
256.9	0.1313	701.6194151	701.6194151	610 807 223.34	\$2 759 243 445.8	
338.3	0.1413	923.8259082	923.8259082	1 026 265 074.90	\$2 758 588 280.7	
422.2	0.1387	1153.006437	1153.006437	1 558 731 084.01	\$2 757 945 042.8	
511.6	0.1362	1397.23323	1397.23323	2 239 410 479.23	\$2 757 287 235.5	
679.2	0.1364	1854.976043	1854.976043	3 821 576 816.08	\$2 756 112 354.1	
840.4	0.1383	2295.30628	2295.30628	5 710 866 476.13	\$2 755 036 332.3	
1003.9	0.1385	2741.65537	2741.65537	7 984 519 918.44	\$2 753 987 177.8	
1167.7	0.1433	3189.134998	3189.134998	10 619 000 618.11	\$2 752 969 262.5	

Flash-drum							
Total volume flow (m3/hr)	Drum-volume	D (m)	H (m)	tw (m)	shell mass (kg)	cost (\$)	EP
#DIV/0!	#DIV/0!	#DIV/0!	#DIV/0!	#DIV/0!	#DIV/0!	#DIV/0!	#DIV/0!
128.9059261	10.74173082	1.90	3.80	0.001601138	289.9578672	8990.865053	\$2 761 837 533.81
201.28444	16.77303239	2.20	4.40	0.001857553	452.7643429	15186.99395	\$2 761 717 037.95
180.193344	15.01551135	2.12	4.24	0.001790265	405.3225424	13490.04158	\$2 761 616 504.51
178.2964277	14.85744132	2.11	4.23	0.001783961	401.0556649	13333.62141	\$2 761 514 697.03
187.8696217	15.65517558	2.15	4.30	0.001815335	422.5893756	14116.41545	\$2 761 396 254.34
179.9173476	14.99251257	2.12	4.24	0.001789351	404.7017228	13467.32394	\$2 761 320 425.87
178.4673753	14.87168638	2.12	4.23	0.001784531	401.4401903	13347.74499	\$2 761 235 208.58
178.6541235	14.88724811	2.12	4.23	0.001785153	401.8602571	13363.16782	\$2 761 148 486.82
176.9411649	14.74450727	2.11	4.22	0.001779429	398.0071696	13221.45813	\$2 761 071 251.50
175.6634577	14.63803593	2.10	4.21	0.001775136	395.1331261	13115.39832	\$2 760 995 544.70
176.2805501	14.68945824	2.11	4.21	0.001777212	396.5211988	13166.66027	\$2 760 913 976.58
176.6517327	14.72038888	2.11	4.22	0.001778459	397.3561278	13197.45987	\$2 760 758 572.45
175.1860222	14.59825123	2.10	4.20	0.001773526	394.0591943	13075.68826	\$2 760 618 544.53
175.1780798	14.59758939	2.10	4.20	0.0017735	394.0413286	13075.02728	\$2 760 475 097.15
173.3337248	14.44389929	2.10	4.19	0.001767253	389.8926813	12921.21437	\$2 760 348 431.34
172.1179508	14.34258884	2.09	4.18	0.001763112	387.1579486	12819.46479	\$2 760 222 255.10
172.4250472	14.36817919	2.09	4.18	0.00176416	387.8487239	12845.19312	\$2 759 957 327.68
171.2643506	14.27145833	2.09	4.17	0.001760192	385.237881	12747.85412	\$2 759 230 697.92
169.1284913	14.09347718	2.08	4.16	0.001752845	380.433531	12568.04313	\$2 758 575 712.66
168.8683874	14.07180272	2.08	4.15	0.001751946	379.8484594	12546.08395	\$2 757 932 496.73
170.5313711	14.21037915	2.08	4.17	0.001757678	383.5891347	12686.24861	\$2 757 274 549.26
169.7989291	14.14934476	2.08	4.16	0.001755158	381.9415973	12624.58239	\$2 756 099 729.49
168.0843478	14.0064687	2.07	4.15	0.00174923	378.0848599	12479.80971	\$2 755 023 852.53
167.3085922	13.94182499	2.07	4.14	0.001746535	376.339894	12414.1139	\$2 753 974 763.65
166.8136159	13.90057862	2.07	4.14	0.001744811	375.2265063	12372.13253	\$2 752 956 890.40

Membrane Cost						
C8 + 2-C8 (kg/hr)	C12-C14 (kg/hr)	wt frac C8	flux	Area	Membrane cost	EP-cost
#DIV/0!	#DIV/0!	#DIV/0!	#DIV/0!	#DIV/0!	#DIV/0!	#DIV/0!
112.2	1050.65	0.096502977	0.925597	2093.901	41 249 849.97	\$2 720 587 683.85
50514.3	2092.99	0.960214898	7.36444	11905.7	234 542 385.93	\$2 527 174 652.03
36680.1	1130.00	0.970113894	7.519785	8380.129	165 088 548.41	\$2 596 527 956.10
35426.4	1050.65	0.971197097	7.536896	8066.335	158 906 803.28	\$2 602 607 893.75
35514.7	1172.85	0.968031414	7.486951	8167.004	160 889 975.43	\$2 600 506 278.92
36449.8	1155.84	0.969264094	7.506376	8349.711	164 489 308.28	\$2 596 831 117.59
35436.6	1137.62	0.968895639	7.500567	8126.992	160 101 745.45	\$2 601 133 463.13
35546.9	1155.61	0.968514111	7.494554	8162.046	160 792 310.53	\$2 600 356 176.29
34413.3	1085.20	0.969429556	7.508986	7879.106	155 218 395.41	\$2 605 852 856.09
33351.1	1200.07	0.965266854	7.443489	7736.338	152 405 858.68	\$2 608 589 686.02
33871.8	1138.79	0.967472971	7.47816	7802.854	153 716 229.89	\$2 607 197 746.69
34129.2	1144.97	0.967540823	7.479228	7860.483	154 851 513.78	\$2 605 907 058.67
33027.1	1186.93	0.965308794	7.444148	7660.165	150 905 247.13	\$2 609 713 297.39
33002.4	1201.61	0.964869384	7.437253	7665.026	151 001 020.42	\$2 609 474 076.73
31783.4	1124.61	0.965825625	7.452262	7359.735	144 986 780.97	\$2 615 361 650.37
30890.8	1142.68	0.964328394	7.428769	7186.799	141 579 934.47	\$2 618 642 320.62
31109.2	1143.67	0.964540559	7.432095	7232.784	142 485 850.40	\$2 617 471 477.28
30305.3	1123.60	0.964249427	7.427531	7052.348	138 931 258.48	\$2 620 299 439.44
28779.6	1122.55	0.962459216	7.399498	6735.179	132 683 021.28	\$2 625 892 691.38
28613.2	1107.54	0.962735055	7.403813	6690.408	131 801 035.61	\$2 626 131 461.13
29792.9	1114.74	0.963933188	7.422574	6940.012	136 718 245.19	\$2 620 556 304.07
29352.1	1050.65	0.96544237	7.446244	6804.932	134 057 163.51	\$2 622 042 565.98
28126.1	1050.65	0.963990326	7.42347	6550.567	129 046 172.23	\$2 625 977 680.30
27571.4	1050.65	0.963292482	7.412538	6435.511	126 779 569.40	\$2 627 195 194.25
27144.8	1106.78	0.96082407	7.373946	6385.46	125 793 568.51	\$2 627 163 321.88

ECONOMIC POTENTIAL AND EQUIPMENT COST FOR THE **GCYC** CATALYST AT VARIED CATALYST LOADS

C₈/Ru: 5000

Reactor Cost (\$\$) & EP						
V (m3)	Conversion	D (m)	H (m)	Cost (\$)	H/D based	EP
#DIV/0!	1.0000	#DIV/0!	#DIV/0!	#DIV/0!	#DIV/0!	#DIV/0!
22.53808544	0.0088	61.55458221	61.55458	6 204 426.46	\$2 619 075 230.03	
154.893672	0.0232	423.0357231	423.0357	235 235 927.78	\$2 617 679 764.44	
135.883826	0.2352	371.1172434	371.1172	183 761 508.80	\$2 617 856 318.32	
18.18414677	0.3225	49.66338248	49.66338	4 138 862.54	\$2 619 135 161.07	
23.86431227	0.3763	65.17668838	65.17669	6 910 900.01	\$2 619 057 452.95	
29.29592924	0.3721	80.01117441	80.01117	10 174 162.43	\$2 618 986 571.89	
35.95840765	0.4520	98.20731073	98.20731	14 974 067.69	\$2 618 903 120.77	
41.72745895	0.4829	113.9633759	113.9634	19 825 124.19	\$2 618 833 350.82	
47.67394082	0.5112	130.2040281	130.204	25 488 143.66	\$2 618 763 430.29	
53.56165656	0.5382	146.284182	146.2842	31 748 176.43	\$2 618 695 903.60	
59.65908926	0.5559	162.9371015	162.9371	38 906 865.55	\$2 618 627 520.51	
71.82145985	0.5918	196.1541927	196.1542	55 207 186.51	\$2 618 495 107.25	
83.85779192	0.6185	229.0270556	229.0271	73 944 016.26	\$2 618 368 432.94	
95.88130694	0.6580	261.8649134	261.8649	95 202 940.17	\$2 618 245 486.13	
107.9633374	0.6809	294.8625849	294.8626	119 085 598.75	\$2 618 125 016.48	
119.7150346	0.6982	326.9580711	326.9581	144 706 680.15	\$2 618 010 407.40	
143.9824079	0.7197	393.235574	393.2356	204 961 235.09	\$2 617 780 535.65	
216.7387661	0.7590	591.9431014	591.9431	443 278 391.58	\$2 617 132 364.70	
289.5297549	0.7860	790.7452098	790.7452	765 338 428.89	\$2 616 526 885.10	
361.8834243	0.8081	988.3529393	988.3529	1 165 629 933.80	\$2 615 954 825.96	
434.5339063	0.8203	1186.771305	1186.771	1 645 935 382.68	\$2 615 403 140.18	
579.7530701	0.8327	1583.384628	1583.385	2 835 153 296.34	\$2 614 351 936.71	
723.7145251	0.8605	1976.562976	1976.563	4 307 686 087.26	\$2 613 361 160.84	
867.4052239	0.8591	2369.001853	2369.002	6 061 594 709.68	\$2 612 411 066.74	
1012.591839	0.8619	2765.526281	2765.526	8 116 138 731.05	\$2 611 482 666.10	

Flash-drum						
Total volume flow (m3/hr)	Drum-volume	D (m)	H (m)	tw (m)	shell mass (kg)	cost (\$)
#DIV/0!	#DIV/0!	#DIV/0!	#DIV/0!	#DIV/0!	#DIV/0!	#DIV/0!
1352.285126	112.6859196	4.16	8.31	0.003505048	3041.797401	71593.23276 \$2 619 003 636.79
3717.448129	309.7749526	5.82	11.64	0.004910052	8361.93776	140698.7047 \$2 617 539 065.74
1630.605912	135.8783906	4.42	8.85	0.003730676	3667.845434	81435.13066 \$2 617 774 883.19
145.4731742	12.1222796	1.98	3.95	0.001666987	327.2238336	10511.7351 \$2 619 124 649.33
143.1858736	11.93167885	1.97	3.93	0.001658204	322.0788351	10306.04855 \$2 619 047 146.90
140.6204604	11.71790296	1.95	3.91	0.001648241	316.3082567	10073.78238 \$2 618 976 498.10
143.8336306	11.98565644	1.97	3.94	0.00166607	323.535884	10364.43095 \$2 618 892 756.34
143.0655735	11.92165424	1.97	3.93	0.001657739	321.8082351	10295.19428 \$2 618 823 055.62
143.0218225	11.91800847	1.96	3.93	0.00165757	321.7098225	10291.24586 \$2 618 753 139.05
142.8310841	11.90211424	1.96	3.93	0.001656833	321.2807804	10274.02657 \$2 618 685 629.57
143.1818142	11.93134058	1.97	3.93	0.001658188	322.0697041	10305.68235 \$2 618 617 214.83
143.6429197	11.9697645	1.97	3.94	0.001659966	323.1069036	10347.2531 \$2 618 484 760.00
143.7562147	11.97920537	1.97	3.94	0.001660402	323.3617466	10357.45899 \$2 618 358 075.48
143.8219604	11.98468396	1.97	3.94	0.001660656	323.5096334	10363.38005 \$2 618 235 122.75
143.9511166	11.99544654	1.97	3.94	0.001661152	323.8001542	10375.0087 \$2 618 114 641.48
143.6580416	11.9710246	1.97	3.94	0.001660024	323.1409183	10348.61551 \$2 618 000 058.79
143.9824079	11.99805405	1.97	3.94	0.001661273	323.8705401	10377.8254 \$2 617 770 157.83
144.4925107	12.04056092	1.97	3.94	0.001663232	325.017953	10423.70808 \$2 617 121 941.00
144.7648774	12.06325724	1.97	3.95	0.001664277	325.6306081	10448.18036 \$2 616 516 436.92
144.7533697	12.0622983	1.97	3.95	0.001664233	325.6047229	10447.14676 \$2 615 944 378.81
144.8446354	12.06990347	1.97	3.95	0.001664582	325.8100138	10455.34317 \$2 615 392 684.83
144.9382675	12.07770583	1.97	3.95	0.001664941	326.0206276	10463.74995 \$2 614 341 472.96
144.742905	12.06142628	1.97	3.95	0.001664193	325.5811839	10446.20681 \$2 613 350 714.63
144.5675373	12.04681288	1.97	3.94	0.00166352	325.186716	10430.4511 \$2 612 400 636.29
144.655977	12.05418256	1.97	3.94	0.001663859	325.3856501	10438.39782 \$2 611 472 227.70

Membrane Cost							
C8 + 2-C8 (kg/hr)	C12-C14 (kg/hr)	wt frac C8	flux	Area	Membrane cost	EP-cost	
#DIV/0!	#DIV/0!	#DIV/0!	#DIV/0!	#DIV/0!	#DIV/0!	#DIV/0!	
739839.2	2515.30	0.996611722	7.94471	155733.5	3 067 950 169.26	-\$448 946 532.47	
1839050.2	12834.15	0.993069681	7.887142	391329.8	7 709 197 593.25	-\$5 091 658 527.52	
1068889.8	1123.38	0.998950124	7.982845	223398.5	4 400 949 907.85	-\$1 783 175 024.66	
6412.0	1135.27	0.849578513	5.753978	2186.093	43 066 033.67	\$2 576 058 615.66	
4221.1	1128.34	0.789074004	4.970899	1793.587	35 333 663.97	\$2 583 713 482.93	
3479.7	1103.88	0.759165347	4.609306	1657.358	32 649 951.42	\$2 586 326 546.68	
3196.3	1154.94	0.734574655	4.324645	1676.928	33 035 482.37	\$2 585 857 273.97	
2415.2	1165.42	0.674520033	3.67739	1622.815	31 969 452.30	\$2 586 853 603.32	
2108.1	1165.06	0.644054298	3.375044	1616.344	31 841 981.72	\$2 586 911 157.33	
1836.6	1152.27	0.614484471	3.098329	1607.805	31 673 753.77	\$2 587 011 875.80	
1635.4	1156.57	0.585749619	2.845226	1635.461	32 218 577.16	\$2 586 398 637.66	
1475.5	1157.85	0.560319531	2.634222	1666.141	32 822 968.92	\$2 585 661 791.08	
1262.4	1163.70	0.520342249	2.327171	1737.528	34 229 301.48	\$2 584 128 774.00	
1098.2	1168.05	0.484580846	2.078041	1817.59	35 806 522.92	\$2 582 428 599.83	
919.2	1171.00	0.439774437	1.799943	1935.456	38 128 489.47	\$2 579 986 152.01	
819.4	1169.10	0.412064209	1.646904	2012.347	39 643 236.01	\$2 578 356 822.77	
744.2	1173.00	0.388174614	1.52659	2093.14	41 234 855.49	\$2 576 535 302.33	
650.8	1178.62	0.355753616	1.380525	2208.651	43 510 426.19	\$2 573 611 514.80	
523.2	1182.37	0.306768363	1.197439	2373.948	46 766 778.21	\$2 569 749 658.70	
440.9	1180.76	0.271878585	1.094631	2469.109	48 641 445.75	\$2 567 302 933.06	
382.4	1184.33	0.244079631	1.029151	2537.277	49 984 358.32	\$2 565 408 326.51	
349.7	1186.17	0.227693418	0.997381	2566.511	50 560 272.18	\$2 563 781 200.77	
312.1	1183.96	0.208618848	0.966777	2579.137	50 808 995.54	\$2 562 541 719.09	
251.4	1175.43	0.17618085	0.93049	2555.642	50 346 145.43	\$2 562 054 490.85	
255.3	1185.15	0.177247476	0.931368	2577.69	50 780 488.59	\$2 560 691 739.11	

C₈/Ru: 7000

Reactor Cost (\$\$) & EP					
V (m3)	Conversion	EP	D (m)	H (m)	EP
#DIV/0!	1.0000	#DIV/0!	#DIV/0!	#DIV/0!	#DIV/0!
2.100079884	0.0507	\$2 700 801 319.82	5.735604	5.735604304	\$2 700 056 407.35
7.397687255	0.0872	\$2 700 702 426.93	20.20409	20.20409185	\$2 700 158 733.76
13.04269486	0.2079	\$2 700 613 001.08	35.62138	35.62137676	\$2 698 706 207.62
18.12878283	0.1841	\$2 700 539 102.61	49.51218	49.51217602	\$2 696 802 558.63
23.75663957	0.2847	\$2 700 462 050.87	64.88262	64.88261957	\$2 694 065 477.16
28.78375774	0.2956	\$2 700 396 297.74	78.61236	78.61236426	\$2 691 076 390.89
34.91125277	0.2955	\$2 700 319 179.05	95.34739	95.34738809	\$2 686 755 414.65
40.20709896	0.3453	\$2 700 254 701.41	109.8111	109.8110656	\$2 682 432 872.31
45.56036163	0.4064	\$2 700 191 232.91	124.4316	124.4315554	\$2 677 518 782.47
51.56595159	0.3835	\$2 700 121 779.86	140.8336	140.8336398	\$2 671 363 649.20
56.71449963	0.4229	\$2 700 063 522.54	154.895	154.895026	\$2 665 553 211.64
68.01549255	0.4740	\$2 699 939 185.11	185.7596	185.7595775	\$2 651 098 281.70
79.18120102	0.5180	\$2 699 820 350.40	216.2546	216.2546487	\$2 634 558 448.90
90.47504064	0.5427	\$2 699 703 523.94	247.0997	247.0996635	\$2 615 585 390.96
101.7350672	0.5729	\$2 699 589 923.42	277.8523	277.8523301	\$2 594 456 860.18
112.9329086	0.5944	\$2 699 479 422.81	308.4352	308.4351609	\$2 571 283 476.07
135.6051249	0.6107	\$2 699 262 104.24	370.3561	370.3560727	\$2 517 866 364.80
204.3135699	0.7259	\$2 698 642 675.74	558.0082	558.0081978	\$2 304 346 933.72
271.7981023	0.7450	\$2 698 074 411.52	742.3177	742.3176506	\$2 021 575 025.26
340.1615081	0.7575	\$2 697 527 101.61	929.0274	929.0274266	\$1 663 727 575.45
408.010624	0.7563	\$2 697 005 398.27	1114.333	1114.332607	\$1 239 324 413.00
544.1938992	0.7873	\$2 696 007 073.21	1486.268	1486.267687	\$184 796 472.55
679.257964	0.7961	\$2 695 065 679.07	1855.146	1855.146051	-\$1 121 319 717.48
814.3477125	0.7976	\$2 694 161 084.09	2224.095	2224.09456	-\$2 680 386 916.18
950.2182847	0.8072	\$2 693 281 175.63	2595.176	2595.175606	-\$4 498 129 842.91

Flash-drum							
Total volume flow (m ³ /hr)	Drum-volume	D (m)	H (m)	tw (m)	shell mass (kg)	cost (\$)	EP
#DIV/0!	#DIV/0!	#DIV/0!	#DIV/0!	#DIV/0!	#DIV/0!	#DIV/0!	#DIV/0!
126.004793	10.4999794	1.88	3.77	0.001589035	283.4321287	8716.674918	\$2 700 792 603.14
177.5444941	14.7947827	2.11	4.22	0.00178145	399.3642838	13271.43271	\$2 700 689 155.50
156.5123383	13.04217315	2.02	4.05	0.001708129	352.055062	11486.79232	\$2 700 601 514.29
145.0302627	12.08537179	1.97	3.95	0.001665293	326.2275592	10472.00765	\$2 700 528 630.60
142.5398374	11.87784465	1.96	3.93	0.001655706	320.625657	10247.71593	\$2 700 451 803.15
138.1620371	11.51304255	1.94	3.88	0.001638579	310.7783391	9849.607073	\$2 700 386 448.13
139.6450111	11.63661877	1.95	3.90	0.001644421	314.1141048	9985.02356	\$2 700 309 194.03
137.8529107	11.48728305	1.94	3.88	0.001637356	310.0829976	9821.306364	\$2 700 244 880.11
136.6810849	11.3896348	1.94	3.87	0.001632703	307.447121	9713.793728	\$2 700 181 519.11
137.5092042	11.45864199	1.94	3.88	0.001635994	309.3098726	9789.810013	\$2 700 111 990.05
136.1147991	11.34244621	1.93	3.87	0.001630445	306.1733315	9661.706065	\$2 700 053 860.83
136.0309851	11.33546199	1.93	3.86	0.001630111	305.9848023	9653.989392	\$2 699 929 531.12
135.7392017	11.31114768	1.93	3.86	0.001628944	305.3284719	9627.110336	\$2 699 810 723.29
135.712561	11.3089277	1.93	3.86	0.001628838	305.2685467	9624.655038	\$2 699 693 899.28
135.6467562	11.3034442	1.93	3.86	0.001628574	305.1205272	9618.589443	\$2 699 580 304.83
135.5194904	11.29283913	1.93	3.86	0.001628065	304.8342584	9606.855286	\$2 699 469 815.96
135.6051249	11.29997506	1.93	3.86	0.001628408	305.0268827	9614.75144	\$2 699 252 489.49
136.2090466	11.35029985	1.93	3.87	0.001630822	306.3853295	9670.381069	\$2 698 633 005.36
135.8990511	11.32446793	1.93	3.86	0.001629584	305.6880332	9641.838505	\$2 698 064 769.68
136.0646032	11.33826339	1.93	3.87	0.001630245	306.0604221	9657.084808	\$2 697 517 444.53
136.0035413	11.3331751	1.93	3.86	0.001630001	305.923071	9651.462257	\$2 696 995 746.80
136.0484748	11.3369194	1.93	3.87	0.001630181	306.0241432	9655.599807	\$2 695 997 417.61
135.8515928	11.32051323	1.93	3.86	0.001629394	305.5812816	9637.466524	\$2 695 056 041.61
135.7246188	11.30993248	1.93	3.86	0.001628886	305.2956693	9625.766346	\$2 694 151 458.33
135.7454692	11.31166995	1.93	3.86	0.001628969	305.3425698	9627.687939	\$2 693 271 547.94

Membrane Cost							
C8 + 2-C8 (kg/hr)	C12-C14 (kg/hr)	wt frac C8	flux	Area	Membrane cost	EP-cost	
#DIV/0!	#DIV/0!	#DIV/0!	#DIV/0!	#DIV/0!	#DIV/0!	#DIV/0!	#DIV/0!
112.4	1026.97	0.098651985	0.924158	2054.789	40 479 347.44	\$2 660 313 255.70	
36891.4	1082.50	0.971493563	7.541583	8392.125	165 324 865.22	\$2 535 364 290.28	
17948.8	1092.24	0.942637879	7.093158	4474.049	88 138 761.35	\$2 612 462 752.94	
9539.1	1112.49	0.895556956	6.395222	2775.928	54 685 785.51	\$2 645 842 845.08	
8381.2	1083.60	0.885513184	6.251742	2523.245	49 707 927.84	\$2 650 743 875.31	
5291.4	1079.22	0.830593985	5.500838	1930.192	38 024 783.97	\$2 662 361 664.16	
5141.6	1095.18	0.824398715	5.419701	1917.924	37 783 112.44	\$2 662 526 081.59	
4704.0	1083.00	0.81285772	5.270483	1830.016	36 051 306.21	\$2 664 193 573.90	
3571.2	1081.83	0.767500256	4.708378	1647.075	32 447 368.67	\$2 667 734 150.45	
3052.2	1096.90	0.735632031	4.33665	1594.603	31 413 669.53	\$2 668 698 320.52	
3072.3	1082.34	0.739484337	4.380568	1580.701	31 139 807.51	\$2 668 914 053.32	
2506.2	1086.33	0.697616746	3.918272	1528.12	30 103 971.37	\$2 669 825 559.75	
2010.8	1090.96	0.648280206	3.415937	1513.392	29 813 817.40	\$2 669 996 905.89	
1686.3	1093.75	0.606568245	3.027047	1530.655	30 153 898.65	\$2 669 540 000.63	
1496.3	1095.59	0.577307098	2.773822	1557.371	30 680 206.78	\$2 668 900 098.05	
1300.3	1087.94	0.544464722	2.50884	1586.571	31 255 438.94	\$2 668 214 377.02	
1176.8	1089.95	0.519154602	2.31851	1629.447	32 100 101.32	\$2 667 152 388.17	
992.5	1102.64	0.473716305	2.007131	1739.743	34 272 940.94	\$2 664 360 064.42	
600.4	1104.83	0.352101556	1.365314	2081.636	41 008 225.06	\$2 657 056 544.62	
541.1	1107.05	0.328324251	1.27243	2158.851	42 529 373.08	\$2 654 988 071.45	
504.4	1100.34	0.314305206	1.222663	2187.456	43 092 885.77	\$2 653 902 861.03	
493.4	1107.53	0.308182859	1.202091	2219.605	43 726 213.75	\$2 652 271 203.86	
413.6	1105.64	0.272264638	1.095643	2311.114	45 528 938.85	\$2 649 527 102.76	
392.2	1105.36	0.261905088	1.069462	2333.854	45 976 932.09	\$2 648 174 526.24	
383.8	1104.85	0.257841122	1.059744	2341.288	46 123 374.85	\$2 647 148 173.09	

C₈/Ru: 10 000

Reactor Cost (\$\$) & EP					
V (m ³)	Conversion	EP	D (m)	H (m)	EP
#DIV/0!	1.000	#DIV/0!	#DIV/0!	#DIV/0!	#DIV/0!
5.8	0.015	\$2 761 782 691.7	\$15.8	\$15.8	\$2 761 493 392.95
13.7	0.068	\$2 761 655 033.4	\$37.5	\$37.5	\$2 759 532 424.20
13.5	0.171	\$2 761 658 445.3	\$36.9	\$36.9	\$2 759 608 457.32
17.7	0.258	\$2 761 597 258.5	\$48.4	\$48.4	\$2 758 028 625.32
23.0	0.333	\$2 761 525 085.9	\$62.7	\$62.7	\$2 755 544 750.73
28.4	0.393	\$2 761 454 083.8	\$77.5	\$77.5	\$2 752 398 557.32
33.9	0.441	\$2 761 384 422.2	\$92.5	\$92.5	\$2 748 592 166.30
39.4	0.477	\$2 761 317 044.3	\$107.5	\$107.5	\$2 744 197 187.68
45.0	0.503	\$2 761 249 603.3	\$123.0	\$123.0	\$2 739 064 262.38
50.7	0.520	\$2 761 184 308.6	\$138.4	\$138.4	\$2 733 368 008.42
56.3	0.522	\$2 761 120 864.3	\$153.7	\$153.7	\$2 727 124 795.09
67.7	0.541	\$2 760 995 335.9	\$184.8	\$184.8	\$2 712 632 278.56
78.8	0.577	\$2 760 876 358.5	\$215.3	\$215.3	\$2 696 157 665.16
90.3	0.607	\$2 760 757 986.2	\$246.5	\$246.5	\$2 677 001 554.38
101.3	0.633	\$2 760 646 775.2	\$276.6	\$276.6	\$2 656 393 679.68
112.1	0.651	\$2 760 539 771.6	\$306.2	\$306.2	\$2 634 097 072.12
135.7	0.684	\$2 760 313 868.7	\$370.5	\$370.5	\$2 578 754 546.49
203.9	0.722	\$2 759 699 002.5	\$556.8	\$556.8	\$2 367 066 270.34
271.9	0.745	\$2 759 126 261.7	\$742.5	\$742.5	\$2 082 327 388.66
339.8	0.755	\$2 758 582 020.2	\$928.1	\$928.1	\$1 726 648 593.34
407.7	0.771	\$2 758 060 488.6	\$1 113.3	\$1 113.3	\$1 302 807 030.10
542.9	0.801	\$2 757 068 815.4	\$1 482.7	\$1 482.7	\$257 291 778.54
678.3	0.804	\$2 756 124 645.4	\$1 852.5	\$1 852.5	-\$1 050 016 500.85
813.6	0.825	\$2 755 218 207.4	\$2 222.1	\$2 222.1	-\$2 610 337 660.59
947.8	0.836	\$2 754 349 263.2	\$2 588.4	\$2 588.4	-\$4 401 924 899.57

Flash-drum								
Total volume flow (m ³ /hr)	Drum-volume	D (m)	H (m)	tw (m)	shell mass (kg)	cost (\$)	EP	#DIV/0!
#DIV/0!	#DIV/0!	#DIV/0!	#DIV/0!	#DIV/0!	#DIV/0!	#DIV/0!	#DIV/0!	#DIV/0!
346.85	28.90	2.64	5.28	0.002226991	780.2	25384.0	\$2 761 757 308	
329.61	27.47	2.60	5.19	0.002189463	741.4	24281.1	\$2 761 630 752	
162.06	13.50	2.05	4.10	0.001728073	364.5	11966.3	\$2 761 646 479	
141.75	11.81	1.96	3.92	0.001652648	318.9	10176.4	\$2 761 587 082	
137.76	11.48	1.94	3.88	0.001636989	309.9	9812.8	\$2 761 515 273	
136.14	11.34	1.93	3.87	0.001630549	306.2	9664.1	\$2 761 444 420	
135.49	11.29	1.93	3.86	0.001627944	304.8	9604.1	\$2 761 374 818	
135.01	11.25	1.93	3.86	0.001626029	303.7	9560.0	\$2 761 307 484	
135.15	11.26	1.93	3.86	0.001626569	304.0	9572.4	\$2 761 240 031	
135.14	11.26	1.93	3.86	0.001626554	304.0	9572.1	\$2 761 174 737	
135.05	11.25	1.93	3.86	0.001626189	303.8	9563.7	\$2 761 111 301	
135.33	11.28	1.93	3.86	0.001627314	304.4	9589.6	\$2 760 985 746	
135.14	11.26	1.93	3.86	0.001626564	304.0	9572.3	\$2 760 866 786	
135.41	11.28	1.93	3.86	0.001627608	304.6	9596.3	\$2 760 748 390	
135.05	11.25	1.93	3.86	0.001626175	303.8	9563.4	\$2 760 637 212	
134.54	11.21	1.93	3.85	0.001624134	302.6	9516.4	\$2 760 530 255	
135.67	11.31	1.93	3.86	0.001628666	305.2	9620.7	\$2 760 304 248	
135.91	11.32	1.93	3.86	0.001629608	305.7	9642.4	\$2 759 689 360	
135.93	11.33	1.93	3.86	0.001629711	305.8	9644.8	\$2 759 116 617	
135.93	11.33	1.93	3.86	0.001629725	305.8	9645.1	\$2 758 572 375	
135.88	11.32	1.93	3.86	0.001629522	305.7	9640.4	\$2 758 050 848	
135.72	11.31	1.93	3.86	0.001628868	305.3	9625.3	\$2 757 059 190	
135.66	11.30	1.93	3.86	0.001628621	305.1	9619.7	\$2 756 115 026	
135.60	11.30	1.93	3.86	0.001628404	305.0	9614.7	\$2 755 208 593	
135.39	11.28	1.93	3.86	0.001627561	304.6	9595.2	\$2 754 339 668	

Membrane Cost							
C8 + 2-C8 (kg/hr)	C12-C14 (kg/hr)	wt frac C8	flux	Area	Membrane cost	EP-cost	
#DIV/0!	#DIV/0!	#DIV/0!	#DIV/0!	#DIV/0!	#DIV/0!	#DIV/0!	
120251.2	1437.05	0.988190687	7.808233	25974.34	511 694 488.91	\$2 250 062 818.75	
138517.9	1152.47	0.991748628	7.865732	29594.7	583 015 582.38	\$2 178 615 169.90	
24430.5	1057.97	0.958492193	7.337594	5789.462	114 052 409.73	\$2 647 594 069.34	
8902.6	1063.66	0.893274082	6.362443	2610.699	51 430 762.90	\$2 710 156 319.24	
5380.5	1070.44	0.834064817	5.54661	1938.413	38 186 742.99	\$2 723 328 530.09	
3761.5	1074.39	0.777830083	4.832982	1667.671	32 853 113.57	\$2 728 591 306.12	
2875.9	1076.51	0.727632735	4.24635	1551.304	30 560 688.08	\$2 730 814 130.07	
2338.1	1077.76	0.684485074	3.780084	1506.081	29 669 803.03	\$2 731 637 681.25	
2010.8	1081.34	0.650296075	3.435562	1500.069	29 551 356.50	\$2 731 688 674.37	
1810.9	1084.15	0.625512323	3.199599	1508.01	29 707 805.27	\$2 731 466 931.28	
1703.8	1084.69	0.611011144	3.066907	1515.364	29 852 671.01	\$2 731 258 629.60	
1661.5	1092.92	0.603204844	2.997119	1531.679	30 174 067.02	\$2 730 811 679.33	
1489.5	1088.11	0.577867777	2.778523	1546.177	30 459 683.86	\$2 730 407 102.36	
1268.3	1093.59	0.536981991	2.451312	1605.861	31 635 456.46	\$2 729 112 933.42	
1102.2	1091.70	0.502399236	2.199157	1662.707	32 755 318.28	\$2 727 881 893.52	
976.5	1088.21	0.472935001	2.002118	1718.733	33 859 045.95	\$2 726 671 209.22	
882.6	1097.92	0.445639551	1.834192	1799.631	35 452 733.53	\$2 724 851 514.51	
742.2	1102.18	0.402407536	1.596974	1924.849	37 919 531.35	\$2 721 769 828.72	
610.0	1101.62	0.356379723	1.383158	2062.424	40 629 743.91	\$2 718 486 873.06	
540.4	1104.62	0.328494315	1.273057	2153.599	42 425 892.25	\$2 716 146 482.88	
504.6	1104.02	0.313689841	1.220563	2196.563	43 272 295.00	\$2 714 778 553.15	
448.9	1103.34	0.289199654	1.1428	2263.819	44 597 227.48	\$2 712 461 962.60	
376.9	1103.62	0.254579361	1.05217	2345.202	46 200 476.30	\$2 709 914 549.43	
361.4	1102.16	0.246957654	1.035254	2356.281	46 418 738.27	\$2 708 789 854.49	
312.2	1100.79	0.220970624	0.985812	2388.948	47 062 284.41	\$2 707 277 383.56	

C₈/Ru: 12 000

Reactor Cost (\$\$) & EP					
V (m3)	Conversion	EP	D (m)	H (m)	EP
#DIV/0!	1.0000	#DIV/0!	#DIV/0!	#DIV/0!	#DIV/0!
#DIV/0!	0.0663	#DIV/0!	#DIV/0!	#DIV/0!	#DIV/0!
#DIV/0!	0.0138	#DIV/0!	#DIV/0!	#DIV/0!	#DIV/0!
#DIV/0!	0.0098	#DIV/0!	#DIV/0!	#DIV/0!	#DIV/0!
155.5540562	0.0123	\$2 783 871 834.67	424.8393	424.8393222	\$2 548 581 639.47
99.18866435	0.0189	\$2 784 410 344.10	270.8978	270.8977571	\$2 684 221 643.04
67.05454866	0.0371	\$2 784 744 547.85	183.1351	183.1351088	\$2 737 212 416.69
52.73568877	0.0512	\$2 784 903 406.19	144.0284	144.0283514	\$2 754 881 516.63
53.65919841	0.0686	\$2 784 892 920.55	146.5506	146.5505821	\$2 753 855 340.46
55.83811499	0.0881	\$2 784 868 322.35	152.5015	152.5015001	\$2 751 371 758.88
60.53406646	0.0871	\$2 784 815 948.01	165.3268	165.3267834	\$2 745 722 606.17
65.71743505	0.1278	\$2 784 759 071.81	179.4833	179.4832693	\$2 739 020 294.73
74.34472771	0.1455	\$2 784 666 343.40	203.0456	203.0455811	\$2 726 790 581.17
84.92125798	0.1637	\$2 784 555 545.43	231.9315	231.9315263	\$2 709 990 119.42
95.15195137	0.1791	\$2 784 450 975.25	259.8729	259.8729439	\$2 691 870 936.03
104.5782051	0.1986	\$2 784 356 607.07	285.6173	285.6173273	\$2 673 571 185.99
115.099352	0.2020	\$2 784 253 263.77	314.352	314.352013	\$2 651 348 441.92
137.3009324	0.2223	\$2 784 041 116.64	374.9876	374.987554	\$2 598 320 091.41
203.7320386	0.2445	\$2 783 442 682.56	556.42	556.4199565	\$2 391 268 026.41
271.2093972	0.2630	\$2 782 874 196.83	740.7098	740.709817	\$2 109 142 443.68
336.8827456	0.2837	\$2 782 347 773.45	920.0727	920.0726797	\$1 767 296 922.06
402.0636093	0.2367	\$2 781 845 350.45	1098.09	1098.090499	\$1 364 038 484.24
540.7303564	0.2480	\$2 780 826 749.74	1476.808	1476.80828	\$299 708 565.34
693.6511122	0.4577	\$2 779 762 653.25	1894.456	1894.455699	-\$1 190 707 176.83
788.6145324	0.2871	\$2 779 125 888.50	2153.814	2153.813739	-\$2 279 376 665.25
959.8731399	0.2721	\$2 778 014 608.34	2621.544	2621.544331	-\$4 551 911 134.71

Flash-drum							
Total volume flow (m ³ /hr)	Drum-volume	D (m)	H (m)	tw (m)	shell mass (kg)	cost (\$)	EP
#DIV/0!	#DIV/0!	#DIV/0!	#DIV/0!	#DIV/0!	#DIV/0!	#DIV/0!	#DIV/0!
#DIV/0!	#DIV/0!	#DIV/0!	#DIV/0!	#DIV/0!	#DIV/0!	#DIV/0!	#DIV/0!
#DIV/0!	#DIV/0!	#DIV/0!	#DIV/0!	#DIV/0!	#DIV/0!	#DIV/0!	#DIV/0!
#DIV/0!	#DIV/0!	#DIV/0!	#DIV/0!	#DIV/0!	#DIV/0!	#DIV/0!	#DIV/0!
1244.43245	103.698556	4.04	8.08	0.003409272	2799.196204	67564.53049	\$2 783 804 270.14
595.1319861	49.5923484	3.16	6.32	0.002666095	1338.675471	39387.98262	\$2 784 370 956.11
321.8618335	26.82074659	2.58	5.15	0.002172173	723.9882107	23778.05247	\$2 784 720 769.80
210.9427551	17.57785978	2.24	4.47	0.001886801	474.4895228	15940.18151	\$2 784 887 466.01
183.9743945	15.3305863	2.14	4.27	0.001802701	413.827546	13799.87655	\$2 784 879 120.67
167.514345	13.95897037	2.07	4.14	0.00174725	376.8027092	12431.55017	\$2 784 855 890.80
161.4241772	13.45147669	2.05	4.09	0.001725814	363.1036335	11911.75598	\$2 784 804 036.26
157.7218441	13.14296127	2.03	4.06	0.001712518	354.7756951	11591.92588	\$2 784 747 479.89
148.6894554	12.39029232	1.99	3.98	0.001679182	334.4584587	10798.78541	\$2 784 655 544.61
145.5792994	12.13112302	1.98	3.95	0.001667392	327.4625491	10521.24693	\$2 784 545 024.18
142.7279271	11.89351816	1.96	3.93	0.001656434	321.0487413	10264.71003	\$2 784 440 710.54
139.4376068	11.61933578	1.95	3.90	0.001643606	313.6475747	9966.11934	\$2 784 346 640.95
138.1192224	11.50947481	1.94	3.88	0.001638441	310.6820328	9845.688874	\$2 784 243 418.08
137.3009324	11.4412867	1.94	3.88	0.001635168	308.8413909	9770.709207	\$2 784 031 345.94
135.8213591	11.31799385	1.93	3.86	0.001629273	305.5132746	9634.680996	\$2 783 433 047.88
135.6046986	11.29993954	1.93	3.86	0.001628406	305.0259238	9614.712139	\$2 782 864 582.12
134.7530983	11.22897568	1.93	3.85	0.00162499	303.1103546	9536.099053	\$2 782 338 237.36
134.0212031	11.16798686	1.92	3.85	0.001622043	301.4640474	9468.377293	\$2 781 835 882.07
135.1825891	11.26476515	1.93	3.86	0.001626715	304.0764409	9575.771049	\$2 780 817 173.97
138.7302224	11.56038944	1.95	3.89	0.001640822	312.0564014	9901.558802	\$2 779 752 751.69
131.4357554	10.9525415	1.91	3.82	0.001611545	295.6484039	9227.954232	\$2 779 116 660.54
137.1247343	11.42660411	1.94	3.88	0.001634468	308.4450552	9754.540863	\$2 778 004 853.80

Membrane Cost							
C8 + 2-C8 (kg/hr)	C12-C14 (kg/hr)	wt frac C8	flux	Area	Membrane cost	EP-cost	
#DIV/0!	#DIV/0!	#DIV/0!	#DIV/0!	#DIV/0!	#DIV/0!	#DIV/0!	#DIV/0!
#DIV/0!	#DIV/0!	#DIV/0!	#DIV/0!	#DIV/0!	#DIV/0!	#DIV/0!	#DIV/0!
#DIV/0!	#DIV/0!	#DIV/0!	#DIV/0!	#DIV/0!	#DIV/0!	#DIV/0!	#DIV/0!
#DIV/0!	2454.59	#DIV/0!	#DIV/0!	#DIV/0!	#DIV/0!	#DIV/0!	#DIV/0!
798911.3	1704.72	0.997870744	7.965229	167523.1	3 300 205 487.51	-\$516 401 217.38	
335056.4	1399.46	0.995840572	7.932156	70694.5	1 392 681 607.08	\$1 391 689 349.03	
140030.6	1119.44	0.992069153	7.870924	29888.48	588 803 146.75	\$2 195 917 623.04	
60739.1	1107.32	0.982095699	7.710288	13368.81	263 365 507.25	\$2 521 521 958.75	
41511.3	1065.13	0.974983094	7.596875	9340.776	184 013 280.94	\$2 600 865 839.73	
29722.7	1080.33	0.964927825	7.438169	6902.017	135 969 742.42	\$2 648 886 148.38	
25385.9	1066.70	0.959675002	7.35602	5993.403	118 070 045.19	\$2 666 733 991.07	
21165.9	1077.79	0.951546183	7.22992	5127.692	101 015 523.08	\$2 683 731 956.81	
14998.2	1064.99	0.933699978	6.957446	3847.959	75 804 786.35	\$2 708 850 758.26	
12770.7	1069.71	0.922710921	6.792655	3395.926	66 899 749.71	\$2 717 645 274.48	
11112.4	1061.01	0.912841826	6.646599	3052.534	60 134 926.20	\$2 724 305 784.34	
9689.0	1048.52	0.902349629	6.493337	2756.03	54 293 798.21	\$2 730 052 842.74	
8751.7	1044.39	0.893386464	6.364054	2565.468	50 539 727.93	\$2 733 703 690.16	
8166.9	1044.14	0.886643153	6.267789	2449.313	48 251 465.30	\$2 735 779 880.63	
7116.1	1038.67	0.872630723	6.070495	2238.911	44 106 543.65	\$2 739 326 504.23	
6310.5	1053.09	0.856987072	5.854608	2096.231	41 295 760.34	\$2 741 568 821.78	
5661.0	1046.12	0.844028834	5.679275	1968.306	38 775 627.05	\$2 743 562 610.31	
5829.0	1038.67	0.848759702	5.742919	1993.082	39 263 719.10	\$2 742 572 162.98	
6660.4	1037.92	0.865175292	5.967032	2150.225	42 359 438.12	\$2 738 457 735.85	
8550.6	1045.38	0.891061309	6.330764	2526.29	49 767 917.29	\$2 729 984 834.40	
3982.5	1037.03	0.793402492	5.024627	1664.984	32 800 178.17	\$2 746 316 482.37	
5404.3	1069.75	0.834763109	5.555846	1942.109	38 259 555.88	\$2 739 745 297.92	

C₈Ru: 14 000

Reactor Cost (\$\$) & EP						
V (m3)	Conversion	EP	D (m)	H (m)	EP	
#DIV/0!	1.0000	#DIV/0!	#DIV/0!	#DIV/0!	#DIV/0!	
2.651258996	0.0501	\$2 802 543 612.45	7.24094956	7.24094956	\$2 802 562 059.99	
7.533991306	0.0731	\$2 802 454 087.57	20.57635679	20.57635679	\$2 801 886 097.72	
13.33115111	0.1251	\$2 802 362 624.82	36.40919008	36.40919008	\$2 800 367 013.50	
18.422422	0.1651	\$2 802 288 927.00	50.31414459	50.31414459	\$2 798 429 899.68	
23.73902423	0.1926	\$2 802 216 238.58	64.83450969	64.83450969	\$2 795 829 009.19	
29.10390033	0.2214	\$2 802 146 144.96	79.48671729	79.48671729	\$2 792 622 888.71	
34.61746255	0.2438	\$2 802 076 763.71	94.54500695	94.54500695	\$2 788 733 303.36	
39.9600829	0.2753	\$2 802 011 622.10	109.1364311	109.1364311	\$2 784 400 422.12	
45.27623228	0.2857	\$2 801 948 515.27	123.6555594	123.6555594	\$2 779 547 185.90	
50.94748666	0.3231	\$2 801 882 807.06	139.1445278	139.1445278	\$2 773 782 562.41	
55.8508972	0.3408	\$2 801 827 170.74	152.5364101	152.5364101	\$2 768 315 923.34	
67.36520862	0.3709	\$2 801 700 173.85	183.9835634	183.9835634	\$2 753 746 757.17	
78.26042909	0.4029	\$2 801 583 969.51	213.7398951	213.7398951	\$2 737 760 269.76	
89.25758165	0.4372	\$2 801 469 923.68	243.7746171	243.7746171	\$2 719 492 039.64	
100.1917584	0.4601	\$2 801 359 291.40	273.6373435	273.6373435	\$2 699 236 218.14	
111.1434244	0.4758	\$2 801 250 881.48	303.5478358	303.5478358	\$2 676 884 298.65	
133.1317788	0.5185	\$2 801 039 389.23	363.6010275	363.6010275	\$2 625 866 253.35	
199.6142404	0.5789	\$2 800 437 489.91	545.1736886	545.1736886	\$2 423 128 323.59	
265.9495657	0.5993	\$2 799 876 389.51	726.3445004	726.3445004	\$2 150 635 612.59	
331.1568368	0.6341	\$2 799 351 787.25	904.4344426	904.4344426	\$1 816 656 128.85	
400.6222459	0.6534	\$2 798 815 267.05	1094.15394	1094.15394	\$1 390 594 358.02	
529.4437207	0.6470	\$2 797 866 504.78	1445.982939	1445.982939	\$413 626 879.57	
662.6843419	0.6528	\$2 796 932 978.71	1809.88123	1809.88123	-\$845 578 381.30	
793.9194612	0.6603	\$2 796 049 777.50	2168.302223	2168.302223	-\$2 326 869 544.32	
926.2413409	0.6741	\$2 795 188 471.79	2529.691305	2529.691305	-\$4 057 609 406.53	

Flash-drum							
Total volume flow (m3/hr)	Drum-volume	D (m)	H (m)	tw (m)	shell mass (kg)	cost (\$)	EP
#DIV/0!	#DIV/0!	#DIV/0!	#DIV/0!	#DIV/0!	#DIV/0!	#DIV/0!	#DIV/0!
159.0755398	13.25576473	2.04	4.07	0.001717403	357.8206652	11709.2111	\$2 802 531 903.24
180.8157913	15.06737989	2.12	4.25	0.001792324	406.7226605	13541.22504	\$2 802 440 546.35
159.9738133	13.33061786	2.04	4.08	0.00172063	359.84122	11786.81793	\$2 802 350 838.00
147.379376	12.2811234	1.98	3.97	0.001674236	331.5115978	10682.16475	\$2 802 278 244.84
142.4341454	11.86903733	1.96	3.92	0.001655297	320.3879159	10238.16261	\$2 802 206 000.41
139.6987216	11.64109447	1.95	3.90	0.001644632	314.2349198	9989.917262	\$2 802 136 155.04
138.4698502	11.53869262	1.94	3.89	0.001639795	311.4707263	9877.762385	\$2 802 066 885.95
137.0059985	11.41670986	1.94	3.87	0.001633996	308.1779738	9743.640708	\$2 802 001 878.46
135.8286968	11.31860531	1.93	3.86	0.001629302	305.52978	9635.357071	\$2 801 938 879.91
135.8599644	11.32121083	1.93	3.86	0.001629427	305.6001125	9638.237782	\$2 801 873 168.83
134.0421533	11.16973263	1.92	3.85	0.001622127	301.5111722	9470.31785	\$2 801 817 700.42
134.7304172	11.22708567	1.93	3.85	0.001624899	303.0593364	9534.002606	\$2 801 690 639.84
134.1607356	11.1796141	1.92	3.85	0.001622606	301.7779083	9481.299528	\$2 801 574 488.21
133.8863725	11.15675142	1.92	3.84	0.001621499	301.1607626	9455.885386	\$2 801 460 467.79
133.55890112	11.1319723	1.92	3.84	0.001620297	300.4918853	9428.317392	\$2 801 349 863.08
133.3721093	11.11389787	1.92	3.84	0.00161942	300.0039916	9408.193212	\$2 801 241 473.29
133.1317788	11.09387113	1.92	3.84	0.001618447	299.4633979	9385.880019	\$2 801 030 003.35
133.0761603	11.08923644	1.92	3.84	0.001618221	299.3382909	9380.71389	\$2 800 428 109.19
132.9747829	11.08078865	1.92	3.84	0.00161781	299.110255	9371.295221	\$2 799 867 018.22
132.4627347	11.03811969	1.92	3.83	0.001615731	297.9584664	9323.678426	\$2 799 342 463.58
133.5407486	11.12795058	1.92	3.84	0.001620102	300.3833247	9423.84072	\$2 798 805 843.21
132.3609302	11.02963631	1.91	3.83	0.001615317	297.7294696	9314.202564	\$2 797 857 190.58
132.5368684	11.04429724	1.92	3.83	0.001616032	298.1252208	9330.576875	\$2 796 923 648.13
132.3199102	11.02621812	1.91	3.83	0.00161515	297.6372003	9310.383645	\$2 796 040 467.12
132.3201916	11.02624156	1.91	3.83	0.001615151	297.6378332	9310.409841	\$2 795 179 161.38

Membrane Cost							
C8 + 2-C8 (kg/hr)	C12-C14 (kg/hr)	wt frac C8	flux	Area	Membrane cost	EP-cost	
#DIV/0!	#DIV/0!	#DIV/0!	#DIV/0!	#DIV/0!	#DIV/0!	#DIV/0!	
23758.0	1026.97	0.958564815	7.338725	5628.806	110 887 472.68	\$2 691 644 430.56	
39245.1	1071.16	0.973431087	7.572255	8873.678	174 811 461.63	\$2 627 629 084.71	
24351.2	1064.90	0.958101211	7.331509	5777.818	113 823 015.82	\$2 688 527 822.17	
14217.8	1062.29	0.930479053	6.908909	3686.082	72 615 808.21	\$2 729 662 436.63	
10560.2	1057.47	0.908977487	6.58991	2938.253	57 883 586.21	\$2 744 322 414.20	
8632.2	1056.05	0.890997041	6.329846	2550.942	50 253 553.27	\$2 751 882 601.78	
7275.3	1058.78	0.872957287	6.07505	2286.424	45 042 562.22	\$2 757 024 323.73	
6236.2	1056.56	0.8551218	5.829174	2085.136	41 077 182.12	\$2 760 924 696.34	
5436.5	1057.38	0.837172247	5.587783	1936.927	38 157 465.58	\$2 763 781 414.33	
4905.4	1063.71	0.821798192	5.385858	1847.155	36 388 946.18	\$2 765 484 222.65	
4182.0	1060.98	0.797637104	5.077532	1720.958	33 902 878.61	\$2 767 914 821.81	
3750.4	1064.78	0.778868881	4.845624	1656.188	32 626 911.40	\$2 769 063 728.45	
3228.0	1063.40	0.752204065	4.527565	1579.742	31 120 915.73	\$2 770 453 572.47	
2768.9	1067.98	0.721655141	4.179659	1529.993	30 140 871.90	\$2 771 319 595.90	
2402.6	1069.91	0.691893807	3.857648	1500.281	29 555 544.69	\$2 771 794 318.39	
2183.5	1070.22	0.671075198	3.642326	1488.839	29 330 127.82	\$2 771 911 345.47	
1963.4	1072.04	0.646828429	3.40185	1487.166	29 297 174.58	\$2 771 732 828.77	
1581.3	1077.07	0.594836565	2.923582	1515.472	29 854 798.92	\$2 770 573 310.27	
1249.1	1074.71	0.537523032	2.455437	1577.32	31 073 207.97	\$2 768 793 810.24	
1112.2	1075.99	0.508265667	2.240343	1627.845	32 068 549.15	\$2 767 273 914.43	
960.0	1083.77	0.469721015	1.981615	1718.943	33 863 177.70	\$2 764 942 665.50	
893.6	1079.52	0.452888505	1.877418	1751.63	34 507 105.83	\$2 763 350 084.75	
907.9	1074.49	0.457970957	1.908317	1731.316	34 106 916.71	\$2 762 816 731.42	
879.2	1077.81	0.449254213	1.855623	1757.725	34 627 176.24	\$2 761 413 290.87	
844.0	1084.19	0.437713868	1.788064	1797.268	35 406 175.73	\$2 759 772 985.65	

CAPITAL COST ESTIMATION FOR GCYC

Total Capital investment		
Equipment		Cost (\$)
Reactor		176 805 386.5
Flash drum		9385.88
Membrane		29297174.58
Heater		2161.5
Column		1531804.8
Agitator		16358.2
Total Equipment cost		207 662 271.57
item	% of purchased equipment	total cost
	Direct cost	
Equipment installation	47	97 601 267.64
Instrumentation and control	18	37 379 208.88
Piping	66	137 057 099.23
Electrical	11	22 842 849.87
Buildings (including services)	6	12 459 736.29
Yard improvements	10	20 766 227.16
Service facilities (installed)	30	62 298 681.47
Land	6	12 459 736.29
total Direct reaction unit plant cost		610 527 078.41
Indirect cost		
Engineering and supervision	33	68 528 549.62
Construction expenses	41	85 141 531.34
Contractor's fee an legal expenses	21	43 609 077.03
Contingency	35	72 681 795.05
total indirect reaction unit plant cost		269 960 953.04
Fixed Capital Investment (FCI)		880 488 031.44
Working capital	86	757 219 707.04
Total Capital Investment		1 637 707 738.48

PRODUCTION COST ESTIMATION FOR GCYC

Raw materials cost					
Material	Price .unit		Feedrate		USD/yr
1-Octene	1.8 USD/kg		3845.95 kg/hr		57 652 307.17
GCYC catalyst	22516.0 USD/kg		0.7597 kgCat/hr		142 455 533.77
Total					200 107 840.95
Labour operations					
Operators/ shift/section	Number of sections	Number of shifts	Hours per year	Wage rate (\$/h)	Direct wages & benefits (DW&B)
2	3	5	8328	30	7495200
Item			Factor	Total cost per year	
Direct salaries and benefits			0.15	1124280	
Operating supplies and services			0.06	449712	
Technical assistance to manufacturing				260000	
Control laboratory				285000	
Total labour-related operations annual cost				2118992	
TOTAL LABOUR-RELATED OPERATIONS ANNUAL COST				9 614 192.00	
Product sales					
ITEM	Cost/unit		Production rate	Revenue/yr	
7-Tetradecene	334.00 USD/Kg		1026.97 kg/hr	2 856 568 114.44	
Maintenance					
			Wage factor (% purchased Capital)	wages & benefits (MW&B)	
			0.035	21 368 447.74	
Item			Factor	Total cost per year	
Salaries and benefits			0.25	5 342 111.94	
materials and services			1	21 368 447.74	
Maintenance overhead			0.05	1 068 422.39	
				27778982.07	
Maintainance and Opeertaion benefits				49 147 429.81	
MAINTENANCE OPERATION SALARIES AND BENEFITS				58 761 621.81	
Overhead					
General plant overhead			0.071	4 172 075.15	
Utilities					
	Input (kw)	Cost/unit		Total Annual cost	
Electricity	40095.27	0.235292419 \$/kwh		78567295.19	

CUMULATIVE DISCOUNTED CASH FLOW ANALYSIS GCYC

Line	Item	0	1	2	3	4	5	6	7	8	9	10	11	12	13	14	15
1	Fixed Capital	-264146409	-352195213	-176097606													
2	Working capital			-757219707													
3	TOTAL CAPITAL INVESTMENT	-264146409	-352195213	-933317313													
4	Inflation Factor	1.000	1.063	1.130	1.201	1.277	1.357	1.443	1.534	1.630	1.733	1.842	1.958	2.082	2.213	2.352	2.500
5	Annual Income (Sales)	0	571313623	1713940869	2856568114	2856568114	2856568114	2856568114	2856568114	2856568114	2856568114	2856568114	2856568114	2856568114	2856568114	2856568114	2856568114
6	<i>Annual manufacturing cost</i>	-	-	-	-	-	-	-	-	-	-	-	-	-	-	-	-
a	Raw materials (Variable cost)	0	0	-45223131	-192288755	-255503683	-271600415	-288711241	-306900049	-326234752	-346787542	-368635157	-391859172	-416546299	-442788716	-470684405	-50037523
b	Labor (fixed cost)	0	0	-3259122	-11548154	-12275688	-13049057	-13871147	-14745029	-15673966	-16661426	-17711096	-18826895	-20012989	-21273808	-22614058	-24038743
c	Utilities (variable cost)	0	0	-88778608	-75497328	-100317075	-106637051	-113355185	-120496561	-128087845	-136157379	-144735294	-153853617	-163546395	-173849818	-184802357	-196444905
d	Maintenance (fixed cost)	0	0	-55535072	-59033782	-62752910	-66706343	-70908843	-75376100	-80124794	-85172656	-90538534	-96242461	-102305736	-108750998	-115602311	-122885256
h	Plant overhead (fixed cost)	0	0	-4714316	-5011317	-5327030	-5662633	-6019379	-6398600	-6801712	-7230220	-7685724	-8169924	-8684630	-9231761	-9813362	-10431604
	TOTAL ANNUAL MANUFACTURING COST																
6T	TOTAL ANNUAL MANUFACTURING COST	0	0	-197510249	-343379336	-436176386	-463655499	-492865795	-523916340	-556923069	-592009223	-629305804	-668952069	-711096050	-755895101	-803516492	-854138031
7	Annual General Expenses	0	0														
a	Administrative	0	0	-12911334	-41174243	-72947034	-77542697	-82427887	-87620844	-93140957	-99008837	-105246394	-111876917	-118925163	-126417448	-134381747	-142847797
b	Distribution/ selling	0	0	-19367000	-61761365	-109420551	-116314046	-123641830	-131431266	-139711436	-148513256	-157869591	-167815375	-178387744	-189626172	-201572621	-214271696
c	R&D	0	0	-32278334	-102935608	-182367585	-193856743	-206069717	-219052110	-232852393	-247522093	-263115985	-279692292	-297312907	-316043620	-335954368	-357119493
	TOTAL ANNUAL GENERAL EXPENSES	0	0	-64556668	-205871215	-364735170	-387713485	-412139435	-438104219	-465704785	-495044187	-526231970	-559384585	-594625813	-632087240	-671908736	-714238986
	TOTAL COST OF PRODUCTION (7T+6T)	0	0	-262066917	-549250552	-800911556	-851368984	-905005230	-962020559	-1022627855	-1087053409	-1155537774	-1228336654	-1305721863	-1387982341	-1475425228	-1568377017
9	Annual Operating Income (5-8)	0	0	309246706	1164690317	2055656559	2005199131	1951562885	1894547555	1833940260	1769514705	1701030340	1628231460	1550846251	1468585774	1381142886	1288191097
	Annual depreciation (fixed Cost)			-41089441	-41089441	-41089441	-41089441	-41089441	-41089441	-41089441	-41089441	-41089441	-41089441	-41089441	-41089441	-41089441	
10	Income before tax (9-10)	0	0	268157264	1123600875	2014567117	1964109689	1910473443	1853458114	1792850818	1728425264	1659940899	1587142019	1509756810	1427496332	1340053445	1247101656
11	Income after tax	0	0	267406424	1120454793	2008926329	1958610182	1905124117	1848268431	1787830836	1723585673	1655293064	1582698021	1505529491	1423499343	1336301295	1243609771
13	Annual cash income (10+12)	0	0	226316983	1079365352	1967836888	1917520740	1864034676	1807178989	1746741395	1682496231	1614203623	1541608580	1464440049	1382409901	1295211854	1202520329
14	Annual Cash flow (3+13)	-264146409	-352195213	-707000331	1079365352	1967836888	1917520740	1864034676	1807178989	1746741395	1682496231	1614203623	1541608580	1464440049	1382409901	1295211854	1202520329
15	Cumulative cash flow	-264146409	-616341622	-1323341953	-243976601	1723860286	3641381027	5505415703	7312594692	9059336087	10741832318	12356035941	13897644521	15362084570	1674494471	1809706325	1924226654
16	Discount factor for % interest	1.00	0.87	0.76	0.66	0.57	0.50	0.43	0.38	0.33	0.28	0.25	0.21	0.19	0.16	0.14	0.12
17	Discounted Cash flow (Present value)	-264146409	-306256707	-534593823	709700239	1125117127	953346702	805873630	679385520	571012860	478270437	399006448	331358316	273714316	224680257	183050553	147783117
18	CUMULATIVE DISCOUNTED CASH FLOW	-264146409	-570403116	-1104996939	-395296700	729820428	1683167129	248904760	3168426279	3739439140	4217709577	4616716025	4948074341	5221788657	5446468914	5629519467	5777302584
19	IRR factor	1.000	0.577	0.333	0.192	0.111	0.064	0.037	0.021	0.012	0.007	0.004	0.002	0.001	0.000	0.000	0.000
20	IRR Discounted cash flow	-264146409	-203197941	-235337603	207288895	218038164	122579923	68749432	38454941	21444477	11917270	6596550	3634700	1992057	1084933	586466	314145
21	CUMULATIVE IRR DISCOUNTED CASH FLOW	-264146409	-467344350	-702681954	-495393059	-277354895	-154774972	-86025539	-47570598	-26126122	-14208851	-7612301	-3977601	-198544	-900611	-314145	0

ECONOMIC POTENTIAL AND EQUIPMENT COST FOR THE GMPP CATALYST AT VARIED TEMPERATURES

40°C

Reactor Cost (\$\$) & EP						
V (m3)	Conversion	D (m)	H (m)	Cost (\$)	H/D based	EP
#DIV/0!	1.0000	#DIV/0!	#DIV/0!	#DIV/0!	#DIV/0!	#DIV/0!
#DIV/0!	0.0034	#DIV/0!	#DIV/0!	#DIV/0!	#DIV/0!	#DIV/0!
#DIV/0!	0.0091	#DIV/0!	#DIV/0!	#DIV/0!	#DIV/0!	#DIV/0!
#DIV/0!	0.0086	#DIV/0!	#DIV/0!	#DIV/0!	#DIV/0!	#DIV/0!
#DIV/0!	0.0085	#DIV/0!	#DIV/0!	#DIV/0!	#DIV/0!	#DIV/0!
#DIV/0!	0.0086	#DIV/0!	#DIV/0!	#DIV/0!	#DIV/0!	#DIV/0!
#DIV/0!	0.0096	#DIV/0!	#DIV/0!	#DIV/0!	#DIV/0!	#DIV/0!
#DIV/0!	0.0077	#DIV/0!	#DIV/0!	#DIV/0!	#DIV/0!	#DIV/0!
#DIV/0!	0.0074	#DIV/0!	#DIV/0!	#DIV/0!	#DIV/0!	#DIV/0!
#DIV/0!	0.0080	#DIV/0!	#DIV/0!	#DIV/0!	#DIV/0!	#DIV/0!
#DIV/0!	0.0076	#DIV/0!	#DIV/0!	#DIV/0!	#DIV/0!	#DIV/0!
#DIV/0!	0.0074	#DIV/0!	#DIV/0!	#DIV/0!	#DIV/0!	#DIV/0!
#DIV/0!	0.0138	#DIV/0!	#DIV/0!	#DIV/0!	#DIV/0!	#DIV/0!
459.4491164	0.0131	1254.818	1254.818	451 481 125.57	\$2 756 085 017.50	
364.0400969	0.0210	994.2431	994.2431	291 063 170.12	\$2 758 682 702.10	
365.3850168	0.0133	997.9163	997.9163	293 094 527.08	\$2 758 645 205.26	
337.8275542	0.0528	922.6531	922.6531	252 800 963.06	\$2 759 419 208.76	
194.591567	0.0639	531.4561	531.4561	89 319 794.79	\$2 763 684 851.10	
278.9754983	0.0637	761.9201	761.9201	176 196 556.62	\$2 761 116 613.08	
370.2056836	0.0593	1011.082	1011.082	300 430 123.59	\$2 758 511 029.22	
431.9606072	0.0985	1179.743	1179.743	401 890 256.70	\$2 756 821 303.55	
476.7993554	0.1064	1302.204	1302.204	484 173 346.19	\$2 755 624 837.72	
625.6103047	0.1149	1708.627	1708.627	808 144 398.65	\$2 751 802 059.60	
763.3581882	0.1308	2084.835	2084.835	1 176 211 785.66	\$2 748 424 428.56	
#DIV/0!	1.0000	#DIV/0!	#DIV/0!	#DIV/0!	#DIV/0!	#DIV/0!
#DIV/0!	1.0000	#DIV/0!	#DIV/0!	#DIV/0!	#DIV/0!	#DIV/0!

Flash-drum							
Total volume flow (m3/hr)	Drum-volume	D (m)	H (m)	tw (m)	shell mass (kg)	cost (\$)	EP
#DIV/0!	#DIV/0!	#DIV/0!	#DIV/0!	#DIV/0!	#DIV/0!	#DIV/0!	#DIV/0!
#DIV/0!	#DIV/0!	#DIV/0!	#DIV/0!	#DIV/0!	#DIV/0!	#DIV/0!	#DIV/0!
#DIV/0!	#DIV/0!	#DIV/0!	#DIV/0!	#DIV/0!	#DIV/0!	#DIV/0!	#DIV/0!
#DIV/0!	#DIV/0!	#DIV/0!	#DIV/0!	#DIV/0!	#DIV/0!	#DIV/0!	#DIV/0!
#DIV/0!	#DIV/0!	#DIV/0!	#DIV/0!	#DIV/0!	#DIV/0!	#DIV/0!	#DIV/0!
#DIV/0!	#DIV/0!	#DIV/0!	#DIV/0!	#DIV/0!	#DIV/0!	#DIV/0!	#DIV/0!
#DIV/0!	#DIV/0!	#DIV/0!	#DIV/0!	#DIV/0!	#DIV/0!	#DIV/0!	#DIV/0!
#DIV/0!	#DIV/0!	#DIV/0!	#DIV/0!	#DIV/0!	#DIV/0!	#DIV/0!	#DIV/0!
#DIV/0!	#DIV/0!	#DIV/0!	#DIV/0!	#DIV/0!	#DIV/0!	#DIV/0!	#DIV/0!
#DIV/0!	#DIV/0!	#DIV/0!	#DIV/0!	#DIV/0!	#DIV/0!	#DIV/0!	#DIV/0!
#DIV/0!	#DIV/0!	#DIV/0!	#DIV/0!	#DIV/0!	#DIV/0!	#DIV/0!	#DIV/0!
#DIV/0!	#DIV/0!	#DIV/0!	#DIV/0!	#DIV/0!	#DIV/0!	#DIV/0!	#DIV/0!
787.6270566	65.63296263	3.47	6.94	0.002927148	1771.66922	48655.13432	\$2 756 036 362.37
546.0601453	45.50319191	3.07	6.14	0.002590705	1228.294462	36841.16406	\$2 758 645 860.93
487.1800224	40.59671127	2.96	5.91	0.002494026	1095.85094	33660.96617	\$2 758 611 544.29
405.3930651	33.78140411	2.78	5.56	0.00234583	911.8813393	28974.96848	\$2 759 390 233.79
194.591567	16.21531527	2.18	4.35	0.001836732	437.7095564	14656.55591	\$2 763 670 194.54
185.9836656	15.49801885	2.14	4.29	0.00180924	418.3471515	13963.48769	\$2 761 102 649.59
185.1028418	15.42461981	2.14	4.28	0.001806379	416.3658479	13891.85136	\$2 758 497 137.37
172.7842429	14.39811096	2.09	4.19	0.001765384	388.6566899	12875.26304	\$2 756 808 428.29
158.9331185	13.24389676	2.04	4.07	0.001716891	357.5003062	11696.89045	\$2 755 613 140.83
156.4025762	13.03302667	2.02	4.05	0.00170773	351.8081657	11477.23544	\$2 751 790 582.36
152.6716376	12.72212756	2.01	4.02	0.001694041	343.415883	11150.77312	\$2 748 413 277.79
#DIV/0!	#DIV/0!	#DIV/0!	#DIV/0!	#DIV/0!	#DIV/0!	#DIV/0!	#DIV/0!
#DIV/0!	#DIV/0!	#DIV/0!	#DIV/0!	#DIV/0!	#DIV/0!	#DIV/0!	#DIV/0!

Membrane Cost						
C8 + 2-C8 (kg/hr)	C12-C14 (kg/hr)	wt frac C8	flux	Area	Membrane cost	EP-cost
#DIV/0!	#DIV/0!	#DIV/0!	#DIV/0!	#DIV/0!	#DIV/0!	#DIV/0!
#DIV/0!	#DIV/0!	#DIV/0!	#DIV/0!	#DIV/0!	#DIV/0!	#DIV/0!
#DIV/0!	#DIV/0!	#DIV/0!	#DIV/0!	#DIV/0!	#DIV/0!	#DIV/0!
#DIV/0!	#DIV/0!	#DIV/0!	#DIV/0!	#DIV/0!	#DIV/0!	#DIV/0!
#DIV/0!	#DIV/0!	#DIV/0!	#DIV/0!	#DIV/0!	#DIV/0!	#DIV/0!
#DIV/0!	#DIV/0!	#DIV/0!	#DIV/0!	#DIV/0!	#DIV/0!	#DIV/0!
#DIV/0!	#DIV/0!	#DIV/0!	#DIV/0!	#DIV/0!	#DIV/0!	#DIV/0!
#DIV/0!	#DIV/0!	#DIV/0!	#DIV/0!	#DIV/0!	#DIV/0!	#DIV/0!
#DIV/0!	#DIV/0!	#DIV/0!	#DIV/0!	#DIV/0!	#DIV/0!	#DIV/0!
#DIV/0!	#DIV/0!	#DIV/0!	#DIV/0!	#DIV/0!	#DIV/0!	#DIV/0!
#DIV/0!	#DIV/0!	#DIV/0!	#DIV/0!	#DIV/0!	#DIV/0!	#DIV/0!
#DIV/0!	#DIV/0!	#DIV/0!	#DIV/0!	#DIV/0!	#DIV/0!	#DIV/0!
#DIV/0!	#DIV/0!	#DIV/0!	#DIV/0!	#DIV/0!	#DIV/0!	#DIV/0!
#DIV/0!	#DIV/0!	#DIV/0!	#DIV/0!	#DIV/0!	#DIV/0!	#DIV/0!
#DIV/0!	#DIV/0!	#DIV/0!	#DIV/0!	#DIV/0!	#DIV/0!	#DIV/0!
1050.67	#DIV/0!	#DIV/0!	#DIV/0!	#DIV/0!	#DIV/0!	#DIV/0!
471100.8	1050.66	0.99777474	7.963664	98813.69	1 946 629 762.46	\$809 406 599.91
298378.6	1050.65	0.996491152	7.942746	62830.76	1 237 765 981.07	\$1 520 879 879.87
256280.4	1050.65	0.995917108	7.933402	54060.69	1 064 995 500.04	\$1 693 616 044.25
197800.9	1050.65	0.994716409	7.913877	41878.24	825 001 363.79	\$1 934 388 870.00
47077.3	1050.65	0.978169638	7.647568	10488.72	206 627 803.32	\$2 557 042 391.23
40922.9	1050.65	0.974968752	7.596648	9208.786	181 413 075.58	\$2 579 689 574.01
40293.0	1050.65	0.974587455	7.590595	9077.826	178 833 175.51	\$2 579 663 961.86
31485.1	1050.65	0.96770793	7.481858	7247.705	142 779 797.30	\$2 614 028 630.99
21581.7	1050.65	0.95357764	7.261316	5194.733	102 336 248.81	\$2 653 276 892.02
19772.4	1050.65	0.949543879	7.19905	4820.775	94 969 275.72	\$2 656 821 306.64
17104.8	1050.65	0.942130319	7.085411	4270.606	84 130 930.80	\$2 664 282 346.99
#DIV/0!	#DIV/0!	#DIV/0!	#DIV/0!	#DIV/0!	#DIV/0!	#DIV/0!
#DIV/0!	#DIV/0!	#DIV/0!	#DIV/0!	#DIV/0!	#DIV/0!	#DIV/0!

50°C

Reactor Cost (\$\$) & EP						
V (m3)	Conversion	D (m)	H (m)	Cost (\$)	H/D based	EP
#DIV/0!	1.0000	#DIV/0!	#DIV/0!	#DIV/0!	#DIV/0!	#DIV/0!
2.148450195	0.0139	5.86771	5.86771	18 199.02	\$2 771 165 268.21	
25.64036691	0.0136	70.02734	70.02734	1 953 848.71	\$2 769 854 711.94	
76.6365073	0.0138	209.3047	209.3047	15 406 555.79	\$2 767 725 567.97	
137.2372614	0.0140	374.8137	374.8137	46 230 873.24	\$2 765 558 989.86	
178.8413465	0.0166	488.4401	488.4401	76 175 329.56	\$2 764 186 927.00	
205.595116	0.0118	561.5083	561.5083	99 083 639.92	\$2 763 338 921.50	
#DIV/0!	0.0040	#DIV/0!	#DIV/0!	#DIV/0!	#DIV/0!	#DIV/0!
#DIV/0!	0.0113	#DIV/0!	#DIV/0!	#DIV/0!	#DIV/0!	#DIV/0!
322.2686476	0.0126	880.1596	880.1596	231 291 183.63	\$2 759 861 758.02	
320.4351592	0.0139	875.1521	875.1521	228 815 673.58	\$2 759 914 186.88	
255.3721787	0.0203	697.4562	697.4562	149 138 303.57	\$2 761 816 997.62	
159.2172735	0.0327	434.8441	434.8441	61 180 540.32	\$2 764 825 107.73	
152.3836296	0.0336	416.1805	416.1805	56 322 442.90	\$2 765 050 965.63	
184.2266985	0.0313	503.1482	503.1482	80 559 130.38	\$2 764 014 297.64	
198.4361002	0.0348	541.956	541.956	92 677 099.38	\$2 763 563 552.72	
267.1668375	0.0182	729.669	729.669	162 394 648.17	\$2 761 465 465.65	
#DIV/0!	0.0032	#DIV/0!	#DIV/0!	#DIV/0!	#DIV/0!	#DIV/0!
#DIV/0!	0.0589	#DIV/0!	#DIV/0!	#DIV/0!	#DIV/0!	#DIV/0!
366.8220482	0.0742	1001.841	1001.841	295 272 341.30	\$2 758 605 170.81	
421.5255834	0.1065	1151.244	1151.244	383 775 963.94	\$2 757 103 239.90	
472.5605696	0.1100	1290.627	1290.627	476 087 340.69	\$2 755 736 949.17	
613.6430745	0.1418	1675.943	1675.943	779 236 151.52	\$2 752 102 153.78	
1064.303944	0.0492	2906.759	2906.759	2 201 434 054.93	\$2 741 434 404.31	
1206.82133	0.1032	3295.993	3295.993	2 790 220 206.24	\$2 738 267 882.68	
1053.14322	0.2300	2876.278	2876.278	2 158 097 833.09	\$2 741 685 838.69	

Flash-drum							
Total volume flow (m ³ /hr)	Drum-volume	D (m)	H (m)	tw (m)	shell mass (kg)	cost (\$)	EP
#DIV/0!	#DIV/0!	#DIV/0!	#DIV/0!	#DIV/0!	#DIV/0!	#DIV/0!	#DIV/0!
128.9070117	10.74182128	1.90	3.80	0.001601143	289.9603091	8990.967189	\$2 771 156 277.25
615.3688058	51.27868259	3.20	6.39	0.002695978	1384.195683	40413.63863	\$2 769 814 298.31
919.6380876	76.63344184	3.65	7.31	0.003082313	2068.611634	54489.14032	\$2 767 671 078.83
1097.898091	91.48784791	3.88	7.75	0.00326983	2469.585367	61859.29963	\$2 765 497 130.56
1073.048079	89.41709643	3.85	7.69	0.003244971	2413.688353	60862.2737	\$2 764 126 064.72
986.8565566	82.23475686	3.74	7.48	0.003155652	2219.81123	57330.19084	\$2 763 281 591.31
#DIV/0!	#DIV/0!	#DIV/0!	#DIV/0!	#DIV/0!	#DIV/0!	#DIV/0!	#DIV/0!
#DIV/0!	#DIV/0!	#DIV/0!	#DIV/0!	#DIV/0!	#DIV/0!	#DIV/0!	#DIV/0!
966.8059429	80.56393922	3.72	7.43	0.003134134	2174.709865	56491.06656	\$2 759 805 266.95
854.4937578	71.20496484	3.57	7.13	0.003007743	1922.077557	51655.32785	\$2 759 862 531.56
612.8932288	51.07239276	3.19	6.38	0.002692358	1378.62718	40288.9019	\$2 761 776 708.72
318.434547	26.5351508	2.57	5.13	0.002164435	716.2789553	23553.95687	\$2 764 801 553.77
261.2290793	21.76821917	2.40	4.80	0.002026181	587.6023621	19658.1497	\$2 765 031 307.48
276.3400477	23.02741618	2.45	4.89	0.00206452	621.5926086	20717.85419	\$2 763 993 579.79
264.5814669	22.04757364	2.41	4.82	0.002034812	595.1431418	19895.31892	\$2 763 543 657.40
320.6002051	26.71561509	2.57	5.14	0.002169331	721.1503342	23695.67151	\$2 761 441 769.98
#DIV/0!	#DIV/0!	#DIV/0!	#DIV/0!	#DIV/0!	#DIV/0!	#DIV/0!	#DIV/0!
#DIV/0!	#DIV/0!	#DIV/0!	#DIV/0!	#DIV/0!	#DIV/0!	#DIV/0!	#DIV/0!
183.4110241	15.28364064	2.13	4.27	0.001800859	412.5603142	13753.87425	\$2 758 591 416.93
168.6102334	14.05029075	2.08	4.15	0.001751052	379.2677741	12524.27602	\$2 757 090 715.63
157.5201899	13.12615742	2.03	4.06	0.001711788	354.3220989	11574.42	\$2 755 725 374.75
153.4107686	12.78371935	2.01	4.02	0.00169677	345.0784663	11215.6994	\$2 752 090 938.08
212.8607888	17.73768953	2.24	4.49	0.001892502	478.8039015	16088.101	\$2 741 418 316.21
201.1368883	16.76073691	2.20	4.40	0.001857099	452.4324437	15175.37663	\$2 738 252 707.30
150.4490315	12.53691779	2.00	4.00	0.00168578	338.4164065	10954.77467	\$2 741 674 883.92

Membrane Cost							
C8 + 2-C8 (kg/hr)	C12-C14 (kg/hr)	wt frac C8	flux	Area	Membrane cost	EP-cost	
#DIV/0!	#DIV/0!	#DIV/0!	#DIV/0!	#DIV/0!	#DIV/0!	#DIV/0!	#DIV/0!
113.0	1050.65	0.097108175	0.925183	2096.242	41 295 974.76	\$2 729 860 302.48	
346851.4	1886.83	0.994589561	7.911815	73463.59	1 447 232 639.89	\$1 322 581 658.41	
563350.6	2700.97	0.995228404	7.922199	119085.5	2 345 984 976.68	\$421 686 102.14	
690414.2	3004.22	0.995667528	7.929341	145749.5	2 871 264 725.34	-\$105 767 594.78	
672261.2	3302.01	0.995112219	7.92031	142158.4	2 800 520 460.96	-\$36 394 396.23	
612278.7	2030.93	0.996693961	7.946049	128850.1	2 538 347 210.52	\$224 934 380.79	
#DIV/0!	#DIV/0!	#DIV/0!	#DIV/0!	#DIV/0!	#DIV/0!	#DIV/0!	#DIV/0!
#DIV/0!	2100.45	#DIV/0!	#DIV/0!	#DIV/0!	#DIV/0!	#DIV/0!	#DIV/0!
598053.2	1945.35	0.996757742	7.947088	125831.9	2 478 889 395.24	\$280 915 871.70	
517416.9	2202.83	0.995760684	7.930857	109197.9	2 151 198 519.88	\$608 664 011.68	
345802.3	1329.57	0.996169831	7.937515	72888.44	1 435 902 255.93	\$1 325 874 452.79	
135435.1	1197.59	0.991234978	7.857416	28981.68	570 939 051.63	\$2 193 862 502.14	
94364.9	1327.69	0.986125504	7.774967	20512.96	404 105 240.16	\$2 360 926 067.32	
105094.2	1385.67	0.986986513	7.788826	22784.74	448 859 442.34	\$2 315 134 137.44	
96831.4	1273.92	0.987014737	7.789281	20991.52	413 532 855.99	\$2 350 010 801.41	
136571.3	1516.19	0.989020104	7.821616	29424.34	579 659 470.74	\$2 181 782 299.24	
#DIV/0!	#DIV/0!	#DIV/0!	#DIV/0!	#DIV/0!	#DIV/0!	#DIV/0!	#DIV/0!
#DIV/0!	1161.39	#DIV/0!	#DIV/0!	#DIV/0!	#DIV/0!	#DIV/0!	#DIV/0!
38880.0	1207.87	0.969869321	7.515925	8889.531	175 123 751.18	\$2 583 467 665.75	
28420.6	1112.62	0.962326433	7.397421	6653.949	131 082 801.93	\$2 626 007 913.70	
20503.3	1103.27	0.94893824	7.189727	5008.675	98 670 904.49	\$2 657 054 470.26	
17564.0	1104.11	0.940856066	7.065983	4403.285	86 744 723.74	\$2 665 346 214.34	
39282.4	1566.07	0.961661478	7.387026	9216.275	181 560 612.77	\$2 559 857 703.44	
46799.0	1147.20	0.976073251	7.614196	10494.91	206 749 688.59	\$2 531 503 018.71	
15467.1	1088.10	0.93427413	6.966119	3960.882	78 029 366.93	\$2 663 645 516.99	

60°C

Reactor Cost (\$\$) & EP						
V (m3)	Conversion	D (m)	H (m)	Cost (\$)	H/D based	EP
#DIV/0!	1.0000	#DIV/0!	#DIV/0!	#DIV/0!	#DIV/0!	#DIV/0!
#DIV/0!	0.0084	#DIV/0!	#DIV/0!	#DIV/0!	#DIV/0!	#DIV/0!
#DIV/0!	0.0097	#DIV/0!	#DIV/0!	#DIV/0!	#DIV/0!	#DIV/0!
#DIV/0!	0.0143	#DIV/0!	#DIV/0!	#DIV/0!	#DIV/0!	#DIV/0!
#DIV/0!	0.0174	#DIV/0!	#DIV/0!	#DIV/0!	#DIV/0!	#DIV/0!
157.6957302	0.0189	430.6885	430.6885	60 082 531.17	\$2 764 875 225.41	
183.0186037	0.0221	499.8487	499.8487	79 565 691.60	\$2 764 052 934.72	
196.6720055	0.0194	537.138	537.138	91 129 348.66	\$2 763 619 152.54	
232.6927832	0.0169	635.5157	635.5157	125 144 682.27	\$2 762 502 277.25	
279.9904757	0.0186	764.6921	764.6921	177 407 513.61	\$2 761 086 767.93	
251.4268381	0.0121	686.681	686.681	144 822 541.71	\$2 761 935 305.25	
242.1112957	0.0222	661.2389	661.2389	134 869 023.07	\$2 762 216 135.91	
226.9160978	0.0259	619.7388	619.7388	119 349 826.48	\$2 762 678 920.93	
245.8755279	0.0308	671.5196	671.5196	138 850 960.95	\$2 762 102 401.95	
220.2807987	0.0249	601.6169	601.6169	112 853 172.26	\$2 762 882 934.43	
239.3148336	0.0330	653.6014	653.6014	131 946 089.77	\$2 762 300 858.25	
238.4035136	0.0348	651.1125	651.1125	131 000 057.12	\$2 762 328 510.53	
262.1520213	0.0401	715.9729	715.9729	156 693 571.41	\$2 761 614 541.55	
334.2381268	0.0590	912.8499	912.8499	247 758 988.02	\$2 759 520 936.10	
397.9069556	0.0590	1086.738	1086.738	344 229 266.23	\$2 757 746 609.88	
471.3589439	0.0840	1287.345	1287.345	473 806 733.41	\$2 755 768 767.44	
514.4787937	0.1038	1405.112	1405.112	558 854 674.47	\$2 754 636 774.44	
611.1073937	0.1669	1669.018	1669.018	773 174 462.17	\$2 752 165 889.00	
757.4690757	0.1222	2068.751	2068.751	1 159 156 403.20	\$2 748 566 180.33	
916.946199	0.1462	2504.305	2504.305	1 662 035 644.55	\$2 744 799 331.83	
1100.001166	0.1071	3004.253	3004.253	2 342 757 282.46	\$2 740 633 704.39	

Flash-drum							
Total volume flow (m3/hr)	Drum-volume	D (m)	H (m)	tw (m)	shell mass (kg)	cost (\$)	EP
#DIV/0!	#DIV/0!	#DIV/0!	#DIV/0!	#DIV/0!	#DIV/0!	#DIV/0!	#DIV/0!
#DIV/0!	#DIV/0!	#DIV/0!	#DIV/0!	#DIV/0!	#DIV/0!	#DIV/0!	#DIV/0!
#DIV/0!	#DIV/0!	#DIV/0!	#DIV/0!	#DIV/0!	#DIV/0!	#DIV/0!	#DIV/0!
#DIV/0!	#DIV/0!	#DIV/0!	#DIV/0!	#DIV/0!	#DIV/0!	#DIV/0!	#DIV/0!
#DIV/0!	#DIV/0!	#DIV/0!	#DIV/0!	#DIV/0!	#DIV/0!	#DIV/0!	#DIV/0!
946.1743815	78.84471121	3.69	7.38	0.00311168	2128.301731	55620.33001	\$2 764 819 605.08
878.4892978	73.20451318	3.60	7.20	0.003035638	1976.052543	52708.87685	\$2 764 000 225.84
786.6880219	65.55471286	3.47	6.94	0.002925984	1769.556977	48612.29138	\$2 763 570 540.25
797.8038282	66.480993	3.48	6.97	0.002939701	1794.560603	49118.14065	\$2 762 453 159.11
839.9714272	69.99481902	3.55	7.09	0.002990607	1889.411378	51011.95845	\$2 761 035 755.97
670.4715684	55.87039579	3.29	6.58	0.002774159	1508.142503	43140.1493	\$2 761 892 165.10
581.0671096	48.42032225	3.14	6.27	0.002644924	1307.038279	38666.90246	\$2 762 177 469.01
453.8321956	37.81783686	2.89	5.78	0.00243577	1020.839146	31791.51327	\$2 762 647 129.42
421.500905	35.12367041	2.82	5.63	0.002376497	948.113924	29925.80734	\$2 762 072 476.15
330.4211198	27.53399843	2.60	5.20	0.002191259	743.2414377	24333.58338	\$2 762 858 600.85
319.0864448	26.58947344	2.57	5.14	0.002165911	717.7453184	23596.65569	\$2 762 277 261.59
286.0842163	23.83939774	2.48	4.95	0.002088506	643.5109053	21388.9206	\$2 762 307 121.61
262.1520213	21.84512794	2.40	4.81	0.002028565	589.6784057	19723.56532	\$2 761 594 817.99
222.8254179	18.56804207	2.28	4.56	0.001921584	501.2180966	16848.15943	\$2 759 504 087.94
198.9534778	16.57879331	2.19	4.39	0.001850355	447.521133	15003.0678	\$2 757 731 606.81
188.5435776	15.71133632	2.15	4.31	0.001817503	424.1053556	14170.91586	\$2 755 754 596.52
171.4929312	14.29050596	2.09	4.18	0.001760975	385.7520448	12767.0443	\$2 754 624 007.40
152.7768484	12.73089478	2.01	4.02	0.00169443	343.6525416	11160.02264	\$2 752 154 728.97
151.4938151	12.62397962	2.00	4.01	0.001689673	340.7665176	11047.05118	\$2 748 555 133.28
152.8243665	12.73485446	2.01	4.02	0.001694606	343.7594276	11164.19932	\$2 744 788 167.63
157.1430238	13.09472817	2.03	4.06	0.00171042	353.4737106	11541.65362	\$2 740 622 162.74

Membrane Cost						
C8 + 2-C8 (kg/hr)	C12-C14 (kg/hr)	wt frac C8	flux	Area	Membrane cost	EP-cost
#DIV/0!	#DIV/0!	#DIV/0!	#DIV/0!	#DIV/0!	#DIV/0!	#DIV/0!
#DIV/0!	#DIV/0!	#DIV/0!	#DIV/0!	#DIV/0!	#DIV/0!	#DIV/0!
#DIV/0!	#DIV/0!	#DIV/0!	#DIV/0!	#DIV/0!	#DIV/0!	#DIV/0!
#DIV/0!	#DIV/0!	#DIV/0!	#DIV/0!	#DIV/0!	#DIV/0!	#DIV/0!
#DIV/0!	2969.47	#DIV/0!	#DIV/0!	#DIV/0!	#DIV/0!	#DIV/0!
486371.0	3031.15	0.993806431	7.899097	103261.2	2 034 245 600.16	\$730 574 004.92
434554.1	3137.25	0.992832281	7.883292	92535.65	1 822 952 214.23	\$941 048 011.62
391400.4	2619.00	0.993353131	7.89174	83213.45	1 639 305 006.82	\$1 124 265 533.44
420319.4	2567.19	0.993929374	7.901093	89204.23	1 757 323 412.96	\$1 005 129 746.15
435794.4	2658.17	0.993937392	7.901223	92486.22	1 821 978 611.92	\$939 057 144.06
386336.9	1819.50	0.995312466	7.923566	81645.99	1 608 426 037.21	\$1 153 466 127.88
289684.4	1757.60	0.993969285	7.901741	61472.12	1 211 000 677.99	\$1 551 176 791.02
199822.2	1794.37	0.991100082	7.855233	42777.55	842 717 764.97	\$1 919 929 364.45
171557.1	1906.02	0.989011954	7.821484	36962.97	728 170 457.78	\$2 033 902 018.37
143725.6	1413.98	0.990257763	7.841609	30848.16	607 708 828.16	\$2 155 149 772.69
119790.4	1444.36	0.988086264	7.806549	25883.13	509 897 697.32	\$2 252 379 564.27
100663.7	1324.83	0.987009969	7.789204	21822.63	429 905 717.64	\$2 332 401 403.96
85598.1	1310.15	0.984924863	7.755665	18676.31	367 923 221.45	\$2 393 671 596.54
61420.5	1177.53	0.981188987	7.695777	13556.79	267 068 793.22	\$2 492 435 294.72
44352.1	1177.53	0.974136988	7.583447	10006.35	197 125 139.13	\$2 560 606 467.68
37187.5	1169.24	0.969516818	7.510363	8511.966	167 685 737.23	\$2 588 068 859.29
25896.0	1137.65	0.957917325	7.328648	6147.927	121 114 162.58	\$2 633 509 844.81
17151.3	1072.74	0.94113595	7.070248	4295.956	84 630 336.07	\$2 667 524 392.91
14049.8	1104.11	0.927139912	6.858798	3682.351	72 542 307.18	\$2 676 012 826.10
15845.5	1089.34	0.935674337	6.987295	4039.435	79 576 862.32	\$2 665 211 305.31
17020.4	1128.63	0.93781298	7.01971	4309.056	84 888 400.26	\$2 655 733 762.48

70°C

Reactor Cost (\$\$) & EP						
V (m3)	Conversion	D (m)	H (m)	Cost (\$)	H/D based	EP
#DIV/0!	1.0000	#DIV/0!	#DIV/0!	#DIV/0!	#DIV/0!	#DIV/0!
#DIV/0!	0.0000	#DIV/0!	#DIV/0!	#DIV/0!	#DIV/0!	#DIV/0!
#DIV/0!	0.0119	#DIV/0!	#DIV/0!	#DIV/0!	#DIV/0!	#DIV/0!
#DIV/0!	0.0043	#DIV/0!	#DIV/0!	#DIV/0!	#DIV/0!	#DIV/0!
#DIV/0!	0.0072	#DIV/0!	#DIV/0!	#DIV/0!	#DIV/0!	#DIV/0!
#DIV/0!	0.0139	#DIV/0!	#DIV/0!	#DIV/0!	#DIV/0!	#DIV/0!
88.06264135	0.0249	240.5111	240.5111	20 023 361.32	\$2 767 296 487.13	
75.5356284	0.0370	206.2981	206.2981	14 991 814.73	\$2 767 767 560.09	
71.24884206	0.0373	194.5903	194.5903	13 427 611.72	\$2 767 932 264.40	
73.58011915	0.0450	200.9573	200.9573	14 268 230.01	\$2 767 842 455.03	
76.09310565	0.0547	207.8206	207.8206	15 201 172.17	\$2 767 746 280.39	
87.03573889	0.0617	237.7065	237.7065	19 585 268.79	\$2 767 334 573.33	
92.23400579	0.0732	251.9036	251.9036	21 849 644.90	\$2 767 142 677.25	
104.5281054	0.0936	285.4805	285.4805	27 665 174.27	\$2 766 697 153.69	
109.0694585	0.0950	297.8836	297.8836	29 975 606.42	\$2 766 535 283.01	
122.8243755	0.1191	335.4501	335.4501	37 501 661.78	\$2 766 052 940.36	
131.3222272	0.1380	358.6589	358.6589	42 544 727.28	\$2 765 760 386.35	
148.4923041	0.1552	405.5527	405.5527	53 640 580.12	\$2 765 180 479.81	
214.4474363	0.2426	585.6852	585.6852	107 283 013.34	\$2 763 063 307.98	
273.9618679	0.3160	748.2272	748.2272	170 272 058.87	\$2 761 264 358.11	
335.8795597	0.3837	917.3328	917.3328	250 058 744.67	\$2 759 474 389.56	
402.9333731	0.4431	1100.466	1100.466	352 476 131.58	\$2 757 609 065.02	
534.1879317	0.5303	1458.94	1458.94	599 916 551.55	\$2 754 125 751.25	
665.1008622	0.6012	1816.481	1816.481	907 038 391.02	\$2 750 819 773.38	
801.5893211	0.6669	2189.25	2189.25	1 289 772 611.12	\$2 747 509 426.83	
933.693852	0.7153	2550.045	2550.045	1 719 750 756.81	\$2 744 411 730.44	

Flash-drum							
Total volume flow (m3/hr)	Drum-volume	D (m)	H (m)	tw (m)	shell mass (kg)	cost (\$)	EP
#DIV/0!	#DIV/0!	#DIV/0!	#DIV/0!	#DIV/0!	#DIV/0!	#DIV/0!	#DIV/0!
#DIV/0!	#DIV/0!	#DIV/0!	#DIV/0!	#DIV/0!	#DIV/0!	#DIV/0!	#DIV/0!
#DIV/0!	#DIV/0!	#DIV/0!	#DIV/0!	#DIV/0!	#DIV/0!	#DIV/0!	#DIV/0!
#DIV/0!	#DIV/0!	#DIV/0!	#DIV/0!	#DIV/0!	#DIV/0!	#DIV/0!	#DIV/0!
#DIV/0!	#DIV/0!	#DIV/0!	#DIV/0!	#DIV/0!	#DIV/0!	#DIV/0!	#DIV/0!
#DIV/0!	#DIV/0!	#DIV/0!	#DIV/0!	#DIV/0!	#DIV/0!	#DIV/0!	#DIV/0!
422.7006785	35.22364754	2.82	5.64	0.00237875	950.8126655	29996.04258	\$2 767 266 491.09
302.1425136	25.17753566	2.52	5.04	0.002126874	679.6320501	22475.21108	\$2 767 745 084.87
244.2817442	20.35599774	2.35	4.70	0.001981382	549.4814372	18440.03278	\$2 767 913 824.37
220.7403575	18.39429399	2.27	4.54	0.001915572	496.5280122	16690.26366	\$2 767 825 764.76
202.9149484	16.90890265	2.21	4.42	0.001862555	456.431969	15315.14425	\$2 767 730 965.25
208.8857733	17.40645149	2.23	4.46	0.001880648	469.8625979	15780.94714	\$2 767 318 792.39
184.4680116	15.3717194	2.14	4.28	0.001804311	414.9378762	13840.13681	\$2 767 128 837.11
179.1910378	14.93198918	2.12	4.24	0.00178694	403.0679793	13407.47369	\$2 766 683 746.21
163.6041877	13.63313696	2.06	4.11	0.001733548	368.0072963	12098.70624	\$2 766 523 184.30
163.765834	13.64660695	2.06	4.11	0.001734119	368.3708995	12112.52866	\$2 766 040 827.83
157.5866727	13.13169744	2.03	4.06	0.001712028	354.4716437	11580.19245	\$2 765 748 806.16
148.4923041	12.3738637	1.99	3.98	0.00167844	334.0149913	10781.26175	\$2 765 169 698.54
142.9649576	11.91326991	1.96	3.93	0.00165735	321.5819119	10286.11322	\$2 763 053 021.87
136.9809339	11.41462122	1.94	3.87	0.001633896	308.1215942	9741.339253	\$2 761 254 616.77
134.3518239	11.19553748	1.92	3.85	0.001623376	302.2077377	9498.987679	\$2 759 464 890.57
134.3111244	11.19214599	1.92	3.85	0.001623212	302.1161892	9495.221159	\$2 757 599 569.79
133.5469829	11.12847009	1.92	3.84	0.001620127	300.397348	9424.419029	\$2 754 116 326.84
133.0201724	11.08457097	1.92	3.84	0.001617994	299.2123532	9375.512585	\$2 750 810 397.86
133.5982202	11.13273969	1.92	3.84	0.001620335	300.5125998	9429.171517	\$2 747 499 997.66
133.384836	11.11495838	1.92	3.84	0.001619471	300.0326186	9409.374355	\$2 744 402 321.07

Membrane Cost						
C8 + 2-C8 (kg/hr)	C12-C14 (kg/hr)	wt frac C8	flux	Area	Membrane cost	EP-cost
#DIV/0!	#DIV/0!	#DIV/0!	#DIV/0!	#DIV/0!	#DIV/0!	#DIV/0!
#DIV/0!	#DIV/0!	#DIV/0!	#DIV/0!	#DIV/0!	#DIV/0!	#DIV/0!
#DIV/0!	#DIV/0!	#DIV/0!	#DIV/0!	#DIV/0!	#DIV/0!	#DIV/0!
#DIV/0!	#DIV/0!	#DIV/0!	#DIV/0!	#DIV/0!	#DIV/0!	#DIV/0!
#DIV/0!	#DIV/0!	#DIV/0!	#DIV/0!	#DIV/0!	#DIV/0!	#DIV/0!
#DIV/0!	1705.48	#DIV/0!	#DIV/0!	#DIV/0!	#DIV/0!	#DIV/0!
209756.6	1374.44	0.993490116	7.893963	44576.47	878 156 431.19	\$1 889 110 059.89
109787.5	1384.57	0.987545707	7.797835	23761.31	468 097 781.91	\$2 299 647 302.97
82370.9	1232.30	0.985260163	7.761052	17953.58	353 685 560.96	\$2 414 228 263.41
65590.8	1192.13	0.982149253	7.711145	14434.29	284 355 429.00	\$2 483 470 335.76
52895.6	1153.48	0.978658689	7.655364	11767.15	231 812 923.37	\$2 535 918 041.88
46295.8	1291.24	0.972865836	7.563299	10486.4	206 582 146.65	\$2 560 736 645.74
39634.5	1208.76	0.97040489	7.524379	9046.883	178 223 598.41	\$2 588 905 238.70
30613.5	1218.38	0.961724564	7.388012	7180.982	141 465 352.68	\$2 625 218 393.53
24826.7	1123.91	0.956690315	7.309575	5917.034	116 565 563.63	\$2 649 957 620.67
21208.8	1142.17	0.948898402	7.189114	5181.661	102 078 718.51	\$2 663 962 109.33
16897.0	1128.75	0.937381429	7.013162	4283.799	84 390 845.41	\$2 681 357 960.75
14050.3	1101.84	0.927281572	6.860919	3680.772	72 511 211.70	\$2 692 658 486.85
10131.9	1075.80	0.904011826	6.517479	2866.058	56 461 337.83	\$2 706 591 684.04
5860.2	1070.47	0.845546424	5.699645	2026.639	39 924 785.64	\$2 721 329 831.13
3988.7	1064.08	0.789404365	4.974987	1692.713	33 346 446.89	\$2 726 118 443.68
2928.0	1073.52	0.731719206	4.292329	1553.731	30 608 497.35	\$2 726 991 072.45
2163.3	1077.15	0.667594357	3.607122	1497.259	29 495 997.67	\$2 724 620 329.17
1479.3	1078.47	0.578354536	2.782608	1531.993	30 180 270.33	\$2 720 630 127.53
1070.6	1084.74	0.496721682	2.159915	1663.146	32 763 968.22	\$2 714 736 029.44
786.4	1085.48	0.420109038	1.689842	1846.195	36 370 040.08	\$2 708 032 280.99

80°C

Reactor Cost (\$\$) & EP						
V (m3)	Conversion	D (m)	H (m)	Cost (\$)	H/D based	EP
#DIV/0!	1.0000	#DIV/0!	#DIV/0!	#DIV/0!	#DIV/0!	#DIV/0!
#DIV/0!	0.0038	#DIV/0!	#DIV/0!	#DIV/0!	#DIV/0!	#DIV/0!
#DIV/0!	0.0086	#DIV/0!	#DIV/0!	#DIV/0!	#DIV/0!	#DIV/0!
49.05183145	0.0196	133.9672	133.9672	6 641 032.15	\$2 768 820 919.91	
40.06104317	0.0295	109.4122	109.4122	4 533 086.38	\$2 769 202 759.93	
40.3908062	0.0404	110.3128	110.3128	4 603 717.44	\$2 769 188 471.34	
43.31246691	0.0493	118.2922	118.2922	5 251 843.68	\$2 769 062 869.27	
46.89573309	0.0650	128.0786	128.0786	6 101 228.40	\$2 768 911 111.26	
49.72033945	0.0904	135.793	135.793	6 812 760.29	\$2 768 793 117.98	
53.33968543	0.1024	145.6779	145.6779	7 778 161.80	\$2 768 643 863.35	
58.16423997	0.1211	158.8545	158.8545	9 158 010.74	\$2 768 448 012.23	
62.70270425	0.1401	171.2496	171.2496	10 552 168.85	\$2 768 266 725.40	
73.32335163	0.1633	200.2561	200.2561	14 174 469.62	\$2 767 852 318.46	
83.35033383	0.2055	227.6411	227.6411	18 050 576.37	\$2 767 472 009.45	
93.31598873	0.2306	254.8587	254.8587	22 335 565.71	\$2 767 103 010.81	
105.0948662	0.2574	287.0284	287.0284	27 948 759.43	\$2 766 676 876.56	
115.7989597	0.2929	316.2627	316.2627	33 558 829.80	\$2 766 297 868.59	
137.2172793	0.3503	374.7591	374.7591	46 218 178.78	\$2 765 559 667.25	
203.1463044	0.4520	554.8202	554.8202	96 869 589.31	\$2 763 415 580.05	
277.0226812	0.6166	756.5867	756.5867	173 877 638.48	\$2 761 174 096.34	
345.2864838	0.5662	943.0244	943.0244	263 430 774.33	\$2 759 208 504.04	
408.9154	0.6069	1116.804	1116.804	362 410 308.20	\$2 757 445 816.74	
545.5975955	0.6408	1490.101	1490.101	624 311 392.55	\$2 753 831 646.79	
687.49892	0.6759	1877.653	1877.653	965 505 726.69	\$2 750 267 854.06	
821.6439427	0.7463	2244.022	2244.022	1 351 304 436.68	\$2 747 032 957.15	
961.6817939	0.7527	2626.484	2626.484	1 818 264 390.42	\$2 743 767 071.48	

Flash-drum						
Total volume flow (m3/hr)	Drum-volume	D (m)	H (m)	tw (m)	shell mass (kg)	cost (\$)
#DIV/0!	#DIV/0!	#DIV/0!	#DIV/0!	#DIV/0!	#DIV/0!	#DIV/0!
#DIV/0!	#DIV/0!	#DIV/0!	#DIV/0!	#DIV/0!	#DIV/0!	#DIV/0!
#DIV/0!	#DIV/0!	#DIV/0!	#DIV/0!	#DIV/0!	#DIV/0!	#DIV/0!
588.6219775	49.04986938	3.15	6.30	0.002656338	1324.032016	39055.08371 \$2 768 781 864.82
320.4883454	26.70629382	2.57	5.14	0.002169078	720.8987197	23688.36112 \$2 769 179 071.57
242.3448372	20.19459529	2.34	4.69	0.001976131	545.1246056	18298.69273 \$2 769 170 172.64
207.8998412	17.32429377	2.23	4.45	0.001877684	467.644866	15704.40223 \$2 769 047 164.86
187.5829324	15.63128575	2.15	4.30	0.001814411	421.9445036	14093.2082 \$2 768 897 018.05
170.4697353	14.20524304	2.08	4.17	0.001757466	383.4504926	12681.06342 \$2 768 780 436.92
160.0190563	13.33438796	2.04	4.08	0.001720792	359.9429885	11790.72211 \$2 768 632 072.63
155.1046399	12.92486964	2.02	4.04	0.001702993	348.8886194	11364.02122 \$2 768 436 648.21
150.4864902	12.54003923	2.00	4.00	0.00168592	338.5006653	10958.08749 \$2 768 255 767.31
146.6467033	12.22006978	1.98	3.96	0.001671457	329.8635415	10616.76289 \$2 767 841 701.70
142.8862866	11.90671426	1.96	3.93	0.001657046	321.4049513	10279.01103 \$2 767 461 730.44
139.9739831	11.66403201	1.95	3.90	0.001645711	314.8540864	10014.98526 \$2 767 092 995.83
140.1264882	11.67674026	1.95	3.90	0.001646309	315.1971277	10028.86538 \$2 766 666 847.69
138.9587516	11.57943277	1.95	3.89	0.001641723	312.5704494	9922.430243 \$2 766 287 946.16
137.2172793	11.43431588	1.94	3.88	0.001634836	308.6532237	9763.034042 \$2 765 549 904.21
135.4308696	11.28545436	1.93	3.86	0.00162771	304.634917	9598.68168 \$2 763 405 981.37
138.5113406	11.54215001	1.94	3.89	0.001639959	311.5640539	9881.555553 \$2 761 164 214.79
138.1145935	11.50908908	1.94	3.88	0.001638391	310.6716206	9845.265228 \$2 759 198 658.77
136.3051333	11.35830676	1.93	3.87	0.001631205	306.6014647	9679.222896 \$2 757 436 137.51
136.3993989	11.36616191	1.93	3.87	0.001631581	306.8135033	9687.894713 \$2 753 821 958.89
137.499784	11.457857	1.94	3.88	0.001635957	309.288683	9788.946323 \$2 750 258 065.11
136.9406571	11.41126496	1.94	3.87	0.001633736	308.0309965	9737.640642 \$2 747 023 219.51
137.3831134	11.44813484	1.94	3.88	0.001635494	309.026247	9778.247489 \$2 743 757 293.23

Membrane Cost							
C8 + C8 (kg/hr)	C12-C14 (kg/hr)	wt frac C8	flux	Area	Membrane cost	EP-cost	
#DIV/0!	#DIV/0!	#DIV/0!	#DIV/0!	#DIV/0!	#DIV/0!	#DIV/0!	#DIV/0!
#DIV/0!	#DIV/0!	#DIV/0!	#DIV/0!	#DIV/0!	#DIV/0!	#DIV/0!	#DIV/0!
#DIV/0!	1050.65	#DIV/0!	#DIV/0!	#DIV/0!	#DIV/0!	#DIV/0!	#DIV/0!
328809.2	1050.65	0.996814872	7.948019	69170.25	1 362 653 833.81	\$1 406 128 031.01	
137093.7	1050.65	0.992394578	7.876197	29232.45	575 879 184.13	\$2 193 299 887.44	
81221.0	1050.65	0.98722956	7.792741	17595.8	346 637 173.80	\$2 422 532 998.85	
56592.9	1050.65	0.981773393	7.705128	12468.65	245 632 367.97	\$2 523 414 796.89	
42066.3	1050.65	0.975632639	7.607193	9446.526	186 096 555.72	\$2 582 800 462.32	
29830.3	1050.65	0.96597759	7.454649	6904.19	136 012 549.79	\$2 632 767 887.13	
22358.1	1050.65	0.955117403	7.285166	5355.347	105 500 334.39	\$2 663 131 738.24	
18844.3	1050.65	0.947190323	7.162861	4629.19	91 195 044.13	\$2 677 241 604.08	
15542.3	1050.65	0.936681274	7.002546	3949.27	77 800 628.26	\$2 690 455 139.05	
12796.9	1050.65	0.924127528	6.81377	3387.141	66 726 683.85	\$2 701 115 017.85	
10108.2	1050.65	0.905846197	6.544182	2841.92	55 985 819.37	\$2 711 475 911.07	
8005.5	1066.41	0.882449446	6.208353	2435.401	47 977 392.35	\$2 719 115 603.47	
6922.7	1080.63	0.864977527	5.964302	2236.456	44 058 178.43	\$2 722 608 669.27	
5864.6	1082.82	0.844139883	5.680764	2038.283	40 154 183.61	\$2 726 133 762.56	
4654.0	1085.19	0.810915101	5.245614	1823.488	35 922 708.84	\$2 729 627 195.37	
3317.4	1099.30	0.751104943	4.514743	1630.486	32 120 572.49	\$2 731 285 408.87	
2087.7	1200.08	0.634991178	3.288478	1666.326	32 826 630.35	\$2 728 337 584.43	
1244.6	1156.61	0.518313544	2.312392	1730.656	34 093 925.10	\$2 725 104 733.67	
1395.4	1143.57	0.54958911	2.548846	1660.193	32 705 807.51	\$2 724 730 330.01	
1157.6	1151.18	0.50140009	2.192207	1755.326	34 579 915.38	\$2 719 242 043.51	
988.2	1169.48	0.457987256	1.908416	1884.335	37 121 395.66	\$2 713 136 669.45	
797.7	1168.41	0.405716679	1.613886	2030.376	39 998 414.71	\$2 707 024 804.80	
575.9	1173.34	0.329231527	1.275779	2285.204	45 018 522.97	\$2 698 738 770.26	

90°C

Reactor Cost (\$\$) & EP					
V (m3)	Conversion	D (m)	H (m)	Cost (\$) H/D based	EP
#DIV/0!	1.0000	#DIV/0!	#DIV/0!	#DIV/0!	#DIV/0!
#DIV/0!	0.0055	#DIV/0!	#DIV/0!	#DIV/0!	#DIV/0!
#DIV/0!	0.0213	#DIV/0!	#DIV/0!	#DIV/0!	#DIV/0!
27.54399837	0.0403	75.22641	75.22641	2 236 406.35	\$2 769 765 104.79
25.89789004	0.0755	70.73067	70.73067	1 991 023.79	\$2 769 842 514.04
28.56542096	0.0893	78.01606	78.01606	2 395 384.58	\$2 769 717 538.60
34.70435468	0.1208	94.78232	94.78232	3 457 992.10	\$2 769 438 340.74
39.42504254	0.1751	107.6752	107.6752	4 398 313.06	\$2 769 230 384.45
44.17498056	0.1685	120.6479	120.6479	5 450 827.67	\$2 769 026 117.95
49.55828108	0.1845	135.3504	135.3504	6 770 941.20	\$2 768 799 850.77
55.64523057	0.2003	151.9747	151.9747	8 424 360.26	\$2 768 549 847.20
61.03389525	0.2260	166.6919	166.6919	10 028 752.09	\$2 768 333 069.83
73.88964644	0.2612	201.8027	201.8027	14 381 641.92	\$2 767 830 574.04
87.3960308	0.3005	238.6905	238.6905	19 738 456.42	\$2 767 321 200.49
95.6399921	0.3457	261.2058	261.2058	23 396 235.29	\$2 767 018 119.83
106.0222167	0.3716	289.5611	289.5611	28 415 698.75	\$2 766 643 745.61
119.1700645	0.3999	325.4697	325.4697	35 425 102.44	\$2 766 179 981.02
146.6836553	0.4469	400.613	400.613	52 415 019.88	\$2 765 240 907.09
223.2704998	0.5615	609.7822	609.7822	115 759 259.44	\$2 762 790 861.04
294.6679344	0.6407	804.7783	804.7783	195 353 696.43	\$2 760 657 553.24
367.6574353	0.7081	1004.123	1004.123	296 541 847.02	\$2 758 581 912.07
436.7426693	0.7347	1192.804	1192.804	410 322 517.71	\$2 756 692 556.95
580.9218076	0.7718	1586.577	1586.577	702 725 589.38	\$2 752 928 754.03
707.6953636	0.7688	1932.812	1932.812	1 019 694 415.08	\$2 749 773 263.37
872.1366614	0.7819	2381.924	2381.924	1 512 175 759.38	\$2 745 843 449.88
905.6124424	0.7449	2473.351	2473.351	1 623 503 218.54	\$2 745 062 438.94

Flash-drum							
Total volume flow (m ³ /hr)	Drum-volume	D (m)	H (m)	tw (m)	shell mass (kg)	cost (\$)	EP
#DIV/0!	#DIV/0!	#DIV/0!	#DIV/0!	#DIV/0!	#DIV/0!	#DIV/0!	#DIV/0!
#DIV/0!	#DIV/0!	#DIV/0!	#DIV/0!	#DIV/0!	#DIV/0!	#DIV/0!	#DIV/0!
#DIV/0!	#DIV/0!	#DIV/0!	#DIV/0!	#DIV/0!	#DIV/0!	#DIV/0!	#DIV/0!
330.5279805	27.54289661	2.60	5.20	0.002191495	743.4816317	24340.47731	\$2 769 740 764.31
207.1831203	17.26456941	2.22	4.45	0.001875524	466.0326914	15648.66692	\$2 769 826 865.38
171.3925258	14.28213917	2.09	4.17	0.001760631	385.5261952	12758.61615	\$2 769 704 779.98
166.5809025	13.8811866	2.07	4.13	0.001743999	374.7030463	12352.37775	\$2 769 425 988.37
157.7001702	13.14115518	2.03	4.06	0.001712439	354.7269422	11590.04476	\$2 769 218 794.40
151.4570762	12.62091816	2.00	4.01	0.001689537	340.6838779	11043.81068	\$2 769 015 074.14
148.6748432	12.38907469	1.99	3.98	0.001679127	334.4255905	10797.48694	\$2 768 789 053.28
148.3872815	12.36511217	1.99	3.98	0.001678044	333.7787561	10771.92308	\$2 768 539 075.28
146.4813486	12.20629078	1.98	3.96	0.001670829	329.4915968	10601.98448	\$2 768 322 467.85
147.7792928	12.31444847	1.99	3.97	0.001675749	332.411161	10717.80836	\$2 767 819 856.23
149.8217671	12.48464785	2.00	3.99	0.001683434	337.0054532	10899.2508	\$2 767 310 301.24
143.4599881	11.95452081	1.97	3.93	0.001659261	322.6954218	10330.76739	\$2 767 007 789.06
141.3629556	11.77977509	1.96	3.91	0.001651137	317.9784076	10141.17909	\$2 766 633 604.43
143.0040774	11.91652977	1.96	3.93	0.001657502	321.6699072	10289.64427	\$2 766 169 691.37
146.6836553	12.22314899	1.98	3.96	0.001671598	329.9466605	10620.06453	\$2 765 230 287.02
148.8469999	12.4034205	1.99	3.98	0.001679775	334.8128355	10812.78197	\$2 762 780 048.26
147.3339672	12.27733949	1.98	3.97	0.001674064	331.4094564	10678.11513	\$2 760 646 875.12
147.0629741	12.25475763	1.98	3.97	0.001673037	330.7998911	10653.9372	\$2 758 571 258.13
145.5808898	12.13125554	1.98	3.95	0.001667398	327.4661265	10521.38945	\$2 756 682 035.56
145.2304519	12.10205356	1.98	3.95	0.001666059	326.6778601	10489.96985	\$2 752 918 264.06
141.5390727	11.79445093	1.96	3.92	0.001651822	318.3745611	10157.14454	\$2 749 763 106.22
145.3561102	12.11252467	1.98	3.95	0.001666539	326.9605128	10501.23962	\$2 745 832 948.64
129.3732061	10.78066926	1.90	3.80	0.00160307	291.0089554	9034.796523	\$2 745 053 404.14

Membrane Cost						
C8 + 2-C8 (kg/hr)	C12-C14 (kg/hr)	wt frac C8	flux	Area	Membrane cost	EP-cost
#DIV/0!	#DIV/0!	#DIV/0!	#DIV/0!	#DIV/0!	#DIV/0!	#DIV/0!
#DIV/0!	#DIV/0!	#DIV/0!	#DIV/0!	#DIV/0!	#DIV/0!	#DIV/0!
#DIV/0!	1347.92	#DIV/0!	#DIV/0!	#DIV/0!	#DIV/0!	#DIV/0!
144067.0	1209.06	0.991677471	7.86458	30787	606 503 944.00	\$2 163 236 820.32
55965.5	1139.50	0.980045597	7.67775	12396.6	244 213 104.57	\$2 525 613 760.81
30408.5	1113.76	0.964667618	7.434088	7067.051	139 220 902.72	\$2 630 483 877.26
22998.0	1126.17	0.953317994	7.257299	5540.212	109 142 174.98	\$2 660 283 813.39
17391.0	1409.38	0.925034463	6.827308	4589.505	90 413 255.28	\$2 678 805 539.12
13342.4	1133.87	0.921674328	6.777227	3560.035	70 132 680.10	\$2 698 882 394.04
11482.9	1109.96	0.911857811	6.632137	3164.607	62 342 767.05	\$2 706 446 286.23
10119.6	1114.10	0.900825164	6.471242	2893.234	56 996 706.03	\$2 711 542 369.25
8891.2	1119.06	0.888209214	6.290069	2652.402	52 252 328.33	\$2 716 070 139.52
7507.7	1145.24	0.867647109	6.001218	2403.104	47 341 142.98	\$2 720 478 713.25
6191.7	1165.29	0.841607498	5.646864	2171.397	42 776 525.48	\$2 724 533 775.76
4882.4	1129.76	0.812086682	5.260604	1904.764	37 523 858.97	\$2 729 483 930.09
3918.5	1117.38	0.778115178	4.836449	1735.387	34 187 114.15	\$2 732 446 490.27
3475.7	1139.83	0.753044035	4.53738	1695.367	33 398 728.10	\$2 732 770 963.27
3032.4	1176.05	0.720551898	4.167424	1683.091	33 156 887.14	\$2 732 073 399.88
2291.6	1192.66	0.657702831	3.508329	1655.248	32 608 377.44	\$2 730 171 670.82
1412.7	1187.42	0.543325737	2.500015	1733.416	34 148 289.83	\$2 726 498 585.29
976.4	1189.72	0.450757887	1.86461	1936.169	38 142 525.09	\$2 720 428 733.04
708.3	1179.94	0.375095302	1.465279	2147.705	42 309 787.90	\$2 714 372 247.66
597.6	1177.77	0.336610753	1.30359	2269.855	44 716 148.81	\$2 708 202 115.25
485.0	1151.20	0.296437051	1.164604	2341.635	46 130 218.45	\$2 703 632 887.78
494.2	1179.42	0.295285553	1.161069	2402.402	47 327 316.79	\$2 698 505 631.85
437.1	1057.80	0.292377584	1.152253	2162.241	42 596 144.98	\$2 702 457 259.17

100°C

Reactor Cost (\$\$) & EP							
V (m3)	Conversion	D (m)	H (m)	Cost (\$)	H/D based	EP	
#DIV/0!	1.0000	#DIV/0!	#DIV/0!	#DIV/0!		#DIV/0!	#DIV/0!
2.148494359	0.0111	5.867831	5.867831	18 199.73	\$2 771 165 264.78		
28.59218517	0.0195	78.08915	78.08915	2 399 619.16	\$2 769 716 296.85		
38.3618831	0.0309	104.7715	104.7715	4 177 294.25	\$2 769 276 762.73		
40.39208501	0.0318	110.3163	110.3163	4 603 992.34	\$2 769 188 415.97		
47.29854243	0.0601	129.1788	129.1788	6 200 442.65	\$2 768 894 199.48		
52.72359524	0.0404	143.9953	143.9953	7 609 590.50	\$2 768 669 122.94		
60.50826073	0.0471	165.2563	165.2563	9 866 481.16	\$2 768 354 041.51		
66.96708825	0.0545	182.8962	182.8962	11 946 328.55	\$2 768 098 767.02		
76.05947723	0.0432	207.7288	207.7288	15 188 504.55	\$2 767 747 563.15		
86.0472206	0.0545	235.0067	235.0067	19 167 855.07	\$2 767 371 320.91		
91.85652842	0.0522	250.8727	250.8727	21 681 300.88	\$2 767 156 537.75		
106.5401407	0.0645	290.9756	290.9756	28 678 064.89	\$2 766 625 267.26		
111.6644066	0.0923	304.9707	304.9707	31 334 810.01	\$2 766 443 396.52		
140.527707	0.0675	383.8003	383.8003	48 343 587.99	\$2 765 447 710.14		
157.7952012	0.0871	430.9602	430.9602	60 154 028.11	\$2 764 871 946.02		
153.3568845	0.1029	418.8385	418.8385	57 002 802.02	\$2 765 018 676.93		
177.136157	0.0829	483.783	483.783	74 811 306.18	\$2 764 241 803.05		
299.2463361	0.1229	817.2825	817.2825	201 117 665.54	\$2 760 524 549.30		
379.7302096	0.1403	1037.095	1037.095	315 173 688.85	\$2 758 246 949.12		
448.2476293	0.1987	1224.225	1224.225	430 945 920.91	\$2 756 383 957.83		
537.530698	0.1894	1468.07	1468.07	607 016 356.94	\$2 754 039 456.51		
720.1312839	0.2171	1966.777	1966.777	1 053 751 603.29	\$2 749 470 126.69		
885.1930048	0.2228	2417.583	2417.583	1 555 154 142.05	\$2 745 538 136.24		
1061.186587	0.2193	2898.245	2898.245	2 189 288 864.98	\$2 741 504 580.39		
1239.402754	0.2193	3384.978	3384.978	2 933 989 246.26	\$2 737 554 753.45		

Flash-drum							
Total volume flow (m3/hr)	Drum-volume	D (m)	H (m)	tw (m)	shell mass (kg)	cost (\$)	EP
#DIV/0!	#DIV/0!	#DIV/0!	#DIV/0!	#DIV/0!	#DIV/0!	#DIV/0!	#DIV/0!
128.9096616	10.7420421	1.90	3.80	0.001601154	289.9662697	8991.216498	\$2 771 156 273.56
686.2124442	57.18208297	3.31	6.63	0.002795701	1543.549647	43902.36349	\$2 769 672 394.49
460.3425972	38.36034863	2.90	5.80	0.002447362	1035.483486	32160.68829	\$2 769 244 602.04
323.1366801	26.92697955	2.58	5.16	0.002175037	726.8558197	23861.16543	\$2 769 164 554.81
283.7912546	23.64832524	2.47	4.94	0.002082912	638.3531727	21231.84105	\$2 768 872 967.64
253.0732571	21.08859452	2.38	4.75	0.002004872	569.2568535	19076.01336	\$2 768 650 046.92
242.0330429	20.16861347	2.34	4.68	0.001975283	544.4232631	18275.89831	\$2 768 335 765.61
229.6014454	19.13268845	2.30	4.60	0.001940868	516.4599288	17357.25471	\$2 768 081 409.77
228.1784317	19.01410871	2.30	4.59	0.00193685	513.2590362	17250.84507	\$2 767 730 312.30
229.4592549	19.12083971	2.30	4.60	0.001940467	516.140089	17346.63392	\$2 767 353 974.28
220.4556682	18.37057083	2.27	4.54	0.001914748	495.8876391	16668.65875	\$2 767 139 869.09
213.0802813	17.75597984	2.24	4.49	0.001893152	479.2976225	16104.99428	\$2 766 609 162.26
191.4246971	15.95142001	2.17	4.33	0.001826714	430.586076	14403.02852	\$2 766 428 993.49
210.7915604	17.56526073	2.24	4.47	0.00188635	474.1494292	15928.49849	\$2 765 431 781.64
210.3936016	17.53209882	2.23	4.47	0.001885162	473.2542702	15897.73163	\$2 764 856 048.29
184.0282614	15.33507502	2.14	4.27	0.001802877	413.9487127	13804.27212	\$2 765 004 872.66
177.136157	14.76075596	2.11	4.22	0.001780083	398.44578	13237.61703	\$2 764 228 565.43
199.4975574	16.62413146	2.20	4.39	0.00185204	448.7449725	15046.07555	\$2 760 509 503.22
189.8651048	15.82145918	2.16	4.32	0.001821739	427.0779669	14277.55738	\$2 758 232 671.57
179.2990517	14.94098998	2.12	4.24	0.001787299	403.3109431	13416.38051	\$2 756 370 541.45
179.1768993	14.93081102	2.12	4.24	0.001786893	403.0361765	13406.30767	\$2 754 026 050.20
180.032821	15.00213497	2.12	4.24	0.001789734	404.9614659	13476.83041	\$2 749 456 649.86
177.038601	14.75262662	2.11	4.22	0.001779756	398.2263399	13229.5335	\$2 745 524 906.71
176.8644312	14.73811305	2.11	4.22	0.001779172	397.8345666	13215.09729	\$2 741 491 365.29
177.0575364	14.7542045	2.11	4.22	0.001779819	398.2689327	13231.10263	\$2 737 541 522.35

Membrane Cost							
C8 + 2-C8 (kg/hr)	C12-C14 (kg/hr)	wt frac C8	flux	Area	Membrane cost	EP-cost	
#DIV/0!	#DIV/0!	#DIV/0!	#DIV/0!	#DIV/0!	#DIV/0!	#DIV/0!	
114.9	1050.65	0.098582041	0.924204	2101.895	41 407 338.29	\$2 729 748 935.27	
397708.0	1729.59	0.995669936	7.92938	83957.29	1 653 958 699.14	\$1 115 713 695.35	
236398.0	1585.07	0.993339575	7.89152	50261.35	990 148 670.90	\$1 779 095 931.15	
138655.7	1306.86	0.990662797	7.848159	29723.02	585 543 508.98	\$2 183 621 045.83	
109506.7	2092.99	0.981245582	7.696682	24166.19	476 073 919.67	\$2 292 799 047.97	
88685.8	1209.95	0.986540538	7.781646	19253.79	379 299 690.04	\$2 389 350 356.88	
80779.1	1219.94	0.985122513	7.75884	17614.11	346 997 905.21	\$2 421 337 860.40	
71730.3	1344.09	0.981606586	7.702458	15811.93	311 494 982.60	\$2 456 586 427.17	
71092.1	1050.65	0.985436565	7.763888	15486.81	305 090 144.02	\$2 462 640 168.28	
71819.9	1196.31	0.983615804	7.73465	15733.58	309 951 446.57	\$2 457 402 527.71	
65452.5	1141.71	0.982855642	7.722462	14372.4	283 136 275.46	\$2 484 003 593.63	
60110.2	1195.29	0.980502654	7.684803	13295.83	261 927 895.99	\$2 504 681 266.27	
44626.6	1195.02	0.973920197	7.580009	10075.11	198 479 665.84	\$2 567 949 327.65	
45245.5	1312.08	0.9718181	7.546715	10282.09	202 557 133.52	\$2 562 874 648.12	
50528.2	1313.61	0.974661177	7.591765	11381.14	224 208 468.82	\$2 540 647 579.48	
35090.3	1146.73	0.968354812	7.492045	8061.232	158 806 277.95	\$2 606 198 594.72	
34489.7	1133.84	0.968171707	7.48916	7927.799	156 177 644.43	\$2 608 050 921.00	
34484.6	1296.70	0.963760546	7.419869	8037.281	158 334 432.57	\$2 602 175 070.65	
24946.3	1312.97	0.949999844	7.206073	6073.417	119 646 317.92	\$2 638 586 353.64	
18455.3	1291.10	0.934615867	6.971283	4720.902	93 001 768.73	\$2 663 368 772.72	
14280.5	1360.43	0.913020719	6.64923	3920.476	77 233 386.63	\$2 676 792 663.57	
14035.6	1332.94	0.913268188	6.652871	3850.106	75 847 083.96	\$2 673 609 565.90	
12160.0	1325.70	0.901695913	6.483857	3466.489	68 289 842.36	\$2 677 235 064.35	
11930.1	1332.70	0.899516236	6.452305	3425.869	67 489 618.09	\$2 674 001 747.20	
12068.2	1332.70	0.900551524	6.46728	3453.518	68 034 305.08	\$2 669 507 217.27	

ECONOMIC POTENTIAL AND EQUIPMENT COST FOR THE GMPP CATALYST AT VARIED
CATALYST LOADS

C₈/Ru: 5000

Reactor Cost (\$\$) & EP							
V (m3)	Conversion	D (m)	H (m)	Cost (\$)	H/D based	EP	
#DIV/0!	1.0000	#DIV/0!	#DIV/0!	#DIV/0!	#DIV/0!	#DIV/0!	
#DIV/0!	0.0000	#DIV/0!	#DIV/0!	#DIV/0!	#DIV/0!	#DIV/0!	
#DIV/0!	0.0071	#DIV/0!	#DIV/0!	#DIV/0!	#DIV/0!	#DIV/0!	
75.59541757	0.0085	206.4614	206.4614	18 238 064.75	\$2 600 861 524.41		
85.02411487	0.0076	232.2124	232.2124	22 764 217.88	\$2 600 762 921.80		
67.31562118	0.0325	183.8481	183.8481	14 654 223.27	\$2 600 950 158.62		
49.97122171	0.0315	136.4782	136.4782	8 354 532.54	\$2 601 143 457.16		
56.26595778	0.0431	153.67	153.67	10 449 601.21	\$2 601 071 954.90		
57.128017	0.0593	156.0244	156.0244	10 753 597.87	\$2 601 062 290.91		
63.08838983	0.0680	172.303	172.303	12 967 042.86	\$2 600 996 242.87		
67.03142062	0.0901	183.0719	183.0719	14 537 756.93	\$2 600 953 238.37		
70.13152767	0.0976	191.5388	191.5388	15 831 744.73	\$2 600 919 782.32		
80.23423936	0.1275	219.1306	219.1306	20 406 041.50	\$2 600 812 723.32		
86.4186355	0.1629	236.0211	236.0211	23 473 500.65	\$2 600 748 529.22		
97.96318429	0.1858	267.5508	267.5508	29 735 888.06	\$2 600 631 083.28		
106.0275404	0.2145	289.5757	289.5757	34 520 409.58	\$2 600 550 691.57		
117.8088275	0.2463	321.752	321.752	42 109 267.83	\$2 600 435 401.67		
139.409976	0.2932	380.7476	380.7476	57 846 155.68	\$2 600 229 776.83		
204.6814627	0.4104	559.013	559.013	119 352 183.76	\$2 599 642 885.21		
264.9397478	0.4977	723.5866	723.5866	194 174 306.11	\$2 599 134 150.60		
337.6177306	0.6193	922.08	922.08	306 722 977.01	\$2 598 550 445.34		
400.7837082	0.5917	1094.595	1094.595	423 862 180.40	\$2 598 063 490.57		
540.8327903	0.7482	1477.088	1477.088	745 921 528.94	\$2 597 034 458.12		
673.6103438	0.7854	1839.722	1839.722	1 128 535 419.15	\$2 596 107 640.71		
809.5362513	0.8133	2210.954	2210.954	1 596 136 248.67	\$2 595 196 158.45		
944.8583377	0.8531	2580.537	2580.537	2 136 376 991.54	\$2 594 318 787.48		

Flash-drum							
Total volume flow (m3/hr)	Drum-volume	D (m)	H (m)	tw (m)	shell mass (kg)	cost (\$)	EP
#DIV/0!	#DIV/0!	#DIV/0!	#DIV/0!	#DIV/0!	#DIV/0!	#DIV/0!	#DIV/0!
#DIV/0!	#DIV/0!	#DIV/0!	#DIV/0!	#DIV/0!	#DIV/0!	#DIV/0!	#DIV/0!
#DIV/0!	#DIV/0!	#DIV/0!	#DIV/0!	#DIV/0!	#DIV/0!	#DIV/0!	#DIV/0!
907.1450108	75.59239375	3.64	7.27	0.002044838	1359.881156	39867.49425	\$2 600 821 656.92
680.192919	56.68047594	3.30	6.61	0.001857708	1019.662261	31761.75305	\$2 600 731 160.05
403.8937271	33.65646428	2.78	5.55	0.00156143	605.4682127	20218.1178	\$2 600 929 940.50
239.8618642	19.98768915	2.33	4.67	0.001312463	359.5716509	11776.47424	\$2 601 131 680.68
225.0638311	18.75456905	2.29	4.57	0.001284898	337.3882446	10914.3236	\$2 601 061 040.58
195.8674869	16.32163768	2.18	4.36	0.001226745	293.6206464	9143.681316	\$2 601 053 147.23
189.2651695	15.77146657	2.16	4.31	0.001212803	283.7232575	8728.960655	\$2 600 987 513.91
178.750455	14.89527541	2.12	4.23	0.001189915	267.9608799	8056.331663	\$2 600 945 182.04
168.3156664	14.02574448	2.07	4.15	0.001166295	252.3183176	7372.975811	\$2 600 912 409.35
160.4684787	13.37183833	2.04	4.08	0.00114788	240.554771	6847.848883	\$2 600 805 875.47
148.1462323	12.34502554	1.99	3.98	0.001117713	222.0827621	6002.026061	\$2 600 742 527.19
146.9447764	12.24490822	1.98	3.97	0.001114683	220.281686	5918.076661	\$2 600 625 165.20
141.3700539	11.78036659	1.96	3.91	0.001100405	211.9247419	5524.904173	\$2 600 545 166.67
141.3705929	11.78041151	1.96	3.91	0.001100406	211.92555	5524.942488	\$2 600 429 876.73
139.409976	11.6170333	1.95	3.90	0.001095296	208.9864322	5385.196481	\$2 600 224 391.63
136.4543085	11.37073752	1.93	3.87	0.0010875	204.5556559	5173.031575	\$2 599 637 712.18
132.4698739	11.03871459	1.92	3.83	0.00107681	198.5826776	4884.086594	\$2 599 129 266.51
135.0470922	11.2534742	1.93	3.86	0.001083748	202.446129	5071.372866	\$2 598 545 373.97
133.5945694	11.13243547	1.92	3.84	0.001079849	200.2686839	4965.995749	\$2 598 058 524.58
135.2081976	11.2668991	1.93	3.86	0.001084179	202.6876385	5083.032684	\$2 597 029 375.09
134.7220688	11.22638999	1.93	3.85	0.001082878	201.9588934	5047.832708	\$2 596 102 592.87
134.9227085	11.2431093	1.93	3.85	0.001083416	202.2596681	5062.36693	\$2 595 191 096.09
134.9797625	11.24786361	1.93	3.85	0.001083568	202.3451965	5066.498306	\$2 594 313 720.98

Membrane Cost							
C8 + 2-C8 (kg/hr)	C12-C14 (kg/hr)	wt frac C8	flux	Area	Membrane cost	EP-cost	
#DIV/0!	#DIV/0!	#DIV/0!	#DIV/0!	#DIV/0!	#DIV/0!	#DIV/0!	
#DIV/0!	#DIV/0!	#DIV/0!	#DIV/0!	#DIV/0!	#DIV/0!	#DIV/0!	
#DIV/0!	1050.65	#DIV/0!	#DIV/0!	#DIV/0!	#DIV/0!	#DIV/0!	
556553.2	1050.65	0.998115785	7.969227	116616	2 297 336 116.63	\$303 485 540.29	
394282.4	1050.65	0.997342378	7.956614	82810.15	1 631 359 962.91	\$969 371 197.14	
196728.5	1050.65	0.994687783	7.913411	41654.84	820 600 404.87	\$1 780 329 535.64	
79445.7	1050.65	0.986947911	7.788205	17226.13	339 354 698.44	\$2 261 776 982.25	
68865.1	1050.65	0.984972694	7.756433	15023.18	295 956 623.92	\$2 305 104 416.66	
47989.7	1050.65	0.978575908	7.654044	10678.53	210 367 112.24	\$2 390 686 034.98	
36726.1	1121.69	0.970363034	7.523718	8384.108	165 166 919.59	\$2 435 820 594.32	
30105.1	1111.95	0.964379953	7.429577	7002.881	137 956 758.11	\$2 462 988 423.93	
23875.1	1098.59	0.956010281	7.299016	5702.533	112 339 906.17	\$2 488 572 503.18	
19320.9	1087.11	0.946731084	7.155812	4753.258	93 639 181.57	\$2 507 166 693.91	
13869.0	1050.65	0.9295799	6.895395	3606.195	71 042 050.97	\$2 529 700 476.22	
10803.7	1074.60	0.909532457	6.598034	3000.471	59 109 277.25	\$2 541 515 887.95	
9024.1	1050.65	0.895714622	6.397489	2624.654	51 705 680.09	\$2 548 839 486.57	
7405.4	1068.23	0.873934642	6.088697	2319.488	45 693 910.52	\$2 554 735 966.21	
6031.4	1067.92	0.849574813	5.753928	2056.383	40 510 747.41	\$2 559 713 644.23	
4201.3	1064.85	0.79779375	5.079496	1727.912	34 039 864.50	\$2 565 597 847.68	
2466.5	1052.75	0.700855745	3.952857	1483.827	29 231 383.19	\$2 569 897 883.33	
1623.1	1081.92	0.600028796	2.969054	1518.438	29 913 223.40	\$2 568 632 150.57	
1084.4	1076.49	0.501835603	2.195234	1640.611	32 320 045.99	\$2 565 738 478.58	
1031.4	1089.60	0.48626973	2.089264	1691.943	33 331 269.09	\$2 563 698 106.00	
507.3	1091.51	0.31729629	1.23297	2161.188	42 575 407.10	\$2 553 527 185.77	
404.2	1094.19	0.269780662	1.089181	2292.913	45 170 387.17	\$2 550 020 708.92	
328.7	1095.45	0.230802141	1.003019	2366.436	46 618 797.43	\$2 547 694 923.55	

C₈Ru: 7000

Reactor Cost (\$\$) & EP							
V (m3)	Conversion	D (m)	H (m)	Cost (\$)	H/D based	EP	
#DIV/0!	1.0000	#DIV/0!	#DIV/0!	#DIV/0!	22 106.57	\$2 688 233 533.10	#DIV/0!
2.148441813	0.0208	5.867687	5.867687				#DIV/0!
#DIV/0!	0.0039	#DIV/0!	#DIV/0!	#DIV/0!			#DIV/0!
#DIV/0!	0.0036	#DIV/0!	#DIV/0!	#DIV/0!			#DIV/0!
#DIV/0!	0.0060	#DIV/0!	#DIV/0!	#DIV/0!			#DIV/0!
86.41993462	0.0183	236.0246	236.0246	23 474 166.18		\$2 687 178 374.41	
65.02552403	0.0255	177.5936	177.5936	13 728 163.97		\$2 687 404 909.01	
61.02957074	0.0382	166.6801	166.6801	12 180 506.03		\$2 687 448 768.37	
60.63701408	0.0419	165.6079	165.6079	12 033 163.04		\$2 687 453 107.52	
66.33036672	0.0514	181.1573	181.1573	14 252 330.33		\$2 687 390 705.15	
70.76902004	0.0558	193.2798	193.2798	16 104 251.24		\$2 687 342 798.17	
74.15342455	0.0708	202.5231	202.5231	17 587 485.92		\$2 687 306 673.73	
83.26596615	0.0902	227.4107	227.4107	21 884 571.60		\$2 687 210 993.41	
92.14547782	0.1139	251.6619	251.6619	26 493 193.41		\$2 687 119 759.03	
100.971054	0.1410	275.7657	275.7657	31 481 225.49		\$2 687 030 807.80	
109.7893537	0.1669	299.8497	299.8497	36 866 583.05		\$2 686 943 471.67	
119.427682	0.1846	326.1733	326.1733	43 207 220.79		\$2 686 849 603.24	
140.6640248	0.2364	384.1726	384.1726	58 831 444.09		\$2 686 647 902.74	
207.5915134	0.4267	566.9607	566.9607	122 572 654.81		\$2 686 047 543.77	
269.4462598	0.5118	735.8944	735.8944	200 450 336.32		\$2 685 526 957.55	
334.9846032	0.5535	914.8886	914.8886	302 226 927.60		\$2 685 000 979.46	
402.3586836	0.6114	1098.896	1098.896	427 009 097.99		\$2 684 481 413.34	
535.3246911	0.6800	1462.045	1462.045	731 658 592.13		\$2 683 503 686.52	
667.8329435	0.7574	1823.943	1823.943	1 110 349 853.93		\$2 682 577 013.63	
801.0551415	0.7853	2187.791	2187.791	1 564 745 120.11		\$2 681 681 940.30	
934.1360651	0.8103	2551.253	2551.253	2 090 883 424.11		\$2 680 817 201.00	

Flash-drum							
Total volume flow (m3/hr)	Drum-volume	D (m)	H (m)	tw (m)	shell mass (kg)	cost (\$)	EP
#DIV/0!	#DIV/0!	#DIV/0!	#DIV/0!	#DIV/0!	#DIV/0!	#DIV/0!	#DIV/0!
128.9065088	10.74177938	1.90	3.80	0.001067067	193.2409152	4622.718348	\$2 688 228 910.38
#DIV/0!	#DIV/0!	#DIV/0!	#DIV/0!	#DIV/0!	#DIV/0!	#DIV/0!	#DIV/0!
#DIV/0!	#DIV/0!	#DIV/0!	#DIV/0!	#DIV/0!	#DIV/0!	#DIV/0!	#DIV/0!
#DIV/0!	#DIV/0!	#DIV/0!	#DIV/0!	#DIV/0!	#DIV/0!	#DIV/0!	#DIV/0!
518.5196077	43.20823891	3.02	6.04	0.001697026	777.3013522	25302.4442	\$2 687 153 071.96
312.1225154	26.00916921	2.55	5.10	0.001432875	467.8960055	15713.07757	\$2 687 389 195.93
244.118283	20.34237652	2.35	4.70	0.001320181	365.9523547	12020.48443	\$2 687 436 747.88
207.898334	17.32416817	2.23	4.45	0.001251364	311.655825	9885.285016	\$2 687 443 222.23
198.9911002	16.58192838	2.19	4.39	0.001233231	298.3031865	9337.937417	\$2 687 381 367.21
188.7173868	15.72581984	2.16	4.31	0.001211632	282.9020884	8694.294057	\$2 687 334 103.87
177.9682189	14.83009168	2.11	4.23	0.001188176	266.788247	8005.667697	\$2 687 298 668.06
166.5319323	13.87710592	2.07	4.13	0.00116216	249.644361	7254.485212	\$2 687 203 738.92
157.9636763	13.16311314	2.03	4.06	0.001141876	236.7998766	6678.07897	\$2 687 113 080.95
151.456581	12.62087689	2.00	4.01	0.001125977	227.045233	6231.932871	\$2 687 024 575.87
146.3858049	12.19832912	1.98	3.96	0.001113268	219.4437441	5878.926065	\$2 686 937 592.74
143.3132184	11.94229049	1.97	3.93	0.001105424	214.8376972	5662.643571	\$2 686 843 940.59
140.6640248	11.72153318	1.95	3.91	0.00109857	210.8663491	5474.670637	\$2 686 642 428.07
138.3943423	11.53240054	1.94	3.89	0.001092629	207.463918	5312.496623	\$2 686 042 231.27
134.7231299	11.22647842	1.93	3.85	0.001082881	201.9604842	5047.909601	\$2 685 521 909.64
133.9938413	11.16570679	1.92	3.85	0.001080924	200.8672237	4995.007466	\$2 684 995 984.45
134.1195612	11.17618304	1.92	3.85	0.001081262	201.0556876	5004.135309	\$2 684 476 409.21
133.8311728	11.15215163	1.92	3.84	0.001080486	200.6233708	4983.191898	\$2 683 498 703.33
133.5665887	11.13010384	1.92	3.84	0.001079773	200.2267387	4963.961329	\$2 682 572 049.67
133.5091903	11.12532082	1.92	3.84	0.001079619	200.1406939	4959.78747	\$2 681 676 980.51
133.4480093	11.12022262	1.92	3.84	0.001079454	200.0489789	4955.337767	\$2 680 812 245.66

Membrane Cost						
C8 + C8 (kg/hr)	C12-C14 (kg/hr)	wt frac C8	flux	Area	Membrane cost	EP-cost
#DIV/0!	#DIV/0!	#DIV/0!	#DIV/0!	#DIV/0!	#DIV/0!	#DIV/0!
112.6	1050.65	0.096827911	0.925374	2095.16	41 274 643.16	\$2 646 954 267.22
#DIV/0!	#DIV/0!	#DIV/0!	#DIV/0!	#DIV/0!	#DIV/0!	#DIV/0!
#DIV/0!	#DIV/0!	#DIV/0!	#DIV/0!	#DIV/0!	#DIV/0!	#DIV/0!
#DIV/0!	1050.65	#DIV/0!	#DIV/0!	#DIV/0!	#DIV/0!	#DIV/0!
278686.0	1050.65	0.996244161	7.938725	58728.29	1 156 947 317.83	\$1 530 205 754.13
131112.1	1050.65	0.992050363	7.870619	27986.52	551 334 360.98	\$2 136 054 834.95
82489.1	1050.65	0.987423397	7.795864	17859.83	351 838 720.35	\$2 335 598 027.53
56591.8	1050.65	0.981773052	7.705122	12468.42	245 627 946.70	\$2 441 815 275.54
50223.1	1050.65	0.979509099	7.668933	11143.18	219 520 577.19	\$2 467 860 790.02
42877.4	1050.65	0.976082584	7.614345	9615.198	189 419 406.64	\$2 497 914 697.23
35191.8	1050.65	0.971010597	7.533948	8017.577	157 946 265.43	\$2 529 352 402.63
27014.8	1050.65	0.962564459	7.401144	6320.072	124 505 423.86	\$2 562 698 315.06
20888.5	1050.65	0.952110937	7.23864	5051.399	99 512 565.99	\$2 587 600 514.96
16235.9	1050.65	0.939221903	7.041112	4091.821	80 608 879.98	\$2 606 415 695.89
12610.3	1050.65	0.92309148	6.798323	3349.105	65 977 367.15	\$2 620 960 225.59
10413.4	1050.65	0.908353247	6.580779	2903.425	57 197 473.05	\$2 629 646 467.54
8519.3	1050.65	0.890213588	6.318652	2524.248	49 727 679.34	\$2 636 914 748.73
5203.3	1069.03	0.829563399	5.48729	1905.102	37 530 518.40	\$2 648 511 712.87
2330.1	1071.73	0.684953005	3.784953	1497.95	29 509 610.53	\$2 656 012 299.11
1663.6	1073.30	0.607837248	3.038394	1501.276	29 575 128.54	\$2 655 420 855.91
1350.1	1077.68	0.556096172	2.60036	1556.028	30 653 753.82	\$2 653 822 655.39
1012.3	1079.11	0.484037859	2.074445	1680.332	33 102 547.03	\$2 650 396 156.30
708.9	1080.35	0.396198671	1.5658	1904.511	37 518 867.26	\$2 645 053 182.40
479.3	1082.40	0.306906097	1.19789	2172.837	42 804 895.28	\$2 638 872 085.23
401.5	1082.77	0.270510666	1.091068	2267.325	44 666 298.35	\$2 636 145 947.31

C₈/Ru: 10 000

Reactor Cost (\$\$) & EP					
V (m3)	Conversion	D (m)	H (m)	Cost (\$) H/D based	EP
#DIV/0!	1.0000	#DIV/0!	#DIV/0!	#DIV/0!	#DIV/0!
#DIV/0!	0.0000	#DIV/0!	#DIV/0!	#DIV/0!	#DIV/0!
#DIV/0!	0.0119	#DIV/0!	#DIV/0!	#DIV/0!	#DIV/0!
#DIV/0!	0.0043	#DIV/0!	#DIV/0!	#DIV/0!	#DIV/0!
#DIV/0!	0.0072	#DIV/0!	#DIV/0!	#DIV/0!	#DIV/0!
#DIV/0!	0.0139	#DIV/0!	#DIV/0!	#DIV/0!	#DIV/0!
88.06264135	0.0249	240.5111	240.5111	24 322 793.73	\$2 751 983 873.75
75.5356284	0.0370	206.2981	206.2981	18 210 869.36	\$2 752 114 409.75
71.24884206	0.0373	194.5903	194.5903	16 310 799.42	\$2 752 160 049.91
73.58011915	0.0450	200.9573	200.9573	17 331 915.95	\$2 752 135 163.41
76.09310565	0.0547	207.8206	207.8206	18 465 180.20	\$2 752 108 513.07
87.03573889	0.0617	237.7065	237.7065	23 790 633.62	\$2 751 994 427.57
92.23400579	0.0732	251.9036	251.9036	26 541 218.40	\$2 751 941 252.48
104.5281054	0.0936	285.4805	285.4805	33 605 462.96	\$2 751 817 796.30
109.0694585	0.0950	297.8836	297.8836	36 411 992.97	\$2 751 772 941.36
122.8243755	0.1191	335.4501	335.4501	45 554 049.06	\$2 751 639 282.48
131.3222272	0.1380	358.6589	358.6589	51 679 965.68	\$2 751 558 214.72
148.4923041	0.1552	405.5527	405.5527	65 158 329.06	\$2 751 397 520.54
214.4474363	0.2426	585.6852	585.6852	130 318 909.10	\$2 750 810 844.64
273.9618679	0.3160	748.2272	748.2272	206 833 013.65	\$2 750 312 349.18
335.8795597	0.3837	917.3328	917.3328	303 751 561.42	\$2 749 816 342.48
402.9333731	0.4431	1100.466	1100.466	428 160 092.83	\$2 749 299 454.37
534.1879317	0.5303	1458.94	1458.94	728 731 120.74	\$2 748 334 215.64
665.1008622	0.6012	1816.481	1816.481	1 101 798 411.03	\$2 747 418 117.33
801.5893211	0.6669	2189.25	2189.25	1 566 713 633.72	\$2 746 500 808.44
933.693852	0.7153	2550.045	2550.045	2 089 017 036.07	\$2 745 642 425.67

Flash-drum							
Total volume flow (m ³ /hr)	Drum-volume	D (m)	H (m)	tw (m)	shell mass (kg)	cost (\$)	EP
#DIV/0!	#DIV/0!	#DIV/0!	#DIV/0!	#DIV/0!	#DIV/0!	#DIV/0!	#DIV/0!
#DIV/0!	#DIV/0!	#DIV/0!	#DIV/0!	#DIV/0!	#DIV/0!	#DIV/0!	#DIV/0!
#DIV/0!	#DIV/0!	#DIV/0!	#DIV/0!	#DIV/0!	#DIV/0!	#DIV/0!	#DIV/0!
#DIV/0!	#DIV/0!	#DIV/0!	#DIV/0!	#DIV/0!	#DIV/0!	#DIV/0!	#DIV/0!
#DIV/0!	#DIV/0!	#DIV/0!	#DIV/0!	#DIV/0!	#DIV/0!	#DIV/0!	#DIV/0!
#DIV/0!	#DIV/0!	#DIV/0!	#DIV/0!	#DIV/0!	#DIV/0!	#DIV/0!	#DIV/0!
422.7006785	35.22364754	2.82	5.64	0.001585298	633.6613004	21088.50783	\$2 751 962 785.24
302.1425136	25.17753566	2.52	5.04	0.001417438	452.9352041	15192.9732	\$2 752 099 216.78
244.2817442	20.35599774	2.35	4.70	0.001320476	366.1973959	12029.82118	\$2 752 148 020.09
220.7403575	18.39429399	2.27	4.54	0.001276617	330.9070202	10658.18768	\$2 752 124 505.22
202.9149484	16.90890265	2.21	4.42	0.001241285	304.1853411	9580.239835	\$2 752 098 932.83
208.8857733	17.40645149	2.23	4.46	0.001253342	313.1360736	9945.379926	\$2 751 984 482.19
184.4680116	15.3717194	2.14	4.28	0.001202469	276.5319434	8423.990366	\$2 751 932 828.49
179.1910378	14.93198918	2.12	4.24	0.001190891	268.621348	8084.828347	\$2 751 809 711.48
163.6041877	13.63313696	2.06	4.11	0.001155309	245.2554435	7058.893407	\$2 751 765 882.46
163.765834	13.64660695	2.06	4.11	0.001155689	245.4977638	7069.728724	\$2 751 632 212.75
157.5866727	13.13169744	2.03	4.06	0.001140967	236.2347189	6652.433566	\$2 751 551 562.29
148.4923041	12.3738637	1.99	3.98	0.001118583	222.6015507	6026.156585	\$2 751 391 494.38
142.9649576	11.91326991	1.96	3.93	0.001104528	214.3156269	5638.012634	\$2 750 805 206.62
136.9809339	11.41462122	1.94	3.87	0.001088897	205.3451086	5210.967591	\$2 750 307 138.22
134.3518239	11.19553748	1.92	3.85	0.001081885	201.4038675	5020.989648	\$2 749 811 321.49
134.3111244	11.19214599	1.92	3.85	0.001081776	201.3428557	5018.037096	\$2 749 294 436.33
133.5469829	11.12847009	1.92	3.84	0.001079721	200.1973481	4962.535732	\$2 748 329 253.11
133.0201724	11.08457097	1.92	3.84	0.001078299	199.4076181	4924.198264	\$2 747 413 193.13
133.5982202	11.13273969	1.92	3.84	0.001079859	200.2741567	4966.261179	\$2 746 495 842.18
133.384836	11.11495838	1.92	3.84	0.001079283	199.9542772	4950.742302	\$2 745 637 474.93

Membrane Cost						
C8 + 2-C8 (kg/hr)	C12-C14 (kg/hr)	wt frac C8	flux	Area	Membrane cost	EP-cost
#DIV/0!	#DIV/0!	#DIV/0!	#DIV/0!	#DIV/0!	#DIV/0!	#DIV/0!
#DIV/0!	#DIV/0!	#DIV/0!	#DIV/0!	#DIV/0!	#DIV/0!	#DIV/0!
#DIV/0!	#DIV/0!	#DIV/0!	#DIV/0!	#DIV/0!	#DIV/0!	#DIV/0!
#DIV/0!	#DIV/0!	#DIV/0!	#DIV/0!	#DIV/0!	#DIV/0!	#DIV/0!
#DIV/0!	#DIV/0!	#DIV/0!	#DIV/0!	#DIV/0!	#DIV/0!	#DIV/0!
#DIV/0!	1705.48	#DIV/0!	#DIV/0!	#DIV/0!	#DIV/0!	#DIV/0!
209756.6	1374.44	0.993490116	7.893963	44576.47	878 156 431.19	\$1 873 806 354.05
109787.5	1384.57	0.987545707	7.797835	23761.31	468 097 781.91	\$2 284 001 434.87
82370.9	1232.30	0.985260163	7.761052	17953.58	353 685 560.96	\$2 398 462 459.13
65590.8	1192.13	0.982149253	7.711145	14434.29	284 355 429.00	\$2 467 769 076.22
52895.6	1153.48	0.978658689	7.655364	11767.15	231 812 923.37	\$2 520 286 009.47
46295.8	1291.24	0.972865836	7.563299	10486.4	206 582 146.65	\$2 545 402 335.54
39634.5	1208.76	0.970404089	7.524379	9046.883	178 223 598.41	\$2 573 709 230.08
30613.5	1218.38	0.961724564	7.388012	7180.982	141 465 352.68	\$2 610 344 358.79
24826.7	1123.91	0.956690315	7.309575	5917.034	116 565 563.63	\$2 635 200 318.83
21208.8	1142.17	0.948898402	7.189114	5181.661	102 078 718.51	\$2 649 553 494.25
16897.0	1128.75	0.937381429	7.013162	4283.799	84 390 845.41	\$2 667 160 716.88
14050.3	1101.84	0.927281572	6.860919	3680.772	72 511 211.70	\$2 678 880 282.68
10131.9	1075.80	0.904011826	6.517479	2866.058	56 461 337.83	\$2 694 343 868.80
5860.2	1070.47	0.845546424	5.699645	2026.639	39 924 785.64	\$2 710 382 352.58
3988.7	1064.08	0.789404365	4.974987	1692.713	33 346 446.89	\$2 716 464 874.60
2928.0	1073.52	0.731719206	4.292329	1553.731	30 608 497.35	\$2 718 685 938.99
2163.3	1077.15	0.667594357	3.607122	1497.259	29 495 997.67	\$2 718 833 255.44
1479.3	1078.47	0.578354536	2.782608	1531.993	30 180 270.33	\$2 717 232 922.80
1070.6	1084.74	0.496721682	2.159915	1663.146	32 763 968.22	\$2 713 731 873.96
786.4	1085.48	0.420109038	1.689842	1846.195	36 370 040.08	\$2 709 267 434.85

C₈/Ru: 12000

Reactor Cost (\$\$) & EP				Cost (\$) H/D based		EP
V (m3)	Conversion	D (m)	H (m)	#DIV/0!	#DIV/0!	#DIV/0!
#DIV/0!	1.0000	#DIV/0!	#DIV/0!			
2.148437607	0.0359	5.867676	5.867676		22 106.49	\$2 778 264 635.87
9.522632292	0.0350	26.00761	26.00761		366 498.35	\$2 778 131 916.48
18.86464393	0.0395	51.52191	51.52191		1 330 483.76	\$2 777 993 143.42
27.38359898	0.0465	74.78834	74.78834		2 686 850.04	\$2 777 878 723.95
35.2307021	0.0448	96.21985	96.21985		4 321 453.70	\$2 777 779 598.44
42.81484052	0.0458	116.9332	116.9332		6 241 991.94	\$2 777 687 947.35
50.57353196	0.0458	138.1232	138.1232		8 545 463.27	\$2 777 597 501.93
68.64225875	0.0227	187.4714	187.4714		15 203 654.43	\$2 777 396 777.88
86.149665	0.0278	235.2865	235.2865		23 335 900.95	\$2 777 212 262.83
87.53539694	0.0373	239.0711	239.0711		24 048 874.99	\$2 777 197 998.08
89.00864466	0.0443	243.0947	243.0947		24 817 921.30	\$2 777 182 881.87
90.18814708	0.4822	246.3161	246.3161		25 441 820.62	\$2 777 170 815.68
87.91845064	0.1076	240.1173	240.1173		24 247 737.70	\$2 777 194 062.90
108.9067972	0.1170	297.4393	297.4393		36 309 644.81	\$2 776 983 250.18
121.5843942	0.1258	332.0635	332.0635		44 690 569.97	\$2 776 859 912.67
123.9040982	0.1671	338.399	338.399		46 312 249.09	\$2 776 837 630.15
148.4143756	0.1739	405.3399	405.3399		65 093 852.32	\$2 776 606 949.91
213.4274752	0.2066	582.8995	582.8995		129 152 379.68	\$2 776 028 320.51
278.6117904	0.3410	760.9268	760.9268		213 503 665.94	\$2 775 483 082.27
338.496871	0.4030	924.4811	924.4811		308 231 047.60	\$2 775 004 510.70
402.9577046	0.4234	1100.532	1100.532		428 208 856.44	\$2 774 507 978.85
538.1504592	0.4935	1469.762	1469.762		738 959 612.85	\$2 773 514 581.60
675.4891636	0.7048	1844.853	1844.853		1 134 479 291.73	\$2 772 555 766.46
797.809682	0.6443	2178.927	2178.927		1 552 810 220.05	\$2 771 734 474.37
931.1503018	0.6384	2543.098	2543.098		2 078 297 030.79	\$2 770 867 421.69

Flash-drum							
Total volume flow (m3/hr)	Drum-volume	D (m)	H (m)	tw (m)	shell mass (kg)	cost (\$)	EP
#DIV/0!	#DIV/0!	#DIV/0!	#DIV/0!	#DIV/0!	#DIV/0!	#DIV/0!	#DIV/0!
128.9062564	10.74175835	1.90	3.80	0.001067066	193.2405369	4622.699736	\$2 778 260 013.17
228.543175	19.04450277	2.30	4.59	0.001291485	342.6040526	11119.0243	\$2 778 120 797.46
226.3757272	18.86388935	2.29	4.58	0.00128739	339.3548792	10991.6542	\$2 777 982 151.76
219.0687918	18.25500242	2.27	4.53	0.001273386	328.4012129	10558.62197	\$2 777 868 165.33
211.3842126	17.61464644	2.24	4.48	0.001258319	316.881429	10096.92799	\$2 777 769 501.52
205.5112345	17.12525117	2.22	4.43	0.001246556	308.0773765	9739.534142	\$2 777 678 207.81
202.2941278	16.85716967	2.21	4.41	0.001240017	303.2546827	9542.029045	\$2 777 587 959.90
235.3448872	19.61128945	2.32	4.64	0.001304172	352.8003498	11515.62474	\$2 777 385 262.26
258.448995	21.53655475	2.39	4.79	0.001345525	387.4352103	12829.79377	\$2 777 199 433.04
233.4277252	19.45153234	2.31	4.63	0.001300621	349.9263744	11404.30656	\$2 777 186 593.77
213.6207472	17.80101686	2.25	4.49	0.001262742	320.2341689	10231.98298	\$2 777 172 649.88
180.3762942	15.03075659	2.12	4.25	0.001193511	270.3981397	8161.351373	\$2 777 162 654.33
150.717344	12.55927627	2.00	4.00	0.001124142	225.9370591	6180.76791	\$2 777 187 882.14
163.3601959	13.61280512	2.05	4.11	0.001154734	244.8896806	7042.530264	\$2 776 976 207.65
162.1125256	13.50883676	2.05	4.10	0.001151787	243.0193255	6958.702848	\$2 776 852 953.97
148.6849179	12.38991421	1.99	3.98	0.001119066	222.8902938	6039.577209	\$2 776 831 590.57
148.4143756	12.36736992	1.99	3.98	0.001118387	222.4847298	6020.724834	\$2 776 600 929.19
142.2849835	11.85660767	1.96	3.92	0.001102774	213.2962927	5589.851814	\$2 776 022 730.65
139.3058952	11.60836025	1.95	3.90	0.001095023	208.8304069	5377.756059	\$2 775 477 704.51
135.3987484	11.28277771	1.93	3.86	0.001084688	202.9732891	5096.816416	\$2 774 999 413.89
134.3192349	11.19282184	1.92	3.85	0.001081798	201.355014	5018.625503	\$2 774 502 960.23
134.5376148	11.21101944	1.93	3.85	0.001082384	201.6823826	5034.463337	\$2 773 509 547.14
135.0978327	11.2577024	1.93	3.86	0.001083884	202.5221929	5075.045751	\$2 772 550 691.42
132.9682803	11.0802468	1.92	3.84	0.001078159	199.3298277	4920.418648	\$2 771 729 553.95
133.0214717	11.08467924	1.92	3.84	0.001078303	199.4095657	4924.292889	\$2 770 862 497.40

Membrane Cost							
C8 + 2-C8 (kg/hr)	C12-C14 (kg/hr)	wt frac C8	flux	Area	Membrane cost	EP-cost	
#DIV/0!	#DIV/0!	#DIV/0!	#DIV/0!	#DIV/0!	#DIV/0!	#DIV/0!	
112.5	1050.65	0.096687209	0.925471	2094.615	41 263 915.42	\$2 736 996 097.76	
71352.9	1050.65	0.985489021	7.764731	15541.1	306 159 761.58	\$2 471 961 035.87	
69803.1	1050.65	0.985171634	7.75963	15218.46	299 803 689.21	\$2 478 178 462.56	
64370.5	1211.52	0.981526674	7.701179	14193.08	279 603 615.80	\$2 498 264 549.52	
59084.2	1050.65	0.982528503	7.71722	12987.16	255 846 978.10	\$2 521 922 523.41	
54885.0	1050.65	0.98121689	7.696223	12113.23	238 630 586.14	\$2 539 047 621.67	
52584.8	1050.65	0.98041135	7.683344	11634.57	229 200 979.47	\$2 548 386 980.43	
76216.1	1050.65	0.986402352	7.779422	16553.66	326 107 011.21	\$2 451 278 251.05	
92735.5	1050.65	0.988797434	7.818021	19993.58	393 873 598.22	\$2 383 325 834.82	
74845.3	1050.65	0.986156763	7.77547	16268.25	320 484 427.65	\$2 456 702 166.12	
60683.3	1050.65	0.982981075	7.724472	13320	262 403 930.94	\$2 514 768 718.95	
29422.8	1131.99	0.962952244	7.407212	6875.004	135 437 575.17	\$2 641 725 079.16	
7250.8	1142.47	0.863881425	5.949183	2351.366	46 321 915.98	\$2 730 865 966.15	
19913.4	1103.13	0.947511099	7.167787	4886.794	96 269 843.76	\$2 680 706 363.89	
17877.6	1115.55	0.941265517	7.072222	4475.994	88 177 089.01	\$2 688 675 864.96	
14254.2	1050.65	0.931352085	6.922046	3685.049	72 595 455.93	\$2 704 236 134.64	
10937.6	1084.56	0.909786592	6.601756	3035.089	59 791 256.26	\$2 716 809 672.92	
9678.2	1050.65	0.902073233	6.489328	2755.522	54 283 785.63	\$2 721 738 945.02	
6485.6	1062.18	0.859272347	5.885857	2137.27	42 104 212.84	\$2 733 373 491.67	
3553.0	1063.69	0.769597695	4.733516	1625.529	32 022 912.51	\$2 742 976 501.38	
2799.7	1063.49	0.724715091	4.213714	1528.042	30 102 426.69	\$2 744 400 533.54	
2393.8	1069.59	0.691173251	3.850059	1499.29	29 536 017.59	\$2 743 973 529.55	
3026.4	1067.11	0.739317542	4.378661	1558.141	30 695 380.14	\$2 741 855 311.27	
823.1	1074.47	0.433781104	1.765615	1791.27	35 288 012.14	\$2 736 441 541.82	
929.1	1073.73	0.463900901	1.944983	1716.257	33 810 255.20	\$2 737 052 242.20	

C₈/Ru: 14000

Reactor Cost (\$\$) & EP						
V (m3)	Conversion	D (m)	H (m)	Cost (\$)	H/D based	EP
#DIV/0!	1.0000	#DIV/0!	#DIV/0!	#DIV/0!	#DIV/0!	#DIV/0!
2.148481831	0.0075	5.867797	5.867797	22 107.35	\$2 796 270 855.45	
#DIV/0!	0.0113	#DIV/0!	#DIV/0!	#DIV/0!	#DIV/0!	#DIV/0!
#DIV/0!	0.0131	#DIV/0!	#DIV/0!	#DIV/0!	#DIV/0!	#DIV/0!
127.1129707	0.0127	347.1628	347.1628	48 600 237.17	\$2 794 813 163.92	
123.5558562	0.0174	337.4479	337.4479	46 067 065.15	\$2 794 847 190.46	
87.66378915	0.0218	239.4218	239.4218	24 115 444.21	\$2 795 202 899.24	
87.4813341	0.0284	238.9234	238.9234	24 020 870.17	\$2 795 204 774.28	
84.21296212	0.0338	229.9971	229.9971	22 356 354.31	\$2 795 238 497.04	
130.7962845	0.0692	357.2225	357.2225	51 290 299.40	\$2 794 778 130.27	
139.4432844	0.0867	380.8386	380.8386	57 872 224.52	\$2 794 696 646.72	
101.5307833	0.0564	277.2944	277.2944	31 811 168.93	\$2 795 062 543.37	
113.3081793	0.0645	309.4601	309.4601	39 126 683.28	\$2 794 946 340.89	
109.5873996	0.0680	299.2981	299.2981	36 738 788.34	\$2 794 982 778.93	
117.4486511	0.0820	320.7683	320.7683	41 866 792.23	\$2 794 906 072.80	
126.0310776	0.0882	344.208	344.208	47 823 036.00	\$2 794 823 492.67	
136.51682	0.0990	372.846	372.846	55 602 894.54	\$2 794 724 107.48	
158.6210206	0.1132	433.2156	433.2156	73 793 252.35	\$2 794 519 414.03	
226.0644977	0.1677	617.4129	617.4129	143 952 275.60	\$2 793 926 495.86	
286.2757059	0.2088	781.858	781.858	224 714 891.06	\$2 793 426 987.03	
348.5969333	0.2546	952.0657	952.0657	325 805 592.39	\$2 792 931 761.43	
410.8064741	0.2906	1121.968	1121.968	444 074 877.76	\$2 792 454 874.09	
548.3601805	0.3556	1497.646	1497.646	765 622 351.85	\$2 791 447 966.31	
681.0389086	0.4694	1860.01	1860.01	1 152 122 201.71	\$2 790 524 114.49	
804.8412023	0.4247	2198.131	2198.131	1 578 722 271.16	\$2 789 694 284.19	
940.5385746	0.4730	2568.739	2568.739	2 117 993 323.43	\$2 788 813 569.70	

Flash-drum							
Total volume flow (m3/hr)	Drum-volume	D (m)	H (m)	tw (m)	shell mass (kg)	cost (\$)	EP
#DIV/0!	#DIV/0!	#DIV/0!	#DIV/0!	#DIV/0!	#DIV/0!	#DIV/0!	#DIV/0!
128.9089099	10.74197946	1.90	3.80	0.001067074	193.2445147	4622.895432	\$2 796 266 232.56
#DIV/0!	#DIV/0!	#DIV/0!	#DIV/0!	#DIV/0!	#DIV/0!	#DIV/0!	#DIV/0!
#DIV/0!	#DIV/0!	#DIV/0!	#DIV/0!	#DIV/0!	#DIV/0!	#DIV/0!	#DIV/0!
1016.903766	84.73859082	3.78	7.56	0.00212419	1524.418094	43491.39508	\$2 794 769 672.52
741.335137	61.77545696	3.40	6.80	0.001911781	1111.319217	34040.02495	\$2 794 813 150.43
420.7861879	35.06411304	2.82	5.63	0.001582901	630.7913297	21000.62306	\$2 795 181 898.61
349.9253364	29.15927828	2.65	5.30	0.001488533	524.565384	17625.53719	\$2 795 187 148.75
288.7301558	24.05988389	2.48	4.97	0.001396146	432.8290332	14483.03596	\$2 795 224 014.01
392.3888534	32.69776315	2.75	5.50	0.001546461	588.2215094	19677.66854	\$2 794 758 452.60
371.8487583	30.98615703	2.70	5.40	0.001518992	557.4303042	18696.75241	\$2 794 677 949.97
243.67388	20.30534442	2.35	4.69	0.001319379	365.28616	11995.08788	\$2 795 050 548.28
226.6163586	18.88394116	2.29	4.58	0.001287846	339.7156045	11005.81891	\$2 794 935 335.07
187.8641137	15.65471659	2.15	4.30	0.001209803	281.6229654	8640.21412	\$2 794 974 138.71
176.1729767	14.68049415	2.11	4.21	0.001184168	264.0970388	7889.055219	\$2 794 898 183.75
168.0414368	14.00289293	2.07	4.15	0.001165661	251.9072261	7354.791969	\$2 794 816 137.87
163.820184	13.65113593	2.06	4.11	0.001155817	245.5792387	7073.3709	\$2 794 717 034.10
158.6210206	13.21788965	2.03	4.07	0.001143458	237.7852871	6722.735878	\$2 794 512 691.30
150.7096651	12.55863639	2.00	4.00	0.001124123	225.9255479	6180.235907	\$2 793 920 315.62
143.137853	11.92767729	1.97	3.93	0.001104973	214.5748107	5650.243752	\$2 793 421 336.79
139.4387733	11.61943298	1.95	3.90	0.001095371	209.0296016	5387.254721	\$2 792 926 374.18
136.9354914	11.4108345	1.94	3.87	0.001088776	205.2769867	5207.696392	\$2 792 449 666.39
137.0900451	11.42371346	1.94	3.87	0.001089186	205.5086748	5218.82023	\$2 791 442 747.49
136.2077817	11.35019445	1.93	3.87	0.001086844	204.1860931	5155.252644	\$2 790 518 959.24
134.1402004	11.1779029	1.92	3.85	0.001081317	201.0866273	5005.633481	\$2 789 689 278.56
134.3626535	11.19643992	1.92	3.85	0.001081914	201.420102	5021.775226	\$2 788 808 547.93

Membrane Cost						
C8 + 2-C8 (kg/hr)	C12-C14 (kg/hr)	wt frac C8	flux	Area	Membrane cost	EP-cost
#DIV/0!	#DIV/0!	#DIV/0!	#DIV/0!	#DIV/0!	#DIV/0!	#DIV/0!
114.4	1050.65	0.098164433	0.924477	2100.301	41 375 924.10	\$2 754 890 308.46
#DIV/0!	#DIV/0!	#DIV/0!	#DIV/0!	#DIV/0!	#DIV/0!	#DIV/0!
#DIV/0!	2398.97	#DIV/0!	#DIV/0!	#DIV/0!	#DIV/0!	#DIV/0!
633234.0	2439.40	0.99616249	7.937396	133476.5	2 629 486 648.45	\$165 283 024.08
437463.4	1464.72	0.996662951	7.945544	92070.08	1 813 780 479.16	\$981 032 671.27
208419.8	1349.62	0.993566198	7.895198	44282.07	872 356 843.26	\$1 922 825 055.35
157740.8	1360.02	0.991451834	7.860927	33732.42	664 528 753.03	\$2 130 658 395.72
113930.4	1403.20	0.987833578	7.802475	24636.12	485 331 574.85	\$2 309 892 439.15
91099.5	2286.92	0.975511225	7.605264	20465.3	403 166 480.03	\$2 391 591 972.58
68535.4	2427.37	0.965793731	7.451761	15871.59	312 670 393.78	\$2 482 007 556.19
59919.5	1514.27	0.975351241	7.602722	13467.49	265 309 481.94	\$2 529 741 066.34
54293.7	1351.58	0.975710853	7.608436	12189.38	240 130 717.14	\$2 554 804 617.93
42116.6	1167.16	0.973034592	7.565972	9534.739	187 834 352.26	\$2 607 139 786.46
33785.4	1145.55	0.967205304	7.473949	7789.485	153 452 864.26	\$2 641 445 319.49
28010.8	1115.02	0.961717202	7.387897	6570.622	129 441 255.35	\$2 665 374 882.52
24970.5	1132.15	0.956627041	7.308592	5952.496	117 264 170.36	\$2 677 452 863.75
21307.5	1090.09	0.951330048	7.226584	5165.551	101 761 353.35	\$2 692 751 337.94
15638.7	1099.45	0.934314812	6.966733	4004.316	78 885 029.20	\$2 715 035 286.43
10246.9	1082.47	0.904454405	6.523916	2894.311	57 017 930.38	\$2 736 403 406.41
7620.4	1068.31	0.877045523	6.132255	2361.465	46 520 854.68	\$2 746 405 519.50
5833.3	1066.11	0.845478917	5.698738	2017.833	39 751 311.51	\$2 752 698 354.88
4612.0	1082.60	0.809890336	5.232523	1813.849	35 732 822.10	\$2 755 709 925.39
3180.8	1086.07	0.745465594	4.449311	1598.34	31 487 293.21	\$2 759 031 666.03
2317.4	1085.04	0.68109869	3.744976	1514.226	29 830 247.69	\$2 759 859 030.87
2491.5	1085.38	0.696558491	3.907015	1525.849	30 059 226.81	\$2 758 749 321.12

CAPITAL COST ESTIMATION FOR GMPP

Total Capital investment		
Equipment		Cost (\$)
Reactor		31 811 168.93
Flash drum		11995.08788
Membrane		265309481.94
column		1510617.08
Heater		6171.044358
Mixer		48010.94483
Total Equipment cost		298 697 445.02
item	% of purchased equipment	total cost
Direct cost		
Equipment installation	47	140 387 799.16
Instrumentation and control	18	53 765 540.10
Piping	66	197 140 313.72
Electrical	11	32 856 718.95
Buildings (including services)	6	17 921 846.70
Yard improvements	10	29 869 744.50
Service facilities (installed)	30	89 609 233.51
Land	6	17 921 846.70
total Direct reaction unit plant cost		878 170 488.37
Indirect cost		
Engineering and supervision	33	98 570 156.86
Construction expenses	41	122 465 952.46
Contractor's fee an legal expenses	21	62 726 463.45
Contingency	35	104 544 105.76
total indirect reaction unit plant cost		388 306 678.53
Fixed Capital Investment (FCI)		1 266 477 166.90
Working capital	86	1 089 170 363.53
Total Capital Investment		2 355 647 530.43

OPERATIONAL COSTS ESTIMATION GMPP CATALYST

Raw materials cost					
Material	Price/unit		Feedrate		USD/yr
1-Octene	1.8 USD/kg		4330.47 kg/hr		64 915 459.98
GMPP catalyst	20995.66 USD/kg		0.86503054 kgCat/hr		151 252 195.81
Total					216 167 655.79
Labour operations					
Operators/shift/section	Number of sections	Number of shifts	Hours per year	Wage rate (\$/h)	Direct wages & benefits (DW&B)
2	3	5	8328	30	7495200
Item	Factor	Total cost per year			
Direct salaries and benefits	0.15	1124280			
Operating supplies and services	0.06	449712			
Technical assistance to manufacturing		260000			
Control laboratory		285000			
Total labour-related operations annual cost		2118992			
TOTAL LABOUR-RELATED OPERATIONS ANNUAL COST		9 614 192.00			
Product sales					
ITEM	Cost/unit		Production rate		Revenue/yr
7-Tetradecene	334.00 USD/Kg		1050.64568 kg/hr		2 922 425 592.59
Maintenance					
			Wage factor (% purchased Capital)	wages & benefits (MW&B)	
			0.035	30 735 967.09	
Item	Factor	Total cost per year			
Salaries and benefits	0.25	7 683 991.77			
materials and services	1	30 735 967.09			
Maintenance overhead	0.05	1 536 798.35			
		39956757.22			
Maintnance and Operataion benefits		70 692 724.31			
MAINTENANCE OPERATION SALARIES AND BENEFITS		80 306 916.31			
Overhead					
General plant overhead			0.071		5 701 791.06
Utilities					
	Input (kw)	Cost/unit		Total Annual cost	
Electricity	42186.42	0.235292419 \$/kwh		82664925.71	

Line	Item	-	1	2	3	4	5	6	7	8	9	10	11	12	13	14	15
1	Fixed Capital	-379 943 150	-506 590 867	-253 295 433													
2	Working capital			-1 089 170 364													
3	TOTAL CAPITAL INVESTMENT	-379 943 150	-506 590 867	-1 342 465 797													
4	Inflation Factor	1.000	1.063	1.130	1.201	1.277	1.357	1.443	1.534	1.630	1.733	1.842	1.958	2.082	2.213	2.352	2.500
5	Annual Income (Sales)	-		584 485 119	1 753 455 356	2 922 425 593	2 922 425 593	2 922 425 593	2 922 425 593	2 922 425 593	2 922 425 593	2 922 425 593	2 922 425 593	2 922 425 593	2 922 425 593	2 922 425 593	2 922 425 593
6	<i>Annual manufacturing cost</i>	-	-	-	-	-	-	-	-	-	-	-	-	-	-	-	-
a	Raw materials (Variable cost)	-	-	-73 278 825	-207 721 042	-276 009 335	-293 397 923	-311 881 992	-331 530 558	-352 416 983	-374 619 253	-398 220 266	-423 308 143	-449 976 556	-478 325 079	-508 459 559	-540 492 511
b	Labor (fixed cost)	-	-	-3 259 122	-11 548 154	-12 275 688	-13 049 057	-13 871 147	-14 745 029	-15 673 966	-16 661 426	-17 711 096	-18 826 895	-20 012 989	-21 273 808	-22 614 058	-24 038 743
c	Utilities (variable cost)	-	-	-93 408 803	-79 434 846	-105 549 052	-112 198 643	-119 267 157	-126 780 988	-134 768 190	-143 258 586	-152 283 877	-161 877 761	-172 076 060	-182 916 852	-194 440 614	-206 690 372
d	Maintenance (fixed cost)	-	-	-79 880 587	-84 913 064	-90 262 587	-95 949 130	-101 993 925	-108 419 542	-115 249 974	-122 510 722	-130 228 897	-138 433 318	-147 154 617	-156 425 358	-166 280 155	-176 755 805
h	Plant overhead (fixed cost)	-	-	-6 442 847	-6 848 747	-7 280 218	-7 738 871	-8 226 420	-8 744 685	-9 295 600	-9 881 223	-10 503 740	-11 165 475	-11 868 900	-12 616 641	-13 411 489	-14 256 413
6T	TOTAL ANNUAL MANUFACTURING COST	-	-	-256 270 184	-390 465 854	-491 376 880	-522 333 624	-555 240 642	-590 220 802	-627 404 713	-666 931 210	-708 947 876	-753 611 592	-801 089 123	-851 557 737	-905 205 875	-962 233 845
7	<i>Annual General Expenses</i>	-	-														
a	Administrative	-	-	-13 209 001	-42 123 505	-74 628 810	-79 330 425	-84 328 242	-89 640 921	-95 288 299	-101 291 462	-107 672 824	-114 456 212	-121 666 953	-129 331 971	-137 479 885	-146 141 118
b	Distribution/ selling	-	-	-19 813 502	-63 185 258	-111 943 215	-118 995 637	-126 492 363	-134 461 381	-142 932 448	-151 937 193	-161 509 236	-171 684 318	-182 500 430	-193 997 957	-206 219 828	-219 211 677
c	R&D	-	-	-33 022 503	-105 308 763	-186 572 025	-198 326 062	-210 820 604	-224 102 302	-238 220 747	-253 228 655	-269 182 060	-286 140 530	-304 167 383	-323 329 928	-343 699 714	-365 352 795
7T	TOTAL ANNUAL GENERAL EXPENSES	-	-	-66 045 006	-210 617 526	-373 144 050	-396 652 125	-421 641 209	-448 204 605	-476 441 495	-506 457 309	-538 364 120	-572 281 059	-608 334 766	-646 659 856	-687 399 427	-730 705 591
8	TOTAL COST OF PRODUCTION (7T+6T)	-	-	-322 315 191	-601 083 380	-864 520 930	-918 985 748	-976 881 851	-1 038 425 407	-1 103 846 208	-1 173 388 519	-1 247 311 996	-1 325 892 651	-1 409 423 888	-1 498 217 593	-1 592 605 302	-1 692 939 436
9	Annual Operating Income (5-8)	-	-	262 169 928	1 152 371 976	2 057 904 663	2 003 439 844	1 945 543 742	1 884 000 185	1 818 579 385	1 749 037 074	1 675 113 597	1 596 532 941	1 513 001 704	1 424 207 999	1 329 820 291	1 229 486 157
10	Annual depreciation (fixed Cost)	-	-	-59 102 268	-59 102 268	-59 102 268	-59 102 268	-59 102 268	-59 102 268	-59 102 268	-59 102 268	-59 102 268	-59 102 268	-59 102 268	-59 102 268	-59 102 268	
11	Income before tax (9-10)	-	-	203 067 660	1 093 269 708	1 998 802 395	1 944 337 576	1 886 441 474	1 824 897 918	1 759 477 117	1 689 934 806	1 616 011 329	1 537 430 673	1 453 899 436	1 365 105 731	1 270 718 023	1 170 383 889
12	Income after tax	-	-	202 499 071	1 090 208 553	1 993 205 748	1 938 893 431	1 881 159 438	1 819 788 203	1 754 550 581	1 685 202 988	1 611 486 497	1 533 125 868	1 449 828 518	1 361 283 435	1 267 160 013	1 167 106 814
13	<i>Annual cash income (10+12)</i>	-	-	143 396 803	1 031 106 285	1 934 103 480	1 879 791 163	1 822 057 170	1 760 685 936	1 695 448 313	1 626 100 721	1 552 384 230	1 474 023 600	1 390 726 250	1 302 181 168	1 208 057 745	1 108 004 546
14	Annual Cash flow (3+13)	-379 943 150	-506 590 867	-1 199 068 994	1 031 106 285	1 934 103 480	1 879 791 163	1 822 057 170	1 760 685 936	1 695 448 313	1 626 100 721	1 552 384 230	1 474 023 600	1 390 726 250	1 302 181 168	1 208 057 745	1 108 004 546
15	Cumulative cash flow	-379 943 150	-886 534 017	-2 085 603 011	-1 054 496 726	879 606 755	2 759 397 918	4 581 455 088	6 342 141 024	8 037 589 337	9 663 690 058	11 216 074 288	12 690 097 888	14 080 824 138	15 383 005 305	16 591 063 050	17 699 067 597
16	Discount factor for % interest	1.000	0.870	0.756	0.658	0.572	0.497	0.432	0.376	0.327	0.284	0.247	0.215	0.187	0.163	0.141	0.123
17	Discounted Cash flow (Present value)	-379 943 150	-440 513 797	-906 668 427	677 969 120	1 105 829 942	934 588 434	787 725 596	661 907 059	554 245 061	462 239 313	383 725 640	316 831 383	259 936 680	211 640 844	170 733 180	136 167 648
18	CUMULATIVE DISCOUNTED CASH FLOW	-379 943 150	-820 456 947	-1 727 125 374	-1 049 156 254	56 673 688	991 262 122	1 778 987 718	2 440 894 777	2 995 139 838	3 457 379 151	3 841 104 791	4 157 936 174	4 417 872 854	4 629 513 698	4 800 246 878	4 936 414 526
19	IRR factor	1.000	0.651	0.424	0.276	0.180	0.117	0.076	0.050	0.032	0.021	0.014	0.009	0.006	0.004	0.002	0.002
20	iRR Discounted cash flow	-379 943 150	-329 750 750	-508 043 670	284 373 250	347 210 979	219 660 406	138 590 229	87 172 790	54 640 170	34 111 700	21 197 448	13 101 386	8 046 053	4 903 894	2 961 323	1 767 942
21	CUMULATIVE IRR DISCOUNTED CASH FLOW	-379 943 150	-709 693 900	-1 217 737 569	-933 364 319	-586 153 341	-366 492 935	-227 902 705	-140 729 916	-86 089 746	-51 978 046	-30 780 598	-17 679 212	-9 633 159	-4 729 265	-1 767 942	-0

CAPITAL COST ESTIMATION FOR HG2

Total Capital investment		
Equipment	Cost (\$)	
Reactor		92380023.67
Flash drum		9286.71
Membrane		29895030.98
Heater		10131.8
column		1572164.9
Agitator		15835.596
Total Equipment cost	123 882 473.58	
item	% of purchased equipment	total cost
Direct cost		
Equipment installation	47	58 224 762.58
Instrumentation and control	18	22 298 845.24
Piping	66	81 762 432.56
Electrical	11	13 627 072.09
Buildings (including services)	6	7 432 948.41
Yard improvements	10	12 388 247.36
Service facilities (installed)	30	37 164 742.07
Land	6	7 432 948.41
total Direct reaction unit plant cost	364 214 472.33	
Indirect cost		
Engineering and supervision	33	40 881 216.28
Construction expenses	41	50 791 814.17
Contractor's fee an legal expenses	21	26 015 319.45
Contingency	35	43 358 865.75
total indirect reaction unit plant cost	161 047 215.66	
Fixed Capital Investment (FCI)	525 261 687.98	
Working capital	86	451 725 051.66
Total Capital Investment	976 986 739.65	

Raw materials cost					
Material	Price/unit		Feedrate		USD/yr
1-Octene	1.8 USD/kg		2263.57 kg/hr		33 931 811.05
HG2 catalyst	28746.0 USD/kg		0.5426 kgCat/hr		129 908 470.61
Total					163 840 281.65
Labour operations					
Operators/shift/section	Number of sections	Number of shifts	Hours per year	Wage rate (\$/h)	Direct wages & benefits (DW&B)
2	3	5	8328	30	7495200
Item			Factor	Total cost per year	
Direct salaries and benefits			0.15	1124280	
Operating supplies and services			0.06	449712	
Technical assistance to manufacturing				260000	
Control laboratory				285000	
Total labour-related operations annual cost				2118992	
TOTAL LABOUR-RELATED OPERATIONS ANNUAL COST				9 614 192.00	
Product sales					
ITEM	Cost/unit		Production rate		Revenue/yr
7-Tetradecene	334.00 USD/Kg		1050.65 kg/hr		2 922 425 592.59
	58.59649123				
Maintenance					
			Wage factor (% purchased Capital)	wages & benefits (MW&B)	
			0.035	12 747 506.53	
Item			Factor	Total cost per year	
Salaries and benefits			0.25	3 186 876.63	
materials and services			1	12 747 506.53	
Maintenance overhead			0.05	637 375.33	
				16571758.49	
Maintnance and Opeertaion benefits				29 319 265.02	
MAINTENANCE OPERATION SALARIES AND BENEFITS					
				38 933 457.02	
Overhead					
General plant overhead			0.071	2 764 275.45	
Utilities					
	Input (kw)	Cost/unit		Total Annual cost	
Electricity	40095.27	0.235292419 \$/kwh		78567295.19	

Line	Item	0	1	2	3	4	5	6	7	8	9	10	11	12	13	14	15
1	Fixed Capital	-157 578 506	-210 104 675	-105 052 338													
2	Working capital			-451 725 052													
3	TOTAL CAPITAL INVESTMENT	-157 578 506	-210 104 675	-556 777 389													
4	Inflation Factor	1.000	1.063	1.130	1.201	1.277	1.357	1.443	1.534	1.630	1.733	1.842	1.958	2.082	2.213	2.352	2.500
5	Annual Income (Sales)	-		584 485 119	1 753 455 356	2 922 425 593	2 922 425 593	2 922 425 593	2 922 425 593	2 922 425 593	2 922 425 593	2 922 425 593	2 922 425 593	2 922 425 593	2 922 425 593	2 922 425 593	2 922 425 593
6	<i>Annual manufacturing cost</i>	-	-	-	-	-	-	-	-	-	-	-	-	-	-	-	-
a	Raw materials (Variable cost)	-	-	-37 026 888	-157 438 327	-209 196 177	-222 375 536	-236 385 195	-251 277 462	-267 107 943	-283 935 743	-301 823 695	-320 838 587	-341 051 418	-362 537 658	-385 377 530	-409 656 315
b	Labor (fixed cost)	-	-	-3 259 122	-11 548 154	-12 275 688	-13 049 057	-13 871 147	-14 745 029	-15 673 966	-16 661 426	-17 711 096	-18 826 895	-20 012 989	-21 273 808	-22 614 058	-24 038 743
c	Utilities (variable cost)	-	-	-88 778 608	-75 497 328	-100 317 075	-106 637 051	-113 355 185	-120 496 561	-128 087 845	-136 157 379	-144 735 294	-153 853 617	-163 546 395	-173 849 818	-184 802 357	-196 444 905
d	Maintenance (fixed cost)	-	-	-33 129 861	-35 217 042	-37 435 715	-39 794 165	-42 301 198	-44 966 173	-47 799 042	-50 810 382	-54 011 436	-57 414 157	-61 031 248	-64 876 217	-68 963 419	-73 308 114
h	Plant overhead (fixed cost)	-	-	-3 123 546	-3 320 329	-3 529 510	-3 751 869	-3 988 236	-4 239 495	-4 506 584	-4 790 498	-5 092 300	-5 413 115	-5 754 141	-6 116 652	-6 502 001	-6 911 627
6T	TOTAL ANNUAL MANUFACTURING COS	-	-	-165 318 024	-283 021 181	-362 754 165	-385 607 678	-409 900 961	-435 724 722	-463 175 379	-492 355 428	-523 373 820	-556 346 371	-591 396 192	-628 654 153	-668 259 364	-710 359 704
7	<i>Annual General Expenses</i>	-	-	-	-	-	-	-	-	-	-	-	-	-	-	-	-
a	Administrative	-	-	-13 209 001	-42 123 505	-74 628 810	-79 330 425	-84 328 242	-89 640 921	-95 288 299	-101 291 462	-107 672 824	-114 456 212	-121 666 953	-129 331 971	-137 479 885	-146 141 118
b	Distribution/ selling	-	-	-19 813 502	-63 185 258	-111 943 215	-118 995 637	-126 492 363	-134 461 381	-142 932 448	-151 937 193	-161 509 236	-171 684 318	-182 500 430	-193 997 957	-206 219 828	-219 211 677
c	R&D	-	-	-33 022 503	-105 308 763	-186 572 025	-198 326 062	-210 820 604	-224 102 302	-238 220 747	-253 228 655	-269 182 060	-286 140 530	-304 167 383	-323 329 928	-343 699 714	-365 352 795
7T	TOTAL ANNUAL GENERAL EXPENSES	-	-	-66 045 006	-210 617 526	-373 144 050	-396 652 125	-421 641 209	-448 204 605	-476 441 495	-506 457 309	-538 364 120	-572 281 059	-608 334 766	-646 659 856	-687 399 427	-730 705 591
8	TOTAL COST OF PRODUCTION (7T+6T)	-	-	-231 363 030	-493 638 706	-735 898 215	-782 259 803	-831 542 170	-883 929 327	-939 616 874	-998 812 737	-1 061 737 940	-1 128 627 430	-1 199 730 958	-1 275 314 009	-1 355 658 791	-1 441 065 295
9	Annual Operating Income (5-8)	-	-	353 122 088	1 259 816 649	2 186 527 378	2 140 165 790	2 090 883 422	2 038 496 266	1 982 808 718	1 923 612 855	1 860 687 653	1 793 798 162	1 722 694 634	1 647 111 584	1 566 766 801	1 481 360 298
10	Annual depreciation (fixed Cost)	-	-	-24 512 212	-24 512 212	-24 512 212	-24 512 212	-24 512 212	-24 512 212	-24 512 212	-24 512 212	-24 512 212	-24 512 212	-24 512 212	-24 512 212	-24 512 212	-24 512 212
11	Income before tax (9-10)	-	-	328 609 876	1 235 304 437	2 162 015 165	2 115 653 578	2 066 371 210	2 013 984 054	1 958 296 506	1 899 100 643	1 836 175 441	1 769 285 950	1 698 182 422	1 622 599 372	1 542 254 589	1 456 848 085
12	Income after tax	-	-	236 599 111	889 419 195	1 556 650 919	1 523 270 576	1 487 787 271	1 450 068 519	1 409 973 484	1 367 352 463	1 322 046 317	1 273 885 884	1 222 691 344	1 168 271 548	1 110 423 304	1 048 930 622
13	Annual cash income (10+12)	-	-	212 086 899	864 906 983	1 532 138 707	1 498 758 364	1 463 275 059	1 425 556 307	1 385 461 272	1 342 840 251	1 297 534 105	1 249 373 672	1 198 179 132	1 143 759 336	1 085 911 092	1 024 418 409
14	Annual Cash flow (3+13)	-157 578 506	-210 104 675	-344 690 490	864 906 983	1 532 138 707	1 498 758 364	1 463 275 059	1 425 556 307	1 385 461 272	1 342 840 251	1 297 534 105	1 249 373 672	1 198 179 132	1 143 759 336	1 085 911 092	1 024 418 409
15	Cumulative cash flow	-157 578 506	-367 683 182	-712 373 672	152 533 311	1 684 672 018	3 183 430 382	4 646 705 441	6 072 261 748	7 457 723 020	8 800 563 271	10 098 097 376	11 347 471 048	12 545 650 180	13 689 409 515	14 775 320 608	15 799 739 017
16	Discount factor for % interest	1.0000	0.8696	0.7561	0.6575	0.5718	0.4972	0.4323	0.3759	0.3269	0.2843	0.2472	0.2149	0.1869	0.1625	0.1413	0.1229
17	Discounted Cash flow (Present value)	-157 578 506	-182 699 718	-260 635 532	568 690 381	876 005 278	745 147 790	632 614 189	535 919 418	452 909 747	381 719 009	320 730 586	268 544 403	223 948 247	185 892 868	153 470 357	125 895 373
18	CUMULATIVE DISCOUNTED CASH FLOW	-157 578 506	-340 278 224	-600 913 755	-32 223 375	843 781 904	1 588 929 694	2 221 543 883	2 757 463 301	3 210 373 048	3 592 092 057	3 912 822 643	4 181 367 047	4 405 315 294	4 591 208 162	4 744 678 519	4 870 573 892
19	IRR factor	1.0000	0.5246	0.2752	0.1444	0.0758	0.0397	0.0209	0.0109	0.0057	0.0030	0.0016	0.0008	0.0004	0.0002	0.0001	0.0001
20	IRR Discounted cash flow	-157 578 506	-110 226 749	-94 870 648	124 888 730	116 065 518	59 564 573	30 509 400	15 593 491	7 950 687	4 042 834	2 049 423	1 035 277	520 879	260 856	129 931	64 305
21	CUMULATIVE IRR DISCOUNTED	-157 578 506	-267 805 255	-362 675 903	-237 787 173	-121 721 655	-62 157 083	-31 647 683	-16 054 192	-8 103 505	-4 060 671	-2 011 248	-975 972	-455 092	-194 236	-64 305	0

GCYC DISTILLATION COLUMN SIMULATION RESULTS

Distillation stream results (WUCOL) GCYC			
	WUCOLFED	WUCOLTOP	WUCOLBOT
Substream: MIXED			
Mole Flow kmol/hr			
C14	5.229829	0.000522983	5.229306
01-Oct-01	10.08127	10.07926	0.00201626
CIS-2-01	8.81E-05	8.81E-05	3.12E-08
ETHYL-01	0.299072	0.299072	3.58E-14
PROPY-01	0.0390406	0.0390406	3.64E-13
1-BUT-01	0.0272477	0.0272477	8.82E-12
6-TRI-01	0.1919867	0.00021922	0.1917675
6-DOD-01	0.0592896	0.000920935	0.0583687
Total Flow kmol/hr	15.92783	10.44637	5.481459
Total Flow kg/hr	2214.845	1142.914	1071.932
Total Flow l/min	59.57548	26.44267	30.26436
Temperature C	150	3.095261	262.7565
Pressure bar	3.899793	1	1.5
Vapor Frac	0	0	0
Liquid Frac	1	1	1
Solid Frac	0	0	0
Enthalpy cal/mol	-31405.95	-29284.26	-38008.68
Enthalpy cal/gm	-225.8526	-267.6617	-194.3622
Enthalpy cal/sec	-138950	-84976.18	-57873.06
Entropy cal/mol-K	-193.8121	-174.5041	-252.9832
Entropy cal/gm-K	-1.39378	-1.594988	-1.293662
Density mol/cc	0.00445592	0.00658429	0.00301866
Density gm/cc	0.6196188	0.720372	0.5903158
Average MW	139.0551	109.4077	195.5559
Liq Vol 60F l/min	49.83985	26.79832	23.04153

Distillation block (WUCOL) results GCYC	
Minimum reflux ratio	0.017988608
Actual reflux ratio	0.055
Minimum number of stages	6.64238995
Number of actual stages	24.974727
Feed stage	11.5888798
Number of actual stages above feed	10.5888798
Reboiler heating required	27184.8884 cal/sec
Condenser cooling required	31081.749 cal/sec
Distillate temperature	3.0952615 C
Bottom temperature	262.756485 C
Distillate to feed fraction	0.655856478

Distillation Column Sizing									
Design parameters								Cost	
R/Rm	3.28	Rm	0.01679	H	115.0	ft	V top	56.029	ft/hr
N/Nm	3.8	R	0.055	U	100	Btu/ft ² h.° F	V bottom	64.127	ft/hr
% recovery	0.998	Tray spacing	24 in	D	7.67	ft	H vap	52711.67	btu
%purity	0.95	Nmin	6.62	Fm	3.67	solid ss	H liq	68415.62	btu
E ₀	0.5	Nactual	25	Fp	1	-	delta T	110	° F
H/D	15	-		Fc	3.67	-			
								Total	\$1 531 804.85 \$/yr

GMPP DISTILLATION COLUMN SIMULATION RESULTS

Distillation stream results (WUCOL) GMPP				Distillation block (WUCOL) results GMPP			
	WUCOLFED	WUCOLTOP	WUCOLBOT				
Substream: MIXED				Minimum reflux ratio	0.018723		
Mole Flow kmol/hr				Actual reflux ratio	0.055		
C14	5.349847	0.000534985	5.349312	Minimum number of stages	6.602248		
01-Oct-01	12.27649	12.27403	0.0024553	Number of actual stages	25.1871		
CIS-2-01	0	0	0	Feed stage	11.69558		
ETHYL-01	0.3446172	0.3446172	4.08E-14	Number of actual stages above feed	10.69558		
PROPY-01	0.0204538	0.0204538	1.89E-13	Reboiler heating required	28994.75 cal/sec		
1-BUT-01	0.0547841	0.0547841	1.76E-11	Condenser cooling required	37646.69 cal/sec		
6-TRI-01	0.0889946	0.000101301	0.0888933	Distillate temperature	6.64217 C		
6-DOD-01	0.1099835	0.00170633	0.1082771	Bottom temperature	262.698 C		
Total Flow kmol/hr	18.24517	12.69623	5.548938	Distillate to feed fraction	0.695868		
Total Flow kg/hr	2476.533	1391.344	1085.189				
Total Flow l/min	67.01065	32.30246	30.62949				
Temperature C	150	6.64217	262.698				
Pressure bar	3.970372	1	1.5				
Vapor Frac	0	0	0				
Liquid Frac	1	1	1				
Solid Frac	0	0	0				
Enthalpy cal/mol	-30160.79	-29180.98	-38015.79				
Enthalpy cal/gm	-222.2013	-266.281	-194.3876				
Enthalpy cal/sec	-152860	-102910	-58596.46				
Entropy cal/mol-K	-188.712	-174.1661	-253.0911				
Entropy cal/gm-K	-1.390283	-1.589293	-1.29414				
Density mol/cc	0.00453788	0.0065507	0.00301939				
Density gm/cc	0.615955	0.717873	0.5904925				
Average MW	135.7364	109.5872	195.567				
Liq Vol 60F l/min	55.92989	32.60403	23.32586				

Distillation Column Sizing								Cost		
Design parameters								tower	\$1 458 382.4 (\$/Yr)	
R/Rm	3.28	Rm	0.01679	H	115.0	ft	V t	65.536	ft/hr	
N/Nm	3.8	R	0.055	U	100	Btu/ft ² h.° F	V b	63.941	ft/hr	
% recovery	0.998	ray spacinc	24 in	D	7.67	ft	H vap	26307.22	btu	condenser 12671.46 \$/yr
%purity	0.95	Nmin	6.62	Fm	3.67	solid ss	Hliq	52984.23	btu	reboiler 39563.26 \$/yr
E0	0.5	Nactual	25	Fp	1	-	delta T	110	° F	
H/D	15			Fc	3.67	-				Total \$1 510 617.08 \$/yr

HG2 DISTILLATION COLUMN SIMULATION RESULTS

Distillation stream results (WUCOL) HG2			
	WUCOLFED	WUCOLTOP	WUCOLBOT
Substream: MIXED			
Mole Flow kmol/hr			
C14	5.349837	0.000534984	5.349302
01-Oct-01	11.67423	11.6719	0.00233485
CIS-2-01	0.0990886	0.0990535	3.51E-05
ETHYL-01	0.3245418	0.3245418	3.89E-14
PROPY-01	0.1048388	0.1048388	9.80E-13
1-BUT-01	0.1362685	0.1362685	4.42E-11
6-TRI-01	0.4809693	0.000549486	0.4804198
6-DOD-01	0.2829545	0.00439475	0.2785598
Total Flow	18.45273	12.34208	6.110652
Total Flow	2528.219	1342.985	1185.234
Total Flow	68.24987	31.18003	33.45317
Temperat	150	5.309883	260.4484
Pressure b	4.109477	1	1.5
Vapor Frac	0	0	0
Liquid Frac	1	1	1
Solid Frac	0	0	0
Enthalpy c	-30680.2	-28928.66	-37900.23
Enthalpy c	-223.9258	-265.8555	-195.4002
Enthalpy c	-157260	-99177.75	-64331.97
Entropy ca	-190.3219	-172.7912	-250.8283
Entropy ca	-1.389104	-1.587958	-1.293182
Density m	0.00450617	0.00659722	0.00304438
Density gr	0.617393	0.7178659	0.5904942
Average N	137.0106	108.8135	193.962
Liq Vol 60	57.01527	31.51579	25.49948

Distillation block (WUCOL) results HG2		
Minimum reflux ratio	0.017364	
Actual reflux ratio	0.05	
Minimum number of stages	6.619727	
Number of actual stages	27.11786	
Feed stage	12.5181	
Number of actual stages above feed	11.5181	
Reboiler heating required	29869.51 cal/sec	
Condenser cooling required	36119.92 cal/sec	
Distillate temperature	5.309883 C	
Bottom temperature	260.4484 C	
Distillate to feed fraction	0.668848	

Distillation Column Sizing											Cost	
Design parameters										Cost		
R/Rm	2.98	Rm	0.01679	H	119.6	ft	V top	0.062	ft/hr	tower	\$1 570 349.4	Cost (\$/Yr)
N/Nm	3.9	R	0.05	U	100	Btu/ft ² h. ^o F	V bottom	0.071	ft/hr	condenser	417.88	\$/yr
% recovery	0.998	Tray spacing	24 in	D	7.97	ft	H vap	26254.8459	btu	reboiler	1397.63	\$/yr
%purity	0.95	Nmin	6.62	Fm	3.67	solid ss	H liq	52430.2637	btu			
E ₀	0.5	Nactual	26	Fp	1	-	delta T	110	° F			
H/D	15			Fc	3.67	-				Total	\$1 572 164.86	\$/yr

APPENDIX E: Simulations and Regression algorithms

Programmable MATLAB code

```

function [temp,paropty,rSQ,MSE] = Bootfunction3_CD_plots(nboots)
%Bootfunct function that determines optimal regression coefficients for a
reaction
% ODEsystem and bootstraps the coeficients to determine the 95% confidence
% intervals
%% bootfunct returns an array of the optimal regression coefficients obtained
during the execuction of nboots trials.

%% import excel data an define variables
global Cexp0;% initial concentrations
global GC;% experimental data
global tspan;%time span

%read excel file
GC = xlsread('Mock data workbook2.xlsx','Sheet2','A2:D26');
Cexp0(1)=GC(1,2);% 1-octene
Cexp0(2)=GC(1,3);%Primary metathesis Products
Cexp0(3)=GC(1,4);% Side metathesis products

tspan =GC(:,1);%interval for the odesolver

%initial k values
k1=0.01;
k2=0.001;
k3=0.01;
%k4=0.001;

k0= [k1,k2,k3];% k4];

%create Temporary matrice ase a space holder
temp = zeros(nboots,3);

%% STEP2-determine beta-hat as paropty
%choose leverberg marquart and display iterations
options = optimset('Algorithm','Levenberg-Marquardt','Display','iter',
'Tolfun',1e-10,'tolx',1e-10);

%supply the basis values to LSQnonlin
[paropty]=lsqnonlin(@minimiz,k0, [], [],options);

%%STEP3
%solve ode with initial guessed k values
[t,C]=ode45(@lsqparafit2,tspan,Cexp0,'',k0);

%slove ode with optimised parameters get y hat
[t,C_hat]=ode45(@lsqparafit2,tspan,Cexp0,'',paropty);

```

```

%% STEP4-Calculate the residuals and centre them
e1 =GC(:,2)-C_hat(:,1);
e2 =GC(:,3)-C_hat(:,2);
e3 =GC(:,4)-C_hat(:,3);
e = [e1,e2,e3];
e_mean =sum(e)/numel(e);

e_tilde1= e1-e_mean(1);
e_tilde2=e2-e_mean(2);
e_tilde3=e3-e_mean(3);
e_tilde = [e_tilde1,e_tilde2,e_tilde3];

%% Initialise Bootstrap
for i=1:nboots;

%% Step 5 Sample with replacement from e-tilde
e_star1 =datasample(e_tilde1,numel(e_tilde1));
e_star2 =datasample(e_tilde2,numel(e_tilde2));
e_star3 =datasample(e_tilde3,numel(e_tilde3));

e_star= [e_star1,e_star2,e_star3];

global Cstar;

%bootstrap sample
Cstar1=C_hat(:,1)+e_star1;
Cstar2=C_hat(:,2)+e_star2;
Cstar3=C_hat(:,3)+e_star3;

Cstar= [Cstar1,Cstar2,Cstar3];

%% Step7 Solve for paropt star and repeat nboot times
[paropt_star] =lsqnonlin(@minimiz_star,k0, [], [],options);
temp(i,:)= [paropt_star];
end
%% Step 6 create a function that solves the odes with Cstar and returns the
residuals vector
function [ lsq_star] = minimiz_star (par2)
    %solving ode with initial valuesk0
    global Cstar0
    Cstar0(1)=Cstar(1,1);% initial conditions for minimiz_star
    Cstar0(2)=Cstar(1,2);
    Cstar0(3)=Cstar(1,3);
    [t,C2]=ode45(@lsqparafit,tspan,Cstar0,'',par2);
    lsq_star = [C2(:,1)-Cstar1; C2(:,2)-Cstar2;C2(:,3)-Cstar3];
end
%% Plot the calculated confidence intervals,
kll= [0.035976781    0.00422493656    0.02856908];
[t,C_ll]=ode45(@lsqparafit2,tspan,Cexp0,'',kll);

kul= [0.032176781    0.004693656658    0.03956908];
[t,C_ul]=ode45(@lsqparafit2,tspan,Cexp0,'',kul);

%% Step 8-Create the curve fit
expD= xlsread('Mock data workbook2.xlsx','Sheet2','B2:D26');

```

```

%% Plot results
% Create figure
figure1 = figure('Name','Experimental and Predicted Concentration profiles',...
    'Color', [0.933333337306976 0.933333337306976 0.933333337306976]);

% Create axes
axes1 = axes('Parent',figure1,'YMinorTick','on','XMinorTick','on',...
    'FontName','Arial',...
    'PlotBoxAspectRatio',[1 0.85 1],...
    'Position',[0.127803806734993 0.0946938775510203 0.775 0.815]);

xlim(axes1,[0 360]);
box(axes1,'on');
hold(axes1,'on');

Y= [C_hat C_ul C_ll expD];
X=tspan;
plot1=plot(X,Y,'Parent',axes1);

% Create multiple lines using matrix input to plot
set(plot1(1), 'LineWidth',1,'Color', [0 0 0]);
set(plot1(2), 'LineWidth',1,'Color', [0 0 0]);
set(plot1(3), 'LineWidth',1,'Color', [0 0 0]);
set(plot1(4), 'LineStyle',':','Color', [1 0 1]);
set(plot1(5), 'LineStyle',':','Color', [1 0 1]);
set(plot1(6), 'LineStyle',':','Color', [1 0 1]);
set(plot1(7), 'LineStyle',':','Color', [1 0 1]);
set(plot1(8), 'LineStyle',':','Color', [1 0 1]);
set(plot1(9), 'LineStyle',':','Color', [1 0 1]);
set(plot1(10),...
    'MarkerFaceColor', [0.501960813999176 0.501960813999176
0.501960813999176],...
    'Marker','o',...
    'LineStyle','none',...
    'Color', [0 0 0]);
set(plot1(11),...
    'MarkerFaceColor', [0.501960813999176 0.501960813999176
0.501960813999176],...
    'Marker','o',...
    'LineStyle','none',...
    'Color', [0 0 0]);
set(plot1(12),...
    'MarkerFaceColor', [0.501960813999176 0.501960813999176
0.501960813999176],...
    'Marker','o',...
    'LineStyle','none',...
    'Color', [0 0 0]);

% Create xlabel
xlabel('Time (mins)', 'FontWeight', 'bold');

% Create ylabel
ylabel('Percentage', 'FontWeight', 'bold', 'FontSize', 12);

% Create title
title('Experimental Vs Predicted Reaction Concentration', 'FontSize', 12);

% Create legend

```

```
%legend1 = legend( [plot1(2),plot1(4),plot1(10)], {'Model','Conf. Interval','Exp. Data'});
```

```
end
```



```
function [ dC ] = lsqparafit2(t,C,par,[],varargin)
%Rate equations are described in this function
k1=par(1);
k3=par(3);
k2=par(2);
%k4=par(4);

dC8_dt = -k1*((C(1)*exp(-k3.*t)))-k2*(C(1)*exp(-k3.*t));
dCPMP_dt= k1*((C(1)*exp(-k3.*t)));
dCSP_dt= k2*((C(1)*exp(-k3.*t)));

dC= [dC8_dt;dCPMP_dt;dCSP_dt];
end
```



```
function [ lsq ] = minimiz( par,varargin )
%Objective function definition
GC = xlsread('Mock data workbook2.xlsx','Sheet2','A2:D26');

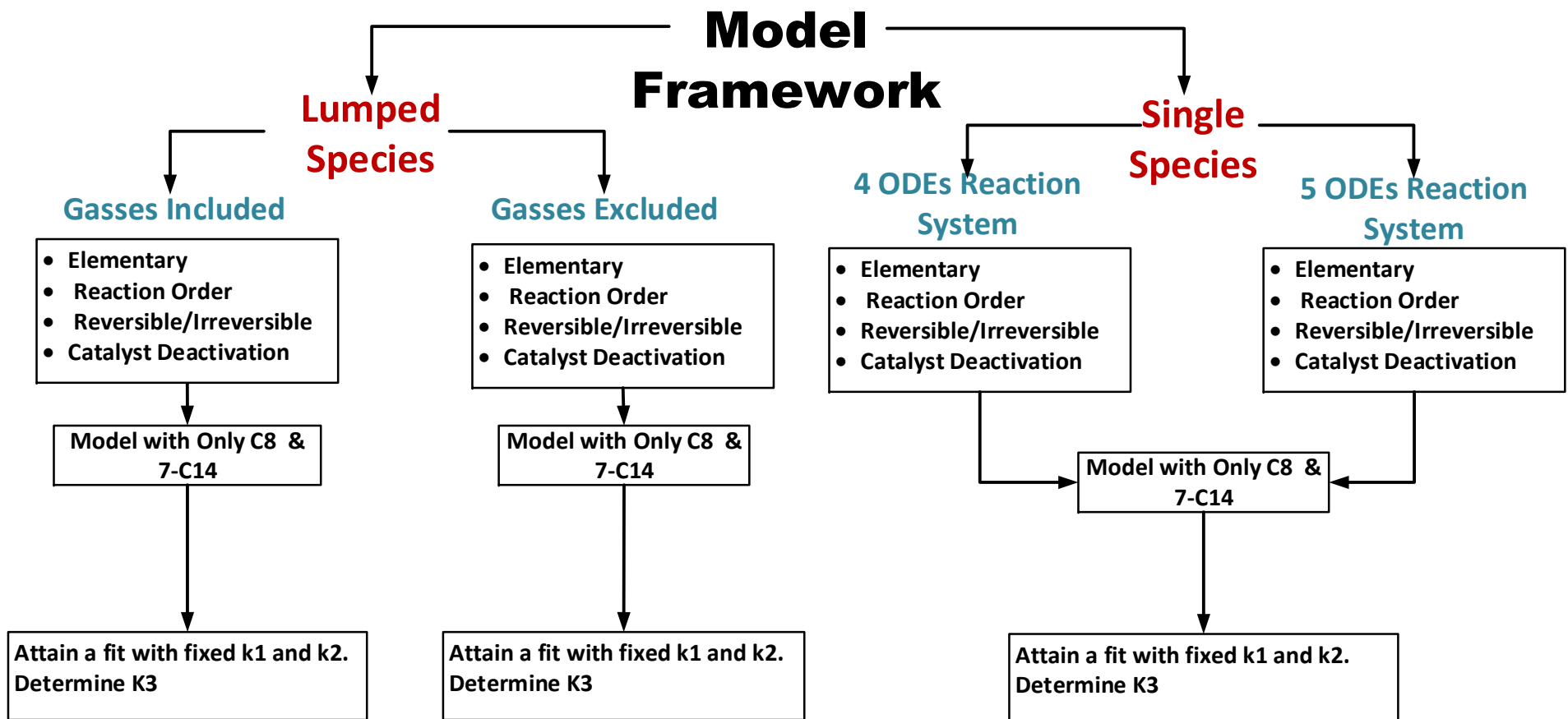
Cexp0(1)=GC(1,2);% 1-octene
Cexp0(2)=GC(1,3);%Primary metathesis Products
Cexp0(3)=GC(1,4);% Side metathesis products

tspan = [0;1;2.5;5;7.5;10;12.5;15;17.5;20;22.5;25;30;35;40;45;50;60;90;120;150;180;240;300;360];
%solving ode with initial valuesk0
[t,C]=ode45(@lsqparafit2,tspan,Cexp0,[],par);

lsq = [1.* (C(:,1)-GC(:,2)); 1.* (C(:,2)-GC(:,3));1.* ( C(:,3)-GC(:,4))];
```

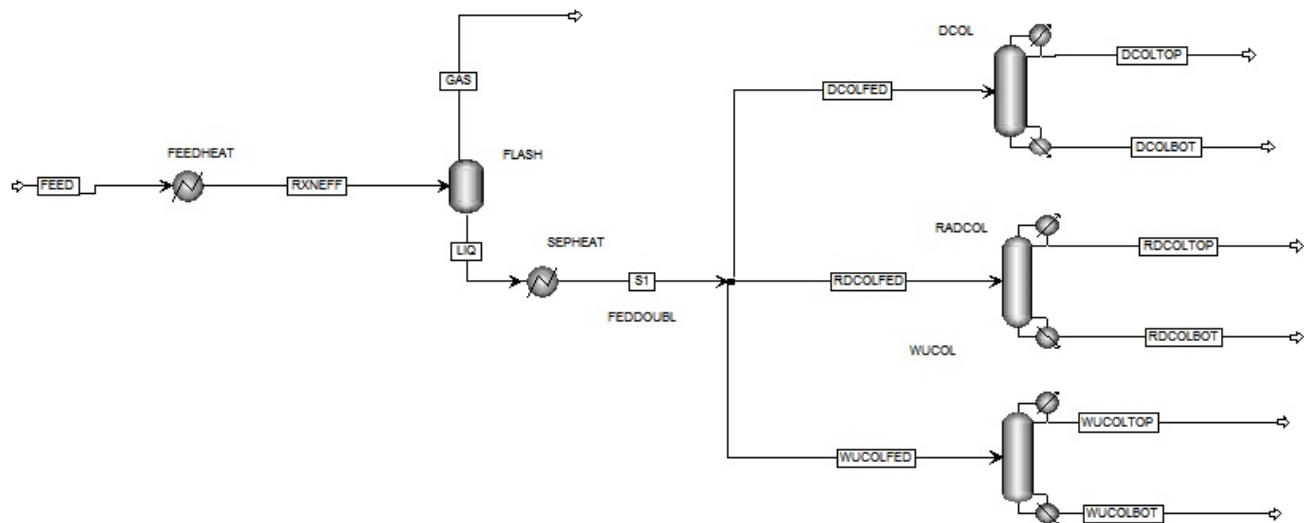
```
end
```

MODEL FRAMEWORK REACTION KINTEC STUDY



ASPEN PROCESS SIMULATION DETAILS

Simulation Flowsheet



PROPERTY METHOD DECISION TREE RESULTS

Aspen method's assistant [1]:

Component type (polarity):	Hydrocarbon system
Real or Assays?	Real

Therefore, possible property methods are:

Soave-Reidlich-Kwong
LK-Plocker
or Peng Robinson

[1] E.C. Carlson, Don't gamble with physical properties for simulations, Chem. Eng. Prog. 92 (1996) 35–46.

Input Summary created by Aspen Plus**DYNAMICS**

DYNAMICS RESULTS=ON

IN-UNITS MET PRESSURE=bar TEMPERATURE=C DELTA-T=C PDROP=bar &
INVERSE-PRES='1/bar'

DEF-STREAMS CONVEN ALL**MODEL-OPTION**

DATABANKS 'APV88 PURE32' / 'APV88 AQUEOUS' / 'APV88 SOLIDS' / &

'APV88 INORGANIC' / 'APEOSV88 AP-EOS' / 'APV88 ASPENPCD' &
'APV88 BIODIESEL' / 'APV88 COMBUST' / &
'APV88 ELECPURE' / 'APV88 EOS-LIT' / 'APV88 ETHYLENE' / &
'APV88 HYSYS' / 'APV88 INITIATO' / 'APV88 NRTL-SAC' / &
'APV88 PC-SAFT' / 'APV88 POLYMER' / 'APV88 POLYPCSF' / &
'APV88 PURE20' / 'APV88 PURE22' / 'APV88 PURE24' / &
'APV88 PURE25' / 'APV88 PURE26' / 'APV88 PURE27' / &
'APV88 PURE28' / 'APV88 SEGMENT' / 'FACTV88 FACTPCD' / &
'NISTV88 NIST-TRC'

PROP-SOURCES 'APV88 PURE32' / 'APV88 AQUEOUS' / 'APV88 SOLIDS' &

/ 'APV88 INORGANIC' / 'APEOSV88 AP-EOS' / &
'APV88 ASPENPCD' / 'APV88 BIODIESEL' / 'APV88 COMBUST' &
'APV88 ELECPURE' / 'APV88 EOS-LIT' / 'APV88 ETHYLENE' &
'APV88 HYSYS' / 'APV88 INITIATO' / 'APV88 NRTL-SAC' &
'APV88 PC-SAFT' / 'APV88 POLYMER' / 'APV88 POLYPCSF' &
'APV88 PURE20' / 'APV88 PURE22' / 'APV88 PURE24' / &
'APV88 PURE25' / 'APV88 PURE26' / 'APV88 PURE27' / &
'APV88 PURE28' / 'APV88 SEGMENT' / 'FACTV88 FACTPCD' / &
'NISTV88 NIST-TRC'

COMPONENTS

C14 C14H28-N6 /
1-OCT-01 C8H16-16 /
CIS-2-01 C8H16-D7 /
ETHYL-01 C2H4 /
PROPY-01 C3H6-2 /
1-BUT-01 C4H8-1 /
6-TRI-01 C13H26-N8 /
6-DOD-01 C12H24-N24

SOLVE

RUN-MODE MODE=SIM

FLOWSCHEET

BLOCK FLASH IN=RXNEFF OUT=GAS LIQ
BLOCK FEEDHEAT IN=FEED OUT=RXNEFF
BLOCK SEPHEAT IN=LIQ OUT=S1

BLOCK WUCOL IN=WUCOLFED OUT=WUCOLTOP WUCOLBOT
PROPERTIES RK-SOAVE
PROP-DATA RSKBV-1
IN-UNITS MET PRESSURE=bar TEMPERATURE=C DELTA-T=C PDROP=bar &
 INVERSE-PRES='1/bar'
PROP-LIST RSKBV
BPVAL PROPY-01 1-BUT-01 -3.700000E-3 0.0 0.0 -273.1500000 &
 726.8500000
BPVAL 1-BUT-01 PROPY-01 -3.700000E-3 0.0 0.0 -273.1500000 &
 726.8500000
PROP-SET PS-2 TBUB KVL KVL2 MOLEFRAC UNITS='C' &
 SUBSTREAM=MIXED COMPS=6-TRI-01 1-OCT-01 PHASE=V L1 L2

STREAM FEED

SUBSTREAM MIXED TEMP=70.00000000 PRES=1.013250000 &
 MOLE-FLOW=24.128
MOLE-FLOW C14 5.35 / 1-OCT-01 11.8 / CIS-2-01 0.1 / &
 ETHYL-01 5.35 / PROPY-01 0.481 / 1-BUT-01 0.283 / &
 6-TRI-01 0.481 / 6-DOD-01 0.283

BLOCK FEEDHEAT HEATER

PARAM TEMP=33.00000000 PRES=1.013250000 DPPARMOPT=NO

BLOCK SEPHEAT HEATER

PARAM TEMP=150. VFRAC=0. DPPARMOPT=NO

BLOCK FLASH FLASH2

PARAM TEMP=33.00000000 PRES=1.000000000

BLOCK WUCOL DSTWU

PARAM LIGHTKEY=1-OCT-01 RECOVL=0.9998 HEAVYKEY=C14 &
 RECOVH=0.0001 PTOP=1.000000000 PBOT=1.500000000 RR=0.05

BLOCK RADCOL RADFRAC

PARAM NSTAGE=26 ALGORITHM=STANDARD MAXOL=25 DAMPING=NONE
COL-CONFIG CONDENSER=TOTAL
RATESEP-ENAB CALC-MODE=EQUILIBRIUM
FEEDS RDCOLFED 10
PRODUCTS RDCOLTOP 1 L / RDCOLBOT 26 L
P-SPEC 1 1.000000000
COL-SPECS D:F=0.99 MOLE-RR=0.05
DB:F-PARAMS COMPS=1-OCT-01
SC-REFLUX OPTION=0

BLOCK FEDDOUBL DUPL**DESIGN-SPEC DS-1**

DEFINE PURITY MASS-FRAC STREAM=RDCOLTOP SUBSTREAM=MIXED &
 COMPONENT=1-OCT-01
SPEC "PURITY" TO "0.95"
TOL-SPEC "0.002"

VARY BLOCK-VAR BLOCK=RADCOL VARIABLE=NSTAGE SENTENCE=PARAM
LIMITS "6" "30" STEP-SIZE=1.

DESIGN-SPEC DS-2

```
DEFINE RECOVERY BLOCK-VAR BLOCK=RADCOL VARIABLE=D:F &
SENTENCE=COL-SPECS
SPEC "RECOVERY" TO "0.9997"
TOL-SPEC "0.00001"
VARY BLOCK-VAR BLOCK=RADCOL VARIABLE=NSTAGE SENTENCE=PARAM
LIMITS "5" "35" STEP-SIZE=0.5
```

EO-CONV-OPTI

STREAM-REPOR MOLEFLOW



A reader lives a thousand lives before he dies, said Jojen. The man who never reads lives only one~

George R R Martin (A Song of Ice and Fire)

